THE MALE AND FEMALE BRAIN: MOLECULAR MECHANISMS OF SEX DIFFERENCES

EDITED BY: Laura Musazzi and Jordan Marrocco

PUBLISHED IN: Frontiers in Molecular Neuroscience and
Frontiers in Human Neuroscience

frontiers Research Topics

frontiers

ISSN 1664-8714
ISBN 978-2-88971-887-0
DOI 10.3389/978-2-88971-887-0

About Frontiers

Frontiers is more than just an open-access publisher of scholarly articles: it is a pioneering approach to the world of academia, radically improving the way scholarly research is managed. The grand vision of Frontiers is a world where all people have an equal opportunity to seek, share and generate knowledge. Frontiers provides immediate and permanent online open access to all its publications, but this alone is not enough to realize our grand goals.

Frontiers Journal Series

The Frontiers Journal Series is a multi-tier and interdisciplinary set of open-access, online journals, promising a paradigm shift from the current review, selection and dissemination processes in academic publishing. All Frontiers journals are driven by researchers for researchers; therefore, they constitute a service to the scholarly community. At the same time, the Frontiers Journal Series operates on a revolutionary invention, the tiered publishing system, initially addressing specific communities of scholars, and gradually climbing up to broader public understanding, thus serving the interests of the lay society, too.

Dedication to Quality

Each Frontiers article is a landmark of the highest quality, thanks to genuinely collaborative interactions between authors and review editors, who include some of the world's best academicians. Research must be certified by peers before entering a stream of knowledge that may eventually reach the public - and shape society; therefore, Frontiers only applies the most rigorous and unbiased reviews.
Frontiers revolutionizes research publishing by freely delivering the most outstanding research, evaluated with no bias from both the academic and social point of view. By applying the most advanced information technologies, Frontiers is catapulting scholarly publishing into a new generation.

What are Frontiers Research Topics?

Frontiers Research Topics are very popular trademarks of the Frontiers Journals Series: they are collections of at least ten articles, all centered on a particular subject. With their unique mix of varied contributions from Original Research to Review Articles, Frontiers Research Topics unify the most influential researchers, the latest key findings and historical advances in a hot research area! Find out more on how to host your own Frontiers Research Topic or contribute to one as an author by contacting the Frontiers Editorial Office: frontiersin.org/about/contact

THE MALE AND FEMALE BRAIN: MOLECULAR MECHANISMS OF SEX DIFFERENCES

Topic Editors:
Laura Musazzi, University of Milano Bicocca, Italy
Jordan Marrocco, The Rockefeller University, United States

Citation: Musazzi, L., Marrocco, J., eds. (2021). The Male and Female Brain: Molecular Mechanisms of Sex Differences. Lausanne: Frontiers Media SA. doi: 10.3389/978-2-88971-887-0

Table of Contents

frontiers in Human Neuroscience

CASE REPORT
published: 14 November 2017
doi: 10.3389/fnhum.2017.00528

Brain Maturation, Cognition and Voice Pattern in a Gender Dysphoria Case under Pubertal Suppression

Maiko A. Schneider[1], Poli M. Spritzer[1,2,3], Bianca Machado Borba Soll[1], Anna M. V. Fontanari[1], Marina Carneiro[4], Fernanda Tovar-Moll[4,5], Angelo B. Costa[1,6], Dhiordan C. da Silva[1], Karine Schwarz[1], Maurício Anes[7], Silza Tramontina[1,8] and Maria I. R. Lobato[1,9]*

[1] Gender Identity Program, Hospital de Clinicas de Porto Alegre, Universidade Federal do Rio Grande do Sul, Porto Alegre, Brazil, [2] Department of Physiology, Universidade Federal do Rio Grande do Sul, Porto Alegre, Brazil, [3] Service of Endocrinology, Hospital de Clínicas de Porto Alegre, Porto Alegre, Brazil, [4] Instituto D'Or de Pesquisa e Ensino, Rio de Janeiro, Porto Alegre, Brazil, [5] Institute for Biomedical Sciences, Federal University of Rio de Janeiro, Rio de Janeiro, Brazil, [6] Graduate Program in Psychology, Pontifícia Universidade Católica do Rio Grande do Sul, Porto Alegre, Brazil, [7] Division of Medicine Physics, Hospital de Clínicas de Porto Alegre, Porto Alegre, Brazil, [8] Child and Adolescent Psychiatry Service, Hospital de Clínicas de Porto Alegre, Porto Alegre, Brazil, [9] Psychiatry and Forensic Medicine Service, Hospital de Clínicas de Porto Alegre, Porto Alegre, Brazil

Introduction: Gender dysphoria (GD) (DMS-5) is a condition marked by increasing psychological suffering that accompanies the incongruence between one's experienced or expressed gender and one's assigned gender. Manifestation of GD can be seen early on during childhood and adolescence. During this period, the development of undesirable sexual characteristics marks an acute suffering of being opposite to the sex of birth. Pubertal suppression with gonadotropin releasing hormone analogs (GnRHa) has been proposed for these individuals as a reversible treatment for postponing the pubertal development and attenuating psychological suffering. Recently, increased interest has been observed on the impact of this treatment on brain maturation, cognition and psychological performance.

Objectives: The aim of this clinical report is to review the effects of puberty suppression on the brain white matter (WM) during adolescence. WM Fractional anisotropy, voice and cognitive functions were assessed before and during the treatment. MRI scans were acquired before, and after 22 and 28 months of hormonal suppression.

Methods: We performed a longitudinal evaluation of a pubertal transgender girl undergoing hormonal treatment with GnRH analog. Three longitudinal magnetic resonance imaging (MRI) scans were performed for diffusion tensor imaging (DTI), regarding Fractional Anisotropy (FA) for regions of interest analysis. In parallel, voice samples for acoustic analysis as well as executive functioning with the Wechsler Intelligence Scale (WISC-IV) were performed.

Results: During the follow-up, white matter fractional anisotropy did not increase, compared to normal male puberty effects on the brain. After 22 months of pubertal suppression, operational memory dropped 9 points and remained stable after 28 months of follow-up. The fundamental frequency of voice varied during the first year; however, it remained in the female range.

OPEN ACCESS

Edited by:
Jordan Marrocco, Rockefeller University, United States

Reviewed by:
Robert-Paul Juster, Columbia University Medical Center, United States
Shau-Ming Wei, National Institutes of Health (NIH), United States

***Correspondence:**
Maiko A. Schneider
maikoschneider@hcpa.edu

Received: *21 June 2017*
Accepted: *18 October 2017*
Published: *14 November 2017*

Citation:
Schneider MA, Spritzer PM, Soll BMB, Fontanari AMV, Carneiro M, Tovar-Moll F, Costa AB, da Silva DC, Schwarz K, Anes M, Tramontina S and Lobato MIR (2017) Brain Maturation, Cognition and Voice Pattern in a Gender Dysphoria Case under Pubertal Suppression. Front. Hum. Neurosci. 11:528. doi: 10.3389/fnhum.2017.00528

Conclusion: Brain white matter fractional anisotropy remained unchanged in the GD girl during pubertal suppression with GnRHa for 28 months, which may be related to the reduced serum testosterone levels and/or to the patient's baseline low average cognitive performance.Global performance on the Weschler scale was slightly lower during pubertal suppression compared to baseline, predominantly due to a reduction in operational memory. Either a baseline of low average cognition or the hormonal status could play a role in cognitive performance during pubertal suppression. The voice pattern during the follow-up seemed to reflect testosterone levels under suppression by GnRHa treatment.

Keywords: gender dysphoria, pubertal suppression, white matter, WISC-IV, cognition

INTRODUCTION

Gender dysphoria (GD), according to DMS-5 (APA-2013), is a condition marked by increasing psychological suffering that accompanies the incongruence between one's experienced or expressed gender and one's assigned gender. Diagnostic criteria consider the individual's developmental history and fit it for two different diagnoses: childhood (pre-pubertal) and adolescence or adulthood, the last share the same DSM-5 (APA-2013) diagnostic criteria. Clinical management is focused on therapy for attenuating dysphoric feelings about the body, as well as body incongruence. These interventions range from biopsychosocial approaches to hormonal treatment and sex-reassignment surgery in adulthood (Coleman et al., 2012).

Childhood and adolescence is a critical time for the development of mental disorders. In this period, GD youths are at high risk of having a clinical diagnosis of depression (Resiner et al., 2015), suicide, self-harm and eating disorders (Connolly et al., 2016; Feder et al., 2017), which are strongly related to dysphoric feelings and to different levels of transphobia exposition (Acerlus et al., 2016).

Preventing the development of secondary sex characteristics is a crucial part of the treatment for alleviating gender inconformity in adolescence (Cohen-Kettenis et al., 2011; Coleman et al., 2012). It is considered a transient and reversible intervention (Smith et al., 2014) and should be prescribed to GD individuals in the Tanner 2–3 stages of puberty development under parents' consent (Tanner, 1962; Hembree et al., 2009; Coleman et al., 2012). Recently, increased interest has been observed on the impact of pubertal suppression on brain maturation, cognition and psychological performance (Staphorsius et al., 2015; Hough et al., 2017, 2019). In our study, we aim to evaluate the WM fractional anisotropy and the IQ scale in a longitudinal case during pubertal suppression.

Case Presentation

An 11-year-old individual, designated a boy at birth, was referred to the Gender Identity Program (PROTIG). The patient fit the criteria for male-to-female (MtF) GD (DSM-5) and gender incongruence (ICD-11 inventory) (Robles et al., 2016), which was translated and adapted for the Brazilian population (Soll et al., 2017). At admission, current psychosis, mood disorders, anxiety and global development disorders were excluded.

The patient was born at term, of normal weight, displayed a male phenotype, and experienced no intercurrences during pregnancy. The parents confirmed normal neuropsychomotor development for each of the developmental milestones. At age three, they noticed some female behaviors and sought out psychological treatment. They were informed about a possible DG diagnosis, and the child was kept in psychotherapy to "reverse the desire of belonging to the opposite sex" until age seven. The patient and parents report that she made efforts to behave as a boy during this treatment. At nine, she assumed her gender identity and reported believing that she was born the wrong sex, and she wanted to be a girl.

At 11 years and 11 months old, she weighed 35.5 kg, was 145.5 cm in height and was in Tanner stage 2, according to male characteristics. The patient's bone age was compatible with the chronological age for both male and female standards. The biochemical and hormonal laboratory tests were normal for age, born-sex, and Tanner stage (testosterone 182 ng/dl, LH 3.3 and FSH 2.2 IU/L). After written consent of the parents and patient for using GnRHa and for publication of data to scientific article, she started receiving Leuprorelin 3.75 mg IM/every 28 days. In the next months, the GnRHa doses were adjusted according to the clinical signs and hormone levels (last testosterone under GnRHa 29 ng/dl). The affective and social domains improved during the GnRH treatment; however, the teachers and school counselors reported some difficulties, specifically in math and exact sciences.

This study was carried out in accordance with the recommendations of the Endocrine Society Clinical Practice Guideline for the Endocrine Treatment of Transsexual Persons (2009, updated in 2017), the Standards of Care for the health of transsexual, transgender and gender-nonconforming people, of the WPATH, (World Professional Association for Transgender Health), 7th ed, 2012, and the local Research Ethics Committee from Hospital de Clinicas de Porto Alegre, with written informed consent from all subjects and their caretakers. All subjects gave written informed consent in accordance with the Declaration of Helsinki. The protocol was approved by the local Research Ethics Committee from Hospital de Clínicas de Porto Alegre.

Physical Exams and Laboratory Results

Before treatment and during different periods of follow-up, in addition to endocrinological monitoring, specific assessments were performed to evaluate the neuropsychiatric status during GnRHa administration.

Psychological Evaluation

A standard psychological protocol and psychiatric evaluations were applied for personality traits, parental style, life-long depressive symptomatology, and overall intellectual performance assessment at study admission. House-Tree-Person (HTP) (Buck, 2003); Kiddie-Sads-Present and Lifetime (K-SADS-PL) Brazilian version 1.0 (Brasil and Bordin, 1996); Parental Styles Inventory (PIS) (Gomide, 2006); Wechsler Intelligence Scale for Childhood (Brazilian validated version) (WISC-IV) (Rueda et al., 2013) were the chosen instruments.

The K-SADS-PL matched only for major depressive disorder at five, which was the age of the "conversion therapy." The HTP was normal for age, signaling the desire to belong to the opposite sex (female), and the PIS was at percentile 95, which is the optimal parental style. During the clinical follow-up, that included weekly appointments with a psychotherapist, the patient did not match clinical criteria for psychiatric comorbidities.

Three evaluations were performed for the WISC-IV: T0, prior to GnRHa treatment, T1, 22 months and T2, 28 months after pubertal suppression. The same version of the test was applied by the same professional, and they were performed in the same environment at all set points.

Longitudinal Cognitive WISC-IV Evaluation

Comparing the periods of follow-up, a reduction on Global IQ (GIQ) during pubertal suppression was observed. In T1, the GIQ was lower than before hormonal treatment (T0), and this finding was sustained by the third WISC-IV evaluation (**Table 1**).

According to the results obtained through the cognitive evaluations, the patient presented a decrease in their overall intellectual performance after the onset of pubertal block, pointing to immaturity in her cognitive development (**Table 1**).

Neuroimaging

A DTI protocol was used to assess the brain's white matter FA, which is an indirect evaluation of neuronal fascicule integrity and maturation. The WM microstructure maturation during puberty was previously reported (Menzies et al., 2015; Pangelinan et al., 2016). The Magnetic Resonance Imaging (MRI) scans were done on a Philips Achieva 1.5T (Bethesda/Netherlands, 2009) with a dedicated 8 channels head coil. The diffusion weighted MRI images were acquired using a single-shot spin-echo echo-planar imaging (SE-EPI) sequence: TR/TE/Flip, angle/Pixel Band with (11,500 ms/80 ms/90/1784 Hz); b-value of 0 and 800 s/mm² with 32 directions; voxel sizes: $2 \times 2 \times 2$ mm^3 (high resolution); matrix sizes $112 \times 112 \times 70$, no gaps between slices; and Field of View between 224×224 mm. The data were collected at T0, T1, and T2.

The images weighted by the diffusion tensor were initially inspected for the identification of possible artifacts generated during acquisition. After the quality control, the diffusion images and non-weighted diffusion images were co-registered for the correction of movement and distortions caused by eddy currents. From the co-registered images, non-cerebral tissue was removed with the brain extraction tool (FMRIB's Software Library, FSL version 5.0). The six diffusion tensor elements (3 auto-vectors: v1, v2 and v3 and 3 auto-values λ1, λ2 e λ3) and consequent fractional anisotropy (FA) maps were calculated using the DTIFIT, adjusting the data for a tensor diffusion model for each voxel. The colored FA map was used for visualization of the tensor orientation, respecting the white matter tract anatomy.

To extract the mean FA value of the genu of the corpus callosum (CC), the white matter (WM) John Hopkins University Atlas JHU-ICBM-labels-1 mm was co-registered with each individual FA map (from T0, T1, and T2). The JHU-FA image, which the JHU-ICBM-labels-1 mm is aligned with, and the FSL FA template were co-registered using an affine transformation to reduce any misalignment between the chosen atlas and the FSL FA template. The JHU atlas was co-registered to this template by applying the resulted affine-registration matrix to the JHU-ICBM-labels-1 mm (**Figure 1**). After non-linearly registering the FA template to each individual FA map, the genu of the CC from the template-aligned JHU-ICBM-labels-1 mm could also be non-linearly transformed to each individual FA space. Finally, the mean FA from this region of interest (ROI) at each time point could be extracted and compared.

Similarly, further mean FA estimates were performed for the hippocampal cingulate fascicule and the splenium of the CC, bilateral, using the JHU-ICBM-labels-1 mm. The FA estimates were also performed for the bilateral uncinate fascicule from the WM atlas JHU-ICBM-tracts-prob-1 mm, which has better fascicule representation, following the steps described above. **Figure 2** presents similar FA values for the different ROIs during the follow-up. The mean FA values of the CC's splenium was 0.710 ± 0.159 before treatment, 0.707 ± 0.166 for T1, and 0.704 ± 0.162 for T2. The mean FA values for the hippocampal cingulate fascicule for T0, T1, and T2 were: 0.356 ± 0.141 (l:left) 0.371 ± 0.151 (r:right); 0.374 ± 0.143 (l), 0.381 ± 0.164 (r); and 0.394 ± 0.143 (l) 0.383 ± 0.150 (r), respectively. For the uncinate fascicule, the results of mean FA values for T0, T1, and T2 were: 0.409 ± 0.180 (l), 0.418 ± 0.183 (r); 0.443 ± 0.202 (l), 0.454 ± 0.175 (r); and 0.410 ± 0.179 (l), 0.412 ± 0.179 (r), respectively.

The FA of the genu of the CC, using the JHU tract probe in MATLAB, presented small variations between T0, T1, and T2 ($T_0 = 0.523473$; $T_1 = 0.507267$; $T_3 = 0.491564$), toward FA reduction. After adjusting by the JHU tract probe FSL, the analyses were similar among the periods of assessment ($T_0 = 0.504 \pm 0.216$; $T_1 = 0.493 \pm 0.205$; $T_2 = 0.502 \pm 0.2066$), as well as after the JHU/Labels, 1 mm ($T_0 = 0.59 \pm 0.221$; $T_1 = 0.583 \pm 0.210$; $T_2 = 0.591 \pm 0.207$), without a reduction trend (**Figure 2**).

Voice Evaluation

The voice collections were performed at four time points (before treatment and the eighth, seventeenth, and twentieth

TABLE 1 | The results of the longitudinal evaluation of the Weschler Scale of Intelligence.

	Composite scaled score	Percentile rank	Confidence interval 95%	Qualitative description
T0-Admission (11 years and 10 months old)				
Global IQ (GIQ)	80	9	76–86	Low Average
Comprehension Index (VCI)	101	53	94–108	Average
Perceptual Reasoning Index (PRI)	79	8	73–88	Borderline
Working Memory Index (WMI)	83	13	77–91	Low Average
Processing Speed Index (PSI)	68	2	63–81	Extremely Low
T1- (13 Years and 3 Months Old)				
Global IQ (GIQ)	71	3	67–77	Borderline
Comprehension Index (VCI)	91	27	84–99	Average
Perceptual Reasoning Index (PRI)	73	4	68–82	Borderline
Working Memory Index (WMI)	68	2	63–77	Extremely Low
Processing Speed Index (PSI)	74	4	68–86	Borderline
T2- (14 Years and 2 Months Old)				
Global IQ (GIQ)	70	2	66–76	Borderline
Comprehension Index (VCI)	86	18	80–94	Low Average
Perceptual Reasoning Index (PRI)	77	6	71–86	Borderline
Working Memory Index (WMI)	74	4	69–83	Borderline
Processing Speed Index (PSI)	64	1	59–77	Extremely Low

A Global IQ reduction is observed. At the end of 28 months of treatment, speed processing and memory remain lower than before GnRHa treatment.

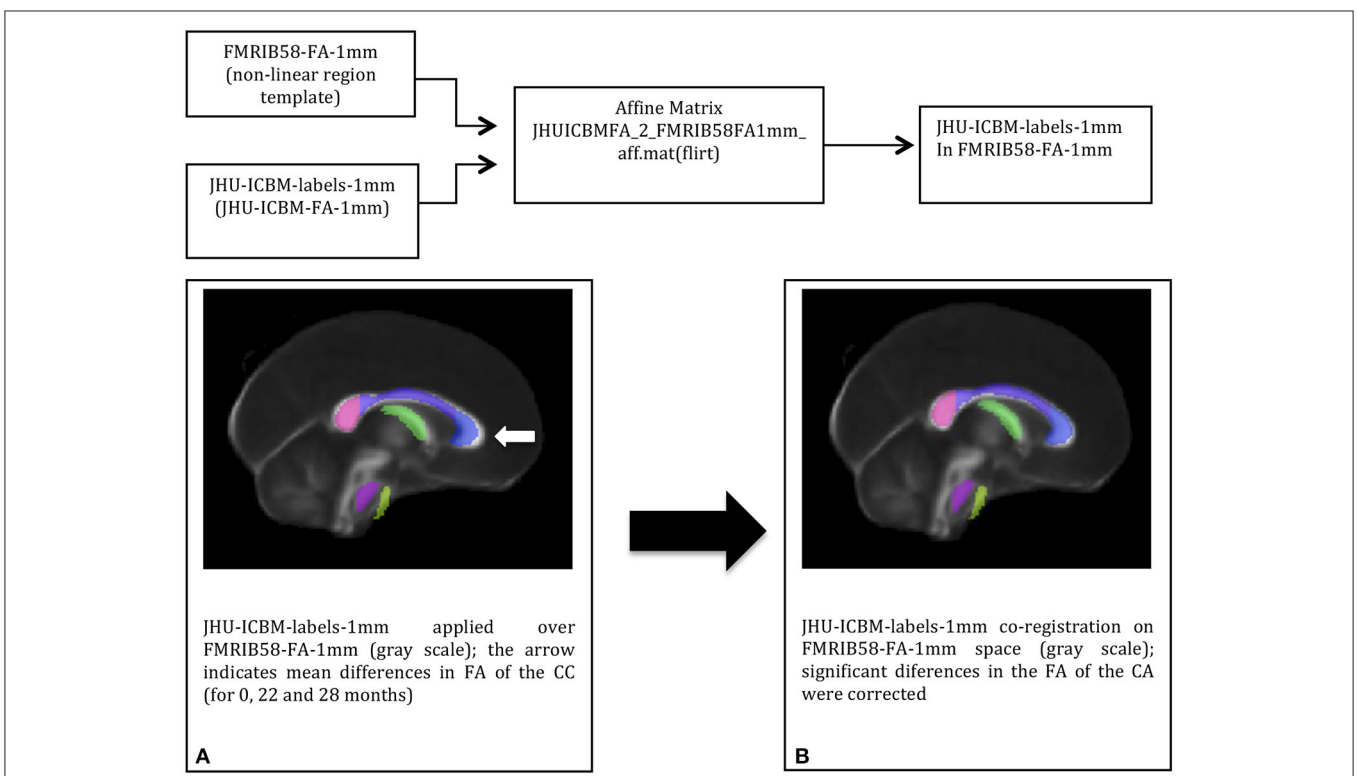

FIGURE 1 | The DTI-based white matter atlas JHU-ICBM-labels-1 mm (colored in transparency) before **(A)** and after **(B)** affine-co-registration with the FSL FA template (in gray scale): co-registration corrected the misalignments (white arrow) between the two images before the atlas transformation to the individual space.

month of treatment) by means of a sustained vowel/a/. The voice was recorded directly on the computer. The microphone was positioned at an angle of 90° from the mouth, and the same distance of 4 cm between the microphone and mouth was maintained to avoid signal interference. The patient was instructed to emit the vowel sound in a usual tone and intensity. For the acoustic analysis, the first 5 s of the vowel/a/ were used, excluding the beginning of the broadcast so that the vocal attack did not interfere with the data analysis.

The measurements were obtained through the Multidimensional Voice Program Advanced software (MVDPA), Kay Pentax®. We considered the following measures: the mean fundamental frequency (f0) that corresponds to the velocity of the vocal fold vibration (number of glottal cycles per second), the maximum fundamental frequency (FHI), and the minimum fundamental frequency (flo). This measure is directly related to the length, tension, rigidity and mass of the vocal folds during their interaction with the subglottic pressure, which reflects the biomechanical characteristics of the vocal folds. Normal values vary according to sex, age, and physical and laryngeal structures. In Brazil, the reference values are: 80–150 Hz for men, 150–250 Hz for women and above 250 Hz for children (Campisi et al., 2002).

Other measures used were those of frequency disturbance *(jitter)*. The measure of jitter is the fundamental frequency variation in consecutive cycles that reflects the irregularity of the mucosa vibration of the vocal folds. There are different ways to extract these measures, such as those used in this study: Jitter percentage (Jitt), average relative frequency of disturbance (RFD), and pitch perturbation quotient (PPQ). The intensity or shimmer disturbance corresponds to the amplitude variation in consecutive cycles that is present to a certain degree in all vocal samples.

The period of collection of the vocal samples and the results of the acoustic measurements of the voice are shown in **Table 2**. The voice f0 varied during the first 17 months of treatment, with a decrease of approximately 30 Hz. Then, in the last assessment there was an increase in the f0. The shimmer was not modified. The other measures (jitter and PPQ) also confirmed the variability in the fundamental frequency that occurred during the evaluation period.

BACKGROUND

Hypothesis of Puberty Suppression Impact in Brain White Matter

Several studies have been performed in recent years regarding brain changes during puberty, especially when evaluating sex differences (Menzies et al., 2015; Pangelinan et al., 2016; Seunarine et al., 2016; Juraska and Willing, 2017). The DTI approaches are a useful tool for evaluating WM microstructure regarding brain maturation. Sex steroids have been observed to impact axons myelinization and WM microstructure (Mishra et al., 2013; Pesaresi et al., 2015; Pangelinan et al., 2016), in part due to their effects on axonal protein synthesis (Pesaresi et al., 2015). Previous studies have found a positive correlation between age and FA in boys during puberty (Wang et al., 2012), which can be related to the effects of testosterone in axons (Lebel et al., 2008). Other DTI measures, such as the mean diffusivity (MD) and magnetic transfer ratio (MTR) are similarly related to WM maturation (Menzies et al., 2015; Pangelinan et al., 2016) regarding pubertal development. In addition, MD and FA show a trend to be inversely correlated (Clayden et al., 2012; Seunarine et al., 2016). Taken together, these findings suggest a role between puberty and brain maturation, and WM maturation related to androgen exposure during puberty may, at least in part, be accessed by FA. Although there is not a consensus about FA, several studies used it as an experimental measure (Lebel et al., 2008; Clayden et al., 2012; Wang et al., 2012; Menzies et al., 2015; Seunarine et al., 2016).

Cognitive Skills from Childhood to Adolescence under Normal Circumstances

The Wechsler tests are among the most widely used instruments for ascertaining intelligence in different populations (Mishra et al., 2013). Evidence for Wechsler Scale validation, considering age as a criterion, is grounded on a theoretic and practical presuppose that intelligence grows between the ages of 8 and 16. The validation for the Brazilian population demonstrated that most of the WISC-IV subtests had a positive and significant correlation with age, indicating that there is a trend for IQ augmentation (Rueda et al., 2013) with aging. The IQ temporal stability between the test and re-test is more reliable according to the individual's age at the first testing (Schuerger and Witt, 1989).

Review of Similar Cases: Pubertal Suppression

Staphorsius et al. (2015) conducted a study in a GD adolescent group under hormonal suppression to investigate the impact of pubertal suppression on executive function (EF). They compared GD adolescents under GnRHa treatment to GD adolescents undergoing physiological puberty and compared them to male and female control groups. They used the Tower of London test and found a negative impact of pubertal suppression on EF. However, they also associate this outcome with a lower IQ before GnRHa treatment.

Recently, studies have shown additional data regarding the impact of steroid deprivation during puberty (Costa et al., 2015; Wojniusz et al., 2016; Hough et al., 2019). In an animal study with pre-pubertal castrated sheep (Hough et al., 2019), researchers reported an impairment in long-term spatial memory that was not reversed by subsequent hormone replacement treatment. Additionally, a global IQ decrease (WISC-III) was reported in a longitudinal follow-up of girls with central precocious puberty (Schuerger and Witt, 1989) treated with GnRHa. Finally, a third study correlated verbal skill impairment to pubertal suppression in a GD group (Costa et al., 2015).

DISCUSSION

In the present study, we report the lack of significant variation in brain WM FA during pubertal suppression with GnRHa

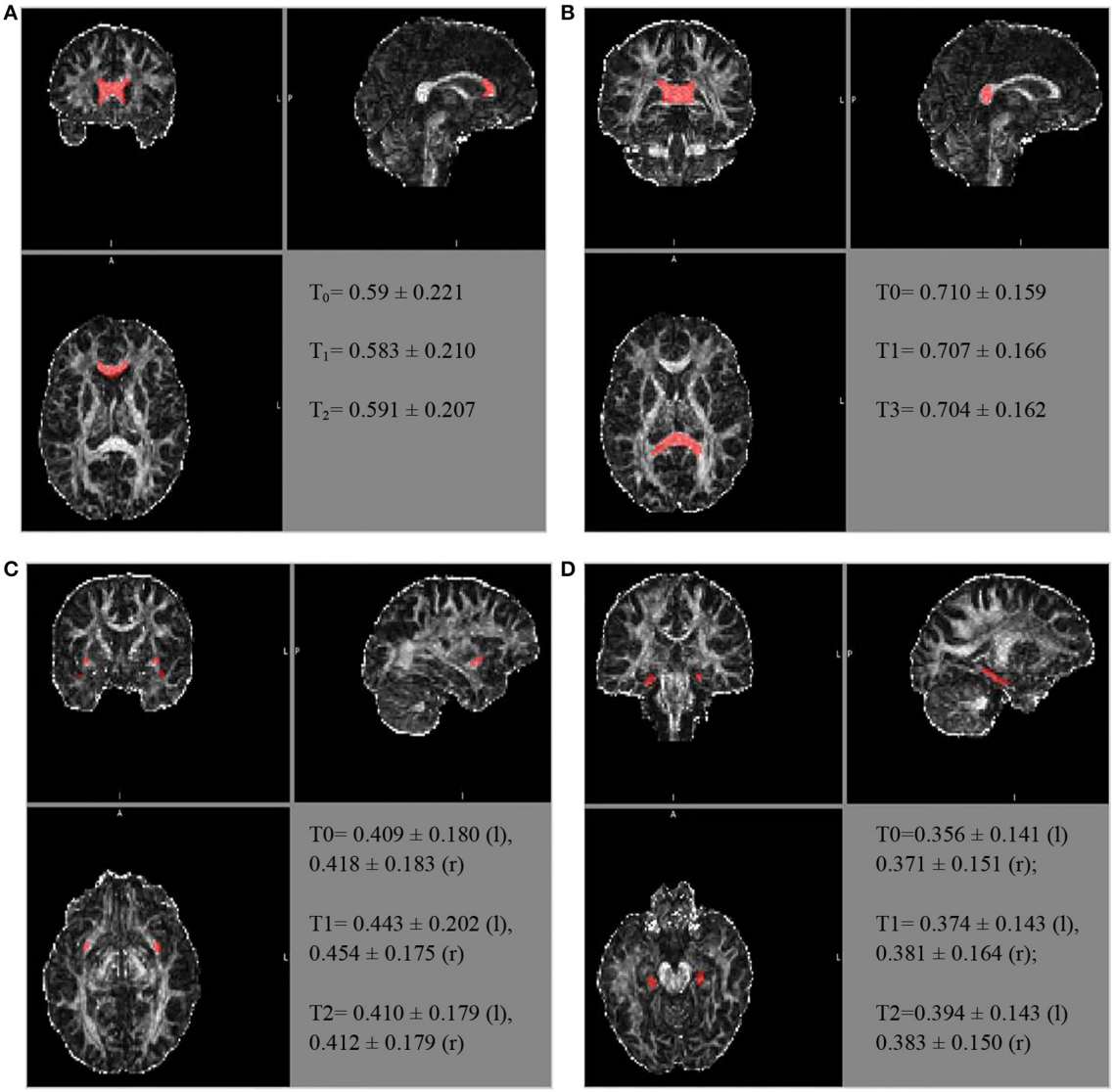

FIGURE 2 | The longitudinal FA variation for different regions of interest. The atlas showing the locations for the **(A)** genu of the CC, **(B)** splenium of the CC, **(C)** uncinate fascicule right r/l, and **(D)** cingulate hippocampal fascicule r/l.

treatment for 28 months in a GD girl. WM brain maturation in some areas during physiological pubertal progression in boys has been previously reported (Menzies et al., 2015; Pangelinan et al., 2016). However, the effects of blocking puberty on brain development and cognition in GD youths still lack conclusive studies (Vries et al., 2011; Wojniusz et al., 2016). The differences in the cognitive skills of boys, girls and GD individuals were previously partially attributed to sexual steroid arousal (Soleman et al., 2013). To our knowledge, this is the first case reporting brain WM and WISC-IV variations during pubertal suppression in a GD youth.

The white matter's FA augmentation during adolescence was previously related to the pubertal stage in male groups (Lebel et al., 2008). Furthermore, Herting et al. (2017) have recently reported a robust statistical model investigating the age-by-sex interaction and gonadal correlation with Fractional Anisotropy, and FA seems to be associated with pubertal development (Herting et al., 2017). The above-mentioned ROIs were chose considering prior publications. The splenium and genu of the CC show an earlier and more rapid increase in FA approximately 11 years old, while variations in FA in other areas are slower, such as for the uncinate and cingulate (Lebel et al., 2008). Other DTI studies also identified continuous WM microstructural developmental changes during adolescence to adulthood (Giorgio et al., 2010). The Tanner stage is an accurate parameter for pubertal evaluation. Prior studies associated this scale to CC's structure and morphology (Chavarria et al., 2014). The results presented here show no increase in the WM FA in

TABLE 2 | The longitudinal vocal acoustic measures according to the period of collection of the vocal sample.

Voice acoustic measures	Time 1 before GnRHa	Time 2 after 8 mo GnRHa	Time 3 after 17 mo GnRHa	Time 4 after 20 mo GnRHa	Threshold value
Mean fundamental frequency (Hz)	218.682	192.181	187.643	222.98	Average in Brazil: 150–250 Hz for women; 80–150 Hz for men; above 250 Hz for children.
Maximum fundamental frequency (Hz)	229.100	217.98	278.979	242.234	–
Minimum fundamental frequency (Hz)	207.321	174.799	91.64	214.564	–
Jitter percentage (Jitt) (%)	1.196	0.943	1.341	0.729	1.040*
Average relative frequency of disturbance (RFD) (%)	0.718	0.488	0.781	0.435	0.680*
Pitch perturbation quotient (PPQ) (%)	0.725	0.682	0.868	0.438	0.840*
Shimmer (dB)	0.343	0.356	0.528	0.232	0.350*

**Threshold Value: mean values offered by the acoustic analysis program.*

a GD girl with suppressed serum testosterone on brain plasticity during male puberty.

The patient's GIQ (global IQ) was further slightly reduced during the follow-up with GnRHa treatment. In fact, the low average GIQ together with impairment in the perceptual organization of intelligence and processing speed index presented even before treatment (T0) suggest that any neurodevelopmental immaturity may have been potentiated by pubertal suppression. Some changes at the functional levels in IQ (e.g., operational memory and EF) can be generally explained by the psychosocial environment or psychopathological status (Cunha, 2000; Roughan and Hadwin, 2011; Zhang et al., 2013; Cromheeke et al., 2014; Li et al., 2016). However, the GD girl did not fully meet any criteria for psychiatric comorbidity during the evaluations. Furthermore, she has shown an improvement in her affective and social life due to the prevention of sexual secondary characteristics arousal.

Some questions emerge from these findings, especially regarding the influence of sex steroids on cognition during puberty. It is likely that the structural and microstructural changes in the brain during adolescence, as discussed above, may interfere on the achievement of complete cognitive potential. Indeed, IQ was recently associated with inter-hemispheric and intra-hemispheric connectivity. Children with high IQ were also those who presented higher FA in some bundles, such as the CC genu and splenium (Nusbaum et al., 2017). These findings highlight the importance of gonadal steroids in brain structure and cognition, and seems to be in accordance with prior study (Seunarine et al., 2016). Neuronal plasticity conferred from sex steroids during puberty may be critical, especially during this period.

Also, it is well known that the brain has different androgen receptor (AR) density, or even lack of AR, along specific areas of white matter and gray matter (Swinft-Gallant and Monks, 2017; Wong et al., 2017). In addition, there might be a synchronism between gray matter and WM development during adolescence (Moura et al., 2017), and these substances might response intrinsically to sex steroids during physiological puberty. In this sense, a plausible explanation for the GIQ decrease should consider a disruption of the synchronic development of brain areas by pubertal suppression. Nevertheless, this is only a speculative discussion about cognition and testosterone. Cognition is more than WISC-IV subtests, and at the present the mechanism for the GIQ decrease observed in this case remains uncertain.

Finally, the patient described here presented a decrease of approximately 30 Hz in the fundamental frequency of the voice during the first year of GnRHa treatment, remaining in the female range. Sex hormones have a substantial influence on voice quality, and testosterone may induce chances in vocal folds, which are parallel to voice pattern changes for fundamental frequencies. At puberty, boys' vocal fold grows up to 1 cm, leading to an average lowering of the fundamental frequency by one octave. In girls, the vocal fold grows less than 4 mm. In this case, the fundamental frequency variation occurred mainly in the first year, and the mean fundamental frequency maintained in the female range during the pubertal suppression. Thus, the testosterone influences over the fundamental frequency results in

changes in the voice tone (Nygren et al., 2013; Hari Kumar et al., 2016).

One limitation of the present study is the lack of a paired control without hormone intervention. However, this case report points out the timing interactions between brain maturity, as assessed by FA, cognition and pubertal suppression, and provides us some clues that brain maturation depends also on sex steroids.

CONCLUSION

Brain white matter fractional anisotropy remained unchanged in a GD girl during pubertal suppression with GnRHa treatment for 28 months, which may be related to reduced serum testosterone levels. The global performance in the Weschler scale was slightly lower during pubertal suppression compared with baseline, predominantly due to the reduction in operational memory. Either a baseline of a low average cognition or the hormonal status could play a role in cognitive performance during pubertal suppression. The variation in voice frequency was consistent with the testosterone levels and peripheral testosterone effects, as seen in vocal folds. Further longitudinal clinical studies comparing DTI parameters and cognition among TG adolescents under puberty suppression and age-matched controls with physiological pubertal development are needed in order to confirm the present findings and support the hypothesis on the impact of sex hormones on cognition and brain maturity during developmental stages.

AUTHOR CONTRIBUTIONS

MS: data collection, MRI acquisitions, clinical interview, and literature review. BS: psychologist, WISC-IV evaluation, HTP and Parental stile evaluation. PS: endocrinological follow up, pubertal suppression follow-up. AF: logistics concerns and literature review. MC: DTI analysis and technical support. FT-M DTI analysis and technical support, supervised methodological issues about neuroimage. AC: Ethics and familiar follow up. DdS: literature review, writing manuscript. KS: voice follow up, MRI acquisitions. MA: MRI acquisitions, quality control of MRIs. ST: Childhood psychiatrist evaluated the child during all follow up. ML: chief of the Gender Identity program, family follow up, clinical interviews, literature review, writing the case report. MS, PS, KS, and BS: writing the manuscript. All authors had access to the data and had a role in writing the manuscript. All the authors read and approved the final manuscript.

FUNDING

This work was supported in part by a grant from the Conselho Nacional de Desenvolvimento Científico e Tecnológico (CNPq/INCT465482/2014-7), Porto Alegre, Brazil.

REFERENCES

Acerlus, J., Claes, L., Witcomb, G. L., Marshall, E., and Bouman, W. P. (2016). Risk factors for non-suicidal self-injury among trans youth. *J. Sex. Med*. 13, 402–412. doi: 10.1016/j.jsxm.2016.01.003

Brasil, H. H. A., and Bordin, I. A. S. (1996). *"Entrevista Diagnóstica: Kiddie-Sads Referente ao Momento Presente ao Longo Da Vida. Versão 1.0 [S.I.:s.n.]" Versão Brasileira da Schedule for Affective Disorders and Schizophrenia for School-Age Children-Present and Lifetime Version (K-SADS-PL)*. São Paulo.

Buck, J. N. (2003). *H-T-P: Casa – Árvore – Pessoa. Técnica Projetiva de Desenho: Manual e Guia de Interpretação, 1st Edn*. São Paulo: Vetor.

Campisi, P., Tewfik, T. L., Manoukian, J. J., Schloss, M. D., Pelland-Blais, E., and Sadeghi, N. (2002). Computer-Assisted voice analysis. *Arch. Otolaryngol. Head Neck Surg.* 128, 156–160. doi: 10.1001/archotol.128.2.156

Chavarria, M. C., Sánchez, F. J., Chou, Y. Y., Thompson, P. M., and Luders, E. (2014). Puberty in the *Corpus callosum*. *Neuroscience* 265, 1–8. doi: 10.1016/j.neuroscience.2014.01.030

Clayden, J. D., Jentschke, S., Muñoz, M., Cooper, J. M., Chadwick, M. J., Banks, T., et al. (2012). Normative development of white matter tracts: similarities and differences in relation to age, gender, and intelligence. *Cereb. Cortex* 22, 1738–1747. doi: 10.1093/cercor/bhr243

Cohen-Kettenis, P. T., Schagen, S. E., Steensma, T. D., de Vries, A. L., and Delemarre-van de Waal, H. A. (2011). Puberty suppression in a gender-dysphoric adolescent: a 22-year follow-up. *Arch. Sex. Behav.* 40, 843–847. doi: 10.1007/s10508-011-9758-9

Coleman, E., Bockting, W., Botzer, M., Cohen-Kettenis, P., DeCuypere, G., Feldman, J., et al. (2012). Standards of care for the health of transsexual, transgender, and gender-nonconforming people, version 7. *Int. J. Trans.* 13, 165–232. doi: 10.1080/15532739.2011.700873

Connolly, M. D., Zervos, M. J., Barone, C. J., Johnson, C. C., and Joseph, C. L. (2016). The mental health of transgender youth: advances in understanding. *J. Adolesc. Heal.* 59, 489–495. doi: 10.1016/j.jadohealth.2016.06.012

Costa, R., Dunsford, M., Skagerberg, E., Holt, V., Carmichael, P., and Colizzi, M. (2015). Psychological support, puberty suppression, and psychosocial functioning in adolescents with gender dysphoria. *J. Sex. Med*. 12, 2206–2214. doi: 10.1111/jsm.13034

Cromheeke, S., Herpoel, L. A., and Mueller, S. C. (2014). Childhood abuse is related to working memory impairment for positive emotion in female university students. *Child Maltreat.* 19, 38–48. doi: 10.1177/1077559513511522

Cunha, J. A. (2000). *Escalas Wechsler*. Porto Alegre: JA Cunha and cols. (Org.). Psicodiagnóstico - V.

Feder, S., Isserlin, L., Seale, E., Hammond, N., and Norris, M. L. (2017). Exploring the association between eating disorders and gender dysphoria in youth. *Eat. Disord*. 10, 1–8. doi: 10.1080/10640266.2017.1297112

Giorgio, A., Watkins, K. E., Chadwick, M., James, S., Winmill, L., Douaud, G., et al. (2010). Longitudinal changes in white matter microsctructure during adolescence. *Neuroimage* 49, 94–103. doi: 10.1016/j.neuroimage.2009.08.003

Gomide, P. I. C. (2006). *Inventário de Estilos Parentais (IEP), Modelo Teórico, Manual e Aplicaçãoo, Apuração E Interpretaçãoo*. Petrópolis: Vozes.

Hari Kumar, K. V., Garg, A., Ajai Chandra, N. S., Singh, S. P., and Datta, R. (2016). Voice and endocrinology. *Indian J. Endocrinol. Metab*. 20, 590–594. doi: 10.4103/2230-8210.190523

Hembree, W. C., Cohen-Kettenis, P., Delemarre-van de Waal, H. A., Gooren, L. J., Meyer, W. J. III, Spack, N. P., et al. (2009). Endocrine treatment of transsexual persons: an Endocrine Society clinical practice guideline. *J. Clin. Endocrinol. Metab*. 94, 3132–3154. doi: 10.1210/jc.2009-0345

Herting, M. M., Kim, R., Uban, K. A., Kan, E., Binley, A., and Sowell, E. R. (2017). Longitudinal changes in pubertal maturation and white matter microstructure. *Psychoneuroendocrinology* 81, 70–79. doi: 10.1016/j.psyneuen.2017.03.017

Hough, D., Bellingham, M., Haraldsen, I. R., McLaughlin, M., Rennie, M., Robinson, J. E., et al (2019). Spatial memory is impaired by peripubertal GnRH agonist treatment and testosterone replacement in sheep. *Psychoneuroendocrinology* 75, 173–182. doi: 10.1016/j.psyneuen.2016.10.016

Hough, D., Bellingham, M., Haraldsen, I. R., McLaughlin, M., Robinson, J. E., Solbakk, A. K., et al (2017). A reduction in long-term spatial memory persists after discontinuation of peripubertal GnRH agonist treatment in sheep. *Psychoneuroendocrinology* 77, 1–8. doi: 10.1016/j.psyneuen.2016.11.029

Juraska, J. M., and Willing, J. (2017). Pubertal onset as a critical transition for neural development and cognition. *Brain Res.* 1654, 87–94. doi: 10.1016/j.brainres.2016.04.012

Lebel, C., Walker, L., Leemans, A., Phillips, L., and Beaulieu, C. (2008). Microstructural maturation of the human brain from childhood to adulthood. *Neuroimage* 40, 1044–1055. doi: 10.1016/j.neuroimage.2007.12.053

Li, M., Zhong, N., Lu, S., Wang, G., Feng, L., and Hu, B. (2016). Cognitive behavioral performance of untreated depressed patients with mild depressive symptoms. *PLoS ONE* 11:e0146356. doi: 10.1371/journal.pone.0146356

Menzies, L., Goddings, A.-L., Kirstie, J., Whitaker, K. J., Blakemore, S.-J., and Viner, R. M. (2015). The effects of puberty on white matter development in boys. *Dev. Cogn. Neurosci.* 11, 116–128. doi: 10.1016/j.dcn.2014.10.002

Mishra, V., Cheng, H., Gong, G., He, Y., Dong, Q., and Huang, H. (2013). Differences of inter-tract correlations between neonates and children around puberty: a study based on microstructural measurements with DTI. *Front. Hum. Neurosci.* 7:721. doi: 10.3389/fnhum.2013.00721

Moura, L. M., Crossley, N. A., Zugman, A., Pan, P. M., Gadelha, A., Del Aquilla, M. A. G., et al. (2017). Coordinated brain development: exploring the synchrony between changes in grey and white matter during childhood maturation. *Brain Imaging Behav.* 11, 808–817. doi: 10.1007/s11682-016-9555-0

Nusbaum, F., Hannoun, S., Kocevar, G., Stamile, C., Fourneret, P., Revol, O., et al. (2017). Hemispheric differences in white matter microstructure between two profiles of children with high intelligence quotient vs. controls: a tract-based spatial statistics study. *Front. Neurosci.* 11:173. doi: 10.3389/fnins.2017.00173

Nygren, U., Nyström, H. F., Falhmmar, H., Hagenfeldt, K., Nordenskjöld, A., and Södersten, M. (2013). Voice problems due to virilization in adult women with congenital adrenal hyperplasia due to 21-hydroxilase deficiency. *Clin. Endocrinol. (Oxf).* 79, 859–866. doi: 10.1111/cen.12226

Pangelinan, M. M., Leonard, G., Perron, M., Pike, G. B., Richer, L., Veillette, S., et al. (2016). Puberty and testosterone shape the corticospinal tract during male adolescence. *Brain Struct. Funct.* 221, 1083–1094. doi: 10.1007/s00429-014-0956-9

Pesaresi, M., Soon-Shiong, R., French, L., Kaplan, D. R., Miller, F. D., and Paus, T. (2015). Axon diameter and axonal transport: *in vivo* and *in vitro* effects of androgens. *Neuroimage* 115, 191–201. doi: 10.1016/j.neuroimage.2015.04.048

Resiner, S. L., Vetters, R., Leclerc, M., Zaslow, S., Wolfrum, S., Shumer, D., et al. (2015). Mental health of transgender youth in care at an adolescent urban community health center: a matched retrospective cohort study. *J. Adolesc. Heal.* 56, 274–279. doi: 10.1016/j.jadohealth.2014.10.264

Robles, R., Fresán, A., Vega-Ramírez, H., Cruz-Islas, J., Rodríguez-Pérez, V., Domínguez-Martínez, T., et al. (2016). Removing transgender identity from the classification of mental disorders: a Mexican field study for ICD-11. *Lancet Psychiatry* 3, 850–859. doi: 10.1016/S2215-0366(16)30165-1

Roughan, L., and Hadwin, J. A. (2011). The impact of working memory training in young people with social, emotional and behavioural difficulties. *Learn. Indiv. Differ.* 21, 759–764. doi: 10.1016/j.lindif.2011.07.011

Rueda, F. J. M., Noronha, A. P. P., Sisto, F. F., Santos, A. A. A., and Castro, N. R. (2013). *Escala Wechsler de Inteligência para Crianças – 4ª Edição (WISC-IV): Manual Técnico*. São Paulo: Casa do Psicólogo.

Schuerger, J. M., and Witt, A. C. (1989). The temporal stability of individuality tests inteligence. *J. Clin. Psychol.* 45, 249–302.

Seunarine, K. K., Clayden, J. D., Jentschke, S., Muñoz, M., Cooper, J. M., Chadwick, M. J., et al. (2016). Sexual dimorphism in white matter developmental trajectories using tract-based spatial statistics. *Brain Connect.* 6, 37–47. doi: 10.1089/brain.2015.0340

Smith, K. P., Madison, C. M., and Milne, N. M. (2014). Gonadal suppressive and cross-sex hormone therapy for gender dysphoria in adolescence and adults. *Pharmacotherapy* 34, 1282–1297. doi: 10.1002/phar.1487

Soll, B. M., Robles-García, R., Brandelli-Costa, A., Mori, D., Mueller, A., Vaitses-Fontanari, A. M., et al. (2017). Gender incongruence: a comparative study using ICD-10 and DSM-5 diagnostic criteria. *Rev. Bras. Psiquiatr.* 24, 568–567. doi: 10.1590/1516-4446-2016-2224

Soleman, R. S., Schagen, S. E., Veltman, D. J., Kreukels, B. P., Cohen-Kettenis, P. T., Lambalk, C. B., et al. (2013). Sex differences in verbal fluency during adolescence: a functional magnetic resonance imaging study in gender dysphoric and control boys and girls. *J. Sex. Med.* 10, 1969–1977. doi: 10.1111/jsm.12083

Staphorsius, A. S., Kreukels, B. P., Cohen-Kettenis, P. T., Veltman, D. J., Burke, S. M., Schagen, S. E., et al. (2015). Puberty suppression and executive functioning: an fMRI-study in adolescents with gender dysphoria. *Psychoneuroendocrinology* 56, 190–199. doi: 10.1016/j.psyneuen.2015.03.007

Swinft-Gallant, A., and Monks, D. A. (2017). Androgenic mechanisms of sexual differentiation of the nervous system and behavior. *Front. Neuroendocrinol.* 46, 32–45. doi: 10.1016/j.yfrne.2017.04.003

Tanner, J. M. (1962). *Growth at Adolescence*. Oxford: Blackwell.

Vries, A. L., Steensma, T. D., Doreleijers, T. A., and Cohen-Kettenis, P. T. (2011). Puberty suppression in adolescents with gender identity disorder: a prospective follow-up study. *J. Sex. Med.* 8, 2276–2283. doi: 10.1111/j.1743-6109.2010.01943.x

Wang, Y., Adamson, C., Yuan, W., Altaye, M., Rajagopal, A., Byars, A. W., et al. (2012). Sex Differences in white matter development during adolescence: a DTI study. *Brain Res.* 1478, 1–15. doi: 10.1016/j.brainres.2012.08.038

Wojniusz, S., Callens, N., Sütterlin, S., Andersson, S., De Schepper, J., Gies, I., et al. (2016). Cognitive, emotional, and psychosocial functioning of girls treated with pharmacological puberty blockage for idiopathic central precocious puberty. *Front. Psychol.* 7:1053. doi: 10.3389/fpsyg.2016.01053

Wong, A. P., French,. L., Leonard, G., Perron, M., Pike, G. B., Richer, L., et al. (2017). Inter-regional variations in gene expression and age-related cortical thinning in the adolescent brain. *Cereb. Cortex.* 25, 1–10. doi: 10.1093/cercor/bhx186

Zhang, J. N., Xiong, K. L., Qiu, M. G., Zhang, Y., Xie, B., Wang, J., et al. (2013). Negative emotional distraction on neural circuits for working memory in patients with posttraumatic stress disorder. *Brain Res.* 531, 94–101. doi: 10.1016/j.brainres.2013.07.042

Conflict of Interest Statement: The authors declare that the research was conducted in the absence of any commercial or financial relationships that could be construed as a potential conflict of interest.

frontiers in Molecular Neuroscience

ORIGINAL RESEARCH
published: 16 March 2018
doi: 10.3389/fnmol.2018.00083

Stable Density and Dynamics of Dendritic Spines of Cortical Neurons Across the Estrous Cycle While Expressing Differential Levels of Sensory-Evoked Plasticity

*Bailin H. Alexander[1], Heather M. Barnes[1,2], Emma Trimmer[1], Andrew M. Davidson[1,3], Benard O. Ogola[1], Sarah H. Lindsey[1,4] and Ricardo Mostany[1,4]**

[1]Department of Pharmacology, Tulane University School of Medicine, Tulane University, New Orleans, LA, United States, [2]Neuroscience Program, Brain Institute, Tulane University, New Orleans, LA, United States, [3]Department of Cell and Molecular Biology, Tulane University, New Orleans, LA, United States, [4]Brain Institute, Tulane University, New Orleans, LA, United States

Periodic oscillations of gonadal hormone levels during the estrous cycle exert effects on the female brain, impacting cognition and behavior. While previous research suggests that changes in hormone levels across the cycle affect dendritic spine dynamics in the hippocampus, little is known about the effects on cortical dendritic spines and previous studies showed contradictory results. In this *in vivo* imaging study, we investigated the impact of the estrous cycle on the density and dynamics of dendritic spines of pyramidal neurons in the primary somatosensory cortex of mice. We also examined if the induction of synaptic plasticity during proestrus, estrus, and metestrus/diestrus had differential effects on the degree of remodeling of synapses in this brain area. We used chronic two-photon excitation (2PE) microscopy during steady-state conditions and after evoking synaptic plasticity by whisker stimulation at the different stages of the cycle. We imaged apical dendritic tufts of layer 5 pyramidal neurons of naturally cycling virgin young female mice. Spine density, turnover rate (TOR), survival fraction, morphology, and volume of mushroom spines remained unaltered across the estrous cycle, and the values of these parameters were comparable with those of young male mice. However, while whisker stimulation of female mice during proestrus and estrus resulted in increases in the TOR of spines (74.2 ± 14.9% and 75.1 ± 12.7% vs. baseline, respectively), sensory-evoked plasticity was significantly lower during metestrus/diestrus (32.3 ± 12.8%). In males, whisker stimulation produced 46.5 ± 20% increase in TOR compared with baseline—not significantly different from female mice at any stage of the cycle. These results indicate that, while steady-state density and dynamics of dendritic spines of layer 5 pyramidal neurons in the primary somatosensory cortex of female mice are constant during the estrous cycle, the susceptibility of these neurons to sensory-evoked structural plasticity may be dependent on the stage of the cycle. Since dendritic spines are more plastic during proestrus and estrus than during metestrus/diestrus, certain stages of the cycle could be more suitable for forms of memory requiring *de novo* formation and elimination of spines and other stages for forms of

OPEN ACCESS

Edited by:
Jordan Marrocco, Rockefeller University, United States

Reviewed by:
Deepak Prakash Srivastava, King's College London, United Kingdom
Pirta Elina Hotulainen, Minerva Institute for Medical Research, Finland
Volker Scheuss, Max Planck Institute of Neurobiology (MPG), Germany

***Correspondence:**
Ricardo Mostany
rmostany@tulane.edu

Received: *01 November 2017*
Accepted: *01 March 2018*
Published: *16 March 2018*

Citation:
Alexander BH, Barnes HM, Trimmer E, Davidson AM, Ogola BO, Lindsey SH and Mostany R (2018) Stable Density and Dynamics of Dendritic Spines of Cortical Neurons Across the Estrous Cycle While Expressing Differential Levels of Sensory-Evoked Plasticity. Front. Mol. Neurosci. 11:83. doi: 10.3389/fnmol.2018.00083

memory where retention and/or repurposing of already existing synaptic connections is more pertinent.

Keywords: synaptic plasticity, estrous cycle, two-photon imaging, pyramidal neurons, female, estrogens, dendritic spines

INTRODUCTION

Over the past 40 years it has been well established that gonadal hormones exert influence on brain structure and function in both the developing and the adult brain (Luine and Rodriguez, 1994; McEwen and Alves, 1999; Brinton, 2009; Srivastava et al., 2013). It is also well known that brain functions depend on the maintenance of synaptic contacts, as well as on the ability to modify, eliminate, and create new synapses between neurons to establish adaptive connections in a changing environment (Holtmaat and Svoboda, 2009). This degree of adaptability is defined as synaptic plasticity, and it is paramount for any type of learning and form of memory. Dendritic spines are essential components of cortical circuits, functioning as the main postsynaptic structure receiving excitatory inputs in pyramidal neurons in the neocortex and as the anatomical substrate for memory storage (Yuste and Bonhoeffer, 2001). These neuronal structures have been used as a proxy of the computing capabilities of the cortical circuitry and can undergo rapid and extensive changes during learning (Xu et al., 2009; Lai et al., 2012; Moczulska et al., 2013; Kuhlman et al., 2014) and after sensory manipulations (Zuo et al., 2005; Miquelajauregui et al., 2015) or brain injury (Mostany et al., 2010). Several studies have reported changes in spine density in the hippocampus at different stages of the estrous cycle, with higher levels of estrogen during proestrus corresponding to higher densities of dendritic spines (Woolley et al., 1990; Woolley and McEwen, 1992; Kato et al., 2013). However, results from studies in the cerebral cortex are more arguable, with studies reporting higher density of dendritic spines during proestrus (Chen et al., 2009) and studies reporting no differences in density in relation to the stage of the estrous cycle (Markham and Juraska, 2002; Prange-Kiel et al., 2008).

Regardless of the results, these studies used fixed tissues, a methodology that does not allow tracking spine density and dynamics longitudinally, and no *in vivo* studies are available on the effects of fluctuating hormone levels on cortical plasticity. The advent of *in vivo* two-photon excitation (2PE) imaging (Denk et al., 1990; Svoboda and Yasuda, 2006) has allowed the precise, longitudinal examination of dendritic spines in the same animal. Several 2PE imaging studies have shown that sensory manipulations affect the dynamics of dendritic spines of different cortical areas in mice, showing increases in the turnover ratios of dendritic spines after monocular deprivation (Hofer et al., 2009) or whisker trimming (Trachtenberg et al., 2002). However, it is unknown whether these changes in the dynamics of dendritic spines in response to a sensory-dependent manipulation are similar in magnitude or duration in females across the estrous cycle.

The goal of the present *in vivo* study was to characterize the changes in dendritic spine density and dynamics of cortical pyramidal neurons of naturally cycling female mice and of male mice to better understand whether the mechanisms regulating memory and learning are enhanced or weakened at specific stages of the cycle and whether these mechanisms are different between female and male mice. These are important pieces of information that are still missing in the neurophysiology of the female brain. Based on the results from previous studies, we wanted to test the hypothesis that dendritic spine density of L5 pyramidal neurons varies during the estrous cycle as a consequence of the oscillating levels of endogenous estrogen. We also wanted to test if synaptic plasticity was differentially expressed in L5 pyramidal neurons across the estrous cycle. Finally, we wanted to test the hypothesis that both, dendritic spine density and dynamics, are different between female and male due to the effect of endogenous hormones associated with the estrous cycle in female mice. We found that dendritic spine density is constant across the estrous cycle in females and similar in magnitude to the density found in males. We also found that in steady-state conditions, the dynamics of dendritic spines are not affected by the stage of the cycle and are comparable to the dynamics observed in males. Finally, we found that the response of these neurons to sensory-evoked structural plasticity is dependent on the stage of the cycle.

MATERIALS AND METHODS

Animals

We used GFP-M transgenic mice expressing GFP under the Thy-1 promoter (The Jackson Laboratory; IMSR Cat# JAX:007788, RRID:IMSR_JAX:007788). These mice express GFP in sparse subsets of projection pyramidal track-type layer 5 (L5) pyramidal neurons in the cortex (Feng et al., 2000). All animals were virgin and group caged. Food and water was available *ad libitum* and all cages were kept in a 12-h light/dark cycle. The study was carried out in accordance with the recommendations of the NIH Office of Laboratory Animal Welfare's *Public Health Service Policy on Humane Care and Use of Laboratory Animals* and *Guide for the Care and Use of Laboratory Animals* and all the procedures described were approved by the Institutional Animal Care and Use Committee of Tulane University.

Droplet Digital PCR

Four GFP-M female mice (3.7 ± 0.2 months of age) were decapitated and immediately dissected on ice, and the primary somatosensory cortex was removed from both hemispheres. Tissues were immediately immerged in RNA*later* Stabilization Solution (Invitrogen Cat# AM7020) and kept at 4°C for 24 h before freezing. Tissues from the left hemisphere were used

for droplet digital PCR (ddPCR). RNA was isolated using the RNeasy mini kit (Qiagen). Purity and concentration of RNA was determined using the nanodrop before being subjected to ddPCR as previously described (Liu et al., 2017). Briefly, approximately 40 ng of RNA was combined with Taqman primers and probes as well as Mastermix (Bio-Rad) to create a 20 μl working reaction mixture (Hindson et al., 2011). The following PrimePCR Primers were used: G protein-coupled estrogen receptor 1 (ER) 1 (GPER/GPR30; Bio-Rad Unique Assay ID: dMmuCPE5103030), ER alpha (ERα, ESR1; Bio-Rad Unique Assay ID: dMmuCPE5092741), ER beta (ERβ, ESR2; Bio-Rad Unique Assay ID: dMmuCPE5092742), and aromatase/CYP19A1 (Bio-Rad Unique Assay ID: dMmuCPE5097863). Each working reaction mixture was then fractionated into approximately 20,000 individual 1 nl droplets by oil emulsion microfluidics. During thermal cycling, each droplet comprises an individual PCR reaction. If the target sequence is present, a fluorescent reporter probe is released. Droplets were analyzed via the QX200 droplet reader (BioRad), which samples and singularizes each reaction mixture, flowing droplets at a rate of 1000 droplets/s past a two-color fluorescence detector. The ratio of positive to negative droplets allows the system to compute the concentration of a target sequence via Poisson distribution statistics.

Western Blot Detection of Classic Nuclear ERs

The tissues from the right hemispheres from the same animals used for the ddPCR were used for immunoblotting assays. Samples were homogenized in NP40 Cell Lysis Buffer (ThermoFisher Cat# FNN0021). Following a 10-min centrifugation at 10,000 rpm, protein concentration was quantified using Pierce BCA Protein Assay Kit (ThermoFisher Cat# 23225). For gel electrophoresis, 100 μg of protein was loaded into 10% SDS-polyacrylamide gels (Invitrogen Cat# NP0315BOX) and was resolved at 150 V for approximately 90 min. Next, the gels were blotted to nitrocellulose membrane (Bio-Rad Cat# 1620115) via iBlot System (Invitrogen). Blots were washed once with DI water then incubated in 5% milk solution at room temperature for 2 h. They were subsequently incubated overnight at 4°C with the primary antibody (1:1000 in Odyssey Blocking Buffer; Li-Cor Biosciences Cat# 927-40100). Next, the blots were washed with TBST (3 × 10 min) then incubated for 2 h at room temperature with the secondary antibody (1:1000 in 5% milk in TBST solution). Immunoblotting was done using anti-ER α (Santa Cruz Biotechnology Cat# sc-71064, RRID:AB_1122667) and anti-ER β (Abcam Cat# ab288, RRID:AB_303379), each paired with a secondary anti-mouse antibody (Santa Cruz Biotechnology Cat# sc-516102, RRID:AB_2687626) conjugated to horseradish peroxidase. Immunoreactive bands were visualized using SuperSignal West Pico Kit (ThermoFisher Cat# 34580).

Cranial Window Surgery for *in Vivo* Imaging

Chronic glass-covered cranial windows were implanted as described previously (Mostany and Portera-Cailliau, 2008; Holtmaat et al., 2009) at least 3 weeks before the beginning of the *in vivo* imaging of dendritic spines (**Figure 1A**). The average age at the time of entering the experiment was 3.5 ± 0.9 months (mean ± SD; range 2.1–4.8 months) and 3.1 ± 0.7 months (range 2.3–4.4 months) for the female and male mice, respectively. Briefly, mice were anesthetized (isoflurane, 5% for induction, 1.5% for maintenance via nose cone) and placed on a stereotaxic frame. Dexamethasone (0.2 mg/kg; MWI/VetOne) and carprofen (Rimadyl® 5 mg/kg; Zoetis, Inc.) were administered subcutaneously to reduce brain edema and local tissue inflammation. A 4 mm-diameter craniotomy was performed with a pneumatic dental drill over the primary somatosensory cortex, 3 mm lateral to the midline and 1.95 mm caudal to Bregma. A round glass coverslip (5 mm #1; Electron Microscopy Sciences) was gently laid over the dura mater, covering the exposed brain and part of the skull and glued to the latter with cyanoacrylate-based glue. A layer of dental acrylic (Lang Dental Mfg. Co., Inc.) was then applied throughout the skull surface and up to the edges of the coverslip. A titanium bar (9.5 × 3.2 × 1.1 mm) was embedded in the dental acrylic to secure the mouse onto the stage of the microscope for imaging.

Vaginal Cytology

Female mouse estrous cycles were tracked beginning 2 weeks post-cranial window surgery using a wet smear technique as previously described (Caligioni, 2009). Briefly, a standard 10 μl pipette loaded with 10 μl of 0.9% saline solution was used to flush the vaginal cavity at approximately the same time each day, 10 am ± 1 h. The samples were scored on an inverted light microscope (Fisher Scientific Company LLC) and assigned to a stage of the estrous cycle (**Figure 1B**). Smears that contained primarily nucleated epithelial cells and absence or very low numbers of leukocytes were classified as proestrus (P). Smears that contained predominantly cornified squamosal cells were classified as estrus (E), and those containing abundant numbers of cornified cells and/or significant amounts of leukocytes were classified as metestrus/diestrus (M/D; Caligioni, 2009). All female mice were followed through two complete cycles before imaging was started to ensure the animal was cycling regularly. Females that showed irregular estrous cycles (i.e., stayed 50% of time in one stage, skipped stages, or average cycle length was ≥7 days) were excluded from the study. Once the females entered the *in vivo* imaging regime, the lavages were performed immediately after the *in vivo* imaging session and while the female was still anesthetized.

Intrinsic Optical Signal Imaging

The precise location of the primary somatosensory cortex barrel field (S1BF) was mapped through the cranial window preparation using intrinsic optical signal (IOS) imaging, as previously described (Johnston et al., 2013). Briefly, the mice were anesthetized with isoflurane (0.75%–1.0% via nose cone) and secured to the IOS rig using the titanium head bar. LED array light sources (Thorlabs) of green (525 nm) and red (630 nm) were used to visualize the vasculature and for the

IOS imaging, respectively. Imaging was performed at 30 frames per second using a Pantera 1M60 camera (Dalsa) and custom routines written in MATLAB (MathWorks; RRID:SCR_001622). The camera was focused to approximately 350 μm below the dura surface using a tandem of objective lenses (135 mm and 50 mm) arranged in a front-to-front configuration. The vibrissae contralateral to the cranial window were bundled and fixed with dental wax to a glass microelectrode coupled to a piezo bender actuator (Physik Instrumente). Imaging sessions consisted of 30 trials, taken 20 s apart, of mechanical stimulation in the rostro-caudal direction for 1.5 s at 10 Hz. Frames 0.9 s before onset of stimulation (baseline) and 1.5 s after stimulation (response) were collected. Stimulated cortical areas (barrel cortex) were identified by dividing the response signal by the averaged baseline signal (ΔR/R) for every trial and then summing all trials.

High Resolution *in Vivo* Two-Photon Imaging

Imaging of dendritic spines was done under isoflurane anesthesia (1%–1.5%) with a custom-built two-photon microscope, using a Ti:Sapphire laser (Chameleon Ultra II; Coherent Inc.) tuned to 910 nm, a 40× 0.8 NA water immersion objective (Olympus), and ScanImage 3.8 software (RRID:SCR_014307; Pologruto et al., 2003) written in MATLAB (MathWorks; RRID:SCR_001622). Mice were secured to the microscope using the titanium head bar. Guided by the maps obtained with the IOS imaging, we scanned the S1BF area searching for L5 pyramidal neurons with apical dendritic tufts clearly identifiable and not obscured by large blood vessels. On the first day of imaging, low magnification image stacks (512 × 512 pixels, 0.72 μm/pixel, 5 μm *z* steps) were collected down to the soma, at least 450 μm from the pia, to ensure all cells studied were L5 pyramidal neurons. The apical dendritic tufts of L5 pyramidal neurons were imaged every 24 h (**Figure 1A**), ranging between 8 am and 12 pm for all the mice imaged. High magnification images (512 × 512 pixels, 0.152 μm/pixel, 1.5 μm *z* steps) of dendritic segments in L1 (within the first 100 μm from the pia mater) were collected on each day of imaging for the analysis of dendritic spines. After female mice demonstrated that they were having regular menstrual cycles, they were imaged daily for 1–3 additional menstrual cycles (average: 2.1 ± 0.8 cycles/female) for an average of 12.4 ± 2.5 days for assessment of steady-state dynamics of dendritic spines (**Figure 1A**). Imaging of male mice began 3 weeks post-cranial window surgery, and they were imaged consecutively for 7 days for assessment of steady-state dynamics of dendritic spines.

Sensory-Evoked Synaptic Plasticity

Once the female mice completed the *in vivo* imaging regime for the study of steady-state density and dynamics of dendritic spines across the estrous cycle, they were randomly assigned to one of the experimental groups (P_{St}, E_{St}, or M/D_{St}) based on the stage of the cycle at which the female mouse was going to experience the induction of synaptic plasticity. Daily imaging continued until the assigned estrous stage was detected after the two-photon imaging session. At that moment we induced sensory-evoked plasticity by rhythmic sensory whisker stimulation (RWS; **Figure 1A**) following a stimulation protocol previously described to induce long term plasticity (Mégevand et al., 2009; Gambino et al., 2014). Briefly, at the conclusion

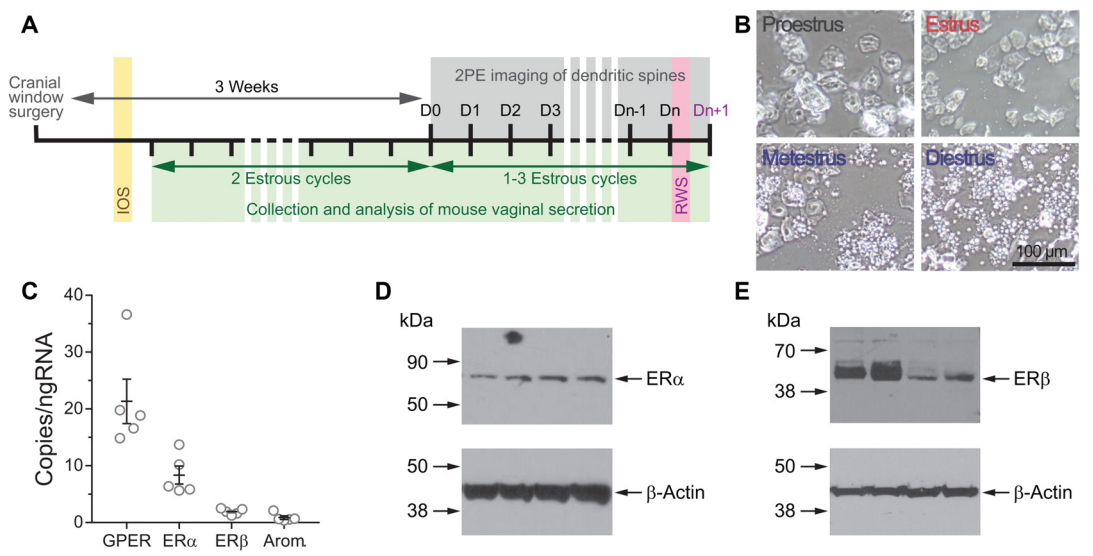

FIGURE 1 | (A) Experimental design for time-lapse two-photon imaging of dendrites during the estrous cycle. **(B)** Representative photomicrographs of vaginal cytology from mice at the different stages of the estrous cycle. **(C)** Copies per ng of RNA of transcripts for G protein-coupled estrogen receptor (GPER), estrogen receptor α (ERα), ERβ, and aromatase in the somatosensory cortex of Thy1 GFP-M female mice determined by droplet digital PCR (ddPCR). **(D,E)** The expression of ERα **(D)** and ERβ **(E)** in the somatosensory cortex of Thy1 GFP-M female mice was confirmed by Western blot.

of the 2PE imaging session, and after assessing the stage cycle, mice were lightly anesthetized (0.75%–1% isoflurane) and attached to the rig using the titanium head bar. The vibrissae contralateral to the cranial window were bundled and fixed with dental wax to a glass microelectrode coupled to a piezo bender actuator which continuously vibrated the whiskers with rostro-caudal deflections (2 mm) at a rate of 8 Hz for 10 min. Male mice underwent whisker stimulation immediately after the last imaging session of the baseline period (day 7). All mice underwent one final imaging session 24 h after the stimulation.

Analysis

Spine density and dynamics from 2PE images were determined using spine analysis software written in MATLAB (kindly provided by Drs. T. O'Connor and K. Svoboda, Janelia Campus). All visible spines were scored, including those on the z-axis which clearly protruded beyond the noise of the dendritic shaft. Scoring of dendritic spines was done blind to both the estrous cycle and sex. Within each cycle, the data obtained for a given stage was averaged if that particular estrous stage lasted for more than 1 day. Values for each of the stages from consecutive cycles were averaged. We analyzed dendritic spines from n = 15 cells (n = 10 female mice) and n = 10 cells (n = 6 male mice) and tracked a total of 5890 distinct dendritic spines over 6–18 imaging sessions. For display purposes only, best projections of the dendritic segments were obtained, where the best focal plane is identified and overlaid in Adobe Photoshop CC (Adobe Systems Inc.; RRID:SCR_014199), preserving all the elements in the segment, and a median filter (radius of 1) was applied. The fold-change in spine density was defined as the density calculated the day after the stimulation divided by the average spine density computed during the steady-state imaging regime. We defined turnover rate (TOR) of dendritic spines as: combined number of gained and lost spines divided by two-times the total number of spines ([#gained spines + #lost spines]/2 × total number of spines). The fold-change in TOR was defined as the TOR computed the day after the stimulation divided by the average TOR computed during the steady-state imaging regime. New persistent spines were defined as newly-formed spines that were still present 24 h after their initial formation. The survival function over a period of 6 days of dendritic spines present at a given day was obtained by fitting the survival fraction plots to a single exponential decay curve. Survival fraction and half-life were calculated as follows: survival fraction = plateau + unstable fraction X $e^{-t/\tau}$, where t is the time (days) and τ (tau) is the time constant. Rate constant (K) = $1/\tau$. Volumetric estimations of dendritic spines and sorting of dendritic spine subtypes were completed using custom written routines in MATLAB and ImageJ (RRID:SCR_003070)[1] as previously described (Mostany et al., 2013). Briefly, dendritic spine volumes were calculated by total integrated brightness (TIB) and normalized using the mean TIB of the adjacent dendritic shaft. Dendritic spines were classified (stubby, thin or mushroom) using a semiautomated unsupervised method. The examiner drew a line manually from the center of the dendritic shaft to the tip of the spine and the pixel intensity for the profile was obtained. A custom written MATLAB routine used the brightness intensity data to determine the spine type based on several criteria including presence or absence of a spine head and overall spine length. Volumetric estimations were limited to stable mushroom spines across three consecutive stages of the estrous cycle in female mice and in male mice. All cells that were used for volumetric analysis were also analyzed for dendritic spine subtypes (n = 15 cells in n = 10 female mice). An average of 19 randomly selected stable mushroom spines (range 16–23) were tracked in each cell across the three estrous cycle stages and in male mice (285 individual mushroom spines) for volumetric comparison. For dendritic spine sorting for the population study, an average of 460 dendritic spines per stage of the cycle (92 dendritic spines/mouse) were scored. For longitudinal analyses of dendritic spine morphology, a total of 876 spines were scored.

[1]http://rsb.info.nih.gov/ij/

Statistics

Statistical differences between groups were calculated with repeated measures one-way or two-way ANOVA followed by a Tukey's multiple comparison test when applicable. A Student's t test (unpaired or paired when appropriate) was used to compare single parameters between two groups. The extra sum-of-squares F test was used to compare the best-fit values for the survival function parameters, i.e., plateau and rate constant K. Differences in proportions between groups was computed using a Chi-square test. All statistical analyses were performed with GraphPad Prism (GraphPad Software; RRID:SCR_002798). All data are presented as the mean ± SEM, unless otherwise stated. Significance was set at $p < 0.05$. In the figures, $^{*}p < 0.05$, $^{**}p < 0.01$, and $^{***}p < 0.001$.

RESULTS

The Primary Somatosensory Cortex Barrel Field Is a Putative Estrogen-Sensitive Area

While several studies have previously shown the presence of ERα and ERβ receptors in total cerebral cortex lysates of mice (Sharma and Thakur, 2006), in the somatosensory cortex (Mitra et al., 2003), as well as their mRNAs from mouse total cerebral cortex (Thakur and Sharma, 2007) and mouse primary visual cortex (Jeong et al., 2011), there is no data about the expression of these receptors in the somatosensory cortex of Thy1 GFP-M mice. The expression of aromatase mRNA has been detected in the visual cortex (Jeong et al., 2011) and in the cingulate and secondary motor cortex (Stanić et al., 2014) of mice. However, the expression of this enzyme has not been reported in the Thy1 GFP-M mice used in this study. The expression of RNA transcripts for ERs ERα and ERβ, GPER, and aromatase was confirmed by ddPCR (**Figure 1C**). Western blot assays confirmed the expression of the two classic ERs ERα and ERβ (**Figures 1D,E**). These results indicate that the primary

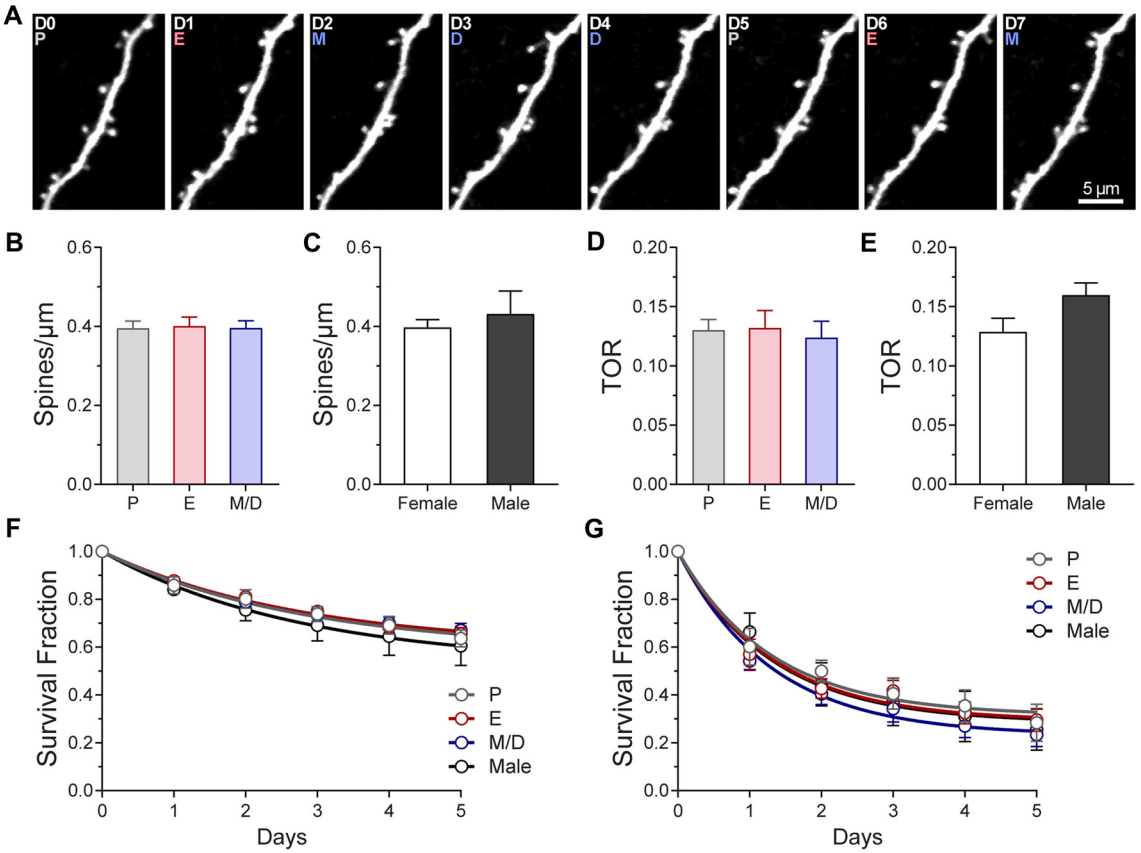

FIGURE 2 | Density and turnover of dendritic spines of L5 pyramidal neurons in primary somatosensory cortex barrel field (S1BF) across the estrous cycle. **(A)** Representative high-resolution two-photon microscopy images acquired *in vivo* of an apical dendritic segment from a L5 pyramidal neuron across two estrous cycles. All the images are best projections (3–6 slices, 1.5 µm apart). The day of imaging and the stage of the cycle are shown in the upper left corner. **(B)** Density of dendritic spines in S1BF at the different stages of the estrous cycle. **(C)** Average density of dendritic spines in female and male mice. **(D)** Turnover rate (TOR) of dendritic spines in S1BF at the different stages of the estrous cycle. **(E)** Average TOR of dendritic spines in female and male mice. **(F,G)** Survival fraction of all the spines present **(F)** or new persistent spines formed **(G)** at different stages of the estrous cycle and in male mice. P, Proestrus; E, Estrus; M/D, Metestrus/Diestrus.

somatosensory cortex of the transgenic Thy1 GFP-M mice is a putative estrogen-sensitive area.

Density, Turnover, Survival Fraction, Morphology, and Volume of Dendritic Spines in the Somatosensory Cortex of Adult Female Mice Does Not Differ Between Stages of the Estrous Cycle

We used high-resolution *in vivo* two-photon imaging of layer (L) 5 pyramidal neurons through a cranial window preparation to monitor the density, dynamics, size, and morphology of individual dendritic spines in the primary somatosensory cortex barrel field (S1BF) of GFP-M female mice across the estrous cycle. To characterize the steady-state density and dynamics of dendritic spines, imaging sessions were performed at 24-h intervals through the estrous cycle (**Figures 1A**, **2A**). To further assess whether sex-differences in density and dynamics of dendritic spines exist in S1BF, male mice were imaged daily for 7 days to obtain the same metrics. No differences in dendritic spine density (# spines/µm) were found between any stages of the estrous cycle in regularly cycling females (P: 0.39 ± 0.02; E: 0.40 ± 0.02, M/D: 0.40 ± 0.02 spines/µm; p = 0.57, repeated measures one-way ANOVA; **Figure 2B**). Additionally, the average dendritic spine density across all the stages in females did not differ from the average density observed in males (0.40 ± 0.02 spines/µm in females vs. 0.43 ± 0.06 spine/µm in males; p = 0.53, unpaired t test; **Figure 2C**). Dendritic spine dynamics were explored in terms of turnover ratio (TOR) over 24 h, i.e., the combined fraction of dendritic spines that appears or disappears between consecutive imaging sessions, 24 h apart, to assess overall change. This measurement was obtained for each stage of the estrous cycle and showed no significant differences between stages (P: 0.13 ± 0.01; E: 0.13 ± 0.02; M/D: 0.12 ± 0.01; p = 0.63, repeated measures one-way ANOVA; **Figure 2D**). When the averaged TOR for female and male mice were compared, we did not find differences either (0.13 ± 0.01 in females vs. 0.16 ± 0.01 in males; p = 0.09, unpaired t-test;

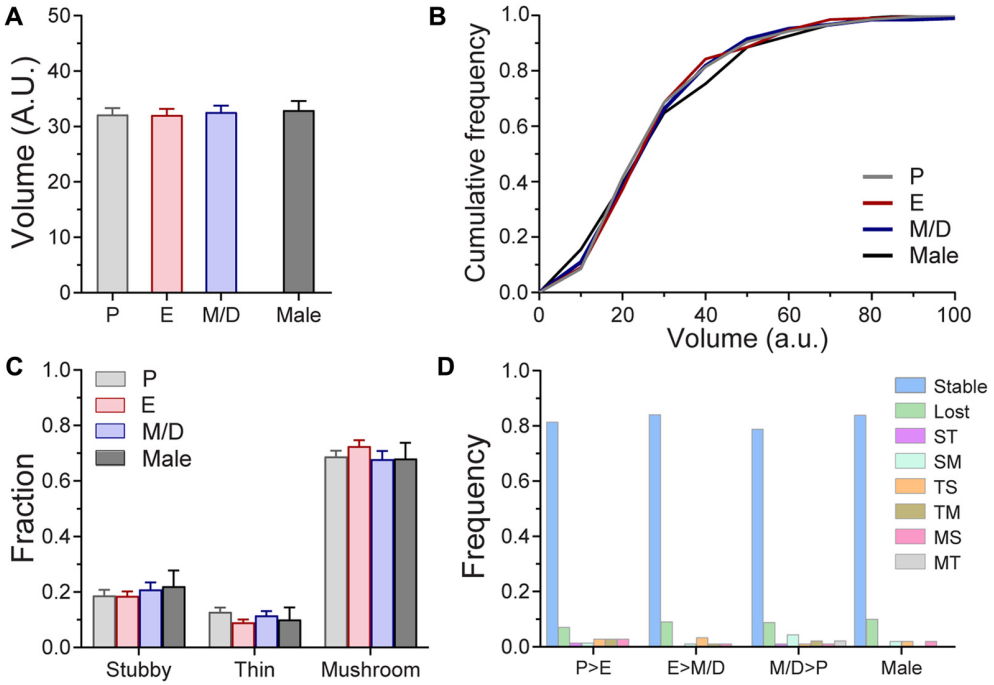

FIGURE 3 | Volume of mushroom spines and morphology of dendritic spines of L5 pyramidal neurons in S1BF across the estrous cycle and male mice in steady-state conditions. **(A)** Volume of mushroom dendritic spines at the different stages of the estrous cycle and male mice. **(B)** Cumulative frequency distribution of the volume of mushroom spines at different stages of the estrous cycle and male mice. **(C)** Distribution of stubby, thin and mushroom spines at different stages of the estrous cycle and in male mice. **(D)** Frequency of spine type transitions between stages of the estrous cycle and in male mice. P, Proestrus; E, Estrus; M/D, Metestrus/Diestrus; ST, Stubby > Thin; SM, Stubby > Mushroom; TS, Thin > Stubby; TM, Thin > Mushroom; MS, Mushroom > Stubby; MT, Mushroom > Thin.

Figure 2E). To determine whether dendritic spines present or formed at a given stage of the estrous cycle were more stable than when this occurred at any of the other stages, we computed the survival function over a period of 6 days of two populations of spines: (1) all the dendritic spines present on the first occurrence of a given stage of the estrous cycle; and (2) new persistent spines formed on the first occurrence of each stage of the cycle. There were no differences in either the fraction of persistent spines (i.e., plateau; $p = 0.6569$, extra sum-of-squares F test) or rate constant K ($p = 0.6621$; extra sum-of-squares F test) between stages or comparable data from male mice (**Figure 2F**) when all the spines present at a given day were tracked. We did not find differences either for new persistent spines ($p = 0.4721$ and $p = 0.4546$ for fraction of persistent spines and K, respectively, extra sum-of-squares F test; **Figure 2G**). These data suggest that the stability of dendritic spines during steady-state conditions does not depend on the phase of the estrous cycle at which the spine was formed.

Next, we seek to elucidate whether oscillations in endogenous hormones, despite the fact that they do not influence the density or dynamics of dendritic spines, may still induce changes at the spine level, either by affecting the volume of mushroom spines or changing the proportions of the three main subtypes of dendritic spines. We used volumetric estimation and an unbiased semi-automated classification scheme (see "Materials and Methods" section) to analyze these parameters across the estrous cycle. We tracked and compared the volume of 210 individual spines across three consecutive stages of the estrous cycle and we did not find differences between stages (P: 32.12 ± 1.2; E: 32.07 ± 1.1; M/D: 32.57 ± 11.2; AU; $p = 0.79$, repeated measures one-way ANOVA; **Figure 3A**), or when the comparison included male mice (Males: 32.93 ± 1.6 AU; $p = 0.9669$, one-way ANOVA; **Figure 3A**). The medians and the 25% and 75% percentiles of the distributions of the volume of dendritic spines at different stages of the cycle and males were comparable (Medians: P: 27.64; E: 28.13; M/D: 29.66; Male: 30.6; 25% Percentiles: P: 20.63; E: 20.43; M/D: 20.08; Male: 18.49. Average: 19.91; and 75% Percentiles: P: 40.09; E: 39.99; M/D: 40.73; Male: 43.67; **Figure 3B**). Regarding the morphological subtypes of dendritic spines, analysis of the proportions of the presence of each subtypes at the population level indicated that there was no difference in the proportions of the stubby, thin, and mushroom spines between stages of the estrus cycle and male mice ($p = 0.3754$, χ^2 test; **Figure 3C**). Taking advantage of the longitudinal aspect of our study we tracked the morphology of individual dendritic spines during the estrous cycle. Dendritic spines were tracked over the transitions from P > E, E > M/D, and from M/D > P. Depending on the morphology of the spine before and after those transitions, these were classified as: stubby > stubby (stable stubby), stubby > thin (ST),

stubby > mushroom (SM), stubby > lost, thin > thin (stable thin), thin > stubby (TS), thin > mushroom (TM), thin > lost, mushroom > mushroom (stable mushroom), mushroom > stubby (MS), mushroom > thin (MT), and mushroom > lost. The fraction of stable spines (stable stubby, stable thin, and stable mushroom) was very similar for all the cycle transitions (P > E: 0.81 ± 0.07; E > M/D: 0.82 ± 0.1; M/D > P: 0.80 ± 0.12) as well as for males over a 24 h period (0.82 ± 0.08; $p = 0.6614$, one-way ANOVA), indicating that, regardless of the stage of the cycle or the sex of the animal, ∼81% of the dendritic spines do not transition to other types of spines over a 24-h period (**Figure 3D**). The fraction of dendritic spines that were lost ranged between 0.071 and 0.088 in the females and it was 0.095 for males. The rest of the transitions (ST, SM, TS, TM, MS, and MT) presented very low frequencies (less than 0.04). Chi-square test did not find statistical differences between stages of the cycle or sex (χ^2 $p = 0.9017$).

Despite the unique hormonal fluctuations of female mice our findings indicate that there are no observable changes in steady-state dendritic spine density, dynamics, survival, volume, or morphology in L5 pyramidal neurons of S1BF across the estrous cycle. Our results also indicate that spine density and dynamics in these neurons are comparable between female and male mice.

Differential Effect of Sensory-Evoked Plasticity on the Dynamics of Dendritic Spines in S1BF L5 Pyramidal Neurons During the Estrous Cycle

While our results indicate that the estrous cycle does not have an effect on steady-state structural synaptic plasticity in L5 pyramidal neurons of S1BF, little is known about the effects of changing levels of endogenous hormones on experience-dependent synaptic plasticity in the cerebral cortex. Furthermore, no chronic *in vivo* studies have been performed to assess whether any particular stage of the estrous cycle favors synaptic plasticity or not. To answer this question, once the baseline imaging of dendritic spines during the estrous cycle was completed, females were randomly assigned to an experimental group based on the stage of the cycle (P_{St}, E_{St}, or M/D_{St}) at which the mouse would undergo rhythmic whisker stimulation to induce sensory-evoked plasticity. Spine density and TOR of individual cells were compared pre- and post-stimulation. Data from the steady-state imaging sessions prior to the whisker stimulation were

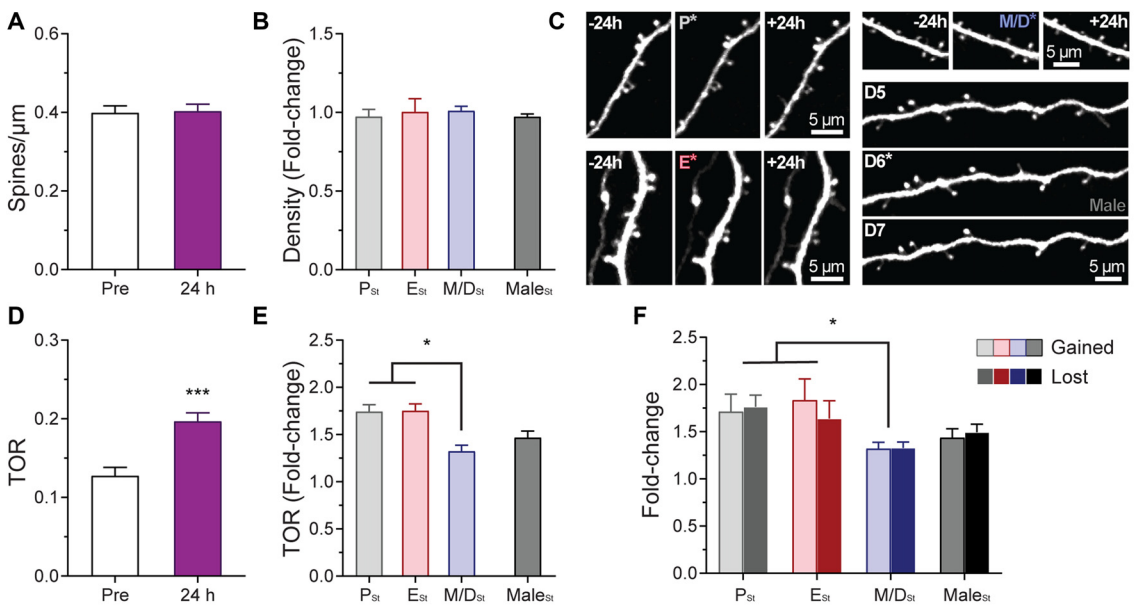

FIGURE 4 | Effects of sensory-evoked plasticity on density and turnover of dendritic spines of L5 pyramidal neurons in S1BF at different stages of the estrous cycle. **(A)** Effect of rhythmic whisker stimulation on the density of dendritic spines when the data from the steady-state imaging sessions prior to the whisker stimulation were averaged to serve as a baseline (Pre vs. 24 h). **(B)** Change in the density of dendritic spines at 24 h based on the stage of the cycle at which the stimulation occurred. Data from male mice is also included in the analysis. **(C)** Representative *in vivo* two-photon images of apical dendritic segments from L5 pyramidal neurons taken 24 h apart depicting differences in relative changes of turnover ratio after whisker stimulation at different stages of the cycle and in male mice. Stimulation ocurred at P (top-left image sequence), E (bottom-left image sequence); M/D (top-right image sequence); and after the imaging session on the 6th day in male mice (bottom-right image sequence). Whisker stimulation was performed immediately following the 2PE imaging session depicted with an asterisk in the image. All are best projections (3–5 slices, 1.5 µm apart). **(D)** Effect of rhythmic whisker stimulation on the TOR of dendritic spines when the data from the steady-state imaging sessions prior to the whisker stimulation were averaged to serve as a baseline (Pre vs. 24 h). **(E)** Change in the TOR of dendritic spines at 24 h based on the stage of the cycle at which the stimulation occurred. **(F)** Changes in the gained and lost ratios based on the stage of the cycle at which the stimulation occurred. Data from male mice is also included in these two analyses. P_{St}, E_{St}, M/D_{St}, and $Male_{St}$: Stimulation at proestrus, estrus, metestrus/diestrus, and after the imaging session on 6th day in male mice, respectively. $^*p < 0.05$ and $^{***}p < 0.001$.

averaged to serve as a baseline (Pre) for comparison to the day after the whisker stimulation (24 h). Whisker stimulation did not affect density of dendritic spines either when pooling the data from the different stages together (Pre: 0.40 ± 0.06; 24 h: 0.40 ± 0.06; p = 0.72, paired t test; **Figure 4A**) or when comparisons were done as the fold-change in density based on the stage of the cycle of the mouse and the sex (p = 0.8451; **Figure 4B**). On the other hand, whisker stimulation increased the TOR of dendritic spines when combining the data from all the cells regardless of the stage at stimulation (PRE: 0.13 ± 0.03; 24 h: 0.20 ± 0.04; $p < 0.001$, paired t test; **Figures 4C,D**). Furthermore, when we divided the results based upon the stage of the cycle the female was in at the moment of the induction of plasticity, we found differential increases in TOR among stages. The fold-changes in TOR after the stimulation relative to the steady-state TOR were significantly larger when females were stimulated during P (P_{St}: 1.74 ± 0.15) and E (E_{St}: 1.75 ± 0.13) than when females were stimulated in the M/D stage (M/D_{St}: 1.32 ± 0.13; $p < 0.01$ vs. P_{St} and E_{St}, one-way ANOVA; **Figures 3C,E**). The fold-change in TOR found in males (1.47 ± 0.2) did not significantly differ from the values obtained for any of the female stages (**Figure 4E**). When we analyzed the independent contributions of the two factors that define TOR, we found that rates at which the values for gained and lost spines changed after the whisker stimulation were comparable at each estrous stage and in males (p = 0.8479, two-way ANOVA) whereas these values were different between stages and with males (p = 0.0074, two-way ANOVA; $p < 0.05$ for P_{St} vs. M/D_{St} and E_{St} vs. M/D_{St}, Sidak's multiple comparisons test; **Figure 4F**). Interestingly, when the data for fold-change in TOR were grouped based on the stage of the estrous cycle at which the female was in 24 h after the stimulation—when the *in vivo* imaging was performed—we failed to find any differences between stages (P_{St}: 1.52 ± 0.26; E_{St}: 1.73 ± 0.12; M/D_{St}: 1.55 ± 0.31; p = 0.21, one-way ANOVA; not shown).

Similarly to the analysis carried out during the *in vivo* imaging of steady-state plasticity, we studied the potential variations in volume in mushroom spines after the stimulation. Volume of individual dendritic spines were recorded before and after stimulation and the fold-change in volume was analyzed as a function of the stage of the cycle the female was in during the

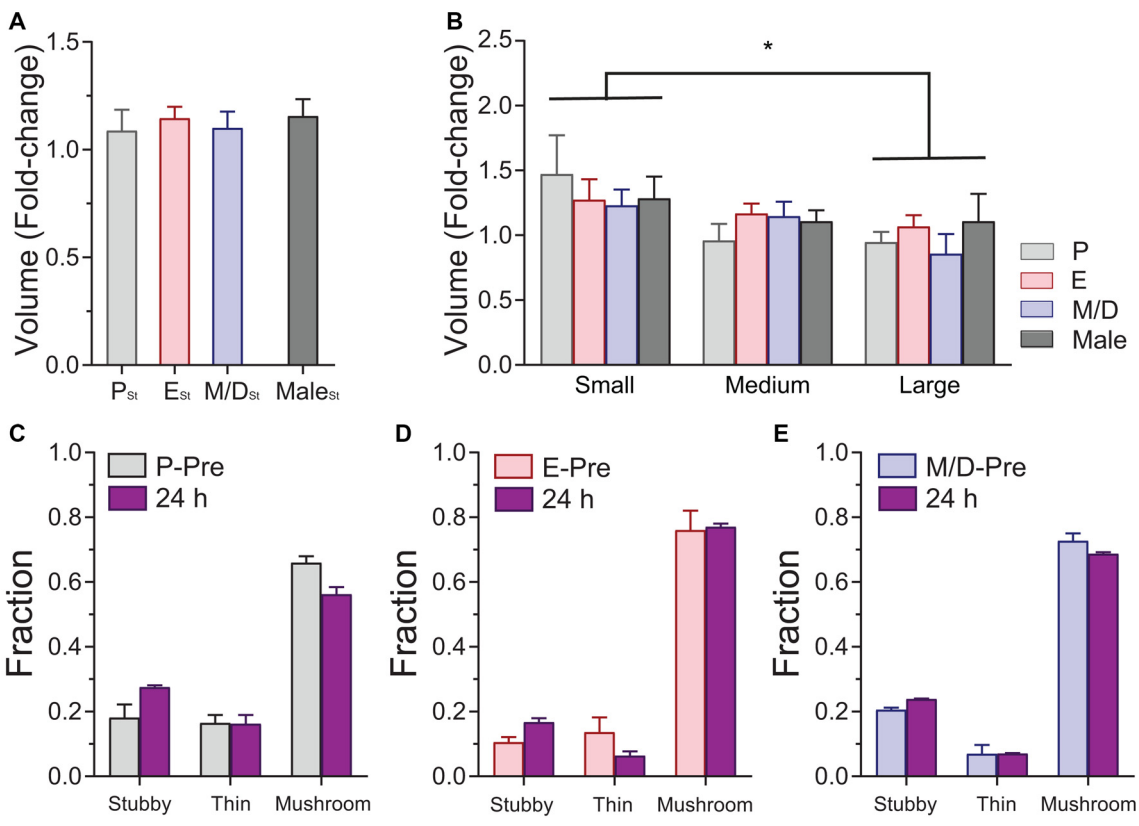

FIGURE 5 | Effects of sensory-evoked plasticity on volume and morphology of dendritic spines of L5 pyramidal neurons in S1BF at different stages of the estrous cycle and in male mice. **(A)** Changes in the volume of mushroom spines at 24 h based on the stage of the cycle at which the stimulation occurred. **(B)** Differential effect of stimulation on the relative volume increase of dendritic spines. Small spines increase their volume relatively more than larger spines regardless of the stage of the cycle when the stimulation occurred or the sex. **(C–E)** Distribution of stubby, thin, and mushroom spines before (P-Pre, Proestrus Pre; E-Pre, Estrous Pre; and M/D-Pre, Metestrus/Diestrus Pre) and 24 h after sensory evoked plasticity at different stages of the estrous cycle. P_{St}, E_{St}, and M/D_{St}: Stimulation at proestrus, estrus, and metestrus/diestrus, respectively. *$p < 0.05$.

stimulation or sex. We could not find differences in spine volume fold-change between groups after stimulation (p = 0.9096, one-way ANOVA; **Figure 5A**). In an attempt to unmask if stimulation produces differential effects on spines depending on the spines size and if this effect was influenced by the stage of the estrous cycle the female was in at the time of the stimulation, we divided the population of spines of each experimental group in three size groups (small, medium, and large) based on the parameters of the distributions obtained during the steady-state conditions (averaged 25% percentile: 19.91; averaged 75% percentile: 41.12). Small spines were those with initial volume (volume measured at the imaging session immediately preceding the whisker stimulation) between 0 and 19.91 AU. Medium spines were those with initial volumes between 19.91 and 41.12 AU, and large spines those with a volume bigger than 41.12 AU. Data from male mice was divided in the same fashion. Analysis of the estrous stage/sex and spine size effects on the fold-change in volume was performed. The main effect of the factor size of the spines was statistically significant (p = 0.0116, two-way ANOVA; small vs. large, p = 0149, Tukey's multiple comparisons test; **Figure 5B**), whereas there was no main effect due to the stage of the cycle or the sex or to the interaction size∗estrous cycle/sex (p = 0.8042 and p = 0.7185, respectively, two-way ANOVA). These data indicate that smaller spines increase their relative size more than larger spines regardless of the stage of the cycle of the sex. Analysis of the proportions of the different types of dendritic spines at the population level showed no differences between estrous stages after the stimulation, regardless of the stage during the stimulation (χ^2 p values: P_{St}: 0.29; E_{St}: 0.24; M/D_{St}: 0.83; **Figures 5C–E**) or the stage 24 h after the stimulation (χ^2 p values: P_{St24}: 0.59; E_{St24}: 0.16; M/D_{St24}: 0.50; not shown). When we tracked the morphology of individual dendritic spines before and 24 h after the stimulation at different stages of the cycle, we did not find an effect of the stimulation on the frequencies of the transitions when comparing the frequencies obtained between stages of the cycle or sex (p = 0.9678, χ^2 test; not shown).

Our results indicate that sensory-evoked plasticity does not result in changes in the density and morphology of dendritic spines at any stage of the estrous cycle in female mice, and comparable results were obtained in male mice. However, we find differential degrees of TOR of dendritic spines across the cycle after sensory stimulation. Small dendritic spines increase their relative size in response to sensory-evoked plasticity to a larger degree than large spines regardless of the stage of the cycle or the sex of the mouse.

DISCUSSION

The present *in vivo* imaging study finds that oscillatory levels of endogenous gonadal hormones during the estrous cycle do not have an effect on the steady-state density, dynamics, survival fraction, morphology, and volume of dendritic spines of L5 pyramidal neurons in S1BF. Our results suggest, however, that sensory-evoked synaptic plasticity may be differentially affected by the levels of gonadal hormones across the estrous cycle.

The estrous—or reproductive—cycle, characterized by cyclical alterations in the female reproductive track and in sexual receptivity, is regulated by the production and release of hormones by the brain, pituitary gland, and gonads. The effects of gonadal hormones on brain function have been widely described (Luine, 2008; Frick, 2009). In particular, the effects of exogenous estrogen on the hippocampus and cortex (Gould et al., 1990; Daniel et al., 1997; Woolley, 1998; Hao et al., 2006; Chen et al., 2009) suggest that these brain areas may be susceptible to changes in the levels of this hormone occurring during the different stages of the estrous cycle. In this regard, our results indicate that, similar to what has been reported for the visual cortex (Jeong et al., 2011), the somatosensory cortex of mice is equipped with the machinery to be sensitive to endogenous estrogens regardless of its source—i.e., brain-derived or circulating estrogen, and to the exposure to xenoestrogens like BPA (Kelly et al., 2014). However, very little is known about changes in the density or in the dynamics of dendritic spines in the cortex during endogenous oscillations of estrogens. The few studies examining the changes in density of dendritic spines in the cerebral cortex during the estrous cycle describe contradictory results, reporting either no differences across the cycle in the neocortex (Prange-Kiel et al., 2008) and in the prefrontal cortex of rats (Markham and Juraska, 2002), or higher density of dendritic spines during P in the primary somatosensory cortex of female rats (Chen et al., 2009). While these studies are comprehensive analyses of the density of dendritic spines throughout the estrous cycle, they lack the longitudinal aspect that *in vivo* studies provide. Our study following the same apical dendritic segments (within the first 100 mm from the pia mater) of L5 pyramidal neurons in S1BF during the estrous cycle (in several instances, up to three cycles) indicates that in the absence of significant sensory stimulation—limited to the social interaction with their cagemates and the exploration of the physical features of the home cage—the density of dendritic spines is stable during steady-state conditions with no significant changes across the different stages of the cycle. To the best of our knowledge this is the first comprehensive *in vivo* study on dendritic spine density, dynamics, survival fraction, size, and morphology done throughout the estrous cycle in normally cycling female mice. The fact that our study was done in young (2–5 months old) mice (most of the studies done in the cortex used rats) and limited to the apical dendrites of L5 pyramidal neurons has also to be taken into consideration when comparing these results with previously reported data. It is important to note that unaltered spine density does not rule out unaltered spine dynamics, as it has been previously observed (Trachtenberg et al., 2002; Keck et al., 2008). In fact, the rates at which dendritic spines are formed and eliminated could be different from day to day, not affecting, however, the overall density if both rates are equalized. These potential shifts are undetectable to fixed tissue studies. Our *in vivo* approach allowed us to test whether TOR varies from one stage of the cycle to another or stays constant throughout

the cycle. We find that the TOR over 24 h does not change during the different stages of the estrous cycle suggesting that in steady-state conditions the naturally occurring oscillations in the levels of circulating estrogens do not influence the rate at which dendritic spines are formed and eliminated. We also find that these measurements, density and TOR, from cycling female mice are comparable to male mice, indicating that apical dendrites of L5 pyramidal neurons in S1BF of female and male mice have similar densities of dendritic spines and rewire cortical connections at similar rates. Another question we were able to answer was if dendritic spines formed at different stages of the cycle show varied degrees of spine stability. We analyzed the survival fraction of newly-formed spines that were formed at different phases of the cycle and lasted at least 24 h (new persistent spines). We found that this metric was not altered across the estrous cycle, suggesting that the oscillating levels of circulating estrogen during the cycle do not have an effect on the persistence of cortical synapses. The fact that spine morphology and volume of mushroom spines were unaltered during the estrous cycle reinforces the notion of a very stable, yet plastic, steady-state cortical micro-circuitry not altered by endogenous oscillations of gonadal hormones. The discrepancies with the previously reported results (Chen et al., 2009) may arise due to different subtypes of neurons examined. While in the present study we imaged non-adapting pyramidal track-type L5 pyramidal neurons exclusively (Hattox and Nelson, 2007; Popescu et al., 2017), there is no information about the subtype of L5 pyramidal neurons they examined. Furthermore, while our *in vivo* preparation is non-invasive, the *ex vivo* preparation described by Chen et al. (2009) requires slicing of the brain which severs almost all the horizontal projections onto these neurons and probably affects the natural occurrence of synaptic plasticity in the cortical circuits.

Rearrangement of the connections of neuronal circuits is necessary for synaptic plasticity, and hence for memory and learning. We wondered if changes in hormone levels during the estrous cycle may have a differential effect on the degree of rewiring of the L5 pyramidal neurons in S1BF after sensory-evoked synaptic plasticity by rhythmic whisker stimulation (Mégevand et al., 2009; Gambino et al., 2014). The plasticity-inducing protocol produced a generalized increase in TOR of dendritic spines, regardless of the stage of the cycle at which the female mice were stimulated. However, this increase in TOR was higher when the mice were stimulated during P and E than when the mice were stimulated during M/D, suggesting that indeed, some stages of the cycle (P and E) may favor the formation and elimination of synaptic connections, i.e., rewiring, to adapt to and integrate new information in the cortical microcircuits, while other stages (M and D) may favor the use of pre-existing connections. The fact that during steady-state conditions we did not find differences in TOR but we do after whisker stimulation is in agreement with the idea that gonadal hormones may serve as primers for synaptic plasticity, contingent to the co-occurrence of sustained synaptic activity within a time window (Srivastava and Penzes, 2011). In this sense, *in vitro* studies using cultured cortical neurons have shown rapid and transient increases in connectivity after treatment with estradiol (Srivastava et al., 2008). As the authors suggest, these results support the idea of a two-step model of estrogen-induced synaptic plasticity. In this view, formation of new non-functional dendritic protrusions is induced by elevated levels of estrogens leading some of them to form stable synapses after subsequent presynaptic stimulation, therefore contributing to remodeling of cortical circuits. The levels of gonadal estrogen at M and D are low and have been low for more than 24 h (Kato et al., 2013), probably outside of the sensitive window for plasticity elicited by the high levels of estrogen during P, and may explain the attenuated evoked-synaptic plasticity detected at M/D. Regarding the size and morphology of dendritic spines, we did not find differences in the volume or proportion of the three types of spines after stimulation, even when we sub-analyzed the results based on the stage of the cycle when the female was stimulated. It is important to note that while estrogens have been extensively studied and implicated in synaptogenesis and synaptic plasticity, the synergistic or antagonistic potential effects of the rest of the gonadal hormones should be considered when interpreting these results. In addition, the 24-h interval regime of our *in vivo* study may have missed events, e.g., transient spines, volume oscillations, etc. so we cannot draw any conclusion about differential immediate effects of evoked-plasticity during estrous cycle.

In summary, our findings indicate that steady-state density and dynamics of dendritic spines of L5 pyramidal neurons in the primary somatosensory cortex of female mice are constant during the estrous cycle; however, the susceptibility of these neurons to sensory-evoked structural plasticity is dependent on the current stage of the cycle. Since the dendritic spines of these neurons undergo higher degree of remodeling during proestrus and estrus than during metestrus/diestrus, it is possible that certain stages of the cycle could favor forms of memory requiring *de novo* formation and elimination of dendritic spines, i.e., rewiring of cortical circuits, while other stages are more suitable for forms of memory where retention or repurposing of already existing synaptic connections—or just changes is the strength of the synaptic contact—is more pertinent.

AUTHOR CONTRIBUTIONS

BHA, ET and RM performed the cranial window surgeries; BHA, HMB, ET and AMD collected the *in vivo* two-photon imaging data; AMD, BOO and SHL performed the ddPCR and the Western Blot experiments; HMB, ET, AMD, BOO, SHL and RM analyzed the data; HMB and ET contributed to the drafting and editing of the manuscript; BHA, AMD and RM contributed to the writing of the manuscript. All the authors contributed to the design of the experiments.

FUNDING

This work was supported by a DeBakey Scholars Research Fellowship to BHA and by grants from the National

Institute on Aging (5R01AG047296), Louisiana Board of Regents RCS (LEQSF(2016-19)-RD-A-24), Louisiana Board of Regents Pfund NSF EPSCoR (LEQSF-EPS(2015)-PFUND-416), COBRE on Aging and Regenerative Medicine (5P20GM103629), and by a 2016 Spring Carol Lavin Bernick Faculty Grant of Tulane University to RM.

ACKNOWLEDGMENTS

We would like to thank Drs. Jill Daniel, Damek Homiack, and Laura Schrader for guidance and helpful discussion. We would like also to thank the Tulane Hypertension and Renal Center of Excellence for the use of their facilities (COBRE, P30GM103337).

REFERENCES

Brinton, R. D. (2009). Estrogen-induced plasticity from cells to circuits: predictions for cognitive function. *Trends Pharmacol. Sci.* 30, 212–222. doi: 10.1016/j.tips.2008.12.006

Caligioni, C. S. (2009). Assessing reproductive status/stages in mice. *Curr. Protoc. Neurosci.* 48:4I:A.4I.1–A.4I.8. doi: 10.1002/0471142301.nsa04is48

Chen, J.-R., Yan, Y.-T., Wang, T.-J., Chen, L.-J., Wang, Y.-J., and Tseng, G.-F. (2009). Gonadal hormones modulate the dendritic spine densities of primary cortical pyramidal neurons in adult female rat. *Cereb. Cortex* 19, 2719–2727. doi: 10.1093/cercor/bhp048

Daniel, J. M., Fader, A. J., Spencer, A. L., and Dohanich, G. P. (1997). Estrogen enhances performance of female rats during acquisition of a radial arm maze. *Horm. Behav.* 32, 217–225. doi: 10.1006/hbeh.1997.1433

Denk, W., Strickler, J., and Webb, W. (1990). Two-photon laser scanning fluorescence microscopy. *Science* 248, 73–76. doi: 10.1126/science.2321027

Feng, G., Mellor, R., Bernstein, M., Keller-Peck, C., Nguyen, Q., Wallace, M., et al. (2000). Imaging neuronal subsets in transgenic mice expressing multiple spectral variants of GFP. *Neuron* 28, 41–51. doi: 10.1016/s0896-6273(00)00084-2

Frick, K. M. (2009). Estrogens and age-related memory decline in rodents: what have we learned and where do we go from here? *Horm. Behav.* 55, 2–23. doi: 10.1016/j.yhbeh.2008.08.015

Gambino, F., Pagès, S., Kehayas, V., Baptista, D., Tatti, R., Carleton, A., et al. (2014). Sensory-evoked LTP driven by dendritic plateau potentials *in vivo*. *Nature* 515, 116–119. doi: 10.1038/nature13664

Gould, E., Woolley, C. S., Frankfurt, M., and McEwen, B. S. (1990). Gonadal steroids regulate dendritic spine density in hippocampal pyramidal cells in adulthood. *J. Neurosci.* 10, 1286–1291.

Hao, J., Rapp, P. R., Leffler, A. E., Leffler, S. R., Janssen, W. G., Lou, W., et al. (2006). Estrogen alters spine number and morphology in prefrontal cortex of aged female rhesus monkeys. *J. Neurosci.* 26, 2571–2578. doi: 10.1523/JNEUROSCI.3440-05.2006

Hattox, A. M., and Nelson, S. B. (2007). Layer V neurons in mouse cortex projecting to different targets have distinct physiological properties. *J. Neurophysiol.* 98, 3330–3340. doi: 10.1152/jn.00397.2007

Hindson, B. J., Ness, K. D., Masquelier, D. A., Belgrader, P., Heredia, N. J., Makarewicz, A. J., et al. (2011). High-throughput droplet digital PCR system for absolute quantitation of DNA copy number. *Anal. Chem.* 83, 8604–8610. doi: 10.1021/ac202028g

Hofer, S. B., Mrsic-Flogel, T. D., Bonhoeffer, T., and Hübener, M. (2009). Experience leaves a lasting structural trace in cortical circuits. *Nature* 457, 313–317. doi: 10.1038/nature07487

Holtmaat, A., Bonhoeffer, T., Chow, D., Chuckowree, J., De Paola, V., Hofer, S., et al. (2009). Long-term, high-resolution imaging in the mouse neocortex through a chronic cranial window. *Nat. Protoc.* 4, 1128–1144. doi: 10.1038/nprot.2009.89

Holtmaat, A., and Svoboda, K. (2009). Experience-dependent structural synaptic plasticity in the mammalian brain. *Nat. Rev. Neurosci.* 10, 647–658. doi: 10.1038/nrn2699

Jeong, J.-K., Tremere, L. A., Burrows, K., Majewska, A. K., and Pinaud, R. (2011). The mouse primary visual cortex is a site of production and sensitivity to estrogens. *PLoS One* 6:e20400. doi: 10.1371/journal.pone.0020400

Johnston, D., Denizet, M., Mostany, R., and Portera-Cailliau, C. (2013). Chronic *in vivo* imaging shows no evidence of dendritic plasticity or functional remapping in the contralesional cortex after stroke. *Cereb. Cortex* 23, 751–762. doi: 10.1093/cercor/bhs092

Kato, A., Hojo, Y., Higo, S., Komatsuzaki, Y., Murakami, G., Yoshino, H., et al. (2013). Female hippocampal estrogens have a significant correlation with cyclic fluctuation of hippocampal spines. *Front. Neural Circuit.* 7:149. doi: 10.3389/fncir.2013.00149

Keck, T., Mrsic-Flogel, T., Vaz Afonso, M., Eysel, U., Bonhoeffer, T., and Hübener, M. (2008). Massive restructuring of neuronal circuits during functional reorganization of adult visual cortex. *Nat. Neurosci.* 11, 1162–1167. doi: 10.1038/nn.2181

Kelly, E. A., Opanashuk, L. A., and Majewska, A. K. (2014). The effects of postnatal exposure to low-dose bisphenol-A on activity-dependent plasticity in the mouse sensory cortex. *Front. Neuroanat.* 8:117. doi: 10.3389/fnana.2014.00117

Kuhlman, S. J., O'Connor, D. H., Fox, K., and Svoboda, K. (2014). Structural plasticity within the barrel cortex during initial phases of whisker-dependent learning. *J. Neurosci.* 34, 6078–6083. doi: 10.1523/JNEUROSCI.4919-12.2014

Lai, C., Franke, T., and Gan, W.-B. (2012). Opposite effects of fear conditioning and extinction on dendritic spine remodelling. *Nature* 483, 87–91. doi: 10.1038/nature10792

Liu, J., Edgington-Giordano, F., Dugas, C., Abrams, A., Katakam, P., Satou, R., et al. (2017). Regulation of nephron progenitor cell self-renewal by intermediary metabolism. *J. Am. Soc. Nephrol.* 28, 3323–3335. doi: 10.1681/ASN.2016111246

Luine, V. N. (2008). Sex steroids and cognitive function. *J. Neuroendocrinol.* 20, 866–872. doi: 10.1111/j.1365-2826.2008.01710.x

Luine, V., and Rodriguez, M. (1994). Effects of estradiol on radial arm maze performance of young and aged rats. *Behav. Neural Biol.* 62, 230–236. doi: 10.1016/s0163-1047(05)80021-4

Markham, J. A., and Juraska, J. M. (2002). Aging and sex influence the anatomy of the rat anterior cingulate cortex. *Neurobiol. Aging* 23, 579–588. doi: 10.1016/s0197-4580(02)00004-0

McEwen, B. S., and Alves, S. E. (1999). Estrogen actions in the central nervous system. *Endocr. Rev.* 20, 279–307. doi: 10.1210/er.20.3.279

Mégevand, P., Troncoso, E., Quairiaux, C., Muller, D., Michel, C., and Kiss, J. (2009). Long-term plasticity in mouse sensorimotor circuits after rhythmic whisker stimulation. *J. Neurosci.* 29, 5326–5335. doi: 10.1523/JNEUROSCI.5965-08.2009

Miquelajauregui, A., Kribakaran, S., Mostany, R., Badaloni, A., Consalez, G. G., and Portera-Cailliau, C. (2015). Layer 4 pyramidal neurons exhibit robust dendritic spine plasticity *in vivo* after input deprivation. *J. Neurosci.* 35, 7287–7294. doi: 10.1523/JNEUROSCI.5215-14.2015

Mitra, S. W., Hoskin, E., Yudkovitz, J., Pear, L., Wilkinson, H. A., Hayashi, S., et al. (2003). Immunolocalization of estrogen receptor β in the mouse brain: comparison with estrogen receptor α. *Endocrinology* 144, 2055–2067. doi: 10.1210/en.2002-221069

Moczulska, K., Tinter-Thiede, J., Peter, M., Ushakova, L., Wernle, T., Bathellier, B., et al. (2013). Dynamics of dendritic spines in the mouse auditory cortex during memory formation and memory recall. *Proc. Natl. Acad. Sci. U S A* 110, 18315–18320. doi: 10.1073/pnas.1312508110

Mostany, R., Anstey, J. E., Crump, K. L., Maco, B., Knott, G., and Portera-Cailliau, C. (2013). Altered synaptic dynamics during normal brain aging. *J. Neurosci.* 33, 4094–4104. doi: 10.1523/JNEUROSCI.4825-12.2013

Mostany, R., Chowdhury, T., Johnston, D., Portonovo, S., Carmichael, S., and Portera-Cailliau, C. (2010). Local hemodynamics dictate long-term dendritic plasticity in peri-infarct cortex. *J. Neurosci.* 30, 14116–14126. doi: 10.1523/JNEUROSCI.3908-10.2010

Mostany, R., and Portera-Cailliau, C. (2008). A craniotomy surgery procedure for chronic brain imaging. *J. Vis. Exp.* 12:680. doi: 10.3791/680

Pologruto, T., Sabatini, B., and Svoboda, K. (2003). ScanImage: flexible software for operating laser scanning microscopes. *Biomed. Eng. Online* 2:13. doi: 10.1186/1475-925X-2-13

Popescu, I. R., Le, K. Q., Palenzuela, R., Voglewede, R., and Mostany, R. (2017). Marked bias towards spontaneous synaptic inhibition distinguishes non-adapting from adapting layer 5 pyramidal neurons in the barrel cortex. *Sci. Rep.* 7:14959. doi: 10.1038/s41598-017-14971-z

Prange-Kiel, J., Jarry, H., Schoen, M., Kohlmann, P., Lohse, C., Zhou, L., et al. (2008). Gonadotropin-releasing hormone regulates spine density via its regulatory role in hippocampal estrogen synthesis. *J. Cell Biol.* 180, 417–426. doi: 10.1083/jcb.200707043

Sharma, P. K., and Thakur, M. K. (2006). Expression of estrogen receptor (ER) α and β in mouse cerebral cortex: effect of age, sex and gonadal steroids. *Neurobiol. Aging* 27, 880–887. doi: 10.1016/j.neurobiolaging.2005.04.003

Srivastava, D. P., and Penzes, P. (2011). Rapid estradiol modulation of neuronal connectivity and its implications for disease. *Front. Endocrinol. (Lausanne)* 2:77. doi: 10.3389/fendo.2011.00077

Srivastava, D. P., Woolfrey, K. M., and Penzes, P. (2013). Insights into rapid modulation of neuroplasticity by brain estrogens. *Pharmacol. Rev.* 65, 1318–1350. doi: 10.1124/pr.111.005272

Srivastava, D. P., Woolfrey, K. M., Woolfrey, K., Jones, K. A., Shum, C. Y., Lash, L. L., et al. (2008). Rapid enhancement of two-step wiring plasticity by estrogen and NMDA receptor activity. *Proc. Natl. Acad. Sci. U S A* 105, 14650–14655. doi: 10.1073/pnas.0801581105

Stanić, D., Dubois, S., Chua, H. K., Tonge, B., Rinehart, N., Horne, M. K., et al. (2014). Characterization of aromatase expression in the adult male and female mouse brain. I. Coexistence with oestrogen receptors α and β androgen receptors. *PLoS One* 9:e90451. doi: 10.1371/journal.pone.0090451

Svoboda, K., and Yasuda, R. (2006). Principles of two-photon excitation microscopy and its applications to neuroscience. *Neuron* 50, 823–839. doi: 10.1016/j.neuron.2006.05.019

Thakur, M. K., and Sharma, P. K. (2007). Transcription of estrogen receptor α and β in mouse cerebral cortex: effect of age, sex, 17β-estradiol and testosterone. *Neurochem. Int.* 50, 314–321. doi: 10.1016/j.neuint.2006.08.019

Trachtenberg, J., Chen, B., Knott, G., Feng, G., Sanes, J., Welker, E., et al. (2002). Long-term *in vivo* imaging of experience-dependent synaptic plasticity in adult cortex. *Nature* 420, 788–794. doi: 10.1038/nature01273

Woolley, C. S. (1998). Estrogen-mediated structural and functional synaptic plasticity in the female rat hippocampus. *Horm. Behav.* 34, 140–148. doi: 10.1006/hbeh.1998.1466

Woolley, C. S., Gould, E., Frankfurt, M., and McEwen, B. S. (1990). Naturally occurring fluctuation in dendritic spine density on adult hippocampal pyramidal neurons. *J. Neurosci.* 10, 4035–4039.

Woolley, C. S., and McEwen, B. S. (1992). Estradiol mediates fluctuation in hippocampal synapse density during the estrous cycle in the adult rat. *J. Neurosci.* 12, 2549–2554.

Xu, T., Yu, X., Perlik, A., Tobin, W., Zweig, J., Tennant, K., et al. (2009). Rapid formation and selective stabilization of synapses for enduring motor memories. *Nature* 462, 915–919. doi: 10.1038/nature08389

Yuste, R., and Bonhoeffer, T. (2001). Morphological changes in dendritic spines associated with long-term synaptic plasticity. *Annu. Rev. Neurosci.* 24, 1071–1089. doi: 10.1146/annurev.neuro.24.1.1071

Zuo, Y., Yang, G., Kwon, E., and Gan, W.-B. (2005). Long-term sensory deprivation prevents dendritic spine loss in primary somatosensory cortex. *Nature* 436, 261–265. doi: 10.1038/nature03715

Conflict of Interest Statement: The authors declare that the research was conducted in the absence of any commercial or financial relationships that could be construed as a potential conflict of interest.

frontiers in Molecular Neuroscience

REVIEW
published: 05 June 2018
doi: 10.3389/fnmol.2018.00197

Sex Differences in Psychiatric Disease: A Focus on the Glutamate System

Megan M. Wickens[1], *Debra A. Bangasser*[1,2] *and Lisa A. Briand*[1,2*]

[1] *Department of Psychology and Neuroscience Program, Temple University, Philadelphia, PA, United States,* [2] *Neuroscience Program, Temple University, Philadelphia, PA, United States*

Alterations in glutamate, the primary excitatory neurotransmitter in the brain, are implicated in several psychiatric diseases. Many of these psychiatric diseases display epidemiological sex differences, with either males or females exhibiting different symptoms or disease prevalence. However, little work has considered the interaction of disrupted glutamatergic transmission and sex on disease states. This review describes the clinical and preclinical evidence for these sex differences with a focus on two conditions that are more prevalent in women: Alzheimer's disease and major depressive disorder, and three conditions that are more prevalent in men: schizophrenia, autism spectrum disorder, and attention deficit hyperactivity disorder. These studies reveal sex differences at multiple levels in the glutamate system including metabolic markers, receptor levels, genetic interactions, and therapeutic responses to glutamatergic drugs. Our survey of the current literature revealed a considerable need for more evaluations of sex differences in future studies examining the role of the glutamate system in psychiatric disease. Gaining a more thorough understanding of how sex differences in the glutamate system contribute to psychiatric disease could provide novel avenues for the development of sex-specific pharmacotherapies.

Keywords: sex differences, glutamate, ADHD, Alzheimer's disease, schizophrenia, autism spectrum disorders (ASD), depression

OPEN ACCESS

Edited by:
Jordan Marrocco,
Rockefeller University, United States

Reviewed by:
Christina Dalla,
National and Kapodistrian University of Athens, Greece
Maarten Van Den Buuse,
La Trobe University, Australia

***Correspondence:**
Lisa A. Briand
lbriand@temple.edu

Received: *27 March 2018*
Accepted: *18 May 2018*
Published: *05 June 2018*

Citation:
Wickens MM, Bangasser DA and Briand LA (2018) Sex Differences in Psychiatric Disease: A Focus on the Glutamate System. Front. Mol. Neurosci. 11:197. doi: 10.3389/fnmol.2018.00197

INTRODUCTION

Accumulating data indicate that disruptions in glutamate neurotransmission are a common underlying pathology in multiple psychiatric diseases including Alzheimer's disease (AD), major depressive disorder (MDD), schizophrenia (SCZ), autism spectrum disorder (ASD), and attention deficit hyperactivity disorder (ADHD) (Magri et al., 2008; Counts et al., 2011; Shimmura et al., 2011; Sokolow et al., 2012; Gray et al., 2015). Furthermore, these diseases all exhibit a sex bias, with increased prevalence of ASD and SCZ in men and increased prevalence of MD and AD in women (Fombonne, 2005; Noble, 2005; Markham, 2012; Mielke et al., 2014). Although little work has been done to elucidate baseline sex differences in the glutamate system, it is clear from work in these disease populations that sex differences must be considered. To promote a better understanding of these sex biases in disease along with sex differences in treatment response, we must first gain a better understanding of sex differences in the glutamate system. To date, very little work has been done to elucidate these differences. This review will focus on the sex differences in the glutamate system that have been revealed in clinical populations and preclinical studies of glutamatergic sex

differences, highlighting how much more work is needed to obtain a clear picture of how sex differences in the glutamate system contribute to disease.

THE GLUTAMATE SYSTEM

Glutamate is the primary excitatory neurotransmitter in the brain and it is essential for normal brain development and plasticity. Glutamate receptors come in two types, ionotropic ligand-gated ion channels and metabotropic, G-protein coupled receptors. These receptor subtypes can be even further subdivided. Currently there are 8 identified metabotropic glutamate receptors: mGluR1-8, and 3 identified ionotropic glutamate receptor subtypes: a-amino-3-hydroxy-5-methyl-4-isoxazolepropionic acid (AMPA) receptors, *N*-methyl-D-aspartate (NMDA) receptors, and kainate receptors. These receptor subtypes can be further divided based upon their subunit composition. AMPA receptors may be calcium-permeable or calcium-impermeable, depending on the absence or presence of the GluA2 subunit, respectively (Hanley, 2014). NMDA receptors are composed of two GluN1 and two GluN2 (or rarely GluN3 subunits). The four subtypes of GluN2 subunits (GluN2A-2D) confer functional diversity with each GluN2 subunit exhibiting unique biophysical, pharmacological and signaling properties (Paoletti et al., 2013; Sanz-Clemente et al., 2013; Wyllie et al., 2013; Ferreira et al., 2017). After being cleared from the synapse by excitatory amino acid transporters (EEATs), glutamate is converted to glutamine. As the levels of both glutamate and glutamine can be measured using proton magnetic resonance spectroscopy (MRS) in humans, many studies have examined these amino acids as potential biomarkers for psychiatric disease (Shimmura et al., 2011; Chiu et al., 2018; Sheikh-Bahaei et al., 2018).

SEX DIFFERENCES IN GLUTAMATE SYSTEMS

Baseline Differences

The little work that has been done in humans to elucidate sex differences in the glutamate system has led to somewhat mixed results. MRS studies have demonstrated a slight increase in glutamate concentration within the parietal gray matter of men compared to women, while no differences were detected in the frontal gray or white matter or the basal ganglia (Sailasuta et al., 2008). However, when looking more carefully at specific brain regions, women seem to exhibit higher levels of glutamate compared to men. Specifically, women exhibit increased glutamate levels in the striatum and cerebellum compared to men (Zahr et al., 2013). There also appears to be increases in glutamate within the sensorimotor cortex and anterior cingulate cortex (ACC) of women (Grachev and Apkarian, 2000). Along with these studies examining glutamate within the brain, studies have also shown sex differences in serum glutamate concentration (Stover and Kempski, 2005; Teichberg et al., 2009). In contrast to the majority of studies examining glutamate in the brain, studies in blood have revealed higher glutamate concentrations in men compared to women (Zlotnik et al., 2011). As glutamate is present in many tissues in the body, these differences in serum glutamate may not reflect changes within the central nervous system (Shulman et al., 2006).

Sex differences in the glutamate system are more readily examined in rodent models. Several brain regions in rodents show sex differences in glutamate concentrations, including higher glutamate in the lateral hypothalamus and habenula of males and higher glutamate in the medial preoptic area of females (Frankfurt et al., 1984). Along with these overall sex differences in glutamate levels there are also changes in glutamate concentration across the estrous cycle (Frankfurt et al., 1984). These changes are brain region specific, with higher levels observed in the lateral septum during proestrus—the phase of the cycle where ovarian hormones are highest—compared to estrus; in the medial septum and diagonal band of Broca during proestrus compared to diestrus; and lower in the anterior hypothalamic area during proestrus compared to diestrus (Frankfurt et al., 1984).

Sex differences are also observed in synaptic glutamate signaling. Under basal conditions, female rats show larger hippocampal AMPR receptor synaptic responses, possibly due to enhanced phosphorylation of the GluA2 subunit (Monfort et al., 2015). However, this enhanced glutamate signaling may occlude further plasticity. Female rats show a reduction in the magnitude of tetanus-induced long-term potentiation (LTP) compared to male rats and this reduction is associated with a decrease in tetanus-induced phosphorylation of GluA1 (Monfort et al., 2015). As the phosphorylation of GluA1 AMPA subunits is involved in the insertion of GluA1-containing AMPR receptors into the synapse, this could reflect a mechanism for this diminished synaptic plasticity (Man et al., 2007). Along with these alterations in AMPA receptor signaling, sex differences also exist in NMDA receptor signaling. For example, NMDA antagonism increases prefrontal dopamine in male rats but decreases levels in females (Locklear et al., 2016). This may reflect a leftward shift in the dose response curve since females seem to be more sensitive to NMDA receptor manipulations. Female rats are more sensitive to excitotoxic damage following administration of an NMDA receptor antagonist, MK-801 (Wozniak et al., 1998) and exhibit a greater behavioral response to ketamine, an NDMA receptor antagonist (McDougall et al., 2017). This increase in NMDA sensitivity may be the result of increased receptor expression as female rats exhibit higher levels of both NR1 and NR2B NMDA subunits (Wang et al., 2015). Along with these changes in ionotropic glutamate signaling, there also appear to be basal sex differences in the metabotropic glutamate receptor system, with female rats exhibiting higher levels of mGluR2/3 and mGluR5 within the hippocampus along with increased mGluR5 in the prefrontal cortex (Wang et al., 2015). Steroid hormones may influence this overall increase in glutamatergic transmission. The neurosteroid, 17β-estradiol (E2) is known to potentiate excitatory transmission by increasing the probability of glutamate release in females (Smejkalova and Woolley, 2010).

Changes Across the Lifespan

While relatively subtle sex differences in glutamate exist in healthy younger individuals, more dramatic sex differences seem to emerge with age. When examining glutamate levels in the brain across the lifespan, men exhibit a clear decline in glutamate from age 21 to age 70 within the basal ganglia and the parietal gray matter that is not present in women (Sailasuta et al., 2008). However, in the ACC, women show a more pronounced age-related decline (between ages 19 and 56) in glutamate levels compared to men (Hädel et al., 2013). Healthy men have been shown to have higher levels of glutamine (Gln) in the ACC, compared to healthy women (Tayoshi et al., 2009). In serum, women exhibit an increase in glutamate concentration as they age (from age 20 to 80), whereas men do not (Kouchiwa et al., 2012). Along with these age-related changes in glutamate levels, there appear to be changes in glutamate receptors as well. Over the course of aging (age 25 vs. age 70), men exhibit an increase in the distribution of mGluR1 in the cerebellum, parietal cortex, putamen, amygdala, and hippocampus (Sakata et al., 2017). Women do not show these aging-related differences in mGluR1 distribution (Sakata et al., 2017). Postmortem tissue analysis has demonstrated that glutamate related gene expression, including genes that code for glutamate receptors and trafficking proteins, decrease over the first 50 years of life within the prefrontal cortex (Choi et al., 2009). However, no studies have yet been adequately powered to detect normal sex differences in these effects nor have more advanced ages been examined. Nevertheless, studies on aging and disease provide us with some insight into potential differences.

Similar to the changes in the glutamate system that occur across the lifespan in humans, rodents also exhibit developmental changes in glutamate. Glutamate concentrations rise over the first 3 months of life in both male and female mice (Kulak et al., 2010). These changes in the glutamate system do not stop when animals reach adulthood. Glutamate concentrations decrease over the course of aging in the hippocampus, cortex, and striatum (Duarte et al., 2014). Although there were no sex differences in the total glutamate concentrations, the authors report a significant interaction between age and brain region in the ratio of glutamine/glutamate, which may reflect differences in glutamatergic transmission between neurons and glial cells (Duarte et al., 2014). Decreased levels of GluA1, GluN2A, and GluN2B glutamate receptor subunit levels over the course of aging (6 mo vs. 24 mos) have been correlated with poorer cognitive performance in male rats, but these studies have not been done in females (Ménard et al., 2015).

Taken together, although much more work is needed to fully understand sex differences in the glutamate system, there appears to be an overall increase in glutamate transmission in females. This increase may be subtle in young adulthood but during aging glutamate transmission decreases in males and the sex difference is amplified. These alterations in glutamate transmission at different ages could contribute to sex differences in incidence, symptomology, and treatment response for many psychiatric diseases. However, much more work is needed to examine differences within the glutamate system in different brain regions in males and females and determine whether there is in fact an overall increase in glutamate tone in females or if the differences are more subtle.

SEX DIFFERENCES IN GLUTAMATE SYSTEMS IN DISEASE

Alzheimer's Disease

Alzheimer's disease (AD) is the leading cause of dementia and it is more likely to affect women than men, with nearly two-thirds of AD cases being women (Mielke et al., 2014). AD is characterized by accumulation of amyloid beta (Aβ) oligomers that are able to block glutamate uptake, leading to increased glutamate levels (Mattson et al., 1992; Domingues et al., 2007). This increased glutamate can lead to excitotoxicity and neurodegeneration. Dampening glutamate transmission can be helpful in the treatment of AD, as the non-competitive NMDA receptor antagonist memantine shows efficacy in the management of moderate-to-severe AD (Reisberg et al., 2003; Winblad et al., 2007). This increase in glutamate levels could more severely impact women with AD as they exhibit lower levels of GluA2-containing AMPR receptor subunits during late mild cognitive impairment compared to men at the same point in the progression of AD (Counts et al., 2011). Reduced levels of GluA2-containing AMPR receptor subunits could result in a greater proportion of GluA2-lacking, Ca^{2+}-permeable AMPA receptors, and thus, increased vulnerability to excitotoxicity due to increased calcium conductance (Counts et al., 2011). To date, there are no studies that have examined whether glutamatergic drug treatments for AD exhibit similar effectiveness in men and women (Canevelli et al., 2017). Future work examining these sex differences in treatment response could provide insight into mechanistic differences in AD progression in men and women.

Just as sex differences are seen in patients with AD, sex differences are observed in AD phenotypes in mouse models of the disease. In the triple transgenic mouse model of AD (3xTg-AD), impairments in spatial memory and inhibitory avoidance tasks appear earlier in female mice than male mice (Clinton et al., 2007). Among 3xTgAD mice, both males and females show deficits in working memory, short-term memory, and increased anxiety-like behavior by 12 months of age, though female mutants show additional impairments in reference memory (Blázquez et al., 2014). This same early onset of cognitive deficits is also seen in two other mouse models of AD, tTa:APPsi mice, in which amyloid precursor protein (APP) expression is driven by the tetracycline transactivator (Melnikova et al., 2016) and APP(SW) mice which overexpress human APP (King et al., 1999). Furthermore, female mice exhibit greater deficits in cognitive function following overexpression of corticotropin releasing factor (CRF) in the presence of human APP compared to males (Bangasser et al., 2017). These differences in behavioral phenotypes are accompanied by differences in pathology. In another AD mouse model, the APP/PS1 transgenic line, female mice show an increase in plasma levels of amyloid protein with age, while males do not (Ordóñez-Gutiérrez et al., 2015). Female APP/PS1 mice also exhibit higher levels of parenchymal Aβ, particularly in the hippocampus, along with higher levels of

phosphorylated tau and proinflammatory cytokines compared to male mutant mice (Jiao et al., 2016).

Building upon the work done in clinical studies, preclinical mouse models have found a role for glutamate in AD symptomatology. Learning deficits and amyloid plaque formation are among the AD symptoms implicated by disruptions in the glutamatergic system. Rats given a competitive NMDA receptor blocker showed deficits in reversal learning, yet no changes in the initial acquisition of a spatial memory task (Zhang et al., 2014), suggesting that NMDA receptors are at least partially involved in the learning deficits associated with AD. NMDA receptors have also been examined in mouse models. Treatment with memantine decreases amyloid plaque formation in APP/PS1-21 mice (Scholtzova et al., 2008). However, when treated with memantine, APP/PS1-21 mice performed similarly to WT controls in the object recognition test (Scholtzova et al., 2008). GluCEST and ^{1}H MRS imaging of the APP-PS1 mouse model showed decreased glutamate levels throughout the brain (compared to WT controls), but the largest difference was observed in the hippocampus (Haris et al., 2013). This suggests that glutamate, and especially NMDA receptors, may be involved in the pathogenesis of AD (Monfort et al., 2015).

Furthermore, glutamatergic sex differences have been observed in preclinical models of AD. Reductions in glutamate within the dorsal hippocampus are seen only in male McGill-R-Thy1-APP rats and not females (Nilsen et al., 2014). Sex differences in AD development could be due to an interaction of glutamatergic systems with sex hormones. Estrogen is thought to play a protective role against cognitive impairments in female, and potentially male, rodents (Li C. et al., 2004; Frye et al., 2005; Carroll et al., 2007). It is hypothesized that estrogen is an underlying factor of sex differences in cognitive deficits following stress in rodents (Luine et al., 2007). After repeated stress, female rats show normal PFC glutamatergic transmission (Wei et al., 2014), suggesting that estrogen may be protective of PFC-mediated functioning. Furthermore, E2 treatment ameliorates Aβ-induced deficits in synaptic plasticity (Logan et al., 2011). However, as women age, their estrogen levels decline and this decline in estrogen may increase vulnerability (Barron and Pike, 2012). To date, the studies done in mouse and rat models of AD have not taken declining estrogen levels into account.

Major Depressive Disorder

Women are nearly twice as likely as men to develop MDD and among those diagnosed with MDD, women experience more severe symptoms than men (Kornstein et al., 1995). Although the efficacy of SSRIs has focused the depression field on the serotonergic system, recent work on the efficacy of ketamine in treating MDD has led to increased interest in the glutamatergic system (Berman et al., 2000). Individuals with MDD have lower levels of both glutamate and glutamine in several brain regions including the ACC, dorsolateral prefrontal cortex (dlPFC), dorsomedial amygdala, and hippocampus (Auer et al., 2000; Michael et al., 2003a,b; Block et al., 2009). While the majority of studies have found this relationship, a few studies have not detected differences in glutamate metabolites (either glutamate or glutamine) in MDD (Binesh et al., 2004; Milne et al., 2009; Price et al., 2009). It is possible that some of the disparities in findings regarding glutamate levels and MDD are due to inconsistencies among participants between studies i.e., the ratio of men to women in the study and whether women were pre- or post- menopause (Gray et al., 2015). However, to date, none of these studies have examined potential sex differences in glutamate metabolite levels in MDD patients. Women with MDD have been shown to have higher levels of glutamate receptor gene expression postmortem, particularly in both AMPA and NMDA receptor subunit expression Additionally, women with postpartum depression exhibit an increase in prefrontal glutamate compared to healthy controls (McEwen et al., 2012). Thus, there is evidence for increased dysregulation in the glutamate system in women with MDD.

Similar to what has been seen in the clinical population, increased activity in the glutamatergic system has been connected to depression-like behavior in preclinical models. Male rats from the Flinders sensitive line (FSL), a model of depression, exhibit increased glutamatergic synaptic transmission in the hippocampus compared to controls (Gómez-Galán et al., 2013). However, female FSL rats exhibit higher levels of glutamate within the PFC compared to their male FSL counterparts (Kokras et al., 2009). Female rats also exhibit an increase in glutamate in the PFC in response to acute stress whereas males do not (Kokras et al., 2018). Furthermore, antidepressant administration increases cortical glutamate levels in both male and female FSL rats, while only increasing hippocampal glutamate in females (Kokras et al., 2009). Female rats expressing learned helplessness behavior, similarly would have increased glutamate, because they exhibit decreased glutamate uptake in the hippocampus, cortex, and striatum (Almeida et al., 2010). Furthermore, genetic alterations in the glutamate system can lead to depressive symptoms. Decreasing levels of vesicular glutamate transporter with a heterozygous knockout (VGLUT1$^{+/-}$) leads to depressive-like behavior in mice (Tordera et al., 2011). However, chronic mild stress, another model of depression, leads to increased VGLUT1 levels in the hippocampus suggesting that bidirectional dysregulation of the glutamate system can be associated with depressive phenotypes (Garcia-Garcia et al., 2009).

Along with these broad differences in the glutamate system, preclinical models have revealed sex-specific alterations in the glutamate system in models of depression. Following prenatal chronic mild stress, male rats displayed higher expression of mGluR2/3, mGluR5, and NR1 in the prefrontal cortex; while female rats did not (Wang et al., 2015). Neonatal NMDA receptor blockade increases both physiological stress responsivity, CORT response, and anxiety-like behavior in the elevated plus maze in adult male mice, while female mice exhibit a decreased in anxiety-like behavior following the same treatment (Amani et al., 2013). Although the glutamate system of males appears more vulnerable to manipulations early in life, in adulthood, female mice are more sensitive to the antidepressant effects of ketamine, an NMDA receptor antagonist (Carrier and Kabbaj, 2013). Female mice exhibit a decrease in immobility in the forced swim test as well as an antidepressant response in the novelty suppressed feeding test at doses of ketamine that have

no effect in males (Carrier and Kabbaj, 2013). These studies suggest that adult female mice have increased glutamate tone on NMDA receptors that may be leading to increased anxiety and depressive-like behaviors. This increased NMDA receptor tone may be responsible for the increased hippocampal dendritic spine density in females at baseline (Woolley et al., 1990; Shors et al., 2004). This idea is supported by work demonstrating that male and female rats exhibit opposite spine density changes in response to acute stress and these different responses are mediated by NMDA receptor activation (Shors et al., 2004). Further, this could provide a mechanism by which females are hyper-responsive to anxiety provoking stimuli in their environment.

Schizophrenia

In contrast to AD and MDD, SCZ is more prevalent in men, with a male to female ratio of ∼1.4:1.0 (Castle et al., 1993). Furthermore, men exhibit an earlier age of onset, greater symptom severity, and poorer response to treatment (Abel et al., 2010). Although there are many factors contributing to these sex differences, differences in the glutamatergic system are a critical component. Impairments in the glutamatergic system contribute to the pathophysiology of SCZ. (Olney and Farber, 1995; Goff and Coyle, 2001; Coyle et al., 2002; Tsai and Coyle, 2002; Javitt, 2007). However, this contribution appears to be different in men and women. For example, polymorphisms in different glutamate related genes increase the risk for SCZ in males and females. Multiple single-nucleotide polymorphisms (SNPs) in an X-linked gene coding for the AMPA receptor subunit 3, GRIA3, confer increased risk for the development of SCZ in females only (Magri et al., 2008). On the other hand, SNPs in the SAP97 gene that encodes a scaffolding protein involved in membrane targeting of glutamate receptors, is associated with an increased risk of SCZ in males but not females (Uezato et al., 2012).

Along with differences in genetic contributions, sex differences in glutamate related protein expression and metabolites have been found. Glutamine synthetase, an enzyme involved in the maintenance of glutamate levels, is upregulated in women with SCZ but not men (Martins-de-Souza et al., 2010). Additionally, women with SCZ exhibit higher levels of NMDA receptor density compared to men with SCZ (Nudmamud-Thanoi and Reynolds, 2004). NMDA receptor hypofunction is hypothesized to contribute to the pathophysiology of SCZ, therefore increased NMDA receptor density in women with SCZ could be protective and contribute to sex differences in symptomology (Leung and Chue, 2000; Coyle et al., 2002).

Examinations of sex differences in preclinical models of SCZ are few and far between. Much of the research on SCZ has focused on behavioral endophenotypes. Prepulse inhibition of startle (PPI), the reduction of startle produced by a prepulse stimulus, is diminished in patients with SCZ and can be easily modeled in animals (Swerdlow and Geyer, 1998). Female rats exhibit higher levels of PPI compared to males at baseline (Nozari et al., 2015; Zhang X. et al., 2015; Gogos et al., 2017). NMDA receptor antagonist, MK-801, decreases PPI in both intact and gonadectomized male mice whereas female mice only exhibit this decrease following ovariectomy (van den Buuse et al., 2017). This suggests that circulating hormones protect females against NMDA receptor mediated disruption of PPI. In support of this, estradiol treatment following ovariectomy blunts the ability of MK-801 to disrupt PPI (Gogos et al., 2012). Higher doses of MK-801 are able to disrupt PPI in females suggesting that NMDA receptors are still involved in the response in both sexes (Nozari et al., 2015).

In contrast to these static models of behavioral endophenotypes, developmental animal models of SCZ, such as the neonatal hippocampal lesion (nVHL) model, mimic the developmental progression of the disorder. The initial studies describing the nVHL model and the majority of those since then have utilized only the male pups, eliminating the ability to determine whether any sex differences exist (Lipska et al., 1993; Chambers et al., 1996; Flores et al., 1996; Goto and O'Donnell, 2002). An analysis of the literature revealed three papers that examined both males and females after nVHL. Overall, many of the behavioral effects of nVHL are similar in males and females, including deficits in working memory and increased locomotor response to novelty, MK-801 and amphetamine (Beninger et al., 2009; Bychkov et al., 2011). However, following nVHL, male mice exhibit hyperactivity in response to apomorphine, a non-selective dopamine agonist, whereas females do not (Bychkov et al., 2011). Further, following nVHL only male mice exhibit a decrease in phosphorylated extracellular signal-related kinase (pERK), mitrogen activated protein kinase (pMAPK), glycogen synthase kinase 3β (pGSK-3β), and protein kinase B (pAkt) in the accumbens and pERK within the PFC (Bychkov et al., 2011). In contrast, only female mice exhibit a decrease in pAkt and pMAPK in the dorsal striatum following nVHL (Bychkov et al., 2011). Along with these behavioral and molecular sex differences, there are also sex differences in the response to antipsychotics following nVHL. Clozapine can worsen working memory deficits in male nVHL mice whereas a floor effect may limit its effects in female nVHL mice (Levin and Christopher, 2006). However, control females are vulnerable to the memory dampening effects of clozapine whereas males are not (Levin and Christopher, 2006). Along with the nVHL model, neonatal administration of an NMDA receptor antagonist also induces SCZ-like behavior (Stefani and Moghaddam, 2005). However, the SCZ-like phenotypes are influenced by sex and hormonal status, with males and diestrous females exhibiting more consistent endophenotypes compared to proestrous females (Célia Moreira Borella et al., 2016). This could reflect a protective effect of estrogens, as levels of estradiol are highest during proestrus.

Studies utilizing mutant mice have also revealed sex differences that may be relevant to SCZ. The gene neuregulin1 (NRG1) confers an increased risk of SCZ and mutations in NRG1 lead to SCZ-like endophenotypes in mice (Gerlai et al., 2000; Stefansson et al., 2002, 2003, 2004; Li T. et al., 2004). However, there are sex differences in these phenotypes. While male neuregulin deficient mice exhibit deficits in object recognition memory and both contextual and cued fear conditioning, female $Nrg1^{+/-}$ mice do not exhibit any cognitive deficits (Pei et al., 2014). Additionally, male $Nrg1^{+/-}$ mice exhibited a decrease in the GABAergic markers, GAD67 and parvalbumin, while females did not (Pei et al., 2014). Although both male and female NRG1

mutant mice exhibit an increase in exploratory behavior, the specific elements of this behavior differed between males and female mutants (O'Tuathaigh et al., 2006).

Abnormalities in glutamatergic functioning have been associated with SCZ-like symptoms in animals. NMDA receptor hypofunction has been repeatedly cited as a component of SCZ and D-serine, an NMDA receptor co-agonist, may have therapeutic effects (Labrie et al., 2012). Accordingly, disrupting the glutamate system in a variety of ways, including neonatal NMDA antagonism (Stefani and Moghaddam, 2005) or deletion of AMPA GluA1 subunits (Procaccini et al., 2013), can lead to behavioral symptoms of the disease. Neonatal VHL rats also display disruptions in glutamate signaling, with reduced glutamate release in the PFC (Beninger et al., 2009). Furthermore, PCP and MK-801, NMDA receptor antagonists, have long been used to model the positive symptoms of SCZ (Moghaddam and Jackson, 2003). Perinatal treatment with PCP leads to deficits in spatial reference memory in male rats but not females (Andersen and Pouzet, 2004). Furthermore, these deficits were alleviated by treatment with D-serine, an NMDA co-agonist, suggesting that males may be more sensitive to disruptions of NMDA function than females (Andersen and Pouzet, 2004). Copy number variants (CNV) in the synaptic scaffolding molecular (S-SCAM), which controls synaptic AMPA receptor levels, have been linked to risk for SCZ. Transgenic mice with S-SCAM CNVs exhibit behaviors consistent with positive, negative, and cognitive symptoms of SCZ, as well as cellular and morphological abnormalities (Zhang N. et al., 2015). These mice also mimic the human condition because although both males and females show SCZ-like symptoms, male S-SCAM Tg mice generally exhibit more severe symptoms (Zhang N. et al., 2015). Taken together these findings suggest that increased glutamatergic tone in females may be protective and lead to differences in symptomology.

Autism Spectrum Disorder

Similar to the sex bias seen in SCZ, ASD is more common in boys, affecting nearly four times as many boys as it does girls (Fombonne, 2009; Elsabbagh et al., 2012). Individuals with ASD have decreased levels of glutamate metabolites in the basal ganglia and ACC and these decreases are correlated with severity of ASD symptoms (Horder et al., 2013; Tebartz van Elst et al., 2014). In contrast to these decreases in glutamate metabolites in the brain, children with ASD have increased levels of glutamate in plasma and these levels also correlate with symptom severity (Cai et al., 2016). Despite the clear sex bias in the disease, to date, no studies have examined sex differences in metabolite levels (Ford and Crewther, 2016).

Similar to animal models of SCZ, animal models of autism focus on endophenotypes. In particular, autism-like behaviors in rodents have focused on deficits in social behavior. Healthy juvenile male mice exhibit more social exploratory behavior compared to juvenile females (Karlsson et al., 2015; Netser et al., 2017). Following prenatal valproic acid (VPA) treatment, an animal model of autism, male mice show impairments in social behavior in adulthood, while female mice do not (Kim et al., 2013). The prenatal VPA model also leads to male-specific deficits in sensorimotor gating, another phenotype of ASD (Anshu et al., 2017). Similar male-specific effects are seen in the telomerase reverse transcriptase overexpressing mice (TERT-tg). Male TERT-tg mice exhibit impaired social behavior, increased anxiety-like behavior, and lowered seizure threshold, while female TERT-tg mice do not (Kim et al., 2017). Maternal immune challenge also leads to male-specific deficits in social behavior in the contactin-associated protein-like 2 (Cntnap2) mouse model of ASD (Schaafsma et al., 2017). Individuals with ASD exhibit a decrease in striatal activation in response to social and non-social rewards (Scott-Van Zeeland et al., 2010). Male-specific deficits in reward learning are seen following 16p11.2 hemideletion, a gene that is disrupted in ASD (Weiss et al., 2008; Grissom et al., 2018).

Consistent with what has been seen in patients with ASD, preclinical studies demonstrate a clear role for the glutamate system in ASD-like behaviors. Extracellular glutamate concentrations in the lateral septum (LS) increase during social play for both male and female juvenile rats (Bredewold et al., 2015). In a mouse model of a common CNV found in ASD, ubiquitin protein ligase Ube3a, shows deficits in social interaction, impaired communication, and increased incidence of repetitive behaviors are accompanied by impaired glutamate synaptic transmission in male and female mice (Smith et al., 2011). A similar relationship is seen in both male and female Shank2 knockout mice. These mice show reduced social interaction and communication, impaired spatial learning and memory, and increased anxiety-like behavior, which are accompanied by reductions in NMDA receptor function (Won et al., 2012). Furthermore, restoring NMDA receptor function with D-cycloserine reversed the decreased sociability phenotype (Won et al., 2012). However, disruption of Shank3, another gene implicated in human ASD patients, leads to more pronounced reductions in glutamate transmission in male knockout mice and only juvenile males exhibit deficits in social behavior (Yang et al., 2012). As male mice exhibit higher levels of glutamate induced by social play compared to females, there may be sex differences in sensitivity to perturbations in the glutamate system (Bredewold et al., 2015). Furthermore, the increase in glutamatergic tone may be protective in females.

Attention Deficit Hyperactivity Disorder (ADHD)

Attention deficit hyperactivity disorder (ADHD) also shows a strong male bias, affecting nearly 3 times as many boys as girls (Cuffe et al., 2005). Traditionally mechanistic work on ADHD has focused on catecholamine function due to the therapeutic efficacy of stimulants. However, more recently the focus has shifted to the glutamate system due to data from genetic screenings implicating CNVs and SNPs in multiple glutamate receptor subtypes (Turic et al., 2004, 2005; Lesch et al., 2008; Mick et al., 2008; Elia et al., 2011). Furthermore, MRS imaging studies show increased glutamatergic tone in both the frontal cortex and striatum of ADHD patients and this is normalized by pharmacological treatment (Carrey et al., 2003; MacMaster et al., 2003). While

no studies have examined male and female ADHD patients and made direct comparisons, female ADHD patients exhibit a positive correlation between ACC glutamate concentration and impulsivity (Ende et al., 2016). Glutamate may play a role in not only the pathology associated with ADHD but also the treatment response. Polymorphisms in NDMA receptor subunit genes predict better methylphenidate treatment response in children with ADHD (Kim et al., 2016). Notably, while studies discussed above controlled for sex, none of the published clinical studies have examined the influence of sex as an independent variable.

The majority of the work examining animal models of ADHD have either utilized only male mice to assess phenotypes (Archer et al., 1988; Kuwagata and Nagao, 1998; Kuwagata et al., 2004; Mergy et al., 2014) or in many cases where males and females were used data were collapsed preventing any examination of possible sex differences (Shaywitz et al., 1976, 1977; Pappas et al., 1980; Dell'Anna et al., 1991; Row et al., 2002). However, some studies utilizing the spontaneous hypertensive rat (SHR) model of ADHD have reported sex differences in behavioral phenotypes. Notably, while both male and female SHRs showed hyperactivity and sustained attention deficits, male SHRs exhibit greater impulsivity (Berger and Sagvolden, 1998). While there is evidence that male SHRs perform better on conditioned association tasks than female SHRs, this seems to reflect an increase in performance compared to controls in the males rather than a decrement in females (Bucci et al., 2008). Direct comparisons between controls and SHR males and females revealed attention deficits in male SHR rats that were not present in female SHRs, while both sexes exhibited increased inhibitory control and hyperactivity (Bayless et al., 2015). Along with these differences in behavioral phenotypes, animal models have also revealed sex differences in treatment response. Omega-3 polyunsaturated fatty acid supplementation lead to improved reinforcement-controlled attention in male SHRs while not affecting female SHRs (Dervola et al., 2012). These findings may be explained by the effects of sex hormones on fatty acid metabolism, particularly the low level of alpha-linolenic acid to docosahexaenoic acid metabolism in males (Dervola et al., 2012).

Just as alterations in the glutamate system have been implicated in human ADHD patients, animal models of ADHD also exhibit aberrant glutamatergic signaling. SHRs exhibit higher levels of glutamate-evoked norepinephrine release and slower AMPR receptor internalization within the hippocampus compared to controls (Howells and Russell, 2008). Given that there is evidence for increased extracellular glutamate within the hippocampus, these downstream effects could be even greater than they appear (Sterley et al., 2016). This increase in extracellular glutamate may occur outside the hippocampus as well. SHR males have heightened levels of evoked glutamate release in the PFC and striatum compared to controls (Miller et al., 2014). Furthermore, manipulations of the glutamate system can lead to ADHD-like behaviors. Infusion of the NMDA antagonist, 3-(R)-2-carboxypiperazin-4-propyl-1-phosphonic acid, into the mPFC of rats leads to increased impulsivity and compulsivity (Pozzi et al., 2011). Despite this link between glutamate and ADHD behavioral phenotypes and the observed sex differences in preclinical models, differential roles of glutamate or alterations in the glutamate system have not been examined in sex-specific manner.

CONCLUSION

These studies clearly demonstrate a role for dysregulation in the glutamate system in sex biased psychiatric diseases.

TABLE 1 | Sex differences in glutamate systems in disease.

Clinical studies	Symptomology incidence	Serum glu	Brain glu	Glu receptor activity/expression	Response to glu drugs
Baseline	N/A	♂> ♀	♀> ♂	–	N/A
Aging	N/A	↓♀	↓♂	↑♂mGlu1	–
AD	↑♀	–	–	↓♀GluA2	–
MDD	↑♀	–	–	↑♀✖♂	–
Schizophrenia	↑♂	–	–	↑♀✖♂	–
ASD	↑♂	–	–	–	–
ADHD	↑♂	–	–	–	–
Preclinical	**Glutamate concentration**	**Glu receptor expression**	**Glu transmission**	**Synaptic plasticity**	**Response to glu drugs**
Baseline	–	♀> ♂	♀> ♂	♂> ♀	N/A
Aging	↓♂↓♀	↓♂✖♀	–	–	–
AD	↓♂	–	–	–	–
MDD	↑♀> ↑♂	–	–	–	↑♀✖♂
Schizophrenia	–	–	–	–	↑♂✖♀
ASD	–	–	↓♂=↓♀	↓♂=↓♀	–
ADHD	–	–	–	–	–

This table summarizes the studies that have examined sex differences to date. The rows for each disease state reflect changes from control or baseline in each sex, respectively. The line symbolizes that no studies have examined sex differences for the variable in a given disease state. There may be data for changes in one sex or data collapsed across sex that indicate a change from baseline but no studies have explicitly examined sex differences.

The little data that are available suggest that females have increased glutamatergic tone compared to males and this can increase vulnerability in some cases and be protective in others. However, very little work has been done to elucidate potential sex differences in the glutamate system either at baseline or in the disease state (see **Table 1**). Although more imaging and postmortem tissue analysis in clinical populations would be insightful, a basic understanding of sex differences in glutamate signaling is needed. To achieve this, more preclinical studies aimed at determining sex differences are warranted. After a fundamental understanding of baseline differences is reached, examination of how dysfunction in the glutamate system can contribute to psychiatric disease would be more informative. As the majority of preclinical work has been done either only in male rodents or studies that have been underpowered to examine sex differences, much of what we know about glutamate system function and psychiatric disease may only apply to males. The examination of how glutamate dysfunction differentially affects males and females could lead to novel avenues for therapeutic development in these sex biased diseases.

AUTHOR CONTRIBUTIONS

MW, DB, and LB contributed to the conception and design of this review, and edited and revised the manuscript. MW and LB wrote the manuscript. MW, DB, and LB have seen and approve of the final version to be published.

FUNDING

This work was supported by National Institute on Drug Abuse (NIDA) Grant R00 DA033372 (LB), Grant T32 DA007237 (MW), National Science Foundation NSF CAREER IOS-1552416 to (DB) and a Brain & Behavior Research Foundation NARSAD award (LB).

REFERENCES

Abel, K. M., Drake, R., and Goldstein, J. M. (2010). Sex differences in schizophrenia. *Int. Rev. Psychiatry* 22, 417–428. doi: 10.3109/09540261.2010.515205

Almeida, R. F., Thomazi, A. P., Godinho, G. F., Saute, J. A., Wofchuk, S. T., Souza, D. O., et al. (2010). Effects of depressive-like behavior of rats on brain glutamate uptake. *Neurochem. Res.* 35, 1164–1171. doi: 10.1007/s11064-010-0169-4

Amani, M., Samadi, H., Doosti, M. H., Azarfarin, M., Bakhtiari, A., Majidi-Zolbanin, N., et al. (2013). Neonatal NMDA receptor blockade alters anxiety- and depression-related behaviors in a sex-dependent manner in mice. *Neuropharmacology* 73, 87–97. doi: 10.1016/j.neuropharm.2013.04.056

Andersen, J. D., and Pouzet, B. (2004). Spatial memory deficits induced by perinatal treatment of rats with PCP and reversal effect of D-serine. *Neuropsychopharmacology* 29, 1080–1090. doi: 10.1038/sj.npp.1300394

Anshu, K., Nair, A. K., Kumaresan, U. D., Kutty, B. M., Srinath, S., and Laxmi, T. R. (2017). Altered attentional processing in male and female rats in a prenatal valproic acid exposure model of autism spectrum disorder. *Autism Res.* 10, 1929–1944. doi: 10.1002/aur.1852

Archer, T., Danysz, W., Fredriksson, A., Jonsson, G., Luthman, J., Sundstrom, E., et al. (1988). Neonatal 6-hydroxydopamine-induced dopamine depletions: motor activity and performance in maze learning. *Pharmacol. Biochem. Behav.* 31, 357–364. doi: 10.1016/0091-3057(88)90358-9

Auer, D. P., Putz, B., Kraft, E., Lipinski, B., Schill, J., and Holsboer, F. (2000). Reduced glutamate in the anterior cingulate cortex in depression: an *in vivo* proton magnetic resonance spectroscopy study. *Biol. Psychiatry* 47, 305–313. doi: 10.1016/S0006-3223(99)00159-6

Bangasser, D. A., Dong, H., Carroll, J., Plona, Z., Ding, H., Rodriguez, L., et al. (2017). Corticotropin-releasing factor overexpression gives rise to sex differences in Alzheimer's disease-related signaling. *Mol. Psychiatry* 22, 1126–1133. doi: 10.1038/mp.2016.185

Barron, A. M., and Pike, C. J. (2012). Sex hormones, aging, and Alzheimer's disease. *Front. Biosci.* 4, 976–997.

Bayless, D. W., Perez, M. C., and Daniel, J. M. (2015). Comparison of the validity of the use of the spontaneously hypertensive rat as a model of attention deficit hyperactivity disorder in males and females. *Behav. Brain Res.* 286, 85–92. doi: 10.1016/j.bbr.2015.02.029

Beninger, R. J., Tuerke, K. J., Forsyth, J. K., Giles, A., Xue, L., Boegman, R. J., et al. (2009). Neonatal ventral hippocampal lesions in male and female rats: effects on water maze, locomotor activity, plus-maze and prefrontal cortical GABA and glutamate release in adulthood. *Behav. Brain Res.* 202, 198–209. doi: 10.1016/j.bbr.2009.03.044

Berger, D. F., and Sagvolden, T. (1998). Sex differences in operant discrimination behaviour in an animal model of attention-deficit hyperactivity disorder. *Behav. Brain Res.* 94, 73–82. doi: 10.1016/S0166-4328(97)00171-X

Berman, R. M., Cappiello, A., Anand, A., Oren, D. A., Heninger, G. R., Charney, D. S., et al. (2000). Antidepressant effects of ketamine in depressed patients. *Biol. Psychiatry* 47, 351–354. doi: 10.1016/S0006-3223(99)00230-9

Binesh, N., Kumar, A., Hwang, S., Mintz, J., and Thomas, M. A. (2004). Neurochemistry of late-life major depression: a pilot two-dimensional MR spectroscopic study. *J. Magn. Reson. Imaging* 20, 1039–1045. doi: 10.1002/jmri.20214

Blázquez, G., Cañete, T., Tobeña, A., Giménez-Llort, L., and Fernández-Teruel, A. (2014). Cognitive and emotional profiles of aged Alzheimer's disease (3×TgAD) mice: effects of environmental enrichment and sexual dimorphism. *Behav. Brain Res.* 268, 185–201. doi: 10.1016/j.bbr.2014.04.008

Block, W., Traber, F., Von Widdern, O., Metten, M., Schild, H., Maier, W., et al. (2009). Proton MR spectroscopy of the hippocampus at 3 T in patients with unipolar major depressive disorder: correlates and predictors of treatment response. *Int. J. Neuropsychopharmacol.* 12, 415–422. doi: 10.1017/S1461145708009516

Bredewold, R., Schiavo, J. K., van Der Hart, M., Verreij, M., and Veenema, A. H. (2015). Dynamic changes in extracellular release of GABA and glutamate in the lateral septum during social play behavior in juvenile rats: implications for sex-specific regulation of social play behavior. *Neuroscience* 307, 117–127. doi: 10.1016/j.neuroscience.2015.08.052

Bucci, D. J., Hopkins, M. E., Keene, C. S., Sharma, M., and Orr, L. E. (2008). Sex differences in learning and inhibition in spontaneously hypertensive rats. *Behav. Brain Res.* 187, 27–32. doi: 10.1016/j.bbr.2007.08.022

Bychkov, E., Ahmed, M. R., and Gurevich, E. V. (2011). Sex differences in the activity of signalling pathways and expression of G-protein-coupled receptor kinases in the neonatal ventral hippocampal lesion model of schizophrenia. *Int. J. Neuropsychopharmacol.* 14, 1–15. doi: 10.1017/S1461145710000118

Cai, J., Ding, L., Zhang, J. S., Xue, J., and Wang, L. Z. (2016). Elevated plasma levels of glutamate in children with autism spectrum disorders. *Neuroreport* 27, 272–276. doi: 10.1097/WNR.0000000000000532

Canevelli, M., Quarata, F., Remiddi, F., Lucchini, F., Lacorte, E., Vanacore, N., et al. (2017). Sex and gender differences in the treatment of Alzheimer's disease: a systematic review of randomized controlled trials. *Pharmacol. Res.* 115, 218–223. doi: 10.1016/j.phrs.2016.11.035

Carrey, N., MacMaster, F. P., Fogel, J., Sparkes, S., Waschbusch, D., Sullivan, S., et al. (2003). Metabolite changes resulting from treatment in children with ADHD: a 1H-MRS study. *Clin. Neuropharmacol.* 26, 218–221. doi: 10.1097/00002826-200307000-00013

Carrier, N., and Kabbaj, M. (2013). Sex differences in the antidepressant-like effects of ketamine. *Neuropharmacology* 70, 27–34. doi: 10.1016/j.neuropharm.2012.12.009

Carroll, J. C., Rosario, E. R., Chang, L., Stanczyk, F. Z., Oddo, S., Laferla, F. M., et al. (2007). Progesterone and estrogen regulate Alzheimer-like neuropathology in female 3xTg-AD mice. *J. Neurosci.* 27, 13357–13365. doi: 10.1523/JNEUROSCI.2718-07.2007

Castle, D. J., Wessely, S., and Murray, R. M. (1993). Sex and schizophrenia: effects of diagnostic stringency, and associations with and premorbid variables. *Br. J. Psychiatry* 162, 658–664. doi: 10.1192/bjp.162.5.658

Célia Moreira Borella, V., Seeman, M. V., Carneiro Cordeiro, R., Vieira Dos Santos, J., Romario Matos de Souza, M., Nunes de Sousa Fernandes, E., et al. (2016). Gender and estrous cycle influences on behavioral and neurochemical alterations in adult rats neonatally administered ketamine. *Dev. Neurobiol.* 76, 519–532. doi: 10.1002/dneu.22329

Chambers, R. A., Moore, J., McEvoy, J. P., and Levin, E. D. (1996). Cognitive effects of neonatal hippocampal lesions in a rat model of schizophrenia. *Neuropsychopharmacology* 15, 587–594. doi: 10.1016/S0893-133X(96)00132-7

Chiu, P. W., Lui, S. S. Y., Hung, K. S. Y., Chan, R. C. K., Chan, Q., Sham, P. C., et al. (2018). *In vivo* gamma-aminobutyric acid and glutamate levels in people with first-episode schizophrenia: a proton magnetic resonance spectroscopy study. *Schizophr. Res.* 193, 295–303. doi: 10.1016/j.schres.2017.07.021

Choi, K. H., Zepp, M. E., Higgs, B. W., Weickert, C. S., and Webster, M. J. (2009). Expression profiles of schizophrenia susceptibility genes during human prefrontal cortical development. *J. Psychiatry Neurosci.* 34, 450–458.

Clinton, L. K., Billings, L. M., Green, K. N., Caccamo, A., Ngo, J., Oddo, S., et al. (2007). Age-dependent sexual dimorphism in cognition and stress response in the 3xTg-AD mice. *Neurobiol. Dis.* 28, 76–82. doi: 10.1016/j.nbd.2007.06.013

Counts, S. E., Che, S., Ginsberg, S. D., and Mufson, E. J. (2011). Gender differences in neurotrophin and glutamate receptor expression in cholinergic nucleus basalis neurons during the progression of Alzheimer's disease. *J. Chem. Neuroanat.* 42, 111–117. doi: 10.1016/j.jchemneu.2011.02.004

Coyle, J. T., Tsai, G., and Goff, D. C. (2002). Ionotropic glutamate receptors as therapeutic targets in schizophrenia. *Curr. Drug Targets CNS Neurol. Disord.* 1, 183–189. doi: 10.2174/1568007024606212

Cuffe, S. P., Moore, C. G., and McKeown, R. E. (2005). Prevalence and correlates of ADHD symptoms in the national health interview survey. *J. Atten. Disord.* 9, 392–401. doi: 10.1177/1087054705280413

Dell'Anna, M. E., Calzolari, S., Molinari, M., Iuvone, L., and Calimici, R. (1991). Neonatal anoxia induces transitory hyperactivity, permanent spatial memory deficits and CA1 cell density reduction in developing rats. *Behav. Brain Res.* 45, 125–134. doi: 10.1016/S0166-4328(05)80078-6

Dervola, K. S., Roberg, B. A., Woien, G., Bogen, I. L., Sandvik, T. H., Sagvolden, T., et al. (2012). Marine omicron-3 polyunsaturated fatty acids induce sex-specific changes in reinforcer-controlled behaviour and neurotransmitter metabolism in a spontaneously hypertensive rat model of ADHD. *Behav. Brain Funct.* 8:56. doi: 10.1186/1744-9081-8-56

Domingues, A., Almeida, S., da Cruz E Silva, E. F., Oliveira, C. R., and Rego, A. C. (2007). Toxicity of beta-amyloid in HEK293 cells expressing NR1/NR2A or NR1/NR2B N-methyl-D-aspartate receptor subunits. *Neurochem. Int.* 50, 872–880. doi: 10.1016/j.neuint.2007.03.001

Duarte, J. M., Do, K. Q., and Gruetter, R. (2014). Longitudinal neurochemical modifications in the aging mouse brain measured *in vivo* by 1H magnetic resonance spectroscopy. *Neurobiol. Aging* 35, 1660–1668. doi: 10.1016/j.neurobiolaging.2014.01.135

Elia, J., Glessner, J. T., Wang, K., Takahashi, N., Shtir, C. J., Hadley, D., et al. (2011). Genome-wide copy number variation study associates metabotropic glutamate receptor gene networks with attention deficit hyperactivity disorder. *Nat. Genet.* 44, 78–84. doi: 10.1038/ng.1013

Elsabbagh, M., Divan, G., Koh, Y. J., Kim, Y. S., Kauchali, S., Marcin, C., et al. (2012). Global prevalence of autism and other pervasive developmental disorders. *Autism Res.* 5, 160–179. doi: 10.1002/aur.239

Ende, G., Cackowski, S., van Eijk, J., Sack, M., Demirakca, T., Kleindienst, N., et al. (2016). Impulsivity and aggression in female BPD and ADHD patients: association with ACC glutamate and GABA concentrations. *Neuropsychopharmacology* 41, 410–418. doi: 10.1038/npp.2015.153

Ferreira, J. S., Papouin, T., Ladepeche, L., Yao, A., Langlais, V. C., Bouchet, D., et al. (2017). Co-agonists differentially tune GluN2B-NMDA receptor trafficking at hippocampal synapses. *Elife* 6:e25492. doi: 10.7554/eLife.25492

Flores, G., Barbeau, D., Quirion, R., and Srivastava, L. K. (1996). Decreased binding of dopamine D3 receptors in limbic subregions after neonatal bilateral lesion of rat hippocampus. *J. Neurosci.* 16, 2020–2026. doi: 10.1523/JNEUROSCI.16-06-02020.1996

Fombonne, E. (2005). The changing epidemiology of autism. *J. Appl. Res. Intell. Disabilit.* 18, 281–294. doi: 10.1111/j.1468-3148.2005.00266.x

Fombonne, E. (2009). Epidemiology of pervasive developmental disorders. *Pediatr. Res.* 65, 591–598. doi: 10.1203/PDR.0b013e31819e7203

Ford, T. C., and Crewther, D. P. (2016). A comprehensive review of the (1)H-MRS metabolite spectrum in autism spectrum disorder. *Front. Mol. Neurosci.* 9:14. doi: 10.3389/fnmol.2016.00014

Frankfurt, M., Fuchs, E., and Wuttke, W. (1984). Sex differences in gamma-aminobutyric acid and glutamate concentrations in discrete rat brain nuclei. *Neurosci. Lett.* 50, 245–250. doi: 10.1016/0304-3940(84)90493-2

Frye, C. A., Rhodes, M. E., and Dudek, B. (2005). Estradiol to aged female or male mice improves learning in inhibitory avoidance and water maze tasks. *Brain Res.* 1036, 101–108. doi: 10.1016/j.brainres.2004.12.014

Garcia-Garcia, A. L., Elizalde, N., Matrov, D., Harro, J., Wojcik, S. M., Venzala, E., et al. (2009). Increased vulnerability to depressive-like behavior of mice with decreased expression of VGLUT1. *Biol. Psychiatry* 66, 275–282. doi: 10.1016/j.biopsych.2009.02.027

Gerlai, R., Pisacane, P., and Erickson, S. (2000). Heregulin, but not ErbB2 or ErbB3, heterozygous mutant mice exhibit hyperactivity in multiple behavioral tasks. *Behav. Brain Res.* 109, 219–227. doi: 10.1016/S0166-4328(99)00175-8

Goff, D. C., and Coyle, J. T. (2001). The emerging role of glutamate in the pathophysiology and treatment of schizophrenia. *Am. J. Psychiatry* 158, 1367–1377. doi: 10.1176/appi.ajp.158.9.1367

Gogos, A., Kusljic, S., Thwaites, S. J., and van den Buuse, M. (2017). Sex differences in psychotomimetic-induced behaviours in rats. *Behav. Brain Res.* 322, 157–166. doi: 10.1016/j.bbr.2017.01.028

Gogos, A., Kwek, P., and van den Buuse, M. (2012). The role of estrogen and testosterone in female rats in behavioral models of relevance to schizophrenia. *Psychopharmacology* 219, 213–224. doi: 10.1007/s00213-011-2389-y

Gómez-Galán, M., de Bundel, D., van Eeckhaut, A., Smolders, I., and Lindskog, M. (2013). Dysfunctional astrocytic regulation of glutamate transmission in a rat model of depression. *Mol. Psychiatry* 18, 582–594. doi: 10.1038/mp.2012.10

Goto, Y., and O'Donnell, P. (2002). Delayed mesolimbic system alteration in a developmental animal model of schizophrenia. *J. Neurosci.* 22, 9070–9077. doi: 10.1523/JNEUROSCI.22-20-09070.2002

Grachev, I. D., and Apkarian, A. V. (2000). Chemical heterogeneity of the living human brain: a proton MR spectroscopy study on the effects of sex, age, and brain region. *Neuroimage* 11, 554–563. doi: 10.1006/nimg.2000.0557

Gray, A. L., Hyde, T. M., Deep-Soboslay, A., Kleinman, J. E., and Sodhi, M. S. (2015). Sex differences in glutamate receptor gene expression in major depression and suicide. *Mol. Psychiatry* 20, 1057–1068. doi: 10.1038/mp.2015.91

Grissom, N. M., McKee, S. E., Schoch, H., Bowman, N., Havekes, R., O'Brien, W. T., et al. (2018). Male-specific deficits in natural reward learning in a mouse model of neurodevelopmental disorders. *Mol. Psychiatry* 23, 544–555. doi: 10.1038/mp.2017.184

Hädel, S., Wirth, C., Rapp, M., Gallinat, J., and Schubert, F. (2013). Effects of age and sex on the concentrations of glutamate and glutamine in the human brain. *J. Magn. Reson. Imag.* 38, 1480–1487. doi: 10.1002/jmri.24123

Hanley, J. G. (2014). Subunit-specific trafficking mechanisms regulating the synaptic expression of Ca(2+)-permeable AMPA receptors. *Semin. Cell Dev. Biol.* 27, 14–22. doi: 10.1016/j.semcdb.2013.12.002

Haris, M., Nath, K., Cai, K., Singh, A., Crescenzi, R., Kogan, F., et al. (2013). Imaging of glutamate neurotransmitter alterations in Alzheimer's disease. *NMR Biomed.* 26, 386–391. doi: 10.1002/nbm.2875

Horder, J., Lavender, T., Mendez, M. A., O'Gorman, R., Daly, E., Craig, M. C., et al. (2013). Reduced subcortical glutamate/glutamine in adults with autism spectrum disorders: a [^{1}H]MRS study. *Transl. Psychiatry* 3:e279. doi: 10.1038/tp.2013.53

Howells, F. M., and Russell, V. A. (2008). Glutamate-stimulated release of norepinephrine in hippocampal slices of animal models of attention-deficit/hyperactivity disorder (spontaneously hypertensive rat) and depression/anxiety-like behaviours (Wistar-Kyoto rat). *Brain Res.* 1200, 107–115. doi: 10.1016/j.brainres.2008.01.033

Javitt, D. C. (2007). Glutamate and schizophrenia: phencyclidine, N-methyl-D-aspartate receptors, and dopamine-glutamate interactions. *Int. Rev. Neurobiol.* 78, 69–108. doi: 10.1016/S0074-7742(06)78003-5

Jiao, S. S., Bu, X. L., Liu, Y. H., Zhu, C., Wang, Q. H., Shen, L. L., et al. (2016). Sex dimorphism profile of Alzheimer's Disease-type pathologies in an APP/PS1 mouse model. *Neurotox. Res.* 29, 256–266. doi: 10.1007/s12640-015-9589-x

Karlsson, S. A., Haziri, K., Hansson, E., Kettunen, P., and Westberg, L. (2015). Effects of sex and gonadectomy on social investigation and social recognition in mice. *BMC Neurosci.* 16:83. doi: 10.1186/s12868-015-0221-z

Kim, J. I., Kim, J. W., Park, J. E., Park, S., Hong, S. B., Han, D. H., et al. (2016). Association of the GRIN2B rs2284411 polymorphism with methylphenidate response in attention-deficit/hyperactivity disorder. *J. Psychopharmacol.* 31, 1070–1077. doi: 10.1177/0269881116667707

Kim, K. C., Cho, K. S., Yang, S. M., Gonzales, E. L., Valencia, S., Eun, P. H., et al. (2017). Sex differences in autism-like behavioral phenotypes and postsynaptic receptors expression in the prefrontal cortex of TERT transgenic mice. *Biomol. Ther.* 25, 374–382. doi: 10.4062/biomolther.2016.242

Kim, K. C., Kim, P., Go, H. S., Choi, C. S., Park, J. H., Kim, H. J., et al. (2013). Male-specific alteration in excitatory post-synaptic development and social interaction in pre-natal valproic acid exposure model of autism spectrum disorder. *J. Neurochem.* 124, 832–843. doi: 10.1111/jnc.12147

King, D. L., Arendash, G. W., Crawford, F., Sterk, T., Menendez, J., and Mullan, M. J. (1999). Progressive and gender-dependent cognitive impairment in the APP(SW) transgenic mouse model for Alzheimer's disease. *Behav. Brain Res.* 103, 145–162. doi: 10.1016/S0166-4328(99)00037-6

Kokras, N., Antoniou, K., Polissidis, A., and Papadopoulou-Daifoti, Z. (2009). Antidepressants induce regionally discrete, sex-dependent changes in brain's glutamate content. *Neurosci. Lett.* 464, 98–102. doi: 10.1016/j.neulet.2009.08.011

Kokras, N., Pastromas, N., Papasava, D., de Bournonville, C., Cornil, C. A., and Dalla, C. (2018). Sex differences in behavioral and neurochemical effects of gonadectomy and aromatase inhibition in rats. *Psychoneuroendocrinology* 87, 93–107. doi: 10.1016/j.psyneuen.2017.10.007

Kornstein, S. G., Schatzberg, A. F., Yonkers, K. A., Thase, M. E., Keitner, G. I., Ryan, C. E., et al. (1995). Gender differences in presentation of chronic major depression. *Psychopharmacol. Bull.* 31, 711–718.

Kouchiwa, T., Wada, K., Uchiyama, M., Kasezawa, N., Niisato, M., Murakami, H., et al. (2012). Age-related changes in serum amino acids concentrations in healthy individuals. *Clin. Chem. Lab. Med.* 50, 861–870. doi: 10.1515/cclm-2011-0846

Kulak, A., Duarte, J. M., Do, K. Q., and Gruetter, R. (2010). Neurochemical profile of the developing mouse cortex determined by *in vivo* 1H NMR spectroscopy at 14.1 T and the effect of recurrent anaesthesia. *J. Neurochem.* 115, 1466–1477. doi: 10.1111/j.1471-4159.2010.07051.x

Kuwagata, M., and Nagao, T. (1998). Behavior and reproductive function of rat male offspring treated prenatally with 5-bromo-2'-deoxyuridine. *Reprod. Toxicol.* 12, 541–549. doi: 10.1016/S0890-6238(98)00037-9

Kuwagata, M., Muneoka, K. T., Ogawa, T., Takigawa, M., and Nagao, T. (2004). Locomotor hyperactivity following prenatal exposure to 5-bromo-2'-deoxyuridine: neurochemical and behavioral evidence of dopaminergic and serotonergic alterations. *Toxicol. Lett.* 152, 63–71. doi: 10.1016/j.toxlet.2004.03.019

Labrie, V., Wong, A. H., and Roder, J. C. (2012). Contributions of the D-serine pathway to schizophrenia. *Neuropharmacology* 62, 1484–1503. doi: 10.1016/j.neuropharm.2011.01.030

Lesch, K. P., Timmesfeld, N., Renner, T. J., Halperin, R., Roser, C., Nguyen, T. T., et al. (2008). Molecular genetics of adult ADHD: converging evidence from genome-wide association and extended pedigree linkage studies. *J. Neural Transm.* 115, 1573–1585. doi: 10.1007/s00702-008-0119-3

Leung, A., and Chue, P. (2000). Sex differences in schizophrenia, a review of the literature. *Acta Psychiatr. Scand. Suppl.* 401, 3–38. doi: 10.1111/j.0065-1591.2000.0ap25.x

Levin, E. D., and Christopher, N. C. (2006). Effects of clozapine on memory function in the rat neonatal hippocampal lesion model of schizophrenia. *Prog. Neuropsychopharmacol. Biol. Psychiatry* 30, 223–229. doi: 10.1016/j.pnpbp.2005.10.018

Li, C., Brake, W. G., Romeo, R. D., Dunlop, J. C., Gordon, M., Buzescu, R., et al. (2004). Estrogen alters hippocampal dendritic spine shape and enhances synaptic protein immunoreactivity and spatial memory in female mice. *Proc. Natl. Acad. Sci. U.S.A.* 101, 2185–2190. doi: 10.1073/pnas.0307313101

Li, T., Stefansson, H., Gudfinnsson, E., Cai, G., Liu, X., Murray, R. M., et al. (2004). Identification of a novel neuregulin 1 at-risk haplotype in Han schizophrenia Chinese patients, but no association with the Icelandic/Scottish risk haplotype. *Mol. Psychiatry* 9, 698–704. doi: 10.1038/sj.mp.4001485

Lipska, B. K., Jaskiw, G. E., and Weinberger, D. R. (1993). Postpubertal emergence of hyperresponsiveness to stress and to amphetamine after neonatal excitotoxic hippocampal damage: a potential animal model of schizophrenia. *Neuropsychopharmacology* 9, 67–75. doi: 10.1038/npp.1993.44

Locklear, M. N., Cohen, A. B., Jone, A., and Kritzer, M. F. (2016). Sex differences distinguish intracortical glutamate receptor-mediated regulation of extracellular dopamine levels in the prefrontal cortex of adult rats. *Cereb. Cortex* 26, 599–610. doi: 10.1093/cercor/bhu222

Logan, S. M., Sarkar, S. N., Zhang, Z., and Simpkins, J. W. (2011). Estrogen-induced signaling attenuates soluble Abeta peptide-mediated dysfunction of pathways in synaptic plasticity. *Brain Res.* 1383, 1–12. doi: 10.1016/j.brainres.2011.01.038

Luine, V. N., Beck, K. D., Bowman, R. E., Frankfurt, M., and Maclusky, N. J. (2007). Chronic stress and neural function: accounting for sex and age. *J. Neuroendocrinol.* 19, 743–751. doi: 10.1111/j.1365-2826.2007.01594.x

MacMaster, F. P., Carrey, N., Sparkes, S., and Kusumakar, V. (2003). Proton spectroscopy in medication-free pediatric attention-deficit/hyperactivity disorder. *Biol. Psychiatry* 53, 184–187. doi: 10.1016/S0006-3223(02)01401-4

Magri, C., Gardella, R., Valsecchi, P., Barlati, S. D., Guizzetti, L., Imperadori, L., et al. (2008). Study on GRIA2, GRIA3 and GRIA4 genes highlights a positive association between schizophrenia and GRIA3 in female patients. *Am. J. Med. Genet. B Neuropsychiatr. Genet.* 147B, 745–753. doi: 10.1002/ajmg.b.30674

Man, H. Y., Sekine-Aizawa, Y., and Huganir, R. L. (2007). Regulation of {alpha}-amino-3-hydroxy-5-methyl-4-isoxazolepropionic acid receptor trafficking through PKA phosphorylation of the Glu receptor 1 subunit. *Proc. Natl. Acad. Sci. U.S.A.* 104, 3579–3584. doi: 10.1073/pnas.0611698104

Markham, J. A. (2012). Sex steroids and schizophrenia. *Rev. Endocrine Metab. Disord.* 13, 187–207. doi: 10.1007/s11154-011-9184-2

Martins-de-Souza, D., Maccarrone, G., Wobrock, T., Zerr, I., Gormanns, P., Reckow, S., et al. (2010). Proteome analysis of the thalamus and cerebrospinal fluid reveals glycolysis dysfunction and potential biomarkers candidates for schizophrenia. *J. Psychiatr. Res.* 44, 1176–1189. doi: 10.1016/j.jpsychires.2010.04.014

Mattson, M. P., Cheng, B., Davis, D., Bryant, K., Lieberburg, I., and Rydel, R. E. (1992). beta-Amyloid peptides destabilize calcium homeostasis and render human cortical neurons vulnerable to excitotoxicity. *J. Neurosci.* 12, 376–389. doi: 10.1523/JNEUROSCI.12-02-00376.1992

McDougall, S. A., Moran, A. E., Baum, T. J., Apodaca, M. G., and Real, V. (2017). Effects of ketamine on the unconditioned and conditioned locomotor activity of preadolescent and adolescent rats: impact of age, sex, and drug dose. *Psychopharmacology* 234, 2683–2696. doi: 10.1007/s00213-017-4660-3

McEwen, A. M., Burgess, D. T., Hanstock, C. C., Seres, P., Khalili, P., Newman, S. C., et al. (2012). Increased glutamate levels in the medial prefrontal cortex in patients with postpartum depression. *Neuropsychopharmacology* 37, 2428–2435. doi: 10.1038/npp.2012.101

Melnikova, T., Park, D., Becker, L., Lee, D., Cho, E., Sayyida, N., et al. (2016). Sex-related dimorphism in dentate gyrus atrophy and behavioral phenotypes in an inducible tTa:APPsi transgenic model of Alzheimer's disease. *Neurobiol. Dis.* 96, 171–185. doi: 10.1016/j.nbd.2016.08.009

Ménard, C., Quirion, R., Vigneault, E., Bouchard, S., Ferland, G., El Mestikawy, S., et al. (2015). Glutamate presynaptic vesicular transporter and postsynaptic receptor levels correlate with spatial memory status in aging rat models. *Neurobiol. Aging* 36, 1471–1482. doi: 10.1016/j.neurobiolaging.2014.11.013

Mergy, M. A., Gowrishankar, R., Davis, G. L., Jessen, T. N., Wright, J., Stanwood, G. D., et al. (2014). Genetic targeting of the amphetamine and methylphenidate-sensitive dopamine transporter: on the path to an animal

model of attention-deficit hyperactivity disorder. *Neurochem. Int.* 73, 56–70. doi: 10.1016/j.neuint.2013.11.009

Michael, N., Erfurth, A., Ohrmann, P., Arolt, V., Heindel, W., and Pfleiderer, B. (2003a). Metabolic changes within the left dorsolateral prefrontal cortex occurring with electroconvulsive therapy in patients with treatment resistant unipolar depression. *Psychol. Med.* 33, 1277–1284. doi: 10.1017/S0033291703007931

Michael, N., Erfurth, A., Ohrmann, P., Arolt, V., Heindel, W., and Pfleiderer, B. (2003b). Neurotrophic effects of electroconvulsive therapy: a proton magnetic resonance study of the left amygdalar region in patients with treatment-resistant depression. *Neuropsychopharmacology* 28, 720–725. doi: 10.1038/sj.npp.1300085

Mick, E., Neale, B., Middleton, F. A., McGough, J. J., and Faraone, S. V. (2008). Genome-wide association study of response to methylphenidate in 187 children with attention-deficit/hyperactivity disorder. *Am. J. Med. Genet. B Neuropsychiatr. Genet.* 147B, 1412–1418. doi: 10.1002/ajmg.b.30865

Mielke, M. M., Vemuri, P., and Rocca, W. A. (2014). Clinical epidemiology of Alzheimer's disease: assessing sex and gender differences. *Clin. Epidemiol.* 6, 37–48. doi: 10.2147/CLEP.S37929

Miller, E. M., Pomerleau, F., Huettl, P., Gerhardt, G. A., and Glaser, P. E. (2014). Aberrant glutamate signaling in the prefrontal cortex and striatum of the spontaneously hypertensive rat model of attention-deficit/hyperactivity disorder. *Psychopharmacology* 231, 3019–3029. doi: 10.1007/s00213-014-3479-4

Milne, A., MacQueen, G. M., Yucel, K., Soreni, N., and Hall, G. B. (2009). Hippocampal metabolic abnormalities at first onset and with recurrent episodes of a major depressive disorder: a proton magnetic resonance spectroscopy study. *Neuroimage* 47, 36–41. doi: 10.1016/j.neuroimage.2009.03.031

Moghaddam, B., and Jackson, M. E. (2003). Glutamatergic animal models of schizophrenia. *Ann. N.Y. Acad. Sci.* 1003, 131–137. doi: 10.1196/annals.1300.065

Monfort, P., Gomez-Gimenez, B., Llansola, M., and Felipo, V. (2015). Gender differences in spatial learning, synaptic activity, and long-term potentiation in the hippocampus in rats: molecular mechanisms. *ACS Chem. Neurosci.* 6, 1420–1427. doi: 10.1021/acschemneuro.5b00096

Netser, S., Haskal, S., Magalnik, H., and Wagner, S. (2017). A novel system for tracking social preference dynamics in mice reveals sex- and strain-specific characteristics. *Mol. Autism* 8:53. doi: 10.1186/s13229-017-0169-1

Nilsen, L. H., Melø, T. M., Witter, M. P., and Sonnewald, U. (2014). Early differences in dorsal hippocampal metabolite levels in males but not females in a transgenic rat model of Alzheimer's disease. *Neurochem. Res.* 39, 305–312. doi: 10.1007/s11064-013-1222-x

Noble, R. E. (2005). Depression in women. *Metab. Clin. Exp.* 54, 49–52. doi: 10.1016/j.metabol.2005.01.014

Nozari, M., Shabani, M., Farhangi, A. M., Mazhari, S., and Atapour, N. (2015). Sex-specific restoration of MK-801-induced sensorimotor gating deficit by environmental enrichment. *Neuroscience* 299, 28–34. doi: 10.1016/j.neuroscience.2015.04.050

Nudmamud-Thanoi, S., and Reynolds, G. P. (2004). The NR1 subunit of the glutamate/NMDA receptor in the superior temporal cortex in schizophrenia and affective disorders. *Neurosci. Lett.* 372, 173–177. doi: 10.1016/j.neulet.2004.09.035

Olney, J. W., and Farber, N. B. (1995). Glutamate receptor dysfunction and schizophrenia. *Arch. Gen. Psychiatry* 52, 998–1007. doi: 10.1001/archpsyc.1995.03950240016004

Ordóñez-Gutiérrez, L., Antón, M., and Wandosell, F. (2015). Peripheral amyloid levels present gender differences associated with aging in AβPP/PS1 mice. *J. Alzheimers. Dis.* 44, 1063–1068. doi: 10.3233/JAD-141158

O'Tuathaigh, C. M., O'Sullivan, G. J., Kinsella, A., Harvey, R. P., Tighe, O., Croke, D. T., et al. (2006). Sexually dimorphic changes in the exploratory and habituation profiles of heterozygous neuregulin-1 knockout mice. *Neuroreport* 17, 79–83. doi: 10.1097/01.wnr.0000192738.31029.0a

Paoletti, P., Bellone, C., and Zhou, Q. (2013). NMDA receptor subunit diversity: impact on receptor properties, synaptic plasticity and disease. *Nat. Rev. Neurosci.* 14, 383–400. doi: 10.1038/nrn3504

Pappas, B. A., Gallivan, J. V., Dugas, T., Saari, M., and Ings, R. (1980). Intraventricular 6-hydroxydopamine in the newborn rat and locomotor responses to drugs in infancy: no support for the dopamine depletion model of minimal brain dysfunction. *Psychopharmacology* 70, 41–46. doi: 10.1007/BF00432368

Pei, J. C., Liu, C. M., and Lai, W. S. (2014). Distinct phenotypes of new transmembrane-domain neuregulin 1 mutant mice and the rescue effects of valproate on the observed schizophrenia-related cognitive deficits. *Front. Behav. Neurosci.* 8:126. doi: 10.3389/fnbeh.2014.00126

Pozzi, L., Baviera, M., Sacchetti, G., Calcagno, E., Balducci, C., Invernizzi, R. W., et al. (2011). Attention deficit induced by blockade of N-methyl D-aspartate receptors in the prefrontal cortex is associated with enhanced glutamate release and cAMP response element binding protein phosphorylation: role of metabotropic glutamate receptors 2/3. *Neuroscience* 176, 336–348. doi: 10.1016/j.neuroscience.2010.11.060

Price, R. B., Shungu, D. C., Mao, X., Nestadt, P., Kelly, C., Collins, K. A., et al. (2009). Amino acid neurotransmitters assessed by proton magnetic resonance spectroscopy: relationship to treatment resistance in major depressive disorder. *Biol. Psychiatry* 65, 792–800. doi: 10.1016/j.biopsych.2008.10.025

Procaccini, C., Maksimovic, M., Aitta-Aho, T., Korpi, E. R., and Linden, A. M. (2013). Reversal of novelty-induced hyperlocomotion and hippocampal c-Fos expression in GluA1 knockout male mice by the mGluR2/3 agonist LY354740. *Neuroscience* 250, 189–200. doi: 10.1016/j.neuroscience.2013.07.010

Reisberg, B., Doody, R., Stoffler, A., Schmitt, F., Ferris, S., Mobius, H. J., et al. (2003). Memantine in moderate-to-severe Alzheimer's disease. *N. Engl. J. Med.* 348, 1333–1341. doi: 10.1056/NEJMoa013128

Row, B. W., Kheirandish, L., Neville, J. J., and Gozal, D. (2002). Impaired spatial learning and hyperactivity in developing rats exposed to intermittent hypoxia. *Pediatr. Res.* 52, 449–453. doi: 10.1203/00006450-200209000-00024

Sailasuta, N., Ernst, T., and Chang, L. (2008). Regional variations and the effects of age and gender on glutamate concentrations in the human brain. *Magn. Reson. Imaging* 26, 667–675. doi: 10.1016/j.mri.2007.06.007

Sakata, M., Toyohara, J., Ishibashi, K., Wagatsuma, K., Ishii, K., Zhang, M. R., et al. (2017). Age and gender effects of (11)C-ITMM binding to metabotropic glutamate receptor type 1 in healthy human participants. *Neurobiol. Aging* 55, 72–77. doi: 10.1016/j.neurobiolaging.2017.03.022

Sanz-Clemente, A., Nicoll, R. A., and Roche, K. W. (2013). Diversity in NMDA receptor composition: many regulators, many consequences. *Neuroscientist* 19, 62–75. doi: 10.1177/1073858411435129

Schaafsma, S. M., Gagnidze, K., Reyes, A., Norstedt, N., Mansson, K., Francis, K., et al. (2017). Sex-specific gene-environment interactions underlying ASD-like behaviors. *Proc. Natl. Acad. Sci. U.S.A.* 114, 1383–1388. doi: 10.1073/pnas.1619312114

Scholtzova, H., Wadghiri, Y. Z., Douadi, M., Sigurdsson, E. M., Li, Y. S., Quartermain, D., et al. (2008). Memantine leads to behavioral improvement and amyloid reduction in Alzheimer's-disease-model transgenic mice shown as by micromagnetic resonance imaging. *J. Neurosci. Res.* 86, 2784–2791. doi: 10.1002/jnr.21713

Scott-Van Zeeland, A. A., Dapretto, M., Ghahremani, D. G., Poldrack, R. A., and Bookheimer, S. Y. (2010). Reward processing in autism. *Autism Res.* 3, 53–67. doi: 10.1002/aur.122

Shaywitz, B. A., Gordon, J. W., Klopper, J. H., and Zelterman, D. A. (1977). The effect of 6-hydroxydopamine on habituation of activity in the developing rat pup. *Pharmacol. Biochem. Behav.* 6, 391–396. doi: 10.1016/0091-3057(77)90175-7

Shaywitz, B. A., Yager, R. D., and Klopper, J. H. (1976). Selective brain dopamine depletion in developing rats: an experimental model of minimal brain dysfunction. *Science* 191, 305–308. doi: 10.1126/science.942800

Sheikh-Bahaei, N., Sajjadi, S. A., Manavaki, R., McLean, M., O'Brien, J. T., and Gillard, J. H. (2018). Positron emission tomography-guided magnetic resonance spectroscopy in Alzheimer disease. *Ann. Neurol.* 83, 771–778. doi: 10.1002/ana.25202

Shimmura, C., Suda, S., Tsuchiya, K. J., Hashimoto, K., Ohno, K., Matsuzaki, H., et al. (2011). Alteration of plasma glutamate and glutamine levels in children with high-functioning autism. *PLoS ONE* 6:e25340. doi: 10.1371/journal.pone.0025340

Shors, T. J., Falduto, J., and Leuner, B. (2004). The opposite effects of stress on dendritic spines in male vs. female rats are NMDA receptor-dependent. *Eur. J. Neurosci.* 19, 145–150. doi: 10.1046/j.1460-9568.2003.03065.x

Shulman, Y., Grant, S., Seres, P., Hanstock, C., Baker, G., and Tibbo, P. (2006). The relation between peripheral and central glutamate and glutamine in healthy male volunteers. *J. Psychiatry Neurosci.* 31, 406–410.

Smejkalova, T., and Woolley, C. S. (2010). Estradiol acutely potentiates hippocampal excitatory synaptic transmission

through a presynaptic mechanism. *J. Neurosci.* 30, 16137–16148. doi: 10.1523/JNEUROSCI.4161-10.2010

Smith, S. E., Zhou, Y. D., Zhang, G., Jin, Z., Stoppel, D. C., and Anderson, M. P. (2011). Increased gene dosage of Ube3a results in autism traits and decreased glutamate synaptic transmission in mice. *Sci. Transl. Med.* 3:103ra197. doi: 10.1126/scitranslmed.3002627

Sokolow, S., Luu, S. H., Nandy, K., Miller, C. A., Vinters, H. V., Poon, W. W., et al. (2012). Preferential accumulation of amyloid-beta in presynaptic glutamatergic terminals (VGluT1 and VGluT2) in Alzheimer's disease cortex. *Neurobiol. Dis.* 45, 381–387. doi: 10.1016/j.nbd.2011.08.027

Stefani, M. R., and Moghaddam, B. (2005). Transient N-methyl-D-aspartate receptor blockade in early development causes lasting cognitive deficits relevant to schizophrenia. *Biol. Psychiatry* 57, 433–436. doi: 10.1016/j.biopsych.2004.11.031

Stefansson, H., Sarginson, J., Kong, A., Yates, P., Steinthorsdottir, V., Gudfinnsson, E., et al. (2003). Association of neuregulin 1 with schizophrenia confirmed in a Scottish population. *Am. J. Hum. Genet.* 72, 83–87. doi: 10.1086/345442

Stefansson, H., Sigurdsson, E., Steinthorsdottir, V., Bjornsdottir, S., Sigmundsson, T., Ghosh, S., et al. (2002). Neuregulin 1 and susceptibility to schizophrenia. *Am. J. Hum. Genet.* 71, 877–892. doi: 10.1086/342734

Stefansson, H., Steinthorsdottir, V., Thorgeirsson, T. E., Gulcher, J. R., and Stefansson, K. (2004). Neuregulin 1 and schizophrenia. *Ann. Med.* 36, 62–71. doi: 10.1080/07853890310017585

Sterley, T. L., Howells, F. M., Dimatelis, J. J., and Russell, V. A. (2016). Genetic predisposition and early life experience interact to determine glutamate transporter (GLT1) and solute carrier family 12 member 5 (KCC2) levels in rat hippocampus. *Metab. Brain Dis.* 31, 169–182. doi: 10.1007/s11011-015-9742-5

Stover, J. F., and Kempski, O. S. (2005). Anesthesia increases circulating glutamate in neurosurgical patients. *Acta Neurochir.* 147, 847–853. doi: 10.1007/s00701-005-0562-y

Swerdlow, N. R., and Geyer, M. A. (1998). Using an animal model of deficient sensorimotor gating to study the pathophysiology and new treatments of schizophrenia. *Schizophr. Bull.* 24, 285–301. doi: 10.1093/oxfordjournals.schbul.a033326

Tayoshi, S., Sumitani, S., Taniguchi, K., Shibuya-Tayoshi, S., Numata, S., Iga, J., et al. (2009). Metabolite changes and gender differences in schizophrenia using 3-Tesla proton magnetic resonance spectroscopy (1H-MRS). *Schizophr. Res.* 108, 69–77. doi: 10.1016/j.schres.2008.11.014

Tebartz van Elst, L., Maier, S., Fangmeier, T., Endres, D., Mueller, G. T., Nickel, K., et al. (2014). Disturbed cingulate glutamate metabolism in adults with high-functioning autism spectrum disorder: evidence in support of the excitatory/inhibitory imbalance hypothesis. *Mol. Psychiatry* 19, 1314–1325. doi: 10.1038/mp.2014.62

Teichberg, V. I., Cohen-Kashi-Malina, K., Cooper, I., and Zlotnik, A. (2009). Homeostasis of glutamate in brain fluids: an accelerated brain-to-blood efflux of excess glutamate is produced by blood glutamate scavenging and offers protection from neuropathologies. *Neuroscience* 158, 301–308. doi: 10.1016/j.neuroscience.2008.02.075

Tordera, R. M., Garcia-Garcia, A. L., Elizalde, N., Segura, V., Aso, E., Venzala, E., et al. (2011). Chronic stress and impaired glutamate function elicit a depressive-like phenotype and common changes in gene expression in the mouse frontal cortex. *Eur. Neuropsychopharmacol.* 21, 23–32. doi: 10.1016/j.euroneuro.2010.06.016

Tsai, G., and Coyle, J. T. (2002). Glutamatergic mechanisms in schizophrenia. *Annu. Rev. Pharmacol. Toxicol.* 42, 165–179. doi: 10.1146/annurev.pharmtox.42.082701.160735

Turic, D., Langley, K., Mills, S., Stephens, M., Lawson, D., Govan, C., et al. (2004). Follow-up of genetic linkage findings on chromosome 16p13: evidence of association of N-methyl-D aspartate glutamate receptor 2A gene polymorphism with ADHD. *Mol. Psychiatry* 9, 169–173. doi: 10.1038/sj.mp.4001387

Turic, D., Langley, K., Williams, H., Norton, N., Williams, N. M., Moskvina, V., et al. (2005). A family based study implicates solute carrier family 1-member 3 (SLC1A3) gene in attention-deficit/hyperactivity disorder. *Biol. Psychiatry* 57, 1461–1466. doi: 10.1016/j.biopsych.2005.03.025

Uezato, A., Kimura-Sato, J., Yamamoto, N., Iijima, Y., Kunugi, H., and Nishikawa, T. (2012). Further evidence for a male-selective genetic association of synapse-associated protein 97 (SAP97) gene with schizophrenia. *Behav. Brain Funct.* 8:2. doi: 10.1186/1744-9081-8-2

van den Buuse, M., Low, J. K., Kwek, P., Martin, S., and Gogos, A. (2017). Selective enhancement of NMDA receptor-mediated locomotor hyperactivity by male sex hormones in mice. *Psychopharmacology* 234, 2727–2735. doi: 10.1007/s00213-017-4668-8

Wang, Y., Ma, Y., Hu, J., Cheng, W., Jiang, H., Zhang, X., et al. (2015). Prenatal chronic mild stress induces depression-like behavior and sex-specific changes in regional glutamate receptor expression patterns in adult rats. *Neuroscience* 301, 363–374. doi: 10.1016/j.neuroscience.2015.06.008

Wei, J., Yuen, E. Y., Liu, W., Li, X., Zhong, P., Karatsoreos, I. N., et al. (2014). Estrogen protects against the detrimental effects of repeated stress on glutamatergic transmission and cognition. *Mol. Psychiatry* 19, 588–598. doi: 10.1038/mp.2013.83

Weiss, L. A., Shen, Y., Korn, J. M., Arking, D. E., Miller, D. T., Fossdal, R., et al. (2008). Association between microdeletion and microduplication at 16p11.2 and autism. *N. Engl. J. Med.* 358, 667–675. doi: 10.1056/NEJMoa075974

Winblad, B., Jones, R. W., Wirth, Y., Stoffler, A., and Mobius, H. J. (2007). Memantine in moderate to severe Alzheimer's disease: a meta-analysis of randomised clinical trials. *Dement. Geriatr. Cogn. Disord.* 24, 20–27. doi: 10.1159/000102568

Won, H., Lee, H. R., Gee, H. Y., Mah, W., Kim, J. I., Lee, J., et al. (2012). Autistic-like social behaviour in Shank2-mutant mice improved by restoring NMDA receptor function. *Nature* 486, 261–265. doi: 10.1038/nature11208

Woolley, C. S., Gould, E., Frankfurt, M., and McEwen, B. S. (1990). Naturally occurring fluctuation in dendritic spine density on adult hippocampal pyramidal neurons. *J. Neurosci.* 10, 4035–4039. doi: 10.1523/JNEUROSCI.10-12-04035.1990

Wozniak, D. F., Dikranian, K., Ishimaru, M. J., Nardi, A., Corso, T. D., Tenkova, T., et al. (1998). Disseminated corticolimbic neuronal degeneration induced in rat brain by MK-801: potential relevance to Alzheimer's disease. *Neurobiol. Dis.* 5, 305–322. doi: 10.1006/nbdi.1998.0206

Wyllie, D. J., Livesey, M. R., and Hardingham, G. E. (2013). Influence of GluN2 subunit identity on NMDA receptor function. *Neuropharmacology* 74, 4–17. doi: 10.1016/j.neuropharm.2013.01.016

Yang, M., Bozdagi, O., Scattoni, M. L., Wohr, M., Roullet, F. I., Katz, A. M., et al. (2012). Reduced excitatory neurotransmission and mild autism-relevant phenotypes in adolescent Shank3 null mutant mice. *J. Neurosci.* 32, 6525–6541. doi: 10.1523/JNEUROSCI.6107-11.2012

Zahr, N. M., Mayer, D., Rohlfing, T., Chanraud, S., Gu, M., Sullivan, E. V., et al. (2013). *In vivo* glutamate measured with magnetic resonance spectroscopy: behavioral correlates in aging. *Neurobiol. Aging* 34, 1265–1276. doi: 10.1016/j.neurobiolaging.2012.09.014

Zhang, J., Li, Y., Xu, J., and Yang, Z. (2014). The role of N-methyl-D-aspartate receptor in Alzheimer's disease. *J. Neurol. Sci.* 339, 123–129. doi: 10.1016/j.jns.2014.01.041

Zhang, N., Zhong, P., Shin, S. M., Metallo, J., Danielson, E., Olsen, C. M., et al. (2015). S-SCAM, a rare copy number variation gene, induces schizophrenia-related endophenotypes in transgenic mouse model. *J. Neurosci.* 35, 1892–1904. doi: 10.1523/JNEUROSCI.3658-14.2015

Zhang, X., Li, Q., Wong, N., Zhang, M., Wang, W., Bu, B., et al. (2015). Behaviour and prefrontal protein differences in C57BL/6N and 129 X1/SvJ mice. *Brain Res. Bull.* 116, 16–24. doi: 10.1016/j.brainresbull.2015.05.003

Zlotnik, A., Ohayon, S., Gruenbaum, B. F., Gruenbaum, S. E., Mohar, B., Boyko, M., et al. (2011). Determination of factors affecting glutamate concentrations in the whole blood of healthy human volunteers. *J. Neurosurg. Anesthesiol.* 23, 45–49. doi: 10.1097/ANA.0b013e3181f82a8f

Conflict of Interest Statement: The authors declare that the research was conducted in the absence of any commercial or financial relationships that could be construed as a potential conflict of interest.

frontiers in Molecular Neuroscience

ORIGINAL RESEARCH
published: 19 June 2018
doi: 10.3389/fnmol.2018.00214

Endocannabinoid Signaling at Hypothalamic Steroidogenic Factor-1/Proopiomelanocortin Synapses Is Sex- and Diet-Sensitive

*Carolina Fabelo[1], Jennifer Hernandez[2], Rachel Chang[2], Sakara Seng[1], Natalia Alicea[3], Sharon Tian[1], Kristie Conde[1] and Edward J. Wagner[1,2]**

[1]Department of Basic Medical Sciences, College of Osteopathic Medicine, Western University of Health Sciences, Pomona, CA, United States, [2]Graduate College of Biomedical Sciences, Western University of Health Sciences, Pomona, CA, United States, [3]College of Veterinary Medicine, Western University of Health Sciences, Pomona, CA, United States

We tested the hypotheses that steroidogenic factor (SF)-1 neurons in the hypothalamic ventromedial nucleus (VMN) provide sexually disparate, endocannabinoid (EC)- and diet-sensitive glutamatergic input onto proopiomelanocortin (POMC) neurons. Electrophysiological recordings were performed in hypothalamic slices from intact and castrated guinea pigs, along with *in vitro* optogenetic experiments in intact male as well as cycling and ovariectomized female NR5A1-Cre mice. In slices from castrated male and female guinea pigs, depolarized-induced suppression of excitation (DSE) time-dependently reduced the amplitude of evoked excitatory postsynaptic currents (eEPSCs) in POMC neurons generated by electrically stimulating the dorsomedial VMN. Androgen stimulation rapidly enhanced this DSE, which was also found in insulin-resistant, high-fat diet (HFD)-fed males. By contrast, retrograde signaling at VMN/ARC POMC synapses was markedly attenuated in periovulatory females. HFD potentiated central cannabinoid-induced hyperphagia in both males and females, but exerted differential influences on cannabinoid-induced increases in energy expenditure. In NR5A1-Cre mice, the reduction in light-evoked EPSC amplitude caused by postsynaptic depolarization in cycling females was modest in comparison to that seen in intact males. Estradiol attenuated the DSE in light-evoked EPSC amplitude in slices from ovariectomized females. Moreover, the retrograde inhibition of transmission was further accentuated in HFD-fed males. Chemogenetic activation of SF-1 neurons suppressed appetite and increased energy expenditure in males, effects which were attenuated by HFD. Conversely, energy expenditure was increased in estradiol- but not vehicle-treated ovariectomized females. Together with our previous studies indicating that DSE in POMC neurons is EC-mediated, these findings indicate that VMN SF-1/ARC POMC synapses represent a sexually differentiated, EC- and diet-sensitive anorexigenic component within the hypothalamic energy balance circuitry.

Keywords: endocannabinoids, obesity, steroidogenic factor-1, sex differences, estradiol, proopiomelanocortin, testosterone, insulin

OPEN ACCESS

Edited by:
Laura Musazzi,
Università degli Studi di Milano, Italy

Reviewed by:
Michiru Hirasawa,
Memorial University of Newfoundland, Canada
Marco Koch,
Leipzig University, Germany

****Correspondence:***
Edward J. Wagner
ewagner@westernu.edu

Received: *31 March 2018*
Accepted: *30 May 2018*
Published: *19 June 2018*

Citation:
Fabelo C, Hernandez J, Chang R, Seng S, Alicea N, Tian S, Conde K and Wagner EJ (2018) Endocannabinoid Signaling at Hypothalamic Steroidogenic Factor-1/Proopiomelanocortin Synapses Is Sex- and Diet-Sensitive. Front. Mol. Neurosci. 11:214. doi: 10.3389/fnmol.2018.00214

INTRODUCTION

Energy balance is regulated through interactions between the gastrointestinal tract (GI), brainstem and the hypothalamus. The hypothalamic energy balance circuity comprises the arcuate nucleus (ARC), ventromedial nucleus (VMN), lateral hypothalamus (LH), dorsomedial nucleus (DMN) and paraventricular nucleus (PVN) (Berthoud, 2012; Wilson and Enriori, 2015). The ARC is a critical mediator within this energy balance circuitry due to the precise location near the third ventricle in close contact to the median eminence (Belgardt et al., 2009). This allows the ARC to serve as a sensor of global energy homeostatic status of an organism (Belgardt et al., 2009; Berthoud, 2012; Wilson and Enriori, 2015).

Proopiomelanocortin (POMC)/cocaine amphetamine-regulated transcript (CART) neurons in the ARC are an critical anorexigenic component of the hypothalamic energy balance circuitry. The excitability of POMC neurons varies in direct proportion to the ambient glucose concentration (Ibrahim et al., 2003; Claret et al., 2007; Parton et al., 2007), and peripheral hormones such as insulin and leptin are known to influence the mRNA expression and excitability of POMC neurons (Belgardt et al., 2009). Insulin works through the mediobasal hypothalamus to increase lipogenesis and decrease lipolysis in white adipose tissue (Scherer et al., 2011). Leptin is secreted by adipocytes and circulating concentrations will increase with the accumulation of fat (Belgardt et al., 2009; Wilson and Enriori, 2015). Rodents and humans lacking leptin or a functional leptin receptor are immensely obese and hyperglycemic (Chua et al., 1996; Clément et al., 1998; Belgardt et al., 2009), while mice lacking the insulin receptor display a more mild obese phenotype (Brüning et al., 2000). Both leptin and insulin will depolarize POMC neurons via activation of transient receptor potential (TRP)C5 channels, which occurs through insulin and leptin receptor-mediated activation of phosphatidylinositol-3-kinase (PI3K) and leads to increased firing of POMC neurons (Cowley et al., 2003; Qiu et al., 2010, 2014). Leptin and insulin also modulate POMC neuronal firing by presynaptic action on neuropeptide Y (NPY)/agouti-related protein (AgRP) neurons, which will inhibit the release of gamma-amino butyric acid (GABA) from terminals impinging onto POMC neurons (Vong et al., 2011).

POMC neurons receive robust glutamatergic input from the dorsomedial portion of the VMN (Sternson et al., 2005; Krashes et al., 2014). A likely source of this glutamatergic input is from the population of steroidogenic factor (SF)-1 neurons emanating from that dorsomedial region of the VMN that project to the ARC and synapse onto POMC neurons (Lindberg et al., 2013; Cardinal et al., 2014). These neurons are exclusively found in the VMN (Majdic et al., 2002), express leptin, insulin and cannabinoid CB1 receptors, and when these cells are activated they suppress appetite and increase energy expenditure (Dhillon et al., 2006; Klöckener et al., 2011; Cardinal et al., 2014). These inputs are clearly part of what makes the VMN such an important anorexigenic component of the hypothalamic energy balance circuitry, and studies have shown that upon VMN lesion, hyperphagia and obesity occurs (Stricker, 1978).

The endocannabinoid system (ECS) exerts notable effects on energy homeostasis. Several studies have shown that a blockade of the CB1 receptor leads to a suppression of food intake, and central administration of CB1 receptor agonists increase food intake (Jamshidi and Taylor, 2001; Ravinet-Trillou et al., 2003; Verty et al., 2005). The two main endocannabinoids (ECs) are N-arachidonoylethanolamine (AEA) and 2-arachidonylglycerol (2-AG). Among the two, 2-AG is considered to be the most sensitive to changes induced by fasting and feeding in the hypothalamus (Di Marzo et al., 2001; Kirkham et al., 2002), although AEA but not 2-AG levels are elevated by fasting in the olfactory bulb (Soria-Gómez et al., 2014). ECs are known as retrograde messengers, and engage in a form of plasticity that occurs at glutamatergic and GABAergic synapses known as depolarization-induced suppression of excitation (DSE) or inhibition (DSI), respectively (Freund et al., 2003). For example, ECs retrogradely inhibit glutamatergic input onto POMC neurons in the ARC, and GABAergic transmission at melanin-concentrating hormone synapses in the LH (Jo et al., 2005; Borgquist et al., 2015a). EC levels are also influenced by anorexigenic/orexigenic factors such as leptin and ghrelin, respectively (Di Marzo et al., 2001; Kola et al., 2008). In addition, EC signaling is altered by obesity and type II diabetes, and may involve elevated EC tone (Di Marzo et al., 2001; Kim et al., 2013).

Many of the biological processes regulated by cannabinoids are sexually differentiated (Wagner, 2016). Our previous studies have shown that cannabinoid-induced hyperphagia and hypothermia is sexually disparate, with males being more sensitive than females (Diaz et al., 2009). Moreover, estradiol rapidly and markedly attenuates cannabinoid-induced hyperphagia in ovariectomized guinea pigs. It also decreases the magnitude and duration of the cannabinoid-induced hypothermia. These actions can be attributed, at least in part, to diminished cannabinoid-induced presynaptic inhibition of glutamatergic input onto POMC neurons (Kellert et al., 2009). The manner in which estradiol rapidly attenuates cannabinoid-induced presynaptic inhibition of excitatory input onto POMC neurons is due to activation of estrogen receptor subtype (ER)α and the G_q-coupled membrane ER (mER) (Washburn et al., 2013). This attenuating effect of estradiol is due to signaling through two parallel pathways in POMC neurons: one involving protein kinase A and protein kinase C elicited following activation of the Gq-coupled mER, and another pathway involving PI3K and neuronal nitric oxide synthase (nNOS) elicited following activation of ERα. Moreover, estradiol down-regulates CB1 receptors in the hypothalamus (Washburn et al., 2013; Borgquist et al., 2015a; Mela et al., 2016).

By contrast, testosterone replacement in orchidectomized male guinea pigs increases energy intake, which is blocked by the CB1 receptor antagonist, AM251 (Borgquist et al., 2015b). Additionally, testosterone increases inhibitory GABAergic input onto POMC neurons as well as potentiates the EC-mediated retrograde inhibition of spontaneous excitatory postsynaptic current (EPSC) frequency and amplitude via DSE (Borgquist et al., 2015b). This potentiating effect of testosterone is blocked

by the AMPK inhibitor compound C (Borgquist et al., 2015b), which indicates that AMPK plays an important role to the androgenic regulation of EC tone and energy homeostasis. Thus, the activational effects of gonadal hormones differentially modulate EC-mediated inhibition of excitatory input onto POMC neurons, which accounts, at least in part, for the prominent sex differences in the cannabinoid regulation of energy homeostasis. The question arises: from where does this EC-sensitive input originate? As mentioned above, there are several compelling reasons to think that SF-1 neurons in the dorsomedial VMN are a likely source. Therefore, we hypothesized that SF-1 neurons innervate ARC/POMC neurons and provide a source of sexually disparate, EC- and diet-sensitive glutamatergic input onto POMC neurons that serves as the basis for sex differences in the cannabinoid regulation for energy homeostasis.

MATERIALS AND METHODS

Animal Models

Adult male and female Topeka guinea pigs (337–785 g; 35–103 days of age) were either purchased from Elm Hill Breeding Labs (Clemsford, MA, USA) or bred in-house. Intact female guinea pigs were checked daily through two consecutive estrous cycles to identify the period of genital swelling and vaginal opening. This was done to ensure that we performed the electrophysiological and behavioral testing during the periovulatory phase. Male and female NR5A1-Cre mice (18–43 g; 52–144 days of age) were generously provided by Drs. William Krause and Holly Ingraham at the University of California, San Francisco, CA, USA. Intact female NR5A1-Cre mice were checked the day of experimentation by vaginal lavage to evaluate cell cytology to determine the stage of the estrous cycle. Animals were housed under a 12:12 h light/dark cycle, with food and water available *ad libitum*. All procedures were approved by the Western University of Health Sciences' IACUC in accordance with institutional guidelines based on NIH standards.

Diet

Guinea pigs were subdivided and fed either a standard chow (Teklad Global Guinea Pig Diet, Madison, WI, USA), from which 12% of the calories were derived from fat, 31% from protein and 57% from carbohydrates or a "Westernized" high-fat diet (HFD; Newco Distributors Inc., CA, USA), from which 46% of the calories were derived from fat, 18% from protein and 36% from carbohydrates.

NR5A1-Cre mice were similarly subdivided and given continuous access to either a standard rodent chow (Teklad Rodent Diet, Teklad Diets, Madison, WI, USA) from which 18% of the calories were derived from fat, 24% from protein, and 58% from carbohydrates, or a high-fat diet (HFD; Research Diets, New Brunswick, NJ, USA) from which 45% of calories were derived from fat, 20% from protein and 35% from carbohydrates. All animals were kept on their respective diets for a minimum of 5 weeks prior to experimentation.

Surgical Procedures

For some experiments, male guinea pigs were orchidectomized while they were under ketamine/xylazine (87.5 mg/kg and 12.5 mg/kg, respectively; s.c.) anesthesia maintained with 1.5%–2% isoflurane. For other experiments, NR5A1-Cre female mice were ovariectomized while they were under 2% isoflurane anesthesia.

The stereotaxic implantation of a guide cannula into the third ventricle of the guinea pig was performed as previously described (Borgquist et al., 2015a). Briefly, once anesthetized under ketamine/xylazine (87.5 mg/kg and 12.5 mg/kg, respectively; s.c.) maintained with 1.5%–2% isoflurane, an animal was secured in a stereotaxic frame (Stoelting, Wood Dale, IL, USA), and a midline incision was made through the scalp. A hole was then drilled in the skull, through which a 22-gauge guide cannula (Plastics One, Roanoke, VA, USA) was lowered 1 mm above the third ventricle at a 4° angle from the vertical plane using the following coordinates: AP −2.1 mm, ML ± 0.7 mm, DV −9.8 mm, tooth bar −5.5 mm. Three additional holes were drilled to insert anchor screws into the skull. The guide cannula was fastened in place with dental acrylic applied to the surgical field. Finally, a stylet was inserted into the guide cannula to keep the lumen patent. The animals were allowed to recover for 1–2 weeks prior to the start of experimentation.

To focally inject adeno-associated viral vector (AAV) constructs, NR5A1-Cre mice were anesthetized with 2% isoflurane and placed in a stereotaxic frame. An incision was made to expose the skull, and one or two holes were drilled on either side of the mid-sagittal suture so that an injection needle could be slowly lowered into the dorsomedial subdivision of the VMN using the following coordinates: AV −0.6 mm; ML, ± 0.3 mm; and DV, −5.6 mm. A unilateral injection of a Cre recombinase-dependent AAV vector containing cation channelrhodopsin-2 (ChR2; AAV1.EF1a.DIO.ChR2 (E123A).YFP.WPRE.jGH; 7.2×10^{12} genomic copies/mL; 300 nL total volume; University of Pennsylvania Vector Core; Addgene plasmid #35507), or a bilateral injection of a designer receptor exclusively activated by designer drugs (DREADD)-containing AAV vector (pAAV-EF1a-DIO-hM3D(Gq)-mCherry; 3.8×10^{12} genomic copies/mL; 300 nL total volume; University of North Carolina Vector Core; Addgene plasmid #50460) was given over 2 min. The injection needle remained in place for 10 min after infusion to allow for diffusion from the tip, and then slowly removed from the brain to reduce potential spread of the virus. Animals were used for experimentation 2–3 weeks after viral injection, and 1–2 weeks after gonadectomy.

Drugs

All drugs were purchased from Tocris Bioscience/R&D Systems (Minneapolis, MN, USA) unless otherwise stated. For the behavioral experiments, estradiol benzoate (EB; Steraloids, Newport, RI, USA) was initially prepared as a 1 mg/mL stock solution in punctilious ethanol. A known quantity of this stock solution was added to a volume of sesame oil sufficient to produce a final concentration of 100 μg/mL, following evaporation of the ethanol. The

cannabinoid receptor agonist (*R*)-(+)-[2,3-Dihydro-5-methyl-3-(4-morpholinylmethyl)pyrrolo[1,2,3-*de*]-1,4-benzoxazin-6-yl]-1-naphthalenylmethanone mesylate (WIN 55,212-2) was dissolved in cremephor/ethanol/0.9% saline (CES; 1/1/18; v/v/v) at a concentration of 1.5 μg/μL, and delivered centrally in a total volume of 2 μL. Clozapine-N-oxide (CNO) was dissolved in filtered 0.9% saline to a final concentration of 0.3 mg/mL, and delivered systemically in a total volume of 1 mL/kg.

For the electrophysiological experiments, purified guinea pig insulin was purchased from Dr. Al Parlow (Harbor-UCLA Medical Center, Torrance, CA, USA) through the National Hormone and Peptide Program. It was dissolved in 0.01 HCl to a stock concentration of 20 μM, and further diluted with artificial cerebrospinal fluid (aCSF) to a working concentration of 20 nM. Tetrodotoxin (TTX; Alomone Labs, Jerusalem, Israel) was prepared as a 1 mM stock solution in NanoPure H_2O, and diluted further with aCSF to the working concentration of 500 nM. The $GABA_A$ receptor antagonist 6-imino-3-(4-methoxyphenyl)-1(6H)-pyridazinebutanoic acid hydrobromide (SR 95531) was dissolved in Ultrapure H_2O to a stock concentration of 10 mM, and the stock solution was diluted further with artificial cerebrospinal fluid (aCSF) to the working concentration of 10 μM. The membrane impermeant source of testosterone 4-androsten-17 μ-ol-3-one-3 carboxymethyloxime bovine serum albumin (TBSA; Steraloids) was dissolved in DMSO to a stock concentration of 1 mM, and then diluted further with aCSF to a working concentration of 100 nM. The calcium/calmodulin inhibitor N-(10-aminodecyl)-5-chloro-1-naphthalenesulfonamide hydrochloride (A7) was dissolved in NanoPure H_2O to a stock concentration of 3 mM, and further diluted into internal solution (see below), to a working concentration of 30 μM. 1,3,5(10)-Estratrien-3, 17β-diol (17β-estradiol; Steraloids) used for ovariectomized NR5A1-cre mice was dissolved in punctilious ethanol to a stock concentration of 1 mM, which was further diluted to a working concentration of 100 nM. The Akt activator 2-amino-6-chloro-α-cyano-3-(ethoxycarbonyl)-4H-1-benzopyran-4-acetic acid ethyl ester (SC79) was dissolved in NanoPure H_2O to a stock concentration of 10 mM, and the stock concentration was diluted further with aCSF to a working concentration of 10 μM. The androgen receptor antagonist 2-methyl-N-(4-nitro-3-[trifluoromethyl]phenyl)propanamide (Flutamide) was dissolved in NanoPure H_2O to a stock concentration of 10 mM, and further diluted with aCSF to a working concentration of 100 μM. The PI3K inhibitor 2-(4-morpholinyl)-8-(4-aminopheny)l-4H-1-benzopyran-4-one (PI 828) was dissolved in DMSO to a stock concentration of 10 mM, and further diluted with aCSF to a working concentration of 10 μM. CNO was dissolved in NanoPure H_2O to a stock concentration of 5 mM, and further diluted with aCSF to its working concentration of 5 μM. All aliquots of the stock solutions were stocked at −20 degrees Celsius until needed for experimentation.

Hypothalamic Slice Preparation

On the day of experimentation, the animal was briefly anesthetized with 32% isoflurane and rapidly decapitated. The brain was removed from the skull and the hypothalamic area was dissected. We then mounted the hypothalamic block on a cutting platform that was secured in a vibratome well filled with ice-cold, oxygenated (95% O_2, 5% CO_2) aCSF (for guinea pigs: NaCl 124, $NaHCO_3$ 26, dextrose 10, HEPES 10, KCl 5, NaH_2PO_4 2.6, $MgSO_4$ 2, $CaCl_2$ 1; for mice: sucrose 208, $NaHCO_3$ 26, KCl, 2, NaH_2 PO_4 1.25, dextrose 10, HEPES 10, $MgSO_4$ 2, $MgCl_2$ 1, $CaCl_2$ 1; in mM). Four to five coronal slices (300 μm) through the rostrocaudal extent of the ARC were then cut. The slices were transferred to an auxiliary chamber containing room temperature oxygenated aCSF made like that described above for the guinea pig slice preparation and allowed to recover for a minimum of 1 h until the electrophysiological recording.

Electrophysiology

Whole-cell patch clamp electrophysiological recordings from ARC neurons using biocytin-filled electrodes were performed in hypothalamic slices prepared from orchidectomized male guinea pigs, intact male guinea pigs, periovulatory female guinea pigs, gonadally intact male and cycling female NR5A1-Cre mice, and ovariectomized female NR5A1-Cre mice. During recordings, the slices were maintained in a chamber perfused with warmed (35 degrees Celsius), oxygenated aCSF in which we raised the $CaCl_2$ concentration to 2 mM. Artificial CSF and all drugs (diluted with aCSF) were perfused via peristaltic pump at a rate of 1.5 mL/min. Patch electrodes were prepared from borosilicate glass (World Precision Instruments, Sarasota, FL, USA; 1.5 mm OD) pulled on a P-97 Flaming Brown puller (Sutter Instrument Co., Novato, CA, USA), and filled with an internal solution containing the following (in mM): cesium gluconate 128; NaCl 10; $MgCl_2$ 1; EGTA 11; HEPES 10; ATP 1; GTP 0.25; 0.5% biocytin; adjusted to a pH of 7.3 with CsOH; osmolality: 286–320 mOsm. Electrode resistances varied from 3 MΩ to 8 MΩ.

For guinea pig experiments, whole-cell patch clamp recordings were performed using a Multiclamp 700A preamplifier (Axon Instruments, Foster City, CA, USA) that amplified potentials and passed current through the electrode. Membrane currents were recorded in voltage clamp with access resistances ranging from 8 MΩ to 20 MΩ. The signals underwent analog-digital conversion via a Digidata 1322A interface coupled to pClamp 10.5 software (Axon instruments). For the transgenic mouse experiments, recordings were made using an Olympus BX51 W1 fixed stage microscope outfitted with infrared differential interference contrast video imaging. A Multiclamp 700B preamplifier (Molecular Devices) amplified potentials and passed current through the electrode. Membrane currents underwent analog-digital conversion with a Digi-data 1550A interface (Molecular Devices) coupled to pClamp 10.5 software. The access resistance, resting membrane potential (RMP) and input resistance were monitored throughout the course of all recordings. If the access resistance deviated greater than 10% of the original value, the recording was ended. Low-pass filtering of the currents was conducted at a frequency of 2 kHz. The liquid junction potential was calculated to be −10 mV, and corrected for during data analysis using pClamp software. All recordings were performed under a holding potential of

−75 mV. For all electrophysiological recordings, we generated an I/V relationship from a holding potential of −60 mV by delivering voltage commands at 10 mV increments (150 ms in duration) ranging from −50 mV to −130 mV. The expression of intrinsic currents such as the A-type K+ current and the hyperpolarization-activated mixed cation current (Ibrahim et al., 2003; Tang et al., 2005; Conde et al., 2016) provided the first indication that we were recording from POMC neurons.

To assess the postsynaptic actions of purified guinea pig insulin in POMC neurons from chow- and HFD-fed animals, recordings using the whole-cell configuration from holding potentials of −60 mV were performed. Insulin (20 nM) was perfused along with 500 nM TTX until a new steady-state holding current was established (6–8 min). Current-voltage (I/V) relationships were generated using a ramp protocol (75 mV/s) before and immediately following peptide application over a range of potentials extending from −100 mV to −10 mV.

To evoke EPSCs in the guinea pig model, we placed a bipolar tungsten stimulating electrode connected to a SUl5 stimulus isolation unit (Grass Telefactor, Warwick, RI, USA) into the dorsomedial portion of the VMN. Cells received a single stimulation of 18 V magnitude every 1–2 s for 500 μs delivered from a S88 Stimulus Generator (Grass Telefactor, W. Warwick, RI, USA). For the optogenetic experiments, recordings were performed in slices from NR5A1-Cre mice that were injected with a ChR2-containing viral vector into the VMN 2–3 weeks prior to experimentation. Once glutamatergic SF-1-expressing fibers (visualized with eYFP) impinging on ARC neurons were encountered, functional synaptic connectivity was ascertained by applying a photo-stimulus (25–100 ms pulses delivered every 2 s) from a light-emitting diode (LED) blue light source (470 nm) controlled by a variable 2A driver (ThorLabs, Newton, NJ, USA) that directly delivered the light path through the Olympus 40× water-immersion lens to generate a fast EPSC.

EC-mediated retrograde inhibition of excitatory input was assessed via DSE. To elicit the DSE, cells were given a 60-mV depolarization, which lasted 3 s in duration. These pulses were delivered every 60 s for up to 10–15 consecutive trials. After attaining 1–2 min of baseline eEPSC amplitude, we then began to execute the DSE protocol. For all experiments, the electrical stimulation and DSE protocol were executed in the presence of SR 95531(10 μM) to block $GABA_A$ receptor-mediated synaptic input. We used TBSA (100 nM) to determine the potential for rapid membrane-delimited androgenic signaling, which was further evaluated using the androgen receptor antagonist flutamide (10 μM) in conjunction with TBSA (100 nM). A7 (30 μM) was applied via the internal solution in conjunction with bath application of TBSA (100 nm) to confirm the role of calcium/calmodulin in the androgenic enhancement of EC tone. To evaluate whether estradiol abrogates the DSE-changes in EC tone, and whether this occurs via PI3K, we bath administered 17β-estradiol (E_2; 100 nM) to slices generated in ovariectomized NR5A1-Cre mice, or applied the PI3K inhibitor PI 828 (10 μM) to slices obtained from periovulatory, female guinea pigs. To assess the role of PI3K/Akt pathway in the change in EC tone caused by diet-induced obesity/insulin resistance, we bath applied the Akt inhibitor SC79 (10 μM) to slices obtained from chow- and HFD-fed male guinea pigs. Data were analyzed by examining the average post-stimulation amplitude acquired from at least three separate trials over 5 s bins that consisted of data out to 30 s after the DSE stimulus, and then normalizing that to the average EPSC amplitude collected during the baseline period.

Immunohistochemistry

After recording, slices were then processed for immunohistochemistry using various phenotypic markers of ARC POMC neurons. Slices were fixed with 4% paraformaldehyde in Sorenson's phosphate buffer (pH 7.4) for 120–180 min. The slices were then immersed overnight in 20% sucrose dissolved in Sorensen's buffer, and frozen in Tissue-Tek embedding medium (Miles Inc., Elk-hart, IN, USA) the next day. Coronal sections (20 μm) were cut on a cryostat and mounted on chilled slides. These sections were then washed with 0.1 M sodium phosphate buffer (pH 7.4), and then processed with streptavidin-Alexa Flour (AF) 546 (Molecular Probes Inc., Eugene, OR, PA, USA) at a dilution of 1:600. After localizing the biocytin-filled neuron via fluorescence microscopy, the appropriate sections were processed further with polyclonal antibodies directed against α-melanocyte-stimulating hormone (α-MSH, Immunostar Inc., Hudson, WI, USA; 1:200 dilution), β-endorphin (Immunostar Inc.; 1:400 dilution), or cocaine and amphetamine-regulated transcript (CART; Phoenix Pharmaceuticals Inc., Burlingame, CA, USA; 1:200 dilution), and again evaluated using fluorescence immunohistochemistry. At the end of some of the behavioral experiments (see below), animals were anesthetized with 32% isofluorane and rapidly decapitated. Following brain removal, two to three coronal slices (1 mm in thickness) spanning the rostral-caudal extent of the mediobasal hypothalamus were prepared using a mouse brain matrix (Ted Pella Inc., Redding, CA, USA), submersed in Tissue-Tek embedding medium (Miles Inc.) and frozen in isopentane. Twenty micron-thick cryosections were then prepared for subsequent immunohistofluorescent determination of whether DREADD expression occurs in VMN SF-1 neurons using a polyclonal antibody directed against SF-1 and a monoclonal antibody against mCherry (Abcam, Cambridge, MA, USA; 1:300 and 1:500 dilutions, respectively).

Feeding and Metabolic Studies

The feeding and metabolic studies were performed using a four-station Comprehensive Lab Animal Monitoring System (CLAMS; Columbus Instruments, Columbus, OH, USA) from which we monitored cumulative food intake, meal size, and several measures of energy expenditure (O_2 consumption, CO_2 production and respiratory exchange ratio (RER)) as previously described and validated (Farhang et al., 2010; Borgquist et al., 2015a; Conde et al., 2017). These studies were conducted under conditions in which food (standard chow or HFD) and water were available *ad libitum*. The animals were allowed to acclimate in their CLAMS chamber over 1–3 days. Each day they were weighed, handled and returned to their respective chambers. After the acclimation session, we initiated the 5-day monitoring

phase during which the animals were weighed and injected each day and immediately placed back in their feeding chambers. For the guinea pig studies, intact males and periovulatory females were given either the CB1 receptor agonist WIN 55,212-2 (3 μg; I.3.V) or its CES vehicle (2 μL; I.3.V) each morning at 8:00 am. For the NR5A1-Cre mice, gonadally intact males and ovariactomized females were injected daily at 4:00 pm (2–3 h in advance of the nocturnal peak in energy consumption) with either CNO (0.3 mg/kg s.c.), or its 0.9% saline vehicle (1 mL/kg s.c.). Every other day, females were injected with EB (20 μg/kg; s.c.) or its sesame oil vehicle (1 mL/kg; s.c.). Monitoring took place continuously over 24 h. Cumulative food intake was taken as the total amount of food consumed at 1, 2 and 4 h after either CNO, EB or vehicle administration. Meal size is the amount of food eaten in a given hour divided by the number of meals in that same hour. The parameters of energy intake, meal pattern and energy expenditure were continuously written to a computer via an A/D converter.

Statistical Analysis

Comparisons between two groups were made with either the Student's *t*-test, or the Mann-Whitney U test. Comparisons made between more than two groups were performed using either the one-way, repeated measures multifactorial, or rank-transformed multifactorial analysis of variance (ANOVA) followed by the Least Significant Difference (LSD) test, or alternatively via the Kruskal-Wallis test followed by the median-notched box-and-whisker analysis. Differences were considered statistically significant if the alpha probability was 0.05 or less.

RESULTS

Experiment #1: Does Diet Differentially Influence the Cannabinoid Regulation of Energy Homeostasis?

Previous studies have demonstrated that cannabinoid-induced changes in energy intake and core body temperature are sexually differentiated (Diaz et al., 2009), and elevated EC tone and signaling are implicated in diet-induced obesity/insulin resistance (Kim et al., 2013). We wanted to determine whether long-term exposure to a HFD modifies these sex differences. Our 5–8 week exposure paradigm produced frank sex differences in the development of central insulin resistance. This was characterized by the marked blunting of the amplitude of reversible, insulin-induced inward currents due to activation of TRPC channels in POMC neurons (Qiu et al., 2014, 2018) during recordings in slices from HFD-fed male but not periovulatory female guinea pigs (Supplementary Figure S1).

Despite these sex differences in the development of diet-induced insulin resistance, HFD clearly, yet disparately, impacted cannabinoid sensitivity in both males and females. We found significant main effects of sex and diet, and significant interactions between the two factors, on the ability of the cannabinoid receptor agonist WIN 55,212-2 (3 μg; I.3.V) to evoke changes in energy balance. WIN 55,212-2 increased cumulative energy intake in chow-fed males but not perivulatory females; however, the agonist-induced increase in intake was markedly accentuated in both HFD-fed male and periovulatory females (**Figures 1A, 2A**). The HFD-induced potentiation of the hyperphagia caused by WIN 55,212-2 is associated with heightened increases in meal size in both males and periovulatory females (not shown). On the other hand, WIN 55,212-2 increased O_2 consumption in chow-fed males, an effect that was antagonized by the HFD, whereas the agonist was without effect on O_2 consumption in either HFD- or chow-fed periovulatory females (**Figures 1B, 2B**). WIN 55,212-2 also increased CO_2 production in chow-fed males. HFD *per se* decreased CO_2 production, and prevented the agonist-induced increase seen in the chow-fed animals. By contrast, WIN 55,212-2 decreased CO_2 production in chow-fed periovulatory females, an effect that was entirely reversed by the HFD (**Figures 1C, 2C**). In addition, WIN 55,212-2 elevated RER in chow-fed males. HFD *per se* lowered the RER, and blocked the increase caused by the agonist. Conversely, WIN 55,212-2 reduced the RER in chow-fed periovulatory females. HFD *per se* also decreased the RER, and prevented any further decrease caused by the agonist (**Figures 1D, 2D**). Lastly, WIN 55,212-2 increased metabolic heat production in chow-fed males. HFD *per se* lowered metabolic heat production, and markedly attenuated the agonist-induced increase. In periovulatory females, the HFD *per se* also reduced metabolic heat production; however, in contrast to the male, WIN 55,212-2 increased metabolic heat production in both HFD- and chow-fed animals (**Figures 1E, 2E**). Thus, diet disparately modulates sex differences in the cannabinoid regulation of energy intake and expenditure.

Experiment #2: Is There a Sex Difference in Endocannabinoid Signaling at VMN/ARC POMC Synapses, and Does it Involve Rapid Enhancement Through Membrane-Initiated Androgen Receptor Signaling?

The sex difference in the cannabinoid regulation of energy balance can be attributed, at least in part, to disparites in the presynaptic inhibition of glutamatergic input onto POMC neurons (Wagner, 2016). Evidence suggests that the VMN provides a prominent excitatory input that impinges on POMC neurons (Sternson et al., 2005; Krashes et al., 2014). Therefore, to verify the anatomical origin of this cannabinoid-sensitive glutamatergic input, we attempted to evoke EPSCs generated by electrical stimulation of the dorsomedial VMN. We recorded from a total of 132 guinea pig ARC POMC neurons. Stimulation of the dorsomedial VMN in slices from chow-fed gonadally intact males and periovulatory females elicited robust eEPSCs. The amplitude of the eEPSCs observed in POMC neurons generated by electrical stimulation of the dorsomedial VMN exhibited a reduction caused by postsynaptic depolarization in a sex-dependent manner. Thus, the extent of the postsynaptic depolarization-induced reduction in eEPSC amplitude was greater in males than in periovulatory females, an effect that was reversed in recordings from periovulatory females that

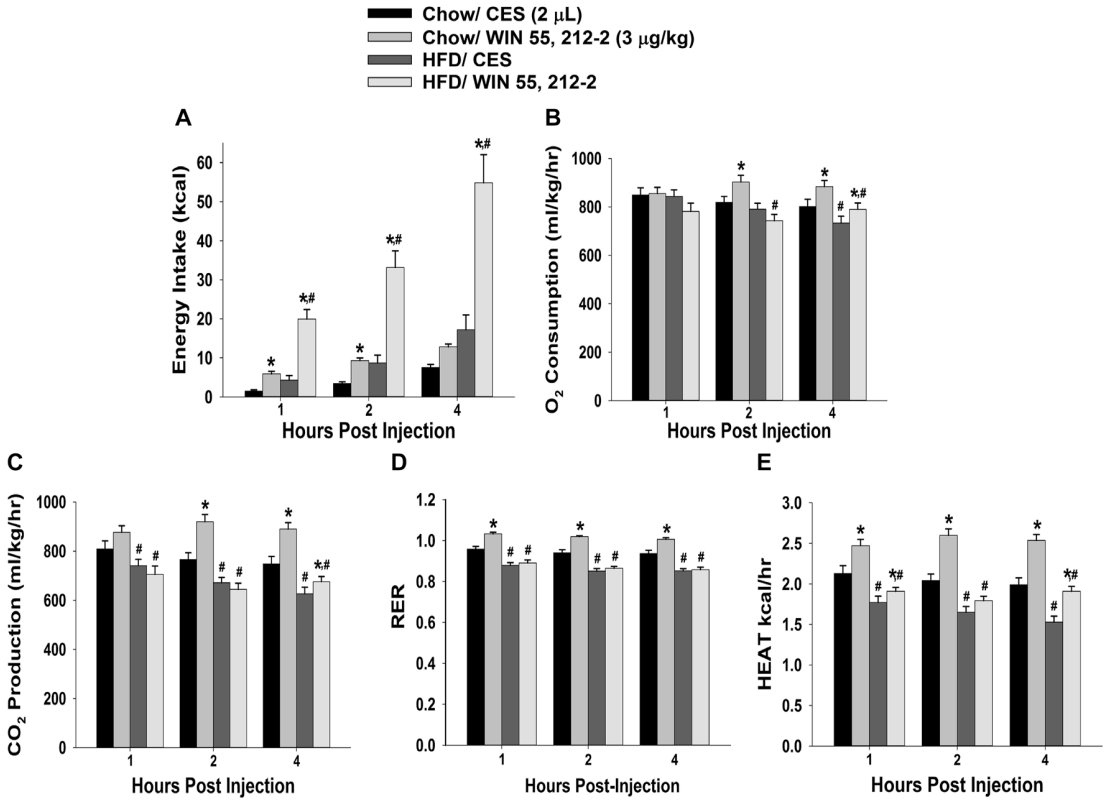

FIGURE 1 | High-fat diet (HFD) potentiates cannabinoid-induced changes in energy intake and but not energy expenditure, in male guinea pigs. Bars represent means and vertical lines 1 SEM of the cumulative energy intake **(A)**, O_2 consumption **(B)**, CO_2 production **(C)**, respiratory exchange ratio (RER; **D)** and metabolic heat production **(E)**, which were measured 1, 2 and 4 h after administration of the cannabinoid receptor agonist WIN 55,212-2 (3 μg; I.3.V) or its cremephor/ethanol/0.9% saline (CES) vehicle (2 μL; I.3.V). $^{*}P < 0.05$ relative to CES treated animals; multifactorial analysis of variance (ANOVA)/least significant difference (LSD); $n = 5$. $^{\#}P < 0.05$ relative to chow-fed animals; repeated measures, multifactorial ANOVA/LSD; $n = 5$.

were pretreated with the PI3K inhibitor PI 828 (**Figure 3**). These data suggest that this glutamatergic input impinging onto POMC neurons in the ARC is significantly attenuated by EC signaling in males compared to females, and that PI3K signaling contributes to this disparity. Due to this apparent sexual disparity, we decided to turn our attention to the androgenic influence on EC signaling within VMN/ARC POMC synapses.

In recordings from males that were orchidectomized in order to remove any confounding influences caused by endogenously produced testosterone, significant main effects of steroid and time were encountered with bath application of the membrane impermeant TBSA (100 nM), which prolonged the extent of the reduction caused by postsynaptic depolarization (**Figure 4**). These data indicate that androgens are involved in increasing EC tone. Due to the rapid time scale over which the TBSA augmented the postsynaptic depolarization-induced reduction in eEPSC amplitude, the possibility exists that this is due to a membrane bound androgen receptor. To further confirm this, we bath applied the classical androgen receptor antagonist flutamide (100 nM; **Figure 4**) along with TBSA. A significant main effect of treatment was found, such that the rapid androgenic augmentation of the reduction in eEPSC amplitude caused by postsynaptic depolarization was blocked with flutamide. Similarly, the calcium/calmodulin antagonist A7 (30 μM; **Figure 4**) abrogated the TBSA-induced enhancement of the decrease in eEPSC amplitude caused by DSE. These data provide further evidence that increases in intracellular Ca^{2+}, in conjunction with the activation of calcium/calmodulin-dependent protein kinase account, at least in part, for the rapid androgenic potentiation of EC-mediated retrograde inhibition. Given this androgenic enhancement of EC tone onto VMN/ARC POMC synapses, which can also be heightened under metabolic conditions such as diet-induced obesity/insulin resistance (Kim et al., 2013), it was of interest to see how diet would influence glutamatergic neurotransmission within this circuit.

Experiment #3: Does Diet Differentially Alter Endocannabinoid Signaling at VMN/ARC POMC Synapses via Alterations in PI3K/Akt Signaling?

Long-term exposure to a "Westernized" HFD causes sexually differentiated insulin resistance that, among other things, is associated with a reduced insulin receptor-mediated activation of TRPC5 channels in POMC neurons from male but not

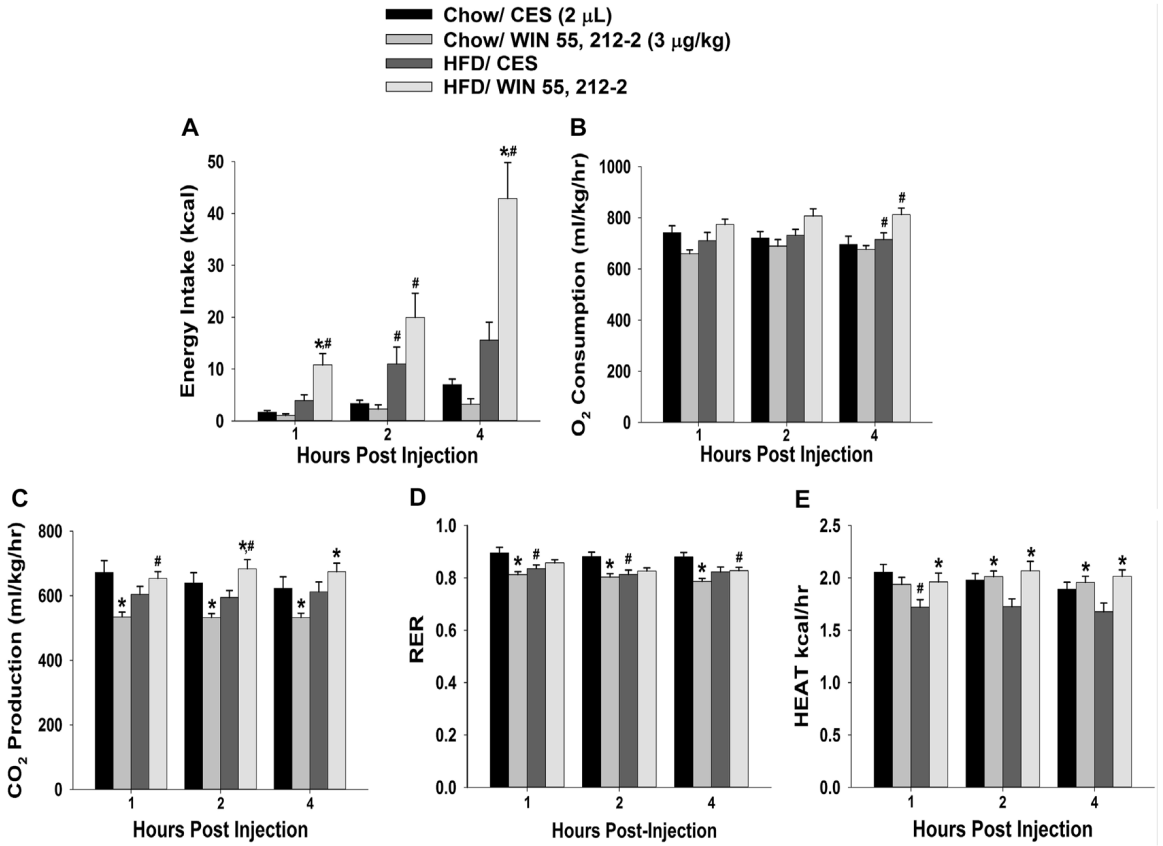

FIGURE 2 | Activation of hypothalamic cannabinoid receptors increases energy intake and various measures of energy expenditure in HFD- but not chow-fed periovulatory female guinea pigs. Bars represent means and vertical lines 1 SEM of the cumulative energy intake **(A)**, O_2 consumption **(B)**, CO_2 production **(C)**, respiratory exchange ratio (RER; **D)** and metabolic heat production **(E)**, which were measured 1, 2 and 4 h after administration of WIN 55,212-2 (3 μg; I.3.V) or its CES vehicle (2 μL; I.3.V). $^{*}P < 0.05$ relative to CES treated animals; multifactorial ANOVA/LSD; $n = 5$. $^{\#}P < 0.05$ relative to chow-fed animals; repeated measures, multifactorial ANOVA/LSD; $n = 5$.

female guinea pigs (Supplementary Figure S1). In addition, the data shown in **Figures 1**, **2** above clearly indicate that diet can profoundly impact the cannabinoid-induced changes in energy intake and expenditure seen in males and females. This suggests that diet-induced insulin resistance could manifest as a dysregulated "sensing" of energy balance—brought on by enhanced cannabinoid sensitivity that creates a state of negative energy balance within the homeostatic energy balance circuitry. We then attempted to resolve these differential dietary influences down to the level of the hypothalamic energy balance circuitry. To test the hypothesis that long-term HFD exposure augments EC signaling within VMN/ARC POMC synapses, we generated eEPSCs via electrical stimulation of the dorsomedial VMN in slices from gonadally intact, chow- or HFD-fed male and periovulatory female guinea pigs. Males fed a HFD exhibited a significant eEPSC amplitude reduction following the DSE as compared to those fed a standard-chow diet (**Figures 5A,B**). Conversely, only a very small percentage (20%) of POMC neurons from HFD-fed periovulatory females displayed any eEPSCs in response to stimulation of the dorsomedial VMN (Supplementary Table S1); effectively precluding any assessment of EC signaling at VMN/ARC POMC synapses in these animals. These data show that a prolonged exposure to a HFD leads to an increase in EC tone and retrograde inhibition that decreases glutamatergic input onto POMC neurons in males; however, in periovulatory females this may involve a dramatic reduction in the number of excitatory inputs emanating from the dorsomedial VMN.

Long-term exposure to a HFD is associated with reduced PI3K/Akt signaling in the ARC of gonadally intact male but not periovulatory female guinea pigs (Qiu et al., 2018). To determine if this reduction in PI3K/Akt signaling contributes to the HFD-induced enhancement of EC tone at VMN/ARC POMC synapses, we then performed recordings in slices from chow- and HFD-fed intact males pre-treated with the Akt activator SC79 (10 μM) or its vehicle. A significant main effect of SC79, as well as a significant interaction between SC79 and diet, were observed. Hence, the postsynaptic depolarization-induced reduction in eEPSC amplitude seen in recordings in slices from chow-fed animals pre-treated with SC79 is retained (**Figure 5C**). However, in animals fed a HFD this effect is completely abrogated (**Figure 5D**). The composite

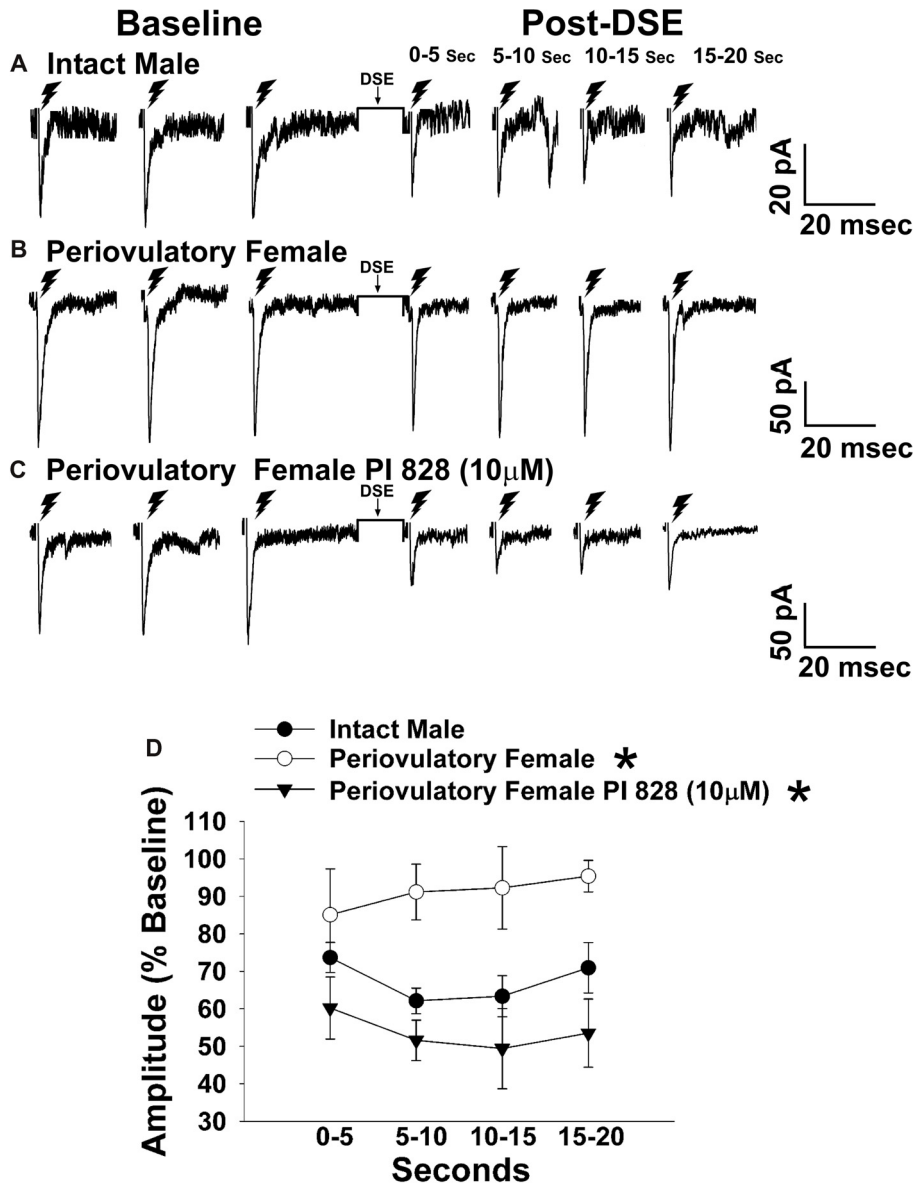

FIGURE 3 | The postsynaptic depolarization-induced reduction in excitatory input onto proopiomelanocortin (POMC) neurons generated by stimulation of the dorsomedial ventromedial nucleus (VMN) is larger in males than in periovulatory females, which is reversed by the phosphatidylinositol-3-kinase (PI3K) inhibitor PI 828. Membrane current traces illustrating the baseline evoked excitatory postsynaptic current (eEPSC) amplitude, and the time-dependent reduction in amplitude at various time points after the depolarized-induced suppression of excitation (DSE) stimulus, in arcuate nucleus (ARC) POMC neurons are shown for the intact male (**A**; $n = 9$) periovulatory female (**B**; $n = 6$) and a slice from a periovulatory female pretreated with PI 828 (10 μM; **(C)** $n = 4$). The composite line graph **(D)** further illustrates the PI3K-dependent sex differences in the retrograde inhibition of excitatory input from the dorsomedial VMN onto ARC POMC neurons under baseline conditions. Lines represent means and lines 1 SEM. *$P < 0.05$; rank-transformed multifactorial ANOVA/LSD; $n = 4$–9.

line graph seen in **Figure 5E** further illustrates the fact that retrograde, EC-mediated decreases in eEPSC amplitude (Conde et al., 2017) were significantly greater in HFD-fed animals compared to chow-fed controls at each time bin, an effect that was completely abolished in the presence of SC79. These data indicate that the HFD-induced enhancement of retrograde, EC-mediated signaling at VMN/ARC POMC synapses is facilitated by the reduction in Akt activation within the mediobasal hypothalamus.

Experiment #4: Does Photostimulation of VMN SF-1 Neurons Elicit a Physiologically Relevant, Sexually Differentiated and EC-Sensitive Source of Glutamatergic Input Onto ARC POMC Neurons?

To this point, we have shown that electrical stimulation of the dorsomedial VMN during electrophysiological recordings from slices obtained from male and female guinea pigs creates

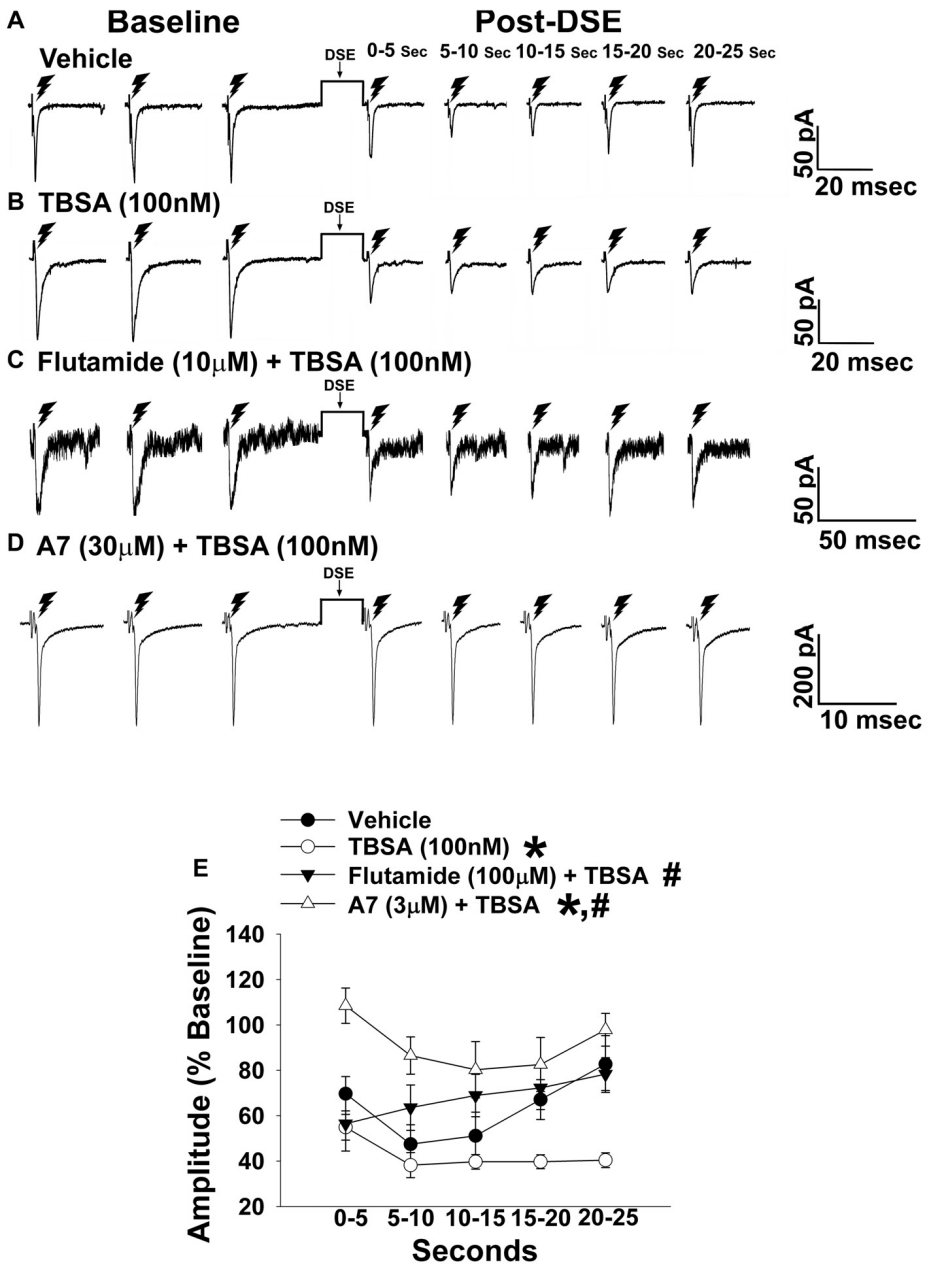

FIGURE 4 | The membrane-impermeant form of testosterone rapidly intensifies endocannabinoid (EC)-mediated reduction in eEPSC amplitude, which is blocked by a classical androgen receptor antagonist, as well as via inhibition of calcium/calmodulin-dependent protein kinase. Current membrane traces showing the decrease in eEPSC amplitude caused by postsynaptic depolarization seen in slices treated with either vehicle (**A**; $n = 6$) or testosterone 4-androsten-17 μ;-ol-3-one-3 carboxymethyloxime bovine serum albumin (TBSA; 100 nM; **B**; $n = 8$). Bath application of flutamide (10 μM) attenuated the rapid potentiating effects of TBSA (100 nM; **C**; $n = 5$) on the reduction in eEPSC amplitude, as did the calcium/calmodulin antagonist A7 administered via the internal solution (30 μM; **D**; $n = 5$). The composite line graph **(E)** shows the enhanced retrograde inhibition caused by TBSA. $^{*}P < 0.05$ relative to vehicle treated slices; rank-transformed multifactorial ANOVA/LSD. $^{\#}P < 0.05$ relative to slices treated with TBSA alone; rank-transformed multifactorial ANOVA/LSD.

a robust eEPSC response. The amplitude is then reduced in a time-dependent manner through retrograde, EC-mediated inhibition of excitatory input onto POMC neurons.

To confirm the excitatory transmission evoked by electrical stimulation of the dorsomedial portion of the VMN is indeed coming from SF-1 neurons, we utilized the transgenic NR5A1-Cre mouse model. We recorded from a total of 137 ARC POMC neurons in these mice, an example of which is represented in **Figure 6**. These animals express cre-recombinase under the control of the NR5A1 promoter, which is the gene that encodes for the SF-1 transcription factor. We injected the VMN with an AAV construct containing ChR2 tagged with a YFP

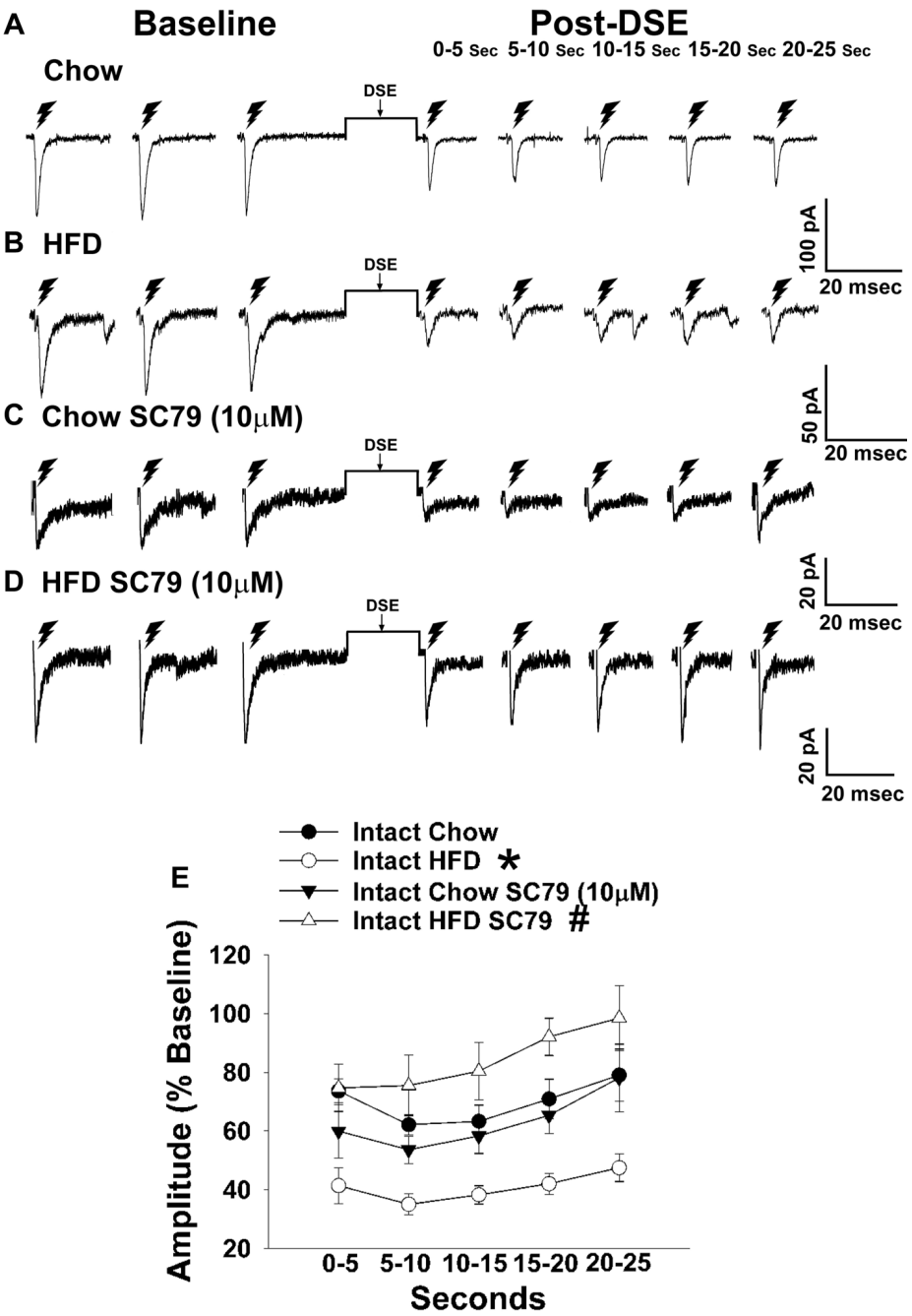

FIGURE 5 | HFD intensifies the reduction in eEPSC amplitude caused by postsynaptic depolarization, which is abrogated by Akt activation. The reduction in eEPSC amplitude caused by the DSE seen in chow-fed animals (**A**; $n = 9$) is further amplified in HFD-fed animals (**B**; $n = 5$). The reduction in eEPSC amplitude caused by postsynaptic depolarization seen during recordings in slices taken from chow-fed animals is unaffected by pretreatment with the Akt activator SC79 (10 μM; **C**; $n = 6$). However, the heightened retrograde signaling observed in slices from HFD-fed animals **(B)** was completely abolished with SC79 (**D**; $n = 5$). The composite line graph further illustrates the heightened postsynaptic depolarization-induced reduction in eEPSC amplitude caused by the HFD, and the impact of reduced PI3K/Akt signaling on the augmented EC tone **(E)**. Lines represent means and vertical lines 1 SEM. $^{*}P < 0.05$ relative to chow-fed animals; rank-transformed multifactorial ANOVA/LSD. $^{\#}P < 0.05$ relative to vehicle-treated slices; rank-transformed multifactorial ANOVA/LSD.

reporter to activate the SF-1 neurons through photstimulation. Two to three weeks later, we performed visualized, whole-cell patch clamp recordings in ARC neurons subsequently identifed as POMC neurons via immunohistofluorescence (**Figures 6A,F**). Upon optogenetic photostimulation, robust light-evoked EPSCs (leEPSCs) are seen (**Figures 6G,I**). By contrast, recordings from NR5A1-Cre mice in which the glutamate transporter Vglut2 is selectively knocked out in SF-1 neurons failed to

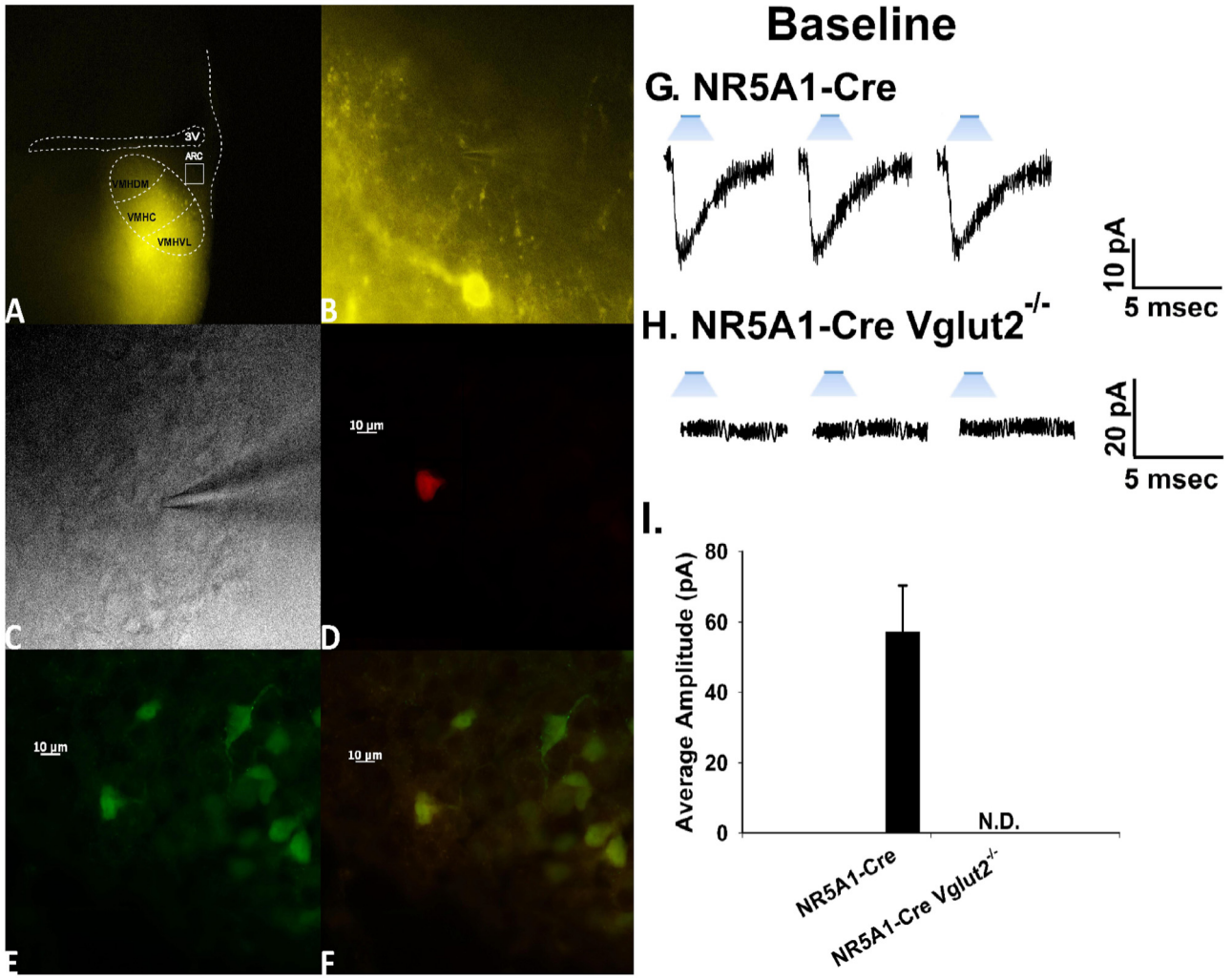

FIGURE 6 | Photostimulation elicits glutamatergic EPSCs at VMN steroidogenic factor (SF-1)/ARC POMC synapses. **(A)** ChR2 labeling in the VMN of a male NR5A1-Cre mouse visualized at ×4 with enhanced yellow fluorescent protein (eYFP) 2 weeks after injection with a ChR2-containing virus. Of note is the gradient extending from the dorsomedial VMN (VMHDM) to the ventrolateral VMN (VMHVL) that is characteristic of the distribution of VMN SF-1 neurons. **(B)** Magnified view of the outlined approximate recorded area in the ARC from **(A)** showing labeling of ChR2-containing fibers in the ARC visualized with eYFP. **(C)** An infrared, differential interference contrast image taken of an ARC neuron in close proximity to the eYFP-labeled fibers seen in **(B)**. **(D)** Biocytin labeling of the cell in **(A)** visualized with streptavidin/Alexa Fluor 546. **(E)** An antibody directed against cocaine- and amphetamine-regulated transcript (CART), a phenotypic marker of POMC neurons, immunolabels the cell in **(C)** as visualized with Alexa Fluor 488. **(F)** A composite overlay of the biocytin/CART labeling seen in the cell in **(A)**. Unless otherwise indicated, all photomicrographs were taken at ×40. A 25-ms stimulus of blue light subsequently delivered to the cell in **(C–F)** elicited robust light-evoked EPSCs (leEPSCs; **G)** that were indiscernible in recordings from NR5A1-cre$^{Vglut2-/-}$ animals **(H)**. This is further illustrated in the composite bar graph in **(I)** Bars represent means and lines 1 SEM of the EPSC amplitude measured in slices from NR5A1-Cre (n = 22) and NR5A1-Cre$^{Vglut2-/-}$ (n = 3) animals.

exhibit any leEPSCs upon photostimulation (**Figures 6H,I**). These results provide a clear indication that glutamatergic input onto POMC neurons is indeed emanating from SF-1-containing neurons in the dorsomedial portion of the VMN. As such, these VMN SF-1/ARC POMC synapses constitute a fundamental component of the hypothalamic energy balance circuitry.

Now that we have clearly demonstrated that VMN SF-1 neurons provide a robust source of glutamatergic input onto POMC neurons, we endeavored to explore whether this input is EC-sensitive and, if so, whether the associated retrograde inhibition is sexually differentiated. **Figure 7** shows representative leEPSCs evoked under basal conditions, and at various time points after the DSE stimulus, during recordings in slices taken from NR5A1-Cre females across the estrous cycle. Recordings during metestrus revealed a significantly lower percentage of cells exhibiting leEPSCs under basal conditions (see Supplementary Table S2). Rank-transformed multifactorial ANOVA revealed significant main effects of sex/cycle and time. The degree of the reduction in leEPSC amplitude caused by postsynaptic depolarization seen in recordings from diestrus (**Figure 7B**) and proestrus (**Figure 7C**) female NR5A1-Cre slices is modest at best. This is especially so when one considers the postsynaptic

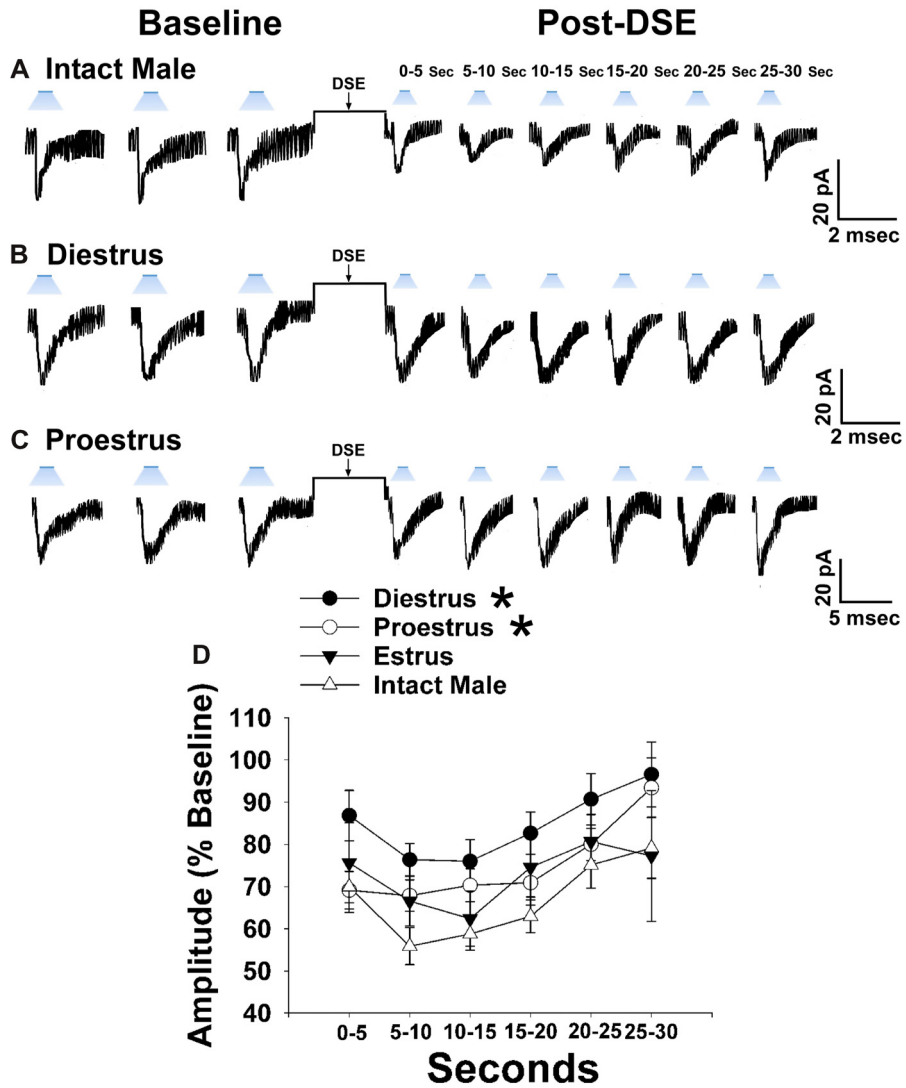

FIGURE 7 | Sex differences in the retrograde inhibition of glutamatergic input at VMN SF-1/ARC POMC synapses in NR5A1-Cre mice. The representative traces of membrane current show that the reduction in leEPSC amplitude caused by postsynaptic depolarization is comparatively larger in gonadally intact males (**A**; $n = 22$) than in diestrus (**B**; $n = 19$) and proestrus (**C**; $n = 21$) females. This can also be seen from the composite line graph **(D)**. Lines represent means and lines 1 SEM. $^*P < 0.05$; rank-transformed multifactorial ANOVA/LSD.

depolarization-induced reduction in leEPSC amplitude seen during recordings from gonadally intact NR5A1-Cre males (**Figure 7A**). Indeed, the decrease in leEPSC amplitude is significantly greater in intact males than in diestrus or proestrus females (**Figure 7D**).

Experiment #5: Does 17β-Estradiol Attenuate Retrograde, EC-Mediated Inhibition of Glutamatergic Input at VMN SF-1/ARC POMC Synapses?

Due to the comparatively modest reduction in leEPSC amplitude caused by the DSE stimulus across the various stages of the estrous cycle, we ovariectomized female NR5A1-Cre mice to determine putative activational effects of ovarian hormones in an environment devoid of any endogenous production. 17β-Estradiol (E_2) has long been known to uncouple $G_{i/o}$-linked receptors from their effector systems (Lagrange et al., 1994, 1996; Qiu et al., 2003). Therefore, we tested the hypothesis that E_2 would attenuate EC signaling at VMN SF-1/ARC POMC synapses. Slices treated with E_2 exhibited a significantly muted decrease in leEPSC amplitude following DSE as compared to those treated with its EtOH vehicle (**Figure 8**). These data indicate that estradiol exerts important activational effects that limit the retrograde inhibition of glutamatergic input onto POMC neurons. This would account, in part, for the sex differences in EC signaling at VMN SF-1/ARC POMC synapses.

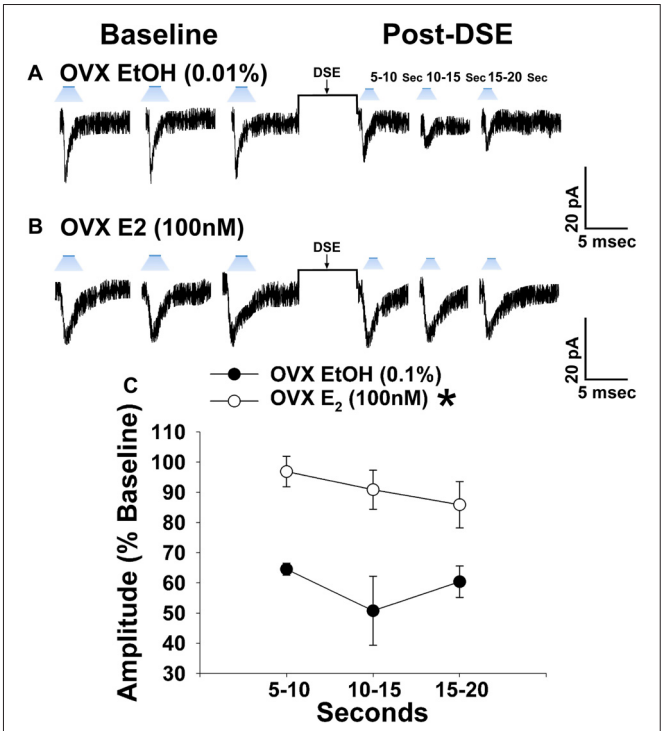

FIGURE 8 | E_2 significantly attenuates retrograde EC inhibition of IeEPSC amplitude in POMC neurons from ovariectomized NR5A1-cre mice. LeEPSC amplitude is reduced post-DSE in recordings from EtOH-treated slices (0.01%; **A**; $n = 5$). However when other slices are treated with E_2 (100 nM; $n = 7$), the degree of reduction is significantly reduced **(B)**. These points are further illustrates by the data shown in the line graph in **(C)** Bars represent means and vertical lines 1 SEM. $^*P < 0.05$; rank-transformed multifactorial ANOVA/LSD.

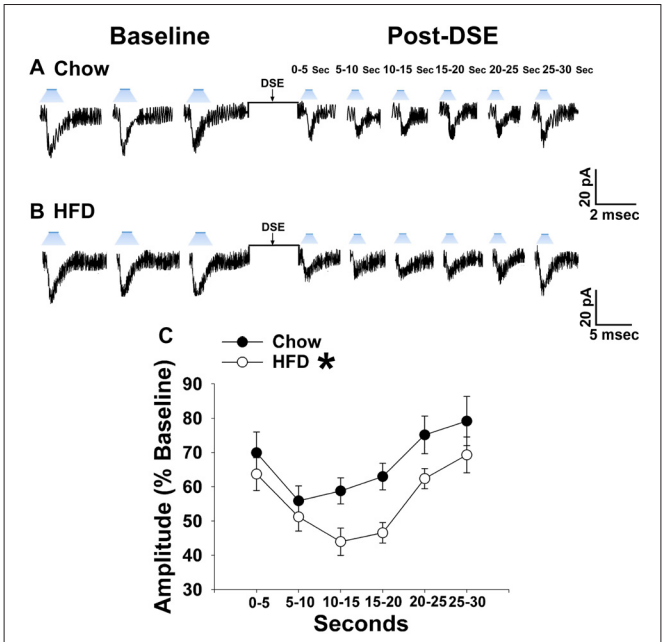

FIGURE 9 | The postsynaptic depolarization-induced reduction in IeEPSC amplitude seen in chow-fed males is even further reduced in HFD-fed animals. **(A)** Representative membrane current trace illustrating that the eEPSC amplitude is reduced post DSE in chow-fed animals ($n = 22$). However, this effect is significantly enhanced in animals fed a HFD (**B**; $n = 19$). A composite line graph showing how the reduction in IeEPSC amplitude caused by postsynaptic depolarization is significantly augmented **(C)**. Lines represent means and vertical lines 1 SEM. $^*P < 0.05$; rank-transformed multifactorial ANOVA/LSD.

Experiment #6: Is EC-Mediated Retrograde Inhibition Occurring at VMN SF-1/ARC POMC Synapses Disparately Enhanced by Diet-Induced Obesity in Male and Female NR5A1-Cre Mice?

As shown in **Figures 1**, **2**, **5** from our guinea pig studies, long-term exposure to a "Westernized" HFD leads to insulin resistance manifested by a sexually differentiated dysregulation of energy balance and enhanced EC signaling at VMN/ARC POMC synapses. We undertook parallel studies using our mouse model to determine whether long-term exposure to a HFD could similarly induce adaptive changes in the retrograde, EC-mediated inhibition of glutamatergic transmission at VMN SF-1/ARC POMC synapses. Notably, HFD-fed NR5A1-Cre mice exhibit an obese phenotype as compared to chow-fed controls (Supplementary Figure S2). The reduction in leEPSC amplitude caused by postsynaptic depolarization is significantly accentuated during recordings in slices taken from NR5A1-Cre males fed a HFD as compared to those taken from chow-fed controls (**Figures 9A–C**). By contrast, we found that only a very small percentage of POMC neurons from ovariectomized, HFD-fed females exhibited leEPSCs under baseline conditions; once again effectively precluding any assessment of dietary or hormonal influences on retrograde EC-mediated signaling (Supplementary Table S3). These data demonstrate that intact male animals fed a HFD exhibit greater retrograde inhibition of glutamatergic neurotransmission at VMN SF-1/ARC POMC synapses, whereas their female counterparts do not, which further substantiates the notion that diet-induced obesity/insulin resistance is associated with a sexually differentiated enhancement of EC tone within the hypothalamic energy balance circuitry.

Experiment #7: Does Chemostimulation of VMN SF-1 Neurons Produce Sex- and Diet-Dependent Changes in Energy Intake and Expenditure?

Through our *in vitro* studies in the NR5A1-Cre mice, we have established the critical role of SF-1 neurons in providing sexually differentiated, EC- and diet-sensitive glutamatergic input onto anorexigenic POMC neurons within the hypothalamic energy balance circuitry. Therefore, it is important to ascertain the importance of these neurons in the regulation of satiety, along with the modulatory influences of sex and diet, with an *in vivo* approach. As proof of principle, we selectively activated SF-1 neurons with DREADD technology to evaluate if they in fact suppress appetite and increase energy expenditure in a sex- and diet-dependent fashion. We injected a G_q-coupled,

M3-DREADD viral vector into the dorsomedial VMN. After 2 weeks of recovery, animals were then treated subcutaneously with either CNO (0.3 kg/mL) or its vehicle saline (0.9%; 0.1 mL/kg) every day at 4 pm for the 5-day duration of the behavioral study. Immunohistofluorescence confirmed that the DREADD was indeed expressed in SF-1 neurons (**Figures 10A,B**), and chemostimulation of SF-1 neurons *in vitro* resulted in a pronounced and reversible inward current in POMC neurons from chow-fed, DREADD-injected but not sham-injected males (**Figures 10C–E**). CNO (0.3 mg/kg; s.c.) decreased cumulative energy intake in chow-fed, DREADD-injected males from two out to 16 h after its administration. In HFD-fed males; however, the CNO-induced decrease in cumulative energy intake was confined to 2–4 h post-injection, after which the animals became refractory to further CNO stimulation (**Figure 11A**). The CNO- and diet-induced changes in food intake were paralleled by similar changes in meal size and the rate of consumption (not shown). In terms of energy expenditure, CNO treatment increased O_2 consumption in males from 1 h to 4 h after injection. However, the CNO-induced increase in O_2 consumption seen in HFD-fed animals was significantly attenuated at 4 h as compared to chow-fed controls (**Figure 11B**). CO_2 production was also significantly increased by CNO in chow-fed males (**Figure 11C**) from 1–4 h post-injection. Animals fed a HFD exhibited a significant decrease in CO_2 production from 2–4 h post injection, and the response to CNO was limited to 1 h after administration. In addition, CNO treatment significantly increased the RER (**Figure 11D**) in chow-fed males out to 2 h post injection. HFD-fed animals displayed significantly decreased RER, and a CNO response that was altogether absent. On the other hand, HFD *per se* increased metabolic heat production, which was further augmented by CNO (**Figure 11E**). The above-described effects of CNO were not seen in chow-fed, sham-injected males (Supplementary Figures S3A–E).

In chow-fed, sesame oil vehicle-treated ovariectomized females, CNO decreased cumulative energy intake up to 2 h post-injection (**Figure 12A**). EB (20 μg/kg; s.c.) also decreased intake for at least 16 h after its administration, which effectively

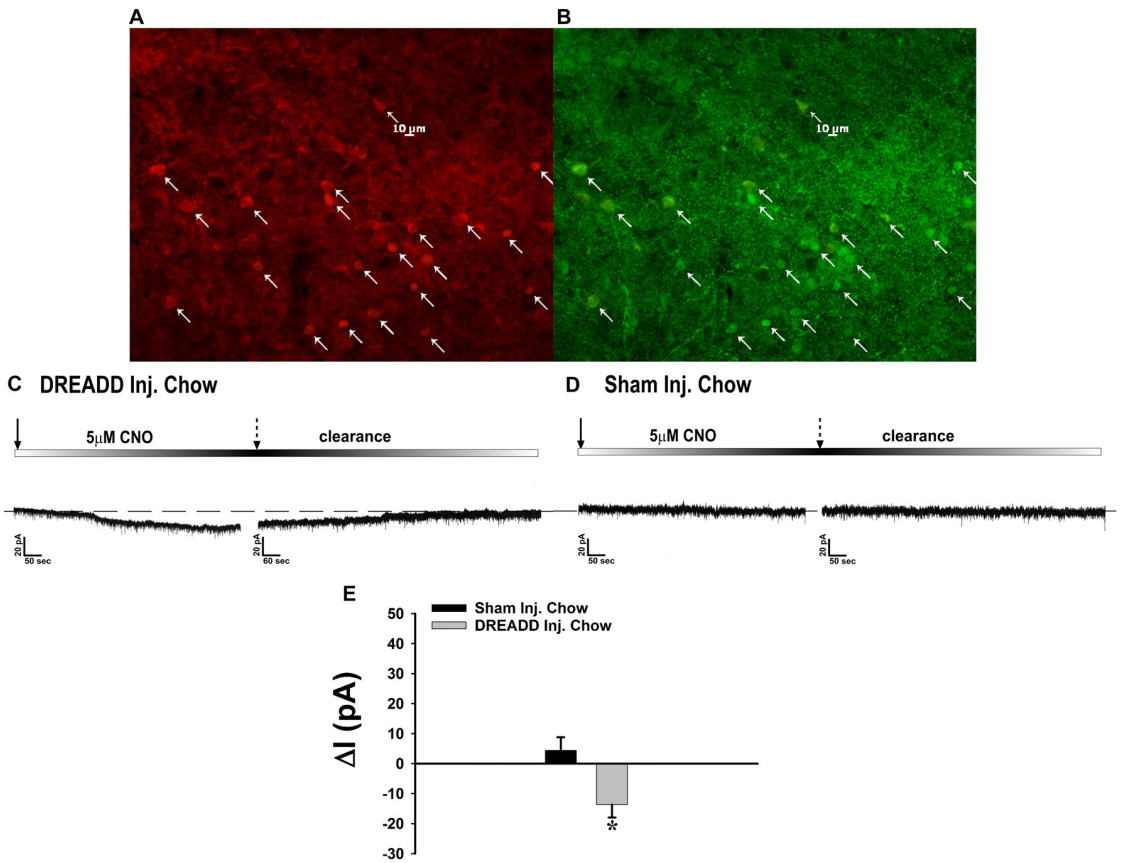

FIGURE 10 | Chemostimulation of VMN SF-1 neurons in male NR5A1-cre mice reversibly stimulates POMC neurons in designer receptor exclusively activated by designer drugs (DREADD)-injected but not sham-injected animals. The color photomicrograph shows the expression of the Gq-M3-DREADD (visualized with mCherry, **A**) in SF-1 neurons (visualized with AF488, **B**). **(C)** Representative traces of membrane current showing that clozapine-N-oxide (CNO) (5 μM) induced a reversible inward current in identified POMC neurons from DREADD-injected animals (n = 13) that was altogether absent in cells from sham-injected animals (**D**; n = 4). The composite bar graph in **(E)** further illustrates the stimulatory effect of CNO in POMC neurons from DREADD-injected animals but not sham-injected animals. Bars represent means and lines 1 SEM of the CNO-induced change in membrane current. *$P < 0.05$; Student's t-test.

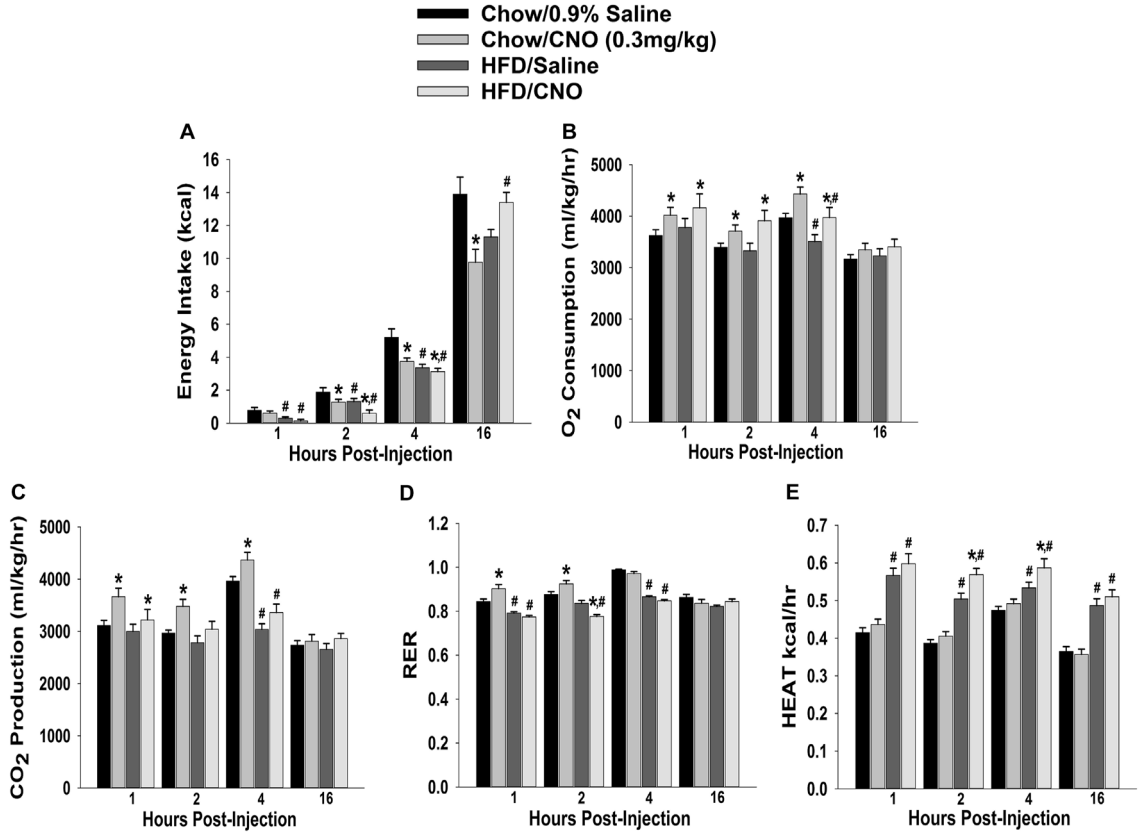

FIGURE 11 | Chemostimulation of VMN SF-1 neurons in male NR5A1-cre mice reduces cumulative energy intake and increases energy expenditure in a diet-sensitive manner. CNO (0.3 mg/kg) significantly decreased cumulative energy intake **(A)**, and increased O_2 consumption **(B)**, CO_2 production **(C)** and RER **(D)** in chow-fed animals, all of which was significantly attenuated in HFD-fed animals. Conversely, CNO increased metabolic heat production in HFD-fed animals **(E)**. Bars represent means and lines 1 SEM of the cumulative food intake, O_2 consumption, CO_2 production, RER and metabolic heat production seen in chow- and HFD-fed NR5A1-Cre mice treated with either CNO (0.3 mg/kg; chow: $n = 8$; HFD: $n = 5$), or its filtered 0.9% saline vehicle (chow: $n = 7$; HFD: $n = 5$). $^{*}P < 0.05$ relative to vehicle-treated animals; multifactorial ANOVA/LSD. $^{\#}P < 0.05$ relative to chow-fed animals; multifactorial ANOVA/LSD.

precluded any further decrease by CNO. In HFD-fed animals, the effect of CNO was more pronounced; lasting from two to at least 16 h post-injection. EB also reduced intake at 16 h post-administration. In terms of metabolism, HFD increased all indices of energy expenditure except RER (**Figures 12B–F**). CNO increased O_2 consumption in EB-treated, chow- and HFD-fed females, whereas in vehicle-treated, chow-fed CNO actually decreased it (**Figure 12B**). CNO also increased CO_2 production in EB-treated, chow- but not HFD-fed females (**Figure 12C**). In addition, CNO decreased rather than increased RER in vehicle-treated, chow-fed animals from 1–2 h post-injection, and in EB-treated, chow-fed animals at 16 h post-administration. HFD *per se* decreased RER, which was further reduced by CNO in both vehicle- and EB-treated animals at 2 h after its injection (**Figure 12D**). Lastly, CNO increased metabolic heat production in EB-treated, chow- and HFD-fed animals from 1–4 and 1–2 h post-injection, respectively. Conversely, CNO decreased metabolic production in vehicle-treated, HFD-fed animals at 4 h post-administration (**Figure 12E**). Thus, these data indicate that chemogenetic activation of SF-1 neurons with CNO effectively decreases food intake and increases energy expenditure in a sex- and diet-dependent manner. With diet-induced obesity/insulin resistance brought on by long-term exposure to a HFD in males, the ability of these neurons to execute their functions becomes impaired, perhaps through augmented EC signaling at VMN SF-1/ARC POMC synapses. In chow-fed, vehicle-treated females, the ability of SF-1 neurons to decrease energy intake and increase energy expenditure is rather muted, again perhaps to a heightened, EC-mediated retrograde inhibition of glutamatergic input onto POMC neurons that is lost following HFD exposure. Finally, estradiol enhances the ability of SF-1 stimulation to increase energy expenditure, an effect that is retained to a large degree in HFD-animals.

DISCUSSION

The results from the present study demonstrate that SF-1 neurons provide a source of sexually disparate, EC-sensitive glutamatergic input onto POMC neurons that account, at least in part, for sex and dietary differences in the cannabinoid regulation for energy homeostasis. These findings are based on the following observations: (1) activation of hypothalamic

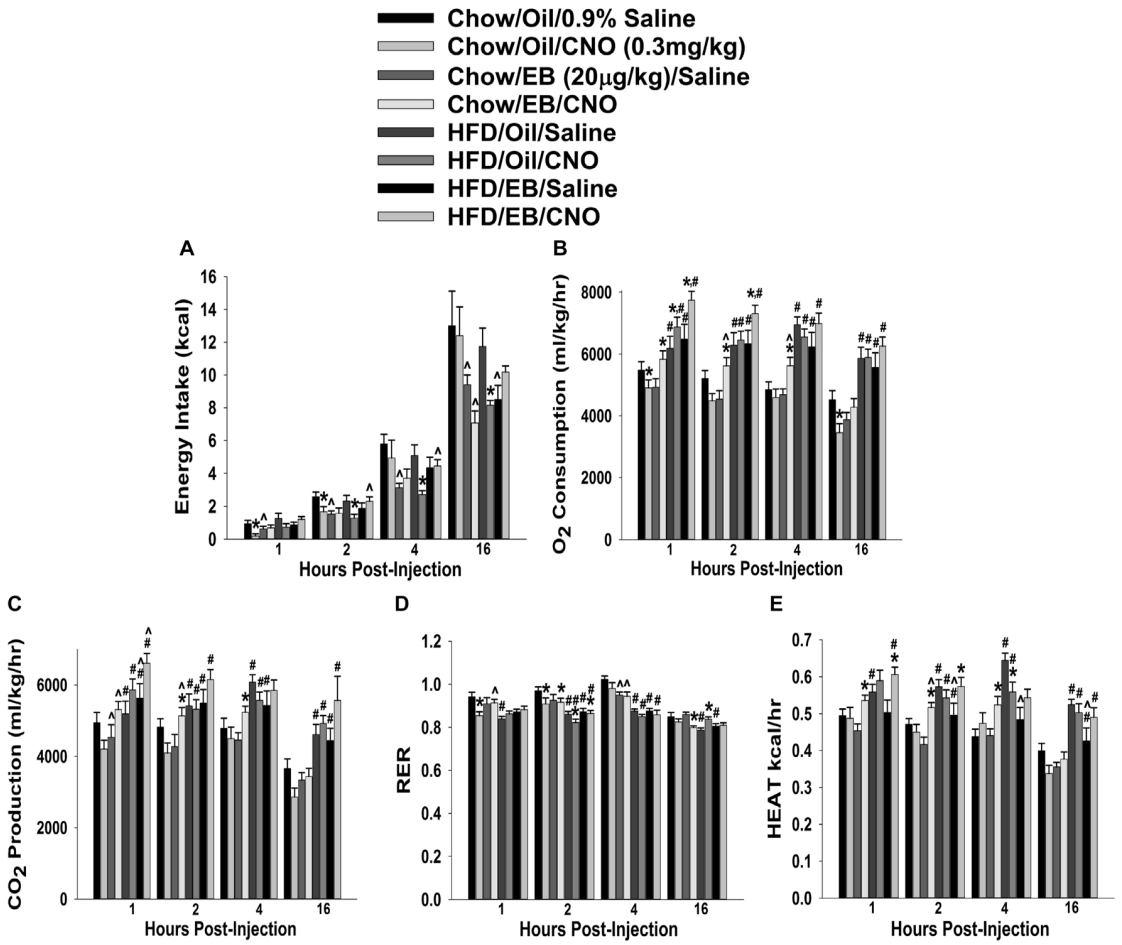

FIGURE 12 | Chemostimulation of VMN SF-1 neurons in ovariectomized NR5A1-cre mice alters cumulative energy intake **(A)**, O_2 consumption **(B)**, CO_2 production **(C)**, RER **(D)** and metabolic heat production **(E)** in an EB- and diet-sensitive manner. CNO (0.3 mg/kg) significantly decreased energy intake in chow-fed oil-treated animals, and to a larger extent in HFD-fed animals. It also increased energy expenditure in chow- and HFD-fed, EB-treated animals. Bars represent means and lines 1 SEM of the cumulative food intake, O_2 consumption, CO_2 production, and RER seen in chow- and HFD-fed NR5A1-Cre mice treated with either CNO (0.3 mg/kg; oil/chow: $n = 5$; oil/HFD: $n = 6$; EB/chow: $n = 6$; EB/HFD: $n = 5$), or its filtered 0.9% saline vehicle (oil/chow: $n = 8$; oil/HFD: $n = 6$; EB/chow: $n = 6$; EB/HFD: $n = 6$). $^*P < 0.05$ relative to saline-treated animals; multifactorial ANOVA/LSD; $n = 5$–8. $^{\#}P < 0.05$ relative to chow-fed animals; multifactorial ANOVA/LSD; $n = 5$–8. $^{\wedge}P < 0.05$ relative to oil-treated animals; multifactorial ANOVA/LSD.

CB1 receptors increases energy intake, alters meal pattern and increases energy expenditure in a sex- and diet-dependent manner; (2) chemogenetic activation of SF-1 neurons stimulates POMC neurons, suppresses food intake, alters meal pattern, and increases energy expenditure in a sex- and diet-dependent fashion; (3) EPSCs in guinea pig POMC neurons evoked by electrical stimulation of the dorsomedial VMN are subject to retrograde, EC-mediated regulation in a manner dictated by sex and dietary conditions; (4) optogenetic photostimulation elicits robust leEPSCs at VMN SF-1/ARC POMC synapses in NR5A1-cre mice that are altogether absent in NR5A1-Cre genetically modified to lack Vglut2 expression in SF-1 neurons; (5) retrograde EC-mediated inhibition of leEPSCs at VMN SF-1/ARC POMC synapses occurs to a greater extent in NR5A1-cre male mice than it does in cycling females; (6) EC tone at VMN SF-1/ARC POMC synapses is rapidly accentuated by androgens acting through membrane initiated signaling in males, an effect that is blocked by the androgen receptor antagonist flutamide and the calcium/Calmodulin inhibitor A7; (7) estradiol rapidly attenuates the EC-mediated reduction in leEPSC amplitude in ovariectomized NR5A1-Cre mice; and (8) HFD augments EC signaling at VMN SF-1/ARC POMC synapses in male guinea pigs and mice, an effect that is blocked with the Akt activator SC79.

Testosterone Increases EC Tone at VMN SF-1/ARC POMC Synapses by Increasing Intracellular Ca^{2+} and Activating Calcium/Calmodulin-Dependent Protein Kinase

We also show presently that androgens rapidly elevate EC tone at VMN SF-1/ARC POMC synapses via membrane-initiated signaling to further suppress glutamatergic input

onto POMC neurons. This is accomplished by increases in intracellular Ca^{2+} and the activation of enzymes like calcium/calmodulin-dependent protein kinase and AMPK. This is consistent with what we have shown previously—namely, that testosterone increases energy intake and expenditure, which is blocked by the CB1 receptor antagonist, AM251, and increases AMPK expression in the ARC (Borgquist et al., 2015b). The membrane-initiated signaling presently observed that leads to the increased intracellular Ca^{2+} concentrations and activation of calcium/calmodulin is consistent with reports describing rapid androgenic signaling in other systems. Mitsuhashi et. al (Mitsuhashi et al., 2016) investigated the signaling pathway through which testosterone stimulates GLUT4-dependent glucose uptake into 3T3-L1 adipocytes. This study also used the membrane-impermeant TBSA that mimicked the testosterone-induced increase in glucose uptake, along with the classical androgen receptor antagonist flutamide, which had no effect. The ability of TBSA to mimic the testosterone-induced rapid increase in glucose uptake brought on by membrane-initiated signaling aligns perfectly with our results in the present study. However, the inability of flutamide to block it contrasts with what we show presently. The increase in glucose uptake was associated with the increased activity of calcium/calmodulin-dependent protein kinase I and II, as well as AMPK, which is exactly what we saw for the androgenic enhancement of EC tone at VMN SF-1/ARC POMC synapses. Other examples of rapid increases in intracellular Ca^{2+} levels elicited by membrane-initiated androgenic signaling are seen in osteoblasts and Sertoli cells, as well as skeletal muscle cells and cardiac myocytes. In all cases, the rapid signaling is triggered by the activation of a G protein-coupled androgen receptor that stimulates phospholipase C, extracellular-regulated kinase 1/2 and AMPK (Estrada et al., 2003; Vicencio et al., 2006; Loss et al., 2011; Wilson et al., 2013). Our findings show that testosterone increases EC tone by increasing intracellular Ca^{2+}, which activates AMPK through calcium/calmodulin-dependent protein kinase to initiate the synthesis of 2-AG via diacylglycerol lipase (DAGL), are entirely consistent with this notion. The 2-AG produced is, in turn, released by the postsynaptic POMC neurons into the synaptic cleft, where it can engage in retrograde inhibition by activating presynaptic CB1 receptors on the terminals of the SF-1 neurons to decrease glutamate release (**Figure 13**).

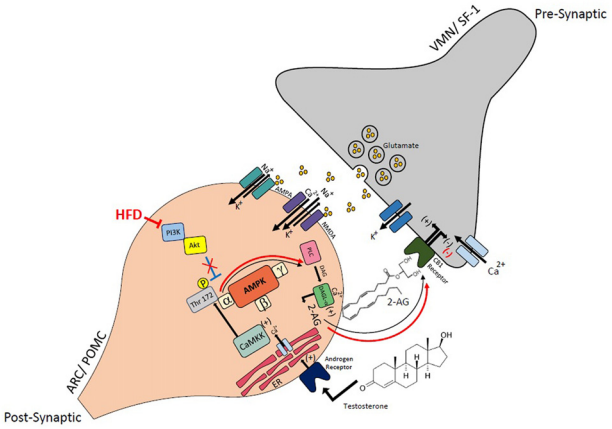

FIGURE 13 | Schematic illustrating the connectivity and EC signaling occurring at VMN SF-1/ARC POMC synapses in males, and how that signaling is rapidly modulated by androgens and influenced by diet. The magnified view of the VMN SF-1/ARC POMC synapse illustrates how testosterone activates a putative membrane androgen receptor to increase intracellular calcium. This increase in intracellular calcium activates calmodulin-dependent protein kinase kinase (CaMKK), which then phosphorylates threonine 172 on the α subunit of the AMPK complex to activate the enzyme. This activation leads to an increased production of 2-arachidonylglycerol (2-AG) through diacylglycerol lipase (DAGL)α, and the 2-AG released can retrogradely activate presynaptic CB1 receptors. This inhibits calcium entry, which decreases glutamatergic input. The resultant relief from the anorexigenic signal leads to hyperphagia. AMPK activity is inhibited by PI3K/Akt signaling, and this inhibition is reduced with HFD-induced obesity/insulin resistance. This further elevates AMPK activity and subsequently EC tone at VMN SF-1/ARC POMC synapses.

EC-Mediated Retrograde Inhibition of Glutamatergic Input at VMN SF-1/ARC POMC Synapses Is Sexually Differentiated and Negatively Modulated by 17β-Estradiol

Our present study shows that the degree of retrograde, EC-mediated inhibition varied depending on the stage of the estrous cycle, with a diminished retrograde inhibition during the diestrus and proestrus stages of the cycle in chow-fed NR5A1-Cre females that was significantly different from that found in estrus females or gonadally intact males. It is known that female rodents consume fewer calories during the periovulatory period straddling the proestrus and estrus stages of the estrous cycle (Asarian and Geary, 2013; Schreiber et al., 2016). This is more or less consistent with our findings that during diestrus and proestrus, when estradiol levels are rising (Asarian and Geary, 2006; Goldman et al., 2007; McLean et al., 2012), the retrograde EC-mediated inhibition of glutamate release at VMN SF-1/ARC POMC synapses is significantly attenuated. It is during this period of the estrous cycle that hypothalamic circuits are most sensitive to the actions of estradiol (Andrews et al., 1981; Gallo and Bona-Gallo, 1985). However, during estrus these same circuits become desensitized due to prolonged exposure to gradually rising levels of estradiol during the preceding stages of the cycle (Andrews et al., 1981; Gallo and Bona-Gallo, 1985). Such is the case in the present study; during estrus the degree of retrograde EC-mediated signaling at VMN SF-1/ARC POMC synapses was significantly higher than that seen during diestrus and proestrus, and comparable to that seen in gonadally intact males.

Estradiol is a potent anorexigenic hormone, and thus plays a critical role in regulating energy homeostasis in large part through the uncoupling of metabotropic $G_{i/o}$–linked receptors, such as μ-opioid and $GABA_B$ receptors, from their effector systems (Lagrange et al., 1994, 1996; Qiu et al., 2003). Hypestrogenic conditions such as those brought on by ovariectomy induce hyperphagia accompanied by increases in weight gain and adiposity, meal size, serum glucose and cholesterol (Geary and Asarian, 1999; Eckel et al., 2002;

Lucas et al., 2003). In recordings from ovariectomized mice, we presently show that E_2 significantly attenuated the postsynaptic depolarization-induced reduction in leEPSC amplitude as compared its EtOH vehicle. This indicates that estradiol is a key modulator that limits retrograde inhibition of glutamatergic input at a critical anorexigenic synapse within the hypothalamic energy circuitry.

Diet-Induced Obesity/Insulin Resistance Profoundly Shapes the Sex Difference in the Cannabinoid-Induced Regulation of Energy Homeostasis

We have demonstrated previously that cannabinoid-induced hyperphagia and hypothermia is sexually differentiated; with males being more sensitive than their female counterparts (Wagner, 2016). This is corroborated by the findings in the present study, where the increases in energy intake, meal size and energy expenditure caused by the cannabinoid receptor agonist WIN 55,212-2 seen in chow-fed intact male guinea pigs are altogether absent in chow-fed periovulatory female guinea pigs. In fact, WIN 55,212-2 decreases rather than increases CO_2 production and the RER in these animals. The increase in energy expenditure seen in males might be due to the sex-dependent expression of mitochondrial CB1 receptors in POMC neurons that have been reported to upregulate uncoupling protein two expression and increase mitochondrial respiration (Koch et al., 2015). By contrast, the agonist-induced hyperphagia and increase in meal size is much more pronounced in HFD-fed males, and equally dramatic increases in energy intake and meal size occur in HFD-fed periovulatory females as well. In addition, the cannabinoid-induced increase in energy expenditure observed in chow-fed males is abrogated in HFD-fed males, whereas in periovulatory females it is observed only in HFD-females. The HFD treatment paradigm produces a sexually differentiated central insulin resistance, where males but not periovulatory females exhibit a marked diminution in the insulin-induced activation of TRPC channels. This is accompanied by equally disparate changes in the ability of insulin to decrease energy intake and increase energy expenditure (Qiu et al., 2018). This differential, diet-induced insulin resistance is not associated with significant changes in adiposity, but it does cause frank dyslipidemia in both males and females (Qiu et al., 2018). This is in keeping with the fact that diet-induced insulin resistance can occur well in advance of any overt changes in body composition (Clegg et al., 2011). Moreover, adaptive changes in the excitability of neurons within the hypothalamic energy balance circuitry, as well as the density of their terminal fields, can be seen within 48 h of HFD exposure (Wei et al., 2015).

The heightened cannabinoid sensitivity that we presently show appears to occur via a different mechanism in males than it does in females. Indeed, intact male guinea pigs and NR5A1-Cre mice fed a HFD both exhibited a significantly more pronounced reduction in eEPSC amplitude at VMN SF-1/ARC POMC synapses following DSE as compared to their respective chow-fed diet controls. This is indicative of enhanced EC tone at these synapses. The diet-induced obesity/insulin resistance seen in our hands is associated with reduced PI3K/Akt signaling in the ARC (Qiu et al., 2018). Since hormones like E_2 act through PI3K/Akt to diminish EC tone at VMN SF-1/ARC POMC synapses (Mela et al., 2016), it stands to reason that decreased ARC PI3K/Akt signaling observed with diet-induced obesity/insulin resistance in males would do just the opposite (**Figure 13**). Both SF-1 and POMC neurons are integral components in the hypothalamic regulation of energy homeostasis under both normophysiologic and metabolically stressed states. Indeed, the knockout of either SF-1 or any one of several components of the melanocortin system (e.g., β-endorphin, melanocortin-4 receptors) leads to hyperphagia, obesity, hyperleptinemia and hyperinsulinemia (Majdic et al., 2002; Appleyard et al., 2003; Cone, 2006). Both SF-1 and POMC neurons are modulated by peripheral hormones like leptin and insulin. They are both depolarized by leptin via PI3K-mediated activation of TRPC5 channels (Dhillon et al., 2006; Hill et al., 2008; Qiu et al., 2010). Knockout of leptin receptors in either of these neurons leads to increased adiposity and hyperleptinemia, as well as increased energy intake and decreased energy expenditure in HFD-fed animals (Balthasar et al., 2004; Dhillon et al., 2006). As shown presently and reported recently, insulin purified from guinea pig and other animal sources also depolarizes POMC neurons via a PI3K-induced activation of TRPC5 channels, and these neurons are a critical substrate in the development of sexually differentiated diet-induced insulin resistance (Qiu et al., 2014, 2018). On the other hand, Humulin and other zinc-containing insulin formulations have been shown previously to hyperpolarize POMC neurons via activation of K_{ATP} channels (Claret et al., 2007; Hill et al., 2008), an effect that can be mimicked by zinc *per se* (Qiu et al., 2014). Insulin also hyperpolarizes SF-1 neurons via PI3K-dependent K_{ATP} channel activation, and the knockout of insulin receptors in these cells protects against insulin resistance (Klöckener et al., 2011). In addition, activation of insulin receptors in the mediobasal hypothalamus promotes lipogenesis, and inhibits lipolysis and hepatic glucose production via suppression of sympathetic outflow to white adipose tissue (Scherer et al., 2011). Moreover, genetic deletion of protein-tyrosine phosphatase 1B in SF-1 neurons exacerbates diet-induced obesity in a sex-dependent manner that is associated with reduced sympathetic tone and energy expenditure in female but not male animals caused by enhanced insulin signaling in these cells (Chiappini et al., 2014). Thus, it is apparent that diet-induced obesity/insulin resistance can produce adaptive changes in the functioning of these neurons, and genetic perturbations in the functioning of these neurons can clearly impact the development of diet-induced obesity/insulin resistance.

On the other hand, we found that POMC neurons from HFD-fed periovulatory female guinea pigs and ovariectomized female NR5A1-Cre mice had substantially less excitatory input from SF-1 neurons. This is consistent with the fact that obese *ob/ob* mice lacking leptin have an increased number of excitatory inputs and a decreased number of inhibitory inputs onto NPY/AgRP neurons, as well as a reduced number of excitatory synapses impinging upon POMC neurons (Pinto et al., 2004). The strength of the excitatory input can also be diminished by

fasting (Sternson et al., 2005). Thus, these adaptive changes in synaptic strength appear to be a hallmark feature of negative energy balance (in the case of fasting) as well dysregulated energy balance (in the case of obesity and insulin/leptin resistance). The question arises: what, then, accounts for the enhanced cannabinoid-induced increases in energy intake and expenditure in HFD-fed females? We have demonstrated previously that E_2 attenuates cannabinoid-induced changes in energy balance and glutamatergic input onto POMC neurons in ovariectomized, chow-fed females (Kellert et al., 2009; Washburn et al., 2013). This is entirely consistent with our present findings, in which activation of hypothalamic cannabinoid receptors was without effect on energy intake and expenditure in chow-fed periovulatory females that are at a stage in their cycle where E_2 predominates (Owen, 1975). The dramatic reduction in excitatory input onto POMC neurons that we presently see in HFD-fed effectively removes the primary neuroanatomical substrate upon which E_2 normally acts to disrupt EC signaling. However, postsynaptic and mitochondrial CB1 receptors are expressed in POMC neurons, and agonist-induced activation reportedly depolarizes these cells to increase energy intake and expenditure (Koch et al., 2015). It is certainly possible that long-term HFD exposure compromises the effectiveness with which E_2 decouples CB1 receptors from their effector systems in POMC neurons; allowing for a more robust response following CB1 receptor activation. As such, both pre- and postsynaptic receptors may play a pivotal role in providing adaptive metabolic flexibility that occurs in response to ever-changing dietary conditions. This is clearly seen in transgenic animals in which the CB1 receptor is selectively knocked in SF-1 neurons, where chow-fed animals exhibit enhanced sympathetic tone, insulin and leptin sensitivity, as well as decreased adiposity, and HFD-fed animals display just the opposite Cardinal et al. (2014). E_2 also increases the hypothalamic expression of ionotropic glutamate receptors (Diano et al., 1997). Thus, it is also plausible that diet-induced obesity/insulin resistance compromises the ability of E_2 to affect this increase.

Our *in vivo* chemogenetic experiments show that activation of SF-1 neurons significantly suppressed food intake and increased energy expenditure in gonadally intact, chow-fed male NR5A1-Cre animals, effects that were appreciably diminished in HFD-fed animals. These *in vivo* chemogenetic findings are largely in keeping with our *in vitro* optogenetic studies, in which animals fed a HFD exhibited augmented EC signaling at VMN SF-1/ARC POMC synapses to further reduce glutamate release onto POMC neurons. SF-1 excitation in ovariectomized females decreased energy intake and increased energy expenditure in an E_2- and diet-dependent manner. Only modest decreases in energy intake caused by SF-1 neuronal activation were observed in chow-fed, vehicle-treated females; reminiscent of the profile seen in obese males. These effects became more robust following HFD exposure. By contrast, SF-1 stimulation elicited prominent increases in energy expenditure in EB-treated females fed either chow or HFD. That fact that these dynamic, diet-induced changes in energy balance can be observed upon SF-1 activation in the absence of functional glutamatergic synapses with POMC neurons strongly indicates that another neuromodulator (or alternatively a different downstream effector) is mediating these effects. Indeed, pituitary adenylate cyclase activating polypeptide (PACAP) is expressed by SF-1 neurons, and it reportedly suppresses energy intake and increases energy expenditure (Segal et al., 2005; Hawke et al., 2009). Future studies will determine whether PACAP is involved in the alterations in energy balance that we observe upon SF-1 neuronal activation in HFD-fed females. It was recently reported that DREADD activation occurs not via CNO, but rather by conversion to clozapine (Gomez et al., 2017). However, clozapine and other neuroleptics increase energy intake and weight gain (Fadel et al., 2002; Weston-Green et al., 2012). Given that, in our hands, chemogenetic activation of SF-1 neurons does just the opposite, we think it is unlikely that clozapine is activating the DREADDS, or any other element of the hypothalamic energy balance circuitry. Collectively, these data further support the notion that long-term exposure to HFD profoundly disrupts the hypothalamic energy balance circuitry, and the sex differences in the cannabinoid regulation of energy homeostasis.

In conclusion, the present study demonstrates that VMN SF-1/ARC POMC synapses represent an important anorexigenic component within the hypothalamic energy balance circuitry. Excitatory neurotransmission occurring at these synapses is inhibited by retrograde, EC-mediated signaling that is sexually differentiated, and enhanced under conditions of diet-induced obesity/insulin resistance in a sex-dependent manner. Collectively, these findings further advance our understanding of the hypothalamic control of energy homeostasis, which in turn will help us to develop rational, gender-based therapies for the treatment of obesity as well as HIV/AIDS- and cancer-related cachexia.

AUTHOR CONTRIBUTIONS

CF, JH and KC performed all stereotaxic and survival surgeries. CF, JH, SS and KC performed all electrophysiological recordings. CF, JH, RC and NA performed all metabolic studies. CF, JH, SS, KC and EW performed data analysis for all electrophysiology and metabolic studies, while NA and ST analyzed data for metabolic studies. CF and EW created all figures and performed all statistical analyses. CF and EW generated the manuscript, while CF, JH, RC, KC and EW edited the final manuscript. EW, CF and JH designed the experiments.

FUNDING

This study was supported by National Institutes of Health PHS Grant DA024314 and intramural funding from Western University of Health Sciences.

SUPPLEMENTARY MATERIAL

The Supplementary Material for this article can be found online at: https://www.frontiersin.org/articles/10.3389/fnmol.2018.00214/full#supplementary-material

REFERENCES

Andrews, W. W., Advis, J. P., and Ojeda, S. R. (1981). The maturation of estradiol-negative feedback in female rats: evidence that the resetting of the hypothalamic "gonadostat" does not precede the first preovulatory surge of gonadotropins. *Endocrinology* 109, 2022–2031. doi: 10.1210/endo-109-6-2022

Appleyard, S. M., Hayward, M., Young, J. I., Butler, A. A., Cone, R. D., Rubinstein, M., et al. (2003). A role for endogenous β-endorphin in energy homeostasis. *Endocrinology* 144, 1753–1760. doi: 10.1210/en.2002-221096

Asarian, L., and Geary, N. (2006). Modulation of appetite by gonadal steroid hormones. *Philos. Trans. R. Soc. Lond. B Biol. Sci.* 361, 1251–1263. doi: 10.1098/rstb.2006.1860

Asarian, L., and Geary, N. (2013). Sex differences in the physiology of eating. *Am. J. Physiol. Regul. Integr. Comp. Physiol.* 305, R1215–R1267. doi: 10.1152/ajpregu.00446.2012

Balthasar, N., Coppari, R., McMinn, J., Liu, S. M., Lee, C. E., Tang, V., et al. (2004). Leptin receptor signaling in POMC neurons is required for normal body weight homeostasis. *Neuron* 42, 983–991. doi: 10.1016/j.neuron.2004.06.004

Belgardt, B. F., Okamura, T., and Brüning, J. C. (2009). Hormone and glucose signalling in POMC and AgRP neurons. *J. Physiol.* 587, 5305–5314. doi: 10.1113/jphysiol.2009.179192

Berthoud, H.-R. (2012). The neurobiology of food intake in an obesogenic environment. *Proc. Nutr. Soc.* 71, 478–487. doi: 10.1017/s0029665112000602

Borgquist, A., Meza, C., and Wagner, E. J. (2015a). Role of neuronal nitric oxide synthase in the estrogenic attenuation of cannabinoid-induced changes in energy homeostasis. *J. Neurophysiol.* 113, 904–914. doi: 10.1152/jn.00615.2014

Borgquist, A., Meza, C., and Wagner, E. J. (2015b). The role of AMP-activated protein kinase in the androgenic potentiation of cannabinoid-induced changes in energy homeostasis. *Am. J. Physiol. Endocrinol. Metab.* 308, E482–E495. doi: 10.1152/ajpendo.00421.2014

Brüning, J. C., Gautam, D., Burks, D. J., Gillette, J., Schubert, M., Orban, P. C., et al. (2000). Role of brain insulin receptor in control of body weight and reproduction. *Science* 289, 2122–2125. doi: 10.1126/science.289.5487.2122

Cardinal, P., André, C., Quarta, C., Bellocchio, L., Clark, S., Elie, M., et al. (2014). CB1 cannabinoid receptor in SF1-expressing neurons of the ventromedial hypothalamus determines metabolic responses to diet and leptin. *Mol. Metab.* 3, 705–716. doi: 10.1016/j.molmet.2014.07.004

Chiappini, F., Catalano, K. J., Lee, J., Peroni, O. D., Lynch, J., Dhaneshwar, A. S., et al. (2014). Ventromedial hypothalamus-specific Ptpn1 deletion exacerbates diet-induced obesity in female mice. *J. Clin. Invest.* 124, 3781–3792. doi: 10.1172/JCI68585

Chua, S. C. Jr., Chung, W. K., Wu-Peng, S., Zhang, Y., Liu, S.-M., Tartaglia, L., et al. (1996). Phenotypes of mouse *diabetes* and rat *fatty* due to mutations in the OB (leptin) receptor. *Science* 271, 994–996. doi: 10.1126/science.271.5251.994

Claret, M., Smith, M. A., Batterham, R. L., Selman, C., Choudhury, A. I., Fryer, L. G. D., et al. (2007). AMPK is essential for energy homeostasis regulation and glucose sensing by POMC and AgRP neurons. *J. Clin. Invest.* 117, 2325–2336. doi: 10.1172/jci31516

Clegg, D. J., Gotoh, K., Kemp, C., Wortman, M. D., Benoit, S. C., Brown, L. M., et al. (2011). Consumption of a high-fat diet induces central insulin resistance independent of adiposity. *Physiol. Behav.* 103, 10–16. doi: 10.1016/j.physbeh.2011.01.010

Clément, K., Vaisse, C., Lahlou, N., Cabrol, S., Pelloux, V., Cassuto, D., et al. (1998). A mutation in the human leptin receptor gene causes obesity and pituitary dysfunction. *Nature* 392, 398–401. doi: 10.1038/32911

Conde, K., Fabelo, C., Krause, W. C., Propst, R., Goethel, J., Fischer, D., et al. (2017). Testosterone rapidly augments retrograde endocannabinoid signaling in proopiomelanocortin neurons to suppress glutamatergic input from steroidogenic factor 1 neurons via upregulation of diacylglycerol lipase-α. *Neuroendocrinology* 105, 341–356. doi: 10.1159/000453370

Conde, K., Meza, C., Kelly, M. J., Sinchak, K., and Wagner, E. J. (2016). Estradiol rapidly attenuates ORL-1 receptor-mediated inhibition of proopiomelanocortin neurons via G_q-coupled, membrane-initiated signaling. *Neuroendocrinology* 103, 787–805. doi: 10.1159/000443765

Cone, R. D. (2006). Studies on the physiological functions of the melanocortin system. *Endocr. Rev.* 27, 736–749. doi: 10.1210/er.2006-0034

Cowley, M. A., Cone, R. D., Enriori, P., Louiselle, I., Williams, S. M., and Evans, A. E. (2003). Electrophysiological actions of peripheral hormones on melanocortin neurons. *Ann. N Y Acad. Sci.* 994, 175–186. doi: 10.1111/j.1749-6632.2003.tb03178.x

Dhillon, H., Zigman, J. M., Ye, C., Lee, C. E., McGovern, R. A., Tang, V., et al. (2006). Leptin directly activates SF1 neurons in the VMH and this action by leptin is required for normal body-weight homeostasis. *Neuron* 49, 191–203. doi: 10.1016/j.neuron.2005.12.021

Di Marzo, V., Goparahu, S. K., Wang, L., Liu, J., Bátkai, S., Járai, Z., et al. (2001). Leptin-regulated endocannabinoids are involved in maintaining food intake. *Nature* 410, 822–825. doi: 10.1038/35071088

Diano, S., Naftolin, F., and Horvath, T. L. (1997). Gonadal steroids target AMPA glutamate receptor-containing neurons in the rat hypothalamus, septum and amygdala: a morphological and biochemical study. *Endocrinology* 138, 778–789. doi: 10.1210/en.138.2.778

Diaz, S., Farhang, B., Hoien, J., Stahlman, M., Adatia, N., Cox, J. M., et al. (2009). Sex differences in the cannabinoid modulation of appetite, body temperature and neurotransmission at POMC synapses. *Neuroendocrinology* 89, 424–440. doi: 10.1159/000191646

Eckel, L. A., Houpt, T. A., and Geary, N. (2002). Estradiol treatment increases CCK-induced c-Fos expression in the brains of ovariectomized rats. *Am. J. Physiol. Regul. Integr. Comp. Physiol.* 283, R1378–R1385. doi: 10.1152/ajpregu.00300.2002

Estrada, M., Espinosa, A., Müller, M., and Jaimovich, E. (2003). Testosterone stimulates intracellular calcium release and mitogen-activated protein kinases via a G protein-coupled receptor in skeletal muscle cells. *Endocrinology* 144, 3586–3597. doi: 10.1210/en.2002-0164

Fadel, J., Bubser, M., and Deutch, A. Y. (2002). Differential activation of orexin neurons by antipsychotic drugs associated with weight gain. *J. Neurosci.* 22, 6742–6746. doi: 10.1523/JNEUROSCI.22-15-06742.2002

Farhang, B., Pietruszewski, L., Lutfy, K., and Wagner, E. J. (2010). The role of the NOP receptor in regulating food intake, meal pattern, and the excitability of proopiomelanocortin neurons. *Neuropharmacology* 59, 190–200. doi: 10.1016/j.neuropharm.2010.05.007

Freund, T. F., Katona, I., and Piomelli, D. (2003). Role of endogenous cannabinoids in synaptic signaling. *Physiol. Rev.* 83, 1017–1066. doi: 10.1152/physrev.00004.2003

Gallo, R. V., and Bona-Gallo, A. (1985). Lack of ovarian steroid negative feedback on pulsatile luteinizing hormone release between estrus and diestrous day 1 in the rat estrous cycle. *Endocrinology* 116, 1525–1528. doi: 10.1210/endo-116-4-1525

Geary, N., and Asarian, L. (1999). Cyclic estradiol treatment normalizes body weight and test meal size in ovariectomized rats. *Physiol. Behav.* 67, 141–147. doi: 10.1016/s0031-9384(99)00060-8

Goldman, J. M., Murr, A. S., and Cooper, R. L. (2007). The rodent estrous cycle: characterization of vaginal cytology and its utility in toxicological studies. *Birth Defects Res. B Dev. Reprod. Toxicol.* 80, 84–97. doi: 10.1002/bdrb.20106

Gomez, J. L., Bonaventura, J., Lesniak, W., Mathews, W. B., Sysa-Shah, P., Rodriguez, L. A., et al. (2017). Chemogenetics revealed: DREADD occupancy and activation via converted clozapine. *Science* 357, 503–507. doi: 10.1126/science.aan2475

Hawke, Z., Ivanov, T. R., Bechtold, D. A., Dhillon, H., Lowell, B. B., and Luckman, S. M. (2009). PACAP neurons in the hypothalamic ventromedial nucleus are targets of central leptin signaling. *J. Neurosci.* 29, 14828–14835. doi: 10.1523/JNEUROSCI.1526-09.2009

Hill, J. W., Williams, K. W., Ye, C., Luo, J., Balthasar, N., Coppari, R., et al. (2008). Acute effects of leptin require PI3K signaling in hypothalamic proopiomelanocortin neurons in mice. *J. Clin. Invest.* 118, 1796–1805. doi: 10.1172/JCI32964

Ibrahim, N., Bosch, M. A., Smart, J. L., Qiu, J., Rubinstein, M., Rønnekleiv, O. K., et al. (2003). Hypothalamic proopiomelanocortin neurons are glucose responsive and express KATP channels. *Endocrinology* 144, 1331–1340. doi: 10.1210/en.2002-221033

Jamshidi, N., and Taylor, D. A. (2001). Anandamide administration into the ventromedial hypothalamus stimulates appetite in rats. *Br. J. Pharmacol.* 134, 1151–1154. doi: 10.1038/sj.bjp.0704379

Jo, Y.-H., Chen, Y.-J. L., Chua, S. C. Jr., Talmage, D. A., and Role, L. W. (2005). Integration of endocannabinoid and leptin signaling in an

appetite-related neural circuit. *Neuron* 48, 1055–1066. doi: 10.1016/j.neuron.2005.10.021

Kellert, B. A., Nguyen, M. C., Nguyen, C., Nguyen, Q. H., and Wagner, E. J. (2009). Estrogen rapidly attenuates cannabinoid-induced changes in energy homeostasis. *Eur. J. Pharmacol.* 622, 15–24. doi: 10.1016/j.ejphar.2009.09.001

Kim, J., Li, Y., and Watkins, B. A. (2013). Fat to treat fat: emerging relationship between dietary PUFA, endocannabinoids, and obesity. *Prostaglandins Other Lipid Mediat.* 104–105, 32–41. doi: 10.1016/j.prostaglandins.2012.11.005

Kirkham, T. C., Williams, C. M., Fezza, F., and Di Marzo, V. (2002). Endocannabinoid levels in rat limbic forebrain and hypothalamus in relation to fasting, feeding and satiation: stimulation of eating by 2-arachidonyl glycerol. *Br. J. Pharmacol.* 136, 550–557. doi: 10.1038/sj.bjp.0704767

Klöckener, T., Hess, S., Belgardt, B. F., Paeger, L., Verhagen, L. A. W., Husch, A., et al. (2011). High-fat feeding promotes obesity via insulin receptor/PI3K-dependent inhibition of SF-1 VMH neurons. *Nat. Neurosci.* 14, 911–918. doi: 10.1038/nn.2847

Koch, M., Varela, L., Kim, J. G., Kim, J. D., Hernández-Nuño, F., Simonds, S. E., et al. (2015). Hypothalamic POMC neurons promote cannabinoid-induced feeding. *Nature* 519, 45–50. doi: 10.1038/nature14260

Kola, B., Farkas, I., Christ-Crain, M., Wittmann, G., Lolli, F., Amin, F., et al. (2008). The orexigenic effect of ghrelin is mediated through central activation of the endogenous cannabinoid system. *PLoS One* 3:e1797. doi: 10.1371/journal.pone.0001797

Krashes, M. J., Shah, B. P., Madara, J. C., Olson, D. P., Strochlic, D. E., Garfield, A. S., et al. (2014). An excitatory paraventricular nucleus to AgRP neuron circuit that drives hunger. *Nature* 507, 238–242. doi: 10.1038/nature12956

Lagrange, A. H., Ronnekleiv, O. K., and Kelly, M. J. (1994). The potency of μ-opioid hyperpolarization of hypothalamic arcuate neurons is rapidly attenuated by 17β-estradiol. *J. Neurosci.* 14, 6196–6204. doi: 10.1523/JNEUROSCI.14-10-06196.1994

Lagrange, A. H., Wagner, E. J., Rønnekleiv, O. K., and Kelly, M. J. (1996). Estrogen rapidly attenuates a $GABA_B$ response in hypothalamic neurons. *Neuroendocrinology* 64, 114–123. doi: 10.1159/000127106

Lindberg, D., Chen, P., and Li, C. (2013). Conditional viral tracing reveals that steroidogenic factor 1-positive neurons of the dorsomedial subdivision of the ventromedial hypothalamus project to the autonomic centers of the hypothalamus and hindbrain. *J. Comp. Neurol.* 521, 3167–3190. doi: 10.1002/cne.23338

Loss, E. S., Jacobus, A. P., and Wassermann, G. F. (2011). Rapid signaling responses in Sertoli cells membranes induced by follicle stimulating hormone and testosterone: calcium inflow and electrophysiological changes. *Life Sci.* 89, 577–583. doi: 10.1016/j.lfs.2011.05.017

Lucas, E. A., Lightfoot, S. A., Hammond, L. J., Devareddy, L., Khalil, D. A., Daggy, B. P., et al. (2003). Soy isoflavones prevent ovariectomy-induced atherosclerotic lesions in Golden Syrian hamster model of postmenopausal hyperlipidemia. *Menopause* 10, 314–321. doi: 10.1097/01.gme.0000051509.84118.fd

Majdic, G., Young, M., Gomez-Sanchez, E., Anderson, P., Szczepaniak, L. S., Dobbins, R. L., et al. (2002). Knockout mice lacking steroidogenic factor 1 are a novel genetic model of hypothalamic obesity. *Endocrinology* 143, 607–614. doi: 10.1210/en.143.2.607

McLean, A. C., Valenzuela, N., Fai, S., and Bennett, S. A. L. (2012). Performing vaginal lavage, crystal violet staining and vaginal cytological evaluation for mouse estrous cycle staging identification. *J. Vis. Exp.* 67:e4389. doi: 10.3791/4389

Mela, V., Vargas, A., Meza, C., Kachani, M., and Wagner, E. J. (2016). Modulatory influences of estradiol and other anorexigenic hormones on metabotropic, Gi/o-coupled receptor function in the hypothalamic control of energy homeostasis. *J. Steroid Biochem. Mol. Biol.* 160, 15–26. doi: 10.1016/j.jsbmb.2015.07.014

Mitsuhashi, K., Senmaru, T., Fukuda, T., Yamazaki, M., Shinomiya, K., Ueno, M., et al. (2016). Testosterone stimulates glucose uptake and GLUT4 translocation through LKB1/AMPK signaling in 3T3–L1 adipocytes. *Endocrine* 51, 174–184. doi: 10.1007/s12020-015-0666-y

Owen, J. A. Jr. (1975). Physiology of the menstrual cycle. *Am. J. Clin. Nutr.* 28, 333–338. doi: 10.1093/ajcn/28.4.333

Parton, L. E., Ye, C. P., Coppari, R., Enriori, P., Choi, B., Zhang, C.-Y., et al. (2007). Glucose sensing by POMC neurons regulates glucose homestasis and is impaired in obesity. *Nature* 449, 228–232. doi: 10.1038/nature06098

Pinto, S., Roseberry, A. G., Liu, H., Diano, S., Shanabrough, M., Cai, X., et al. (2004). Rapid rewiring of arcuate nucleus feeding circuits by leptin. *Science* 304, 110–115. doi: 10.1126/science.1089459

Qiu, J., Bosch, M. A., Meza, C., Navarro, U.-V., Nestor, C. C., Wagner, E. J., et al. (2018). Estradiol protects proopiomelanocortin neurons against insulin resistance. *Endocrinology* 159, 647–664. doi: 10.1210/en.2017-00793

Qiu, J., Bosch, M. A., Tobias, S. C., Grandy, D. K., Scanlan, T. S., Rønnekleiv, O. K., et al. (2003). Rapid signaling of estrogen in hypothalamic neurons involves a novel G-protein-coupled estrogen receptor that activates protein kinase C. *J. Neurosci.* 23, 9529–9540. doi: 10.1523/JNEUROSCI.23-29-09529.2003

Qiu, J., Fang, Y., Rønnekleiv, O. K., and Kelly, M. J. (2010). Leptin excites proopiomelanocortin neurons via activation of TRPC channels. *J. Neurosci.* 30, 1560–1565. doi: 10.1523/JNEUROSCI.4816-09.2010

Qiu, J., Zhang, C., Borgquist, A., Nestor, C. C., Smith, A. W., Bosch, M. A., et al. (2014). Insulin excites anorexigenic proopiomelanocortin neurons via activation of canonical transient receptor potential channels. *Cell Metab.* 19, 682–693. doi: 10.1016/j.cmet.2014.03.004

Ravinet-Trillou, C., Arnone, M., Delgorge, C., Gonalons, N., Keane, P., Maffrand, J.-P., et al. (2003). Anti-obesity effect of SR141716, a CB1 receptor antagonist, in diet-induced obese mice. *Am. J. Physiol. Regul. Integr. Comp. Physiol.* 284, R345–R353. doi: 10.1152/ajpregu.00545.2002

Scherer, T., O'Hare, J., Diggs-Andrews, K., Schweiger, M., Cheng, B., Lindtner, C., et al. (2011). Brain insulin controls adipose tissue lipolysis and lipogenesis. *Cell Metab.* 13, 183–194. doi: 10.1016/j.cmet.2011.01.008

Schreiber, A. L., Arceneaux, K. P. III., Malbrue, R. A., Mouton, A. J., Chen, C. S., Bench, E. M., et al. (2016). The effects of high fat diet and estradiol on hypothalamic prepro-QRFP mRNA expression in female rats. *Neuropeptides* 58, 103–109. doi: 10.1016/j.npep.2016.01.004

Segal, J. P., Stallings, N. R., Lee, C. E., Zhao, L., Socci, N., Viale, A., et al. (2005). Use of laser-capture microdissection for the identification of marker genes for the ventromedial hypothalamic nucleus. *J. Neurosci.* 25, 4181–4188. doi: 10.1523/JNEUROSCI.0158-05.2005

Soria-Gómez, E., Bellocchio, L., Reguero, L., Lepousez, G., Martin, C., Bendahmane, M., et al. (2014). The endocannabinoid system controls food intake via olfactory processes. *Nat. Neurosci.* 17, 407–415. doi: 10.1038/nn.3647

Sternson, S. M., Shepherd, G. M. G., and Friedman, J. M. (2005). Topographic mapping of VMH-arcuate nucleus microcirsuits and their reoganization by fasting. *Nat. Neurosci.* 8, 1356–1363. doi: 10.1038/nn1550

Stricker, E. M. (1978). Hyperphagia. *N. Engl. J. Med.* 298, 1010–1013. doi: 10.1056/NEJM197805042981809

Tang, S. L., Tran, V., and Wagner, E. J. (2005). Sex differences in the cannabinoid modulation of an A-type K^+ current in neurons of the mammalian hypothalamus. *J. Neurophysiol.* 94, 2983–2986. doi: 10.1152/jn.01187.2004

Verty, A. N. A., McGregor, I. S., and Mallet, P. E. (2005). Paraventricular hypothalamic CB_1 cannabinoid receptors are involved in the feeding stimulatory effects of Δ^9-tetrahydrocannabinol. *Neuropharmacology* 49, 1101–1109. doi: 10.1016/j.neuropharm.2005.03.025

Vicencio, J. M., Ibarra, C., Estrada, M., Chiong, M., Soto, D., Parra, V., et al. (2006). Testosterone induces an intracellular calcium increase by a nongenomic mechanism in cultured rat cardiac myocytes. *Endocrinology* 147, 1386–1395. doi: 10.1210/en.2005-1139

Vong, L., Ye, C., Yang, Z., Choi, B., Chua, S. Jr., and Lowell, B. B. (2011). Leptin action of GABAergic neurons prevents obesity and reduces inhibitory tone onto POMC neurons. *Neuron* 71, 142–154. doi: 10.1016/j.neuron.2011.05.028

Wagner, E. J. (2016). Sex differences in cannabinoid-regulated biology: a focus on energy homeostasis. *Front. Neuroendocrinol.* 40, 101–109. doi: 10.1016/j.yfrne.2016.01.003

Washburn, N., Borgquist, A., Wang, K., Jeffery, G. S., Kelly, M. J., and Wagner, E. J. (2013). Receptor subtypes and signal transduction mechanisms contributing to the estrogenic attenuation of cannabinoid-induced changes in energy homeostasis. *Neuroendocrinology* 97, 160–175. doi: 10.1159/000338669

Wei, W., Pham, K., Gammons, J. W., Sutherland, D., Liu, Y., Smith, A., et al. (2015). Diet composition, not calorie intake, rapidly alters intrinsic excitability of hypothalamic AgRP/NPY neurons in mice. *Sci. Rep.* 5:16810. doi: 10.1038/srep16810

Weston-Green, K., Huang, X.-F., and Deng, C. (2012). Alterations to melanocortinergic, GABAergic and cannabinoid neurotransmission associated with olanzapine-induced weight gain. *PLoS One* 7:e33548. doi: 10.1371/journal.pone.0033548

Wilson, C., Contreras-Ferrat, A., Venegas, N., Osorio-Fuentealba, C., Pávez, M., Montoya, K., et al. (2013). Testosterone increases GLUT4-dependent glucose uptake in cardiomyocytes. *J. Cell. Physiol.* 228, 2399–2407. doi: 10.1002/jcp.24413

Wilson, J. L., and Enriori, P. J. (2015). A talk between fat tissue, gut, pancreas and brain to control body weight. *Mol. Cell. Endocrinol.* 418, 108–119. doi: 10.1016/j.mce.2015.08.022

Conflict of Interest Statement: The authors declare that the research was conducted in the absence of any commercial or financial relationships that could be construed as a potential conflict of interest.

frontiers in Molecular Neuroscience

MINI REVIEW
published: 31 July 2018
doi: 10.3389/fnmol.2018.00266

Sex Differences in Synaptic Plasticity: Hormones and Beyond

*Molly M. Hyer, Linda L. Phillips and Gretchen N. Neigh**

Department of Anatomy and Neurobiology, Virginia Commonwealth University, Richmond, VA, United States

Notable sex-differences exist between neural structures that regulate sexually dimorphic behaviors such as reproduction and parenting. While anatomical differences have been well-characterized, advancements in neuroimaging and pharmacology techniques have allowed researchers to identify differences between males and females down to the level of the synapse. Disparate mechanisms at the synaptic level contribute to sex-specific neuroplasticity that is reflected in sex-dependent behaviors. Many of these synaptic differences are driven by the endocrine system and its impact on molecular signaling and physiology. While sex-dependent modifications exist at baseline, further differences emerge in response to stimuli such as stressors. While some of these mechanisms are unifying between sexes, they often have directly opposing consequences in males and females. This variability is tied to gonadal steroids and their interactions with intra- and extra-cellular signaling mechanisms. This review article focuses on the various mechanisms by which sex can alter synaptic plasticity, both directly and indirectly, through steroid hormones such as estrogen and testosterone. That sex can drive neuroplasticity throughout the brain, highlights the importance of understanding sex-dependent neural mechanisms of the changing brain to enhance interpretation of results regarding males and females. As mood and stress responsivity are characterized by significant sex-differences, understanding the molecular mechanisms that may be altering structure and function can improve our understanding of these behavioral and mental characteristics.

Keywords: sex differences, synaptic plasticity, hormones, mood disorders, stress response

OPEN ACCESS

Edited by:
Jordan Marrocco,
Rockefeller University, United States

Reviewed by:
Brian R. Christie,
University of Victoria, Canada
Rebecca M. Shansky,
Independent Researcher, Boston, MA, United States

****Correspondence:***
Gretchen N. Neigh
gretchen.mccandless@vcuhealth.org

Received: *26 April 2018*
Accepted: *13 July 2018*
Published: *31 July 2018*

Citation:
Hyer MM, Phillips LL and Neigh GN (2018) Sex Differences in Synaptic Plasticity: Hormones and Beyond. Front. Mol. Neurosci. 11:266. doi: 10.3389/fnmol.2018.00266

INTRODUCTION

Sex differences in behavior can be observed through both scientific inquiry and casual observations in social settings. Although gender roles have been proposed to account for some of the variability in behavior observed between males and females (Ruble et al., 1993; Aggen et al., 2011), behavioral differences extend beyond socially defined roles to physiological differences and certain well-established sexually dimorphic neural structures. Sex differences in neural structures have been documented in humans (Swaab and Fliers, 1985; Allen et al., 1989; Ruigrok et al., 2014; Catenaccio et al., 2016), but also in animals that do not have the social constructs of humans that define genders, including rodents (Gorski et al., 1978; Campi et al., 2013) and avian species (Nottebohm and Arnold, 1976; Balthazart et al., 2009). Some of the most notable sex differences in neural structure are evident in the hypothalamus of the mammalian brain (Gorski et al., 1978) and the song region in the avian brain (Nottebohm and Arnold, 1976). As these brain regions drive sex-specific reproductive-related behaviors, these findings are somewhat unsurprising.

However, sex differences in neural structures extend beyond brain regions directly involved in reproduction and include structures linked to stress responsivity (for review see McEwen, 2010; Bekhbat and Neigh, 2018) and mood (for review see Bangasser and Valentino, 2014; Gobinath et al., 2015). Over the last three decades, technology and experimental design have advanced the wealth of knowledge regarding sex differences in the brain. Improved imaging techniques along with the elegant use of cell culture and pharmaceutical treatments, have further elucidated sex differences in structure (Phan et al., 2012; Farrell et al., 2015), connectivity (Ingalhalikar et al., 2014), signaling (Skucas et al., 2013; Harte-Hargrove et al., 2015), responsivity (Garrett and Wellman, 2009), and plasticity (Gould et al., 1990; Parducz et al., 2006). Sex differences are evident in adult neurogenesis, the birth of new neurons in adulthood (Ormerod et al., 2004; Tanapat et al., 2005; Mak and Weiss, 2010; Hyer et al., 2017). However, while sex-dependent modifications in adult neurogenesis can have a significant impact on synaptic plasticity (Galea et al., 2006; Livneh and Mizrahi, 2012; Vivar et al., 2016), that discussion is beyond the scope of this mini-review (see: Kempermann et al., 2015). Although these potential mechanisms are important to the understanding of sex differences in neural function, this mini-review focuses specifically on mammalian sex-differences in synaptic plasticity that may contribute to sex differences in neural function.

SEX DIFFERENCES IN STRUCTURAL PLASTICITY

Spine density, sites for synaptic connections (Holtmaat and Svoboda, 2009), and dendritic arborization reflect changes in existing cell structure that can alter neural function and behavioral outcomes. Chronic stress results in differential patterns of dendritic remodeling in the hippocampus (Galea et al., 1997), prefrontal cortex (PFC; Garrett and Wellman, 2009; Farrell et al., 2015) and basolateral amygdala (BLA, Vyas et al., 2002). Clinical neuropsychiatric disorders related to stress exposure, for instance depression (reviewed in Qiao et al., 2016) and anxiety (reviewed in Leuner and Shors, 2013), occur concomitantly with changes in dendritic structure. The prevalence and incidence of depression and anxiety differ between the sexes (Piccinelli and Wilkinson, 2000; Naninck et al., 2011) and may be, in part, driven by sex-dependent dendritic and synaptic plasticity. Sex-differences have been noted in multiple dimensions of neuronal plasticity including neuron structure, dendritic arborization and spine density (Garrett and Wellman, 2009; Farrell et al., 2015) and sex steroids are sufficient to alter many of these parameters (**Figure 1**).

Females

The influence of sex steroids on structural plasticity appears to be more pronounced in females, likely due to cyclical fluctuations in sex steroids. Concentrations of estrogens and progesterone fluctuate across the estrous cycle with peak levels appearing during proestrus and lower levels evident during estrus, metestrus and diestrus (Butcher et al., 1974). The human menstrual cycle shows fluctuations in ovarian steroids as well, with estrogen being lowest early on, then peaking at the end of the follicular phase to initiate ovulation. This peak is followed by a gradual surge in progesterone and a slight rise in estrogen throughout the luteal phase before both drop at the end of the cycle (Protopopescu et al., 2008; Catenaccio et al., 2016). Alterations in spine density are evident in response to changes in ovarian steroid levels across the estrous cycle in female rats. Spine density in area CA1 of the hippocampus peaks during proestrus when ovarian steroids are highest, then declines through the later stages (Woolley et al., 1990). Females generally have double the spine density of males, yet when they are ovariectomized no sex difference is evident, suggesting that the sex difference may be attributable to the activational effects of sex steroids (Gould et al., 1990; Shors et al., 2001). Ovariectomized females display a dramatic decline in spine density in the CA1 region of the hippocampus—a deficit which is reversed with estradiol or progesterone treatment in as low as 40 min (Gould et al., 1990; MacLusky et al., 2005). These changes in spine density appear to have functional implications, such that ovariectomized mice treated with low-dose estradiol demonstrate both improved learning and increased spine density in the CA1 region (Phan et al., 2012).

Sex differences in spine density are not limited to the hippocampus. For instance, female rats have more large spines in the nucleus accumbens than males (Forlano and Woolley, 2010). Sex differences in spine density have also been noted in the BLA, but somewhat surprisingly, testosterone, and not estradiol alone, appears to mediate these effects (Bender et al., 2017). The aromatase enzyme cytochrome P450 (AROM), present throughout the male and female BLA, is capable of converting testosterone to estradiol (Zhao et al., 2007). Administration of letrozole, an AROM inhibitor, to the BLA results in decreased spine density and eliminates long term potentiation (LTP) in females but not males (Bender et al., 2017). Females have greater excitatory synaptic input in the BLA compared to males, specifically in neurons located in the lateral and basal nuclei. The predominance of each nuclei shifts across the estrous cycle driving the balance of excitation-inhibition which is reflected through changes in BLA-dependent emotional memory across the estrous cycle (Blume et al., 2017). Collectively, these findings highlight the significant impact of sex steroids on the regulation of physiology and spine density in females; however, the following section discusses the impact of sex steroids on spine density that is also evident in males.

Males

Although males do not produce estrogen or progesterone in as robust of concentrations as females, both sex steroids are present in males. The main source of estrogen in males is the conversion of testosterone to estrogen via aromatase. Gonadectomy in males reduces spine density in the CA1 region of the hippocampus, and this effect can be reversed through treatment with either testosterone or dihydrotestosterone (DHT). Based on the influence of estradiol demonstrated in females, one may hypothesize that estradiol would be

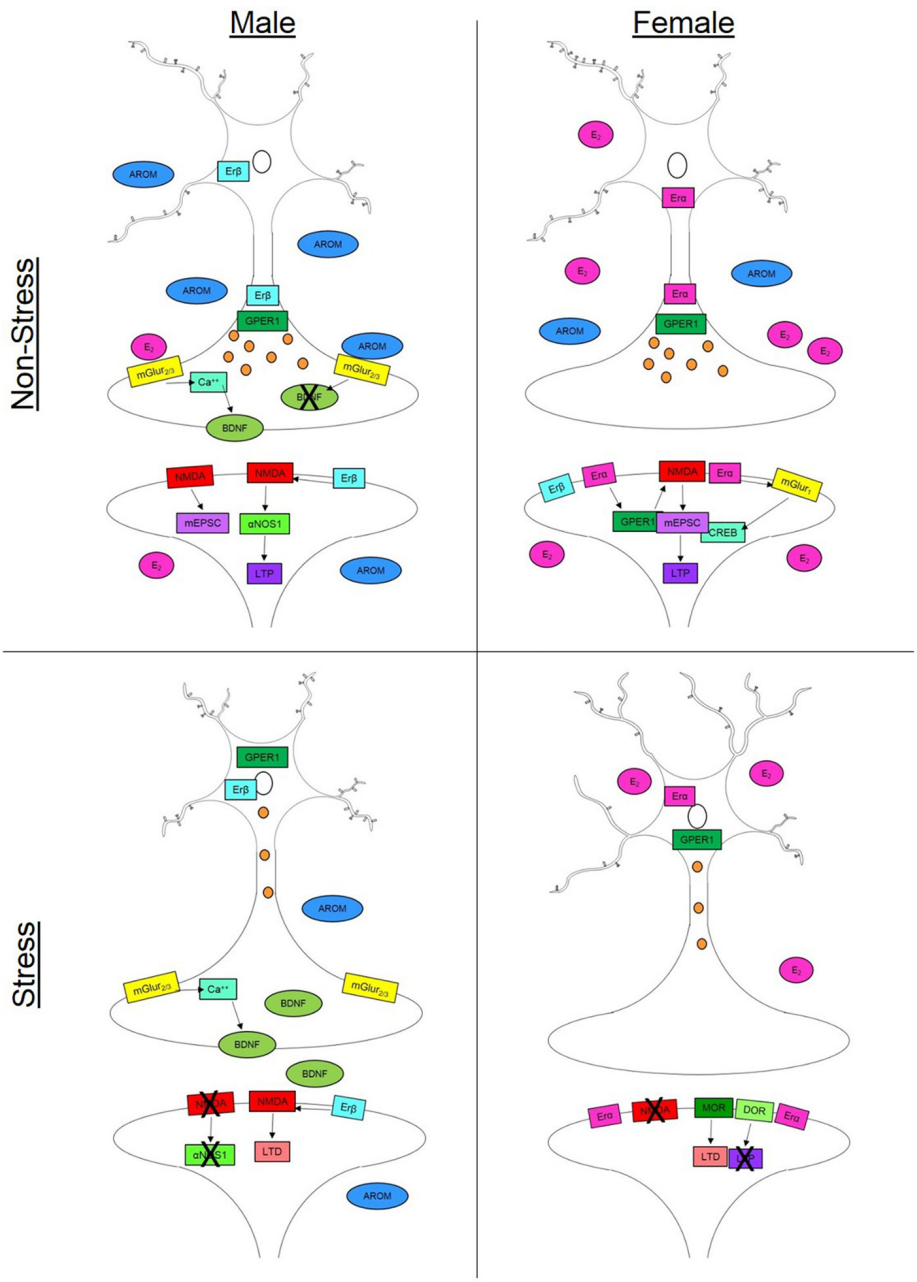

FIGURE 1 | Synaptic plasticity is driven by a variety of sex-specific signaling mechanisms in males and females that can vary throughout the brain. In non-stress conditions, females (top right) have increased spine density compared to males in the hippocampus (top left) but decreased dendritic length in the prefrontal cortex (PFC). This increase in spine density in the female hippocampus can occur via multiple estradiol (E_2)-dependent signaling mechanisms. Binding with estrogen receptor alpha (Erα) or the G-protein coupled estrogen receptor (GPER) can initiate N-methyl-D-aspartate (NMDA) channel signaling increasing mini excitatory postsynaptic currents (mEPCS) which ultimately drive long term potentiation (LTP). Estradiol can also act through Erα on metabotropic glutamate receptor 1 (mGluR1) which in turn drives cAMP response element-binding protein (CREB) phosphorylation in females. In males, NMDA activity is driven by activation of estrogen receptor beta (Erβ). This signaling cascade includes α nitric oxide synthase-1 (αNOS1) which drives LTP in males but not females. In the male presynaptic neuron, E_2-dependent activation of $mGluR_{2/3}$ initiates a calcium (Ca^{++}) signaling cascade which facilitates the release of brain derived neurotrophic factor (BDNF). Testosterone (AROM) can alter the release of BDNF and other aspects of synaptic plasticity in the baso lateral amygdala. In stress conditions, males (bottom left) show decreased dendritic branching in the PFC but slight increases in spine density in the hippocampus. Possibly accounting for this increase is the reduction in circulating steroid hormones which can allow for increased BDNF release in males. Females (bottom right) on the other hand, experience increased dendritic length in the PFC and hippocampus as well as a suppression of spine growth in the hippocampus following stress. Females exhibit changes in opiate receptor (OR) signaling that can drive long term depression (LTD)—specifically through mu- and delta-OR activity. In the presynaptic neuron, axonal labeling of Erα and GPER1 facilitates vesicle transmission down the axon in both males and females. However, in stress conditions (bottom panels), both receptors migrate to the nucleus thereby reducing vesicle trafficking.

equally efficacious in males; however, direct administration of estradiol is not sufficient to restore spine density in gonadectomized males (Leranth et al., 2003). Furthermore, testosterone appears to inhibit LTP and dendritic sprouting in the male hippocampus. Gonadectomy results in increased LTP and dendritic sprouting in CA3 mossy fibers which is dependent on increased brain derived neurotrophic factor (BDNF) signaling through the tyrosine kinase B (TrKB) receptor (Skucas et al., 2013). BDNF plays a well-known role in synaptic plasticity (Lu et al., 2014) and deficits in BDNF signaling in response to stress can be sex-dependent (Yamaura et al., 2013). Treatment with testosterone eliminated both the castration-induced increase in LTP and dendritic sprouting, suggesting that testosterone can act to inhibit BDNF-dependent structural plasticity (Skucas et al., 2013). Taken together, these data suggest that estradiol and testosterone regulate spine density in a sex- and region- dependent manner and that BDNF is a likely target mechanism for these hormones to modify synaptic connections.

Sex Differences in Structural Response to Stress

Dendritic arborization and spine density are both modified by stress and are altered in individuals living with mood disorders. Males overall have more dendritic material than females (Juraska et al., 1985); however, females appear to have more dramatic shifts in dendritic architecture following mildly stressful experiences. For instance, females show increased dendritic length in the dentate gyrus (DG) following the mild stressor of exposure to a novel environment compared to males (Juraska et al., 1985). Interestingly, chronic stress will increase the length and complexity of dendritic arbors in females, possibly making them vulnerable to over-excitation (Farrell et al., 2015), but results in a reduction in dendritic arbors in males in the PFC. The increase is estradiol-dependent as ovariectomized female rats do not demonstrate the stress-induced increase in arborization (Garrett and Wellman, 2009). Chronic stress can also differentially drive subregion-specific plasticity. The dorsal hippocampus demonstrates enhanced markers of plasticity, specifically increased neuropeptide Y and ΔFOSB while the ventral region shows a decline in these same markers following chronic unpredictable stress (Hawley and Leasure, 2012). Further complicating our ability to understand sex differences in dendritic responses to stress, is the observation that the type of stressor impacts the outcome. Unlike chronic stress, acute foot shock generates the opposite effect on spine density in the hippocampus. Following acute foot shock, males have increased spine density in area CA1 of the hippocampus while females in diestrus demonstrate a reduction in dendritic spine density (Shors et al., 2001). Interestingly, regardless of the directionality, both males and females show no changes in spine density in response to acute stress if N-methyl-D-aspartate (NMDA) receptors are antagonized (Shors et al., 2004), suggesting a potentially unifying mechanism for the disparate consequence of stress. It is evident in female hippocampal slices that estradiol-induced LTP is dependent on an increase in the ratio of NMDA transmission to AMPA transmission (Smith and McMahon, 2005). Female rats that underwent inescapable shock to induce learned helplessness can be protected against the stress-induced loss of spines and LTP if treated with estradiol (Bredemann and McMahon, 2014). Thus, function of the hormone-dependent modifications of the NMDA receptor can dramatically alter the outcome of synaptic plasticity following stress.

SEX DIFFERENCES IN MECHANISMS OF SYNAPTIC PLASTICITY

Estrogen Receptors

While changes in spine density and dendritic arborization are evident with cyclic fluctuations of hormones, the mechanisms that drive this structural plasticity are often at the molecular level. As estrogen has a significant impact on structural plasticity, much attention has been given to the mechanisms by which estradiol can modify neuron structure. Estrogens bind with estrogen receptor (Er) α, Erβ and G-protein coupled estrogen receptor 1 (GPER1). These receptors are localized throughout the brain of males and females providing estradiol a site of action to modify neuronal structure (Weiland et al., 1997). GPER1 is located throughout hippocampal neurons along the axon, dendritic tree, spine shafts, and is associated with vesicles in the terminal endings. Although anatomical distribution of GPER1 is similar between males and females, increased circulating estrogen concentrations in females leads to elevated axonal labeling of GPER1 in females as compared to males, suggesting alterations in vesicle transport with increased estradiol levels (Waters et al., 2015).

Unlike GPER1, ERα and ERβ exhibit more notable differences based on sex. Extranuclear ERα distribution in CA1 and CA3 at the ultrastructure level is primarily localized to the dendritic spine heads and at the base of spine shafts. Conversely, ERβ is localized to the soma and dendrite membranes (Mitterling et al., 2010). Regardless of circulating estrogen concentrations, females have higher densities of ERα than males (Shughrue et al., 1997; Mitterling et al., 2010), but ERα-immunoreactivity within females is sensitive to sex steroids concentrations. During diestrus, when circulating estrogen is at a comparatively low concentration, females demonstrate more ERα-immunoreactivity (ir) and ERβ-ir than that observed in proestrus females (Milner et al., 2001; Mitterling et al., 2010). Overall, elevated circulating concentrations of estradiol pair with reduced extranuclear-ir profiles of ERα and ERβ as compared to periods of low estrogen concentrations which are concomitant with elevations in extranuclear-ir (Mitterling et al., 2010). The shifting patterns of Er localization briefly summarized here, suggest a potential mechanism by which neuron structure could be differentially modified across the estrous cycle and lead to hormone-dependent plasticity in females.

While much of the benefits of estradiol are conferred to females, males also experience increased synaptic plasticity with estradiol signaling. Estradiol can drive potentiation of glutamatergic synapses in males as well as females

(Teyler et al., 1980; Wong and Moss, 1992). However, the mechanisms by which the potentiation is initiated are sex-dependent. Estradiol elicits higher amplitude miniature postsynaptic excitatory currents (mEPSCs) in a synapse specific manner (Oberlander and Woolley, 2016). However, while similar results are evident in males, use of ER-selective agonists has identified a sex-dependent mechanism. In males, the potentiation is driven by ERβ while in females it is driven by GPER1. On the other hand, presynaptic potentiation is initiated by ERα in males but ERβ in females (Oberlander and Woolley, 2016).

Estradiol's ability to alter function through Erα and Erβ (Walf and Frye, 2005; Boulware et al., 2013) is partially dependent on activation of metabotropic glutamate receptor 1a (mGluR1a; Boulware et al., 2013). The differing effects of Erα and Erβ are a result of receptor differences- specifically, differing N-terminal regions (Tremblay et al., 1997). This discrepancy results in activation of separate metabotropic glutamate receptors. Signaling through Erα activates mGluR1 which in turn drives cAMP response element-binding protein (CREB) phosphorylation. Erβ activation triggers mGluR2/3 signaling resulting in a downregulation of calcium mediated CREB phosphorylation (Boulware et al., 2005). It is also possible that Erβ activation may result in disinhibition of BDNF-releasing neurons (Blurton-Jones and Tuszynski, 2002) allowing for increased BDNF signaling to drive synaptic plasticity. As Erβ and BDNF are more prevalent in male synaptic plasticity, while Erα appears to drive female-specific plasticity, this may be a primary pathway for sex-dependent synaptic plasticity, allowing for rapid, non-genomic effects of estradiol on hippocampal plasticity (for review see Walf and Frye, 2006). Overall, these data show sex-specific mechanisms by which estradiol interacts with ERα and ERβ to mediate synaptic plasticity.

NMDA Receptor Signaling

In addition to direct action through its own receptors, estradiol can modify NMDA receptor signaling to drive sex-specific plasticity. In female rats, estrogen-dependent increases in spine density are NMDA-dependent (Woolley and Mcewen, 1994). In gonadectomized females, estradiol benzoate treatment increases NMDA binding in area CA1 of the hippocampus compared to males. However, in males, baseline NMDAr binding is elevated in the DG compared to females (Romeo et al., 2005a). These findings suggest that estradiol's interaction with NMDA receptors is dependent on the organizational effects of steroid signaling. DHT treatment to the hippocampus will increase NMDAr binding density in castrated male rats (Romeo et al., 2005b). Both testosterone and DHT have been shown to increase spinogenesis in males (Kovacs et al., 2003; Leranth et al., 2004) suggesting that activation of NMDA receptors by testosterone or its metabolites is necessary for spinogenesis in males while the same is true for estrogen in females. Furthermore, these sex-dependent mechanism may be exacerbated via cholinergic signaling as estradiol acts on NMDA receptors via cholinergic mechanisms in females but not in males (Volosin et al., 2006). Thus, NMDA receptor signaling is a necessary step for synaptic plasticity in both males and females, especially in response to stress (Shors et al., 2004), however the binding affinity and downstream effects are sexually dimorphic further complicating the interpretation of NMDA-dependent effects on synaptic plasticity.

Nitric Oxide

Like its relationship with NMDA receptors, estrogen can act on synaptic plasticity indirectly through nitric oxide in a sex-dependent manner. LTP in males is dependent on α nitric oxide synthase-1 (αNOS1) signaling, however, in females LTP appears not affected in αNOS1 knockouts (Dachtler et al., 2012). This significant sex difference is likely due to the lack of NO and reduced NOS1 expression in the female hippocampus at baseline (Dachtler et al., 2012). However, estradiol application to female mouse derived tissue increases expression of NO in the female brain. Furthermore, NOS levels were altered across the estrous cycle, mirroring fluctuating estradiol levels—specifically, NOS levels were no different from males during proestrus and were lowest during diestrus (Hu et al., 2012). Thus, it is possible that NO-dependent LTP in females may be more likely during proestrous when estradiol is high and availability of NO is increased. However, it seems likely that NO-dependent LTP is a secondary mechanism by which LTP can be initiated in females, yet in males it is far more prominent.

Opioid Receptors

Other mechanisms exist beyond steroid hormone-dependent plasticity, to drive changes in synaptic integrity. In proestrus, female rats have higher mossy fiber transmission in cultured hippocampal CA3 cells following administration of the generic opioid receptor antagonist naloxone. Cultured male tissue, on the other hand, does not show altered signaling. These data implicate the opioid receptor as an inhibitor in hippocampal transmission during peak estradiol levels in females. The mμ-opioid receptor antagonist Cys2, Tyr3, Orn5, Pen7-amide (CTOP) similarly enhances neural transmission, suggesting the mμ-opioid receptor is specifically down-regulating neural firing in females. Females also exhibit low frequency LTP during proestrus, suggesting that activity threshold is reduced when estradiol is elevated (Harte-Hargrove et al., 2015). Thus, a lowered activity threshold during times of peak estradiol supports enhanced learning and memory in proestrous females (Fernandez et al., 2008; Macbeth and Luine, 2010). However, concomitant inhibition of opioid receptors may be necessary to facilitate this estradiol-dependent benefit. Furthering this conclusion, electron microscopy has revealed more δ-opioid receptor-labeled spines in hippocampal pyramidal cells from proestrous females compared to males. Inhibition of δ-opioid receptors with the antagonist naltrinidole impairs low frequency LTP in proestrous females only. Taken together, these data implicate a sex-specific role of the δ-opioid receptor in LTP signaling in hippocampal pyramidal cells (Harte-Hargrove et al., 2015). As the opiate system can be activated by stress (Chaijale et al., 2013), understanding the role these signaling mechanisms play in plasticity can help define the pathways by which stress can modify synaptic plasticity in a sex-specific manner.

CONCLUSION

It is evident that sex differences in synaptic plasticity are driven by both direct and indirect mechanisms of steroid hormones. While these mechanisms exist at the molecular and synaptic levels, they are further reflected in structural differences that ultimately result in sexually-dimorphic behaviors. Recent advances in human neuroimaging have provided insights into the translatability of these sex-differences in synaptic plasticity across mammalian species. Overall changes in white matter, gray matter and cerebral spinal fluid have been observed across the menstrual cycle in human women. Generally, gray and white matter volume appear to increase during the luteal phase when estrogen and progesterone are elevated in women (Catenaccio et al., 2016). Ruigrok et al. (2014) conducted a meta-analysis on gray matter volume and found significant sex-differences with men having more gray matter in the amygdala, hippocampus, parahippocampus, insula, and putamen (Catenaccio et al., 2016). Sex-differences in neural volume are further reflected in a region-specific pattern that fluctuates with the menstrual cycle—similar to what is observed across the rodent estrous cycle. The hippocampus is generally larger in men compared to women, however, during the luteal phase, when estrogen peaks, women see a significant increase in hippocampal volume (Protopopescu et al., 2008). Taken together, these data parallel findings from female rodents that sex-differences evident in certain neural structures are likely dependent on fluctuating hormones in women. Further research is needed to fully elucidate sex-differences in human neuroplasticity, however, it is clear that sex-differences are conserved across mammalian species. By understanding the synaptic mechanisms underlying behavioral differences between males and females, we can derive more information on the source of functional changes as well as their possible dysfunction when, and if, it occurs. Incorporating both males and females into these studies is essential given the extensive sex-differences in synaptic plasticity mechanisms and their functional outcomes.

AUTHOR CONTRIBUTIONS

MH outlined, researched and wrote this review article. In addition, she composed the figure. LP provided editorial comments and suggestions on the research areas to include. GN assisted in the drafting and editing of this manuscript and advised MH, a postdoctoral trainee, during the process.

FUNDING

GN received support from the Office of Extramural Research, National Institutes of Health (grant nos. R01MH110364 and NR014886). LP received support from the Office of Extramural Research, National Institutes of Health (grant no. NS044372 and NS056247). MH is a postdoctoral fellow supported by the Office of Extramural Research, National Institutes of Health (grant no. K12GM093857).

REFERENCES

Aggen, S. H., Kendler, K. S., Kubarych, T. S., and Neale, M. C. (2011). Differential age and sex effects in the assessment of major depression: a population-based twin item analysis of the DSM criteria. *Twin Res. Hum. Genet.* 14, 524–538. doi: 10.1375/twin.14.6.524

Allen, L. S., Hines, M., Shryne, J. E., and Gorski, R. A. (1989). Two sexually dimorphic cell groups in the human brain. *J. Neurosci.* 9, 497–506. doi: 10.1523/JNEUROSCI.09-02-00497.1989

Balthazart, J., Taziaux, M., Holloway, K., Ball, G. F., and Cornil, C. A. (2009). Behavioral effects of brain-derived estrogens in birds. *Ann. N Y Acad. Sci.* 1163, 31–48. doi: 10.1111/j.1749-6632.2008.03637.x

Bangasser, D. A., and Valentino, R. J. (2014). Sex differences in stress-related psychiatric disorders: neurobiological perspectives. *Front. Neuroendocrinol.* 35, 303–319. doi: 10.1016/j.yfrne.2014.03.008

Bekhbat, M., and Neigh, G. N. (2018). Sex differences in the neuro-immune consequences of stress: focus on depression and anxiety. *Brain Behav. Immun.* 67, 1–12. doi: 10.1016/j.bbi.2017.02.006

Bender, R. A., Zhou, L., Vierk, R., Brandt, N., Keller, A., Gee, C. E., et al. (2017). Sex-dependent regulation of aromatase-mediated synaptic plasticity in the basolateral amygdala. *J. Neurosci.* 37, 1532–1545. doi: 10.1523/JNEUROSCI.1532-16.2016

Blume, S. R., Freedberg, M., Vantrease, J. E., Chan, R., Padival, M., Record, M. J., et al. (2017). Systems/Circuits sex-and estrus-dependent differences in rat basolateral amygdala. *J. Neurosci.* 37, 10567–10586. doi: 10.1523/JNEUROSCI.0758-17.2017

Blurton-Jones, M., and Tuszynski, M. H. (2002). Estrogen receptor-β colocalizes extensively with parvalbumin-labeled inhibitory neurons in the cortex, amygdala, basal forebrain, and hippocampal formation of intact and ovariectomized adult rats. *J. Comp. Neurol.* 452, 276–287. doi: 10.1002/cne.10393

Boulware, M. I., Heisler, J. D., and Frick, K. M. (2013). The memory-enhancing effects of hippocampal estrogen receptor activation involve metabotropic glutamate receptor signaling. *J. Neurosci.* 33, 15184–15194. doi: 10.1523/JNEUROSCI.1716-13.2013

Boulware, M. I., Weick, J. P., Becklund, B. R., Kuo, S. P., Groth, R. D., and Mermelstein, P. G. (2005). Estradiol activates group I and II metabotropic glutamate receptor signaling, leading to opposing influences on cAMP response element-binding protein. *J. Neurosci.* 25, 5066–5078. doi: 10.1523/JNEUROSCI.1427-05.2005

Bredemann, T. M., and McMahon, L. L. (2014). 17β estradiol increases resilience and improves hippocampal synaptic function in helpless ovariectomized rats. *Psychoneuroendocrinology* 42, 77–88. doi: 10.1016/j.psyneuen.2014.01.004

Butcher, R. L., Collins, W. E., and Fugo, N. W. (1974). Plasma concentration of LH, FSH, prolactin, progesterone and estradiol-17/3 throughout the 4-day estrous cycle of the rat. *Endocrinology* 94, 1704–1708. doi: 10.1210/endo-94-6-1704

Campi, K. L., Jameson, C. E., and Trainor, B. C. (2013). Sexual dimorphism in the brain of the monogamous california mouse (*Peromyscus californicus*). *Brain Behav. Evol.* 81, 236–249. doi: 10.1159/000353260

Catenaccio, E., Mu, W., and Lipton, M. L. (2016). Estrogen- and progesterone-mediated structural neuroplasticity in women: evidence from neuroimaging. *Brain Struct. Funct.* 221, 3845–3867. doi: 10.1007/s00429-016-1197-x

Chaijale, N. N., Curtis, A. L., Wood, S. K., Zhang, X.-Y., Bhatnagar, S., Reyes, B. A., et al. (2013). Social stress engages opioid regulation of locus coeruleus norepinephrine neurons and induces a state of cellular and physical opiate dependence. *Neuropsychopharmacology* 38, 1833–1843. doi: 10.1038/npp.2013.117

Dachtler, J., Hardingham, N. R., and Fox, K. (2012). The role of nitric oxide synthase in cortical plasticity is sex specific. *J. Neurosci.* 32, 14994–14999. doi: 10.1523/JNEUROSCI.3189-12.2012

Farrell, M. R., Gruene, T. M., and Shansky, R. M. (2015). The influence of stress and gonadal hormones on neuronal structure and function. *Horm. Behav.* 76, 118–124. doi: 10.1016/j.yhbeh.2015.03.003

Fernandez, S. M., Lewis, M. C., Pechenino, A. S., Harburger, L. L., Orr, P. T., Gresack, J. E., et al. (2008). Estradiol-induced enhancement of object memory consolidation involves hippocampal extracellular signal-regulated

kinase activation and membrane-bound estrogen receptors. *J. Neurosci.* 28, 8660–8667. doi: 10.1523/JNEUROSCI.1968-08.2008

Forlano, P., and Woolley, C. (2010). Quantitative analysis of pre- and postsynaptic sex differences in the nucleus accumbens. *J. Comp. Neurol.* 518, 1330–1348. doi: 10.1002/cne.22279

Galea, L. A., McEwen, B. S., Tanapat, P., Deak, T., Spencer, R. L., and Dhabhar, F. S. (1997). Sex differences in dendritic atrophy of CA3 pyramidal neurons in response to chronic restraint stress. *Neuroscience* 81, 689–697. doi: 10.1016/s0306-4522(97)00233-9

Galea, L. A. M., Spritzer, M. D., Barker, J. M., and Pawluski, J. L. (2006). Gonadal hormone modulation of hippocampal neurogenesis in the adult. *Hippocampus* 16, 225–232. doi: 10.1002/hipo.20154

Garrett, J. E., and Wellman, C. L. (2009). Chronic stress effects on dendritic morphology in medial prefrontal cortex: sex differences and estrogen dependence. *Neuroscience* 162, 195–207. doi: 10.1016/j.neuroscience.2009.04.057

Gobinath, A. R., Mahmoud, R., and Galea, L. A. M. (2015). Influence of sex and stress exposure across the lifespan on endophenotypes of depression: focus on behavior, glucocorticoids, and hippocampus. *Front. Neurosci.* 8:420. doi: 10.3389/fnins.2014.00420

Gorski, R. A., Gordon, J. H., Shryne, J. E., and Southam, A. M. (1978). Evidence for a morphological sex difference within the medial preoptic area of the rat brain. *Brain Res.* 148, 333–346. doi: 10.1016/0006-8993(78)90723-0

Gould, E., Woolley, S., Frankfurt, M., and McEwen, B. S. (1990). Gonadal steroids regulate dendritic spine density in hippocampal pyramidal cells in adulthood. *J. Neurosci.* 10, 1286–1291. doi: 10.1523/JNEUROSCI.10-04-01286.1990

Harte-Hargrove, L. C., Varga-Wesson, A., Duffy, A. M., Milner, T. A., and Scharfman, H. E. (2015). Opioid receptor-dependent sex differences in synaptic plasticity in the hippocampal mossy fiber pathway of the adult rat. *J. Neurosci.* 35, 1723–1738. doi: 10.1523/JNEUROSCI.0820-14.2015

Hawley, D. F., and Leasure, J. L. (2012). Region-specific response of the hippocampus to chronic unpredictable stress. *Hippocampus* 22, 1338–1349. doi: 10.1002/hipo.20970

Holtmaat, A., and Svoboda, K. (2009). Experience-dependent structural synaptic plasticity in the mammalian brain. *Nat. Rev. Neurosci.* 10, 647–658. doi: 10.1038/nrn2699

Hu, Y., Wu, D.-L., Luo, C.-X., Zhu, L.-J., Zhang, J., Wu, H.-Y., et al. (2012). Hippocampal nitric oxide contributes to sex difference in affective behaviors. *Proc. Natl. Acad. Sci. U S A* 109, 14224–14229. doi: 10.1073/pnas.1207461109

Hyer, M. M., Khantsis, S., Venezia, A. C., Madison, F. N., Hallgarth, L., Adekola, E., et al. (2017). Estrogen-dependent modifications to hippocampal plasticity in paternal California mice (*Peromyscus californicus*). *Horm. Behav.* 96, 147–155. doi: 10.1016/j.yhbeh.2017.09.015

Ingalhalikar, M., Smith, A., Parker, D., Satterthwaite, T. D., Elliott, M. A., Ruparel, K., et al. (2014). Sex differences in the structural connectome of the human brain. *Proc. Natl. Acad. Sci. U S A* 111, 823–828. doi: 10.1073/pnas.1316909110

Juraska, J. M., Fitch, J. M., Henderson, C., and Rivers, N. (1985). Sex differences in the dendritic branching of dentate granule cells following differential experience. *Brain Res.* 333, 73–80. doi: 10.1016/0006-8993(85)90125-8

Kempermann, G., Song, H., and Gage, F. H. (2015). Neurogenesis in the adult hippocampus. *Cold Spring Harb. Perspect. Biol.* 7:a018812. doi: 10.1101/cshperspect.a018812

Kovacs, E. G., MacLusky, N. J., and Leranth, A. C. (2003). Effects of testosterone on hippocampal CA1 spine synaptic density in the male rat are inhibited by fimbria/fornix transection. *Neuroscience* 122, 807–810. doi: 10.1016/j.neuroscience.2003.08.046

Leranth, C., Hajszan, T., and MacLusky, N. J. (2004). Androgens increase spine synapse density in the CA1 hippocampal subfield of ovariectomized female rats. *J. Neurosci.* 24, 495–499. doi: 10.1523/JNEUROSCI.4516-03.2004

Leranth, C., Petnehazy, O., and MacLusky, N. J. (2003). Gonadal hormones affect spine synaptic density in the CA1 hippocampal subfield of male rats. *J. Neurosci.* 23, 1588–1592. doi: 10.1523/JNEUROSCI.23-05-01588.2003

Leuner, B., and Shors, T. J. (2013). Stress, anxiety, and dendritic spines: what are the connections? *Neuroscience* 251, 108–119. doi: 10.1016/j.neuroscience.2012.04.021

Livneh, Y., and Mizrahi, A. (2012). Experience-dependent plasticity of mature adult-born neurons. *Nat. Neurosci.* 15, 26–28. doi: 10.1038/nn.2980

Lu, B., Nagappan, G., and Lu, Y. (2014). "BDNF and synaptic plasticity, cognitive function, and dysfunction," in *Neurotrophic Factors*, eds G. R. Lewin and B. D. Carter (Berlin, Heidelberg: Springer), 223–250.

Macbeth, A. H., and Luine, V. N. (2010). Changes in anxiety and cognition due to reproductive experience: a review of data from rodent and human mothers. *Neurosci. Biobehav. Rev.* 34, 452–467. doi: 10.1016/j.neubiorev.2009.08.011

MacLusky, N. J., Luine, V. N., Hajszan, T., and Leranth, C. (2005). The 17α and 17β isomers of estradiol both induce rapid spine synapse formation in the CA1 hippocampal subfield of ovariectomized female rats. *Endocrinology* 146, 287–293. doi: 10.1210/en.2004-0730

Mak, G. K., and Weiss, S. (2010). Paternal recognition of adult offspring mediated by newly generated CNS neurons. *Nat. Neurosci.* 13, 753–758. doi: 10.1038/nn.2550

McEwen, B. S. (2010). Stress, sex, and neural adaptation to a changing environment: mechanisms of neuronal remodeling. *Ann. N Y Acad. Sci.* 1204, E38–E59. doi: 10.1111/j.1749-6632.2010.05568.x

Milner, T. A., McEwen, B. S., Hayashi, S., Li, C. J., Alves, L. P., and Reagan, S. E. (2001). Ultrastructural evidence that hippocampal α estrogen receptors are located at extranuclear sites. *J. Comp. Neurol.* 429, 355–371. doi: 10.1002/1096-9861(20010115)429:3<355::aid-cne1>3.3.co;2-r

Mitterling, K. L., Spencer, J. L., Dziedzic, N., Shenoy, S., McCarthy, K., Waters, E. M., et al. (2010). Cellular and subcellular localization of estrogen and progestin receptor immunoreactivities in the mouse hippocampus. *J. Comp. Neurol.* 518, 2729–2743. doi: 10.1002/cne.22361

Naninck, E. F. G., Lucassen, P. J., and Bakker, J. (2011). Sex differences in adolescent depression: do sex hormones determine vulnerability? *J. Neuroendocrinol.* 23, 383–392. doi: 10.1111/j.1365-2826.2011.02125.x

Nottebohm, F., and Arnold, A. (1976). Sexual dimorphism in vocal control areas of the songbird brain. *Science* 194, 211–213. doi: 10.1126/science.959852

Oberlander, J. G., and Woolley, C. S. (2016). 17β-Estradiol acutely potentiates glutamatergic synaptic transmission in the hippocampus through distinct mechanisms in males and females. *J. Neurosci.* 36, 3677–3690. doi: 10.1523/JNEUROSCI.4437-15.2016.

Ormerod, B. K., Lee, T. T. Y., and Galea, L. A. M. (2004). Estradiol enhances neurogenesis in the dentate gyri of adult male meadow voles by increasing the survival of young granule neurons. *Neuroscience* 128, 645–654. doi: 10.1016/j.neuroscience.2004.06.039

Parducz, A., Hajszan, T., MacLusky, N. J., Hoyk, Z., Csakvari, E., Kurunczi, A., et al. (2006). Synaptic remodeling induced by gonadal hormones: neuronal plasticity as a mediator of neuroendocrine and behavioral responses to steroids. *Neuroscience* 138, 977–985. doi: 10.1016/j.neuroscience.2005.07.008

Phan, A., Gabor, C. S., Favaro, K. J., Kaschack, S., Armstrong, J. N., MacLusky, N. J., et al. (2012). Low doses of 17β-estradiol rapidly improve learning and increase hippocampal dendritic spines. *Neuropsychopharmacology* 37, 2299–2309. doi: 10.1038/npp.2012.82

Piccinelli, M., and Wilkinson, G. (2000). Gender differences in depression. Critical review. *Br. J. Psychiatry* 177, 486–492. doi: 10.1192/bjp.177.6.486

Protopopescu, X., Butler, T., Pan, H., Root, J., Altemus, M., Polanecsky, M., et al. (2008). Hippocampal structural changes across the menstrual cycle. *Hippocampus* 18, 985–988. doi: 10.1002/hipo.20468

Qiao, H., Li, M., Xu, C., Chen, H., An, S., and Ma, X. (2016). Dendritic spines in depression: what we learned from animal models. *Neural Plast.* 2016:8056370. doi: 10.1155/2016/8056370

Romeo, R. D., McCarthy, J. B., Wang, A., Milner, T. A., and McEwen, B. S. (2005a). Sex differences in hippocampal estradiol-induced n-methyl-d-spartic acid binding and ultrastructural localization of estrogen receptor-α. *Neuroendocrinology* 81, 391–399. doi: 10.1159/000089557

Romeo, R. D., Staub, D., Jasnow, A. M., Karatsoreos, I. N., Thornton, J. E., and McEwen, B. S. (2005b). Dihydrotestosterone increases hippocampal N-methyl-D-aspartate binding but does not affect choline acetyltransferase cell number in the forebrain or choline transporter levels in the CA1 region of adult male rats. *Endocrinology* 146, 2091–2097. doi: 10.1210/en.2004-0886

Ruble, D. N., Greulich, F., Pomerantz, E. M., and Gochberg, B. (1993). The role of gender-related processes in the development of sex differences in self-evaluation and depression. *J. Affect. Disord.* 29, 97–128. doi: 10.1016/0165-0327(93)90027-h

Ruigrok, A. N. V., Salimi-Khorshidi, G., Lai, M.-C., Baron-Cohen, S., Lombardo, M. V., Tait, R. J., et al. (2014). A meta-analysis of sex differences in human brain structure. *Neurosci. Biobehav. Rev.* 39, 34–50. doi: 10.1016/j.neubiorev.2013.12.004

Shors, T. J., Chua, C., and Falduto, J. (2001). Sex differences and opposite effects of stress on dendritic spine density in the male versus female hippocampus. *J. Neurosci.* 21, 6292–6297. doi: 10.1523/JNEUROSCI.21-16-06292.2001

Shors, T. J., Falduto, J., and Leuner, B. (2004). The opposite effects of stress on dendritic spines in male vs. female rats are NMDA receptor-dependent. *Eur. J. Neurosci.* 19, 145–150. doi: 10.1046/j.1460-9568.2003.03065.x

Shughrue, P. J., Lane, M. V., and Merchenthaler, I. (1997). Comparative distribution of estrogen receptor-α and -β mRNA in the rat central nervous system. *J. Comp. Neurol.* 388, 507–525. doi: 10.1002/(sici)1096-9861(19971201)388:4<507::aid-cne1>3.0.co;2-6

Skucas, V. A., Duffy, A. M., Harte-Hargrove, L. C., Magagna-Poveda, A., Radman, T., Chakraborty, G., et al. (2013). Testosterone depletion in adult male rats increases mossy fiber transmission, LTP, and sprouting in area CA3 of hippocampus. *J. Neurosci.* 33, 2338–2355. doi: 10.1523/JNEUROSCI.3857-12.2013

Smith, C. C., and McMahon, L. L. (2005). Estrogen-induced increase in the magnitude of long-term potentiation occurs only when the ratio of NMDA transmission to AMPA transmission is increased. *J. Neurosci.* 25, 7780–7791. doi: 10.1523/JNEUROSCI.0762-05.2005

Swaab, D. F., and Fliers, E. (1985). A sexually dimorphic nucleus in the human brain. *Science* 228, 1112–1115. doi: 10.1126/science.3992248

Tanapat, P., Hastings, N. B., and Gould, E. (2005). Ovarian steroids influence cell proliferation in the dentate gyrus of the adult female rat in a dose- and time-dependent manner. *J. Comp. Neurol.* 481, 252–265. doi: 10.1002/cne.20385

Teyler, T., Vardaris, R., Lewis, D., and Rawitch, A. (1980). Gonadal steroids: effects on excitability of hippocampal pyramidal cells. *Science* 209, 1017–1018. doi: 10.1126/science.7190730

Tremblay, G. B., Tremblay, A., Copeland, N. G., Gilbert, D. J., Jenkins, N. A., Labrie, F., et al. (1997). Cloning, chromosomal localization, and functional analysis of the murine estrogen receptor β. *Mol. Endocrinol.* 11, 353–365. doi: 10.1210/mend.11.3.9902

Vivar, C., Peterson, B. D., and van Praag, H. (2016). Running rewires the neuronal network of adult-born dentate granule cells. *Neuroimage* 131, 29–41. doi: 10.1016/j.neuroimage.2015.11.031

Volosin, M., Song, W., Almeida, R. D., Kaplan, D. R., Hempstead, B. L., and Friedman, W. J. (2006). Interaction of survival and death dignaling in dasal forebrain neurons: roles of neurotrophins and proneurotrophins. *J. Neurosci.* 26, 7756–7766. doi: 10.1523/JNEUROSCI.1560-06.2006

Vyas, A., Mitra, R., Shankaranarayana Rao, B. S., and Chattarji, S. (2002). Chronic stress induces contrasting patterns of dendritic remodeling in hippocampal and amygdaloid neurons. *J. Neurosci.* 22, 6810–6818. doi: 10.1523/JNEUROSCI.22-15-06810.2002

Walf, A. A., and Frye, C. A. (2005). ERb-Selective estrogen receptor modulators produce antianxiety behavior when administered systemically to ovariectomized rats. *Neuropsychopharmacology* 30, 1598–1609. doi: 10.1038/sj.npp.1300713

Walf, A. A., and Frye, C. A. (2006). A review and update of mechanisms of estrogen in the hippocampus and amygdala for anxiety and depression behavior. *Neuropsychopharmacology* 31, 1097–1111. doi: 10.1038/sj.npp.1301067

Waters, E. M., Thompson, L. I., Patel, P., Gonzales, A. D., Ye, H. Z., Filardo, E. J., et al. (2015). G-protein-coupled estrogen receptor 1 is anatomically positioned to modulate synaptic plasticity in the mouse hippocampus. *J. Neurosci.* 35, 2384–2397. doi: 10.1523/JNEUROSCI.1298-14.2015

Weiland, N. G., Orikasa, C., Hayashi, S., and McEwen, B. S. (1997). Distribution and hormone regulation of estrogen receptor immunoreactive cells in the hippocampus of male and female rats. *J. Comp. Neurol.* 388, 603–612. doi: 10.1002/(sici)1096-9861(19971201)388:4<603::aid-cne8>3.0.co;2-6

Wong, M., and Moss, R. L. (1992). Long-term and short-term electrophysiological effects of on the synaptic properties of hippocampal CA1 neurons estrogen. *J. Neurosci.* 12, 3217–3225. doi: 10.1523/JNEUROSCI.12-08-03217.1992

Woolley, S., Gould, E., Frankfurt, M., and Mcewen, S. (1990). Naturally occurring fluctuation in dendritic spine density on adult hippocampal pyramidal neurons. *J. Neurosci.* 10, 4035–4039. doi: 10.1523/JNEUROSCI.10-12-04035.1990

Woolley, C. S., and Mcewen, B. S. (1994). Estradiol regulates hippocampal dendritic spine density via an N-methyl-D-aspartate receptor-dependent mechanism. *J. Neurosci.* 14, 7680–7687. doi: 10.1523/JNEUROSCI.14-12-07680.1994

Yamaura, K., Bi, Y., Ishiwatari, M., Oishi, N., Fukata, H., and Ueno, K. (2013). Sex differences in stress reactivity of hippocampal BDNF in mice are associated with the female preponderance of decreased locomotor activity in response to restraint stress. *Zoolog. Sci.* 30, 1019–1024. doi: 10.2108/zsj.30.1019

Zhao, C., Fujinaga, R., Tanaka, M., Yanai, A., Nakahama, K., and Shinoda, K. (2007). Region-specific expression and sex-steroidal regulation on aromatase and its mRNA in the male rat brain: immunohistochemical and *in situ* hybridization analyses. *J. Comp. Neurol.* 500, 557–573. doi: 10.1002/cne.21193

Conflict of Interest Statement: The authors declare that the research was conducted in the absence of any commercial or financial relationships that could be construed as a potential conflict of interest.

frontiers in Molecular Neuroscience

ORIGINAL RESEARCH
published: 13 September 2018
doi: 10.3389/fnmol.2018.00338

Oophorectomy Reduces Estradiol Levels and Long-Term Spontaneous Neurovascular Recovery in a Female Rat Model of Focal Ischemic Stroke

Paolo Bazzigaluppi[1]†, Conner Adams[1†], Margaret M. Koletar[1], Adrienne Dorr[1], Aleksandra Pikula[2], Peter L. Carlen[3] and Bojana Stefanovic[1,4]*

[1] Sunnybrook Research Institute, Sunnybrook Health Sciences Centre, Toronto, ON, Canada, [2] Adult Vascular Neurology, Toronto Western Hospital, Toronto, ON, Canada, [3] Fundamental Neurobiology, Krembil Research Institute, Toronto, ON, Canada, [4] Department of Medical Biophysics, University of Toronto, Toronto, ON, Canada

Although epidemiological evidence suggests significant sex and gender-based differences in stroke risk and recovery, females have been widely under-represented in preclinical stroke research. The neurovascular sequelae of brain ischemia in females, in particular, are largely uncertain. We set out to address this gap by a multimodal *in vivo* study of neurovascular recovery from endothelin-1 model of cortical focal-stroke in sham vs. ovariectomized female rats. Three weeks post ischemic insult, sham operated females recapitulated the phenotype previously reported in male rats in this model, of normalized resting perfusion but sustained peri-lesional cerebrovascular hyperreactivity. In contrast, ovariectomized (Ovx) females showed reduced peri-lesional resting blood flow, and elevated cerebrovascular responsivity to hypercapnia in the peri-lesional and contra-lateral cortices. Electrophysiological recordings showed an attenuation of theta to low-gamma phase-amplitude coupling in the peri-lesional tissue of Ovx animals, despite relative preservation of neuronal power. Further, this chronic stage neuronal network dysfunction was inversely correlated with serum estradiol concentration. Our pioneering data demonstrate dramatic differences in spontaneous recovery in the neurovascular unit between Ovx and Sham females in the chronic stage of stroke, underscoring the importance of considering hormonal-dependent aspects of the ischemic sequelae in the development of novel therapeutic approaches and patient recruitment in clinical trials.

Keywords: arterial spin labeling, estrogen, ischemia, ovariectomy, local field potential

OPEN ACCESS

Edited by:
Laura Musazzi,
Università degli Studi di Milano, Italy

Reviewed by:
Samaneh Maysami,
The University of Manchester, United Kingdom
Franca Orsini,
IRCCS - Istituto di Ricerche Farmacologiche Mario Negri, Italy

****Correspondence:***
Paolo Bazzigaluppi
paolo.bazzigaluppi@sri.utoronto.ca

† These authors have contributed equally to this work

Received: *25 May 2018*
Accepted: *28 August 2018*
Published: *13 September 2018*

Citation:
Bazzigaluppi P, Adams C, Koletar MM, Dorr A, Pikula A, Carlen PL and Stefanovic B (2018) Oophorectomy Reduces Estradiol Levels and Long-Term Spontaneous Neurovascular Recovery in a Female Rat Model of Focal Ischemic Stroke. Front. Mol. Neurosci. 11:338. doi: 10.3389/fnmol.2018.00338

INTRODUCTION

Epidemiological evidence suggests lower risk of stroke among *premenopausal* women than among age-matched men (Stegmayr et al., 1997; Sudlow and Warlow, 1997). By the *perimenopausal* years (55- to 64-year olds), the stroke risk for women equalizes to that of age-matched men (Anderson et al., 1991). Once in *post-menopausal* stage, women who experienced stroke show less post-stroke recovery than men: they are more likely than men to be institutionalized, and they tend to suffer worse post-stroke disability (Bushnell, 2008; Petrea et al., 2009). The hormonal profile progression thus plays a major role in determining women's susceptibility and vulnerability to stroke. A recent

report (Levine et al., 2016) suggested that bilateral oophorectomy accelerates aging (particularly of the circulatory system), as measured by increased methylation. Patient studies (Ingelsson et al., 2016; Levine et al., 2016; Rocca et al., 2016, 2017) showed an association between pre-menopausal bilateral oophorectomy and the accumulation rate of cardiovascular diseases and multimorbidity of 18 defined chronic conditions. In the United States, an estimated 2 million women have undergone surgically induced menopause from hysterectomy with removal of the ovaries between 2000 and 2004 alone (Diaz Brinton, 2012), and a more recent survey suggests just below 500,000 new hysterectomies in 2009 (Cohen et al., 2014). Importantly, women undergoing oophorectomy (i.e., surgical menopause) show lower levels of estrogen than age-matched women experiencing natural menopause (Korse et al., 2009). While the epidemiological evidence thus clearly shows that sex and estrogen levels are important factors in the risk of stroke and in its long-term outcome, the mechanism of these dependencies is unclear. In light of the above-mentioned complexity and the slow evolution of cerebrovascular impairments that are thought at the heart of this interaction, examining the mechanism of sex-based differences in stroke risk and its outcomes is exceedingly difficult in humans (Rocca et al., 2017). Preclinical models are hence key as they allow detailed investigation of neurovascular changes in well-controlled conditions. To date, however, estradiol's roles have been investigated almost exclusively *in vitro* (McCullough and Hurn, 2003). With respect to age, experimental stroke has been shown to increase edema and result in larger strokes in middle-aged female animals compared with younger females with intact gonadal function [for review (Manwani and McCullough, 2011)]. However, neurovascular functioning in the chronic stage post ischemia in females, and its dependence on ovariectomy and estrogen decline, has not been evaluated.

In the present work, we modeled the estrogen drop observed in pre-menopausal women following oophorectomy and determined the effects of ovariectomy on spontaneous neurovascular recovery in the chronic stage post focal cortical ischemia. To induce a drop in estrogen levels, we used 7–9 months old retired-breeder female rats [known to best resemble the physiological changes of women in their fourth decade (Sengupta, 2013)], which underwent ovariectomy (Ovx) or sham surgery. Two weeks thereafter, focal cortical stroke was induced by microinjection of Endothelin-1 (ET-1), (Lake et al., 2017) and serum estrogen levels were measured instead of estrous cycle monitoring (Singletary et al., 2005; Weixelbaumer et al., 2014). In our previous report using the same model in the male population (Lake et al., 2017), we reported resting perfusion normalization and sustained cerebrovascular hyperreactivity, associated with increased neuronal excitability, 3 weeks after stroke. In light of the functional nature of these readouts that cannot be captured by post-mortem assays and the fact that T_2-weighted MRI sensitivity parallels histopathology (i.e., cresyl-violet) in detecting stroke volume in the focal cortical ET-1 model (Biernaskie et al., 2001), we used quantitative MRI of cerebral blood flow and intracerebral multielectrode electrophysiological recordings to compare stroke size and neurovascular state in the peri- and contra-lesional cortex 3 weeks following stroke induction. Topographical analysis of local field potentials revealed neuronal deficits within 0.5 mm of the ET-1 injection site in the Ovx group, which were inversely correlated to the level of estradiol at the time of stroke. Despite comparable stroke volumes of the two cohorts, the Ovx females displayed reduced peri-lesional blood flow and widespread exaggerated cerebrovascular responses to hypercapnia when compared to Sham animals. Low estrogen levels were thus shown to be associated with exacerbated long-term neurovascular damage from ischemic stroke.

MATERIALS AND METHODS

All experimental procedures in this study followed the ARRIVE guidelines and were approved by the Animal Care Committee of the Sunnybrook Research Institute, which adheres to the Policies and Guidelines of the Canadian Council on Animal Care and meets all the requirements of the Provincial Statute of Ontario, Animals for Research Act as well as those of the Canadian Federal Health of Animals Act. Animals were housed in pairs on a standard 12-h light/dark cycle. Food and water were freely available. Twenty-five mature female Sprague Dawley rats were purchased from Charles River Canada. They were retired breeders (7–9 months old at the beginning of the study and having had at least one litter), with mean weight at the beginning of the study of 420 $\pm$ 20 g. Animals were randomly assigned to Ovx or Sham groups and the researcher performing MRI and electrophysiology experiment and data analysis was blinded to the surgery level of the animal. Following earlier work (Bernal-Mondragón et al., 2013), we let animals recover from Ovx surgery for 2 weeks before stroke induction surgery. This period was necessary to minimize mortality and to allow a measurable drop in estrogen serum levels to develop [see results, (Laughlin et al., 2000; Strom et al., 2008, 2010)]. In line with 3R principles and to allow recovery from the imaging experiments, we avoided the use of alpha-chloralose anesthesia, which although frequently employed in non-survival studies is associated with prolonged and poor recovery (Silverman and Muir, 1993; Flecknell, 2016). Instead, Propofol anesthesia (see details below) was used throughout all imaging and electrophysiological recordings.

Ovariectomy

Given the expected high mortality of the Ovx procedure, sixteen females were randomly assigned to the Ovx group and eight to the Sham group. Bilateral Ovx was conducted using strict sterile surgical techniques. Rats were anesthetised with isoflurane (5% induction, 2.5% maintenance). A blood sample for serum estradiol measurement was acquired from the lateral tail vein. The bilateral Ovx followed a 2 cm incision being made on each lateral side of the abdomen (between the last rib and hip). The ovary and adjacent uterine horn was isolated and clamped. The ovary and fallopian tube was ligated with 4-0 silk suture and then excised. The abdomen was sutured closed. All rats received subcutaneous local anesthetic (bupivicaine HCl 7 mg/kg, Marcaine, Hospira Healthcare Corp.) along the incision site, analgesic (buprenorphine 0.1 mg/kg, Temgesic, Reckitt Benckiser Healthcare), and antibiotics (enrofloxacin 5 mg/kg, Baytril, Bayer

Inc.). Sham surgeries were conducted exactly in the same way, except that the ovary and uterine horn remained intact. Following surgery, animals were returned to the colony for a 2 weeks recovery period. Six rats died during the first 24 h after the Ovx surgery (three animals chewed the stiches reopening the wound and were hence excluded from the study, and other three died on unknown reasons).

Stroke Induction

Ovx and Sham animals underwent the stroke induction procedure, 2 weeks after surgery, under isoflurane anesthesia (5% induction and 2–2.5% maintenance) following the procedures we described in Lake et al. (2017). In brief, animals were secured in a small animal stereotaxic apparatus (David KOPF Instruments, Tujunga, Los Angeles, CA, United States). A blood sample for serum collection was acquired from the lateral tail vein. Under aseptic condition, two burr holes were drilled over the right sensorimotor cortex (AP +2.3 mm and AP −0.5 mm; ML 2.1 mm) using a high-speed micro-drill (Foredom Electric Co., Bethel Connecticut, United States). A 10-μl Hamilton Syringe (Model 80366, 26-gauge needle with beveled tip) was used to inject 800 pmol of ET-1 (Calbiochem, Millipore, Billerica, MA, United States, dissolved in sterile saline) at −2.3 mm DV (dorsal-ventral) in both locations. One 2-μl aliquot was injected at each location, for a total of 4 μl. The scalp was sutured over the skull. Four Ovx females and two Sham females did not survive stroke induction surgery, leaving six animals in each cohort.

Magnetic Resonance Imaging

The current study was conducted in a 7T horizontal pre-clinical MRI scanner from Bruker BioSpec. The rats were anesthetized with isoflurane, intubated using 14-gauge i.v. catheters, and mechanically ventilated using a rodent ventilator (SAR-830/P, CWE Inc.). Isoflurane was discontinued and intravenous propofol (PharmaScience Inc.) infusion commenced, at a rate of 43 mg/kg/hour. Physiological status was monitored by pulse oximetry (MouseOx Plus MRI compatible, STARR Life Sciences Corp.) and end-tidal capnography (microCapStar, CWE Inc.), with core body temperature maintained using a rectal probe feedback controlled water bed (1025T, Small Animal Instruments Inc.).

T_2-Weighted MRI

A birdcage body coil was used for signal excitation and a quadrature receive-only coil for signal detection. Forty-five coronal images were obtained with a rapid acquisition with relaxation enhancement (RARE) sequence (RARE factor of eight, repetition time/echo time TR/TE of 5500/47 ms, and a matrix size of 128 × 256, flip angle 180), with a nominal in-plane spatial resolution of 0.1 mm × 0.1 mm and a slice thickness of 0.5 mm in under 12 min. Images were imported into Display (from the MNI Minc package developed at the Brain Imaging Centre of the Montreal Neurological Institute) for semi-automated segmentation. Following earlier work (Neumann-Haefelin et al., 2000; Kidwell et al., 2003; van der Zijden et al., 2008; Lake et al., 2017), stroke regions were segmented using a predetermined signal intensity threshold of greater than two standard deviations (SDs) above the mean contra-lesional cortical signal intensity. Following segmentation, stroke volumes were calculated for each animal.

CASL Data Acquisition

For CASL imaging, a custom built labeling coil was placed at the level of the common carotid arteries. The position of the labeling coil relative to the imaging coil was then determined with a localizer acquired using the labeling coil (i.e., Tripilot sequence) to ensure optimal labeling offset in all subjects (**Supplementary Figure S1A**). Shimming was next performed using Fastmap sequence (Bruker) to adjust 1st and 2nd order shims in the brain region to be imaged (containing the stroke volume and relevant brain landmarks of interest, **Supplementary Figure S1B**). The resulting shim was assessed using a PRESS sequence (TE/TR 20/2500 ms, 1 average, 2048 points, 13 ppm spectral width) to measure FWHM of the free induction decay of water. Finally, we collected a 2-min series of CASL-EPI images and evaluated the difference between the control and labeled frames to ensure adequate labeling efficiency. We then proceeded with the collection of the full CASL protocol. Using a 1.5-s adiabatic labeling pulse and a 0.4-s post-labeling delay, single average, single shot continuous arterial spin labeling (CASL) echo planar images (EPI) were obtained with a 0.25 mm × 0.25 mm in-plane resolution, and TR/TE of 2500/9.2 ms, matrix size 80 × 57, 1.4 Partial-FT Acceleration, FOV 20 mm × 20 mm, effective spectral bandwidth 250 MHz (Lake et al., 2017). EPI readout details are reported in the **Supplementary Information**. A single 1.5-mm thick coronal slice was positioned 1 to 2 mm caudally to the caudal ET-1 injection site. CASL was performed during medical air and hypercapnic mixture breathing to measure cerebrovascular reactivity to 10% carbon dioxide, a standard test of cerebrovascular function employed in both preclinical and clinical research. For CO_2 challenges, the composition of inhalant gasses was controlled by programming a gas mixer (GSM-3, CWE Inc.). An initial baseline (4 min of 30% O_2, 70% N_2) was followed by four hypercapnic challenges (1 min each of 10% CO_2, 30% O_2, and 60% N_2) alternating with normocapnic periods (4 min each of 30% O_2, 70% N_2). Oxygen enrichment (30% vs. 21%) was used to compensate for respiratory depression induced by anesthesia. At the end of the MRI experiment, the propofol infusion was discontinued and the animal recovered to colony for 3–4 days, in preparation for electrophysiological recordings.

CASL Data Processing

For analysis of functional MRI experiments, we used Analysis of Functional NeuroImages (AFNI, NIH); CASL data were analyzed as in our previous studies (Lake et al., 2015, 2016, 2017): motion was corrected using 2dImReg; Gaussian blurring of masked gray matter was performed using 3dBlurToFWHM (with full-width half max of 0.55 mm); and generalized linear modeling done using 3dDeconvolve (with FDR correction). Subject-specific hemodynamic response functions were produced by averaging the signal in the left (contra-lateral) cortical gray matter (Kang et al., 2003). A threshold was applied to maps of perfusion signal changes elicited by hypercapnia and resting perfusion to correct for multiple comparisons (false discovery

rate $q < 0.01$). In each animal, peri-lesional ROI and the homologous region in the contralateral hemisphere used as the within-subject reference ROI, were delineated using anatomical local contrast on the EPI and T_2-weighted structural scans (**Figure 3Ai**). Following earlier work, voxels with contrast's effect size exceeding 2 Median Absolute Deviations from contrast's median (estimated independently per surgery group, ROI, and contrast) were excluded from further analysis. Resting perfusion was expressed in absolute units (ml/100 g tissue/min) based on the model of ASL signal described by Hendrich et al. (2001), while assuming a lambda (blood–brain partition coefficient) of 0.9 ml/g (Roberts et al., 1996), longitudinal relaxation time of gray matter at 7T of 1.6 s for neocortex (Guilfoyle et al., 2003), and inversion efficiency of 0.7 following our prior work in this model (Gomez-Smith et al., 2017).

Electrophysiological Data Acquisition

The rats were anesthetized with isoflurane and positioned inside the stereotaxic apparatus. The lateral tail vein was cannulated with a 24-gauge intravenous catheter. Two bilateral craniotomies were created around the ET-1 stroke injection sites from AP +2.3 mm to −4.0 mm and ML ±0.5 mm to ±5.0 mm. After removal of the skull bone, the *dura mater* was excised and the cortical surface kept hydrated with sterile phosphate buffered saline. The continuous infusion of propofol was then commenced at a rate of 43 mg/kg b.w./hour. Physiological status was monitored by pulse oximetry (MouseOx Plus, STARR Life Sciences Corp.), using a rectal probe feedback controlled heating pad (TC-1000 Temperature Controller, CWE Inc.). Two multi-electrode arrays (MEA, MicroProbes, Gaithersburg, MD, United States) comprising 16 Platinum/Iridium electrodes (organized in a grid of evenly spaced 4 rows and 4 columns, tip diameter: 125 μm, impedance: 0.5 MΩ, inter-electrode spacing: 250 μm, for a total MEA width of 1 mm and a total length of 1 mm) were lowered to 250 μm DV into the exposed cortices for intracortical recordings. The MEA Centre was positioned at −1.0 mm AP and −2.5 mm ML to allow for placement of the first row of electrodes ∼0.5 mm posterior to the caudal injection site. Acquisition bandwidth was set to 0.3–5 kHz. Signals were amplified 20× at the head-stage and 50× by the amplifier (Model 3600, A-M Systems, Carlsborg, WA, United States). Data were acquired using a 32-channel SciWorks DataWave Acquisition System, with a sampling rate set to 20 kHz, and stored for offline analysis.

Electrophysiological Data Analysis

Power line noise (60 Hz) and its harmonics were removed via notch filtering before additional filtering using a zero-phase forward and reverse Butterworth infinite impulse response filter with frequency range of ±2 Hz around the stop band (filtfilt.m in Matlab, MathWorks, Natick, MA, United States) to eliminate phase distortions (McGinn and Valiante, 2014). To estimate power, the average signal of each row of four electrodes was computed and then Fast Fourier Transform computed for all 3-s intervals in each 3-min epoch using a non-overlapping running window. The relative power was calculated as the fraction of a specific frequency band power vs. the total power over all frequency bands. Following previous work (Joo et al., 2017; Bazzigaluppi et al., 2018), the frequency bands of interest were defined as: Theta (2–8 Hz), Alpha (10–14 Hz), Beta (15–30 Hz), low Gamma (Laird and Ware, 1982; Bragin et al., 1995; Roberts et al., 1996; Simpkins et al., 1997; Chrobak and Buzsaki, 1998; Hendrich et al., 2001; Guilfoyle et al., 2003; Kang et al., 2003; Lee et al., 2005; Miller et al., 2005; Canolty et al., 2006; Takuma et al., 2007a,b; Hossmann, 2008, 2009; Dudink et al., 2009; Canolty and Knight, 2010; de Hemptinne et al., 2013; Girard et al., 2014; McGinn and Valiante, 2014; Womelsdorf et al., 2014; Lake et al., 2015; Edakawa et al., 2016; Zhang et al., 2016; Barr et al., 2017; Devergnas et al., 2017; Gomez-Smith et al., 2017; Joo et al., 2017; Bazzigaluppi et al., 2018) and high Gamma (62–120 Hz). Power exceeding 2 Median Absolute Deviations from band's median (estimated independently per surgery group, ROI, and contrast) were excluded from further analysis. Neuronal dynamic motifs present in the cortex integrate synaptic input and specify spike output synchronization and have been hypothesized to give rise to these frequency bands (Womelsdorf et al., 2014). The functional interactions between frequency bands have been observed in both animals and humans and are termed cross-frequency coupling [CFC, (Canolty and Knight, 2010) and references therein]. CFC focuses on the properties of the ongoing oscillatory activity itself and reflects the statistical dependence between distinct frequency bands of the ongoing spontaneous electrical activity rather than dependence of the electrical activity on external stimuli. One of the manifestations of CFC is Phase Amplitude Coupling (PAC), where the phase of a low frequency wave (theta) modulates the amplitude of higher frequency band [low and high gamma, (Bragin et al., 1995; Chrobak and Buzsaki, 1998; Lee et al., 2005)]. In the present work, we investigated the phase-amplitude coupling by estimating the Modulation Index (MI) that combines the amplitude envelope of time series (A) of a high-frequency band (low and high gamma, A_{gamma}) with the phase φ(t) of a low-frequency band (theta, φ_{theta}) into one composite signal z(t). We estimated the temporal profile (i.e., time series) of the joint distribution of A_{gamma} and φ_{theta}. To achieve this, following earlier work (Canolty et al., 2006; Bazzigaluppi et al., 2018), we compared the mean of the amplitude of z(t) signal to a set of surrogate means created by offsetting A_{gamma} and φ_{theta} by a large time lag (to create random distributions of amplitudes and phases). The time lag affects only the dependence between A_{gamma} and φ_{theta}, not the distributions of amplitude and phase themselves. We used a set of 50 surrogates to generate a population of spurious MI used to threshold (after Bonferroni correction for multiple comparisons), at an alpha of 0.05, the MI extracted from the raw dataset. The mean over time of this composite signal (the Modulation Index) represents the strength of coupling between the two frequency bands. Raw recordings were re-referenced offline between two neighboring recording sites and modulation index was estimated with an in-house developed Matlab function. Theta band was divided into 0.2 Hz bins, while both gamma bands were binned every 1 Hz. Following previous work (Lake et al., 2017), results of neuronal power and MI population analyses are expressed as *lateralization* (i.e., the ratio of the peri-to contra-lesional values) to evaluate the deficit of the peri-lesional

tissue in relation to the notionally unaffected contralesional hemisphere.

ELISA

Whole blood samples were collected at the beginning of ovariectomy or sham surgery, at the beginning of ET-1 stroke induction surgery, and at the start of MRI sessions. Following clean venipuncture, we collected 300 to 500 μL of whole blood from the lateral tail vein immediately after induction with anesthesia. Samples were kept at 4°C for approximately 45 min to facilitate coagulation. Serum was isolated after centrifugation (21K rpm, 15 min, 4 C), then frozen at −20°C as individual aliquots for each rat and at each time point (serum was not pooled). Each sample of serum was divided into three 25 μL aliquot and assayed for Estradiol (Calbiotech Estradiol Elisa Kit, #ES180S-100) as per manufacturer's instructions. The estradiol reaction was measured at 450 nm absorbance and relative fluorescence fitted to the reference standard curve.

Statistical Analysis

Unless stated otherwise, linear mixed effects (lme) modeling (lme function in R[1]) was used in the statistical analysis. It is particularly well suited for the present data since it produces robust and sensible maximum likelihood estimates in the presence of unbalanced number of subjects in experimental groups, here present due to attrition rates variation (Laird and Ware, 1982). CASL-based estimates of resting perfusion and cerebrovascular reactivity to hypercapnia as well as intracortical electrophysiological recordings-based measurement of spontaneous neuronal activity power and modulation index estimates were modeled as linear functions of the surgery (Sham or Ovx), which is the fixed effect, while subjects were treated as random effects. Results are expressed as mean ± SEM unless specified otherwise.

RESULTS

We employed the endothelin-1 (ET-1) model (Lake et al., 2017) to induce focal ischemia in the right sensorimotor cortex of Sham and Ovx female rats and measured the spontaneous neurovascular recovery in the chronic stage. To model the reduction in circulating estradiol following oophorectomy, we performed Ovx or Sham surgery. When compared to baseline (i.e., before Ovx or Sham surgery), 2 weeks post Ovx (i.e., just before stroke induction), Ovx rats exhibited a 68% drop in blood estradiol concentration (4.3 ± 1.4 pg/ml vs. 1.2 ± 0.4 pg/ml, $p = 0.024$) as shown in **Figure 1Aiii**, whereas Sham animals did not show a significant difference (4.4 ± 1.6 pg/ml vs. 3.5 ± 0.7 pg/ml, $p > 0.05$). Three weeks after ET-1 induction, blood estradiol concentration settled at 1.1 ± 0.2 pg/ml ($n = 3$, $p = 0.6$, vs. baseline) in Ovx animals and at 3.8 ± 1.1 pg/ml ($n = 2$, $p = 0.1$ vs. baseline) in Sham animals. At the study end point, Ovx rats did not show a significant drop in body weight when compared to Sham (414 ± 23 g vs. 475 ± 54 g, $p = 0.23$).

[1]http://www.R-project.org

Peri-Lesional Hypoperfusion and Bilateral Hyperreactivity of Ovx Females

To assess the effects of ovariectomy on stroke volume post ischemic insult, *in vivo* T_2-weighted MR-images were acquired in all animals 3 weeks after insult. Stroke volumes in both cohorts were estimated by segmenting regions of signal hyperintensity in the peri-lesional tissue (Dudink et al., 2009). Ovariectomy did not affect peri-lesional tissue volume, (Ovx: 1654.7 ± 504.6 mm^3, $n = 6$ vs. Sham: 1513.1 ± 414.0 mm^3, $n = 6$, $p = 0.98$, Student's t-test, **Figure 1Aiv**). Given the limited sensitivity of T_2-weighted MRI in predicting vascular and functional recovery [(Girard et al., 2014) and for review (Lake et al., 2016)], CASL MRI data were collected and used to estimate resting brain perfusion and cerebrovascular reactivity to hypercapnia, a standard (pre)clinical test of brain vascular functioning. CASL maps overlaid on structural T_2-weighted MR images from representative Sham and Ovx animals 3 weeks after surgery are shown in **Figure 1** (resting perfusion in **Figure 1B** and cerebrovascular reactivity to hypercapnia in **Figure 1C**). When compared to Sham animals, Ovx rats showed reduced resting perfusion in the peri-lesional cortex (60.9 ± 7.6 ml/min/100 g, $n = 6$, vs. 31.5 ± 5.7 ml/min/100 g, $n = 6$, $p = 0.0026$, Student's t-test), but not in the contralateral cortex (64.1 ± 6.1 ml/min/100 g, $n = 6$, vs. 57.8 ± 8.2 ml/min/100 g, $n = 6$, $p = 0.2975$, Student's t-test), as summarized in **Figure 1Biii**. The lateralization (i.e., the peri-to-contralesional ratio of resting perfusion) was significantly below 1 in the Ovx cohort ($p = 0.0016$), but indistinguishable from 1 in the Sham cohort ($p = 0.25$). Ovx animals showed increased cerebrovascular reactivity to hypercapnia (**Figure 1C**) when compared to Sham animals both in the peri-lesional cortex (76 ± 16.1%, $n = 6$, Sham vs. 116.2 ± 4.9%, $n = 6$, Ovx, $p = 0.0384$, Student's t-test), and in the contra-lateral cortex (41.7 ± 5.8%, $n = 6$, Sham vs. 68.1 ± 7.3%, $n = 6$, Ovx, $p = 0.0254$, Student's t-test), indicating exacerbated cerebrovascular dysfunction in Ovx relative to Sham animals. The lateralization of the cerebrovascular response to hypercapnia was evident both in the Ovx ($n = 6$, $p = 6.3*10^{-5}$) and in the Sham cohort ($n = 6$, $p = 0.0055$), indicating sustained hyper-reactivity of the peri-lesional vasculature in both cohorts.

Preserved Neuronal Power in Ovx Females

Figure 2A shows multi-electrode array recordings from the contralesional hemisphere (**Figure 2Ai**) and from the peri-lesional hemisphere (**Figure 2Aiii**) of an Ovx female (electrode arrays positioning is shown in **Figure 2Aii**). The spontaneous neuronal activity in the peri-ischemic area (orange traces in **Figure 2Aiii**) was attenuated in comparison to that in the caudal area of the ipsilesional hemisphere and to that of the contralesional hemisphere (green traces in **Figures 2Aii,iii**). **Figure 2Bi** displays example traces from the peri-ischemic tissue of a Sham female (magenta trace in **Figure 2Bi**) and the recording from the homologous electrode in the contra-lesional hemisphere (purple trace in **Figure 2Bi**) and their power spectra. Example traces in an Ovx female are enlarged in **Figure 2Bii** (orange for the peri-ischemic and green for the contralesional)

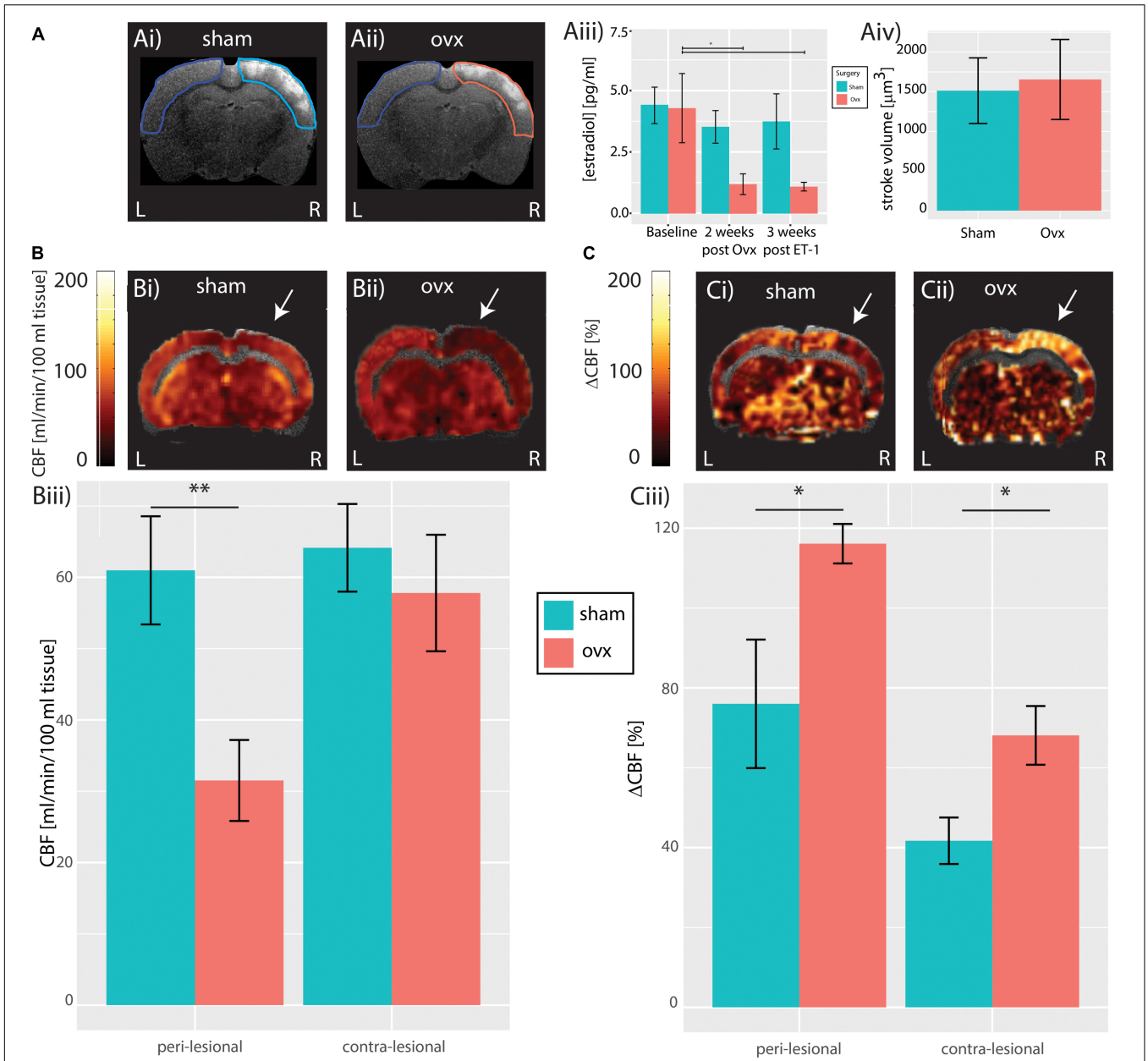

FIGURE 1 | Cerebral hemodynamics. **(A)** Structural T_2-weighted MR images of a Sham **(Ai)** and Ovx subject **(Aii)** showing anatomically identified peri-lesional tissue in turquoise and pink, respectively, and contra-lesional tissue in blue used for estimation of stroke volume; population analysis of T_2-weighted hyperintensity does not reveal difference in stroke volume between Sham and Ovx subjects **(Aiii)**. **(B)** Resting perfusion in a representative Sham **(Bi)** and Ovx **(Bii)** animal. Population analysis revealed reduced blood-flow in the peri-lesional (but not in the contra-lesional) tissue of Ovx subjects compared to that of the Sham group **(Biii)**. White arrow indicate the region of the slice most proximal to ET-1 injection sites. **(C)** Response to hypercapnia in a representative Sham **(Ci)** and Ovx **(Cii)** animals. Population analysis revealed increased response to hypercapnia both in the peri-lesional and in the contra-lesional tissue of Ovx animals compared to the Sham group **(Ciii)**. *$p < 0.05$ and **$p < 0.01$.

alongside their power spectra. **Figure 2C** shows the lateralization of total neuronal power in the Ovx vs. Sham females, revealing a trend toward greater peri- vs. contra-lesional neuronal power attenuation in the Ovx cohort when compared to the Sham group (1.2 ± 0.1, n = 6, vs. 0.8 ± 0.1, n = 6, p = 0.07). There were no differences in the ratio of relative neuronal power of Ovx vs. Sham animals in any of the individual bands (Theta: 0.71 ± 0.17 vs. 0.41 ± 0.05, p = 0.1; Alpha: 0.98 ± 0.3 vs. 0.68 ± 0.8, p = 0.41; Beta: 0.99 ± 0.2 vs. 0.73 ± 0.07, p = 0.28; Low gamma: 1.4 ± 0.2 vs. 0.96 ± 0.14, p = 0.1; High gamma: 1.92 ± 0.35 vs. 1.21 ± 0.18, p = 0.1, Student's t-test). The trend toward decreased power ratio observed in the peri-lesional tissue of Ovx rats was lost at increasing distances from the ET-1 injection site, namely at 0.5, 1, and 1.5 mm from the peri-lesional

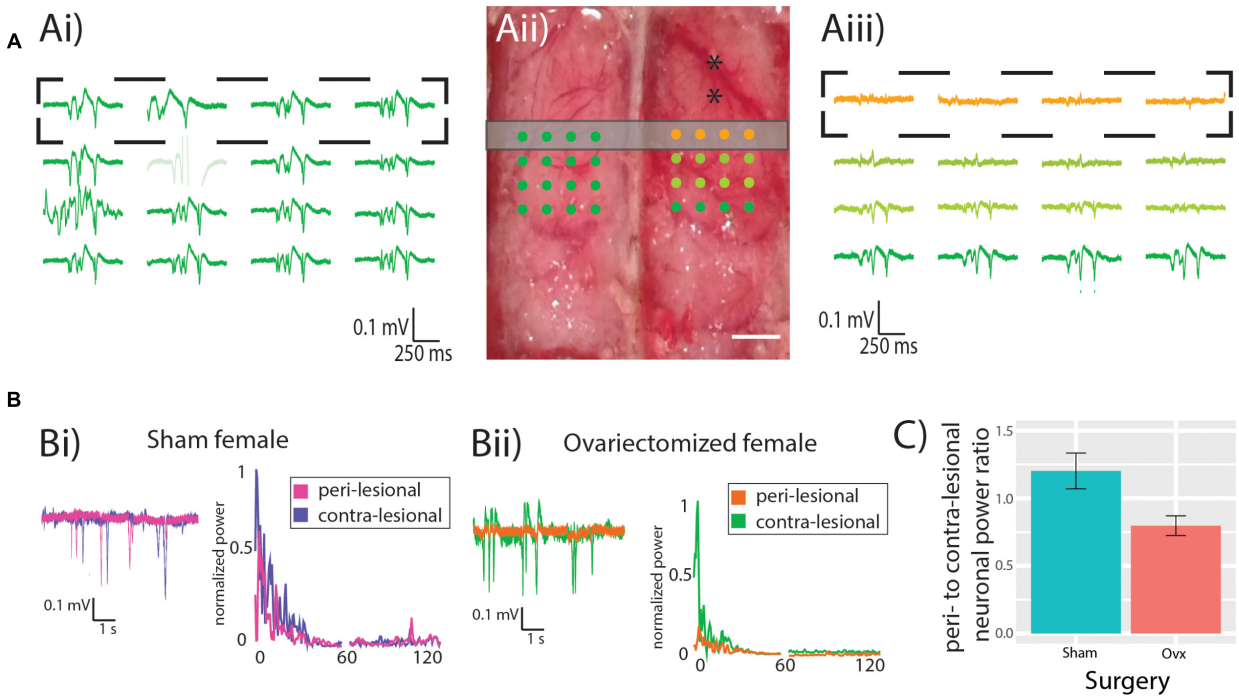

FIGURE 2 | Neuronal power. **(A)** Representative recording from contra- **(Ai)** and ipsi-lesional **(Aiii)** hemispheres, showing in orange the recordings from the peri-lesional tissue. Experimental design showing the MEA location (dots) in relation to the ET-1 injection sites (black asterisks) and the location of the CASL imaging slice (gray rectangle). Scale bar 0.5 mm. **(B)** representative recordings and power spectrum from the peri-lesional and contra-lesional hemisphere of Sham **(Bi)** and Ovx **(Bii)** animal. **(C)** Ovx animals (red bar) show a trend toward reduced neuronal power in the peri-lesional tissue when compared to that of Sham animals (green bar).

tissue, indicating that the neuronal dysfunction was spatially restricted.

Reduced Theta to Low Gamma Phase Amplitude Coupling in Ovx Females

In light of the trends observed in neuronal power and the sensitivity of Cross Frequency Coupling in capturing neuronal dysfunction in pathological models even in the absence of changes in power (de Hemptinne et al., 2013; Edakawa et al., 2016; Zhang et al., 2016; Barr et al., 2017; Devergnas et al., 2017; Bazzigaluppi et al., 2018), we explored Cross Frequency Coupling (CFC) between theta and gamma bands. Contra- and ipsi-lesional MI and sample recordings from a representative Sham animal are displayed in **Figure 3A**, while corresponding data from an Ovx animal are presented in **Figure 3B**. Representative data from the whole MEA are presented in **Supplementary Figure S1**. Population analysis revealed that the average theta to low-gamma MI was significantly reduced in Ovx animals (**Figure 3C**, 0.89 ± 0.10 Sham, $n = 6$, vs. 0.52 ± 0.04 Ovx, $n = 6$, $p = 0.009$, Student's t-test), while theta to high-gamma MI was not affected (**Figure 3C**, 1.04 ± 0.1 Sham, $n = 6$, vs. 0.93 ± 0.1 Ovx, $n = 6$, $p = 0.42$, Student's t-test). Correlating the lateralization in theta to low-gamma MI with the estradiol concentration at the time of ET-1 injection revealed a positive correlation between the two variables (**Figure 3D**, Spearman's rank correlation coefficient rho = 0.67, $p = 0.04$): higher estradiol levels correlated with reduced MI lateralization in the chronic stage. Furthermore, the use of MEA allowed us to describe the topology of the lesion: theta to low-gamma MI lateralization in Sham and Ovx declined at increasing distances from the peri-lesional tissue (tau = −0.7, Spearman's rank correlation, $p = 0.08$; theta to high gamma: tau = 0, Kendall's rank correlation, $p = 1$). The deficit in functional interaction between neuronal ensembles in the chronic stage of injury was thus confined to the tissue within 0.5 mm AP from the injection site.

DISCUSSION

It is known from clinical studies that bilateral oophorectomy in premenopausal women and the consequent drop in ovarian hormonal levels are associated with increased multimorbidity with 18 defined chronic conditions (Levine et al., 2016; Rocca et al., 2017). Furthermore, women approaching menopausal age are subject to an increased risk of stroke and reduced recovery compared to age matched men (Anderson et al., 1991). In the attempt to prevent the pernicious effects of hormonal depletion observed in aging women, estrogen replacement therapy (ERT) has been sporadically attempted as of 1960s. However, following experimental data from the Women's Health Initiative (WHI) and the observational data from the Nurses' Health Study (NHS) (Biernaskie et al., 2001) showing increased risk for secondary

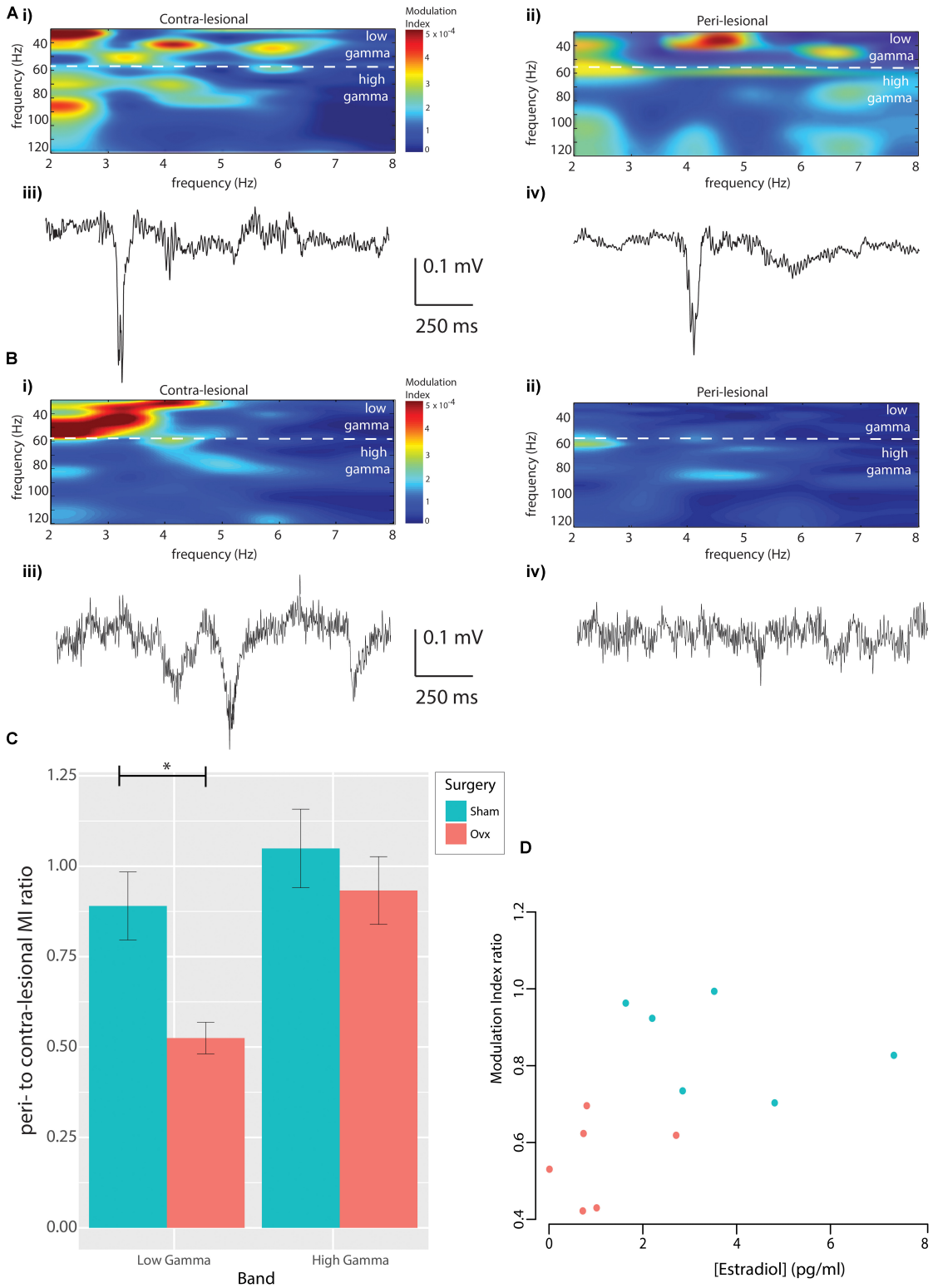

FIGURE 3 | Modulation index. **(A)** Modulation Index from contra-lesional **(Ai)** and peri-lesional **(Aii)** regions of a representative Sham rat, with representative raw data epochs from contra-lesional **(Aiii)** and ipsi-lesional **(Aiv)** regions of the same rat. **(B)** The corresponding data in an Ovx animal. **(C)** Population analysis revealed reduced peri-to-contralesional theta to low-gamma MI ratio in the Ovx vs. Sham cohort, whereas theta to high-gamma MI ratios were indistinguishable. **(D)** Positive correlation between peri-to-contra-lesional theta to low-gamma MI ratio and serum estradiol concentration at stroke-induction (Spearman's correlation, rho = 0.67, $p = 0.04$).

stroke in women older than 50 years supplemented orally with estrogen, it was considered an invariable risk factor for stroke and gradually abandoned. New studies [(Biernaskie et al., 2001) and references therein] proposed and supported the notion of a *timing hypothesis*, which posits that ERT exerts beneficial effects in patients younger than 50 years and starts becoming detrimental for women older than 60, particularly if administered orally. Testing of this hypothesis and the design of novel therapeutic approaches based on hormonal (estrogen alone or in combination with progesterone or allopregnanolone) supplementation requires models that recapitulate the salient phases of focal cerebrovascular occlusion-reperfusion and the drop in ovarian hormones observed in the patient population following bilateral oophorectomy. The present study is the first to link *in vivo* neurovascular function, which has been demonstrated a sensitive assay of brain recovery [for review (Lake et al., 2016)], with circulating estrogen levels at the time of ischemia, providing initial evidence that the evolution of ischemic damage and recovery is affected by estrogen levels in a model of oophorectomy in mature females. Our model of oophorectomy reproduces the faster decrease in estrogen concentration observed in surgically induced menopause [vs. that of natural menopause in women (Korse et al., 2009)] and ET-1 model of focal cortical ischemia produces a precisely targeted necrotic core surrounded by a sizeable region of functionally-challenged peri-ischemic tissue (Hossmann, 2008, 2009). Of note, in our previous study using this stroke model in males, we observed a mortality of ∼12% (Lake et al., 2017) at 48 h post-stroke; in the current study, mortality following stroke injection was 25% in Sham (2 in 8) and 40% in Ovx (4 in 10) females at the same time point (p = 0.52 Chi Squared test), in line with previously reported 35 and 54% of mortality at 6 and 24 h, respectively, in Charles River rats following transient Middle Cerebral Artery occlusion (Simpkins et al., 1997). Although mortality was not significantly different between groups at present, larger cohort studies may reveal the survival as a useful outcome measure of the model.

Neuronal Dysfunction

It was shown by Takuma and collaborators in female Fisher rats that Ovx alone (as well as in combination with restraint-stress) causes pyramidal neurons death in the CA3 and Dentate Gyrus of the hippocampus, associated with cognitive deficits in the novel object recognition test (Takuma et al., 2007a,b). Furthermore, it was previously reported that normo-oestrus female rats have lower death rate (Simpkins et al., 1997) and reduced neuronal death in the hippocampus (Miller et al., 2005; Zhang et al., 2006) and cortex (Fukuda et al., 2000) following global ischemia when compared to estrogen-depleted rats [for review (Brann et al., 2007)]. However, the effect of estrogen depletion/supplementation have mainly been investigated in the early state and by post-mortem assays, which cannot describe functional neuronal recovery (McCullough and Hurn, 2003). In the sole report describing the effect of Ovx on neuronal function in the acute stage of ischemia, Pelligrino et al. (1998) observed larger reduction in neuronal power within the first 30 min following common carotid artery clamping combined with hemorrhagic hypotension in Ovx female rats compared to Sham animals. However, early neuronal dysfunction is not a reliable predictor of long term injury (Moore et al., 2000; Lake et al., 2017; Momosaki et al., 2017). To develop novel therapeutic approaches, it is necessary to have a model that recapitulates the combined effect of estrogen loss and the sequelae of events following ischemia. The present study provides novel data on the consequences of estrogen depletion on neuronal and cerebrovascular recovery in the chronic stage, at 3 weeks post-stroke. Increased excitability in the peri-lesional cortex has been observed in male rats 3 weeks post stroke by us (Lake et al., 2017) and between a week to a month post stroke by others (Schiene et al., 1996; Winship and Murphy, 2008). The role of this increased excitability is still a matter of debate, but it has been hypothesized to be necessary for rewiring of the neuronal network [for review (Rabiller et al., 2015)]. In the present work, we did not observe increased neuronal power in the peri-lesional tissue of either Sham or Ovx females. In the absence of such dynamics in the females, and in the absence of a strong link between neuronal survival on histopathological assays and long-term functioning (Corbett and Nurse, 1998), we focused on the coupling between the phase of slow oscillation (theta) and the amplitude of a faster oscillation (gamma) since PAC has been hypothesized to be a sensitive predictor of cognitive function (Tort et al., 2009; Canolty and Knight, 2010; Lisman and Jensen, 2013). Although the features of excitatory and inhibitory network connectivity underlying PAC have not been established, PAC is known to reflect the temporal coordination of neuronal networks across or within brain regions (Womelsdorf et al., 2014) and has been observed in humans (Palva et al., 2005; Canolty et al., 2006) and rodents [for review (Jensen and Colgin, 2007)]. We focused on the modulation that the theta band (2–8 Hz) exerts on low-gamma band (30–60 Hz) and high-gamma band (60–120 Hz), as its importance has been shown in recent studies of human neocortical injury (Canolty et al., 2006; Jensen and Colgin, 2007). Patients with schizophrenia, Autism Spectrum Disorder, and Parkinson's Disease show reduced phase locking of gamma-band oscillations to theta and beta bands (Uhlhaas and Singer, 2012; Oswal et al., 2013), Mild Cognitive Impairment (Dimitriadis et al., 2015) and Alzheimer's Disease patients, in turn, exhibit reduced coupling between the phase of theta and the amplitude of gamma bands (Poza et al., 2017). Our results show for the first time that in the chronic stage, peri-lesional tissue of Ovx animals presents a ∼40% reduction in theta to low-gamma (but not theta to high-gamma) modulation when compared to that seen in Sham rats. While the difference between low gamma and high gamma bands is still unclear (Ray and Maunsell, 2011), they are known to be modulated independently. In humans, low gamma is mainly modulated by attention (Roh et al., 2016), while high gamma activity is modulated by sensory, motor, and cognitive events (Crone et al., 1998; Edwards et al., 2005). Moreover, the amplitude of both bands, is modulated (though in opposing directions) in relation to the gait cycle (Seeber et al., 2015). Reduced temporo-parietal PAC has been shown to be associated with

dementia and Alzheimer's Disease in patients (Poza et al., 2017), while an increase in subtalamic beta to gamma PAC is associated with increased severity of motor symptoms in Parkinson patients (van Wijk et al., 2016). Moreover, estradiol concentration measured at the time of stroke induction predicted the extent of this deficit, with higher estradiol concentration correlating with less injury (reduced lateralization of the modulation index). This observation lends further support to the importance of estradiol in injury susceptibility/functional recovery.

Cerebrovascular Dysfunction

It was previously reported that estrogen deficiency does not affect resting CBF measured by photoelectric method in urethane or halothane anesthetized animals (Holschneider and Scremin, 1998; Szelke et al., 2008), which have both been shown to depress cortical blood flow (Ueki et al., 1992). Propofol anesthesia, used presently, mildly reduces CBF, preserving normal circulation and metabolism (Oshima et al., 2002). Our experiments show that in the chronic state following ischemic insult, Ovx animals show ∼50% reduction in resting perfusion in the peri-lesional tissue, but not in the contralateral cortex. While we cannot exclude that CBF was reduced at the time of ET-1 injection in Ovx animals, **Figure 1Bii** shows that the resting perfusion in the contralesional (i.e., notionally unaffected hemisphere) 3 weeks after stroke induction was not distinguishable between Ovx and Sham animals. Notwithstanding, further studies on the effects of altered estradiol levels on resting cerebral perfusion are required. Furthermore, the resting CBF is lateralized (attenuated peri-lesionally vs. contra-laterally) in the Ovx but not in the Sham cohort. We have previously reported in the same ET-1 stroke model in adult male rats that resting cerebral blood flow normalizes in the chronic stage post stroke (Lake et al., 2017), just as it did here in the Sham females. However, in the same report we showed that neuronal power was elevated 3 weeks post stroke, supporting the notion of sex-differences in neurovascular recovery [and development in general (Manwani and McCullough, 2011)]. Previous work in the hyperacute stage of stroke showed that Ovx exacerbated CBF drop (measured with laser-Doppler flowmetry LDF) in the first half-hour following common carotid artery clamping combined with hemorrhagic hypotension (Pelligrino et al., 1998), and the increased drop be mediated by reduced nitric oxide synthase activity [for review (Pelligrino and Galea, 2001)]. In the present work we report that in response to hypercapnia, Ovx animals showed a ∼50% increase in cerebrovascular reactivity when compared to Sham animals both peri- and contra-lesionally. Previously it was reported that cerebrovascular responsivity to hypercapnia increases of ∼14% in the absence of cortical damage measured with the photoelectric method (Szelke et al., 2008). Flow response to hypercapnia relies on arteriolar smooth muscle relaxation (Mellander, 1989) and previous *ex vivo* report using the Pressurized Arteriograph Chamber showed that 30 days following Ovx, myogenic reactivity and passive lumen diameter of penetrating arterioles were unaffected while myogenic tone and Blood–Brain Barrier (BBB) permeability to Lucifer Yellow were increased when compared to specimens harvested from control subjects (Cipolla et al., 2009). In a different study, *ex vivo* spectrophotometry revealed increased BBB permeability to Evans Blue following global ischemia-reperfusion in Ovx female rats 3 weeks following surgery (Uzum et al., 2015). In both cases, ERT rescued the increase in BBB permeability. This evidence, together with the observation that BBB is more permeable in reproductively senescent females in the absence of stroke (Bake and Sohrabji, 2004) or acutely after experimental stoke (DiNapoli et al., 2008), indicates that the chronic stage neurovascular damage may be associated with increased BBB permeability.

Study Shortcomings and Translational Potential

As mentioned earlier, epidemiological studies have demonstrated that postmenopausal women have a higher risk of stroke than do age-matched men. While hypertension, diabetes, smoking and obesity are frequent, *modifiable* risk factors in both sexes, biological sex, aging and menopause are *non-modifiable* risk factors. To date, therapeutic exploitation of perimenopausal hormonal influence on cellular and molecular mechanisms underlying neuronal deficits following ischemia has been hindered by the lack of establishment of the neurovascular loss of function in the chronic stage observed in the patient population (Koellhoffer and McCullough, 2013). The present work provides a model that recapitulates the ovariectomy-induced exacerbation of peri-lesional cerebrovascular and neuronal dysfunction, which was found correlated with the circulating estradiol level at the time of stroke induction. PAC is still underutilized as recovery predictor in the clinic; rather, delta and theta bands power have been suggested highly sensitive markers of hypoxia [for review (Rabiller et al., 2015)]. Cerebral blood flow and cerebrovascular reactivity (CVR) mapping provides valuable information in the evaluation of cerebrovascular injury, including arterial stenosis, stroke, small vessel disease, brain tumors, traumatic brain injury, and normal aging [for review (Liu et al., 2017)]. Furthermore, both CBF and CVR can be measured non-invasively and are readily accessible in the patient population (Liu et al., 2017). While a battery of sensitive behavioral tests of sensorimotor function will be necessary to assess the benefits of any therapeutic interventions, the present findings reveal significant effects of ovariectomy on translationally relevant markers of neurovascular recovery from stroke.

AUTHOR CONTRIBUTIONS

PB, AP, PC, and BS designed the study and wrote the manuscript. PB, CA, and MK performed the experiments.

FUNDING

This work was supported by the Canadian Institutes for Health Research, grant number SVB145584 to BS, PC, and AP.

ACKNOWLEDGMENTS

The authors would like to thank Dr. Gillian Einstein (Wilfred and Joyce Posluns Chair in Women's Brain Health and Aging) for careful reading of the manuscript.

SUPPLEMENTARY MATERIAL

The Supplementary Material for this article can be found online at: https://www.frontiersin.org/articles/10.3389/fnmol.2018.00338/full#supplementary-material

REFERENCES

Anderson, K. M., Wilson, P. W., Odell, P. M., and Kannel, W. B. (1991). An updated coronary risk profile, a statement for health professionals. *Circulation* 83, 356–362. doi: 10.1161/01.CIR.83.1.356

Bake, S., and Sohrabji, F. (2004). 17beta-estradiol differentially regulates blood-brain barrier permeability in young and aging female rats. *Endocrinology* 145, 5471–5475. doi: 10.1210/en.2004-0984

Barr, M. S., Rajji, T. K., Zomorrodi, R., Radhu, N., George, T. P., Blumberger, D. M., et al. (2017). Impaired theta-gamma coupling during working memory performance in schizophrenia. *Schizophr. Res.* 189, 104–110. doi: 10.1016/j.schres.2017.01.044

Bazzigaluppi, P., Beckett, T. L., Koletar, M. M., Lai, A. Y., Joo, I. L., Brown, M. E., et al. (2018). Early-stage attenuation of phase-amplitude coupling in the hippocampus and medial prefrontal cortex in a transgenic rat model of Alzheimer's disease. *J. Neurochem.* 144, 669–679. doi: 10.1111/jnc.14136

Bernal-Mondragón, C., Rivas-Arancibia, S., Kendrick, K. M., and Guevara-Guzmán, R. (2013). Estradiol prevents olfactory dysfunction induced by A-β 25-35 injection in hippocampus. *BMC Neurosci.* 14:104. doi: 10.1186/1471-2202-14-104

Biernaskie, J., Corbett, D., Peeling, J., Wells, J., and Lei, H. (2001). A serial MR study of cerebral blood flow changes and lesion development following endothelin-1-induced ischemia in rats. *Magn. Reson. Med.* 46, 827–830. doi: 10.1002/mrm.1263

Bragin, A., Jando, G., Nadasdy, Z., Hetke, J., Wise, K., and Buzsaki, G. (1995). Gamma (40-100 Hz) oscillation in the hippocampus of the behaving rat. *J. Neurosci.* 15(1 Pt 1), 47–60. doi: 10.1523/JNEUROSCI.15-01-00047.1995

Brann, D. W., Dhandapani, K., Wakade, C., Mahesh, V. B., and Khan, M. M. (2007). Neurotrophic and neuroprotective actions of estrogen: basic mechanisms and clinical implications. *Steroids* 72, 381–405. doi: 10.1016/j.steroids.2007.02.003

Bushnell, C. D. (2008). Stroke and the female brain. *Nat. Clin. Pract. Neurol.* 4, 22–33. doi: 10.1038/ncpneuro0686

Canolty, R. T., and Knight, R. T. (2010). The functional role of cross-frequency coupling. *Trends Cognit. Sci.* 14, 506–515. doi: 10.1016/j.tics.2010.09.001

Canolty, R. T., Edwards, E., Dalal, S. S., Soltani, M., Nagarajan, S. S., Kirsch, H. E., et al. (2006). High gamma power is phase-locked to theta oscillations in human neocortex. *Science* 313, 1626–1628. doi: 10.1126/science.1128115

Chrobak, J. J., and Buzsaki, G. (1998). Gamma oscillations in the entorhinal cortex of the freely behaving rat. *J. Neurosci.* 18, 388–398. doi: 10.1523/JNEUROSCI.18-01-00388.1998

Cipolla, M. J., Godfrey, J. A., and Wiegman, M. J. (2009). The effect of ovariectomy and estrogen on penetrating brain arterioles and blood-brain barrier permeability. *Microcirculation* 16, 685–693. doi: 10.3109/10739680903164131

Cohen, S. L., Vitonis, A. F., and Einarsson, J. I. (2014). Updated hysterectomy surveillance and factors associated with minimally invasive hysterectomy. *JSLS* 18:e2014.00096. doi: 10.4293/JSLS.2014.00096

Corbett, D., and Nurse, S. (1998). The problem of assessing effective neuroprotection in experimental cerebral ischemia. *Progr. Neurobiol.* 54, 531–548. doi: 10.1016/S0301-0082(97)00078-6

Crone, N. E., Miglioretti, D. L., Gordon, B., and Lesser, R. P. (1998). Functional mapping of human sensorimotor cortex with electrocorticographic spectral analysis, II. Event-related synchronization in the gamma band. *Brain* 121(Pt 12), 2301–2315. doi: 10.1093/brain/121.12.2301

de Hemptinne, C., Ryapolova-Webb, E. S., Air, E. L., Garcia, P. A., Miller, K. J., Ojemann, J. G., et al. (2013). Exaggerated phase-amplitude coupling in the primary motor cortex in Parkinson disease. *Proc. Natl. Acad. Sci. U.S.A.* 110, 4780–4785. doi: 10.1073/pnas.1214546110

Devergnas, A., Caiola, M., Pittard, D., and Wichmann, T. (2017). Cortical phase-amplitude coupling in a progressive model of parkinsonism in nonhuman primates. *Cereb. Cortex* doi: 10.1093/cercor/bhx314 [Epub ahead of print].

Diaz Brinton, R. (2012). Minireview: translational animal models of human menopause: challenges and emerging opportunities. *Endocrinology* 153, 3571–3578. doi: 10.1210/en.2012-1340

Dimitriadis, S. I., Laskaris, N. A., Bitzidou, M. P., Tarnanas, I., and Tsolaki, M. N. (2015). A novel biomarker of amnestic MCI based on dynamic cross-frequency coupling patterns during cognitive brain responses. *Front. Neurosci.* 9:350. doi: 10.3389/fnins.2015.00350

DiNapoli, V. A., Huber, J. D., Houser, K., Li, X., and Rosen, C. L. (2008). Early disruptions of the blood-brain barrier may contribute to exacerbated neuronal damage and prolonged functional recovery following stroke in aged rats. *Neurobiol. Aging* 29, 753–764. doi: 10.1016/j.neurobiolaging.2006.12.007

Dudink, J., Mercuri, E., Al-Nakib, L., Govaert, P., Counsell, S. J., Rutherford, M. A., et al. (2009). Evolution of unilateral perinatal arterial ischemic stroke on conventional and diffusion-weighted MR imaging. *AJNR Am. J. Neuroradiol.* 30, 998–1004. doi: 10.3174/ajnr.A1480

Edakawa, K., Yanagisawa, T., Kishima, H., Fukuma, R., Oshino, S., Khoo, H. M., et al. (2016). Detection of epileptic seizures using phase-amplitude coupling in intracranial electroencephalography. *Sci. Rep.* 6:25422. doi: 10.1038/srep25422

Edwards, E., Soltani, M., Deouell, L. Y., Berger, M. S., Knight, R. T. (2005). High gamma activity in response to deviant auditory stimuli recorded directly from human cortex. *J. Neurophysiol.* 94, 4269–4280. doi: 10.1152/jn.00324.2005

Flecknell, P. (2016). *Laboratory Animal Anaesthesia – Basic Principles of Anaesthesia*, Chap. 1. Cambridge, MA: Academic Press.

Fukuda, K., Yao, H., Ibayashi, S., Nakahara, T., Uchimura, H., Fujishima, M., et al. (2000). Ovariectomy exacerbates and estrogen replacement attenuates photothrombotic focal ischemic brain injury in rats. *Stroke* 31, 155–160. doi: 10.1161/01.STR.31.1.155

Girard, S., Murray, K. N., Rothwell, N. J., Metz, G. A., and Allan, S. M. (2014). Long-term functional recovery and compensation after cerebral ischemia in rats. *Behav. Brain Res.* 270, 18–28. doi: 10.1016/j.bbr.2014.05.008

Gomez-Smith, M., Janik, R., Adams, C., Lake, E. M., Thomason, L. A. M., Jeffers, M. S., et al. (2017). Reduced cerebrovascular reactivity and increased resting cerebral perfusion in rats exposed to a cafeteria diet. *Neuroscience* 371, 166–177. doi: 10.1016/j.neuroscience.2017.11.054

Guilfoyle, D. N., Dyakin, V. V., O'Shea, J., Pell, G. S., and Helpern, J. A. (2003). Quantitative measurements of proton spin-lattice (T1) and spin-spin (T2) relaxation times in the mouse brain at 7.0 *T. Magn. Reson. Med.* 49, 576–580. doi: 10.1002/mrm.10371

Hendrich, K. S., Kochanek, P. M., Melick, J. A., Schiding, J. K., Statler, K. D., Williams, D. S., et al. (2001). Cerebral perfusion during anesthesia with fentanyl, isoflurane, or pentobarbital in normal rats studied by arterial spin-labeled MRI. *Magn. Reson. Med.* 46, 202–206. doi: 10.1002/mrm.1178

Holschneider, D. P., and Scremin, O. U. (1998). Effects of ovariectomy on cerebral flow of rats. *Neuroendocrinology* 67, 260–268. doi: 10.1159/000054321

Hossmann, K. A. (2009). Pathophysiological basis of translational stroke research. *Folia Neuropathol.* 47, 213–227.

Hossmann, K. A. (2008). Cerebral ischemia: models, methods and outcomes. *Neuropharmacology* 55, 257–270. doi: 10.1016/j.neuropharm.2007.12.004

Ingelsson, E., Lundholmm C., Johansson, A. L., and Altman, D. (2016). Hysterectomy and risk of cardiovascular disease: a population-based cohort study. *Eur. Heart J.* 32, 745–750. doi: 10.1093/eurheartj/ehq477

Jensen, O., and Colgin, L. L. (2007). Cross-frequency coupling between neuronal oscillations. *Trends Cognit. Sci.* 11, 267–269. doi: 10.1016/j.tics.2007.05.003

Joo, I. L., Lai, A. Y., Bazzigaluppi, P., Koletar, M. M., Dorr, A., Brown, M. E., et al. (2017). Early neurovascular dysfunction in a transgenic rat model of Alzheimer's disease. *Sci. Rep.* 7:46427. doi: 10.1038/srep46427

Kang, J. K., Benar, C., Al-Asmi, A., Khani, Y. A., Pike, G. B., Dubeau, F., et al. (2003). Using patient-specific hemodynamic response functions in combined

EEG-fMRI studies in epilepsy. *NeuroImage* 20, 1162–1170. doi: 10.1016/S1053-8119(03)00290-8

Kidwell, C. S., Alger, J. R., and Saver, J. L. (2003). Beyond mismatch: evolving paradigms in imaging the ischemic penumbra with multimodal magnetic resonance imaging. *Stroke* 34, 2729–2735. doi: 10.1161/01.STR.0000097608.38779.CC

Koellhoffer, E. C., and McCullough, L. D. (2013). The effects of estrogen in ischemic stroke. *Trans. Stroke Res.* 4, 390–401. doi: 10.1007/s12975-012-0230-5

Korse, C. M., Bonfrer, J. M., van Beurden, M., Verheijen, R. H., and Rookus, M. A. (2009). Estradiol and testosterone levels are lower after oophorectomy than after natural menopause. *Tumour Biol.* 30, 37–42. doi: 10.1159/000199449

Laird, N. M., and Ware, J. H. (1982). Random-effects models for longitudinal data. *Biometrics* 38, 963–974. doi: 10.2307/2529876

Lake, E. M., Bazzigaluppi, P., Mester, J., Thomason, L. A., Janik, R., Brown, M., et al. (2017). Neurovascular unit remodelling in the subacute stage of stroke recovery. *NeuroImage* 146, 869–882. doi: 10.1016/j.neuroimage.2016.09.016

Lake, E. M., Bazzigaluppi, P., and Stefanovic, B. (2016). Functional magnetic resonance imaging in chronic ischaemic stroke. *Philos. Trans. R. Soc. Lon. Ser. B Biol. Sci.* 371:20150353. doi: 10.1098/rstb.2015.0353

Lake, E. M., Chaudhuri, J., Thomason, L., Janik, R., Ganguly, M., Brown, M., et al. (2015). The effects of delayed reduction of tonic inhibition on ischemic lesion and sensorimotor function. *J. Cereb. Blood Flow Metab.* 35, 1601–1609. doi: 10.1038/jcbfm.2015.86

Laughlin, G. A., Barrett-Connor, E., Kritz-Silverstein, D., and von Muhlen, D. (2000). Hysterectomy, oophorectomy, and endogenous sex hormone levels in older women: the rancho bernardo study. *J. Clin. Endocrinol. Metab.* 85, 645–651. doi: 10.1210/jcem.85.2.6405

Lee, H., Simpson, G. V., Logothetis, N. K., and Rainer, G. (2005). Phase locking of single neuron activity to theta oscillations during working memory in monkey extrastriate visual cortex. *Neuron* 45, 147–156. doi: 10.1016/j.neuron.2004.12.025

Levine, M. E., Lu, A. T., Chen, B. H., Hernandez, D. G., Singleton, A. B., Ferrucci, L., et al. (2016). Menopause accelerates biological aging. *Proc. Natl. Acad. Sci. U.S.A.* 113, 9327–9332. doi: 10.1073/pnas.1604558113

Lisman, J. E., and Jensen, O. (2013). The theta-gamma neural code. *Neuron* 77, 1002–1016. doi: 10.1016/j.neuron.2013.03.007

Liu, P., Li, Y., Pinho, M., Park, D. C., Welch, B. G., and Lu, H. (2017). Cerebrovascular reactivity mapping without gas challenges. *NeuroImage* 146, 320–326. doi: 10.1016/j.neuroimage.2016.11.054

Manwani, B., and McCullough, L. D. (2011). Sexual dimorphism in ischemic stroke: lessons from the laboratory. *Womens Health (Lond.)* 7, 319–339. doi: 10.2217/whe.11.22

McCullough, L. D., and Hurn, P. D. (2003). Estrogen and ischemic neuroprotection: an integrated view. *Trends Endocrinol. Metab. TEM* 14, 228–235. doi: 10.1016/S1043-2760(03)00076-6

McGinn, R. J., and Valiante, T. A. (2014). Phase-amplitude coupling and interlaminar synchrony are correlated in human neocortex. *J. Neurosci.* 34, 15923–15930. doi: 10.1523/JNEUROSCI.2771-14.2014

Mellander, S. (1989). Functional aspects of myogenic vascular control. *J. Hyperten. Suppl.* 7, S21–S30; discussion S1.

Miller, N. R., Jover, T., Cohen, H. W., Zukin, R. S., and Etgen, A. M. (2005). Estrogen can act via estrogen receptor alpha and beta to protect hippocampal neurons against global ischemia-induced cell death. *Endocrinology* 146, 3070–3079. doi: 10.1210/en.2004-1515

Momosaki, S., Ito, M., Yamato, H., Iimori, H., Sumiyoshi, H., Morimoto, K., et al. (2017). Longitudinal imaging of the availability of dopamine transporter and D2 receptor in rat striatum following mild ischemia. *J. Cereb. Blood Flow Metab.* 37, 605–613. doi: 10.1177/0271678X16635183

Moore, A. H., Osteen, C. L., Chatziioannou, A. F., Hovda, D. A., and Cherry, S. R. (2000). Quantitative assessment of longitudinal metabolic changes in vivo after traumatic brain injury in the adult rat using FDG-microPET. *J. Cereb. Blood Flow Metab.* 20, 1492–1501. doi: 10.1097/00004647-200010000-00011

Neumann-Haefelin, T., Kastrup, A., de Crespigny, A., Yenari, M. A., Ringer, T., Sun, G. H., et al. (2000). Serial MRI after transient focal cerebral ischemia in rats: dynamics of tissue injury, blood-brain barrier damage, and edema formation. *Stroke* 31, 1965–1972; discussion 72–73.

Oshima, T., Karasawa, F., and Satoh, T. (2002). Effects of propofol on cerebral blood flow and the metabolic rate of oxygen in humans. *Acta Anaesthesiol. Scand.* 46, 831–835. doi: 10.1034/j.1399-6576.2002.460713.x

Oswal, A., Brown, P., and Litvak, V. (2013). Synchronized neural oscillations and the pathophysiology of Parkinson's disease. *Curr. Opin. Neurol.* 26, 662–670. doi: 10.1097/WCO.0000000000000034

Palva, J. M., Palva, S., and Kaila, K. (2005). Phase synchrony among neuronal oscillations in the human cortex. *J. Neurosci.* 25, 3962–3972. doi: 10.1523/JNEUROSCI.4250-04.2005

Pelligrino, D. A., Santizo, R., Baughman, V. L., and Wang, Q. (1998). Cerebral vasodilating capacity during forebrain ischemia: effects of chronic estrogen depletion and repletion and the role of neuronal nitric oxide synthase. *Neuroreport* 9, 3285–3291. doi: 10.1097/00001756-199810050-00026

Pelligrino, D. A., and Galea, E. (2001). Estrogen and cerebrovascular physiology and pathophysiology. *Jpn. J. Pharmacol.* 86, 137–158. doi: 10.1254/jjp.86.137

Petrea, R. B. A., Seshadri, S., Kelly-Hayes, M., Kase, C., and Wolf, P. (2009). Gender differences in stroke incidence and poststroke disability in the framingham heart study. *Stroke* 40, 1032–1037. doi: 10.1161/STROKEAHA.108.542894

Poza, J., Bachiller, A., Gomez, C., Garcia, M., Nunez, P., Gomez-Pilar, J., et al. (2017). Phase-amplitude coupling analysis of spontaneous EEG activity in Alzheimer's disease. *Conf. Proc. IEEE Eng. Med. Biol. Soc.* 2017, 2259–2262. doi: 10.1109/EMBC.2017.8037305

Rabiller, G., He, J. W., Nishijima, Y., Wong, A., and Liu, J. (2015). Perturbation of brain oscillations after ischemic stroke: a potential biomarker for post-stroke function and therapy. *Int. J. Mol. Sci.* 16, 25605–25640. doi: 10.3390/ijms161025605

Ray, S., and Maunsell, J. H. (2011). Different origins of gamma rhythm and high-gamma activity in macaque visual cortex. *PLoS Biol.* 9:e1000610. doi: 10.1371/journal.pbio.1000610

Roberts, D. A., Rizi, R., Lenkinski, R. E., and Leigh, J. S. Jr. (1996). Magnetic resonance imaging of the brain: blood partition coefficient for water: application to spin-tagging measurement of perfusion. *J. Magnet. Reson. Imaging* 6, 363–366. doi: 10.1002/jmri.1880060217

Rocca, W. A., Gazzuola Rocca, L., Smith, C. Y., Grossardt, B. R., Faubion, S. S, Shuster, L. T., et al. (2017). Bilateral oophorectomy and accelerated aging: cause or effect? *J. Gerontol. Ser. A Biol. Sci. Med. Sci.* 72, 1213–1217. doi: 10.1093/gerona/glx026

Rocca, W. A., Gazzuola-Rocca, L., Smith, C. Y., Grossardt, B. R., Faubion, S. S., Shuster, L. T., et al. (2016). Accelerated accumulation of multimorbidity after bilateral oophorectomy: a population-based cohort study. *Mayo Clin. Proc.* 91, 1577–1589. doi: 10.1016/j.mayocp.2016.08.002

Roh, S. C., Park, E. J., Shim, M., and Lee, S. H. (2016). EEG beta and low gamma power correlates with inattention in patients with major depressive disorder. *J. Affect. Disord.* 204, 124–130. doi: 10.1016/j.jad.2016.06.033

Schiene, K., Bruehl, C., Zilles, K., Qu, M., Hagemann, G., Kraemer, M., et al. (1996). Neuronal hyperexcitability and reduction of GABAA-receptor expression in the surround of cerebral photothrombosis. *J. Cereb. Blood Flow Metab.* 16, 906–914. doi: 10.1097/00004647-199609000-00014

Seeber, M., Scherer, R., Wagner, J., Solis-Escalante, T., and Muller-Putz, G. R. (2015). High and low gamma EEG oscillations in central sensorimotor areas are conversely modulated during the human gait cycle. *NeuroImage* 112, 318–326. doi: 10.1016/j.neuroimage.2015.03.045

Sengupta, P. (2013). The laboratory rat: relating its age with human's. *Int. J. Preven. Med.* 4, 624–630.

Silverman, J., and Muir, W. W. III. (1993). A review of laboratory animal anesthesia with chloral hydrate and chloralose. *Labor. Anim. Sci.* 43, 210–216.

Simpkins, J. W., Rajakumar, G., Zhang, Y. Q., Simpkins, C. E., Greenwald, D., Yu, C. J., et al. (1997). Estrogens may reduce mortality and ischemic damage caused by middle cerebral artery occlusion in the female rat. *J. Neurosurg.* 87, 724–730. doi: 10.3171/jns.1997.87.5.0724

Singletary, S. J., Kirsch, A. J., Watson, J., Karim, B. O., Huso, D. L., Hurn, P. D., et al. (2005). Lack of correlation of vaginal impedance measurements with hormone levels in the rat. *Contemp. Top. Lab. Anim. Sci.* 44, 37–42.

Stegmayr, B., Asplund, K., Kuulasmaa, K., Rajakangas, A. M., Thorvaldsen, P., and Tuomilehto, J. (1997). Stroke incidence and mortality correlated to stroke risk factors in the WHO MONICA Project, an ecological study of 18 populations. *Stroke* 28, 1367–1374. doi: 10.1161/01.STR.28.7.1367

Strom, J. O., Theodorsson, A., and Theodorsson, E. (2008). Substantial discrepancies in 17beta-oestradiol concentrations obtained with three different commercial direct radioimmunoassay kits in rat sera. *Scand. J. Clin. Labor. Investig.* 68, 806–813. doi: 10.1080/00365510802254638

Strom, J. O., Theodorsson, E., Holm, L., and Theodorsson, A. (2010). Different methods for administering 17beta-estradiol to ovariectomized rats result in opposite effects on ischemic brain damage. *BMC Neurosci.* 11:39. doi: 10.1186/1471-2202-11-39

Sudlow, C. L., and Warlow, C. P. (1997). Comparable studies of the incidence of stroke and its pathological types: results from an international collaboration, international stroke incidence collaboration. *Stroke* 28, 491–499. doi: 10.1161/01.STR.28.3.491

Szelke, E., Mersich, T., Szekacs, B., Sandor, P., Komjati, K., and Varbiro, S. (2008). Effects of estrogen and progestin on the CO_2 sensitivity of hemispheric cerebral blood volume. *Menopause* 15, 346–351. doi: 10.1097/gme.0b013e31813c688d

Takuma, K., Hoshina, Y., Arai, S., Himeno, Y., Matsuo, A., Funatsu, Y., et al. (2007a). Ginkgo biloba extract EGb 761 attenuates hippocampal neuronal loss and cognitive dysfunction resulting from chronic restraint stress in ovariectomized rats. *Neuroscience* 149, 256–262. doi: 10.1016/j.neuroscience.2007.07.042

Takuma, K., Matsuo, A., Himeno, Y., Hoshina, Y., Ohno, Y., Funatsu, Y., et al. (2007b). 17beta-estradiol attenuates hippocampal neuronal loss and cognitive dysfunction induced by chronic restraint stress in ovariectomized rats. *Neuroscience* 146, 60–68. doi: 10.1016/j.neuroscience.2007.01.017

Tort, A. B., Komorowski, R. W., Manns, J. R., Kopell, N. J., and Eichenbaum, H. (2009). Theta-gamma coupling increases during the learning of item-context associations. *Proc. Natl. Acad. Sci. U.S.A.* 106, 20942–20947. doi: 10.1073/pnas.0911331106

Ueki, M., Mies, G., and Hossmann, K. A. (1992). Effect of alpha-chloralose, halothane, pentobarbital and nitrous oxide anesthesia on metabolic coupling in somatosensory cortex of rat. *Acta Anaesthesiol. Scand.* 36, 318–322. doi: 10.1111/j.1399-6576.1992.tb03474.x

Uhlhaas, P. J., and Singer, W. (2012). Neuronal dynamics and neuropsychiatric disorders: toward a translational paradigm for dysfunctional large-scale networks. *Neuron* 75, 963–980. doi: 10.1016/j.neuron.2012.09.004

Uzum, G., Bahcekapili, N., Baltaci, A. K., Mogulkoc, R., and Ziylan, Y. Z. (2015). Pre- and post-estrogen administration in global cerebral ischemia reduces blood-brain barrier breakdown in ovariectomized rats. *Acta Physiol. Hung.* 102, 60–66. doi: 10.1556/APhysiol.102.2015.1.6

van der Zijden, J. P., van der Toorn, A., van der Marel, K., and Dijkhuizen, R. M. (2008). Longitudinal in vivo MRI of alterations in perilesional tissue after transient ischemic stroke in rats. *Exp. Neurol.* 212, 207–112. doi: 10.1016/j.expneurol.2008.03.027

van Wijk, B. C., Beudel, M., Jha, A., Oswal, A., Foltynie, T., Hariz, M. I., et al. (2016). Subthalamic nucleus phase-amplitude coupling correlates with motor impairment in Parkinson's disease. *Clin. Neurophysiol.* 127, 2010–2019. doi: 10.1016/j.clinph.2016.01.015

Weixelbaumer, K. M., Drechsler, S., Wehrenpfennig, P., Khadem, A., Bahrami, S., Tichy, A., et al. (2014). Estrus cycle status defined by vaginal cytology does not correspond to fluctuations of circulating estrogens in female mice. *Shock* 41, 145–153. doi: 10.1097/SHK.0000000000000070

Winship, I. R., Murphy, T. H. (2008). In vivo calcium imaging reveals functional rewiring of single somatosensory neurons after stroke. *J. Neurosci.* 28, 6592–6606. doi: 10.1523/JNEUROSCI.0622-08.2008

Womelsdorf, T., Valiante, T. A., Sahin, N. T., Miller, K. J., and Tiesinga, P. (2014). Dynamic circuit motifs underlying rhythmic gain control, gating and integration. *Nat. Neurosci.* 17, 1031–1039. doi: 10.1038/nn.3764

Zhang, X., Zhong, W., Brankack, J., Weyer, S. W., Muller, U. C., Tort, A. B., et al. (2016). Impaired theta-gamma coupling in APP-deficient mice. *Sci. Rep.* 6:21948. doi: 10.1038/srep21948

Zhang, Q. G., Wang, X. T., Han, D., Yin, X. H., Zhang, G. Y., and Xu, T. L. (2006). Akt inhibits MLK3/JNK3 signaling by inactivating Rac1: a protective mechanism against ischemic brain injury. *J. Neurochem.* 98, 1886–1898. doi: 10.1111/j.1471-4159.2006.04020.x

Conflict of Interest Statement: The authors declare that the research was conducted in the absence of any commercial or financial relationships that could be construed as a potential conflict of interest.

frontiers in Molecular Neuroscience

REVIEW
published: 05 October 2018
doi: 10.3389/fnmol.2018.00359

Neurosteroid Metabolites of Gonadal Steroid Hormones in Neuroprotection: Implications for Sex Differences in Neurodegenerative Disease

Ari Loren Mendell and Neil James MacLusky *

Department of Biomedical Sciences, Ontario Veterinary College, University of Guelph, Guelph, ON, Canada

Gonadal steroid hormones are neurotrophic and neuroprotective. These effects are modulated by local metabolism of the hormones within the brain. Such control is necessary to maintain normal function, as several signaling pathways that are activated by gonadal steroid hormones in the brain can also become dysregulated in disease. Metabolites of the gonadal steroid hormones—particularly 3α-hydroxy, 5α-reduced neurosteroids—are synthesized in the brain and can act through different mechanisms from their parent steroids. These metabolites may provide a mechanism for modulating the responses to their precursor hormones, thereby providing a regulatory influence on cellular responses. In addition, there is evidence that the 3α-hydroxy, 5α-reduced neurosteroids are neuroprotective in their own right, and therefore may contribute to the overall protection conferred by their precursors. In this review article, the rapidly growing body of evidence supporting a neuroprotective role for this class of neurosteroids will be considered, including a discussion of potential mechanisms that may be involved. In addition, we explore the hypothesis that differences between males and females in local neurosteroid production may contribute to sex differences in the development of neurodegenerative disease.

Keywords: neurosteroids, sex differences, Alzheimer's disease, neuroprotection, neurodegenerative disease

OPEN ACCESS

Edited by:
Jordan Marrocco,
Rockefeller University, United States

Reviewed by:
Jamie Maguire,
Tufts University School of Medicine, United States
Michael Schumacher,
Institut National de la Santé et de la Recherche Médicale (INSERM), France
Richard G. Hunter,
University of Massachusetts Boston, United States

***Correspondence:**
Neil James MacLusky
nmaclusk@uoguelph.ca

Received: *03 July 2018*
Accepted: *12 September 2018*
Published: *05 October 2018*

Citation:
Mendell AL and MacLusky NJ (2018) Neurosteroid Metabolites of Gonadal Steroid Hormones in Neuroprotection: Implications for Sex Differences in Neurodegenerative Disease. Front. Mol. Neurosci. 11:359. doi: 10.3389/fnmol.2018.00359

INTRODUCTION

Many neurodegenerative diseases—conditions that are characterized by progressive deterioration of cognition, mood, executive function, etc. due to loss of neurons in the central nervous system (CNS)—exhibit sex differences in incidence, onset and severity (for review see Hanamsagar and Bilbo, 2016). For example, while most studies indicate that men are more likely to develop amyotrophic lateral sclerosis (ALS; McCombe and Henderson, 2010) and Parkinson's disease (Baldereschi et al., 2000; Elbaz et al., 2002), the opposite is true for the development of Alzheimer's disease (AD; Seshadri et al., 1997; Plassman et al., 2011; Alzheimer's Association, 2014) and multiple sclerosis (MS; Voskuhl and Gold, 2012), with women comprising approximately two-thirds of patients living with both conditions (Hebert et al., 2013; Hanamsagar and Bilbo, 2016). Several potential causes for sex differences in neurodegenerative disease have been proposed over the years, including interactions between genetic background and environment (for review, Xu et al., 2015),

as well as sex differences in life expectancy and incidence of non-neurodegenerative conditions with high mortality rates (Alzheimer's Association, 2014).

One of the most prominent hypotheses for sex differences in the development of some of these conditions is the profound difference in the timing, extent and duration of decline in the levels of circulating gonadal steroid hormones. In women, the relatively abrupt and drastic menopausal decline in circulating ovarian steroids has been suggested to increase the risk for the development of AD, with a corresponding reduction in risk in estrogen replacement therapy users (Paganini-Hill and Henderson, 1994, 1996; Tang et al., 1996; Kawas et al., 1997), although the relationship is complex because other studies have also shown a positive correlation between estrogen exposure and risk of dementia (Geerlings et al., 2001; Schumacher et al., 2003). This relationship has been further complicated by equivocal findings regarding the role of progesterone on risk of dementia, specifically with respect to its interactions with estrogen in combination therapies (Shumaker et al., 2003; Honjo et al., 2005), with limited investigation of the effects of progesterone independent of estrogen. In men, the natural age-related decline in circulating testosterone levels is much more gradual than the menopausal decline in ovarian steroid hormones observed in women. Declining testosterone levels have been associated with an increased risk for the development of AD and cognitive decline (Hogervorst et al., 2001, 2003, 2004; Yeap et al., 2008; Hsu et al., 2015). Because of these findings, estrogen and testosterone are believed to be neuroprotective in women and men, respectively (for review, see Pike, 2017).

While traditional views of gonadal steroid hormone actions on the brain were predicated on the concept that circulating hormones were required to cross the blood-brain-barrier in order to exert their effects, the discovery of neurosteroids—steroid hormones that are synthesized *de novo* within the nervous system—has broadened the scope of the potential for steroid hormones to impact structure, activity and function of neurons and other cells throughout the CNS. The enzymes necessary for conversion of the primary gonadal steroid hormones to other biologically active metabolites are present in the brain. This raises the possibility that gonadal steroid hormone-mediated neuroprotection, and sex differences in the development of neurodegenerative diseases, may be impacted by neurosteroids that act through distinct mechanisms from their precursors.

In recent years, this hypothesis has gained added impetus from the recognition that the neuroprotective effects of steroids, whether synthesized locally or derived from peripheral steroidogenesis, may be augmented and diversified through local conversion to metabolites with biological properties different from those of their parent hormones. This is a very large and rapidly growing field, with elements beyond the scope of the present article to adequately review. For further information in this area, the reader is referred to a number of excellent recent reviews on the neuroprotective effects of gonadal steroids (Galea et al., 2017; Pike, 2017; Choleris et al., 2018; Giatti et al., 2018). The present review focuses more specifically on the 3α-hydroxy, 5α-reduced metabolites of circulating and neuro-steroids, as well as potential mechanisms through which they may exert neuroprotective effects in the nervous system. In addition, we explore the hypothesis that sex differences in the development of neurodegenerative disease may be partially attributable to differences in neurosteroidogenesis between males and females.

NEUROSTEROIDS

The study of neurosteroids has expanded enormously since the first demonstration that the key enzyme required for the biosynthesis of steroid hormones, the cytochrome P-450 cholesterol side-chain cleavage enzyme (P450scc) was widely distributed throughout the brain (Baulieu and Robel, 1990; Baulieu, 1997; Baulieu et al., 2001). These initial findings suggested that the biosynthetic pathways necessary to synthesize steroid hormones might be expressed within the nervous system. Steroidogenic enzymes including the P450scc, 17α-hydroxylase, 21-hydroxylase, P450 aromatase, 17β-hydroxysteroid dehydrogenase (17β-HSD), 5α-reductase, 3α-hydroxysteroid dehydrogenase (3α-HSD) and 3β-hydroxysteroid dehydrogenase (3β-HSD), are present in many different areas of the brain (Baulieu and Robel, 1990; Melcangi et al., 1996; Mellon and Griffin, 2002; Taves et al., 2011). The diversity of expression of these enzymes in the nervous system allows for the production of the principal steroid hormones, including cortisol (or corticosterone in rodents), progesterone, estradiol and testosterone. This local neurosteroidogenesis, combined with systemically-derived steroids that cross the blood-brain barrier, contribute to the importance of steroid hormones as modulators of neuronal function and survival. These hormones exert sex-specific effects on neural cells, as steroid receptors are differentially expressed throughout the brain in males and females of non-human primates and rodents (Finley and Kritzer, 1999; Milner et al., 2001, 2005; Adams et al., 2002; Nuñez et al., 2003; Tabori et al., 2005; Kritzer, 2006; Sarkey et al., 2008; Wang A. C. J. et al., 2010; Duarte-Guterman et al., 2015; Mogi et al., 2015). However, the influence of these steroid hormones on neural development, activity and survival are not limited to effects mediated via their respective steroid receptor systems. Over the past three decades, the actions of neurosteroid metabolites of gonadal steroid hormones that are synthesized in relatively high concentrations in the brain have received a great deal of attention, due to their ability to act through mechanisms that both converge and diverge from their parent hormones. Of particular interest has been their ability to modulate the activity and sensitivity of specific neurotransmitter receptors, but additional mechanisms by which neurosteroids may affect the function of cells in the brain have also been identified.

3α-HYDROXY, 5α-REDUCED NEUROSTEROIDS AS REGULATORS OF $GABA_A$ RECEPTOR ACTIVITY

Neurosteroid metabolites of gonadal steroid hormones can modulate the effects of neurotransmitters at their receptors, especially the inhibitory neurotransmitter γ-Aminobutyric acid

(GABA; Reddy et al., 2004; Belelli and Lambert, 2005; Reddy, 2008; Reddy and Jian, 2010; Carver and Reddy, 2013). Several neurosteroids are able to allosterically modulate the $GABA_A$ receptor, which is a pentamer of subunits with a chloride ion channel at the core. Neurosteroids with 3α-hydroxy, 5α-reduced structures are positive allosteric modulators of $GABA_A$ receptor activity. This includes metabolites of testosterone, progesterone and 11-deoxycorticosterone that have been sequentially reduced by 5α-reductase and 3α-HSD (most notably 3α-HSD type 3 in the brain) to produce 5α-androstane-3α, 17β-diol (3α-diol), 5α-pregnane-3α-ol-20-one (allopregnanolone) and 3α,21-dihydroxy-5α-pregan-20-one (tetrahydrodeoxycorticosterone, THDOC; **Figure 1**). The 3α-hydroxy, 5α-reduced structure is essential for allosteric modulation of $GABA_A$ activity, as 3β analogs (produced through sequential reduction by 5α-reductase and 3β-HSD) either have negative or null activity at the $GABA_A$ receptor. Importantly, the affinity and relative potency of 3α-hydroxy, 5α-reduced for the $GABA_A$ receptor is highly dependent on the subunit composition of the receptor itself. The $GABA_A$ receptor is a pentamer that is typically composed of two α subunits (α1–6), two β subunits (β1–4), and one additional subunit that is either a γ (γ1–3), δ, ε, π, or θ, or ρ (ρ1–3; Sieghart, 2006; Reddy and Jian, 2010; Belelli et al., 2018). A low-affinity human β3 homopentamer of the $GABA_A$ has been identified as well (Miller and Aricescu, 2014), though this conformation of the receptor does not appear to be neurosteroid-sensitive, probably due to the lack of α subunits (Nik et al., 2017). The subunit composition of the receptor differs depending on its location on the neuronal membrane. For example, receptors containing α1 and γ2 subunits are usually located within synapses, while receptors containing α4/α6 and δ subunits are extrasynaptic, generally being present on or near the cell body of neurons. While most heteropentamers are sensitive to modulation by neurosteroids, extrasynaptic receptors containing δ subunits have been shown to have relatively greater sensitivity. Neurosteroids bind to a distinct site within the core of the ion channel at α- and β-subunit transmembrane domains, whereas GABA itself binds to a site that is between α and β subunits (Hosie et al., 2006).

While the effects of 3α-hydroxy, 5α-reduced neurosteroids via regulation of $GABA_A$ receptor activity are relatively well characterized, other mechanisms have also been proposed. Some identified targets of allopregnanolone include the pregnane-X-receptor (PXR), liver-X-receptor (LXR), membrane progesterone receptor (mPR), N-Methyl-D-Aspartate (NMDA) receptor and L- or T-type calcium channels (Wang et al., 2005; Chen et al., 2011; Frye and Paris, 2011), while the testosterone metabolite 3α-diol has been shown to have negligible affinity for the androgen receptor (AR) and weak affinity for estrogen receptor β (ERβ; Liao et al., 1973; Kuiper et al., 1997; Penning, 1997; Edinger and Frye, 2007). Further work seems warranted in order to continue to identify and characterize mechanisms of action for these neurosteroids.

Because of their ability to modulate multiple signaling pathways, 3α-hydroxy, 5α-reduced neurosteroids have been shown to play important roles in physiological and pathophysiological regulation of stress, mood and feeding behavior (reviewed in Gunn et al., 2011; Mody and Maguire, 2012; Bäckström et al., 2014; Holmberg et al., 2018). In addition, and of particular interest for the focus of this review, 3α-hydroxy, 5α-reduced neurosteroids have been shown to have therapeutic potential for use in treatment of neurodegenerative and neurological diseases.

ALLOPREGNANOLONE IN NEUROPROTECTION

Allopregnanolone in Neuropathic Pain

Neuropathy is a persistent issue in patients undergoing chemotherapy, as well as a common symptom in patients with diabetes. Allopregnanolone has been widely shown to protect against physiological, biochemical and functional alterations associated with peripheral neuropathy. Anti-cancer drugs including Oxaliplatin and Vincristine have been shown to induce alterations to the normal function of peripheral nerves, decrease thermal and mechanical pain thresholds, and reduce sciatic nerve conduction velocity and action potential peak amplitude in adult male Sprague-Dawley rats (Meyer et al., 2010, 2011). In addition, protein markers for myelination of peripheral axons in the sciatic nerve have been found to be decreased by these treatments (Meyer et al., 2010). These effects were restored to normal by treatment with progesterone, 5α-dihydroprogesterone (DHP), or allopregnanolone (Meyer et al., 2010, 2011), with the precursors conceivably achieving these effects at least in part through conversion to allopregnanolone. Allopregnanolone has also been shown to protect against molecular and functional aspects of neuropathic pain induced by median nerve chronic constriction injury (CCI) in male Sprague-Dawley rats (Huang et al., 2016). In this study, treatment with allopregnanolone inhibited astrocytic and microglial ERK phosphorylation in the cuneate nucleus, concurrent with a reduction in pain hypersensitivity. This was also associated with a reduction in glial activation and pro-inflammatory cytokine expression in the cuneate nucleus. The observed protection was apparently exerted through potentiation of $GABA_A$ receptor activity, as bicuculline blocked the effects of allopregnanolone. These effects were proposed to be independent of reverse metabolism to DHP, as the synthetic progestin and allopregnanolone synthesis inhibitor, medroxyprogesterone, reduced allopregnanolone levels in the cuneate nucleus and exacerbated neuropathic pain parameters induced by CCI (Huang et al., 2016). However, it should be noted that the formulation of medroxyprogesterone (medroxyprogesterone acetate) used in the study discussed above has also been shown to impact the activation of other steroid hormone receptors, particularly androgen and glucocorticoid receptors (Stanczyk et al., 2013; Africander et al., 2014), which could have contributed to its effects.

Chronic streptozotocin exposure is a well-established method for induction of type 1 diabetes in rodent models. This provides a valuable model to study the effects of diabetes on peripheral

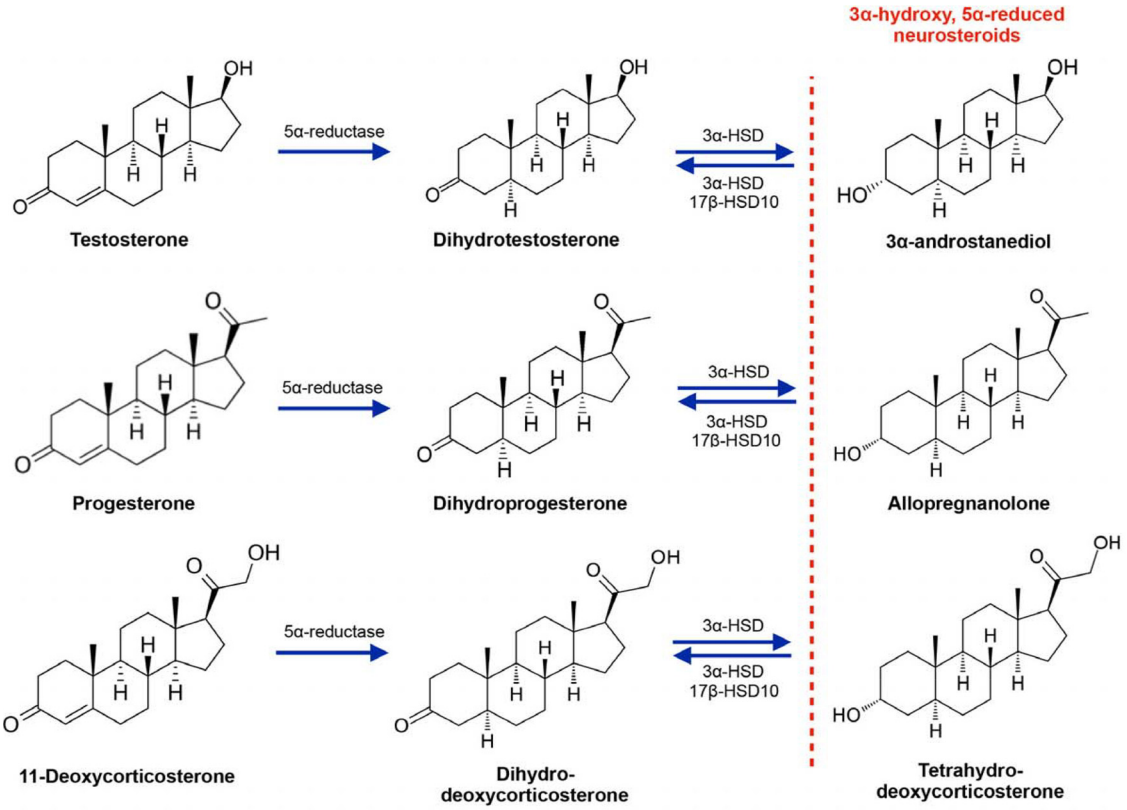

FIGURE 1 | Synthesis of the 3α-hydroxy, 5α-reduced neurosteroid metabolites of testosterone, progesterone and 11-deoxycorticosterone. 3α-HSD, 3α-hydroxysteroid dehydrogenase; 17β-HSD10, 17β-hydroxysteroid dehydrogenase (17β-HSD) type 10.

neuropathy. Using this model in male Sprague-Dawley rats, Leonelli et al. (2007) demonstrated that plasma progesterone levels are reduced in diabetic mice, and chronic treatment with progesterone, DHP, or allopregnanolone were effective in differentially restoring their circulating levels and counteracting impaired nerve conduction velocity of peripheral nerves. This effect was accompanied by an increase in thermal pain threshold and skin innervation density. In this study, levels of myelin protein markers and Na^+/K^+-ATPase activity were increased by progesterone and DHP, but not allopregnanolone (Leonelli et al., 2007).

In addition to peripheral neuropathy, allopregnanolone has been shown to alleviate some deficits in a mouse model of human immunodeficiency virus (HIV) neuropathy. The trans-activator of transcription (Tat) is a neurotoxic protein associated with neurological deficits in HIV patients. By using a mouse model that conditionally expressed Tat, Paris et al. (2016) were able to assess the impact of progesterone and its 5α-reduced metabolites on various neurological and pathophysiological deficits induced by Tat. They found that Tat expression in ovariectomized female mice resulted in an increase in anxiety-like behavior, and this was attenuated by progesterone. However co-treatment with finasteride (a 5α-reductase inhibitor) abolished the progesterone-mediated protection, suggesting that the protective effects were mediated by neurosteroid metabolites as opposed to progesterone itself. In the same study, allopregnanolone partially protected striatal neuronal-glial co-cultures against neurotoxicity and intracellular calcium accumulation induced by Tat treatment.

Allopregnanolone in Amyotrophic Lateral Sclerosis (ALS) and Multiple Sclerosis (MS)

Allopregnanolone is a promising candidate for the treatment of conditions that present with both neuroinflammation and neurodegeneration, as it has been shown to protect against the molecular and neurotoxic consequences of both processes. Two disorders that include both inflammatory and degenerative components are ALS and MS. As such, several studies have been performed in rodent models of these conditions in order to characterize protective effects of allopregnanolone. Deniselle et al. (2012) used Wobbler mice—a model for sporadic ALS—in order to evaluate the effects of chronic progesterone treatment on mitochondrial function. These mice had reductions of mitochondrial complex I and II-III activity, as well as increased levels of mitochondrial neuronal nitric oxide synthase (nNOS), which leads to toxic levels of nitric oxide and results in oxidative stress in the spinal motoneurons of these mice. Progesterone improved mitochondrial complex I activity in the cervical region of the spinal cord, reduced mitochondrial nNOS levels and prevented alterations in amyloid precursor

protein (APP) and MnSOD levels in motoneurons (Deniselle et al., 2012). In a follow up study, the same researchers demonstrated that allopregnanolone was able to produce similar protective effects in the Wobbler mice as progesterone had in the previous study. Both steroids were able to attenuate dysregulations in Akt and c-Jun N-terminal kinase (JNK) phosphorylation, motoneuron vacuolation, BDNF/TrkB mRNA expression, choline acetyltransferase (ChAT) and forelimb grip strength (Meyer et al., 2017). Another study by the same group found that the synthetic progestin Nestorone exerted many of the same beneficial effects in male Wobbler mice as progesterone and allopregnanolone (Meyer et al., 2015). In contrast, however, the effects appeared to be primarily dependent on progesterone receptor signaling, as conversion of Nestorone to its 3α-hydroxy, 5α-reduced was limited, and this metabolite did not possess substantial modulatory activity of the $GABA_A$ receptor (Kumar et al., 2017). Therefore, while allopregnanolone is important for progesterone-mediated neuroprotection in the Wobbler mouse, it does not appear to account for all of its beneficial effects.

One of the earliest studies establishing that neurosteroids may modulate factors related to myelination demonstrated that allopregnanolone treatment stimulated peripheral myelin protein 22 (P22) and myelin protein 0 (P0) gene expression in adult male rats, and in Schwann cell cultures (Melcangi et al., 1999). Based on their findings, it was therefore suggested that endogenous allopregnanolone may promote the expression of myelin proteins within the peripheral nervous system (Melcangi et al., 1999). Demyelination is a major pathophysiological characteristic of disorders with neuroinflammatory components, such as MS, and potential roles for neurosteroids on myelination in the CNS have been investigated. Several studies used the common experimental autoimmune encephalomyelitis (EAE) mice to investigate whether exogenous progesterone treatment could reduce the development of MS-related pathology, with the effects possibly being driven through conversion to allopregnanolone. In male EAE mice, it was demonstrated that administration of a progesterone pellet 1 week prior to EAE induction reduced demyelination, markers of axonal pathology and neuronal dysfunction/degeneration in spinal cord motoneurons (Garay et al., 2007, 2009). Interestingly, in the same EAE animal model, progesterone has recently been shown to modulate the expression of a number of mRNAs coding for enzymes involved in steroidogenesis, suggesting that in addition to acting as a substrate for neurosteroid production, progesterone may itself alter local steroidogenesis in the spinal cord (Garay et al., 2017).

Allopregnanolone in Parkinson's Disease

Parkinson's disease is a neurodegenerative condition with components involving degeneration of areas related to motor control, coordination and cognitive function. The actions of neurosteroids are known to be altered in Parkinson's patients, and this has been related to altered expression of biosynthetic enzymes and receptor subunit targets of neurosteroids. In the substantia nigra (SN) of Parkinson's disease patients, 5α-reductase type 1 and $GABA_A$ receptor subunits α4 and β1 were found to be downregulated, while 3α-HSD type 3 and $GABA_A$ receptor subunit α4 were upregulated in the cuneate nucleus (Luchetti et al., 2010). The latter could potentially be a compensatory response, in order to increase the local synthesis of 3α-hydroxy, 5α-reduced neurosteroids such as allopregnanolone and 3α-diol, along with one of their receptor subunit targets that is more sensitive to these metabolites (Carver and Reddy, 2013).

Studies in animal models have further characterized protective mechanisms of allopregnanolone in Parkinson's disease. The widely employed 1-methyl-4-phenyl-1,2,3,6-tetrahydropyridine (MPTP) lesion mouse model of Parkinson's disease (Meredith and Rademacher, 2011) was used to evaluate protective effects of allopregnanolone. In this study, it was found that allopregnanolone increased tyrosine hydroxylase (TH)-positive cells and total neurons in the SN pars compacta (SNpc) and the locus coeruleus (LC), and increased norepinephrine levels in the striatum of MPTP-lesioned male C57Bl/6J mice (Adeosun et al., 2012). In addition, allopregnanolone increased $BrdU^+$ neurons in the SNpc and improved performance of MPTP-lesioned mice on the rotarod test of balance and coordination (Adeosun et al., 2012).

Allopregnanolone in Ischemia and Traumatic Brain Injury (TBI)

Many peripheral and central conditions can result in cerebral ischemia, and primary gonadal steroids (particularly progesterone) have been shown to have promise in protection during the recovery from ischemic insult (for review see Sayeed and Stein, 2009). Because of the central conversion of progesterone to allopregnanolone, studies have also investigated a potential role for neurosteroid metabolites of gonadal steroid hormones in the protection of neural cells following ischemic insult and reperfusion.

Cardiac arrest is known to result in neuronal cell death as a result of global cerebral ischemia. Some areas of the brain are more susceptible to detrimental consequences of this ischemia than others, including the striatum, cerebellum and CA1 hippocampal subfield. In mice, the cardiac arrest requiring cardiopulmonary resuscitation (CA/CPR) model has been shown to recapitulate many of the effects seen in humans following such an event. In studies investigating cells in one of these vulnerable areas—Purkinje cells of the cerebellum—it was demonstrated that CA/CPR reduced $GABA_A$ receptor expression induced Purkinje cell death, while allopregnanolone was effective in preventing or reversing these consequences (Kelley et al., 2008, 2011). Interestingly, while Purkinje cell death was reduced by both 2 mg/kg and 8 mg/kg doses in adult female C57bl/6 mice, males were only protected by the higher dose (Kelley et al., 2011). Allopregnanolone increased inhibitory neurotransmission in both sexes, but was more effective in females (Kelley et al., 2011), further illustrating the sex difference in susceptibility. Similar experiments have confirmed these effects of allopregnanolone *in vitro*, demonstrating that cultured cerebellar Purkinje cells treated with allopregnanolone had recovered synaptic and total $GABA_A$ receptor current and increased α1 subunit expression that were reduced by oxygen glucose deprivation

(OGD; Kelley et al., 2008). These effects were consistent with an earlier report that demonstrated dose-dependent neuroprotection of cerebellar Purkinje cells by progesterone treatment following OGD, acting through a mechanism that was dependent on conversion to allopregnanolone (Ardeshiri et al., 2006). In that particular study, cultures from male mice required higher concentrations of progesterone to reduce cell death, consistent with the reports *in vivo* (Ardeshiri et al., 2006).

As opposed to the global ischemia induced by CA/CPR, middle cerebral artery occlusion (MCAO) can induce focal cerebral ischemia, which provides a model of ischemic stroke. Allopregnanolone and progesterone have been shown to significantly reduce infarct volume in several brain areas following MCAO in male Sprague-Dawley rats, including in the cerebral cortex (Sayeed et al., 2006, 2007). Interestingly, cortical infarct volume was found to be effectively reduced by a lower dose of allopregnanolone compared to progesterone (Sayeed et al., 2006), suggesting that progesterone may actually exert its effects through a mechanism that is at least partially dependent on conversion to allopregnanolone. Progesterone treatment was also shown to improve rotorod performance in rats following MCAO, indicating a potential role in improving balance and motor coordination during stroke recovery (Sayeed et al., 2007).

Traumatic brain injury (TBI) has aspects of pathology related to both direct damage to neurons from impact, as well as prolonged damage to ischemia or vessels and cells responsible for oxygenation and support of neurons. Using a controlled frontal cortical contusion model of TBI, it has been shown that allopregnanolone reduces the degree of apoptosis and cell loss, learning and memory deficits, and astrocyte infiltration to the site of injury, without affecting the size of the cavity induced by injury itself (Djebaili et al., 2004, 2005). This effect was also achieved with progesterone treatment, but consistent with the studies investigating the two steroid hormones on the effects of ischemia described above, allopregnanolone was effective at lower doses (Djebaili et al., 2004, 2005).

Allopregnanolone in Alzheimer's Disease

While allopregnanolone has been widely studied for both its endogenous role in the development and prevention of neurological and neurodegenerative diseases, as well as its potential use as an exogenous therapeutic, no condition has received more attention with respect to the potential protective applications of allopregnanolone than AD. Over the past two decades, studies from several research groups have investigated the mechanisms by which allopregnanolone may act as a protective and regenerative therapeutic in this disease.

One of allopregnanolone's most intriguing properties, in terms of its potential application to treatment of AD, is its ability to enhance proliferation of neural progenitor cells (NPCs) to create new neurons in the hippocampus. In male triple transgenic AD (3xTg-AD) mice, it has been consistently shown that allopregnanolone increases neurogenesis and promotes the survival of newly generated neural cells (Wang J. M. et al., 2010; Chen et al., 2011; Singh et al., 2012). In addition, allopregnanolone can reduce Aβ pathology in the hippocampus, cortex, and amygdala of male 3xTg-AD mice (Chen et al., 2011), and improve hippocampal-dependent associative learning and memory (Wang J. M. et al., 2010; Singh et al., 2012). An important consideration is that allopregnanolone was most effective if administered prior to the deposition of extraneuronal Aβ plaques (Chen et al., 2011; Singh et al., 2012). In addition, allopregnanolone can reduce the infiltration and activation of microglia and increase myelination of oligodendrocytes (Chen et al., 2011), consistent with reports from rodent models of other conditions (for details, see the neuropathy and ALS/MS sections above). Systems that regulate neurotransmitter levels may able be targets for protection by allopregnanolone. In the SNpc of young 3xTg-AD male mice, TH and total neuron levels were increased to control levels by a single allopregnanolone injection (Sun et al., 2012). Similar findings have been reported in young APPswe/PSEN1 double transgenic male mice, where these changes were accompanied by an increase in proliferation and survival of new neurons in the subventricular zone, and increased neuronal survival in the SNpc (Zhang et al., 2015).

Allopregnanolone promotes proliferation of NPCs in the subgranular zone (SGZ) of the dentate gyrus due to the unique nature of the GABAergic activation of cells in this area (Irwin et al., 2012). The NPCs in the SGZ retain a state similar to that of embryonic neurons, in which the $GABA_A$ receptor populations trigger an efflux of chloride upon opening, thereby depolarizing the cell (Tozuka et al., 2005; Irwin et al., 2012). Additionally, the predominant $GABA_A$ receptor subunits expressed on these cells is consistent with highly neurosteroid-sensitive, extrasynaptic $GABA_A$ receptors (containing α subunits that are often found with δ subunit-containing receptors; Stell et al., 2003; Overstreet Wadiche et al., 2005; Irwin et al., 2012). The depolarization caused by the efflux of chloride upon $GABA_A$ receptor channel opening results in the activation of voltage-dependent L-type calcium channels (Wang et al., 2005). This activates calcium-dependent kinases including the protein kinase A (PKA)/cyclic AMP (cAMP)/cAMP response element binding protein (CREB) pathway, leading to the upregulation of pro-mitotic and suppression of anti-mitotic gene expression (Wang and Brinton, 2008; Irwin et al., 2012). Interestingly, allopregnanolone has also been shown to increase intracellular calcium at low concentrations (EC50 of 10 ± 4 nM) in fetal hypothalamic neurons (Dayanithi and Tapia-Arancibia, 1996). The $GABA_A$ receptor-mediated effects are stereoselective, as 3β stereoisomers and steroids that have a removal, addition or alteration of hydroxyl functional groups, abolishing the effects at the $GABA_A$ receptor, fail to display the induction of proliferation in various *in vitro* and *in vivo* models (Brinton, 1994; Wang et al., 2005; Wang and Brinton, 2008; Karout et al., 2016).

Recent studies have also demonstrated the potential involvement of other mechanisms by which allopregnanolone may protect neural cells independent of proliferation of NPCs. Allopregnanolone has been shown to increase the expression of proteins that promote the clearance and homeostasis of cholesterol, including the LXR, the PXR and methyl-glutaryl-CoA-reductase (HMG-CoA-R; Chen et al., 2011). Interestingly, while the 3α-hydroxy conformation appears to be required to stimulate proliferation, 3β isomers of allopregnanolone and

synthetic analogs (3-O-allyl-allopregnanolone) have been shown to protect hippocampal neurons, neural stem cell cultures, and SH-SY5Y human female neuroblastoma cells from neurotoxicity induced by amyloid β peptide 1-42 (Aβ42) or hydrogen peroxide (H_2O_2; Karout et al., 2016; Lejri et al., 2017). The mechanisms of allopregnanolone and its analogs on neuroprotection *in vitro* appear to have both $GABA_A$ receptor-dependent and -independent components, as these neurosteroids are able to exert protective effects against Aβ42 or H_2O_2-induced toxicity in the absence of functional $GABA_A$ receptors (Lejri et al., 2017; Mendell et al., 2018); although allopregnanolone appears to be more effective at lower concentrations in the presence of functional $GABA_A$ receptors (Grimm et al., 2014; Karout et al., 2016; Mendell et al., 2018). Further studies are required in order to better characterize the $GABA_A$ receptor-independent mechanisms by which allopregnanolone may provide neuroprotection.

TESTOSTERONE METABOLISM IN NEUROPROTECTION

While the majority of studies investigating the potential protective effects of 3α-hydroxy, 5α-reduced neurosteroids have focused on allopregnanolone, other delta-4 3-keto hormonal steroids can also be converted to analogous bioactive metabolites. Recent work has expanded studies to the testosterone-derived structural analog of allopregnanolone, 3α-diol. Several studies have demonstrated that 3α-diol is effective in reducing peripheral neuropathy resulting from different chemical and physical insults (Meyer et al., 2013). Either prophylactic or corrective 3α-diol was shown to suppress paclitaxel-induced thermal and mechanical pain sensitivity, while restoring nerve conduction velocity and action potential peak amplitude in the sciatic nerve, as well as intraepidermal nerve fiber density in male Sprague-Dawley rats (Meyer et al., 2013). There was also evidence that 3α-diol repaired nerve damage in peripheral axons (Meyer et al., 2013). In another study investigating neuropathic pain related to induction of diabetes using streptozotocin injection, either DHT or 3α-diol had analgesic properties in diabetic male Sprague-Dawley rats (Calabrese et al., 2014). Interestingly, the mechanisms by which they improved neuropathic pain had both convergent and divergent components. Both neurosteroids reduced glutamate release, astrocyte infiltration and IL-1β expression. However, DHT increased mechanical nociceptive threshold and reduced over-activation of synapsin-1, syntaxin-1 and P-GluN2B, while 3α-diol increased tactile allodynia threshold and reduced mRNA expression of substance P, toll-like receptor 4, tumor necrosis factor-α, and TSPO (Calabrese et al., 2014). In an earlier study by Magnaghi et al. (2004), 3α-diol was also shown to promote the expression of factors related to peripheral myelination. In male Sprague-Dawley rats, gonadectomy decreased the expression of P0 and P22—two proteins that play a crucial physiological role in the maintenance of the multilamellar structure of peripheral myelin—and the levels of these proteins were recovered by treatment with 3α-diol, while DHT only recovered P0 expression (Magnaghi et al., 2004).

Many studies have evaluated cognitive outcomes after gonadectomy in male animals (for review, see Leonard and Winsauer, 2011). However, a limited number of these studies have evaluated the potential role of 3α-diol in effects that are largely attributed to testosterone, and loss thereof following gonadectomy. In a study using a battery of behavioral tests to evaluate the effects of gonadectomy and replacement with testosterone or 3α-diol in male Fisher-344 rats, Frye et al. (2010) found that age-related decline in performance on cognitive and affective tasks was associated with a decrease in hippocampal 3α-diol levels. Treatment with 3α-diol, but not testosterone, was able to reverse age-related decline in performance. Similar declines in performance were observed after gonadectomy in younger animals, and these were reversed by long-term testosterone replacement using Silastic capsules, which were found to increase both testosterone and 3α-diol levels in the hippocampus (Frye et al., 2010). In another study by the same group, gonadectomized young adult male Long-Evans rats were treated with either testosterone, DHT, or 3α-diol by long-term Silastic capsule implant or acute intrahippocampal infusion (Edinger and Frye, 2004). Animals treated with any of the steroids displayed improved measures of analgesia, less anxiety-like behavior, and increased learning compared to control animals. However, only hippocampal 3α-diol levels were positively correlated with performance on the various tasks, suggesting that effects were primarily mediated through 3α-diol as opposed the androgenic precursors (Edinger and Frye, 2004).

Evidence for a Protective Role of 3α-diol in Alzheimer's Disease

Several *in vitro* studies performed by our group and others have demonstrated that 3α-diol may play an important role in protecting against various molecular and cellular dysfunctions associated with the various pathophysiological processes that occur in the brains of individuals with AD.

Physiological concentrations of 3α-diol are able to protect SH-SY5Y neuroblastoma cells and primary cortical neurons isolated individually from male and female mice against neurotoxicity induced by H_2O_2 or Aβ42 (Mendell et al., 2016, 2018; **Figure 2**). This protection appeared to occur through 3α-diol-mediated inhibition of prolonged ERK phosphorylation induced by the neurotoxins, and was associated with a reduction in caspase-3 activation and cell death (Mendell et al., 2016; **Figure 2**). Interestingly, these effects appeared to be $GABA_A$ receptor-independent, as they were essentially the same in the absence (SH-SY5Y cells) or presence (primary cortical neurons) of functional neurosteroid-sensitive $GABA_A$ receptors, and were not prevented by picrotoxin (Mendell et al., 2018). Allopregnanolone was found to exert effects in both *in vitro* models, but required a 10-fold higher concentration than 3α-diol in the absence of $GABA_A$ receptors, while the effects on ERK phosphorylation were largely prevented by picrotoxin in cells expressing $GABA_A$ receptors (Mendell et al., 2018). These results are consistent with other findings on neurosteroid mediation of mitochondrial bioenergetics, which demonstrated that 10 nM concentrations of 3α-diol, but not allopregnanolone, were effective in improving aspects of mitochondrial function in

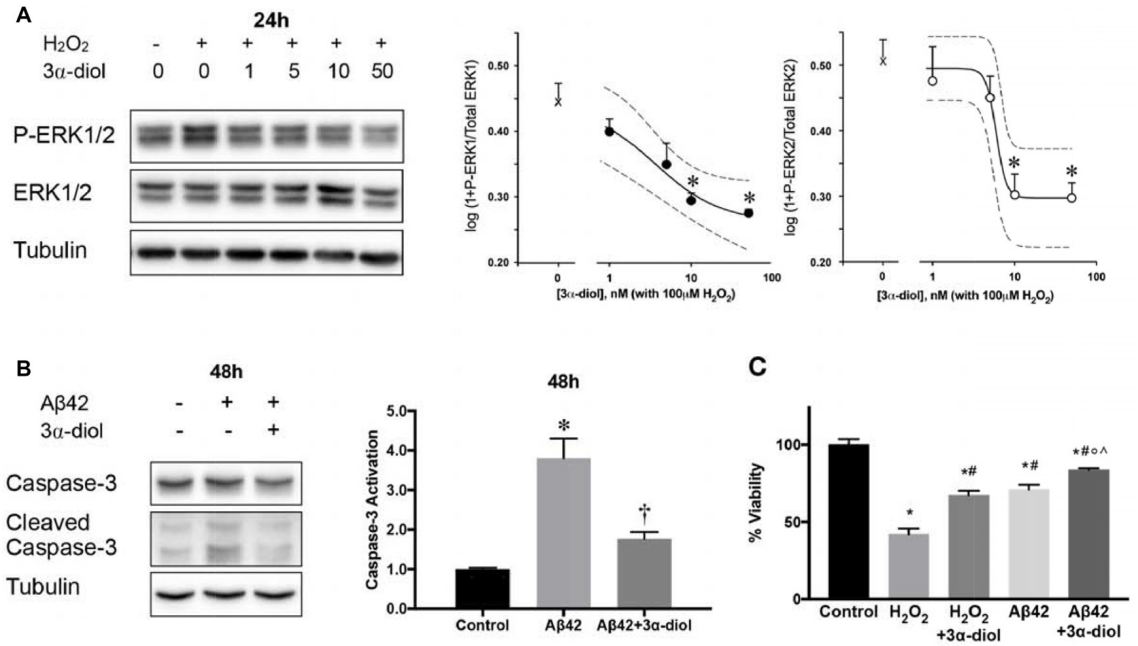

FIGURE 2 | 3α-androstanediol (3α-diol) inhibits ERK phosphorylation induced by hydrogen peroxide (H_2O_2) in a dose-dependent manner in SH-SY5Y cells **(A)**. 3α-diol reduces apoptosis induced by amyloid Beta peptide 1–42 (Aβ42), as indicated by decreased caspase-3 activation **(B)**, and dampens the loss in cellular viability induced by either H_2O_2 or Aβ42 **(C)**. For panel **(A)**, ∗ represents $p < 0.05$ compared to the H_2O_2 group. For panel **(B)**, ∗ and † represent $p < 0.05$ compared to the control and Aβ42 groups, respectively. For panel **(C)**, ∗, #, ∘, and ∧ represent $p < 0.05$ vs. the control, H_2O_2, H_2O_2 + 3α-diol, and Aβ42 groups, respectively. This figure is a compilation of illustrations from Mendell et al. (2016), reproduced by permission of Oxford University Press.

$GABA_A$ receptor deficient SH-SY5Y cells, although both steroids were effective in primary cortical neurons (Grimm et al., 2014). Experiments designed with the aim of identifying the $GABA_A$ receptor-independent mechanisms of 3α-diol action are ongoing, but as discussed above for allopregnanolone, further work will be necessary to characterize these effects.

These observations suggest a potentially important difference between males and females in the role of neurosteroidogenesis in the development of AD. In both men and women with AD, allopregnanolone has been found to decline in circulation and in various brain regions compared to normal control subjects (Bernardi et al., 2000; Yang and He, 2001; Marx et al., 2006; Smith et al., 2006; Naylor et al., 2010). By contrast, the available evidence suggests that neurotoxicity, including neurotoxicity associated with exposure to Aβ, may not reduce 3α-diol levels. In SH-SY5Y human neuroblastoma cells, 3α-diol is not reduced following H_2O_2-induced oxidative stress or exogenous Aβ exposure (Schaeffer et al., 2006, 2008), but increases in cells over-expressing APP (Schaeffer et al., 2006). *In vivo*, limbic brain concentrations of 3α-diol increase with age in wild-type and 3xTg-AD male mice (Caruso et al., 2013a). Consistent with these results, a divergence between plasma levels of allopregnanolone and 3α-diol has been reported in patients with AD, the former being significantly reduced in patients with the disease, while the latter does not appear to change, compared to normal age-matched controls (Smith et al., 2006). Taken together, these observations suggest that differences in the relative production rates of neurosteroids could affect susceptibility to AD. Brain concentrations of allopregnanolone in individuals with AD decline in both sexes, but there is relatively little change (and possibly even a compensatory increase) in brain 3α-diol levels. Higher levels of free androgen in the circulation of males could exacerbate the situation, by providing higher concentrations of testosterone as a substrate for local 3α-diol biosynthesis. If so, females could be at higher risk for disease development as a result of a relatively greater net loss of 3α-hydroxy, 5α-reduced neurosteroids with age. While this hypothesis remains speculative, because there is as yet insufficient direct comparative data on brain levels of different neurosteroids in males and females during both normal and pathological aging, further study of 3α-diol levels in relation to sex differences in the onset and progress of AD seems warranted.

TSPO LIGANDS IN NEUROPROTECTION

The 18 kDa translocator protein (TSPO) is believed to be an important regulator of steroid synthesis by enhancing the translocation of cholesterol into the mitochondria (Papadopoulos et al., 2006; Fan et al., 2015). Along with the steroidogenic acute regulatory protein (StAR), TSPO has been hypothesized to be essential to neurosteroid synthesis (Papadopoulos et al., 2006; Rupprecht et al., 2010), though there have recently been challenges to its necessity for adrenal and gonadal steroidogenesis using conditional TSPO knockout models (Morohaku et al., 2014; Fan et al., 2015). Because of its role in steroidogenesis, TSPO has been increasingly

studied in recent years as a potential therapeutic target in disorders that have shown improvement in preclinical models following neurosteroid manipulation (Rupprecht et al., 2010). Pharmaceutical compounds that are known to act as ligands for TSPO have been shown to induce neurosteroidogenesis, and this has been utilized to determine whether enhanced neurosteroidogenesis may be beneficial in several different models of neurodegenerative and neurological disorders (see Arbo et al., 2015).

Using the TSPO ligand Ro5-4864, Barron et al. (2013) assessed the effects of increasing activity of TSPO on neurosteroidogenesis, Aβ accumulation, gliosis and behavioral impairments in male 3xTg-AD mice, investigating both early (7-month old) and late (24-month old) stages of pathology. Ro5-4864 reduced Aβ load and gliosis in CA1 in gonadectomized (GDX) young adults, and also in intact aged mice. Ro5-4864 also increased brain progesterone and testosterone levels in pooled limbic structures of GDX young adults, but surprisingly decreased progesterone levels in aged mice. In addition, Ro5-4864 improved performance on the Y maze task for hippocampal-dependent working memory in GDX young adults and intact aged mice (Barron et al., 2013).

The TSPO ligand Ro5-4864 has also been investigated for potential application in peripheral neuropathy, which was discussed earlier in this review with respect to its improvement following neurosteroid treatment. In male Sprague-Dawley rats given streptozotocin injections to induce diabetic neuropathy, Ro5-4864 increased levels of pregnenolone, progesterone and DHT in the sciatic nerves, while reversing impairments in nerve conduction velocity, thermal threshold, skin innervation density, P0 mRNA levels, and activity of Na^+/K^+-ATPase (Giatti et al., 2009). As many of these factors were improved in the same way following treatment with DHT or 3α-diol in a previous study (Calabrese et al., 2014), it seems likely that the effects of Ro5-4864 in this study were due to its regulation of endogenous neurosteroidogenesis.

Like Ro5-4864, the TSPO agonist 4'-Chlorodiazepam (4'CD) has been studied for its potential as a neuroprotective agent using *in vitro* models. In SH-SY5Y cells and organotypic hippocampal cultures from early postnatal Wistar rats, 4'CD has been shown to protect against cell death induced by Aβ40 or Aβ42 (Arbo et al., 2016, 2017). This protection appeared to occur through mechanisms involving prevention of Aβ-induced alterations in Survivin and Bax in SH-SY5Y cells (Arbo et al., 2016), while 4'CD increased expression of superoxide dismutase in organotypic cultures, indicating improved antioxidant activity and potential clearance of oxidative free radicals (Arbo et al., 2017). While these studies did not investigate neurosteroid levels following Aβ or 4'CD treatment, it can be inferred that the protective effects observed in these studies were due to increased steroidogenesis, as many others have demonstrated that protection induced by agonism or over-expression of TSPO can be blocked by inhibitors of neurosteroid synthesis (Santoro et al., 2016; Zhang et al., 2016).

Certain ligands for TSPO are used as anxiolytics in humans, as they increase production of inhibitory neurosteroids like allopregnanolone (Li L. et al., 2017). Etifoxine is one such ligand, which acts as an activator of TSPO and also has neurosteroid-like activity as a positive allosteric modulator of the $GABA_A$ receptor (Liere et al., 2017). In a study looking at the impact of acute and chronic effects of etifoxine in male rats, etifoxine acutely increased pregnenolone, progesterone, DHP and allopregnanolone levels in brain tissue and in plasma without impacting testosterone or its metabolites. Concentrations of the neurosteroids peaked 0.5–1 h following injection, and were maintained with daily injections for 15 days (Liere et al., 2017). Through its dual actions of neurosteroid-like activity and stimulation of TSPO activity, etifoxine has been shown to reduce neurological deficits in male mice following intracerebral hemorrhage (ICH) or MCAO-induced hypoxia reperfusion injury (Li H.-D. et al., 2017; Li M. et al., 2017). These improvements were associated with reduced edema, reduced leukocyte infiltration and diminished cell death in the ICH model, reduced infarct volume in the MCAO model, and reduced proinflammatory cytokine production by microglia in both models (Li H.-D. et al., 2017; Li M. et al., 2017).

As TSPO is an important regulator of neurosteroidogenesis, it is interesting to note that increased microglial and astrocytic TSPO immunoreactivity in the hippocampus of AD patients has been reported, with large clusters of TSPO-positive cells localized in close proximity to senile plaques (Cosenza-Nashat et al., 2009). Since TSPO is upregulated in microglia and reactive astrocytes associated with injury (Chechneva and Deng, 2016), this could be a secondary consequence of the cellular damage resulting from Aβ toxicity.

MODULATION OF PRECURSOR ACTIONS BY NEUROSTEROIDS

Aside from their potential role in normalizing pathology-related proteins and intracellular signaling pathways in disease, 3α-hydroxy, 5α-reduced neurosteroids may also act in normal physiological circumstances to dampen cellular responses to their parent hormones, thereby providing an intrinsic regulatory mechanism by which the powerful and potentially harmful actions of steroid hormones may be controlled.

Gonadal steroid hormones exert neurotrophic and neuroprotective actions in the brain through several mechanisms, one of which is rapid and transient activation of intracellular signaling pathways leading to regulation of factors that promote neuronal survival (Nguyen et al., 2005; Zhao and Brinton, 2007; Pike et al., 2008). This includes the phosphoinositide 3-kinase/PI3K/Akt/mammalian target of rapamycin (PI3K/Akt/mTOR) pathway, the Ras/Raf/MEK/ERK pathway and the cAMP/PKA pathway, among others (for review see Foradori et al., 2008; Pike et al., 2008; Srivastava et al., 2011; Galea et al., 2017). However, as discussed above, the neurosteroid metabolites 3α-diol and allopregnanolone inhibit some of these same pathways when they become dysregulated in disease and injury (Huang et al., 2016; Mendell et al., 2016, 2018; **Figure 3**). The same inhibitory mechanisms may limit excessive activation by their precursor hormones—testosterone and progesterone, respectively. In SH-SY5Y human neuroblastoma cells, ERK phosphorylation is rapidly activated by DHT, and

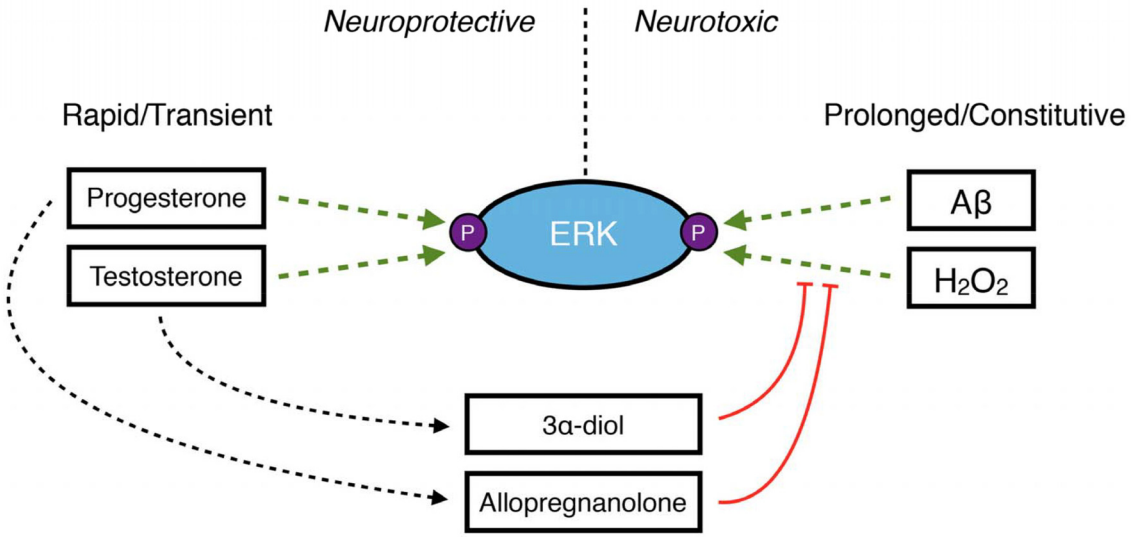

FIGURE 3 | A schematic demonstrating the role of neurosteroids in maintaining the balance of ERK phosphorylation in neuroprotection vs. neurodegeneration. Under normal conditions, the primary gonadal steroid hormones progesterone and testosterone rapidly and transiently increase ERK phosphorylation to protect neurons. However, increased levels of reactive oxygen species like H_2O_2 or accumulation of Aβ42 result in prolonged, dysregulated phosphorylation of ERK, which has detrimental downstream consequences in neurons. Under these conditions, the 3α-hydroxy, 5α-reduced neurosteroids 3α-diol and allopregnanolone may inhibit ERK phosphorylation.

this effect is inhibited by co-treatment with 3α-diol (Mendell et al., 2016). As progesterone has been shown to increase ERK phosphorylation in both *in vitro* neuronal models (Singh, 2001; Nilsen and Brinton, 2003) and *in vivo* in the brain (Orr et al., 2012), it is possible that a similar mechanism exists for progesterone metabolites in the regulation of effects driven by their precursor. While this concept presents an intriguing endogenous regulatory system, further work is necessary to determine whether these mechanisms operate in the brain, and whether any sex differences in these effects may exist.

NEUROSTEROIDOGENESIS, BIOSYNTHETIC ENZYMES AND NEUROSTEROID TARGETS: SEX DIFFERENCES AND RELATIONSHIP TO NEURODEGENERATIVE DISEASE

Neurosteroidogenesis

The availability of information regarding sex and age differences in neurosteroid levels in humans is limited for many reasons, including technical, logistical and ethical considerations. Furthermore, the influence of 5α-reduced neurosteroid levels on neurodegenerative disease, and the impact of disease progression on neurosteroidogenesis, is largely unknown. For example, AD is among the most widely studied neurodegenerative conditions, with known sex differences in incidence and severity of symptoms (Buckwalter et al., 1993; Henderson and Buckwalter, 1994; Ripich et al., 1995; Xing et al., 2015; Ardekani et al., 2016). However, 5α-reduced metabolites of gonadal steroid hormones have not been thoroughly investigated, though allopregnanolone has been consistently shown to be reduced in individuals with AD (Bernardi et al., 2000; Yang and He, 2001; Marx et al., 2006; Smith et al., 2006; Naylor et al., 2010). Studies in humans based on individual measures make causal inferences problematic: whether decreased allopregnanolone contributed to, or was a result of, disease development cannot be definitively stated.

Studies investigating sex differences in production of 3α-hydroxy, 5α-reduced neurosteroids under physiological conditions are limited. However, an important study by Caruso et al. (2013b) demonstrated that there are sex- and region-dependent differences in neurosteroid levels throughout the CNS and in plasma in young adult Sprague-Dawley rats. Measurements were reported in the cerebrospinal fluid (CSF), hippocampus, cerebral cortex, cerebellum, spinal cord and sciatic nerve—all regions that have been discussed in relation to neurosteroid intervention in models of disease throughout this review. Allopregnanolone levels were modestly higher in plasma and throughout the CNS of females, with the exception of the CSF, where levels were higher in males. The pattern of allopregnanolone levels also matched those of its immediate precursors, progesterone and DHP. In contrast, 3α-diol levels were markedly higher in plasma and in all regions of the CNS investigated in male rats. This pattern also matched those of its precursors, testosterone and DHT (Caruso et al., 2013b). While this study provided important insights into sex differences in levels of 3α-hydroxy, 5α-reduced neurosteroids under normal conditions, more of its kind are necessary.

Though many questions remain unanswered, studies using rodent models have helped to provide important insights into the potential roles for neurosteroids in neurodegenerative disease. In another study by Caruso et al. (2013a), neurosteroid levels

were measured in the limbic region of the brain in male 3xTg-AD mice at early (7 months old) and late (24 months old) stages of pathology, compared to age-matched wild-type animals. Pregnenolone, progesterone, testosterone and DHT were all found to decline, while levels of allopregnanolone were unchanged (Caruso et al., 2013a). Interestingly, 3α-diol levels were actually found to increase with age in male mice (Caruso et al., 2013a), which may be particularly important when considered together with reports that male 3xTg-AD mice develop less severe limbic region Aβ pathology and perform better on a task of hippocampal-dependent working memory than age-matched females (Carroll et al., 2010).

Giatti et al. (2010) measured levels of progesterone and testosterone, as well as their 5α-reduced metabolites in the spinal cord, cerebellum, cerebral cortex and plasma in male and female EAE pathogen-free Dark Agouti rats, used as a model of MS. These animals exhibit similar neurological deficiency and pathological severity, though males present with slightly more pronounced inflammation. In all CNS regions, testosterone, DHT and 3α-diol were drastically reduced in male EAE rats, and levels of these neurosteroids ranged from extremely low to undetectable in either control or EAE female rats (Giatti et al., 2010). Progesterone, DHP and allopregnanolone levels were higher in female control rats compared to male controls, but showed a more complex sex- and disease-dependent relationship than testosterone and its metabolites. Progesterone and DHP decreased in both male and female EAE rats in the spinal cord and cerebral cortex, while allopregnanolone actually increased in EAE males and was unaffected in EAE females compared to controls in both brain regions. In the cerebellum, allopregnanolone decreased in EAE females but not males, while progesterone decreased in both male and female EAE rats, and DHP was unaffected (Giatti et al., 2010). This study illustrates the complex nature of alterations to neurosteroidogenesis in disease, in this case using an MS rat model. It is important to note that age was not considered as a factor in this study, which could further compound the interactions between sex- and disease-related effects on neurosteroid levels.

Other studies have investigated changes in neurosteroid levels in rodent models of induced neurological deficits, as opposed to models of disease that occur spontaneously or due to genetic factors. One such study performed by Lopez-Rodriguez et al. (2016) investigated the impact of right orbitofrontal and perirhinal focal lesions in male Swiss-CD1 male mice as a model of TBI on neurosteroid levels in the brain and plasma. The authors reported that progesterone levels were unaffected at time points from 24 h up to 2 weeks following TBI, while testosterone, DHT and 3α-diol exhibited more complex temporal changes. Testosterone levels were significantly increased 2 weeks after injury compared to 24 h, but not significantly different than baseline levels. However, both DHT and 3α-diol were significantly reduced 2 weeks following injury compared to intact controls, while 3α-diol levels were positively correlated with the degree of brain edema, suggesting that a compensatory response may have occurred to increase local neuroprotective activity (Lopez-Rodriguez et al., 2016). Plasma levels of DHT, 3α-diol and 3β-diol were all reduced 2 weeks after TBI, though only plasma DHT and 3α-diol correlated significantly with neurological deficits (Lopez-Rodriguez et al., 2016).

Neurosteroid Biosynthetic Enzymes and Targets

Aside from neurosteroid levels themselves, measurements of expression and functionality of neurosteroidogenic enzymes, as well as targets for neurosteroid action, are important indicators of potential dysfunction in neurodegenerative disease. In both humans with AD (He et al., 2005; Luchetti et al., 2011a) and mouse models of AD (He et al., 2002; Yang et al., 2014; Porcu et al., 2016), 17β-HSD type 10 (17β-HSD10) is known to increase. As this mitochondrial enzyme functions to oxidize 3α-hydroxy, 5α-reduced neurosteroids, especially in the hippocampus (He et al., 2005), increased expression and/or activity of 17β-HSD10 contributes to decreased neurosteroid levels in AD (Yang et al., 2014; Porcu et al., 2016). Concentrations of the 3α-hydroxy, 5α-reduced neurosteroids are at least partially dependent on what has been referred to as a "dual enzyme molecular switch" (He et al., 2005; Yang et al., 2014; Porcu et al., 2016), involving 17β-HSD10 and 3α-HSD type 3 (3α-HSD3), which is predominantly localized to the endoplasmic reticulum. Theoretically, 3α-hydroxy, 5α-reduced neurosteroid levels would be most affected if the increase in 17β-HSD10 was accompanied by a decrease in 3α-HSD3, or if 5α-reductase expression or activity itself was decreased, thereby decreasing availability of precursors. However, data regarding the activity of these enzymes in neurodegenerative diseases is severely limited, with one study reporting increased expression of 3α-HSD3 in the prefrontal cortex of AD patients with both sexes grouped according to Braak stage (Luchetti et al., 2011a), while others have reported increased 5α-reductase expression in 12-month old APP/PS1 double transgenic AD mice (Porcu et al., 2016). Conversely, 3α-HSD3 and 5α-reductase type 1 expression have both been found to decrease in the white matter of patients with MS and in the hindbrain of young adult EAE mice, though all subjects were pooled and sex differences were not evaluated (Noorbakhsh et al., 2011).

As previously discussed, TSPO is an important regulator of neurosteroid synthesis. Interestingly, TSPO has been found to increase in several neurological and neurodegenerative diseases in humans (Porcu et al., 2016; reviewed in Rupprecht et al., 2010). In AD patients, positron emission tomography (PET) scanning using specific ligands for TSPO have demonstrated increased binding in many cortical areas, indicative of increased TSPO expression (Cagnin et al., 2001; Yasuno et al., 2008, 2012; Venneti et al., 2009; Zimmer et al., 2014). TSPO radioligand binding has also been reported to increase with age and pathology in double transgenic APP/PS1 mice (Venneti et al., 2009). In MS and stroke patients, increased TSPO expression has also been found at the sites of white matter lesions and primary lesions, respectively (Gerhard et al., 2005; Versijpt et al., 2005). Similar findings have

been reported in Huntington's disease (Pavese et al., 2006), ALS (Turner et al., 2004) and Parkinson's disease (Gerhard et al., 2006). It has been postulated that increased TSPO expression in these various neurodegenerative and neurological conditions could potentially be a compensatory biological response intended to increase local neurosteroid synthesis (Rupprecht et al., 2010), as TSPO levels have been reported to remain elevated during recovery in some disease models, including EAE mice (Agnello et al., 2000; Chen et al., 2004). The findings from these various studies strongly support a mechanism through which endogenous neurosteroid synthesis may increase locally around lesion sites, to limit neurotoxicity. However, it is important to note that sex was not considered as a biological variable in these studies, as male and female human subjects were grouped together in each case.

In addition to biosynthetic enzymes, the receptor targets for 3α-hydroxy, 5α-reduced neurosteroids may themselves be altered in disease states, thereby reducing the potential effectiveness of endogenous neurosteroids. The expression of some known neurosteroid-sensitive $GABA_A$ receptor subunits–α1, α2, α4, δ—have been shown to decrease in the prefrontal cortex of AD patients (Luchetti et al., 2011b), concurrent with declines in allopregnanolone levels (Bernardi et al., 2000; Marx et al., 2006; Smith et al., 2006; Naylor et al., 2010). However, the decline in $GABA_A$ receptor subunit expression may actually be a consequence of declining neurosteroid levels. Allopregnanolone has been shown to increase hippocampal α4 subunit protein expression in adult female rats (Gulinello et al., 2001; Hsu et al., 2003), and hippocampal synaptic α2 transcript expression in wild-type and progesterone receptor knockout female mice (Reddy et al., 2017). Other novel targets of 3α-hydroxy, 5α-reduced neurosteroids are the PXR and LXR, as discussed above. These proteins are associated with modulation of cholesterol metabolism and homeostasis, which is known to be dysregulated in early and progressive stages of AD (Zelcer et al., 2007). While loss of LXR and PXR was not reported in AD mouse models (Chen et al., 2011), genetic knockout of LXR isoforms exacerbated Aβ pathology in both male and female APP/PS1 double transgenic mice (Zelcer et al., 2007). Allopregnanolone treatment prior to development of Aβ pathology in male 3xTg-AD mice was reported to increase the expression of both LXR and PXR, concurrent with decreased Aβ oligomer accumulation (Chen et al., 2011). These findings provide further evidence that 3α-hydroxy, 5α-reduced neurosteroids, specifically allopregnanolone, may actually promote the expression of their target receptors. Therefore, when levels of these neurosteroids decline in AD, reduced target receptor expression may decline as well. This could indirectly contribute to loss of neuroprotection. For instance, reduced expression or activity of $GABA_A$ receptor subunits associated with decreased allopregnanolone in the brain of AD patients could reduce the effectiveness of other neurosteroids that have not been observed to decline, but protect neurons through the same mechanisms. This includes 3α-diol, which may be an important contributing factor to the observed sex differences in the development and progression of AD.

CONCLUSIONS AND LIMITATIONS

3α-hydroxy, 5α-reduced neurosteroids contribute to the neuroprotective and neurotrophic effects of their precursors, and play important roles in the development—and potential treatment—of neurodegenerative and neurological diseases. While this review has aimed to highlight the sex differences in endogenous production of these neurosteroids and their efficacy for treatment in several rodent models of disease (see **Figure 4**), there remains a substantial lack of information regarding differences in neurosteroidogenesis throughout life in both humans and other preclinical models, especially in relation to sex as a biological variable, since the majority of studies have been performed in males. This is a vital issue to consider, as it will be a

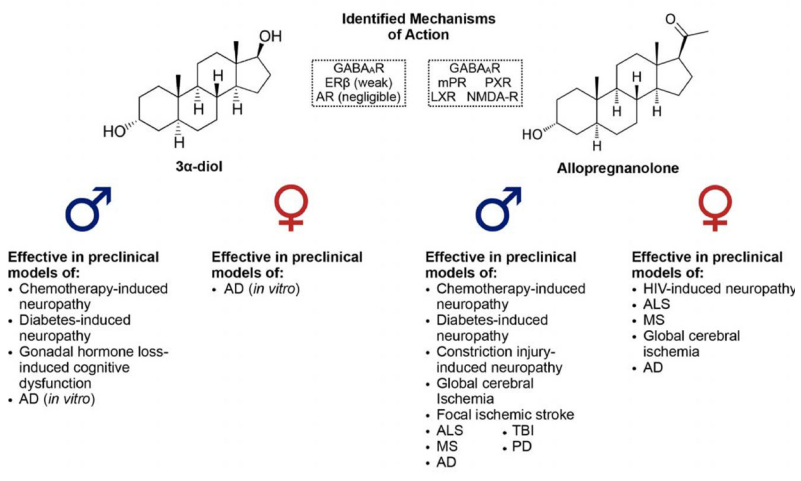

FIGURE 4 | Identified mechanisms of action of 3α-diol and allopregnanolone, along with a list of neurodegenerative/neurological diseases in which these 3α-hydroxy, 5α-reduced neurosteroids have been shown to effectively improve pathology or impairments in preclinical models.

substantial challenge for researchers to fully understand the role of these neurosteroids in sex differences until these questions are answered. The apparent lack of studies concerning both sexes for some of the preclinical disease models discussed should also be considered as a limitation to this review article, and a proposed focus for future studies. Studies incorporating both sexes, investigating age-related changes in neurosteroidogenesis, the onset and progression of disease-related pathology, and potential mechanisms for intervention, are an important priority for future research.

AUTHOR CONTRIBUTIONS

AM and NM wrote the manuscript.

FUNDING

The authors are supported by a Natural Sciences and Engineering Research Council of Canada (NSERC) Alexander Graham Bell Canada Graduate Scholarship to AM, and NSERC Discovery Grant 2015–04537 to NM.

REFERENCES

Adams, M. M., Fink, S. E., Shah, R. A., Janssen, W. G. M., Hayashi, S., Milner, T. A., et al. (2002). Estrogen and aging affect the subcellular distribution of estrogen receptor-α in the hippocampus of female rats. *J. Neurosci.* 22, 3608–3614. doi: 10.1523/jneurosci.22-09-03608.2002

Adeosun, S. O., Hou, X., Jiao, Y., Zheng, B., Henry, S., Hill, R., et al. (2012). Allopregnanolone reinstates tyrosine hydroxylase immunoreactive neurons and motor performance in an MPTP-lesioned mouse model of Parkinson's disease. *PLoS One* 7:e50040. doi: 10.1371/journal.pone.0050040

Africander, D. J., Storbeck, K. H., and Hapgood, J. P. (2014). A comparative study of the androgenic properties of progesterone and the progestins, medroxyprogesterone acetate (MPA) and norethisterone acetate (NET-A). *J. Steroid Biochem. Mol. Biol.* 143, 404–415. doi: 10.1016/j.jsbmb.2014.05.007

Agnello, D., Carvelli, L., Muzio, V., Villa, P., Bottazzi, B., Polentarutti, N., et al. (2000). Increased peripheral benzodiazepine binding sites and pentraxin 3 expression in the spinal cord during EAE: relation to inflammatory cytokines and modulation by dexamethasone and rolipram. *J. Neuroimmunol.* 109, 105–111. doi: 10.1016/s0165-5728(00)00279-4

Alzheimer's Association. (2014). 2014 Alzheimers disease facts and figures. *Alzheimers Dement.* 10, e47–e92. doi: 10.1016/j.jalz.2014.02.001

Arbo, B. D., Benetti, F., Garcia-Segura, L. M., and Ribeiro, M. F. (2015). Therapeutic actions of translocator protein (18 kDa) ligands in experimental models of psychiatric disorders and neurodegenerative diseases. *J. Steroid Biochem. Mol. Biol.* 154, 68–74. doi: 10.1016/j.jsbmb.2015.07.007

Arbo, B. D., Hoppe, J. B., Rodrigues, K., Garcia-Segura, L. M., Salbego, C. G., and Ribeiro, M. F. (2017). 4′-Chlorodiazepam is neuroprotective against amyloid-β in organotypic hippocampal cultures. *J. Steroid Biochem. Mol. Biol.* 171, 281–287. doi: 10.1016/j.jsbmb.2017.04.010

Arbo, B. D., Marques, C. V., Ruiz-Palmero, I., Ortiz-Rodriguez, A., Ghorbanpoor, S., Arevalo, M. A., et al. (2016). 4′-Chlorodiazepam is neuroprotective against amyloid-β through the modulation of survivin and bax protein expression *in vitro*. *Brain Res.* 1632, 91–97. doi: 10.1016/j.brainres.2015.12.018

Ardekani, B. A., Convit, A., and Bachman, A. H. (2016). Analysis of the MIRIAD data shows sex differences in hippocampal atrophy progression. *J. Alzheimers Dis.* 50, 847–857. doi: 10.3233/jad-150780

Ardeshiri, A., Kelley, M., Korner, I., Hurn, P., and Herson, P. (2006). Mechanism of progesterone neuroprotection of rat cerebellar Purkinje cells following oxygen-glucose deprivation. *Eur. J. Neurosci.* 24, 2567–2574. doi: 10.1111/j.1460-9568.2006.05142.x

Bäckström, T., Bixo, M., Johansson, M., Nyberg, S., Ossewaarde, L., Ragagnin, G., et al. (2014). Allopregnanolone and mood disorders. *Prog. Neurobiol.* 113, 88–94. doi: 10.1016/j.pneurobio.2013.07.005

Baldereschi, M., Di Carlo, A., Rocca, W., Vanni, P., Maggi, S., Perissinotto, E., et al. (2000). Parkinson's disease and parkinsonism in a longitudinal study: two-fold higher incidence in men. ILSA Working Group. Italian Longitudinal Study on Aging. *Neurology* 55, 1358–1363. doi: 10.1212/wnl.55.9.1358

Barron, A., Garcia-Segura, L., Caruso, D., Jayaraman, A., Lee, J., Melcangi, R., et al. (2013). Ligand for translocator protein reverses pathology in a mouse model of Alzheimer's disease. *J. Neurosci.* 33, 8891–8897. doi: 10.1523/JNEUROSCI.1350-13.2013

Baulieu, E. E. (1997). Neurosteroids: of the nervous system, by the nervous system, for the nervous system. *Recent Prog. Horm. Res.* 52, 1–32.

Baulieu, E., and Robel, P. (1990). Neurosteroids: a new brain function? *J. Steroid Biochem. Mol. Biol.* 37, 395–403. doi: 10.1016/0960-0760(90)90490-C

Baulieu, E., Robel, P., and Schumacher, M. (2001). Neurosteroids: beginning of the story. *Int. Rev. Neurobiol.* 46, 1–32. doi: 10.1016/s0074-7742(01)46057-0

Belelli, D., Brown, A. R., Mitchell, S. J., Gunn, B. G., Herd, M. B., Phillips, G. D., et al. (2018). Endogenous neurosteroids influence synaptic $GABA_A$ receptors during postnatal development. *J. Neuroendocrinol.* 30:e12537. doi: 10.1111/jne.12537

Belelli, D., and Lambert, J. J. (2005). Neurosteroids: endogenous regulators of the $GABA_A$ receptor. *Nat. Rev. Neurosci.* 6, 565–575. doi: 10.1038/nrn1703

Bernardi, F., Lanzone, A., Cento, R. M., Spada, R. S., Pezzani, I., Genazzani, A. D., et al. (2000). Allopregnanolone and dehydroepiandrosterone response to corticotropin-releasing factor in patients suffering from Alzheimer's disease and vascular dementia. *Eur. J. Endocrinol.* 142, 466–471. doi: 10.1530/eje.0.1420466

Brinton, R. D. (1994). The neurosteroid 3 α-hydroxy-5 α-pregnan-20-one induces cytoarchitectural regression in cultured fetal hippocampal neurons. *J. Neurosci.* 14, 2763–2774. doi: 10.1523/JNEUROSCI.14-05-02763.1994

Buckwalter, J., Sobel, E., Dunn, M., Diz, M., and Henderson, V. (1993). Gender differences on a brief measure of cognitive functioning in Alzheimer's disease. *Arch. Neurol.* 50, 757–760. doi: 10.1001/archneur.1993.00540070069018

Cagnin, A., Brooks, D. J., Kennedy, A. M., Gunn, R. N., Myers, R., Turkheimer, F. E., et al. (2001). *In vivo* measurement of activated microglia in dementia. *Lancet* 358, 461–467. doi: 10.1016/s0140-6736(01)05625-2

Calabrese, D., Giatti, S., Romano, S., Porretta-Serapiglia, C., Bianchi, R., Milanese, M., et al. (2014). Diabetic neuropathic pain: a role for testosterone metabolites. *J. Endocrinol.* 221, 1–13. doi: 10.1530/JOE-13-0541

Carroll, J. C., Rosario, E. R., Kreimer, S., Villamagna, A., Gentzschein, E., Stanczyk, F. Z., et al. (2010). Sex differences in β-amyloid accumulation in 3xTg-AD mice: role of neonatal sex steroid hormone exposure. *Brain Res.* 1366, 233–245. doi: 10.1016/j.brainres.2010.10.009

Caruso, D., Pesaresi, M., Abbiati, F., Calabrese, D., Giatti, S., Garcia-Segura, L. M., et al. (2013a). Comparison of plasma and cerebrospinal fluid levels of neuroactive steroids with their brain, spinal cord and peripheral nerve levels in male and female rats. *Psychoneuroendocrinology* 38, 2278–2290. doi: 10.1016/j.psyneuen.2013.04.016

Caruso, D., Barron, A. M., Brown, M. A., Abbiati, F., Carrero, P., Pike, C. J., et al. (2013b). Age-related changes in neuroactive steroid levels in 3xTg-AD mice. *Neurobiol. Aging* 34, 1080–1089. doi: 10.1016/j.neurobiolaging.2012.10.007

Carver, C. M., and Reddy, D. S. (2013). Neurosteroid interactions with synaptic and extrasynaptic $GABA_A$ receptors: regulation of subunit plasticity, phasic, and tonic inhibition and neuronal network excitability. *Psychopharmacology* 230, 151–188. doi: 10.1007/s00213-013-3276-5

Chechneva, O. V., and Deng, W. (2016). Mitochondrial translocator protein (TSPO), astrocytes and neuroinflammation. *Neural Regen. Res.* 11, 1056–1057. doi: 10.4103/1673-5374.187027

Chen, M. K., Baidoo, K., Verina, T., and Guilarte, T. R. (2004). Peripheral benzodiazepine receptor imaging in CNS demyelination: functional implications of anatomical and cellular localization. *Brain* 127, 1379–1392. doi: 10.1093/brain/awh161

Chen, S., Wang, J. M., Irwin, R. W., Yao, J., Liu, L., and Brinton, R. D. (2011). Allopregnanolone promotes regeneration and reduces β-amyloid

burden in a preclinical model of Alzheimer's disease. *PLoS One* 6:e24293. doi: 10.1371/journal.pone.0024293

Choleris, E., Galea, L. A. M., Sohrabji, F., and Frick, K. M. (2018). Sex differences in the brain: implications for behavioral and biomedical research. *Neurosci. Biobehav. Rev.* 85, 126–145. doi: 10.1016/j.neubiorev.2017.07.005

Cosenza-Nashat, M., Zhao, M., Suh, H., Morgan, J., Morgello, S., and Lee, S. C. (2009). Expression of the translocator protein of 18 kDa by microglia, macrophages and astrocytes based on immunohistochemical localization in abnormal human brain. *Neuropathol. Appl. Neurobiol.* 35, 306–328. doi: 10.1111/j.1365-2990.2008.01006.x

Dayanithi, G., and Tapia-Arancibia, L. (1996). Rise in intracellular calcium via a nongenomic effect of allopregnanolon in fetal rat hypothalamic neurons. *J. Neurosci.* 16, 130–136. doi: 10.1523/JNEUROSCI.16-01-00130.1996

Deniselle, M. C. G., Carreras, M. C., Garay, L., Gargiulo-Monachelli, G., Meyer, M., Poderoso, J. J., et al. (2012). Progesterone prevents mitochondrial dysfunction in the spinal cord of wobbler mice. *J. Neurochem.* 122, 185–195. doi: 10.1111/j.1471-4159.2012.07753.x

Djebaili, M., Guo, Q., Pettus, E., Hoffman, S., and Stein, D. (2005). The neurosteroids progesterone and allopregnanolone reduce cell death, gliosis and functional deficits after traumatic brain injury in rats. *J. Neurotrauma* 22, 106–118. doi: 10.1089/neu.2005.22.106

Djebaili, M., Hoffman, S. W., and Stein, D. G. (2004). Allopregnanolone and progesterone decrease cell death and cognitive deficits after a contusion of the rat pre-frontal cortex. *Neuroscience* 123, 349–359. doi: 10.1016/j.neuroscience.2003.09.023

Duarte-Guterman, P., Lieblich, S. E., Chow, C., and Galea, L. A. M. (2015). Estradiol and GPER activation differentially affect cell proliferation but not GPER expression in the hippocampus of adult female rats. *PLoS One* 10:e0129880. doi: 10.1371/journal.pone.0129880

Edinger, K. L., and Frye, C. A. (2004). Testosterone's analgesic, anxiolytic, and cognitive-enhancing effects may be due in part to actions of its 5α-reduced metabolites in the hippocampus. *Behav. Neurosci.* 118, 1352–1364. doi: 10.1037/0735-7044.118.6.1352

Edinger, K. L., and Frye, C. A. (2007). Androgens' effects to enhance learning may be mediated in part through actions at estrogen receptor-β in the hippocampus. *Neurobiol. Learn. Mem.* 87, 78–85. doi: 10.1016/j.nlm.2006.07.001

Elbaz, A., Bower, J., Maraganore, D., McDonnell, S., Peterson, B., Ahlskog, J., et al. (2002). Risk tables for parkinsonism and Parkinson's disease. *J. Clin. Epidemiol.* 55, 25–31. doi: 10.1016/S0895-4356(01)00425-5

Fan, J., Campioli, E., Midzak, A., Culty, M., and Papadopoulos, V. (2015). Conditional steroidogenic cell-targeted deletion of TSPO unveils a crucial role in viability and hormone-dependent steroid formation. *Proc. Natl. Acad. Sci. U S A* 112, 7261–7266. doi: 10.1073/pnas.1502670112

Finley, S. K., and Kritzer, M. F. (1999). Immunoreactivity for intracellular androgen receptors in identified subpopulations of neurons, astrocytes and oligodendrocytes in primate prefrontal cortex. *J. Neurobiol.* 40, 446–457. doi: 10.1002/(sici)1097-4695(19990915)40:4<446::aid-neu3>3.3.co;2-a

Foradori, C. D., Weiser, M. J., and Handa, R. J. (2008). Non-genomic actions of androgens. *Front. Neuroendocrinol.* 29, 169–181. doi: 10.1016/j.yfrne.2007.10.005

Frye, C. A., Edinger, K. L., Lephart, E. D., and Walf, A. A. (2010). 3α-androstanediol, but not testosterone, attenuates age-related decrements in cognitive, anxiety, and depressive behavior of male rats. *Front. Aging Neurosci.* 2:15. doi: 10.3389/fnagi.2010.00015

Frye, C. A., and Paris, J. J. (2011). Effects of neurosteroid actions at N-methyl-d-aspartate and $GABA_A$ receptors in the midbrain ventral tegmental area for anxiety-like and mating behavior of female rats. *Psychopharmacology* 213, 93–103. doi: 10.1007/s00213-010-2016-3

Galea, L., Frick, K., Hampson, E., Sohrabji, F., and Choleris, E. (2017). Why estrogens matter for behavior and brain health. *Neurosci. Biobehav. Res.* 76, 363–379. doi: 10.1016/j.neubiorev.2016.03.024

Garay, L., Deniselle, M. C. G., Lima, A., Roig, P., and De Nicola, A. F. (2007). Effects of progesterone in the spinal cord of a mouse model of multiple sclerosis. *J. Steroid Biochem. Mol. Biol.* 107, 228–237. doi: 10.1016/j.jsbmb.2007.03.040

Garay, L., Deniselle, M. C. G., Meyer, M., Costa, J. J. L., Lima, A., Roig, P., et al. (2009). Protective effects of progesterone administration on axonal pathology in mice with experimental autoimmune encephalomyelitis. *Brain Res.* 1283, 177–185. doi: 10.1016/j.brainres.2009.04.057

Garay, L., Gonzalez Giqueaux, P., Guennoun, R., Schumacher, M., Gonzalez Deniselle, M. C., and De Nicola, A. F. (2017). Progesterone treatment modulates mRNA OF neurosteroidogenic enzymes in a murine model of multiple sclerosis. *J. Steroid Biochem. Mol. Biol.* 165, 421–429. doi: 10.1016/j.jsbmb.2016.09.001

Geerlings, M., Ruitenberg, A., Witteman, J., van Swieten, J., Hofman, A., van Duijn, C., et al. (2001). Reproductive period and risk of dementia in postmenopausal women. *JAMA* 285, 1475–1481. doi: 10.1001/jama.285.11.1475

Gerhard, A., Pavese, N., Hotton, G., Turkheimer, F., Es, M., Hammers, A., et al. (2006). *In vivo* imaging of microglial activation with [^{11}C](*R*)-PK11195 PET in idiopathic Parkinson's disease. *Neurobiol. Dis.* 21, 404–412. doi: 10.1016/j.nbd.2005.08.002

Gerhard, A., Schwarz, J., Myers, R., Wise, R., and Banati, R. B. (2005). Evolution of microglial activation in patients after ischemic stroke: a [^{11}C]*(R)*-PK11195 PET study. *Neuroimage* 24, 591–595. doi: 10.1016/j.neuroimage.2004.09.034

Giatti, S., D'Intino, G., Maschi, O., Pesaresi, M., Garcia-Segura, L. M., Calza, L., et al. (2010). Acute experimental autoimmune encephalomyelitis induces sex dimorphic changes in neuroactive steroid levels. *Neurochem. Int.* 56, 118–127. doi: 10.1016/j.neuint.2009.09.009

Giatti, S., Garcia-Segura, L. M., Barreto, G. E., and Melcangi, R. C. (2018). Neuroactive steroids, neurosteroidogenesis and sex. *Prog. Neurobiol.* doi: 10.1016/j.pneurobio.2018.06.007 [Epub ahead of print].

Giatti, S., Pesaresi, M., Cavaletti, G., Bianchi, R., Carozzi, V., Lombardi, R., et al. (2009). Neuroprotective effects of a ligand of translocator protein-18kDa (Ro5–4864) in experimental diabetic neuropathy. *Neuroscience* 164, 520–529. doi: 10.1016/j.neuroscience.2009.08.005

Grimm, A., Schmitt, K., Lang, U. E., Mensah-Nyagan, A. G., and Eckert, A. (2014). Improvement of neuronal bioenergetics by neurosteroids: implications for age-related neurodegenerative disorders. *Biochim. Biophys. Acta* 1842, 2427–2438. doi: 10.1016/j.bbadis.2014.09.013

Gulinello, M., Gong, Q. H., Li, X., and Smith, S. S. (2001). Short-term exposure to a neuroactive steroid increases α4 $GABA^A$receptor subunit levels in association with increased anxiety in the female rat. *Brain Res.* 910, 55–66. doi: 10.1016/s0006-8993(01)02565-3

Gunn, B. G., Brown, A. R., Lambert, J. J., and Belelli, D. (2011). Neurosteroids and $GABA_A$ receptor interactions: a focus on stress. *Front. Neurosci.* 5:131. doi: 10.3389/fnins.2011.00131

Hanamsagar, R., and Bilbo, S. (2016). Sex differences in neurodevelopmental and neurodegenerative disorders: focus on microglial function and neuroinflammation during development. *J. Steroid Biochem. Mol. Biol.* 160, 127–133. doi: 10.1016/j.jsbmb.2015.09.039

He, X. Y., Wegiel, J., and Yang, S. Y. (2005). Intracellular oxidation of allopregnanolone by human brain type 10 17β-hydroxysteroid dehydrogenase. *Brain Res.* 1040, 29–35. doi: 10.1016/j.brainres.2005.01.022

He, X. Y., Wen, G. Y., Merz, G., Lin, D., Yang, Y. Z., Mehta, P., et al. (2002). Abundant type 10 17β-hydroxysteroid dehydrogenase in the hippocampus of mouse Alzheimer's disease model. *Mol. Brain Res.* 99, 46–53. doi: 10.1016/s0169-328x(02)00102-x

Hebert, L. E., Weuve, J., Scherr, P. A., and Evans, D. A. (2013). Alzheimer disease in the United States (2010–2050) estimated using the 2010 census. *Neurology* 80, 1778–1783. doi: 10.1212/WNL.0b013e31828726f5

Henderson, V., and Buckwalter, J. (1994). Cognitive deficits of men and women with Alzheimer's disease. *Neurology* 44, 90–96. doi: 10.1212/wnl.44.1.90

Hogervorst, E., Bandelow, S., Combrinck, M., and Smith, A. D. (2004). Low free testosterone is an independent risk factor for Alzheimer's disease. *Exp. Gerontol.* 39, 1633–1639. doi: 10.1016/j.exger.2004.06.019

Hogervorst, E., Combrinck, M., and Smith, A. (2003). Testosterone and gonadotropin levels in men with dementia. *Neuro Endocrinol. Lett.* 24, 203–208.

Hogervorst, E., Williams, J., Budge, M., Barnetson, L., Combrinck, M., and Smith, A. (2001). Serum total testosterone is lower in men with Alzheimer's disease. *Neuro Endocrinol. Lett.* 22, 163–168.

Holmberg, E., Sjöstedt, J., Malinina, E., Johansson, M., Turkmen, S., Ragagnin, G., et al. (2018). Allopregnanolone involvement in feeding regulation, overeating

and obesity. *Front. Neuroendocrinol.* 48, 70–77. doi: 10.1016/j.yfrne.2017.07.002

Honjo, H., Iwasa, K., Kawata, M., Fushiki, S., Hosoda, T., Tatsumi, H., et al. (2005). Progestins and estrogens and Alzheimer's disease. *J. Steroid Biochem. Mol. Biol.* 93, 305–308. doi: 10.1016/j.jsbmb.2004.12.001

Hosie, A. M., Wilkins, M. E., da Silva, H. M. A., and Smart, T. G. (2006). Endogenous neurosteroids regulate $GABA_A$receptors through two discrete transmembrane sites. *Nature* 444, 486–489. doi: 10.1038/nature05324

Hsu, B., Cumming, R. G., Waite, L. M., Blyth, F. M., Naganathan, V., Le Couteur, D. G., et al. (2015). Longitudinal relationships between reproductive hormones and cognitive decline in older men: the concord health and ageing in men project. *J. Clin. Endocrinol. Metab.* 100, 2223–2230. doi: 10.1210/jc.2015-1016

Hsu, F.-C., Waldeck, R., Faber, D. S., and Smith, S. S. (2003). Neurosteroid effects on GABAergic synaptic plasticity in hippocampus. *J. Neurophysiol.* 89, 1929–1940. doi: 10.1152/jn.00780.2002

Huang, C., Chen, S., Lue, J., Chang, C., Wen, W., and Tsai, Y. (2016). Neurosteroid allorpegnanolone suppresses median nerve injury-induced mechanical hypersensitivity and glial extracellular signal—regulated kinase activation through γ-aminobutyric acid type A receptor modulation in the rat cuneate nucleus. *Anesthesiology* 125, 1202–1218. doi: 10.1097/aln.0000000000001360

Irwin, R. W., Wang, J. M., Chen, S., and Brinton, R. D. (2012). Neuroregenerative mechanisms of allopregnanolone in Alzheimer's disease. *Front. Endocrinol.* 3:117. doi: 10.3389/fendo.2011.00117

Karout, M., Miesch, M., Geoffrey, P., Kraft, S., Hofmann, H., and Mensah-Nyagan, A. G. (2016). Novel analogs of allopregnanolone show improved efficiency and specificity in neuroprotection and stimulation of proliferation. *J. Neurochem.* 139, 782–794. doi: 10.1111/jnc.13693

Kawas, C., Resnick, S., Morrison, A., Brookmeyer, R., Corrada, M., Zonderman, A., et al. (1997). A prospective study of estrogen replacement therapy and the risk of developing Alzheimer's disease: the Baltimore Longitudinal Study of Aging. *Neurology* 48, 1517–1521. doi: 10.1212/WNL.48.6.1517

Kelley, M., Kuroiwa, M., Taguchi, N., and Herson, P. (2011). Sex difference in sensitivity to allopregnanolone neuroprotection in mice correlates with effect on spontaneous inhibitory post synaptic currents. *Neuropharmacology* 61, 724–729. doi: 10.1016/j.neuropharm.2011.05.017

Kelley, M. H., Taguchi, N., Ardeshiri, A., Kuroiwa, M., Hurn, P. D., Traystman, R. J., et al. (2008). Ischemic insult to cerebellar Purkinje cells causes diminished $GABA_A$ receptor function and allopregnanolone neuroprotection is associated with $GABA_A$ receptor stabilization. *J. Neurochem.* 107, 668–678. doi: 10.1111/j.1471-4159.2008.05617.x

Kritzer, M. F. (2006). Regional, laminar and cellular distribution of immunoreactivity for ERβ in the cerebral cortex of hormonally intact, postnatally developing male and female rats. *Cereb. Cortex* 16, 1181–1192. doi: 10.1093/cercor/bhj059

Kuiper, G. G., Carlsson, B., Grandien, K., Enmark, E., Häggblad, J., Nilsson, S., et al. (1997). Comparison of the ligand binding specificity and transcript tissue distribution of estrogen receptors α and β. *Endocrinology* 138, 863–870. doi: 10.1210/en.138.3.863

Kumar, N., Fagart, J., Liere, P., Mitchell, S. J., Knibb, A. R., Petit-Topin, I., et al. (2017). Nestorone®as a novel progestin for nonoral contraception: structure-activity relationships and brain metabolism studies. *Endocrinology* 158, 170–182. doi: 10.1210/en.2016-1426

Lejri, I., Grimm, A., Miesch, M., Geoffroy, P., Eckert, A., and Mensah-Nyagan, A. G. (2017). Allopregnanolone and its analog BR 297 rescue neuronal cells from oxidative stress-induced death through bioenergetic improvement. *Biochim. Biophys. Acta* 1863, 631–642. doi: 10.1016/j.bbadis.2016.12.007

Leonard, S. T., and Winsauer, P. J. (2011). The effects of gonadal hormones on learning and memory in male mammals: a review. *Curr. Zool.* 57, 543–558. doi: 10.1093/czoolo/57.4.543

Leonelli, E., Bianchi, R., Cavaletti, G., Caruso, D., Crippa, D., Garcia-Segura, L. M., et al. (2007). Progesterone and its derivatives are neuroprotective agents in experimental diabetic neuropathy: a multimodal analysis. *Neuroscience* 144, 1293–1304. doi: 10.1016/j.neuroscience.2006.11.014

Li, H.-D., Li, M., Shi, E., Jin, W.-N., Wood, K., Gonzales, R., et al. (2017). A translocator protein 18 kDa agonist protects against cerebral ischemia/reperfusion injury. *J. Neuroinflammation* 14:151. doi: 10.1186/s12974-017-0921-7

Li, L., Wang, W., Zhang, L.-M., Jiang, X.-Y., Sun, S., Sun, L.-J., et al. (2017). Overexpression of the 18 kDa translocator protein (TSPO) in the hippocampal dentate gyrus produced anxiolytic and antidepressant-like behavioural effects. *Neuropharmacology* 125, 117–128. doi: 10.1016/j.neuropharm.2017.06.023

Li, M., Ren, H., Sheth, K. N., Shi, F. D., and Liu, Q. (2017). A TSPO ligand attenuates brain injury after intracerebral hemorrhage. *FASEB J.* 31, 3278–3287. doi: 10.1096/fj.201601377rr

Liao, S., Liang, T., Fang, S., Castañeda, E., and Shao, T. (1973). Steroid structure and rogenic activity. Specificities involved in the receptor binding and nuclear retention of various androgens. *J. Biol. Chem.* 248, 6154–6162.

Liere, P., Pianos, A., Oudinet, J. P., Schumacher, M., and Akwa, Y. (2017). Differential effects of the 18-kDa translocator protein (TSPO) ligand etifoxine on steroidogenesis in rat brain, plasma and steroidogenic glands: pharmacodynamic studies. *Psychoneuroendocrinology* 83, 122–134. doi: 10.1016/j.psyneuen.2017.05.022

Lopez-Rodriguez, A. B., Acaz-Fonseca, E., Spezzano, R., Giatti, S., Caruso, D., Viveros, M. P., et al. (2016). Profiling neuroactive steroid levels after traumatic brain injury in male mice. *Endocrinology* 157, 3983–3993. doi: 10.1210/en.2016-1316

Luchetti, S., Bossers, K., Frajese, G., and Swaab, D. (2010). Neurosteroid biosynthetic pathway changes in substantia nigra and caudate nucleus in Parkinson's disease. *Brain Pathol.* 20, 945–951. doi: 10.1111/j.1750-3639.2010.00396.x

Luchetti, S., Bossers, K., Van de Bilt, S., Agrapart, V., Morales, R. R., Frajese, G. V., et al. (2011a). Neurosteroid biosynthetic pathways changes in prefrontal cortex in Alzheimer's disease. *Neurobiol. Aging* 32, 1964–1976. doi: 10.1016/j.neurobiolaging.2009.12.014

Luchetti, S., Huitinga, I., and Swaab, D. F. (2011b). Neurosteroid and GABA-A receptor alterations in Alzheimer's disease, Parkinson's disease and multiple sclerosis. *Neuroscience* 191, 6–21. doi: 10.1016/j.neuroscience.2011.04.010

Magnaghi, V., Ballabio, M., Gonzalez, L. C., Leonelli, E., Motta, M., and Melcangi, R. C. (2004). The synthesis of glycoprotein Po and peripheral myelin protein 22 in sciatic nerve of male rats is modulated by testosterone metabolites. *Mol. Brain Res.* 126, 67–73. doi: 10.1016/j.molbrainres.2004.03.009

Marx, C. E., Trost, W. T., Shampine, L. J., Stevens, R. D., Hulette, C. M., Steffens, D. C., et al. (2006). The neurosteroid allopregnanolone is reduced in prefrontal cortex in Alzheimer's disease. *Biol. Psychiatry* 60, 1287–1294. doi: 10.1016/j.biopsych.2006.06.017

McCombe, P. A., and Henderson, R. D. (2010). Effects of gender in amyotrophic lateral sclerosis. *Gend. Med.* 7, 557–570. doi: 10.1016/j.genm.2010.11.010

Melcangi, R., Froelichsthal, P., Martini, L., and Vescovi, A. (1996). Steroid metabolizing enzymes in pluripotential progenitor central nervous system cells: effect of differentiation and maturation. *Neuroscience* 72, 467–475. doi: 10.1016/0306-4522(95)00522-6

Melcangi, R. C., Magnaghi, V., Cavarretta, I., Zucchi, I., Bovolin, P., D'Urso, D., et al. (1999). Progesterone derivatives are able to influence peripheral myelin protein 22 and P0 gene expression: possible mechanisms of action. *J. Neurosci. Res.* 56, 349–357. doi: 10.1002/(sici)1097-4547(19990515)56:4<349::aid-jnr3>3.3.co;2-8

Mellon, S., and Griffin, L. (2002). Neurosteroids: biochemistry and clinical significance. *Trends Endocrinol. Metab.* 13, 35–43. doi: 10.1016/s1043-2760(01)00503-3

Mendell, A. L., Chung, B. Y. T., Creighton, C. E., Kalisch, B. E., Bailey, C. D. C., and MacLusky, N. J. (2018). Neurosteroid metabolites of testosterone and progesterone differentially inhibit ERK phosphorylation induced by amyloid β in SH-SY5Y cells and primary cortical neurons. *Brain Res.* 1686, 83–93. doi: 10.1016/j.brainres.2018.02.023

Mendell, A. L., Creighton, C. E., Kalisch, B. E., and MacLusky, N. J. (2016). 5α-androstane-3α, 17β-diol inhibits neurotoxicity in SH-SY5Y human neuroblastoma cells and mouse primary cortical neurons. *Endocrinology* 157, 4570–4578. doi: 10.1210/en.2016-1508

Meredith, G. E., and Rademacher, D. J. (2011). MPTP mouse models of Parkinson's disease: an update. *J. Parkinsons Dis.* 1, 19–33. doi: 10.3233/JPD-2011-11023

Meyer, L., Patte-Mensah, C., Taleb, O., and Mensah-Nyagan, A. G. (2010). Cellular and functional evidence for a protective action of neurosteroids against

vincristine chemotherapy-induced painful neuropathy. *Cell. Mol. Life Sci.* 67, 3017–3034. doi: 10.1007/s00018-010-0372-0

Meyer, L., Patte-Mensah, C., Taleb, O., and Mensah-Nyagan, A. G. (2011). Allopregnanolone prevents and suppresses oxaliplatin-evoked painful neuropathy: multi-parametric assessment and direct evidence. *Pain* 152, 170–181. doi: 10.1016/j.pain.2010.10.015

Meyer, L., Patte-Mensah, C., Taleb, O., and Mensah-Nyagan, A. G. (2013). Neurosteroid 3α-androstanediol efficiently counteracts paclitaxel-induced peripheral neuropathy and painful symptoms. *PLoS One* 8:e80915. doi: 10.1371/journal.pone.0080915

Meyer, M., Garay, L. I., Kruse, M. S., Lara, A., Gargiulo-Monachelli, G., Schumacher, M., et al. (2017). Protective effects of the neurosteroid allopregnanolone in a mouse model of spontaneous motoneuron degeneration. *J. Steroid Biochem. Mol. Biol.* 174, 201–216. doi: 10.1016/j.jsbmb.2017.09.015

Meyer, M., Gonzalez Deniselle, M. C., Garay, L., Sitruk-Ware, R., Guennoun, R., Schumacher, M., et al. (2015). The progesterone receptor agonist Nestorone holds back proinflammatory mediators and neuropathology in the wobbler mouse model of motoneuron degeneration. *Neuroscience* 308, 51–63. doi: 10.1016/j.neuroscience.2015.09.007

Miller, P. S., and Aricescu, A. R. (2014). Crystal structure of a human $GABA_A$ receptor. *Nature* 512, 270–275. doi: 10.1038/nature13293

Milner, T. A., Ayoola, K., Drake, C. T., Herrick, S. P., Tabori, N. E., McEwen, B. S., et al. (2005). Ultrastructural localization of estrogen receptor β immunoreactivity in the rat hippocampal formation. *J. Comp. Neurol.* 491, 81–95. doi: 10.1002/cne.20724

Milner, T. A., McEwen, B. S., Hayashi, S., Li, C. J., Reagan, L. P., and Alves, S. E. (2001). Ultrastructural evidence that hippocampal α estrogen receptors are located at extranuclear sites. *J. Comp. Neurol.* 429, 355–371. doi: 10.1002/1096-9861(20010115)429:3<355::aid-cne1>3.3.co;2-r

Mody, I., and Maguire, J. (2012). The reciprocal regulation of stress hormones and $GABA_A$ receptors. *Front. Cell. Neurosci.* 6:4. doi: 10.3389/fncel.2012.00004

Mogi, K., Takanashi, H., Nagasawa, M., and Kikusui, T. (2015). Sex differences in spatiotemporal expression of AR, ERα, and ERβ mRNA in the perinatal mouse brain. *Neurosci. Lett.* 584, 88–92. doi: 10.1016/j.neulet.2014.10.028

Morohaku, K., Pelton, S. H., Daugherty, D. J., Butler, W. R., Deng, W., and Selvaraj, V. (2014). Translocator protein/peripheral benzodiazepine receptor is not required for steroid hormone biosynthesis. *Endocrinology* 155, 89–97. doi: 10.1210/en.2013-1556

Naylor, J. C., Kilts, J. D., Hulette, C. M., Steffens, D. C., Blazer, G., Ervin, J. F., et al. (2010). Allopregnanolone levels are reduced in temporal cortex in patients with Alzheimer's disease compared to cognitively intact control subjects. *Biochim. Biophys. Acta* 1801, 951–959. doi: 10.1016/j.bbalip.2010.05.006

Nguyen, T.-V. V., Yao, M., and Pike, C. J. (2005). Androgens activate mitogen-activated protein kinase signaling: role in neuroprotection. *J. Neurochem.* 94, 1639–1651. doi: 10.1111/j.1471-4159.2005.03318.x

Nik, A. M., Pressly, B., Singh, V., Antrobus, S., Hulsizer, S., Rogawski, M. A., et al. (2017). Rapid throughput analysis of $GABA_A$ receptor subtype modulators and blockers using $DiSBAC_1(3)$ membrane potential red dye. *Mol. Pharmacol.* 92, 88–99. doi: 10.1124/mol.117.108563

Nilsen, J., and Brinton, R. D. (2003). Divergent impact of progesterone and medroxyprogesterone acetate (Provera) on nuclear mitogen-activated protein kinase signaling. *Proc. Natl. Acad. Sci. U S A* 100, 10506–10511. doi: 10.1073/pnas.1334098100

Noorbakhsh, F., Ellestad, K. K., Maingat, F., Warren, K. G., Han, M. H., Steinman, L., et al. (2011). Impaired neurosteroid synthesis in multiple sclerosis. *Brain* 134, 2703–2721. doi: 10.1093/brain/awr200

Nuñez, J. L., Huppenbauer, C. B., McAbee, M. D., Juraska, J. M., and DonCarlos, L. L. (2003). Androgen receptor expression in the developing male and female rat visual and prefrontal cortex. *J. Neurobiol.* 56, 293–302. doi: 10.1002/neu.10236

Orr, P. T., Rubin, A. J., Fan, L., Kent, B. A., and Frick, K. M. (2012). The progesterone-induced enhancement of object recognition memory consolidation involves activation of the extracellular signal-regulated kinase (ERK) and mammalian target of rapamycin (mTOR) pathways in the dorsal hippocampus. *Horm. Behav.* 61, 487–495. doi: 10.1016/j.yhbeh.2012.01.004

Overstreet Wadiche, L., Bromberg, D., Bensen, A., and Westbrook, G. (2005). GABAergic signaling to newborn neurons in dentate gyrus. *J. Neurophysiol.* 94, 4528–4532. doi: 10.1152/jn.00633.2005

Paganini-Hill, A., and Henderson, V. (1994). Estrogen deficiency and risk of Alzheimer's disease in women. *Am. J. Epidemiol.* 140, 256–261. doi: 10.1093/oxfordjournals.aje.a117244

Paganini-Hill, A., and Henderson, V. (1996). Estrogen replacement therapy and risk of alzheimer disease. *Arch. Intern. Med.* 156, 2213–2217. doi: 10.1001/archinte.156.19.2213

Papadopoulos, V., Baraldi, M., Guilarte, T., Knudsen, T., Lacapère, J., Lindemann, P., et al. (2006). Translocator protein (18kDa): new nomenclature for the peripheral-type benzodiazepine receptor based on its structure and molecular function. *Trends Pharmacol. Sci.* 27, 402–409. doi: 10.1016/j.tips.2006.06.005

Paris, J. J., Zou, S. P., Hahn, Y. K., Knapp, P. E., and Hauser, K. F. (2016). 5α-reduced progestogens ameliorate mood-related behavioral pathology, neurotoxicity, and microgliosis associated with exposure to HIV-1 Tat. *Brain Behav. Immun.* 55, 202–214. doi: 10.1016/j.bbi.2016.01.007

Pavese, N., Gerhard, A., Tai, Y., Ho, A., Turkheimer, F., Barker, R., et al. (2006). Microglial activation correlates with severity in Huntington disease: a clinical and PET study. *Neurology* 66, 1638–1643. doi: 10.1212/01.wnl.0000222734.56412.17

Penning, T. M. (1997). Molecular endocrinology of hydroxysteroid dehydrogenases. *Endocr. Rev.* 18, 281–305. doi: 10.1210/edrv.18.3.0302

Pike, C. J. (2017). Sex and the development of Alzheimer's disease. *J. Neurosci. Res.* 95, 671–680. doi: 10.1002/jnr.23827

Pike, C. J., Nguyen, T. V. V., Ramsden, M., Yao, M., Murphy, M. P., and Rosario, E. R. (2008). Androgen cell signaling pathways involved in neuroprotective actions. *Horm. Behav.* 53, 693–705. doi: 10.1016/j.yhbeh.2007.11.006

Plassman, B., Langa, K., McCammon, R., Fisher, G., Potter, G., Burke, J., et al. (2011). Incidence of dementia and cognitive impairment, not dementia in the United States. *Ann. Neurol.* 70, 418–426. doi: 10.1002/ana.22362

Porcu, P., Barron, A., Frye, C., Walf, A., Yang, S., He, X., et al. (2016). Neurosteroidogenesis today: novel targets for neuroactive steroid synthesis and action and their relevance for translational research. *J. Neuroendocrinol.* 28:12351. doi: 10.1111/jne.12351

Reddy, D. S. (2008). Mass spectrometric assay and physiological-pharmacological activity of androgenic neurosteroids. *Neurochem. Int.* 52, 541–553. doi: 10.1016/j.neuint.2007.05.019

Reddy, D. S., Castaneda, D. C., Malley, B. W. O., and Rogawski, M. A. (2004). Anticonvulsant activity of progesterone and neurosteroids in progesterone receptor knockout mice. *J. Pharmacol. Exp. Ther.* 310, 230–239. doi: 10.1124/jpet.104.065268

Reddy, D. S., Gangisetty, O., and Wu, X. (2017). PR-independent neurosteroid regulation of α2-GABA-A receptors in the hippocampus subfields. *Brain Res.* 1659, 142–147. doi: 10.1016/j.brainres.2017.01.030

Reddy, D. S., and Jian, K. (2010). The testosterone-derived neurosteroid androstanediol is a positive allosteric modulator of $GABA_A$ receptors. *J. Pharmacol. Exp. Ther.* 334, 1031–1041. doi: 10.1124/jpet.110.169854

Ripich, D., Petrill, S., Whitehouse, P., and Ziol, E. (1995). Gender differences in language of AD patients: a longitudinal study. *Neurology* 45, 299–302. doi: 10.1212/wnl.45.2.299

Rupprecht, R., Papadopoulos, V., Rammes, G., Baghai, T. C., Fan, J., Akula, N., et al. (2010). Translocator protein (18 kDa) (TSPO) as a therapeutic target for neurological and psychiatric disorders. *Nat. Rev. Drug Discov.* 9, 971–988. doi: 10.1038/nrd3295

Santoro, A., Mattace Raso, G., Taliani, S., Da Pozzo, E., Simorini, F., Costa, B., et al. (2016). TSPO-ligands prevent oxidative damage and inflammatory response in C6 glioma cells by neurosteroid synthesis. *Eur. J. Pharm. Sci.* 88, 124–131. doi: 10.1016/j.ejps.2016.04.006

Sarkey, S., Azcoitia, I., Garcia-Segura, L. M., Garcia-Ovejero, D., and DonCarlos, L. L. (2008). Classical androgen receptors in non-classical sites in the brain. *Horm. Behav.* 53, 753–764. doi: 10.1016/j.yhbeh.2008.02.015

Sayeed, I., Guo, Q., Hoffman, S. W., and Stein, D. G. (2006). Allopregnanolone, a progesterone metabolite, is more effective than progesterone in reducing cortical infarct volume after transient middle cerebral artery occlusion. *Ann. Emerg. Med.* 47, 381–389. doi: 10.1016/j.annemergmed.2005.12.011

Sayeed, I., and Stein, D. G. (2009). Progesterone as a neuroprotective factor in traumatic and ischemic brain injury. *Prog. Brain Res.* 175, 219–237. doi: 10.1016/s0079-6123(09)17515-5

Sayeed, I., Wali, B., and Stein, D. G. (2007). Progesterone inhibits ischemic brain injury in a rat model of permanent middle cerebral artery occlusion. *Restor. Neurol. Neurosci.* 25, 151–159.

Schaeffer, V., Patte-Mensah, C., Eckert, A., and Mensah-Nyagan, A. G. (2006). Modulation of neurosteroid production in human neuroblastoma cells by Alzheimer's disease key proteins. *J. Neurobiol.* 66, 868–881. doi: 10.1002/neu.20267

Schaeffer, V., Patte-Mensah, C., Eckert, A., and Mensah-Nyagan, A. G. (2008). Selective regulation of neurosteroid biosynthesis in human neuroblastoma cells under hydrogen peroxide-induced oxidative stress condition. *Neuroscience* 151, 758–770. doi: 10.1016/j.neuroscience.2007.11.032

Schumacher, M., Weill-Engerer, S., Liere, P., Robert, F., Franklin, R., Garcia-Segura, L., et al. (2003). Steroid hormones and neurosteroids in normal and pathological aging of the nervous system. *Prog. Neurobiol.* 71, 3–29. doi: 10.1016/j.pneurobio.2003.09.004

Seshadri, S., Wolf, P., Beiser, A., Au, R., McNulty, K., White, R., et al. (1997). Lifetime risk of dementia and Alzheimer's disease. The impact of mortality on risk estimates in the Framingham Study. *Neurology* 49, 1498–1504. doi: 10.1212/wnl.49.6.1498

Shumaker, S. A., Legault, C., Rapp, S. R., Thal, L., Wallace, R. B., Ockene, J. K., et al. (2003). Estrogen plus progestin and the incidence of dementia and mild cognitive impairment in postmenopausal women: the women's health initiative memory study: a randomized controlled trial. *JAMA* 289, 2651–2662. doi: 10.1001/jama.289.20.2651

Sieghart, W. (2006). Structure, pharmacology and function of $GABA_A$ receptor subtypes. *Adv. Pharmacol.* 54, 231–263. doi: 10.1016/s1054-3589(06)54010-4

Singh, M. (2001). Ovarian hormones elicit phosphorylation of Akt and extracellular-signal regulated kinase in explants of the cerebral cortex. *Endocrine* 14, 407–415. doi: 10.1385/endo:14:3:407

Singh, C., Liu, L., Wang, J. M., Irwin, R. W., Yao, J., Chen, S., et al. (2012). Allopregnanolone restores hippocampal-dependent learning and memory and neural progenitor survival in aging 3xTgAD and nonTg mice. *Neurobiol. Aging* 33, 1493–1506. doi: 10.1016/j.neurobiolaging.2011.06.008

Smith, C., Wekstein, D., Markesbery, W., and Frye, C. (2006). 3α,5α-THP: a potential plasma neurosteroid biomarker in Alzheimer's disease and perhaps non-Alzheimer's dementia. *Psychopharmacology* 186, 481–485. doi: 10.1007/s00213-005-0186-1

Srivastava, D., Waters, E., Mermelstein, P., Kramár, E., Shors, T., and Liu, F. (2011). Rapid estrogen signaling in the brain: implications for the fine-tuning of neuronal circuitry. *J. Neurosci.* 31, 16056–16063. doi: 10.1523/jneurosci.4097-11.2011

Stanczyk, F. Z., Hapgood, J. P., Winer, S., and Mishell, D. R. Jr. (2013). Progestogens used in postmenopausal hormone therapy: differences in their pharmacological properties, intracellular actions and clinical effects. *Endocr. Rev.* 34, 171–208. doi: 10.1210/er.2012-1008

Stell, B., Brickley, S., Tang, C., Farrant, M., and Mody, I. (2003). Neuroactive steroids reduce neuronal excitability by selectively enhancing tonic inhibition mediated by delta subunit-containing $GABA_A$ receptors. *Proc. Natl. Acad. Sci. U S A* 100, 14439–14444. doi: 10.1073/pnas.2435457100

Sun, C., Ou, X., Farley, J. M., Stockmeier, C., Bigler, S., Brinton, R. D., et al. (2012). Allopregnanolone increases the number of dopaminergic neurons in substantia nigra of a triple transgenic mouse model of Alzheimer's disease. *Curr. Alzheimer Res.* 9, 473–480. doi: 10.2174/156720512800492567

Tabori, N. E., Stewart, L. S., Znamensky, V., Romeo, R. D., Alves, S. E., McEwen, B. S., et al. (2005). Ultrastructural evidence that androgen receptors are located at extranuclear sites in the rat hippocampal formation. *Neuroscience* 130, 151–163. doi: 10.1016/j.neuroscience.2004.08.048

Tang, M., Jacobs, D., Stern, Y., Marder, K., Schofield, P., Gurland, B., et al. (1996). Effect of oestrogen during menopause on risk and age at onset of Alzheimer's disease. *Lancet* 348, 429–432. doi: 10.1016/s0140-6736(96)03356-9

Taves, M., Gomez-Sanchez, C., and Soma, K. (2011). Extra-adrenal glucocorticoids and mineralocorticoids: evidence for local synthesis, regulation and function. *Am. J. Physiol. Endocrinol. Metab.* 301, E11–E24. doi: 10.1152/ajpendo.00100.2011

Tozuka, Y., Fukuda, S., Namba, T., Seki, T., and Hisatsune, T. (2005). GABAergic excitation promotes neuronal differentiation in adult hippocampal progenitor cells. *Neuron* 47, 803–815. doi: 10.1016/j.neuron.2005.08.023

Turner, M. R., Cagnin, A., Turkheimer, F. E., Miller, C. C. J., Shaw, C. E., Brooks, D. J., et al. (2004). Evidence of widespread cerebral microglial activation in amyotrophic lateral sclerosis: an [^{11}C](R)-PK11195 positron emission tomography study. *Neurobiol. Dis.* 15, 601–609. doi: 10.1016/j.nbd.2003.12.012

Venneti, S., Lopresti, B. J., Wang, G., Hamilton, R. L., Mathis, C. A., Klunk, W. E., et al. (2009). PK11195 labels activated microglia in Alzheimer's disease and *in vivo* in a mouse model using PET. *Neurobiol. Aging* 30, 1217–1226. doi: 10.1016/j.neurobiolaging.2007.11.005

Versijpt, J., Debruyne, J. C., Van Laere, K. J., De Vos, F., Keppens, J., Strijckmans, K., et al. (2005). Microglial imaging with positron emission tomography and atrophy measurements with magnetic resonance imaging in multiple sclerosis: a correlative study. *Mult. Scler.* 11, 127–134. doi: 10.1191/1352458505ms1140oa

Voskuhl, R., and Gold, S. (2012). Sex-related factors in multiple sclerosis susceptibility and progression. *Nat. Rev. Neurol.* 8, 255–263. doi: 10.1038/nrneurol.2012.43

Wang, J. M., and Brinton, R. D. (2008). Allopregnanolone-induced rise in intracellular calcium in embryonic hippocampal neurons parallels their proliferative potential. *BMC Neurosci.* 9:S11. doi: 10.1186/1471-2202-9-s2-s11

Wang, A. C. J., Hara, Y., Janssen, W. G. M., Rapp, P. R., and Morrison, J. H. (2010). Synaptic estrogen receptor-α levels in prefrontal cortex in female rhesus monkeys and their correlation with cognitive performance. *J. Neurosci.* 30, 12770–12776. doi: 10.1523/JNEUROSCI.3192-10.2010

Wang, J. M., Johnston, P., Ball, B., and Brinton, R. (2005). The neurosteroid allopregnanolone promotes proliferation of rodent and human neural progenitor cells and regulates cell-cycle gene and protein expression. *J. Neurosci.* 25, 4706–4718. doi: 10.1523/jneurosci.4520-04.2005

Wang, J. M., Singh, C., Liu, L., Irwin, R. W., Chen, S., Chung, E. J., et al. (2010). Allopregnanolone reverses neurogenic and cognitive deficits in mouse model of Alzheimer's disease. *Proc. Natl. Acad. Sci. U S A* 107, 6498–6503. doi: 10.1073/pnas.1001422107

Xing, Y., Tang, Y., and Jia, J. (2015). Sex differences in neuropsychiatric symptoms of Alzheimer's disease: the modifying effect of apolipoprotein E ϵ4 status. *Behav. Neurol.* 2015:275256. doi: 10.1155/2015/275256

Xu, W., Tan, L., Wang, H., Jiang, T., Tan, M., Tan, L., et al. (2015). Meta-analysis of modifiable risk factors for Alzheimer's disease. *J. Neurol. Neurosurg. Psychiatry* 86, 1299–1306. doi: 10.1136/jnnp-2015-310548

Yang, S.-Y., and He, X.-Y. (2001). Role of type 10 17ß-hydroxysteroid dehydrogenase in the pathogenesis of Alzheimer's disease. *Adv. Exp. Med. Biol.* 487, 101–110. doi: 10.1007/978-1-4615-1249-3_8

Yang, S. Y., He, X. Y., Isaacs, C., Dobkin, C., Miller, D., and Philipp, M. (2014). Roles of 17β-hydroxysteroid dehydrogenase type 10 in neurodegenerative disorders. *J. Steroid Biochem. Mol. Biol.* 143, 460–472. doi: 10.1016/j.jsbmb.2014.07.001

Yasuno, F., Kosaka, J., Ota, M., Higuchi, M., Ito, H., Fujimura, Y., et al. (2012). Increased binding of peripheral benzodiazepine receptor in mild cognitive impairment-dementia converters measured by positron emission tomography with [^{11}C]DAA1106. *Psychiatry Res.* 203, 67–74. doi: 10.1016/j.pscychresns.2011.08.013

Yasuno, F., Ota, M., Kosaka, J., Ito, H., Higuchi, M., Doronbekov, T. K., et al. (2008). Increased binding of peripheral benzodiazepine receptor in Alzheimer's disease measured by positron emission tomography with [11C]DAA1106. *Biol. Psychiatry* 64, 835–841. doi: 10.1016/j.biopsych.2008.04.021

Yeap, B. B., Almeida, O. P., Hyde, Z., Chubb, S. A., Hankey, G. J., Jamrozik, K., et al. (2008). Higher serum free testosterone is associated with better cognitive function in older men, while total testosterone is not. The Health In Men Study. *Clin. Endocrinol.* 68, 404–412. doi: 10.1111/j.1365-2265.2007.03055.x

Zelcer, N., Khanlou, N., Clare, R., Jiang, Q., Reed-Geaghan, E. G., Landreth, G. E., et al. (2007). Attenuation of neuroinflammation and Alzheimer's disease pathology by liver x receptors. *Proc. Natl. Acad. Sci. U S A* 104, 10601–10606. doi: 10.1073/pnas.0701096104

Zhang, H., Ma, L., Yin, Y. L., Dong, L. Q., Cheng, G. G., Ma, Y. Q., et al. (2016). Over-expression of TSPO in the hippocampal CA1 area alleviates cognitive dysfunction caused by lipopolysaccharide in mice. *Brain Res.* 1646, 402–409. doi: 10.1016/j.brainres.2016.06.001

Zhang, P., Xie, M. Q., Ding, Y. Q., Liao, M., Qi, S. S., Chen, S. X., et al. (2015). Allopregnanolone enhances the neurogenesis of midbrain dopaminergic neurons in APPswe/PSEN1 mice. *Neuroscience* 290, 214–226. doi: 10.1016/j.neuroscience.2015.01.019

Zhao, L., and Brinton, R. D. (2007). Estrogen receptor α and β differentially regulate intracellular Ca^{2+} dynamics leading to ERK phosphorylation and estrogen neuroprotection in hippocampal neurons. *Brain Res.* 1172, 48–59. doi: 10.1016/j.brainres.2007.06.092

Zimmer, E., Leuzy, A., Benedet, A., Breitner, J., Gauthier, S., and Rosa-Neto, P. (2014). Tracking neuroinflammation in Alzheimer's disease: the role of positron emission tomography imaging. *J. Neuroinflammation* 11:120. doi: 10.1186/1742-2094-11-120

Conflict of Interest Statement: The authors declare that the research was conducted in the absence of any commercial or financial relationships that could be construed as a potential conflict of interest.

frontiers in Molecular Neuroscience

REVIEW
published: 15 October 2018
doi: 10.3389/fnmol.2018.00374

Sexually Dimorphic Effects of Aromatase on Neurobehavioral Responses

Dusti A. Shay[1], Victoria J. Vieira-Potter[1] and Cheryl S. Rosenfeld[2,3,4]**

[1] Nutrition and Exercise Physiology, University of Missouri, Columbia, MO, United States, [2] Bond Life Sciences Center, University of Missouri, Columbia, MO, United States, [3] Thompson Center for Autism and Neurobehavioral Disorders, University of Missouri, Columbia, MO, United States, [4] Department of Biomedical Sciences, University of Missouri, Columbia, MO, United States

Aromatase is the enzyme responsible for converting testosterone to estradiol. In mammals, aromatase is expressed in the testes, ovaries, brain, and other tissues. While estrogen is traditionally associated with reproduction and sexual behavior in females, our current understanding broadens this perspective to include such biological functions as metabolism and cognition. It is now well-recognized that aromatase plays a vital lifetime role in brain development and neurobehavioral function in both sexes. Thus, ongoing investigations seek to highlight potentially vital sex differences in the role of aromatase, particularly regarding its centrally mediated effects. To characterize the role of aromatase in mediating such functions, effects of aromatase inhibitor (AI) treatments on humans and animal models have been determined. Aromatase knockout (ArKO) mice that systemically lack the enzyme have also been employed. Humans possessing mutations in the gene encoding aromatase, *CYP19*, have also provided critical insight into how aromatase affects brain function in a possible sex-dependent manner. A better understanding of how AIs, used to treat breast cancer and other clinical conditions, may detrimentally affect neurobehavioral responses will likely promote development of future therapies to combat these effects. Herein, we will provide a critical review of the current knowledge of sex differences in aromatase regulation of various neurobehavioral functions. Although many species have been used to better understand the functions of aromatase, this review focuses on rodent models and humans. Critical gaps in our present understanding of this area will be considered, and important future research directions will be discussed.

Keywords: estrogen, brain, testosterone, ArKO, locomotor activity, breast cancer, Alzheimer's disease, memory

OPEN ACCESS

Edited by:
Laura Musazzi,
Università degli Studi di Milano, Italy

Reviewed by:
Antonella Peruffo,
Università degli Studi di Padova, Italy
Takayoshi Ubuka,
Monash University Malaysia, Malaysia
Luis Miguel Garcia-Segura,
Consejo Superior de Investigaciones Científicas (CSIC), Spain

****Correspondence:***
Victoria J. Vieira-Potter
vieirapotterv@missouri.edu
Cheryl S. Rosenfeld
rosenfeldc@missouri.edu

Received: *16 June 2018*
Accepted: *21 September 2018*
Published: *15 October 2018*

Citation:
Shay DA, Vieira-Potter VJ and Rosenfeld CS (2018) Sexually Dimorphic Effects of Aromatase on Neurobehavioral Responses. Front. Mol. Neurosci. 11:374. doi: 10.3389/fnmol.2018.00374

INTRODUCTION

Aromatase (encoded by the *Cyp19*/*CYP19* gene) is the rate-limiting enzyme responsible for the unidirectional conversion of androgens to estrogen (E2) in gonadal and extra-gonadal tissues (Blakemore and Naftolin, 2016). It is required for E2 synthesis in males and females in steroidogenic tissues/organs, such as gonad, adipose tissue, bone, and brain (Nelson and Bulun, 2001). In mammalian females, aromatase activity in extra-ovarian tissues provides the sole source of E2

post-natural or surgical menopause (or ovariectomy in animal models). Yet, aromatase is essential throughout the lifespan in males and females.

Naftolin et al. (1971, 1972) discovered aromatase activity in the hypothalamus of the human fetus and went on to establish aromatase activity in the rat brain as well. These findings led to the "aromatization hypothesis," which proposes that developmental expression of aromatase in certain brain regions at critical time windows is required for permanent masculinization (Naftolin et al., 1972; Wright et al., 2010). This hypothesis challenged the previously accepted "organizational-activational hypothesis," postulating that sexual differentiation is driven primarily by the presence or absence of testosterone (T) in the fetal brain in response to XY or XX chromosomal status, respectively (Wright et al., 2010). However, we now recognize the synergistic relationship between androgens and E2 to orchestrate masculinization and feminization of the brain, as well as the potential for genetic (e.g., absence of a Y chromosome) and epigenetic influences (e.g., DNA methylation and/or chromatin modifications) to affect these physiological responses in several brain regions, including the hypothalamus, amygdala, and pre-optic area (Konkle and McCarthy, 2011; Matsuda et al., 2011; McCarthy et al., 2017; Rosenfeld, 2017).

In order to disentangle the complex interactions driving neurobehavioral responses to aromatase activity, research to date has utilized genetic (i.e., manipulation of the aromatase gene, *Cyp19*) and pharmacologic [i.e., aromatase inhibitor (AI) therapy] means. However, species comparisons of aromatase function pose problems due to sometimes stark inter-species differences. For example, rodent species exhibit short gestational period and tend to be polygynous, whereas, humans have long pregnancy duration and most societies are monogamous and biparental; this makes investigation of the precise role of aromatase during gestation difficult. Even so, early post-natal brain development in rodents resembles the critical window for human fetal brain development that occurs during the third trimester (Rice and Barone, 2000; Selevan et al., 2000; Howdeshell, 2002) making the rodent model appropriate for investigation of how aromatase affects brain development specifically. Thus, this review will focus on sex differences in aromatase expression and activity in the brain of mammalian species only. However, it is important to note that non-mammalian species are also known to express aromatase in the brain, and research in non-mammalian species (e.g., birds and fish) has also proven useful; the reader is referred to these cited references for further analyses on those species (Balthazart, 1997; Cao et al., 2012; Vahaba and Remage-Healey, 2018).

Aromatase-specific whole-body knock-out (ArKO) mice (bred on the C57Bl6 background) have been developed that constitutively lack aromatase activity throughout all stages of development. This has been a useful animal model to discern the role of aromatase in physiology and behavior of both sexes (Boon et al., 2010; Borbelyova et al., 2017). There are also 15 known cases of aromatase deficiency in humans (8 men, 7 women) (Boon et al., 2010). In women, aromatase deficiency is typically diagnosed early in life due to pseudo-hermaphroditism at birth and the absence of pubertal menstruation in females, with E2 supplementation generally being curative (Boon et al., 2010). In men, aromatase deficiency tends to be diagnosed later in life with pubertal development being typically normal, although infertility tends to progress with maturity (Boon et al., 2010).

Pharmacologically, AI (Anastrozole, Letrozole) can be administered to down-regulate aromatase activity. AI are primarily used as adjuvant hormone therapy in pre- and post-menopausal women with breast cancer and in less frequent cases of male metastatic breast cancer but are also employed in the treatment of other hormonal conditions (Phillips et al., 2011; Bulun et al., 2012). In boys and girls, AI can assist in the treatment of a number of sex hormone-related conditions in which E2 is over-expressed (Wit et al., 2011). In adolescent males, AI can be used to correct short stature due to pubertal delay (Wit et al., 2011). In sexually mature men, AI can be used to assist with low sperm count and motility, which often contributes to infertility (Schlegel, 2012; Borbelyova et al., 2017). In later adulthood, males often experience a slow, but steady decline in serum T, thus increasing their ratio of E2 to T, which may result in enlarged or painful breasts in men (Tan et al., 2014). This can be treated with an AI to reduce the amount of androgens being converted to E2 and ultimately increase serum T concentrations that naturally decline with age (Tan et al., 2014; Borbelyova et al., 2017).

SEX DIFFERENCES IN THE DISTRIBUTION AND REGULATION OF AROMATASE

CYP19/Cyp19 is widely expressed in the central nervous system (CNS) of both sexes, as well as in different neuronal cell types, with levels of mRNA expression being greatest in regions associated with sexual differentiation and corresponding closely with expression of E2 receptor alpha (ESR1) and beta (ESR2), as well as androgen receptors (AR) (Martinez-Cerdeno et al., 2006; Roselli et al., 2009; Bowers et al., 2010; Wright et al., 2010; Stanic et al., 2014; Tabatadze et al., 2014; Fester et al., 2017; Lorsch et al., 2018). Predominant brain regions in male and female species expressing *Cyp19* are illustrated in **Figure 1**. The presence of aromatase in various neural cell types suggests that the enzyme functions in an autocrine and paracrine fashion, and in some instances, independently of circulating sex hormone levels and presumably contribute to sex differences in the development of neurons during gestation and following injury and will be discussed in later sections.

Sex differences in *Cyp19* expression in rodent brains and varies by region. Tabatadze et al. (2014) found that in comparing intact and gonadectomized male and female Sprague-Dawley rats, intact males had the highest levels of *Cyp19* gene expression in the amygdala, bed nucleus of stria terminalis (BNST), and pre-optic area, while no sex differences were observed in the dorsal hippocampus and cingulate cortex (Tabatadze et al., 2014). Similarly, Stanic et al. (2014) determined that female mice have lower aromatase protein expression in BNST and medial amygdala, when compared to males (Lorsch et al., 2018). Furthermore, steroidal control of *Cyp19/CYP19* expression may

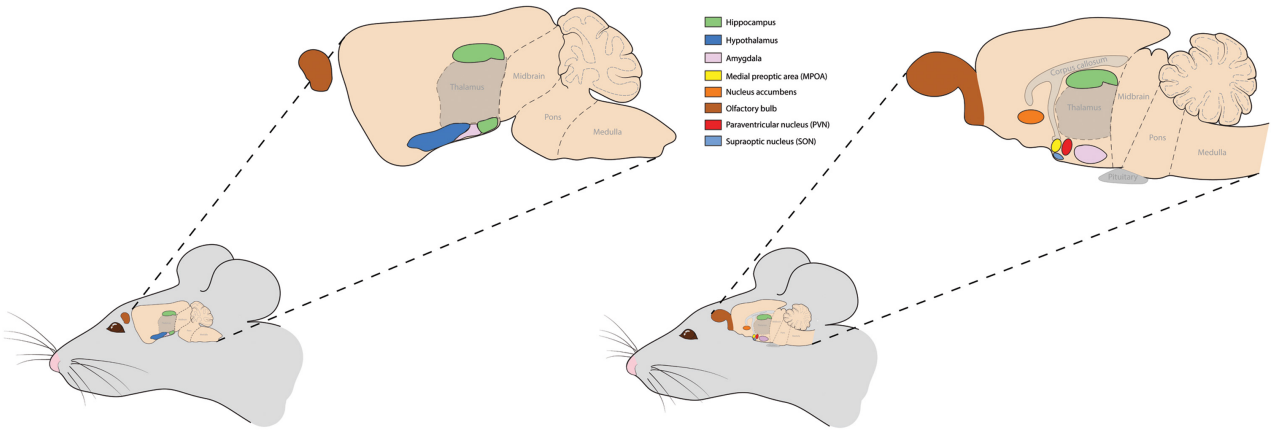

FIGURE 1 | Predominant brain regions expressing aromatase or the *Cyp19* gene in mice and likely other animals. Two sagittal brain sections are illustrated to show the various brain regions, including the olfactory bulbs, hippocampus, hypothalamus, amygdala, and nucleus accumbens. Within the hypothalamus, the medial preoptic area (MPOA), paraventricular nucleus, and supraoptic nucleus express high amounts of this enzyme. These brain regions are highlighted as aromatase expression in them guides many of the behaviors discussed herein and in many cases do so in a sex-dependent manner.

be sex-specific. Adult, male Sprague-Dawley rats (∼60 days old) have higher aromatase activity in specific micro-dissected sub-regions of the hypothalamus and amygdala compared to females, while other subsections displayed no sex differences (Roselli et al., 1985). After castration, brain regions with high or moderate aromatase activity decreased to levels comparable to females, and were restored after treatment with T (Roselli et al., 1985).

Similar to the animal species described above, the adult human brain exhibits aromatase expression in several regions, in particular the hippocampus, amygdala, hypothalamus, frontal cortex, and temporal lobe, whereas no sex differences have been identified to date (Sasano et al., 1998; Stoffel-Wagner et al., 1999; Yague et al., 2006). However, PET studies with [*N*-methyl-^{11}C]vorozole have revealed that humans uniquely possess high levels of aromatase in the thalamus and medulla (inferior olive), but that study did not investigate sex differences in aromatase expression in those two brain regions (Biegon et al., 2010). In human pituitary tissue, there was a non-significant trend for males to show elevated levels of aromatase expression compared to females, but limited sample tissue prevented definitive conclusions from being drawn (Kadioglu et al., 2008). Caution should be taken in interpreting those findings due to the difficulty in performing experiments in human subjects and the limited availability of human brain tissue; however, it is notable that abundant human data demonstrate sex differences in cognitive functions, such as learning and memory, addiction, and motivation, as well as in various pathologies such as epilepsy, Alzheimer's, schizophrenia, anxiety and depression (Beyenburg et al., 1999; Cherrier et al., 2001, 2005; Butler et al., 2010; Blakemore and Naftolin, 2016; Op de Macks et al., 2016; Alarcon et al., 2017). Thus, aromatase likely plays a vital role in modulating these sexually dimorphic differences.

The regulation of *CYP19/Cyp19* expression and aromatase activity in the brain involves genomic, non-genomic, and epigenetic factors. This regulation can vary throughout the lifespan, as well as between sexes, (Boon et al., 2010; McCarthy et al., 2017) and might play an important role (pre and postnatally) in sexual programming of the brain, along with hormone status and even neuroimmune mediation (e.g., reactive oxygen species (ROS), cytokines, and prostanoids) (Konkle and McCarthy, 2011; McCarthy et al., 2017).

There is mounting evidence that aromatase is also rapidly regulated via non-genomic mechanisms involving direct phosphorylation of the aromatase enzyme under conditions that promote protein phosphorylation, in particular high levels of calcium, magnesium, and ATP (Balthazart et al., 2003; Fester et al., 2017). These findings suggest that non-genomic regulation of aromatase can rapidly increase local E2 levels within the brain, thereby allowing for quick neurobehavioral responses to fluctuating environmental conditions (Balthazart et al., 2003; Fester et al., 2017). Interestingly, a protein heavily involved in brain synaptic plasticity, synaptopodin, is directly regulated by E2 and is expressed more strongly in female vs. male hippocampus (Fester et al., 2017). Non-genomic regulation of aromatase is responsible for the effect on synaptopodin, since an increase in intracellular calcium release inhibited aromatase activity in the hippocampus and downregulated synaptopodin expression in males and females, as discussed in more detail in a later section (Fester et al., 2017).

SEX DIFFERENCES IN AROMATASE DURING CRITICAL PERIODS OF DEVELOPMENT

Evidence suggests that there are two aromatase systems that exist within the adult mammalian brain: a gonad-sensitive hypothalamic system, and a non-gonad-sensitive limbic system (Naftolin, 1994). Brain regions responsible for sexual differentiation and behavior, such as the hypothalamus and medial preoptic area, are dependent on gonadal function and sex-steroid secretion, supporting the aromatization hypothesis.

In other brain regions, such as the cerebral cortex, amygdala, and hippocampus, aromatase activity is present but is gonad-function independent. These areas in adult rats also do not respond to removal of T or E2 under experimental conditions (Abdelgadir et al., 1994). In 2–3 year old rams (*Ovis aries)*, castration decreases aromatase expression in the hypothalamus but not in the amygdala (Roselli et al., 1998).

A critical embryonic window exists during which the brain is programmed to be either masculinized or feminized (McCarthy et al., 2017). This critical period in rats is predominantly during the last 5–7 days of gestation with rodent gestation lasting approximately 21 days but recent evidence suggests that this critical period can extend into the post-natal period (Wright et al., 2010; Nugent et al., 2015). During the critical period of short-gestation mammals (e.g., rodents), males are exposed to higher levels of E2 than females, as demonstrated by greater concentrations of T coupled with an increase in aromatase activity (Lephart, 1996). After the critical period, the brain cannot be reprogrammed with endogenous or exogenous T or E2, although it may still be vulnerable to epigenetic influences (McCarthy et al., 2017). This study revealed that pharmacological inhibition of DNA methyltransferase mimics the action of E2 in masculinizing the brain, even if administration occurs after the so-called critical period (Nugent et al., 2015).

During the development of long-gestation mammals (e.g., primates, sheep, and guinea pigs), aromatase may also affect brain regions not typically associated with sexual differentiation, such as the hippocampus, cortex, and amygdala. These areas also must be programmed at critical windows of time. For instance, in sheep which typically have a 147–150 day gestation period, the brain is sculpted between 60 and 90 gestational days; whereas in non-human primates with a 165 gestational period, this occurs at 40–60 gestational days (Roselli and Resko, 1986; Roselli et al., 2014). These effects are not always androgen-dependent, and both gene expression and enzyme activity may fluctuate throughout the lifespan within individual brain regions and across species (Roselli and Resko, 1986; Connolly et al., 1994; Roselli et al., 2003). Male and female rhesus macaques (*Macaca mulatta*) were gonadectomized at 98–103 days gestation and were surgically removed from the uterus at 120 days of gestation (Roselli and Resko, 1986). In the cerebral cortex and amygdala aromatase activity was significantly greater in males than females, but similar sex differences were not observed in the preoptic area or hypothalamus (Roselli and Resko, 1986). Conversely, analysis of fetal sheep brain (at gestational days 53, 65, 85, 100, 120, and 135) by Roselli and Stormshak (2012) revealed that *Cyp19* expression levels in the amygdala was similar across days tested in males and females (Roselli and Stormshak, 2012). This study also revealed that both sexes demonstrated a similar temporal pattern of *Cyp19* expression in the preoptic area, suggesting that in both non-human primates and sheep aromatase expression in this brain region is not influenced by sexually dimorphic factors.

It is important to also recognize that steroid hormones exert an activational role at the time of sexual maturity that varies across animal species (Bell, 2018). Studies of sex differences in central aromatase during puberty are extremely limited, especially in mammals. One study gonadectomized male and female Sprague-Dawley rats at post-natal day (PND) 30 (considered prepubertal), and by PND56 (post-pubertal), identified significantly reduced aromatase activity in the BNST, medial preoptic nucleus, and preoptic area, but not in the anterior hypothalamus or medial amygdala in both sexes (Roselli and Klosterman, 1998). Relative sex differences in aromatase activity in these brain regions were observed, as males showed higher basal levels at the outset. In contrast, a similar study in intact mice found no sex differences in *Cyp19* mRNA expression in the BNST and hypothalamus during the peripubertal phase (PND 20–60) (Kanaya et al., 2018). In sheep, prenatal exposure to 1,4,6-androstatriene-3,17-dione (ATD) did not affect the pubertal development of females, but caused a significant decrease in mounting behavior of males at 18 months of age without inducing feminization of males (e.g., receptive behavior and luteinizing hormone LH surge mechanism) (Roselli et al., 2006). Taken together, the limited available evidence suggests that central aromatase deficiency may affect males more than females, at least regarding sexual behaviors.

AROMATASE AND SOCIOSEXUAL BEHAVIORS

Sociosexual behaviors such as lordosis, mounting, and preference for non-volatile pheromones (and potentially volatile odors from urine/bedding) assists in mate selection and reproduction in several mammalian species. These behaviors may be regulated by aromatase. In rodents, olfaction detection and perception are considered socio-cognitive behaviors in that odor recognition of same and different sex individuals guides subsequent socio-behavioral responses, i.e., fighting or mating behaviors. Two olfactory systems exist in rodents and likely mediate diverging purposes (Bakker, 2003). The main olfactory system is primarily associated with detection of volatile odors and is traditionally associated with finding food and detection of predators (Bakker, 2003). The accessory olfactory system detects non-volatile pheromones and assists in mate selection and reproductive behaviors and is known to be sexually dimorphic (Bakker, 2003).

When examined separately, Bakker (2003) found genotype (ArKO vs. WT), but no sex differences in the role of aromatase in the development of the main olfactory pathway, and a lack of an effect on the accessory olfactory pathway (Bakker, 2003). The findings suggest that aromatase is important for development of the main olfactory system in both sexes, but not the accessory olfactory system (Bakker, 2003).

In a separate but supporting study using the same mouse model, Bakker et al. (2010) applied urinary odors directly to the nasal region of all mice tested in order to activate both the main and accessory olfactory systems. Here, the investigators detected both genotype and sex differences. In response to urinary odors of opposite sex conspecifics, wild-type (WT) females exhibited a significant increase in hypothalamic c-fos expression of kisspeptin neurons (an upstream regulator of gonadotropin releasing hormone- GnRH secretion), while such responses were blunted in ArKO females (Bakker et al., 2010). In WT males, minimal increase in c-fos expression was noted, while no increase

was evident in ArKO males in response to the odor cues of estrus females (Bakker, 2003; Bakker et al., 2010). Taken together, a sex difference may exist in the role of aromatase in mate selection, possibly via influence on kisspeptin neurons, regulated secondarily the GnRH/LH system. Interestingly, expression of kisspeptin mRNA (*Kiss1*) and kisspeptin neuronal activity were reduced in both ArKO males and females, seemingly contradicting the previous findings by Bakker et al. (2010) that suggests kisspeptin neurons are essential for regulating GnRH in the hypothalamus and indirectly, the LH surge. The conflicting findings suggest aromatase plays a role in this pathway but is not the primary enzyme involved. (Szymanski and Bakker, 2012).

However, further examination of the GnRH/LH system by Szymanski and Bakker (2012) determined that administration of E2 + progesterone to WT and ArKO females and ArKO males (between 3 and 6 months of age) successfully produced an LH surge (considered a female pattern of secretion). However, in WT males, defeminization occurred normally, thus rendering them unable to produce a later LH surge in response to these ovary-associated hormones (Szymanski and Bakker, 2012).

Pharmacological manipulation of aromatase has also been utilized to examine the effects of the removal of E2 during gestation on later adult sexual behaviors. Olvera-Hernandez et al. (2015) reported a feminized-pattern of results in male Wistar rats after prenatal exposure to Letrozole (0.56 μg/kg of the dam) with 30% of males showing same-sex preference and 33% displaying lordosis. However, 44% of treated males also displayed a completely masculinized pattern of sexual behavior, i.e., mounting behaviors, intromission, and ejaculation toward receptive females (Olvera-Hernandez et al., 2015), suggestive that some males might be resistant to the effects of this AI. The mechanism by which prenatal exposure to AI affects adult sexual behavior could be epigenetic in origin (Matsuda et al., 2011; Nugent et al., 2015; McCarthy et al., 2017).

In support of an epigenetic component and E2 signaling on adult socio-sexual behaviors, El Hajj Chehadeh et al. (2014) observed decreased *Cyp19* expression in the olfactory bulbs of 21-day old female rat pups whose mothers were fed a methyl-donor deficient diet throughout gestation (El Hajj Chehadeh et al., 2014). In addition, these same pups also exhibited impaired olfactory discrimination during the lactation and weaning periods (El Hajj Chehadeh et al., 2014). While olfactory cues in the diet primarily triggers the main olfactory system in rodents, pheromones are also likely implicated in pup interaction with dams (as with mate selection later in life) and thus, further investigation is necessary to elucidate the effects of DNA methylation and E2/E2 receptor signaling on the accessory olfactory system and sexual behaviors later in life.

Other rodent models have been used to understand how systemic and central aromatase activity regulates other socio-sexual behaviors, in particular prairie voles (*Microtus ochrogaster*) that are monogamous and demonstrate biparental care. Conflicting parenting results have been obtained in prairie voles treated with AI, which are likely due to when the animals were exposed to the pharmaceutical agent. Female virgin prairie voles normally exhibit infanticidal behavior when exposed to pups, while virgin males exhibit normal parental behaviors (Lonstein and De Vries, 2000). In this study, prenatal exposure to AIs (via subcutaneous injection of 1 mg ATD on gestational days 15–19) or post-natal exposure to the same AI (0.5 mg ATD on PND1-7) did not alter the parental or infanticidal behaviors of the prairie voles in adulthood (Lonstein and De Vries, 2000). However, female offspring prenatally exposed to ATD had higher levels of parental care compared to T propionate-treated females. On the other hand, treatment of male prairie voles with ATD (subcutaneous injection of 0.5 mg for PND8-14) or flutamide (0.5 mg for PND8-14) reduced alloparental behavior in 21-day old males with ATD-treated males demonstrating an increase in sniffing behavior but also an increase in latency to lick and huddle the pups, whereas flutamide-treated males had increased latency to enter the pup cage and probability of retreat from initial contact (Kramer et al., 2009).

To test effects of developmental exposure to AI on later reproductive behaviors in prairie voles, male and female pups were treated daily with ATD (injection 0.5 mg on PND1-7) or vehicle control (Northcutt and Lonstein, 2008). ATD-treated females were the recipients of fewer mounts and thrusts, suggestive of reduced attractiveness to males. Males treated neonatally with ATD showed a demasculinized pattern in tyrosine hydroxylases expression in the anteroventral periventricular preoptic area and ESR1 expression in the medial preoptic area. Female guinea pigs (*Cavia porcellus*) subjected to prenatal ATD exposure had decreased mounting activity but comparable responses were not observed in males subjected to similar AI exposure (Roy, 1992). However, another study testing the effects of developmental exposure to ATD in guinea pigs (gestational day 30 to day 55) reported that both males and females were irresponsive to the negative feedback effects of E2 benzoate or LH secretion, and ATD-treated males demonstrated increased lordosis behavior compared to control males (Choate and Resko, 1994). However, no changes in mounting or lordosis behavior were evident in ATD-treated female guinea pigs (Choate and Resko, 1994).

Taken together, the above data provide mixed results as to the role of an early prenatal aromatase surge in guiding later sociosexual behaviors. The results are muddled by the fact that different AI and doses have been tested, variation in developmental exposure periods, and specific tests used to measure sociosexual behaviors. Moreover, the studies have used different animal models that demonstrate divergent reproductive strategies (polygynous vs. monogamous) that assuredly will influence the outcome. The ideal experiment should test the same AI dose at the same gestational period in rodent models displaying these two types of mating systems.

SEX-SPECIFIC ROLE OF AROMATASE IN STRESS-, ANXIETY-, AND DEPRESSIVE-LIKE BEHAVIORS

Anxiety and depression are two of the most widely diagnosed mental illnesses today with women being more likely to be diagnosed than men (Altemus et al., 2014). While animals do not experience stress or depressive behaviors per se, behavioral

tests, such as the elevated plus maze EPM, tail suspension test, and forced swim test (FST), can be used to measure behaviors that are suggestive of anxiety- and depressive-like behaviors. In the EPM, decreased entries into the open arms might suggest anxiety-like behaviors, and increased time spent immobile in the tail suspension test and FST are indicative of depressive-like behaviors in that the animal is giving up trying to escape an aversive (water or suspension) stimulus. These emotive behaviors are considered amygdala-dependent (Gray, 1999) and are collectively considered in this section. With the usage of such rodent tests, there is still limited data comparing aromatase regulation of male and female responses in these categories. Most current studies have examined males or females only, making sex comparisons across reports difficult due to non-uniform procedures to measure these behaviors, such as type of test, genetic or pharmacological manipulation, AI administered, time and duration of AI administration, or even species/rodent strain.

Kokras et al. (2018) showed that female Wistar rats (3 months old) enter the center of an open field test (OFT), indicative of lower anxiety levels, more often than males, but this affect was eliminated by ovariectomy or Letrozole treatment (intraperitoneal injection of 1 mg/kg letrozole for 8 days) indicating that systemic E2, and not central aromatase activity, may be responsible for the primary anxiolytic effect observed in females (Kokras et al., 2018). In a separate study, Letrozole (1 mg/kg subcutaneously for 14 days) induced an anxiogenic effect in intact male Lewis rats which spent, on average, 95% less time in the open arms of the EPM when compared to control males, while intact females given the same AI did not differ significantly from controls, suggesting AI-induced anxiety-like behaviors in males but not females (Borbelyova et al., 2017).

Using the ArKO mouse model, Dalla et al. (2004, 2005), demonstrated that genotype (ArKO vs. WT) did not affect male performance, but female ArKO mice displayed more passive behaviors (e.g., decreased mobility) during the FST, an inherently stressful behavioral test for terrestrial animals that is designed to measure depressive-like behaviors, indicative of elevated depressive-like behaviors (Dalla et al., 2004, 2005). However, Kokras et al. (2018) found that Letrozole did not affect behavior of either sex in this test, although aromatase activity was decreased in the hypothalamus of male rats after behavioral testing (Kokras et al., 2018). This study demonstrated that genotype did not affect male performance, but female ArKO mice displayed more passive behaviors (e.g., decreased mobility) during the FST, indicative of elevated depressive-like behaviors (Dalla et al., 2004, 2005). In contrast, male but not female ArKO mice showed an age-related reduction in the prepulse inhibition of the acoustic startle test, which measures ability of rodents to habituate to an external stimulus (van den Buuse et al., 2003). Collectively, these findings suggest that central E2 synthesis may differentially affect specific aspects of mental health with a potentially greater role in female rover male rodents.

In contrast to the above findings, a study with Sprague-Dawley rats found that acute stress decreased circulating E2 and T in females, while these hormones remained unchanged or in some cases increased, whereas no differences in hypothalamic *Cyp19* mRNA expression were detected (Lu et al., 2015). There is increasing recognition that stressful events during pre- and/or post-natal development may contribute to future development of anxiety or depression in adulthood; whether sex plays a role in the relationship between stress and development is not fully known and is an important area for future work. Such sex-specific developmental programming [known as the developmental origin of adult health and disease (DOHaD) concept (Weinstock, 2007; Wadhwa et al., 2009)] may involve aromatase activity. In support of this notion, maternal stressors, such as prolonged restraint, suppresses aromatase activity in the hypothalamus and amygdala of the male rat (unspecified strain) offspring, causing developmental changes in these brain regions potentially contributing to future anxiety, depression, or learning deficits (Weinstock, 2007). Only a few studies have examined the role of aromatase in the fetal brain as a potential mediator of prenatal programming effects. One of those studies tested how exposure of female Wistar dams to ATD during late gestation would affect later offspring anxiety and emotional behaviors when tested at 1 month of age in the OFT and EPM and found that maternal exposure to ATD increased anxiety-like behaviors in both sexes (Ordyan et al., 2007). With the increased incidence of anxiety and depression in adults, as well as attention deficit disorder in children, further research in this area is vital to understanding the effects of this increase in diagnoses and possible involvement of aromatase in offspring and even descendants through transgenerational inheritance.

SEXUALLY DIMORPHIC EFFECTS OF AROMATASE: POSSIBLE ROLE IN ALZHEIMER'S DISEASE?

The presence of aromatase in mammalian hippocampus suggests that E2 plays a role in learning and memory (Overk et al., 2012; Vierk et al., 2012; El Hajj Chehadeh et al., 2014). Deficits in learning and memory are also a hallmark of Alzheimer's disease (AD) and sex differences have been observed with women overall being at an increased risk (Medway et al., 2014). The Epistasis Project by Medway et al. (2014) determined that 3 of the 4 single-nucleotide polymorphisms (SNPs) of *CYP19* tested were associated with increased risk for AD in women but not in men (Medway et al., 2014). Another human cohort study, OPTIMA, examined nine polymorphisms in the *CYP19* gene in 207 cases of AD, 23 cases of mild cognitive impairments (MCI), and 233 control men and women. Consistent findings between those polymorphisms and both AD and MCI cases were observed, and significant interactions between select polymorphisms and sex were also noted. Remarkably, all associations between *CYP19* polymorphisms and AD were identified exclusively in women (Butler et al., 2010). Three SNPs (res12907866, rs17601241, and rs4646) in *CYP19* were assessed in 319 AD patients and 110 controls representing men and women, and the investigators determined that while none of these CYP19 SNPs increased the risk for AD, women with the rs4636 genotype carrying a T allele were more likely to have an earlier-onset of AD (Corbo et al., 2009).

While aromatase suppression has been associated with increased risk for AD as summarized above, meta-analyses have been inconclusive about potential sex differences (Roselli et al., 1998; Medway et al., 2014; Prange-Kiel et al., 2016). Rodent studies have been somewhat useful in shedding light on the effects of aromatase on risk for AD-like signs, especially in females. Sex differences in intact 5xFAD mice (a mouse model for AD) were observed such that the hippocampi of female (but not male) mice had significantly lower *Cyp19* expression and protein activity when compared to WT counterparts (Prange-Kiel et al., 2016). Sex differences were also observed with Anastrozole administration (0.4 mg/animal/day via solid hydration gel matrix) to intact 9-month-old female 3xTgAD mice (another mouse model of AD), which significantly increased $A\beta_{1-40/42}$-immunoreactivity (a marker of AD pathology) in the hippocampus of intact AI-treated mice (Overk et al., 2012). No significant differences were seen between gonadectomized males and females with or without anastrozole-treatment, suggesting that these effects are due to systemic E2 rather than local aromatase activity (Overk et al., 2012).

In another study, aromatase inhibition completely abolished long-term potentiation (LTP); an electrophysiological parameter of memory, in the hippocampus of 12-week old female C57Bl/6 mice, while treated males of the same age only experienced a 20% reduction in LTP after 7 days (Vierk et al., 2012). Surprisingly, ovariectomy reduced this effect in females with Letrozole producing only a 50% decrease in LTP after 7 days of treatment, suggesting that central aromatase activity and gonadal estrogen work synergistically to modify LTP in the hippocampus of females (Vierk et al., 2012). In neonatal (PND0) Sprague-Dawley rats, exogenous E2 has been shown to promote cell proliferation and survival in hippocampi of females but not males, and this effect persists through PND21 (Bowers et al., 2010). Surprisingly, subcutaneous injection of the AI formestane (100μg/0.1 mL in sesame oil at PND0) significantly decreased hippocampal cell proliferation in male Sprague-Dawley rats but had no effect on females (Bowers et al., 2010).

To further examine potential interactions between aromatase suppression and AD, APP23-ArKO mice have been generated in order to assess the interactions between an increased risk for AD (as in the APP23 mouse model) and a systemic absence of E2 (as occurs in the ArKO model) (McAllister et al., 2010; Li et al., 2013). App/Cyp19 heterozygous ovariectomized females have reduced Aβ plaques and reduced expression of β-secretase 1 (BACE1, enzyme responsible for cleavage of amyloid precursor protein- APP) mRNA and protein expression following E2 or genistein treatment (Li et al., 2013). On the other hand, APP/ArKO males show reduced brain plague formation, enhanced cognitive functions, increased neprilysin, involved in Aβ clearance), and reduced BACE (McAllister et al., 2010). Collective findings in this male line suggests that elevated T due to absence of CYP19 protects against AD-like signs (McAllister et al., 2010). Elevated T might confer protection against this disease in males by suppressing BACE1 activity resulting in reduced β-amyloid production and increased neprilysin to stimulate degradation of any existing β-amyloid within the brain. Overall, the results reveal that the mechanisms by which aromatase, and thus sex hormones, affect cognition and risk for AD are complex and may involve aromatase mediated differences and/or changes in spine synapse density, *CYP19* gene expression, and aromatase activity (Fester et al., 2017).

SEX-SPECIFIC REGULATION OF LOCOMOTOR ACTIVITY BY AROMATASE

Possibly the most limited area of research on sex differences in aromatase is in its effects on physical/locomotor activity. It is known from many rodent studies that intact females are significantly more active than age-matched males (Hong et al., 2009) and preclinical studies in rodents have implicated central E2 signaling in mediating increased physical activity in females (Xu et al., 2015). Moreover, studies in rodents and women provide evidence that aromatase activity may directly affect physical activity, and this effect of aromatase may be sex-specific. Not surprisingly, the ArKO female mouse model demonstrates compromised physical activity (Jones et al., 2001). Notably, this phenotype of ArKO females is even more pronounced than similar observations in ovariectomized WT females, who lack gonadal E2 but presumably have normal aromatase enzyme activity and E2 synthesis in the brain (Jones et al., 2000). It is uncertain whether ArKO males are also significantly less active than WT controls, as only females have been tested to date. There is, however, limited evidence involving pharmacological AI in male mice. In one study, administration of AI (SC 500μl bolus with 250 mg/kg exemestane + injection of Letrozole at 0.5 μg/μl for 7 days) had no effect on voluntary wheel running, while orchidectomy reduced wheel running (Bowen et al., 2011). These findings imply that systemic androgens/T, and not E2, affects wheel running in male mice. While ArKO mice of both sexes have been shown to be metabolically dysfunctional (Jones et al., 2000, 2001), the evidence suggests that aromatase activity offers some metabolic protection in both sexes, but affects physical activity behavior only in females.

Few studies have examined the mechanisms by which aromatase affects physical activity directly, so much of the available evidence includes secondary measurements of locomotor activity as assessed in association with another major outcome (i.e., anxiety-like, depressive-like, or schizophrenia-like behaviors). One experiment conducted in an attempt to understand the role of E2 in schizophrenia discovered that female and male ArKO mice experienced reduced psychotropic drug-induced hyperactivity in an OFT after administration of apomorphine, MK-801, and amphetamine while WT counterparts were unaffected, although this effect was not as pronounced in male ArKO mice (Chavez et al., 2009). Thus, these results lend support for the idea that males and females are potentially differentially affected by aromatase deletion and consequent locomotor activity. This sexually dimorphic difference is possibly explained by an increased density of dopamine transporters in the caudate putamen of male but not female ArKO mice when compared to WT mice, potentially

allowing for a compensatory dopaminergic upregulation in male (but not female) ArKO mice (Chavez et al., 2009).

In contrast, a separate study showed that aromatase inhibition administered via subcutaneous injection had no effect on locomotor activity of neither male nor female middle-aged rats (15 months) when tested in the EPM, which measures both anxiety-like and exploratory behavior (Borbelyova et al., 2017). Similarly, Kokras et al. (2018), who studied younger (i.e., 3 month old) Wistar rats, also reported no sex differences in locomotor activity when measured during an OFT (Kokras et al., 2018). Other reports confirm that locomotor activity is not affected by AI in either sex when it is assessed in an OFT or EPM (Dalla et al., 2004, 2005). However, it is important to consider that all of those above studies only assessed locomotor activity as it relates to other behavioral readouts (i.e., during EPM and OFT assessments of anxiety and/or depressive behaviors) which represents a major confounding variable when assessing spontaneous or motivated physical activity. The role of aromatase activity *per se* on sex differences in physical activity requires more investigation. Better understanding the sex-specific effects of aromatase on physical activity (e.g., potentially decreased motivation to exercise in one or both sexes) may lend insight into the mechanisms driving physical activity, as well as potential side effects of aromatase inhibition in humans. Our current studies seek to examine for potential sex-differences in motivated physical activity using an ArKO mouse model.

NEUROPROTECTIVE ROLE OF AROMATASE FOLLOWING BRAIN INJURY

Sex differences in recovery following brain injury and ischemia have been reported (Melcangi et al., 2016). Rodent studies have often concluded that females experience better outcomes in recovery than males (Chavez et al., 2009; Bowen et al., 2011). While the vast majority of work has investigated the neuroprotective effects of E2 (Zhang et al., 2014; Pietranera et al., 2015) the fact that aromatase is expressed in the brain of males and females, and thus contributes to the production of neuroestrogen, potentially implicates a neuroprotective role of aromatase in both sexes.

How aromatase may contribute to recovery from traumatic brain injury or stroke may depend on the level of aromatase expression in that particular brain region, as well as the cell type (e.g., astrocytes of the human temporal cortex), as discussed earlier. Since astrocytes following brain injury or ischemia become reactive, aromatase activity by these cells in particular may mediate neuronal recovery from injury (Garcia-Segura et al., 1999; Melcangi et al., 2016) Indeed, evidence supports the hypothesis that the protective effects of astrocytes is due to E2 availability (i.e., dependent upon aromatase activity), although whether sex differences exist remains unclear (Garcia-Segura et al., 1999).

Lavaque et al. (2006) examined *Cyp19*, P450scc (an enzyme involved in the conversion of cholesterol to pregnenolone, the first step in steroid hormone production), and StAR (regulates cholesterol transport in the mitochondria) expression in the cerebellum of male and female Wistar albino rats at several days of early development (i.e., PND 1, 5, 10, 15, 20, and 30). In both males and females, peak *Cyp19* expression occurred at PND5, with males exhibiting higher expression than females at all ages. In females, an increase in aromatase at PND10 was sequentially followed by an increase in P450scc and StAR (Lavaque et al., 2006). However, the increases in these three enzymes (i.e., aromatase, P450 scc and StAR) were synchronous in males at PND10 and significantly higher than females. Previous studies in males examined the effects of central E2 on neuronal death after administration of 3-acetylpyridine (3-AP - a toxin that produces degeneration of inferior olivary neurons and the consequent degeneration of climbing fiber afferents to cerebellar Purkinje cells) (Lavaque et al., 2006). They found that inhibition of aromatase increased the neurodegenerative effect of 3-AP, while administration of exogenous E2 decreases the effects of 3AP, again supporting the idea that E2 is neuroprotective and that aromatase activity correlates with this neuroprotection (Lavaque et al., 2006). In that study, an increase in P450scc and StAR mRNA was observed in adult male Wistar rats after injection of 3-AP (dose, 60 mg/kg in saline) in the cerebellum (Lavaque et al., 2006). Taken with the findings from previous studies, the evidence suggests that aromatase, StAR, and P450scc all work in tandem to increase steroidogenesis in response to cellular damage (Lavaque et al., 2006). The fact that aromatase, P450scc, and StAR remain unchanged in female rats throughout the estrous cycle suggests that, at least in the cerebellum, it is local and not gonadal E2 production that provides neuroprotection following brain injury and in neurodegenerative diseases (Lavaque et al., 2006; Garcia-Segura, 2008).

CONCLUSION

Aromatase is the key enzyme in the E2 production pathway, and its marked expression in the brain highlights its potential importance in many neurobehavioral functions. While differences in aromatase expression and activity may not translate directly to behavioral differences, animal studies indicate that aromatase expression and activity is necessary for proper neurobehavioral development in both males and females. Later in life, sex differences in aromatase may affect risk for neurological diseases, such as depression and AD, which tend to be greater in females than males (Dalla et al., 2004; Ordyan et al., 2007; Overk et al., 2012; Lu et al., 2015; Alarcon et al., 2017; Kokras et al., 2018). Research continues to elucidate the mechanisms by which aromatase affects neurobehavioral programming and sex differences in cognitive and other neurological disorders.

In addition to sociosexual, emotive, and cognitive behaviors regulated by aromatase, emerging evidence suggests aromatase might also affect motivational physical activity. Ovary-intact female rodents are more active than male counterparts (Martin et al., 2003; Afonso et al., 2013) and E2 is known to affect physical activity (Hong et al., 2009; McAllister et al., 2010; Xu et al., 2015). Not surprising, ArKO mice are known to exhibit suppressed

physical activity compared to WT. Whether this translates to humans is not clear, but it is noteworthy that AI drugs have been shown to reduce physical activity in humans, a finding with important relevance to women receiving AI to treat breast cancer and other disorders.

Preclinical studies using ArKO and AI-treated rodent models have unraveled some of the multifaceted mechanisms by which aromatase can induce behavioral sex differences. Gonadectomized animal models have also helped tease apart systemic from central effects of aromatase. However, creation of brain-region specific aromatase knockout mice would allow for even more precise assessments on how this enzyme regulates various brain regions and corresponding behaviors in a sex-dependent manner.

While rodent models have provided insight into the role of aromatase in the brain and sex differences, there are potential drawbacks, including differences in gestational period, which might limit translation to humans. Non-invasive methods to image the human brain will aide in our understanding the role aromatase in various brain regions and sex differences. One rapidly evolving method to image in a non-invasive manner the human brain *in vivo* is near-infrared spectro-imaging (Toronov et al., 2005). Structural brain features are determined by spatial light bundles derived from photons traveling to light source detectors placed on top of the head. Positron emission tomography (PET) and a radiolabeled competitive inhibitor of aromatase can also be used to *in vivo* image brain aromatase (Moraga-Amaro et al., 2018). For instance, administration of [^{11}C]vorozole and PET performed in female baboons revealed the highest uptake of this compound was detected in the amygdala followed by the preoptic area and hypothalamus, basal ganglia, and cortical areas (Pareto et al., 2013). As mentioned previously, PET studies with [*N*-methyl-^{11}C]vorozole have revealed high levels of aromatase in the thalamus and medulla (inferior olive) of humans, which has not been identified in these brain regions of other species (Biegon et al., 2010). In combination with these imaging modalities, it is also important to measure directly enzyme and steroid concentrations in the various brain regions of rodent models and in humans where possible.

Future research with enhanced transgenic and imaging technologies will continue to improve our understanding of the relationship between aromatase and neurobehavioral functions. Such methodologies will help unveil the role of this enzyme in normal cognitive aging, mental illness, neurodegenerative disease, and even traumatic brain injury, and whether those relationships are sex specific. A better understanding of how aromatase contributes to the etiology of such cognitive diseases may lead to improved treatment strategies in men and women.

AUTHOR CONTRIBUTIONS

DS, VV-P, and CR researched the area, wrote the original manuscript, and reviewed the final manuscript. DS and CR helped prepare the figure.

FUNDING

CR was supported in part by NIEHS 1R01ES025547-A1.

ACKNOWLEDGMENTS

We are grateful to Donald L. Connor's assistance in preparing the figure.

REFERENCES

Abdelgadir, S. E., Resko, J. A., Ojeda, S. R., Lephart, E. D., Mcphaul, M. J., and Roselli, C. E. (1994). Androgens regulate aromatase cytochrome P450 messenger ribonucleic acid in rat brain. *Endocrinology* 135, 395–401. doi: 10.1210/endo.135.1.8013375

Afonso, V. M., Shams, W. M., Jin, D., and Fleming, A. S. (2013). Distal pup cues evoke dopamine responses in hormonally primed rats in the absence of pup experience or ongoing maternal behavior. *J. Neurosci.* 33, 2305–2312. doi: 10.1523/JNEUROSCI.2081-12.2013

Alarcon, G., Cservenka, A., and Nagel, B. J. (2017). Adolescent neural response to reward is related to participant sex and task motivation. *Brain Cogn.* 111, 51–62. doi: 10.1016/j.bandc.2016.10.003

Altemus, M., Sarvaiya, N., and Neill Epperson, C. (2014). Sex differences in anxiety and depression clinical perspectives. *Front. Neuroendocrinol.* 35, 320–330. doi: 10.1016/j.yfrne.2014.05.004

Bakker, J. (2003). Sexual differentiation of the neuroendocrine mechanisms regulating mate recognition in mammals. *J. Neuroendocrinol.* 15, 615–621. doi: 10.1046/j.1365-2826.2003.01036.x

Bakker, J., Pierman, S., and Gonzalez-Martinez, D. (2010). Effects of aromatase mutation (ArKO) on the sexual differentiation of kisspeptin neuronal numbers and their activation by same versus opposite sex urinary pheromones. *Horm. Behav.* 57, 390–395. doi: 10.1016/j.yhbeh.2009.11.005

Balthazart, J. (1997). Steroid control and sexual differentiation of brain aromatase. *J. Steroid Biochem. Mol. Biol.* 61, 323–339. doi: 10.1016/S0960-0760(97)80030-1

Balthazart, J., Baillien, M., Charlier, T. D., Cornil, C. A., and Ball, G. F. (2003). Multiple mechanisms control brain aromatase activity at the genomic and non-genomic level. *J. Steroid Biochem. Mol. Biol.* 86, 367–379. doi: 10.1016/S0960-0760(03)00346-7

Bell, M. R. (2018). Comparing postnatal development of gonadal hormones and associated social behaviors in rats, mice, and humans. *Endocrinology* 159, 2596–2613. doi: 10.1210/en.2018-00220

Beyenburg, S., Stoffel-Wagner, B., Watzka, M., Blumcke, I., Bauer, J., Schramm, J., et al. (1999). Expression of cytochrome P450scc mRNA in the hippocampus of patients with temporal lobe epilepsy. *Neuroreport* 10, 3067–3070. doi: 10.1097/00001756-199909290-00035

Biegon, A., Kim, S. W., Alexoff, D. L., Jayne, M., Carter, P., Hubbard, B., et al. (2010). Unique distribution of aromatase in the human brain: in vivo studies with PET and [N-methyl-11C]vorozole. *Synapse* 64, 801–807. doi: 10.1002/syn.20791

Blakemore, J., and Naftolin, F. (2016). Aromatase: contributions to physiology and disease in women and men. *Physiology* 31, 258–269. doi: 10.1152/physiol.00054.2015

Boon, W. C., Chow, J. D., and Simpson, E. R. (2010). The multiple roles of estrogens and the enzyme aromatase. *Prog. Brain Res.* 181, 209–232. doi: 10.1016/S0079-6123(08)81012-6

Borbelyova, V., Domonkos, E., Csongova, M., Kacmarova, M., Ostatnikova, D., Celec, P., et al. (2017). Sex-dependent effects of letrozole on anxiety in middle-aged rats. *Clin. Exp. Pharmacol. Physiol.* 44(Suppl. 1), 93–98. doi: 10.1111/1440-1681.12731

Bowen, R. S., Ferguson, D. P., and Lightfoot, J. T. (2011). Effects of aromatase inhibition on the physical activity levels of male mice. *J. Steroids Horm. Sci.* 1, 1–7. doi: 10.4172/2157-7536.S1-001

Bowers, J. M., Waddell, J., and Mccarthy, M. M. (2010). A developmental sex difference in hippocampal neurogenesis is mediated by endogenous oestradiol. *Biol. Sex Differ.* 1:8. doi: 10.1186/2042-6410-1-8

Bulun, S. E., Chen, D., Moy, I., Brooks, D. C., and Zhao, H. (2012). Aromatase, breast cancer and obesity: a complex interaction. *Trends Endocrinol. Metab.* 23, 83–89. doi: 10.1016/j.tem.2011.10.003

Butler, H. T., Warden, D. R., Hogervorst, E., Ragoussis, J., Smith, A. D., and Lehmann, D. J. (2010). Association of the aromatase gene with Alzheimer's disease in women. *Neurosci. Lett.* 468, 202–206. doi: 10.1016/j.neulet.2009.10.089

Cao, M., Duan, J., Cheng, N., Zhong, X., Wang, Z., Hu, W., et al. (2012). Sexually dimorphic and ontogenetic expression of dmrt1, cyp19a1a and cyp19a1b in *Gobiocypris rarus*. *Comp. Biochem. Physiol. A Mol. Integr. Physiol.* 162, 303–309. doi: 10.1016/j.cbpa.2012.03.021

Chavez, C., Gogos, A., Jones, M. E., and Van Den Buuse, M. (2009). Psychotropic drug-induced locomotor hyperactivity and prepulse inhibition regulation in male and female aromatase knockout (ArKO) mice: role of dopamine D1 and D2 receptors and dopamine transporters. *Psychopharmacology* 206, 267–279. doi: 10.1007/s00213-009-1604-6

Cherrier, M. M., Asthana, S., Plymate, S., Baker, L., Matsumoto, A. M., Peskind, E., et al. (2001). Testosterone supplementation improves spatial and verbal memory in healthy older men. *Neurology* 57, 80–88. doi: 10.1212/WNL.57.1.80

Cherrier, M. M., Matsumoto, A. M., Amory, J. K., Ahmed, S., Bremner, W., Peskind, E. R., et al. (2005). The role of aromatization in testosterone supplementation: effects on cognition in older men. *Neurology* 64, 290–296. doi: 10.1212/01.WNL.0000149639.25136.CA

Choate, J. V., and Resko, J. A. (1994). Prenatal inhibition of aromatase activity affects luteinizing hormone feedback mechanisms and reproductive behaviors of adult guinea pigs. *Biol. Reprod.* 51, 1273–1278. doi: 10.1095/biolreprod51.6.1273

Connolly, P. B., Roselli, C. E., and Resko, J. A. (1994). Aromatase activity in developing guinea pig brain: ontogeny and effects of exogenous androgens. *Biol. Reprod.* 50, 436–441. doi: 10.1095/biolreprod50.2.436

Corbo, R. M., Gambina, G., Ulizzi, L., Moretto, G., and Scacchi, R. (2009). Genetic variation of CYP19 (aromatase) gene influences age at onset of Alzheimer's disease in women. *Dement. Geriatr. Cogn. Disord.* 27, 513–518. doi: 10.1159/000221832

Dalla, C., Antoniou, K., Papadopoulou-Daifoti, Z., Balthazart, J., and Bakker, J. (2004). Oestrogen-deficient female aromatase knockout (ArKO) mice exhibit depressive-like symptomatology. *Eur. J. Neurosci.* 20, 217–228. doi: 10.1111/j.1460-9568.2004.03443.x

Dalla, C., Antoniou, K., Papadopoulou-Daifoti, Z., Balthazart, J., and Bakker, J. (2005). Male aromatase-knockout mice exhibit normal levels of activity, anxiety and "depressive-like" symptomatology. *Behav. Brain Res.* 163, 186–193. doi: 10.1016/j.bbr.2005.04.020

El Hajj Chehadeh, S., Pourie, G., Martin, N., Alberto, J. M., Daval, J. L., Gueant, J. L., et al. (2014). Gestational methyl donor deficiency alters key proteins involved in neurosteroidogenesis in the olfactory bulbs of newborn female rats and is associated with impaired olfactory performance. *Br. J. Nutr.* 111, 1021–1031. doi: 10.1017/S0007114513003553

Fester, L., Zhou, L., Ossig, C., Labitzke, J., Blaute, C., Bader, M., et al. (2017). Synaptopodin is regulated by aromatase activity. *J. Neurochem.* 140, 126–139. doi: 10.1111/jnc.13889

Garcia-Segura, L. M. (2008). Aromatase in the brain: not just for reproduction anymore. *J. Neuroendocrinol.* 20, 705–712. doi: 10.1111/j.1365-2826.2008.01713.x

Garcia-Segura, L. M., Wozniak, A., Azcoitia, I., Rodriguez, J. R., Hutchison, R. E., and Hutchison, J. B. (1999). Aromatase expression by astrocytes after brain injury: implications for local estrogen formation in brain repair. *Neuroscience* 89, 567–578. doi: 10.1016/S0306-4522(98)00340-6

Gray, T. S. (1999). Functional and anatomical relationships among the amygdala, basal forebrain, ventral striatum, and cortex. An integrative discussion. *Ann. N. Y. Acad. Sci.* 877, 439–444. doi: 10.1111/j.1749-6632.1999.tb09281.x

Hong, J., Stubbins, R. E., Smith, R. R., Harvey, A. E., and Nunez, N. P. (2009). Differential susceptibility to obesity between male, female and ovariectomized female mice. *Nutr. J.* 8:11. doi: 10.1186/1475-2891-8-11

Howdeshell, K. L. (2002). A model of the development of the brain as a construct of the thyroid system. *Environ. Health Perspect.* 110(Suppl. 3), 337–348. doi: 10.1289/ehp.02110s3337

Jones, M. E., Thorburn, A. W., Britt, K. L., Hewitt, K. N., Misso, M. L., Wreford, N. G., et al. (2001). Aromatase-deficient (ArKO) mice accumulate excess adipose tissue. *J. Steroid Biochem. Mol. Biol.* 79, 3–9. doi: 10.1016/S0960-0760(01)00136-4

Jones, M. E., Thorburn, A. W., Britt, K. L., Hewitt, K. N., Wreford, N. G., Proietto, J., et al. (2000). Aromatase-deficient (ArKO) mice have a phenotype of increased adiposity. *Proc. Natl. Acad. Sci. U.S.A.* 97, 12735–12740. doi: 10.1073/pnas.97.23.12735

Kadioglu, P., Oral, G., Sayitoglu, M., Erensoy, N., Senel, B., Gazioglu, N., et al. (2008). Aromatase cytochrome P450 enzyme expression in human pituitary. *Pituitary* 11, 29–35. doi: 10.1007/s11102-007-0065-3

Kanaya, M., Morishita, M., and Tsukahara, S. (2018). Temporal expression patterns of genes related to sex steroid action in sexually dimorphic nuclei during puberty. *Front. Endocrinol.* 9:213. doi: 10.3389/fendo.2018.00213

Kokras, N., Pastromas, N., Papasava, D., De Bournonville, C., Cornil, C. A., and Dalla, C. (2018). Sex differences in behavioral and neurochemical effects of gonadectomy and aromatase inhibition in rats. *Psychoneuroendocrinology* 87, 93–107. doi: 10.1016/j.psyneuen.2017.10.007

Konkle, A. T., and McCarthy, M. M. (2011). Developmental time course of estradiol, testosterone, and dihydrotestosterone levels in discrete regions of male and female rat brain. *Endocrinology* 152, 223–235. doi: 10.1210/en.2010-0607

Kramer, K. M., Perry, A. N., Golbin, D., and Cushing, B. S. (2009). Sex steroids are necessary in the second postnatal week for the expression of male alloparental behavior in prairie voles (*Microtus ochragaster*). *Behav. Neurosci.* 123, 958–963. doi: 10.1037/a0016927

Lavaque, E., Mayen, A., Azcoitia, I., Tena-Sempere, M., and Garcia-Segura, L. M. (2006). Sex differences, developmental changes, response to injury and cAMP regulation of the mRNA levels of steroidogenic acute regulatory protein, cytochrome p450scc, and aromatase in the olivocerebellar system. *J. Neurobiol.* 66, 308–318. doi: 10.1002/neu.20221

Lephart, E. D. (1996). A review of brain aromatase cytochrome P450. *Brain Res. Brain Res. Rev.* 22, 1–26. doi: 10.1016/0165-0173(96)00002-1

Li, R., He, P., Cui, J., Staufenbiel, M., Harada, N., and Shen, Y. (2013). Brain endogenous estrogen levels determine responses to estrogen replacement therapy via regulation of BACE1 and NEP in female Alzheimer's transgenic mice. *Mol. Neurobiol.* 47, 857–867. doi: 10.1007/s12035-012-8377-3

Lonstein, J. S., and De Vries, G. J. (2000). Influence of gonadal hormones on the development of parental behavior in adult virgin prairie voles (*Microtus ochrogaster*). *Behav. Brain Res.* 114, 79–87. doi: 10.1016/S0166-4328(00)break00192-3

Lorsch, Z. S., Loh, Y. E., Purushothaman, I., Walker, D. M., Parise, E. M., Salery, M., et al. (2018). Estrogen receptor alpha drives pro-resilient transcription in mouse models of depression. *Nat. Commun.* 9:1116. doi: 10.1038/s41467-018-03567-4

Lu, J., Wu, X. Y., Zhu, Q. B., Li, J., Shi, L. G., Wu, J. L., et al. (2015). Sex differences in the stress response in SD rats. *Behav. Brain Res.* 284, 231–237. doi: 10.1016/j.bbr.2015.02.009

Martin, S., Jones, M., Simpson, E., and Van Den Buuse, M. (2003). Impaired spatial reference memory in aromatase-deficient (ArKO) mice. *Neuroreport* 14, 1979–1982. doi: 10.1097/01.wnr.0000089571.45990.eb

Martinez-Cerdeno, V., Noctor, S. C., and Kriegstein, A. R. (2006). Estradiol stimulates progenitor cell division in the ventricular and subventricular zones of the embryonic neocortex. *Eur. J. Neurosci.* 24, 3475–3488. doi: 10.1111/j.1460-9568.2006.05239.x

Matsuda, K. I., Mori, H., Nugent, B. M., Pfaff, D. W., Mccarthy, M. M., and Kawata, M. (2011). Histone deacetylation during brain development is essential for permanent masculinization of sexual behavior. *Endocrinology* 152, 2760–2767. doi: 10.1210/en.2011-0193

McAllister, C., Long, J., Bowers, A., Walker, A., Cao, P., Honda, S., et al. (2010). Genetic targeting aromatase in male amyloid precursor protein transgenic mice down-regulates beta-secretase (BACE1) and prevents Alzheimer-like pathology

and cognitive impairment. *J. Neurosci.* 30, 7326–7334. doi: 10.1523/jneurosci.1180-10.2010

McCarthy, M. M., Nugent, B. M., and Lenz, K. M. (2017). Neuroimmunology and neuroepigenetics in the establishment of sex differences in the brain. *Nat. Rev. Neurosci.* 18, 471–484. doi: 10.1038/nrn.2017.61

Medway, C., Combarros, O., Cortina-Borja, M., Butler, H. T., Ibrahim-Verbaas, C. A., De Bruijn, R. F., et al. (2014). The sex-specific associations of the aromatase gene with Alzheimer's disease and its interaction with IL10 in the Epistasis Project. *Eur. J. Hum. Genet.* 22, 216–220. doi: 10.1038/ejhg.2013.116

Melcangi, R. C., Giatti, S., and Garcia-Segura, L. M. (2016). Levels and actions of neuroactive steroids in the nervous system under physiological and pathological conditions: sex-specific features. *Neurosci. Biobehav. Rev.* 67, 25–40. doi: 10.1016/j.neubiorev.2015.09.023

Moraga-Amaro, R., Van Waarde, A., Doorduin, J., and De Vries, E. F. J. (2018). Sex steroid hormones and brain function: PET imaging as a tool for research. *J. Neuroendocrinol.* 30:e12565 doi: 10.1111/jne.12565

Naftolin, F. (1994). Brain aromatization of androgens. *J. Reprod. Med.* 39, 257–261.

Naftolin, F., Ryan, K. J., and Petro, Z. (1971). Aromatization of androstenedione by limbic system tissue from human foetuses. *J. Endocrinol.* 51, 795–796. doi: 10.1677/joe.0.0510795

Naftolin, F., Ryan, K. J., and Petro, Z. (1972). Aromatization of androstenedione by the anterior hypothalamus of adult male and female rats. *Endocrinology* 90, 295–298. doi: 10.1210/endo-90-1-295

Nelson, L. R., and Bulun, S. E. (2001). Estrogen production and action. *J. Am. Acad. Dermatol.* 45, S116–S124. doi: 10.1067/mjd.2001.117432

Northcutt, K. V., and Lonstein, J. S. (2008). Sex differences and effects of neonatal aromatase inhibition on masculine and feminine copulatory potentials in prairie voles. *Horm. Behav.* 54, 160–169. doi: 10.1016/j.yhbeh.2008.02.008

Nugent, B. M., Wright, C. L., Shetty, A. C., Hodes, G. E., Lenz, K. M., Mahurkar, A., et al. (2015). Brain feminization requires active repression of masculinization via DNA methylation. *Nat. Neurosci.* 18, 690–697. doi: 10.1038/nn.3988

Olvera-Hernandez, S., Chavira, R., and Fernandez-Guasti, A. (2015). Prenatal letrozole produces a subpopulation of male rats with same-sex preference and arousal as well as female sexual behavior. *Physiol. Behav.* 139, 403–411. doi: 10.1016/j.physbeh.2014.11.060

Op de Macks, Z. A., Bunge, S. A., Bell, O. N., Wilbrecht, L., Kriegsfeld, L. J., Kayser, A. S., et al. (2016). Risky decision-making in adolescent girls: the role of pubertal hormones and reward circuitry. *Psychoneuroendocrinology* 74, 77–91. doi: 10.1016/j.psyneuen.2016.08.013

Ordyan, N. E., Pivina, S. G., and Akulova, V. K. (2007). Effects of impaired testosterone metabolism during prenatal ontogenesis on the level of anxiety and behavior of rats in a novel environment. *Neurosci. Behav. Physiol.* 37, 435–441. doi: 10.1007/s11055-007-0032-5

Overk, C. R., Lu, P. Y., Wang, Y. T., Choi, J., Shaw, J. W., Thatcher, G. R., et al. (2012). Effects of aromatase inhibition versus gonadectomy on hippocampal complex amyloid pathology in triple transgenic mice. *Neurobiol. Dis.* 45, 479–487. doi: 10.1016/j.nbd.2011.08.035

Pareto, D., Biegon, A., Alexoff, D., Carter, P., Shea, C., Muench, L., et al. (2013). In vivo imaging of brain aromatase in female baboons: [11C]vorozole kinetics and effect of the menstrual cycle. *Mol. Imaging* 12, 518–524. doi: 10.2310/7290.2013.00068

Phillips, K. A., Ribi, K., and Fisher, R. (2011). Do aromatase inhibitors have adverse effects on cognitive function? *Breast Cancer Res.* 13:203. doi: 10.1186/bcr2806

Pietranera, L., Brocca, M. E., Roig, P., Lima, A., Garcia-Segura, L. M., and De Nicola, A. F. (2015). Estrogens are neuroprotective factors for hypertensive encephalopathy. *J. Steroid Biochem. Mol. Biol.* 146, 15–25. doi: 10.1016/j.jsbmb.2014.04.001

Prange-Kiel, J., Dudzinski, D. A., Prols, F., Glatzel, M., Matschke, J., and Rune, G. M. (2016). Aromatase expression in the hippocampus of AD patients and 5xFAD mice. *Neural Plast.* 2016:9802086. doi: 10.1155/2016/9802086

Rice, D., and Barone, S. Jr. (2000). Critical periods of vulnerability for the developing nervous system: evidence from humans and animal models. *Environ. Health Perspect.* 108(Suppl. 3), 511–533.

Roselli, C. E., Horton, L. E., and Resko, J. A. (1985). Distribution and regulation of aromatase activity in the rat hypothalamus and limbic system. *Endocrinology* 117, 2471–2477. doi: 10.1210/endo-117-6-2471

Roselli, C. E., and Klosterman, S. A. (1998). Sexual differentiation of aromatase activity in the rat brain: effects of perinatal steroid exposure. *Endocrinology* 139, 3193–3201. doi: 10.1210/endo.139.7.6101

Roselli, C. E., Reddy, R. C., Estill, C. T., Scheldrup, M., Meaker, M., Stormshak, F., et al. (2014). Prenatal influence of an androgen agonist and antagonist on the differentiation of the ovine sexually dimorphic nucleus in male and female lamb fetuses. *Endocrinology* 155, 5000–5010. doi: 10.1210/en.2013-2176

Roselli, C. E., and Resko, J. A. (1986). Effects of gonadectomy and androgen treatment on aromatase activity in the fetal monkey brain. *Biol. Reprod.* 35, 106–112. doi: 10.1095/biolreprod35.1.106

Roselli, C. E., Resko, J. A., and Stormshak, F. (2003). Estrogen synthesis in fetal sheep brain: effect of maternal treatment with an aromatase inhibitor. *Biol. Reprod.* 68, 370–374. doi: 10.1095/biolreprod.102.007633

Roselli, C. E., Schrunk, J. M., Stadelman, H. L., Resko, J. A., and Stormshak, F. (2006). The effect of aromatase inhibition on the sexual differentiation of the sheep brain. *Endocrine* 29, 501–511

Roselli, C. E., and Stormshak, F. (2012). Ontogeny of cytochrome p450 aromatase mRNA expression in the developing sheep brain. *J. Neuroendocrinol.* 24, 443–452. doi: 10.1111/j.1365-2826.2011.02260.x

Roselli, C. E., Stormshak, F., and Resko, J. A. (1998). Distribution and regulation of aromatase activity in the ram hypothalamus and amygdala. *Brain Res.* 811, 105–110. doi: 10.1016/S0006-8993(98)00995-0

Roselli, C. E., Liu, M., and Hurn, P. D. (2009). Brain aromatization: classic roles and new perspectives. *Semin. Reprod. Med.* 27, 207–217. doi: 10.1055/s-0029-1216274

Rosenfeld, C. S. (2017). Sex-dependent differences in voluntary physical activity. *J. Neurosci. Res.* 95, 279–290. doi: 10.1002/jnr.23896

Roy, M. M. (1992). Effects of prenatal testosterone and ATD on reproductive behavior in guinea pigs. *Physiol. Behav.* 51, 105–109. doi: 10.1016/0031-9384(92)90210-S

Sasano, H., Takashashi, K., Satoh, F., Nagura, H., and Harada, N. (1998). Aromatase in the human central nervous system. *Clin. Endocrinol.* 48, 325–329. doi: 10.1046/j.1365-2265.1998.00390.x

Schlegel, P. N. (2012). Aromatase inhibitors for male infertility. *Fertil. Steril.* 98, 1359–1362. doi: 10.1016/j.fertnstert.2012.10.023

Selevan, S. G., Kimmel, C. A., and Mendola, P. (2000). Identifying critical windows of exposure for children's health. *Environ. Health Perspect.* 108(Suppl. 3), 451–455.

Stanic, D., Dubois, S., Chua, H. K., Tonge, B., Rinehart, N., Horne, M. K., et al. (2014). Characterization of aromatase expression in the adult male and female mouse brain. I. Coexistence with oestrogen receptors alpha and beta, and androgen receptors. *PLoS One* 9:e90451. doi: 10.1371/journal.pone.0090451

Stoffel-Wagner, B., Watzka, M., Schramm, J., Bidlingmaier, F., and Klingmuller, D. (1999). Expression of CYP19 (aromatase) mRNA in different areas of the human brain. *J. Steroid Biochem. Mol. Biol.* 70, 237–241. doi: 10.1016/S0960-0760(99)00114-4

Szymanski, L., and Bakker, J. (2012). Aromatase knockout mice show normal steroid-induced activation of gonadotrophin-releasing hormone neurones and luteinising hormone surges with a reduced population of kisspeptin neurones in the rostral hypothalamus. *J. Neuroendocrinol.* 24, 1222–1233. doi: 10.1111/j.1365-2826.2012.02334.x

Tabatadze, N., Sato, S. M., and Woolley, C. S. (2014). Quantitative analysis of long-form aromatase mRNA in the male and female rat brain. *PLoS One* 9:e100628. doi: 10.1371/journal.pone.0100628

Tan, R. B., Guay, A. T., and Hellstrom, W. J. (2014). Clinical use of aromatase inhibitors in adult males. *Sex Med. Rev.* 2, 79–90. doi: 10.1002/smrj.23

Toronov, V. Y., Zhang, X., Fabiani, M., Gratton, G., and Webb, A. G. (2005). Signal and image processing techniques for functional near-infrared imaging of the human brain. *Proc. SPIE Int. Soc. Opt. Eng.* 5696, 117–124. doi: 10.1117/12.593345

Vahaba, D. M., and Remage-Healey, L. (2018). Neuroestrogens rapidly shape auditory circuits to support communication learning and perception: evidence from songbirds. *Horm. Behav.* doi: 10.1016/j.yhbeh.2018.03.007 [Epub ahead of print].

van den Buuse, M., Simpson, E. R., and Jones, M. E. (2003). Prepulse inhibition of acoustic startle in aromatase knock-out mice: effects of age and gender. *Genes Brain Behav.* 2, 93–102. doi: 10.1034/j.1601-183X.2003.00014.x

Vierk, R., Glassmeier, G., Zhou, L., Brandt, N., Fester, L., Dudzinski, D., et al. (2012). Aromatase inhibition abolishes LTP generation in female but not in male mice. *J. Neurosci.* 32, 8116–8126. doi: 10.1523/JNEUROSCI.5319-11.2012

Wadhwa, P. D., Buss, C., Entringer, S., and Swanson, J. M. (2009). Developmental origins of health and disease: brief history of the approach and current focus on epigenetic mechanisms. *Semin. Reprod. Med.* 27, 358–368. doi: 10.1055/s-0029-1237424

Weinstock, M. (2007). Gender differences in the effects of prenatal stress on brain development and behaviour. *Neurochem. Res.* 32, 1730–1740. doi: 10.1007/s11064-007-9339-4

Wit, J. M., Hero, M., and Nunez, S. B. (2011). Aromatase inhibitors in pediatrics. *Nat. Rev. Endocrinol.* 8, 135–147. doi: 10.1038/nrendo.2011.161

Wright, C. L., Schwarz, J. S., Dean, S. L., and Mccarthy, M. M. (2010). Cellular mechanisms of estradiol-mediated sexual differentiation of the brain. *Trends Endocrinol. Metab.* 21, 553–561. doi: 10.1016/j.tem.2010.05.004

Xu, P., Cao, X., He, Y., Zhu, L., Yang, Y., Saito, K., et al. (2015). Estrogen receptor-alpha in medial amygdala neurons regulates body weight. *J. Clin. Invest.* 125, 2861–2876. doi: 10.1172/jci80941

Yague, J. G., Munoz, A., De Monasterio-Schrader, P., Defelipe, J., Garcia-Segura, L. M., and Azcoitia, I. (2006). Aromatase expression in the human temporal cortex. *Neuroscience* 138, 389–401. doi: 10.1016/j.neuroscience.2005.11.054

Zhang, Q. G., Wang, R., Tang, H., Dong, Y., Chan, A., Sareddy, G. R., et al. (2014). Brain-derived estrogen exerts anti-inflammatory and neuroprotective actions in the rat hippocampus. *Mol. Cell. Endocrinol.* 389, 84–91. doi: 10.1016/j.mce.2013.12.019

Conflict of Interest Statement: The authors declare that the research was conducted in the absence of any commercial or financial relationships that could be construed as a potential conflict of interest.

frontiers in Molecular Neuroscience

ORIGINAL RESEARCH
published: 30 October 2018
doi: 10.3389/fnmol.2018.00389

TPH2 Deficiency Influences Neuroplastic Mechanisms and Alters the Response to an Acute Stress in a Sex Specific Manner

Paola Brivio[1], *Giulia Sbrini*[1], *Polina Peeva*[2], *Mihail Todiras*[2], *Michael Bader*[2,3], *Natalia Alenina*[2,4] *and Francesca Calabrese*[1]*

[1]Department of Pharmacological and Biomolecular Sciences, University of Milan, Milan, Italy, [2]Cardiovascular and Metabolic Diseases, Max-Delbrück-Center for Molecular Medicine (MDC), Berlin, Germany, [3]Charite-University Medicine, Berlin, Germany, [4]Institute of Translational Biomedicine, St. Petersburg State University, St. Petersburg, Russia

Dysregulations of the central serotoninergic system have been implicated in several psychopathologies, characterized by different susceptibility between males and females. We took advantage of tryptophan hydroxylase 2 (TPH2) deficient rats, lacking serotonin specifically in the brain, to investigate whether a vulnerable genotype can be associated with alterations of neuronal plasticity from the early stage of maturation of the brain until adulthood. We found a significant increase, in both gene and protein expression, of the neurotrophin brain-derived neurotrophic factor (BDNF), in the prefrontal cortex (PFC) of adult TPH2-deficient ($TPH2^{-/-}$) male and female rats in comparison to wild type ($TPH2^{+/+}$) counterparts. Interestingly, a development-specific pattern was observed during early postnatal life: whereas the increase in *Bdnf* expression, mainly driven by the modulation of *Bdnf* isoform IV was clearly visible after weaning at postnatal day (pnd) 30 in both sexes of $TPH2^{-/-}$ in comparison to $TPH2^{+/+}$ rats, at early stages (pnd1 and pnd10) *Bdnf* expression levels did not differ between the genotypes, or even were downregulated in male $TPH2^{-/-}$ animals at pnd10. Moreover, to establish if hyposerotonergia may influence the response to a challenging situation, we exposed adult rats to an acute stress. Although the pattern of corticosterone release was similar between the genotypes, neuronal activation in response to stress, quantified by the expression of the immediate early genes activity regulated cytoskeleton associated protein (*Arc*) and Fos Proto-Oncogene (*cFos*), was blunted in both sexes of animals lacking brain serotonin. Interestingly, although upregulation of *Bdnf* mRNA levels after stress was observed in both genotypes, it was less pronounced in $TPH2^{-/-}$ in comparison to $TPH2^{+/+}$ rats. In summary, our results demonstrated that serotonin deficiency affects neuroplastic mechanisms following a specific temporal pattern and influences the response to an acute stress.

Keywords: serotonin, TPH2, Bdnf, neuroplasticity, stress, immediate early gene

OPEN ACCESS

Edited by:
Jordan Marrocco,
Rockefeller University, United States

Reviewed by:
Mariano Soiza-Reilly,
CONICET Instituto de Fisiología, Biología Molecular y Neurociencias (IFIBYNE), Argentina
Jocelien D. A. Olivier,
University of Groningen, Netherlands
Jean-Pierre Hornung,
Université de Lausanne, Switzerland

***Correspondence:**
Francesca Calabrese
francesca.calabrese@unimi.it

Received: *09 July 2018*
Accepted: *04 October 2018*
Published: *30 October 2018*

Citation:
Brivio P, Sbrini G, Peeva P, Todiras M, Bader M, Alenina N and Calabrese F (2018) TPH2 Deficiency Influences Neuroplastic Mechanisms and Alters the Response to an Acute Stress in a Sex Specific Manner. Front. Mol. Neurosci. 11:389. doi: 10.3389/fnmol.2018.00389

Abbreviations: 5-HT, 5-hydroxytryptamine; *Arc*, activity regulated cytoskeleton associated protein; ANOVA, analysis of variance; BL, baseline; BDNF, brain-derived neurotrophic factor; CNS, central nervous systems; PLSD, Fisher's Protected Least Significant Difference; *cFOS*, Fos Proto-Oncogene; mBDNF, mature BDNF; pnd, postnatal day; PFC, prefrontal cortex; RT-PCR, real-time polymerase chain reaction; SERT, serotonin transporter; SEM, standard error mean; TPH2, tryptophan hydroxylase 2.

INTRODUCTION

Serotonin 5-hydroxytryptamine (5-HT) was originally discovered as cardiovascular hormone but has later gained prominence as neurotransmitter or neuromodulator widely distributed in the central nervous system (CNS) and peripheral nervous systems. Nevertheless, by far the highest amounts of the monoamine are produced in the intestine and released into the blood stream, where it is taken up by platelets which transport it through the circulation and release it at sites of their activation.

5-HT biosynthesis occurs from the essential aminoacid tryptophan in two steps, and tryptophan hydroxylase 2 (TPH2) is the rate-limiting enzyme in this process. As it has been discovered in 2003 (Walther et al., 2003), 5-HT is produced by two different enzymes, TPH1 and TPH2, in the gut and in the brain, respectively. Since in adulthood it cannot pass the blood-brain barrier, these two enzymes define two 5-HT systems with independent regulation and different function. Although in the adult brain 5-HT is produced only by serotonergic neurons in raphe nuclei, during development there are other sources of this monoamine, including maternal 5-HT, that is actively transported through the placental brush border cells via the serotonin transporter (SERT; Cool et al., 1990; Carrasco et al., 2000; Kliman et al., 2018). Moreover, until postnatal day (pnd) 12, the blood-brain barrier is immature (Ribatti et al., 2006) and 5-HT, produced by TPH1 starting at embryonic day 14 in rodents (Côté et al., 2007) can reach the brain. In the early phases of embryonic and postnatal life, 5-HT is a trophic factor that modulates not only cell proliferation, migration and differentiation in the brain and in peripheral tissues (Azmitia, 2001; Buznikov et al., 2001; Gaspar et al., 2003) but also cell survival and synaptogenesis, through its role in the connective organization of the CNS (Gaspar et al., 2003).

Altered 5-HT concentration in the CNS have been implicated in several psychopathologies (H. M., 1994; Brewerton, 1995; Heninger, 1995), characterized by a different susceptibility between males and females such as psychiatric disorders (Breslau et al., 1997; Young and Korszun, 2010), as well as in an altered antidepressant response and tolerance among males and females (Kornstein et al., 2000). Moreover, serotonergic pathways, serotonin synthesis (Nishizawa et al., 1997), the levels of 5-HT metabolites (Gottfries et al., 1974), as well as the expression and activity of different receptors and transporters (Jovanovic et al., 2008) are modulated by sex. In this work we investigate the impact of sex on susceptibility to alterations in the serotonergic system using a new animal model deficient in brain serotonin synthesis, TPH2-deficient ($TPH2^{-/-}$) rats (Kaplan et al., 2016).

Hence, we used male and female $TPH2^{-/-}$ rats to investigate the influence of brain serotonin depletion on neuronal plasticity, in particular on the brain-derived neurotrophic factor (BDNF) from early life until adulthood. Indeed, it is well known that there is a correlation between 5-HT and BDNF (Martinowich and Lu, 2008), the main players in modulation of neurogenesis and neuroplastic mechanisms across lifespan (Homberg et al., 2014). Accordingly, we previously demonstrated that SERT knockout rats showed impaired neuroplasticity starting from the third week of life until adulthood (Calabrese et al., 2013). Moreover, in order to evaluate if hyposerotonergia may alter the response to a challenging condition, we exposed adult $TPH2^{-/-}$ and wild type ($TPH2^{+/+}$) rats to an acute stress focusing on BDNF modulations, since it is known that there is a strong relationship between acute stress response and neuroplasticity (Calabrese et al., 2009) and that 5-HT may be involved in the regulation of *Bdnf* expression during challenges (Foltran and Diaz, 2016). All the molecular analyses were conducted in the prefrontal cortex (PFC), a brain area involved in modulation of mood disorders and strictly connected not only with the neuromodulatory serotonin actions but also with BDNF (Duman and Monteggia, 2006).

MATERIALS AND METHODS

Animals

Animals were kept under standardized conditions with an artificial 12/12-h light/dark cycle (lights on at 6 a.m.), room temperature of 22°C, and approximately 80% humidity with access to food (Ssniff, Soest, Germany) and water *ad libitum*. Male and female TPH2-deficient ($TPH2^{-/-}$) and wild type ($TPH2^{+/+}$) rats on the dark agouti background (Kaplan et al., 2016) were used in the experiments. A cohort of adult (12–14 weeks of age) $TPH2^{+/+}$ and $TPH2^{-/-}$ male and female animals (6–14 animals for each experimental group) was used for the basal measurements. A second cohort of adult male and female $TPH2^{+/+}$ and $TPH2^{-/-}$ rats (4–7 per sex per condition, see below "Stress Procedure" section) was used for the stress experiment. For the developmental analysis male and female rats were sacrificed at pnd 1, 10 and 30 (5–10 animals per age, sex and genotype). All procedures were approved by the ethical committee of the local government (LAGeSo, Berlin, Germany).

Stress Procedure

Adult male and female $TPH2^{+/+}$ and $TPH2^{-/-}$ rats were exposed to acute restraint stress: rats were placed in an air-accessible apparatus for 1 h. The size of the container was similar to the size of the animal, which made the animal almost immobile in it. Half of the stressed animals were sacrificed immediately at the end of the stress session (stress0'), while the other groups were sacrificed 60 min after the end of the stress (stress60'). Unstressed animals served as control group (baseline, BL). Animals were sacrificed by decapitation and trunk blood was collected for the analysis of plasma corticosterone levels.

Brain Tissue Collection

Animals were sacrificed by decapitation and brain regions of interest were rapidly dissected, frozen on dry ice and stored at −80°C for the molecular analyses. Dissections were performed according to the atlas of Paxinos and Watson (1998). In detail, frontal lobe for pnd1-10-30 rats and PF for adult rats were dissected from 2-mm-thick slices (PF defined as Cg1, Cg3 and

IL subregions corresponding to plates 6–9 (approximate weight 8 mg)). The left hemisphere was taken for protein whereas the right was taken for RNA.

RNA Preparation and Gene Expression Analysis by Quantitative Real-Time PCR

Total RNA was isolated by a single step of guanidinium isothiocyanate/phenol extraction using PureZol RNA isolation reagent (Bio-Rad Laboratories, Italy) according to the manufacturer's instructions and quantified by spectrophotometric analysis. Following total RNA extraction, the samples were processed for real-time polymerase chain reaction (RT-PCR) to assess total *Bdnf*, long 3′-UTR *Bdnf* and the exons IV and VI, activity regulated cytoskeleton associated protein (*Arc*) and Fos Proto-Oncogene (*cFOS*) mRNA levels. An aliquot of each sample was treated with DNAse (Life Technologies, Italy) to avoid DNA contamination. RNA was analyzed by TaqMan qRT-PCR instrument (CFX384 real time system, Bio-Rad Laboratories, Italy) using the iScript^{TM} one-step RT-PCR kit for probes (Bio-Rad Laboratories, Italy). Samples were run in 384 well formats in triplicate as multiplexed reactions with a normalizing internal control (36B4). Primers and probes (**Tables 1A, B**) were purchased from Eurofins MWG-Operon (Germany) and Life Technologies (Italy). Thermal cycling was initiated with an incubation at 50°C for 10 min (RNA reverse transcription) and then at 95°C for 5 min (TaqMan polymerase activation). After this initial step, 39 cycles of PCR were performed. Each PCR cycle consisted of heating the samples at 95°C for 10 s to enable the melting process and then for 30 s at 60°C for the annealing and extension reactions. A comparative cycle threshold method was used to calculate the relative target gene expression (Livak and Schmittgen, 2001).

Protein Extraction and Western Blot Analysis

Western blot analysis was used to investigate mature BDNF in the crude synaptosomal fraction. Tissues were manually homogenized using a glass-glass potter in a pH 7.4 cold buffer containing 0.32 M sucrose, 0.1 mM EGTA, 1 mM HEPES solution in the presence of a complete set of protease (Roche) and phosphatase (Sigma-Aldrich) inhibitors. The total homogenate was centrifuged at 2,500 rpm for 10 min at 4°C. The supernatant obtained was further centrifuged at 10,000 *g* for 15 min at 4°C to obtain the pellet corresponding to the crude synaptosomal fraction which was re-suspended in a buffer (20 mM HEPES, 0.1 mM dithiothreitol, 0.1 mM EGTA) with protease and phosphatase inhibitors. Total protein content was measured according to the Bradford Protein Assay procedure (Bio-Rad Laboratories), using bovine serum albumin as a calibration standard. Equal amounts of protein were run under reducing conditions on the criterion TGX precast gels (Bio-Rad Laboratories) and then electrophoretically transferred onto nitrocellulose membranes (Bio-Rad Laboratories). The blots were blocked with 10% nonfat dry milk and then incubated with the primary antibodies (mature BDNF: 1:1,000 (Icosagen), 4° O/N; β-actin 1:10,000 (Sigma), 4°C, O/N). Membranes were then incubated for 1 h at room temperature with the appropriate secondary antibody (mature BDNF: anti-mouse, 1:1,000, RT, 1 h; β-actin: anti-mouse1:10,000). Immunocomplexes were visualized by chemiluminescence using the Western Lightning Clarity ECL (Bio-Rad Laboratories) and the Chemidoc MP imaging system (Bio-Rad Laboratories). BDNF expression was quantified by the evaluation band densities, normalized to the β-actin (ImageLab, Bio-Rad Laboratories).

Analysis of Plasma Corticosterone Levels

Samples of blood from each rat were collected in MiniCollect K3EDTA (Greiner Bio-One GmbH, Frickenhausen, Deutschland) tubes. Plasma was separated by centrifugation for 10 min at 1,300 *g*, 4° and corticosterone was determined by an enzyme-linked immunosorbent assay (ELISA) using a commercial kit (IBL international, Hamburg, Germany) according to the manufacturers' instructions.

Statistical Analyses

All the statistical analyses were conducted by using "IBM SPSS Statistics, version 24." The effects of genotype and sex were analyzed with the two-way analysis of variance (ANOVA) with genotype and sex as independent factors. When appropriate, differences between the individual groups were analyzed by Fisher's protected least significant difference (PLSD). The effects of stress, genotype and sex in the acute stress experiments were analyzed with three-way ANOVA with Fisher's PLSD. Significance for all tests was assumed for $p < 0.05$. Data are presented as means ± standard error mean (SEM). For graphic clarity, all qPCR and western blot results are normalized to male TPH2$^{+/+}$ values that are taken as 100%.

RESULTS

Analysis of *Bdnf* Transcripts and BDNF Protein Levels in the PFC of TPH2$^{-/-}$ Male and Female Adult Rats

We first investigated whether the mRNA expression of total *Bdnf* was modulated by the lack of serotonin, in the PF of both male and female adult rats. As shown in **Figure 1A**, we found a significant effect of the genotype ($F_{(1-52)} = 10.232$, $p < 0.01$) but not of the sex and interaction genotype × sex. *Post hoc* analysis revealed an increase of total *Bdnf* mRNA levels both in TPH2$^{-/-}$ male rats (+23%, $p < 0.05$ vs. TPH2$^{+/+}$) and in TPH2$^{-/-}$ female rats (+25%, $p < 0.05$ vs. TPH2$^{+/+}$). However, no difference was found between the sexes for both genotypes.

To assess if the changes in total *Bdnf* mRNA were paralleled by alterations in BDNF protein, we investigated the levels of the mature form of BDNF (mBDNF) in crude synaptosomal fraction (**Figure 1B**). Two-way ANOVA showed a significant effect of the genotype ($F_{(1-27)} = 17.673$, $p < 0.001$) with no genotype × sex interaction. As revealed by *post hoc* analysis, the levels of mBDNF were significantly increased in both male (+78%, $p < 0.05$ vs. TPH2$^{+/+}$/male) and female (+139%, $p < 0.01$ vs. TPH2$^{+/+}$/female) TPH2$^{-/-}$ rats in comparison to the TPH2$^{+/+}$ counterparts (**Figure 1B**).

TABLE 1A | Sequences of forward and reverse primers and probes used in real-time polymerase chain reaction (RT-PCR) analysis and purchased from Eurofins MWG-Operon (Germany; **A**) and from Life Technologies, which did not disclose the sequences **(B)**.
(A) Forward and reverse primers and probes purchased from Eurofins MWG-Operon (Germany).

Gene	Forward primer	Reverse primer	Probe
Arc	GGTGGGTGGCTCTGAAGAAT	ACTCCACCCAGTTCTTCACC	GATCCAGAACCACATGAATGGG
cFos	TCCTTACGGACTCCCCAC	CTCCGTTTCTCTTCCTCTTCAG	TGCTCTACTTTGCCCCTTCTGCC
Total Bdnf	AAGTCTGCATTACATTCCTCGA	GTTTTCTGGAGGGACAGTTTAT	TGTGGTTTGTTGCCGTTGCCAAG
36b4	TTCCCACTGGCTGAGGT	CGCAGCCGCTGC	AAGGCCTTCCTGGCCGATCCATC

TABLE 1B | (B) Forward and reverse primers and probes purchased from Life Technologies.

Gene	Accession number	Assay ID
Bdnf Long 3'UTR	EF125675	Rn02531967_s1
Bdnf isoform IV	EF125679	Rn01484927_m1
Bdnf isoform VI	EF125680	Rn01484928_m1

Based on the enhancement of total *Bdnf* levels found in TPH2$^{-/-}$ rats, we decided to evaluate if serotonin-deficiency in the CNS differently affects the expression of major *Bdnf* transcripts. In particular, we quantified the expression levels of long 3'UTR *Bdnf* transcripts, and isoforms IV and VI to establish their contribution to the observed modulation in total *Bdnf*.

Bdnf long 3'UTR was significantly modulated by the genotype ($F_{(1-53)} = 4.703$, $p < 0.05$), with an up-regulation of *Bdnf* long 3'UTR mRNA levels specifically in male TPH2$^{-/-}$ in comparison to TPH2$^{+/+}$ rats (+28%, $p < 0.05$ vs. TPH2$^{+/+}$/male). Moreover, the significant effect of the sex ($F_{(1-53)} = 5.884$, $p < 0.05$) reflected the increased expression of *Bdnf* long 3'UTR in female TPH2$^{+/+}$ in comparison to male counterparts (+30%, $p < 0.05$ vs. TPH2$^{+/+}$/male; **Figure 1C**). On the contrary, two-way ANOVA did not show a significant genotype × sex interaction.

Similarly to the results obtained for the total form of the neurotrophin, we observed a significant effect of the genotype ($F_{(1-54)} = 14.017$, $p < 0.05$) for *Bdnf* isoform IV (**Figure 1D**), with no effect of sex and genotype × sex interaction. Accordingly, we found a significant upregulation of *Bdnf* IV expression in TPH2$^{-/-}$ of both sexes (male: +39%, $p < 0.01$ vs. TPH2$^{+/+}$/male; female: +27%, $p < 0.05$ vs. TPH2$^{+/+}$/female).

On the contrary, as shown in **Figure 1E**, we found a significant genotype × sex interaction ($F_{(1-53)} = 4.580$, $p < 0.05$) for *Bdnf* isoform VI. Indeed, *Bdnf* VI increased only in male TPH2$^{-/-}$ rats (+22%, $p < 0.05$ vs. TPH2$^{+/+}$/male).

Analysis of *Bdnf T*ranscripts in the Frontal Lobe of TPH2$^{-/-}$ Male and Female Rats During Postnatal Development

To evaluate the impact of serotonin deficiency during development on *Bdnf* expression, we investigated its mRNA levels in TPH2$^{+/+}$ and TPH2$^{-/-}$ rats at different ages of life, namely pnd 1, 10 and 30 (**Figure 2**).

In male rats, we found a significant effect of the age ($F_{(2-43)} = 107.444$, $p < 0.001$) that is reflected by a significant increase of total *Bdnf* transcripts in both genotypes, at pnd10 compared to pnd1 rats (TPH2$^{+/+}$/pnd10: +1657%, $p < 0.001$ vs. TPH2$^{+/+}$/pnd1; TPH2$^{-/-}$/pnd10: +1467%, $p < 0.01$ vs. TPH2$^{-/-}$/pnd1) but also at pnd30 compared to pnd10 animals (TPH2$^{+/+}$/pnd30: +59%, $p < 0.001$ vs. TPH2$^{+/+}$/pnd10; TPH2$^{-/-}$/pnd30: +240%, $p < 0.001$ vs. TPH2$^{-/-}$/pnd10; **Figure 2A**). Moreover, we found a significant age × genotype interaction ($F_{(2-43)} = 7.115$, $p < 0.01$). Indeed, the developmental profiles of the *Bdnf* expression differed between the genotypes, with an equal expression at pnd1, decreased total *Bdnf* mRNA levels in TPH2$^{-/-}$ at pnd10 (−43%, $p < 0.01$ vs. TPH2$^{+/+}$/pnd10), and a significant increase at pnd30 (+22%, $p < 0.05$ vs. TPH2$^{+/+}$/ pnd30).

Similarly, we observed a significant effect of the age ($F_{(2-45)} = 297.514$, $p < 0.001$) for *Bdnf* long 3'UTR transcripts with an upregulation from pnd10 to pnd30 in both TPH2$^{+/+}$ (TPH2$^{+/+}$/pnd30: +1315%, $p < 0.001$ vs. TPH2$^{+/+}$/pnd10) and TPH2$^{-/-}$ rats (TPH2$^{-/-}$/pnd30: +1355%, $p < 0.001$ vs. TPH2$^{-/-}$/pnd10; **Figure 2B**).

Moreover, we found a significant effect of age ($F_{(2-46)} = 287.421$, $p < 0.001$) for *Bdnf* isoform IV, with an increase in both genotypes from pnd10 to pnd30 (TPH2$^{+/+}$/pnd30: +940%, $p < 0.001$ vs. TPH2$^{+/+}$/pnd10; TPH2$^{-/-}$/pnd30: +1587%, $p < 0.001$ vs. TPH2$^{-/-}$/pnd10). Furthermore, there was a significant effect of the genotype ($F_{(1-46)} = 8.667$, $p < 0.01$) and a significant genotype × age interaction ($F_{(2-46)} = 10.602$, $p < 0.001$) with an upregulation of *Bdnf* isoform IV at pnd30 in TPH2$^{-/-}$ rats (+43%, $p < 0.001$ vs. TPH2$^{+/+}$/pnd30; **Figure 2C**).

Similarly, *Bdnf* isoform VI was significantly modulated by the age ($F_{(2-46)} = 823.232$, $p < 0.001$) with an increase both in TPH2$^{+/+}$ and TPH2$^{-/-}$ from pnd1 to pnd10 (TPH2$^{+/+}$/pnd10: +486, $p < 0.01$ vs. TPH2$^{+/+}$/pnd1; TPH2$^{-/-}$/pnd10: +473, $p < 0.05$ vs. TPH2$^{-/-}$/pnd1) and also from pnd10 to pnd30 (TPH2$^{+/+}$/pnd30: +570%, $p < 0.001$ vs. TPH2$^{+/+}$/pnd10; TPH2$^{-/-}$/pnd30: +1072%, $p < 0.001$ vs. TPH2$^{-/-}$/pnd10). Moreover, we found a significant effect of the genotype ($F_{(1-46)} = 10.912$, $p < 0.01$) and a significant genotype × age interaction ($F_{(2-46)} = 19.039$, $p < 0.001$) with an upregulation of *Bdnf* isoform VI only at pnd30 in TPH2$^{-/-}$ in comparison to TPH2$^{+/+}$ rats of the same age (+30%, $p < 0.001$ vs. TPH2$^{+/+}$/pnd30; **Figure 2D**).

As shown in **Figure 2E**, in female rats, we found a significant effect of the age ($F_{(2-41)} = 105.889$, $p < 0.001$) for total *Bdnf* mRNA levels with a significant increase among the three ages. Actually, we observed an enhancement from pnd1 to pnd10 only in TPH2$^{-/-}$ rats (TPH2$^{-/-}$/pnd10: +1624%, $p < 0.01$ vs. TPH2$^{-/-}$/pnd1), while starting from pnd10, an upregulation of total *Bdnf* mRNA levels was seen in both genotypes (TPH2$^{+/+}$/pnd30: +170%, $p < 0.001$ vs. TPH2$^{+/+}$/pnd10; TPH2$^{-/-}$/pnd30: +241%, $p < 0.001$ vs. TPH2$^{-/-}$/pnd10). Moreover, we found a significant increase of total *Bdnf* in

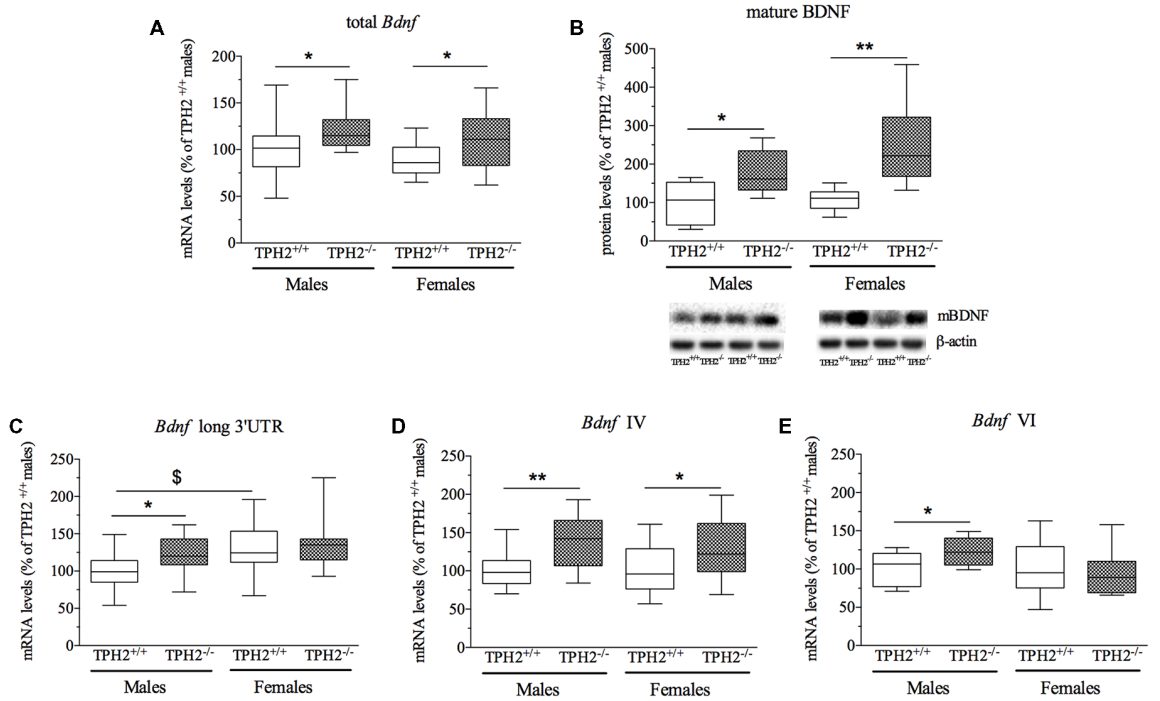

FIGURE 1 | Analysis of brain-derived neurotrophic factor (*Bdnf*) transcripts mRNA levels **(A,C,D,E)** and mature BDNF protein levels **(B)** in the crude synaptosomal fraction of prefrontal cortex (PFC) of tryptophan hydroxylase 2 ($TPH2^{+/+}$) and $TPH2^{-/-}$ adult male and female rats. The data, expressed as % of $TPH2^{+/+}$ male rats, represent the mean ± standard error mean (SEM) of at least 14 independent determinations for the RNA and six for the western blot. $^{*}p < 0.05$, $^{**}p < 0.01$ vs. $TPH2^{+/+}$ of the same sex; $^{\$}p < 0.05$ vs. $TPH2^{+/+}$/male (two-way analysis of variance (ANOVA) with Fisher's protected least significant difference (PLSD).

$TPH2^{-/-}$ rats compared to $TPH2^{+/+}$ (+64%, $p < 0.001$ vs. $TPH2^{+/+}$/ pnd30) only at pnd30, as supported by the significant effect of the genotype ($F_{(1-41)}$ = 8,400, $p < 0.01$) and of the interaction age × genotype ($F_{(2-41)}$ = 9.843, $p < 0.001$).

With respect to *Bdnf* long 3'UTR (**Figure 2F**), we observed a significant effect of the age ($F_{(2-43)}$ = 292.426, $p < 0.001$) with a robust upregulation at pnd30 compared to pnd10 in both $TPH2^{+/+}$ ($TPH2^{+/+}$/pnd30: +1601%, $p < 0.001$ vs. $TPH2^{+/+}$/pnd10) and $TPH2^{-/-}$ ($TPH2^{-/-}$/pnd30: +1210%, $p < 0.001$ vs. $TPH2^{-/-}$/pnd10), but we didn't find any significant interaction of age × genotype.

Similarly, *Bdnf* isoform IV was significantly modulated by the age ($F_{(2-43)}$ = 217.038, $p < 0.001$), but not by the genotype in young female rats. Accordingly, we observed an increase in both genotypes from pnd10 to pnd30 ($TPH2^{+/+}$/pnd30: +1484%, $p < 0.001$ vs. $TPH2^{+/+}$/pnd10; $TPH2^{-/-}$/pnd30: +1676%, $p < 0.001$ vs. $TPH2^{-/-}$/pnd10). Furthermore, the lack of serotonin at pnd30 induced an upregulation of *Bdnf* isoform IV in comparison to $TPH2^{+/+}$/pnd30 (+25%, $p < 0.01$ vs. $TPH2^{+/+}$/pnd30; **Figure 2G**).

In line with what was observed for *Bdnf* long 3'UTR transcripts, *Bdnf* isoform VI was significantly modulated by the age ($F_{(2-42)}$ = 535.298, $p < 0.001$) with the increase, both in $TPH2^{+/+}$ and $TPH2^{-/-}$, from pnd10 to pnd30 ($TPH2^{+/+}$/pnd30: +2105%, $p < 0.001$ vs. $TPH2^{+/+}$/pnd10; $TPH2^{-/-}$/pnd30: +5705%, $p < 0.001$ vs. $TPH2^{-/-}$/pnd10; **Figure 2H**).

Analysis of Stress Responsiveness in $TPH2^{-/-}$ Male and Female Adult Rats

In order to evaluate if the lack of serotonin influences the response to an acute stress challenge, we exposed the animals to 1 h of restraint stress and sacrificed them immediately at the end of the stress session (stress0') or 1 h later (stress60').

In male rats, plasma corticosterone levels were significantly modulated by the acute stress ($F_{(1-27)}$ = 60.729, $p < 0.001$). Indeed, we found a strong increase in corticosterone levels in rats of both genotypes at stress0' time point in comparison to BL conditions (unstressed rats; $TPH2^{+/+}$/stress0': +99%, $p < 0.001$ vs. $TPH2^{+/+}$/BL; $TPH2^{-/-}$/stress0': +98%, $p < 0.001$ vs. $TPH2^{-/-}$/BL), while a significant decrease was observed in the group of rats killed at stress60' time point compared to BL groups of the same genotype ($TPH2^{+/+}$/stress60': −61%, $p < 0.01$ vs. $TPH2^{+/+}$/BL; $TPH2^{-/-}$/stress60': −54%, $p < 0.05$ vs. $TPH2^{-/-}$/BL) as well as to stress0' groups ($TPH2^{+/+}$/stress60': −81%, $p < 0.001$ vs. $TPH2^{+/+}$/stress0'; $TPH2^{-/-}$/stress60': −77%, $p < 0.001$ vs. $TPH2^{-/-}$/stress0'; **Figure 3A**).

As shown in **Figure 3B**, female rats showed high heterogeneity in corticosterone levels at BL and in response to stress. Statistical analysis revealed significant modulation of plasma corticosterone levels by acute stress only in $TPH2^{-/-}$ rats ($F_{(1-42)}$ = 5.239, $p < 0.05$), with an upregulation of corticosterone levels in stress0' group compared to BL (+82%, $p < 0.05$ vs. $TPH2^{-/-}$/BL) and a decrease at stress60' time

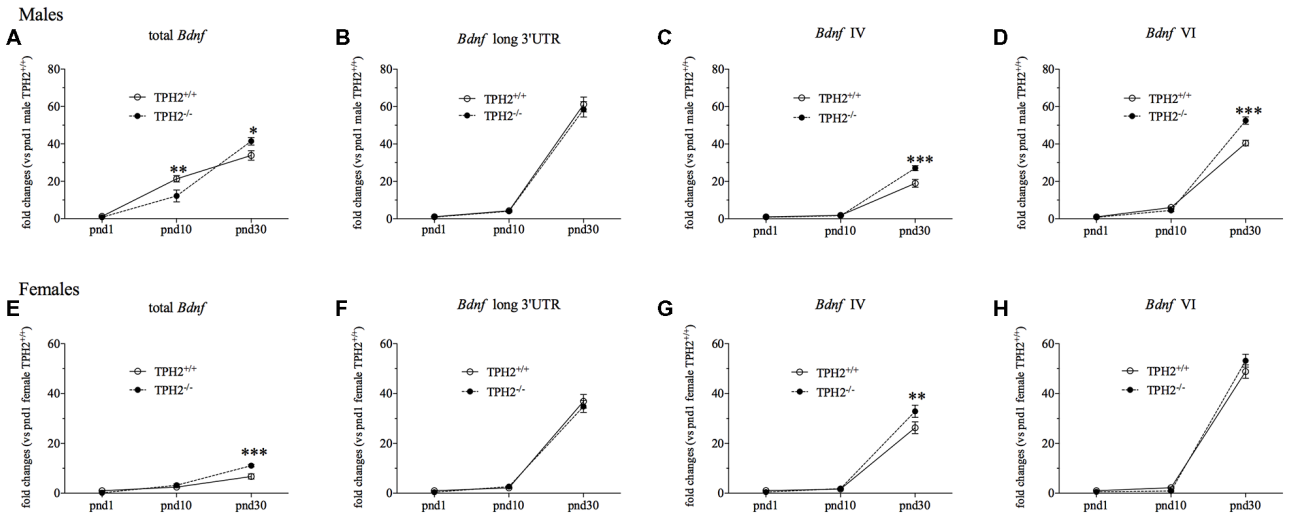

FIGURE 2 | Developmental analysis of total *Bdnf* **(A,E)**, *Bdnf* long 3'UTR **(B,F)**, *Bdnf* isoform IV **(C,G)** and *Bdnf* isoform VI **(D,H)** mRNA levels in TPH2$^{-/-}$ male and female rats at postnatal days (pnd) 1, 10 and 30. The data, expressed as fold change to TPH2$^{+/+}$/pnd1, are the mean ± SEM of at least five independent determinations. $^{*}p < 0.05$, $^{**}p < 0.01$, $^{***}p < 0.001$ vs. TPH2$^{+/+}$ rats/same pnd (two-way ANOVA with Fisher's PLSD).

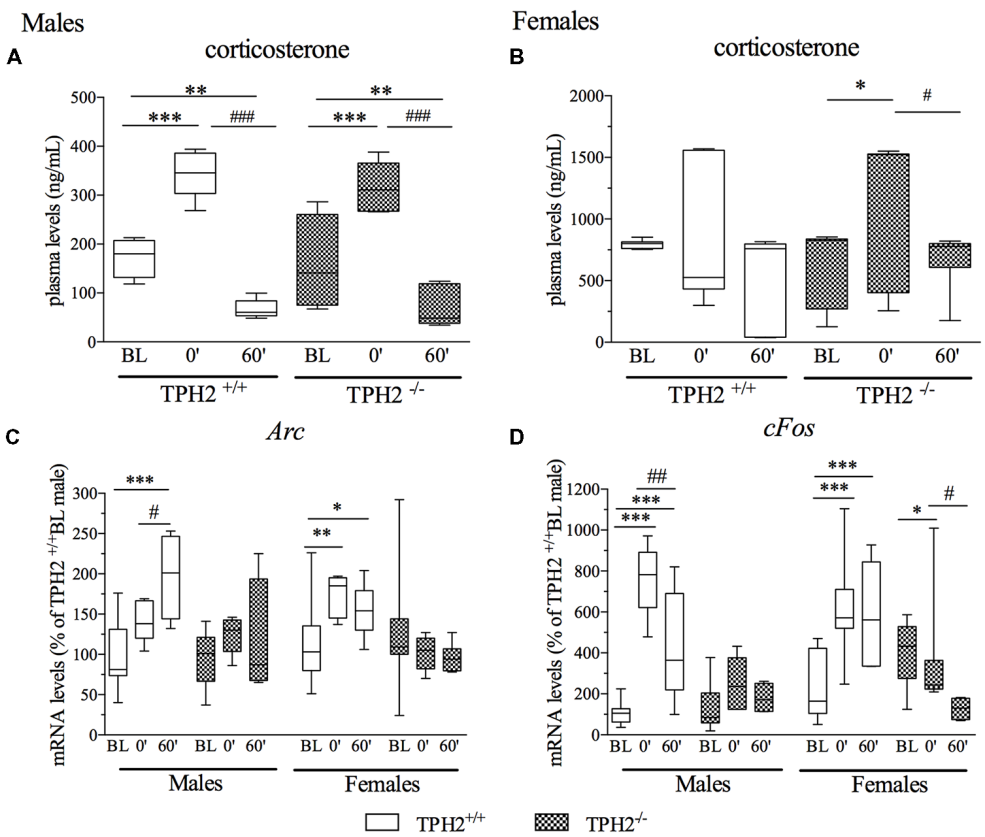

FIGURE 3 | Analysis of corticosterone plasma levels **(A,B)** and activity regulated cytoskeleton associated protein (*Arc*: **C**) and Fos Proto-Oncogene (*cFos*: **D**) mRNA levels in the PFC of TPH2$^{+/+}$ and TPH2$^{-/-}$ adult male and female rats, exposed to an acute restraint stress. The corticosterone data represent the mean ± SEM of at least four independent determinations. Gene expression data are expressed as mean % of TPH2$^{+/+}$/baseline (BL) males ± SEM of at least four independent determinations. $^{*}p < 0.05$, $^{**}p < 0.01$, $^{***}p < 0.001$ vs. BL/same genotype; $^{\#}p < 0.05$, $^{\#\#}p < 0.01$; $^{\#\#\#}p < 0.001$ vs. stress0'/same genotype (two-way ANOVA with Fisher's PLSD panel **A,B**; three-way ANOVA with Fisher's PLSD panel **C,D**).

point with respect to TPH2$^{-/-}$/stress0' (−50%, $p < 0.05$ vs. TPH2$^{-/-}$/stress0').

Analysis of the Immediate Early Genes *Arc* and *cFos* Following Stress

Since we previously demonstrated the implication of the immediate early genes in the response to acute stress (Molteni et al., 2008) and their modulation due to the deletion of the SERT (Molteni et al., 2010), here, we measured two markers of neuronal activation, *Arc* and *cFos*, in order to evaluate if the lack of serotonin in the CNS influenced the response to the restraint stress.

As shown in **Figure 3C**, three-way ANOVA did not reveal a significant genotype × stress × sex interaction ($F_{(2-101)} = 1.668$, $p > 0.05$) on the expression of *Arc*. Nevertheless, we found a significant effect of the stress ($F_{(2-101)} = 5.692$, $p < 0.01$) with a genotype × stress interaction ($F_{(2-101)} = 7.181$, $p < 0.01$). Accordingly, *Arc* mRNA levels were increased by stress exposure only in the TPH2$^{+/+}$ rats of both sexes (TPH2$^{+/+}$/stress60'/male: +97%, $p < 0.001$ vs. TPH2$^{+/+}$/BL/male; TPH2$^{+/+}$/stress60'/male: +38%, $p < 0.05$ vs. TPH2$^{+/+}$/stress0'/male; TPH2$^{+/+}$/stress0'/female: +54%, $p < 0.01$ vs. TPH2$^{+/+}$/BL/female; TPH2$^{+/+}$/stress60'/female: +42%, $p < 0.01$ vs. TPH2$^{+/+}$/BL/female). Interestingly, this stress-mediated upregulation of *Arc* expression was completely blunted in TPH2$^{-/-}$ rats.

Similarly, *cFos* expression was not significantly modulated by genotype × stress × sex interaction ($F_{(2-90)} = 2.170$, $p > 0.05$). However, a significant effect of the stress ($F_{(2-90)} = 20.596$, $p < 0.001$) with a genotype × stress interaction ($F_{(2-90)} = 19.110$, $p < 0.001$) was observed. *Post hoc* analysis revealed a strong increase in *cFos* mRNA levels in TPH2$^{+/+}$ male rats at both time points after stress in comparison to BL (TPH2$^{+/+}$/stress0'/male: +662%, $p < 0.001$ vs. TPH2$^{+/+}$/BL/male; TPH2$^{+/+}$/stress60'/male: +336%, $p < 0.01$ vs. TPH2$^{+/+}$/BL/male). The upregulation of the *cFos* mRNA levels peaked at stress0' was markedly attenuated 1 h later (−43%, $p < 0.01$ vs. TPH2$^{+/+}$/stress0'/male), confirming previously published data (Durchdewald et al., 2009). In female, acute challenge induced an upregulation of *cFos* mRNA levels in the TPH2$^{+/+}$/stress0' rats (+160%, $p < 0.001$ vs. TPH2$^{+/+}$/BL/female) and stress60' group (+145%, $p < 0.01$ vs. TPH2$^{+/+}$/BL/female). This characteristic pattern was again not observed in TPH2$^{-/-}$ female rats; moreover, 1 h after the stress exposure we found a significant downregulation of *cFos* mRNA levels in TPH2$^{-/-}$ rats (TPH2$^{-/-}$/stress60'/female: −67%, $p < 0.01$ vs. TPH2$^{-/-}$/BL/female; TPH2$^{-/-}$/stress60'/female: −65%, $p < 0.01$ vs. TPH2$^{-/-}$/ stress0'/female; **Figure 3D**).

Analysis of *Bdnf* Transcripts Following Stress

The three-way ANOVA revealed no effect of the interaction genotype × stress × sex ($F_{(2-99)} = 1.754$, $p > 0.05$) on total *Bdnf*

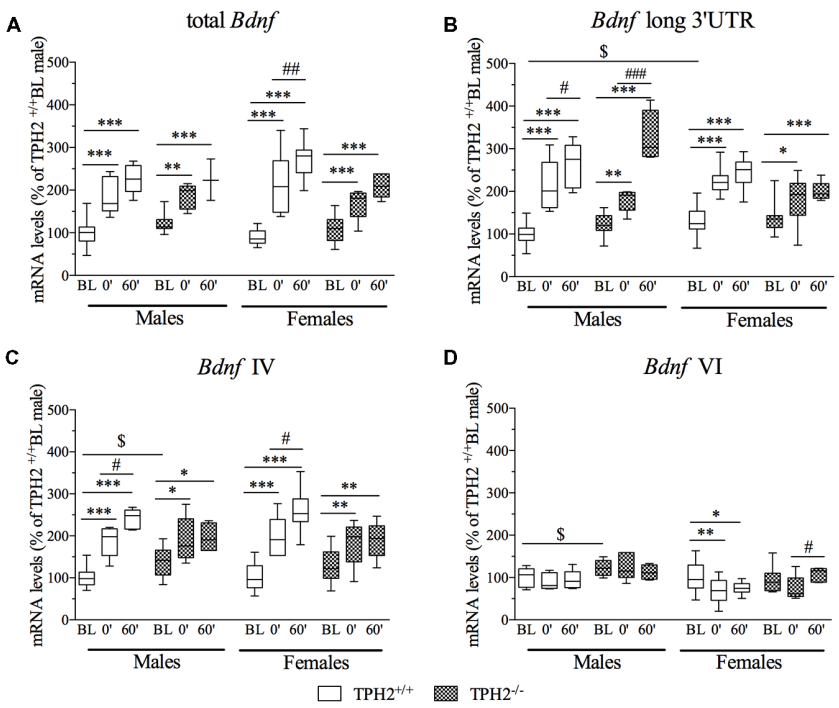

FIGURE 4 | Analysis of total *Bdnf*, **(A)** *Bdnf* long 3'UTR, **(B)** *Bdnf* isoform IV and **(C)** *Bdnf* isoform VI **(D)** mRNA levels in the PFC of TPH2$^{+/+}$ and TPH2$^{-/-}$ adult male and female rats, exposed to an acute restraint stress. The data, expressed as % of TPH2$^{+/+}$/BL males, represent the mean ± SEM of at least four independent determinations. $^{*}p < 0.05$, $^{**}p < 0.01$, $^{***}p < 0.001$ vs. BL/same genotype; $^{\#}p < 0.05$, $^{\#\#}p < 0.01$; $^{\#\#\#}p < 0.001$ vs. stress0'/same genotype, $^{\$}p < 0.05$ vs. TPH2$^{+/+}$ /BL/male (three-way ANOVA with Fisher's PLSD).

gene expression (**Figure 4A**). However, we found a significant effect of stress ($F_{(2-99)}$ = 112.032, $p < 0.001$). Accordingly, total *Bdnf* was increased in both TPH2$^{+/+}$ and TPH2$^{-/-}$ male rats exposed to the acute stress and sacrificed at time point stress0' (TPH2$^{+/+}$/Stress0': +87%, $p < 0.001$ vs. TPH2$^{+/+}$/BL; TPH2$^{-/-}$/Stress0': +51%, $p < 0.01$ vs. TPH2$^{-/-}$/BL) and at time 60' (TPH2$^{+/+}$/stress60': +127%, $p < 0.001$ vs. TPH2$^{+/+}$/BL; TPH2$^{-/-}$/Stress60': +82%, $p < 0.001$ vs. TPH2$^{-/-}$/BL).

In the female rats, the exposure to stress increased the expression of total *Bdnf*, at both time points, in TPH2$^{+/+}$ (TPH2$^{+/+}$/stress0': +146%, $p < 0.001$ vs. TPH2$^{+/+}$/BL; TPH2$^{+/+}$/stress60': +203%, $p < 0.001$ vs. TPH2$^{+/+}$/BL) as well as in TPH2$^{-/-}$ (TPH2$^{-/-}$/stress0': +51%, $p < 0.01$ vs. TPH2$^{-/-}$/BL; TPH2$^{-/-}$/stress60': +88%, $p < 0.001$ vs. TPH2$^{-/-}$/BL). Moreover, TPH2$^{+/+}$stressed rats sacrificed 1 h after the stress exposure had higher mRNA levels compared to the stress0' groups (TPH2$^{+/+}$/stress60': +23%, $p < 0.01$ vs. TPH2$^{+/+}$/stress0').

Furthermore, the significant genotype × stress interaction ($F_{(2-98)}$ = 6.490, $p < 0.01$) indicates that the upregulation found in TPH2$^{+/+}$ was higher than the one observed in TPH2$^{-/-}$ rats.

Bdnf long 3'UTR mRNA levels (**Figure 4B**) were significantly modulated by the interaction genotype × stress × sex ($F_{(2-101)}$ = 3.203, $p < 0.05$). In particular, we found a significant genotype × sex interaction ($F_{(2-101)}$ = 7.205, $p < 0.01$) reflecting an upregulation of *Bdnf* long 3'UTR expression in female TPH2$^{+/+}$/BL compared to the male counterpart (TPH2$^{+/+}$/BL: +30%, $p < 0.05$ vs. TPH2$^{+/+}$/BL). Moreover, the significant effect of stress ($F_{(2-101)}$ = 109.926, $p < 0.001$) indicated that *Bdnf* long 3'UTR was increased after the acute challenge in male (TPH2$^{+/+}$/stress0'/male: +112%, $p < 0.001$ vs. TPH2$^{+/+}$/BL/male; TPH2$^{+/+}$/stress60'/male: +161%, $p < 0.001$ vs. TPH2$^{+/+}$/BL/male; TPH2$^{-/-}$/stress0'/male: +46%, $p < 0.01$ vs. TPH2$^{-/-}$/BL/male; TPH2$^{-/-}$/stress60'/male: +165%, $p < 0.001$ vs. TPH2$^{-/-}$/BL/male) and in female (TPH2$^{+/+}$/stress0'/female: +73%, $p < 0.001$ vs. TPH2$^{+/+}$/BL/female; TPH2$^{+/+}$/stress60'/female: +88%, $p < 0.001$ vs. TPH2$^{+/+}$/BL/female; TPH2$^{-/-}$/stress0'/female: +31%, $p < 0.05$ vs. TPH2$^{-/-}$/BL/female; TPH2$^{-/-}$/stress60'/female: +46%, $p < 0.001$ vs. TPH2$^{-/-}$/BL/female), independently from the genotype.

Moreover, in male rats the up-regulation observed 1 h after the stress exposure was significantly higher than the effect found at time 0' in both genotype (TPH2$^{+/+}$/stress60'/male: +23%, $p < 0.001$ vs. TPH2$^{+/+}$/stress0'/male; TPH2$^{-/-}$/stress60'/male: 81%, $p < 0.001$ vs. TPH2$^{-/-}$/stress0'/male).

Finally, the significant genotype × stress interaction ($F_{(2-101)}$ = 4,368, $p < 0.05$) indicates that the increase in expression of *Bdnf* long 3'UTR due to stress exposure was more robust in TPH2$^{+/+}$ than in TPH2$^{-/-}$ rats.

Analysis of *Bdnf* isoform IV mRNA levels (**Figure 4C**) revealed no effect of the genotype × stress × sex interaction ($F_{(2-101)}$ = 0.094, $p > 0.05$), but a significant effect of stress ($F_{(2-101)}$ = 66.292, $p < 0.001$). In male, *Bdnf* isoform IV expression was upregulated by stress in TPH2$^{+/+}$ rats (TPH2$^{+/+}$/stress0'/male: +88%, $p < 0.001$ vs. TPH2$^{+/+}$/BL/male; TPH2$^{+/+}$/stress60'/male: +141%, $p < 0.001$ vs. TPH2$^{+/+}$/BL/male) with a further increase from stress point 0' to 60' (TPH2$^{+/+}$/stress60'/male: +28%, $p < 0.05$ vs. TPH2$^{+/+}$/stress0'/male) and in TPH2$^{-/-}$ (TPH2$^{-/-}$/stress0'/male: +37%, $p < 0.01$ vs. TPH2$^{-/-}$/BL/male; TPH2$^{-/-}$/stress60"/male: +41%, $p < 0.01$ vs. TPH2$^{-/-}$/BL/male). Moreover, *Bdnf* IV was increased in unstressed TPH2$^{-/-}$ in comparison to TPH2$^{+/+}$ rats (TPH2$^{-/-}$/BL/male: +39%, $p < 0.01$ vs. TPH2$^{+/+}$/BL/male).

In female, exposure to the acute stress increased the *Bdnf* isoform IV mRNA levels in both genotypes (TPH2$^{+/+}$/stress0'/female: +98%, $p < 0.001$ vs. TPH2$^{+/+}$/BL/female; TPH2$^{+/+}$/stress60'/female: +152%, $p < 0.001$ vs. TPH2$^{+/+}$/BL/female; TPH2$^{+/+}$/stress60'/female: +27%, $p < 0.05$ vs. TPH2$^{+/+}$/stress0'/female; TPH2$^{-/-}$/stress0'/female: +39%, $p < 0.05$ vs. TPH2$^{-/-}$/BL/female; TPH2$^{-/-}$/stress60'/female: +46%, $p < 0.01$ vs. TPH2$^{-/-}$/BL/female). Similar to total *Bdnf* and *Bdnf* long 3'UTR, the significant genotype × stress interaction ($F_{(2-101)}$ = 11.065, $p < 0.001$) was also observed for the *Bdnf* isoform IV, suggesting a different response to the challenging situation in the two genotypes in terms of magnitude of the effect.

Similarly, *Bdnf* isoform VI mRNA levels (**Figure 4D**) were not affected by the genotype × stress × sex interaction ($F_{(2-100)}$ = 1.741, $p > 0.05$). However, the significant effect of the genotype ($F_{(2-100)}$ = 10.338, $p < 0.01$) supports the slightly higher mRNA levels found in unstressed male TPH2$^{-/-}$ compared to unstressed TPH2$^{+/+}$ male rats (TPH2$^{-/-}$/BL/male: +22%, $p < 0.05$ vs. TPH2$^{+/+}$/BL/male).

Moreover, in females, isoform VI expression was downregulated specifically in TPH2$^{+/+}$ rats (TPH2$^{+/+}$/stress0'/female: −32%, $p < 0.05$ vs. TPH2$^{+/+}$/BL/female; TPH2$^{+/+}$/stress60'/female: −26%, $p < 0.05$ vs. TPH2$^{+/+}$/BL/female), while its levels were increased in TPH2$^{-/-}$ stressed rats sacrificed 1 h after the stress exposure in comparison to the animals of the same genotype killed immediately after the acute stress (TPH2$^{+/+}$/stress60'/female: +45%, $p < 0.05$ vs. TPH2$^{-/-}$/stress0'/female).

DISCUSSION

The results of the present study highlight that the deletion of *Tph2* profoundly affects neuroplastic mechanisms from the first stage of life until adulthood and influences the response to an acute stress.

We found a significant increase of total *Bdnf* mRNA levels in both adult TPH2$^{-/-}$ male and female rats. Interestingly, the contribution of different *Bdnf* isoforms to this increase is sex-specific: in male TPH2$^{-/-}$ rats, it is due to enhancement of all *Bdnf* transcripts investigated, while in females only the isoform IV is upregulated.

These results are in line with our previous data obtained in a rat model with increased extracellular 5-HT levels, SERT-deficient rats (Molteni et al., 2010; Calabrese et al., 2013). While hyperserotonergia induced by SERT-deletion (Homberg et al., 2007; Olivier et al., 2008) impairs neuronal plasticity in the PFC and hippocampus by downregulation of *Bdnf*, serotonin

depletion in the adult CNS has an opposite effect, confirming the strict dependence of *Bdnf* expression on serotonergic status.

These effects were mirrored, at translational level, by an upregulation of the mature form of BDNF protein levels in the crude synaptosomal fraction in both male and female TPH2$^{-/-}$ rats. The enhancement of the protective form of the neurotrophin, that regulates synaptic connections and plasticity (Martinowich et al., 2007) may be indicative for an increase in the pool of the neurotrophin ready for the release (Poo, 2001; Lau et al., 2010). This suggests a potential compensatory mechanism in the brain to deal with the absence of the trophic contribution of serotonin, confirming data previously obtained in PFC (Kronenberg et al., 2016) and hippocampus (Migliarini et al., 2013) of TPH2-deficient mice.

Furthermore, it's well known that ontogenesis is a critical period for brain adaptability and plasticity. Several lines of evidence support the fundamental role of 5-HT during neurodevelopment (Lauder, 1993; Gaspar et al., 2003) as well as that BDNF is a crucial molecule in promoting CNS growth and in the establishment of neural circuitry including the serotoninergic system (Mamounas et al., 1995). Accordingly, we observed a stepwise increase in *Bdnf* expression from pnd1 to pnd30 in wild type animals as previously demonstrated (Calabrese et al., 2013). Although a similar profile was observed in TPH2$^{-/-}$ rats, the comparison between the two genotypes revealed a significant increase in total *Bdnf* mRNA levels in both male and female TPH2$^{-/-}$ rats at pnd30. In males, this effect was paralleled by an upregulation of *Bdnf* isoform IV and VI, while in females this effect was, again, restricted to the specific effect on the expression of the isoform IV. However, no differences between genotypes at earlier time points (at birth and at pnd10), or even downregulation in *Bdnf* expression levels in TPH2$^{-/-}$ in comparison to TPH2$^{+/+}$ pnd10 male rats were observed, suggesting that peripheral sources may compensate for the lack of central 5-HT synthesis during the early postnatal periods of life. Indeed, the blood brain barrier is not fully functional before pnd12 (Ribatti et al., 2006) and 5-HT from the placenta at embryonic stages (Cool et al., 1990; Carrasco et al., 2000) and from the peripheral blood after birth may easily enter the brain. Accordingly, Vitalis et al. (2007) demonstrated that the embryonic transient 5-HT depletion did not modify cortical BDNF levels until PND21 in pups. In summary, these results suggest that the activation of trophic mechanisms set in motion to compensate the serotonin synthesis deficiency in the CNS became more evident starting from pnd30, when there is no more supply of 5-HT from alternative sources, such as placenta and peripheral blood.

Moreover, the different regulation of *Bdnf* isoforms we found in females in comparison to males may be due to the fact that different transcripts may have different subcellular localization (Chiaruttini et al., 2008) and are controlled by specific intracellular pathways (Aid et al., 2007).

Among these, sex hormones are known to contribute to BDNF modulations (Chan and Ye, 2017), in line with the finding that estrogens can induce *Bdnf* expression by activating their receptors and may modify the neurotrophin activity through methylation of the *Bdnf* promoter IV and V in the hippocampus (Moreno-Piovano et al., 2014). Moreover, sex steroids influence serotonergic neurotransmission (Dalla et al., 2005; Kokras et al., 2009). Indeed, for example it has been demonstrated that androgens facilitate the 5-HT binding to its transporter SERT, while estrogens seem to delay it (Kranz et al., 2015). Due to the limited information available on the functional role of each *Bdnf* transcript, it is not feasible to draw clear-cut conclusions on the consequences exerted by differences in isoform expression between male and female.

Seeing that, in basal condition, 5-HT deficiency was in some way compensated by neuroplastic mechanisms and considering the well-established relationship between the serotonergic system and the stress reactivity (Chen and Miller, 2012; Homberg et al., 2014) we then tested if the lack of central serotonin affects the ability to cope with more dynamic conditions. So, we exposed adult rats to 1 h of restraint stress and we sacrificed them immediately at the end of the stress session or 1 h later. We observed that corticosterone release was differently modulated by stress in wild type males and females and it was affected by lack of 5-HT in a sex specific manner. Indeed, as expected from the literature (Adzic et al., 2009; Molteni et al., 2009) stress exposure induced a strong release of corticosterone immediately after the restraint stress in TPH2$^{+/+}$ male rats and a significant decrease 1 h later, while in females this pattern was not so pronounced and was statistically significant only in TPH2$^{-/-}$, but not in TPH2$^{+/+}$ rats. Corticosterone levels in females are highly influenced by the estrus cycle (Atkinson and Waddell, 1997) and by the stress (Figueiredo et al., 2002). Since females used in our study were not synchronized, high variability in the corticosterone levels in female rats of both genotypes might originate from different estrus cycle stages.

Furthermore, the implication of neuronal activation in response to acute stress can be evaluated by the expression of immediate early genes (Ons et al., 2004; Molteni et al., 2008), in order to assess a different outcome to the acute restraint stress exposure driven by 5-HT deficiency, we measured two markers of neuronal activation, *Arc* and *cFos*. As expected, in both males and female wild type rats we observed a clear stress response, with the slow increase in *Arc* expression during and 1 h after stress and quick upregulation at stress0 and downregulation 1 h later in *cFos* expression, confirming previously published data (Durchdewald et al., 2009). Interestingly in both males and females, the lack of 5-HT in the CNS influenced the response to the challenging condition by preventing the upregulation of both the immediate early genes mRNA levels found in TPH2$^{+/+}$ rats. Seen that Arc mediates the translation between neuronal activation-induced changes into sustained structural and functional modification at synaptic levels (Alberi et al., 2011), the lack of activation observed in TPH2$^{-/-}$ rats may reflect an incorrect translation of the stimulus into a more stable outcome.

Moreover, we have previously shown that hyperserotonergia, evoked by the lack of SERT, has an opposite effect on the stress-induced neuronal activation, leading to a more pronounced upregulation of *Arc* in SERT-deficient rats in comparison to wild types (Molteni et al., 2008). So, these opposite responses

in the neuronal activation of PFC induced by acute stress in hyper- (SERT-deficient) and hyposerotonergic (TPH2-deficient) rats further support an important role of 5-HT in stress response. Accordingly, it was recently shown that the 5-HT_2 receptor antagonist ketanserin also blocks *Arc* induction in the PFC in response to a stress paradigm (Benekareddy et al., 2011). Remarkably, this serotonin effect on neuronal activation seems to be completely independent from the classical stress response via the hypothalamus-pituitary adrenal axis which is hardly affected by the absence of serotonin.

Finally, we found that, despite the increased levels of BDNF observed in $TPH2^{-/-}$, rats, this compensatory mechanism was not enough to restore the normal ability to react to the acute stress challenge, probably because of the complexity of the system and circuit involved that may be BDNF-independent. Even if *Bdnf* transcripts were upregulated in both genotypes in response to stress, the effects found in $TPH2^{+/+}$ were stronger than those induced in the $TPH2^{-/-}$ rats. The fact that BDNF is upregulated by stress in the PFC even in the absence of serotonin, while the immediate early genes are not, suggests distinct stress-modulated neural circuits whereby one is serotonergic, and another is 5-HT independent.

Taken together our findings suggest that 5-HT deficiency in the brain modulates neuroplasticity probably to compensate for the lack of trophic support provided by serotonin starting after weaning until adulthood. Nevertheless, in response to a stressful condition the system is not able to properly respond by setting in motion the strategies to cope with an acute challenge.

AUTHOR CONTRIBUTIONS

FC and NA: conception and study design. PB, PP, MT and GS performed experiments. PB, PP, FC and NA performed data analysis and interpretation of the data. PB drafted and FC, NA and MB critically revised the manuscript. All authors critically reviewed the content and approved the final version for publication.

FUNDING

This work was supported by grants from MIUR Progetto Eccellenza to FC; by the DAAD-MIUR Joint Mobility Program to NA and FC; by German Federal Ministry of Education and Research under the framework of the EU-ERA-NET NEURON project RESPOND to MB and NA; by an RSF Grant 14-50-00069 to NA; and PB was supported by the cycle XXXI of the doctorate in Experimental and Clinical Pharmacological Sciences, Department of Pharmacological and Biomolecular Sciences, Universita' degli Studi di Milano.

REFERENCES

Adzic, M., Djordjevic, A., Demonacos, C., Krstic-Demonacos, M., and Radojcic, M. B. (2009). The role of phosphorylated glucocorticoid receptor in mitochondrial functions and apoptotic signalling in brain tissue of stressed Wistar rats. *Int. J. Biochem. Cell Biol.* 41, 2181–2188. doi: 10.1016/j.biocel.2009.04.001

Aid, T., Kazantseva, A., Piirsoo, M., Palm, K., and Timmusk, T. (2007). Mouse and rat BDNF gene structure and expression revisited. *J. Neurosci. Res.* 85, 525–535. doi: 10.1002/jnr.21139

Alberi, L., Liu, S., Wang, Y., Badie, R., Smith-Hicks, C., Wu, J., et al. (2011). Activity-induced Notch signaling in neurons requires Arc/Arg3.1 and is essential for synaptic plasticity in hippocampal networks. *Neuron* 69, 437–444. doi: 10.1016/j.neuron.2011.01.004

Atkinson, H. C., and Waddell, B. J. (1997). Circadian variation in basal plasma corticosterone and adrenocorticotropin in the rat: sexual dimorphism and changes across the estrous cycle. *Endocrinology* 138, 3842–3848. doi: 10.1210/endo.138.9.5395

Azmitia, E. C. (2001). Modern views on an ancient chemical: serotonin effects on cell proliferation, maturation and apoptosis. *Brain Res. Bull.* 56, 413–424. doi: 10.1016/s0361-9230(01)00614-1

Benekareddy, M., Vadodaria, K. C., Nair, A. R., and Vaidya, V. A. (2011). Postnatal serotonin type 2 receptor blockade prevents the emergence of anxiety behavior, dysregulated stress-induced immediate early gene responses and specific transcriptional changes that arise following early life stress. *Biol. Psychiatry* 70, 1024–1032. doi: 10.1016/j.biopsych.2011.08.005

Breslau, N., Davis, G. C., Andreski, P., Peterson, E. L., and Schultz, L. R. (1997). Sex differences in posttraumatic stress disorder. *Arch. Gen. Psychiatry* 54, 1044–1048. doi: 10.1001/archpsyc.1997.01830230082012

Brewerton, T. D. (1995). Toward a unified theory of serotonin dysregulation in eating and related disorders. *Psychoneuroendocrinology* 20, 561–590. doi: 10.1016/0306-4530(95)00001-5

Buznikov, G. A., Lambert, H. W., and Lauder, J. M. (2001). Serotonin and serotonin-like substances as regulators of early embryogenesis and morphogenesis. *Cell Tissue Res.* 305, 177–186. doi: 10.1007/s004410100408

Calabrese, F., Guidotti, G., Middelman, A., Racagni, G., Homberg, J., and Riva, M. A. (2013). Lack of serotonin transporter alters BDNF expression in the rat brain during early postnatal development. *Mol. Neurobiol.* 48, 244–256. doi: 10.1007/s12035-013-8449-z

Calabrese, F., Molteni, R., Racagni, G., and Riva, M. A. (2009). Neuronal plasticity: a link between stress and mood disorders. *Psychoneuroendocrinology* 34, S208–S216. doi: 10.1016/j.psyneuen.2009.05.014

Carrasco, G., Cruz, M. A., Gallardo, V., Miguel, P., Dominguez, A., and Gonzalez, C. (2000). Transport and metabolism of serotonin in the human placenta from normal and severely pre-eclamptic pregnancies. *Gynecol. Obstet. Invest.* 49, 150–155. doi: 10.1159/000010237

Chan, C. B., and Ye, K. (2017). Sex differences in brain-derived neurotrophic factor signaling and functions. *J. Neurosci. Res.* 95, 328–335. doi: 10.1002/jnr.23863

Chen, G. L., and Miller, G. M. (2012). Advances in tryptophan hydroxylase-2 gene expression regulation: new insights into serotonin-stress interaction and clinical implications. *Am. J. Med. Genet. B Neuropsychiatr. Genet.* 159B, 152–171. doi: 10.1002/ajmg.b.32023

Chiaruttini, C., Sonego, M., Baj, G., Simonato, M., and Tongiorgi, E. (2008). BDNF mRNA splice variants display activity-dependent targeting to distinct hippocampal laminae. *Mol. Cell. Neurosci.* 37, 11–19. doi: 10.1016/j.mcn.2007.08.011

Cool, D. R., Leibach, F. H., and Ganapathy, V. (1990). Modulation of serotonin uptake kinetics by ions and ion gradients in human placental brush-border membrane vesicles. *Biochemistry* 29, 1818–1822. doi: 10.1021/bi00459a022

Côté, F., Fligny, C., Bayard, E., Launay, J. M., Gershon, M. D., Mallet, J., et al. (2007). Maternal serotonin is crucial for murine embryonic development. *Proc. Natl. Acad. Sci. U S A* 104, 329–334. doi: 10.1073/pnas.0606722104

Dalla, C., Antoniou, K., Drossopoulou, G., Xagoraris, M., Kokras, N., Sfikakis, A., et al. (2005). Chronic mild stress impact: are females more vulnerable? *Neuroscience* 135, 703–714. doi: 10.1016/j.neuroscience.2005.06.068

Duman, R. S., and Monteggia, L. M. (2006). A neurotrophic model for stress-related mood disorders. *Biol. Psychiatry* 59, 1116–1127. doi: 10.1016/j.biopsych.2006.02.013

Durchdewald, M., Angel, P., and Hess, J. (2009). The transcription factor Fos: a Janus-type regulator in health and disease. *Histol. Histopathol.* 24, 1451–1461. doi: 10.14670/HH-24.1451

Figueiredo, H. F., Dolgas, C. M., and Herman, J. P. (2002). Stress activation of cortex and hippocampus is modulated by sex and stage of estrus. *Endocrinology* 143, 2534–2540. doi: 10.1210/endo.143.7.8888

Foltran, R. B., and Diaz, S. L. (2016). BDNF isoforms: a round trip ticket between neurogenesis and serotonin? *J. Neurochem.* 138, 204–221. doi: 10.1111/jnc.13658

Gaspar, P., Cases, O., and Maroteaux, L. (2003). The developmental role of serotonin: news from mouse molecular genetics. *Nat. Rev. Neurosci.* 4, 1002–1012. doi: 10.1038/nrn1256

Gottfries, C. G., Roos, B. E., and Winblad, B. (1974). Determination of 5-hydroxytryptamine, 5-hydroxyindoleacetic acid and homovanillic acid in brain tissue from an autopsy material. *Acta Psychiatr. Scand.* 50, 496–507. doi: 10.1111/j.1600-0447.1974.tb09711.x

Heninger, G. R. (1995). "The fourth generation of progress," in *Psychopharmacology*, eds F. E. Williams and D. J. Katz (New York, NY: Raven Press), 471–482.

H. M., V. P. (1994). "Current therapeutics approaches to panic and other anxiety disorders," in *International Academsy for Biomedical and Drug Research*, eds G. Darcourt, J. Mendlewicz, G. Racagni and N. Brunello, 144–150.

Homberg, J. R., Molteni, R., Calabrese, F., and Riva, M. A. (2014). The serotonin-BDNF duo: developmental implications for the vulnerability to psychopathology. *Neurosci. Biobehav. Rev.* 43, 35–47. doi: 10.1016/j.neubiorev.2014.03.012

Homberg, J. R., Olivier, J. D., Smits, B. M., Mul, J. D., Mudde, J., Verheul, M., et al. (2007). Characterization of the serotonin transporter knockout rat: a selective change in the functioning of the serotonergic system. *Neuroscience* 146, 1662–1676. doi: 10.1016/j.neuroscience.2007.03.030

Jovanovic, H., Lundberg, J., Karlsson, P., Cerin, A., Saijo, T., Varrone, A., et al. (2008). Sex differences in the serotonin 1A receptor and serotonin transporter binding in the human brain measured by PET. *Neuroimage* 39, 1408–1419. doi: 10.1016/j.neuroimage.2007.10.016

Kaplan, K., Echert, A. E., Massat, B., Puissant, M. M., Palygin, O., Geurts, A. M., et al. (2016). Chronic central serotonin depletion attenuates ventilation and body temperature in young but not adult Tph2 knockout rats. *J. Appl. Physiol.* 120, 1070–1081. doi: 10.1152/japplphysiol.01015.2015

Kliman, H. J., Quaratella, S. B., Setaro, A. C., Siegman, E. C., Subha, Z. T., Tal, R., et al. (2018). Pathway of maternal serotonin to the human embryo and fetus. *Endocrinology* 159, 1609–1629. doi: 10.1210/en.2017-03025

Kokras, N., Antoniou, K., Dalla, C., Bekris, S., Xagoraris, M., Ovestreet, D. H., et al. (2009). Sex-related differential response to clomipramine treatment in a rat model of depression. *J. Psychopharmacol.* 23, 945–956. doi: 10.1177/0269881108095914

Kornstein, S. G., Schatzberg, A. F., Thase, M. E., Yonkers, K. A., McCullough, J. P., Keitner, G. I., et al. (2000). Gender differences in treatment response to sertraline versus imipramine in chronic depression. *Am. J. Psychiatry* 157, 1445–1452. doi: 10.1176/appi.ajp.157.9.1445

Kranz, G. S., Wadsak, W., Kaufmann, U., Savli, M., Baldinger, P., Gryglewski, G., et al. (2015). High-dose testosterone treatment increases serotonin transporter binding in transgender people. *Biol. Psychiatry* 78, 525–533. doi: 10.1016/j.biopsych.2014.09.010

Kronenberg, G., Mosienko, V., Gertz, K., Alenina, N., Hellweg, R., and Klempin, F. (2016). Increased brain-derived neurotrophic factor (BDNF) protein concentrations in mice lacking brain serotonin. *Eur. Arch. Psychiatry Clin. Neurosci.* 266, 281–284. doi: 10.1007/s00406-015-0611-3

Lau, A. G., Irier, H. A., Gu, J., Tian, D., Ku, L., Liu, G., et al. (2010). Distinct 3′UTRs differentially regulate activity-dependent translation of brain-derived neurotrophic factor (BDNF). *Proc. Natl. Acad. Sci. U S A* 107, 15945–15950. doi: 10.1073/pnas.1002929107

Lauder, J. M. (1993). Neurotransmitters as growth regulatory signals: role of receptors and second messengers. *Trends Neurosci.* 16, 233–240. doi: 10.1016/0166-2236(93)90162-f

Livak, K. J., and Schmittgen, T. D. (2001). Analysis of relative gene expression data using real-time quantitative PCR and the $2^{-\Delta\Delta CT}$ method. *Methods* 25, 402–408. doi: 10.1006/meth.2001.1262

Mamounas, L. A., Blue, M. E., Siuciak, J. A., and Altar, C. A. (1995). Brain-derived neurotrophic factor promotes the survival and sprouting of serotonergic axons in rat brain. *J. Neurosci.* 15, 7929–7939. doi: 10.1523/jneurosci.15-12-07929.1995

Martinowich, K., and Lu, B. (2008). Interaction between BDNF and serotonin: role in mood disorders. *Neuropsychopharmacology* 33, 73–83. doi: 10.1038/sj.npp.1301571

Martinowich, K., Manji, H., and Lu, B. (2007). New insights into BDNF function in depression and anxiety. *Nat. Neurosci.* 10, 1089–1093. doi: 10.1038/nn1971

Migliarini, S., Pacini, G., Pelosi, B., Lunardi, G., and Pasqualetti, M. (2013). Lack of brain serotonin affects postnatal development and serotonergic neuronal circuitry formation. *Mol. Psychiatry* 18, 1106–1118. doi: 10.1038/mp.2012.128

Molteni, R., Calabrese, F., Cattaneo, A., Mancini, M., Gennarelli, M., Racagni, G., et al. (2009). Acute stress responsiveness of the neurotrophin BDNF in the rat hippocampus is modulated by chronic treatment with the antidepressant duloxetine. *Neuropsychopharmacology* 34, 1523–1532. doi: 10.1038/npp.2008.208

Molteni, R., Calabrese, F., Mancini, M., Racagni, G., and Riva, M. A. (2008). Basal and stress-induced modulation of activity-regulated cytoskeletal associated protein (Arc) in the rat brain following duloxetine treatment. *Psychopharmacology Berl.* 201, 285–292. doi: 10.1007/s00213-008-1276-7

Molteni, R., Cattaneo, A., Calabrese, F., Macchi, F., Olivier, J. D., Racagni, G., et al. (2010). Reduced function of the serotonin transporter is associated with decreased expression of BDNF in rodents as well as in humans. *Neurobiol. Dis.* 37, 747–755. doi: 10.1016/j.nbd.2009.12.014

Moreno-Piovano, G. S., Varayoud, J., Luque, E. H., and Ramos, J. G. (2014). Long-term ovariectomy increases BDNF gene methylation status in mouse hippocampus. *J. Steroid Biochem. Mol. Biol.* 144, 243–252. doi: 10.1016/j.jsbmb.2014.08.001

Nishizawa, S., Benkelfat, C., Young, S. N., Leyton, M., Mzengeza, S., de Montigny, C., et al. (1997). Differences between males and females in rates of serotonin synthesis in human brain. *Proc. Natl. Acad. Sci. U S A* 94, 5308–5313. doi: 10.1073/pnas.94.10.5308

Olivier, J. D., Van Der Hart, M. G., Van Swelm, R. P., Dederen, P. J., Homberg, J. R., Cremers, T., et al. (2008). A study in male and female 5-HT transporter knockout rats: an animal model for anxiety and depression disorders. *Neuroscience* 152, 573–584. doi: 10.1016/j.neuroscience.2007.12.032

Ons, S., Marti, O., and Armario, A. (2004). Stress-induced activation of the immediate early gene Arc (activity-regulated cytoskeleton-associated protein) is restricted to telencephalic areas in the rat brain: relationship to c-fos mRNA. *J. Neurochem.* 89, 1111–1118. doi: 10.1111/j.1471-4159.2004.02396.x

Paxinos, G., and Watson, C. (1998). *The Rat Brain in Stereotaxic Coordinates*. San Diego: Academic Press.

Poo, M. M. (2001). Neurotrophins as synaptic modulators. *Nat. Rev. Neurosci.* 2, 24–32. doi: 10.1038/35049004

Ribatti, D., Nico, B., Crivellato, E., and Artico, M. (2006). Development of the blood-brain barrier: a historical point of view. *Anat. Rec. B New Anat.* 289, 3–8. doi: 10.1002/ar.b.20087

Vitalis, T., Cases, O., Passemard, S., Callebert, J., and Parnavelas, J. G. (2007). Embryonic depletion of serotonin affects cortical development. *Eur. J. Neurosci.* 26, 331–344. doi: 10.1111/j.1460-9568.2007.05661.x

Walther, D. J., Peter, J. U., Bashammakh, S., Hötnagl, H., Voits, M., Fink, H., et al. (2003). Synthesis of serotonin by a second tryptophan hydroxylase isoform. *Science* 299:76. doi: 10.1126/science.1078197

Young, E., and Korszun, A. (2010). Sex, trauma, stress hormones and depression. *Mol. Psychiatry* 15, 23–28. doi: 10.1038/mp.2009.94

Conflict of Interest Statement: The authors declare that the research was conducted in the absence of any commercial or financial relationships that could be construed as a potential conflict of interest.

frontiers in Molecular Neuroscience

ORIGINAL RESEARCH
published: 17 December 2018
doi: 10.3389/fnmol.2018.00460

Geostatistical Analysis of White Matter Lesions in Multiple Sclerosis Identifies Gender Differences in Lesion Evolution

Robert Marschallinger[1,2], Mark Mühlau[3,4], Viola Pongratz[3,4], Jan S. Kirschke[4,5], Simon Marschallinger[6], Paul Schmidt[3,4] and Johann Sellner[2,3]*

[1] Geoinformatics Z_GIS, University of Salzburg, Salzburg, Austria, [2] Department of Neurology, Christian Doppler Medical Center, Paracelsus Medical University, Salzburg, Austria, [3] Department of Neurology, Klinikum Rechts der Isar, Technische Universität München, Munich, Germany, [4] TUM Neuroimaging Center, Klinikum Rechts der Isar, Technische Universität München, Munich, Germany, [5] Institute of Neuroradiology, Klinikum Rechts der Isar, Technische Universität München, Munich, Germany, [6] Fachhochschule für Gesundheitsberufe Oberösterreich GmbH, Linz, Austria

Multiple sclerosis (MS) is a chronic inflammatory demyelinating disease of the central nervous system with presumed autoimmune origin. The development of lesions within the gray matter and white matter, which are highly variable with respect to number, total volume, morphology and spatial evolution and which only show a limited correlation with clinical disability, is a hallmark of the disease. Population-based studies indicate a distinct outcome depending on gender. Here, we studied gender-related differences in the evolution of white matter MS-lesions (MS-WML) in early MS by using geostatistical methods. Within a 3 years observation period, a female and a male MS patient group received disease modifying drugs and underwent standardized annual brain magnetic resonance imaging, accompanied by neurological examination. MS-WML were automatically extracted and the derived binary lesion masks were subject to geostatistical analysis, yielding quantitative spatial-statistics metrics on MS-WML pattern morphology and total lesion volume (TLV). Through the MS-lesion pattern discrimination plot, the following differences were disclosed: corresponding to gender and MS-WML pattern morphology at baseline, two female subgroups (F1, F2) and two male subgroups (M1, M2) are discerned that follow a distinct MS-WML pattern evolution in space and time. F1 and M1 start with medium-level MS-WML pattern smoothness and TLV, both behave longitudinally quasi-static. By contrast, F2 and M2 start with high-level MS-WML pattern smoothness and medium-level TLV. F2 and M2 longitudinal development is characterized by strongly diminishing MS-WML pattern smoothness and TLV, i.e., continued shrinking and break-up of MS-WML. As compared to the male subgroup M2, the female subgroup F2 shows continued, increased MS-WML pattern smoothness and TLV. Data from neurological examination suggest a correlation of MS-WML pattern morphology metrics and EDSS. Our results justify detailed studies on gender-related differences.

Keywords: multiple sclerosis, geostatistics, 4D analysis, lesion segmentation, white matter lesion evolution, gender differences, time series analysis

OPEN ACCESS

Edited by:
Laura Musazzi,
University of Milan, Italy

Reviewed by:
David F. Tate,
University of Missouri-St. Louis, United States
Svenja Caspers,
Heinrich-Heine-Universität Düsseldorf, Germany

****Correspondence:***
Robert Marschallinger
robert.marschallinger@sbg.ac.at

Received: *02 July 2018*
Accepted: *28 November 2018*
Published: *17 December 2018*

Citation:
Marschallinger R, Mühlau M, Pongratz V, Kirschke JS, Marschallinger S, Schmidt P and Sellner J (2018) Geostatistical Analysis of White Matter Lesions in Multiple Sclerosis Identifies Gender Differences in Lesion Evolution. Front. Mol. Neurosci. 11:460. doi: 10.3389/fnmol.2018.00460

INTRODUCTION

Multiple sclerosis (MS) is an inflammatory and neurodegenerative autoimmune disease of the central nervous system (CNS), characterized by demyelination and axonal degeneration. Magnetic resonance imaging (MRI) plays a central role in the diagnosis and management of patients with MS: focal hyperintense lesions seen on T2 and FLAIR MRI sequences throughout the CNS are key features of the disorder. MRI is the key tool to assess dissemination in space (DIS) and dissemination in time (DIT) (Thompson et al., 2018). Moreover, MRI is used to monitor disease activity and to evaluate therapeutic responses. Yet, changes in T2 lesion volume are poor predictors of subsequent disease evolution in many cases, a situation often referred to as the "clinicoradiological paradox" (Louapre, 2018). The heterogeneity of the disease may also be impacted by gender differences: while the incidence of MS is consistently greater in females, men have been reported to develop a more severe disease phenotype characterized by a worse clinical outcome and faster accumulation of disability (Tomassini and Pozzilli, 2009; Shirani et al., 2012). Gender, however, does not influence relapse and burden of brain lesions (Dolezal et al., 2013; Harbo et al., 2013; Kalincik et al., 2013). In this regard, Schoonheim (2014) studied gender differences in brain MRI using diffusion tensor imaging, which enables the evaluation of white matter (WM) tracts. They found that WM of male patients was both more extensively and also more severely affected compared to female patients. A combined usage of novel imaging techniques and spatial-statistics models may provide further insights to the pathophysiological background of gender differences in disease course and lesion evolution. Based on geostatistical metrics (Marschallinger et al., 2016), we established a methodology to study MS-WML pattern characteristics including lesion pattern morphology. Here, we tested our geostatistical methodology in a longitudinal group consisting of men and women in order to evaluate gender-related changes and differences in MS-WML evolution.

MATERIALS AND METHODS

Patient Groups

To study the spatiotemporal evolution of MS-WML patterns, we evaluated two groups of early-stage MS patients: groups consist of women ("F": n = 53) and men ("M": n = 36), respectively. The association of WML with MS was checked by an experienced neuroradiologist. During the 3-year study period, F and M group members received disease modifying drug (DMD) and underwent four MRI investigations (MRI1, MRI2, MRI3, MRI4) under standardized conditions: identical 3T MRI scanner, identical protocols (see below) and 1 year time interval between each MRI1-MRI2-MRI3-MRI4. Additional criteria for F and M group inclusion were: time from first reported MS symptoms to MRI1 less than 2 years and time from MS-diagnosis to MRI1 less than 1 year. Members of both groups were checked for EDSS at all times of MRI scans and for disease course at MRI1, MRI2, and MRI4. Two-sample t-test and Fisher F-test indicate equal means and variances ($\alpha = 0.05$) of groups F and M; we therefore assume an identical age structure of both groups. **Table 1** summarizes group ages, MRI investigation intervals and the development of clinical status in the time interval from MRI1 to MRI4. Average investigation interval in both groups was about 1 year $\pm$ 1 month. Average EDSS for groups F and M increased slightly. Both groups started with a mix of clinically isolated syndrome (CIS) and relapsing-remitting MS (RRMS). As indicated by **Table 1**, both groups were affected by marked shifts in disease type, from CIS to RRMS.

MRI Protocols

All subjects underwent MRI scanning at the identical 3T scanner (Philips Achieva) using identical protocols. A 3D gradient echo T1w sequence was acquired using magnetization-prepared 180 degrees radiofrequency pulses and rapid gradient-echo sampling with a spatial resolution of 1.0 mm $\times$ 1.0 mm $\times$ 1.0 mm, a repetition time (TR) of 9 ms, and an echo time (TE) of 4 ms. For the segmentation of MS-WML, also a 3D FLAIR sequence was acquired with a spatial resolution of 1.0 mm $\times$ 1.0 mm $\times$ 1.5 mm, a TR of 10^4 ms, a TE of 140 ms, and a time to inversion of 2750 ms (Righart et al., 2017).

Software

Lesions were segmented with the lesion growth algorithm (LGA, Schmidt et al., 2012) as implemented in the LST toolbox for SPM. The algorithm first segments the T1 images into the three main tissue classes cerebrospinal fluid (CSF), gray matter (GM) and WM. This information is then combined with the coregistered FLAIR intensities in order to calculate lesion belief maps. By thresholding these maps with a pre-chosen initial threshold (kappa), an initial binary lesion map is obtained which is subsequently grown along voxels that appear hyperintense in the FLAIR image. The result is a lesion probability map in MNI-space that can be thresholded to derive a MS-WML mask (MS-lesion voxels = 1, other voxels = 0). Data were acquired with the identical MRI scanner that was used for LGA development in 2012 and protocols also were exactly the same. Hence we worked with a kappa of 0.3, originally determined in 2012 by matching LST segmentation with expert manual segmentation. Empirical variograms of MS-WML masks were calculated with GSLIB (Deutsch and Journel, 1997). Variogram model fitting and longitudinal analysis were performed with R[1], statistics on group age structures and results of variography and Gaussian Mixture Models were done with XLSTAT[2]. Voxler was used for MS-WML pattern visualization, 2D graphics were created with R and Grapher (Golden Software[3]).

Lesion Discrimination Plot (LDP, for Detailed Methodology See Marschallinger et al., 2016)

MS-WML pattern morphology was quantified by means of geostatistical variography. Geostatistics is a collection of algorithms for the analysis, modeling, and simulation of

[1]https://cran.r-project.org

[2]https://www.xlstat.com

[3]http://www.goldensoftware.com

TABLE 1 | Descriptive statistics of ages, MRI acquisition intervals and clinical parameters of groups F and M.

	n	Age(y)		Lag(d)		EDSS1		EDSS4		DType1(%)		DType4(%)	
		avg	std	avg	std	avg	std	avg	std	CIS	RRMS	CIS	RRMS
F	53	33,3	9,0	369	32	1,3	1,0	1,4	1,4	58	42	6	94
M	36	35,1	9,7	365	31	1,2	1,2	1,3	1,3	50	50	14	86

n: number of group members. Age(y): average (avg) and standard deviation (std) of group ages, years. Lag(d): average and standard deviation between MRI1-MRI2, MRI2-MRI3, MRI3-MRI4, days. EDSS1, EDSS4: group average and standard deviation of EDSS at MRI1 and MRI4. DType1, DType4: disease course of group members at MRI1 and MRI4, per cent.

multidimensional data in a variety of disciplines (Caers, 2010). Variography is the central explorative data analysis (EDA) tool of geostatistics for measuring spatial correlation (Gringarten and Deutsch, 1999). The empirical variogram is calculated as follows (Eq. 1):

$$\gamma(h) = \frac{1}{2n(h)} \cdot \sum_{i=1}^{n} (z(x_i) - z(x_i + h))^2 \quad (1)$$

Eq. 1: z(x) value of variable z at some 3D location x, here: voxel with z = binary variable (1 or 0); h lag vector of 3D separation between two relevant voxels (units: mm); n(h) number of voxel pairs [z(x), z(x+h)] at lag h; γ(h) empirical variogram value for lag h.

Computing, for a binary MS-WML pattern (i.e., a MS-WML mask with lesion voxels = 1, other voxels = 0), empirical variograms in x (left–right), y (posterior–anterior), and z (inferior–superior) directions, important aspects of the MS-WML pattern's morphology are sensitively captured in terms of 3D correlation. Then, fitting a variogram model function (Cressie, 1993) to each of the x,y,z directional empirical variograms, the 3D morphology of the MS-WML pattern can be expressed by just two parameters per direction (x,y,z): the variogram range $\boldsymbol{a}$ and the variogram sill $\boldsymbol{c}$, i.e., $\boldsymbol{a}_x$, $\boldsymbol{a}_y$, $\boldsymbol{a}_z$ and $\boldsymbol{c}_x$, $\boldsymbol{c}_y$, $\boldsymbol{c}_z$. The exponential variogram model function (Eq. 2) was found suitable for modeling variograms of binary MS-WML patterns (Marschallinger et al., 2014).

$$\gamma(h) = c \cdot \left(1 - \frac{e(-3 \cdot |h|)}{a}\right) \quad (2)$$

Eq. 2: c sill; a range; h lag vector of separation; γ(h) model variogram value for lag h.

Variogram model function fitting was performed with R, yielding high-quality matching results with r^2 typically 0.98. In consequence, derived parameters $\boldsymbol{a}$ and $\boldsymbol{c}$ are considered robust and significant. The variogram measures spatial correlation, which for binary patterns expresses spatial continuity. For 3D patterns, a high value of spatial correlation can be interpreted as surface smoothness while low spatial correlation points to surface complexness (Kourgli et al., 2004; Trevisani et al., 2009). The surface complexness of biological structures (like MS-WML patterns) is conveniently expressed as the ratio of surface area to enclosed volume (Schmidt-Nielson, 1984). For a binary MS-WML pattern, the variogram model range $\boldsymbol{a}$ is proxy of MS-WML pattern surface smoothness and the variogram model sill $\boldsymbol{c}$ is substitute of total lesion volume (TLV) (Marschallinger et al., 2016): the higher $\boldsymbol{a}$, the higher is the overall spatial correlation and the smoother (i.e., less geometrically complex) is the MS-WML pattern's surface; the higher $\boldsymbol{c}$, the higher is TLV. Compare **Figure 1A** for examples – pattern 518 is "complex," pattern 238 is "smooth." The MS-Lesion Discrimination Plot (LDP) aims at mapping above 3D variography data to a dimension-reduced, well-arranged 2D space spanned by $\boldsymbol{A}$ on the abscissa, and $\boldsymbol{C}$ on the ordinate. For clarity of the LDP plot, each MS-WML pattern is displayed as a single point with $\boldsymbol{A}$ = avg(ln($\boldsymbol{a}_x$), ln($\boldsymbol{a}_y$), ln($\boldsymbol{a}_z$)) and $\boldsymbol{C}$ = avg(ln($\boldsymbol{c}_x$), ln($\boldsymbol{c}_y$), ln($\boldsymbol{c}_z$)). The advantage of logarithmic scaling is that MS-WML patterns with both mild and severe lesion load can be mapped in a single space (see **Figures 1A**, **2**). When working with MS-WML patterns that are normalized to MNI space – recall that LGA results are already in MNI space – relative positions in the LDP can be interpreted in terms of DIS. Working with longitudinal data in MNI space, the LDP framework also enables straightforward graphical representation of MS-WML pattern evolution (DIT) in the individual MS disease course. This facilitates EDA of DIS and DIT, in single patient follow-up and intra- or inter-group data (Marschallinger et al., 2009, 2014).

RESULTS

As an example for practical LDP application, follow-up MRI data of two male patients (labeled "Patient1" and "Patient2," both from group M) are contrasted in **Figures 1A,B** and in **Table 2**. **Figure 1A** shows axial projections of the MS-WML patterns derived from four successive MRIs (MRI1, MRI2, MRI3, MRI4) for Patient1 (patterns 518–521; 518 is an example of "complex pattern") and Patient2 (patterns 238–241; 238 is an example of "smooth pattern"). **Figure 1B** gives the corresponding positions in the LDP; positions were connected by vectors to highlight patient-specific MS-WML pattern evolution paths. Since time lags between MRI exams are equal (1 year), the LDP also suggests dynamics of pattern geometry change – with long vectors signaling rapid change (due to logarithmic scaling of the LDP, visual matching of vector lengths and of evolution path directions is semi-quantitative only, however). **Table 2** indicates that both patients start with similar TLV (at MRI1, Patient1: 4.90 cm^3, Patient2: 4.05 cm^3). In **Figure 1A**, MRI1 of Patient1 shows many scattered small- to medium-sized lesions while Patient2 has much of TLV accumulated in one big lesion. Progressing from MRI1 to MRI4, Patient1 shows steadily increasing TLV as well as increasing MS-WML pattern smoothness, which is due

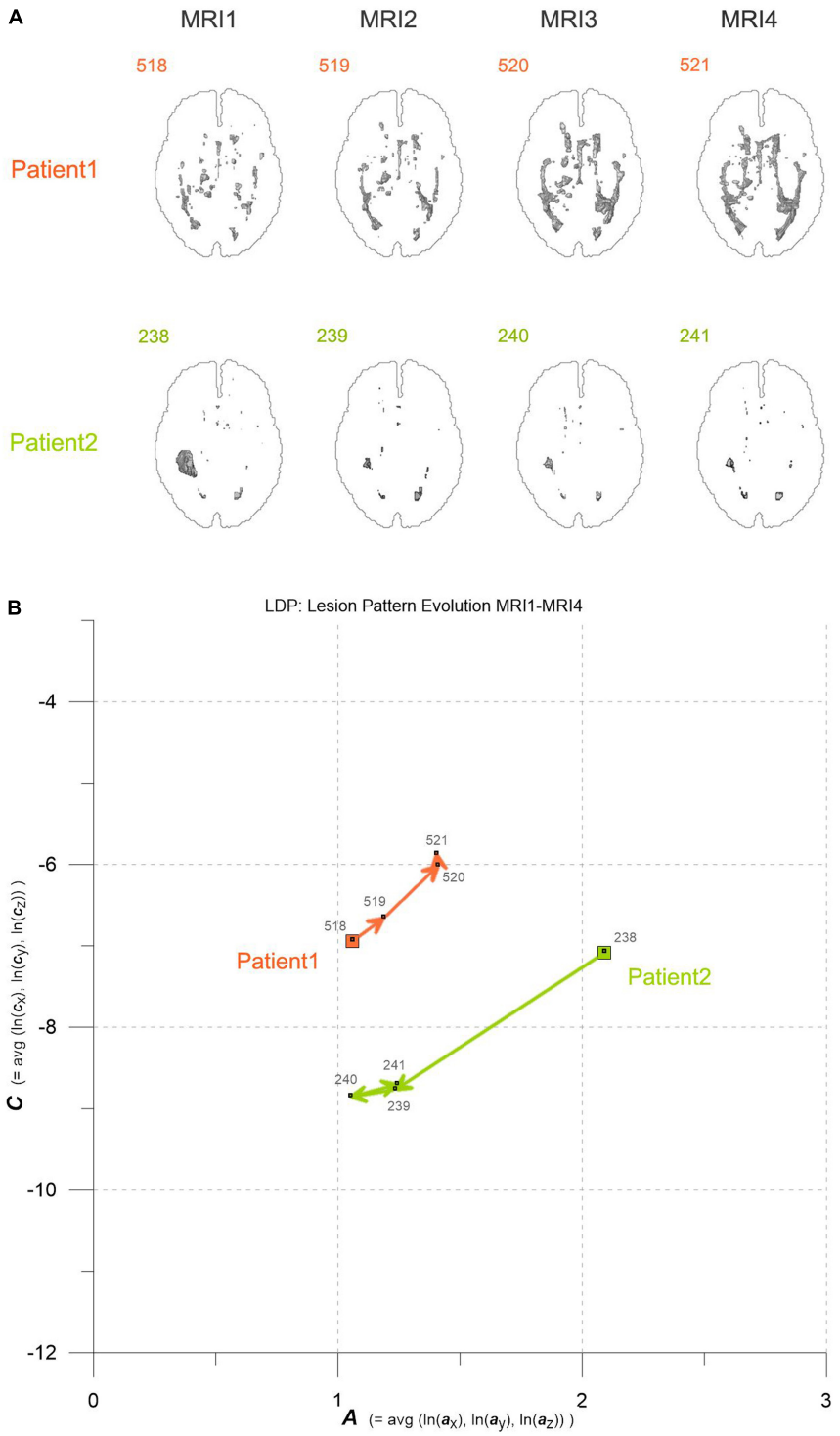

FIGURE 1 | (A) Axial projections of evolving MS-WML patterns of two patients, documented by MRI1-MRI2-MRI3-MRI4. Numbers identify MS-WML patterns. Compare with **Table 2** and **(B)**. **(B)** Abstraction of MS-WML pattern evolution in **(A)** to LDP framework. Numbers identify MS-WML patterns. Compare **Table 2**, see text for details.

to lesion confluence. Most prominent changes occur between MRI2 and MRI3, ending up with a TLV of 9.16 cm^3 at MRI4. As opposed, Patient2 shows decreasing TLV, mainly because the big lesion rapidly shrinks between MRI1 and MRI2. From MRI2 to MRI4, Patient2 MS-WML pattern remains visually almost unchanged with a final TLV of 0.61 cm^3. **Figure 1B** illustrates

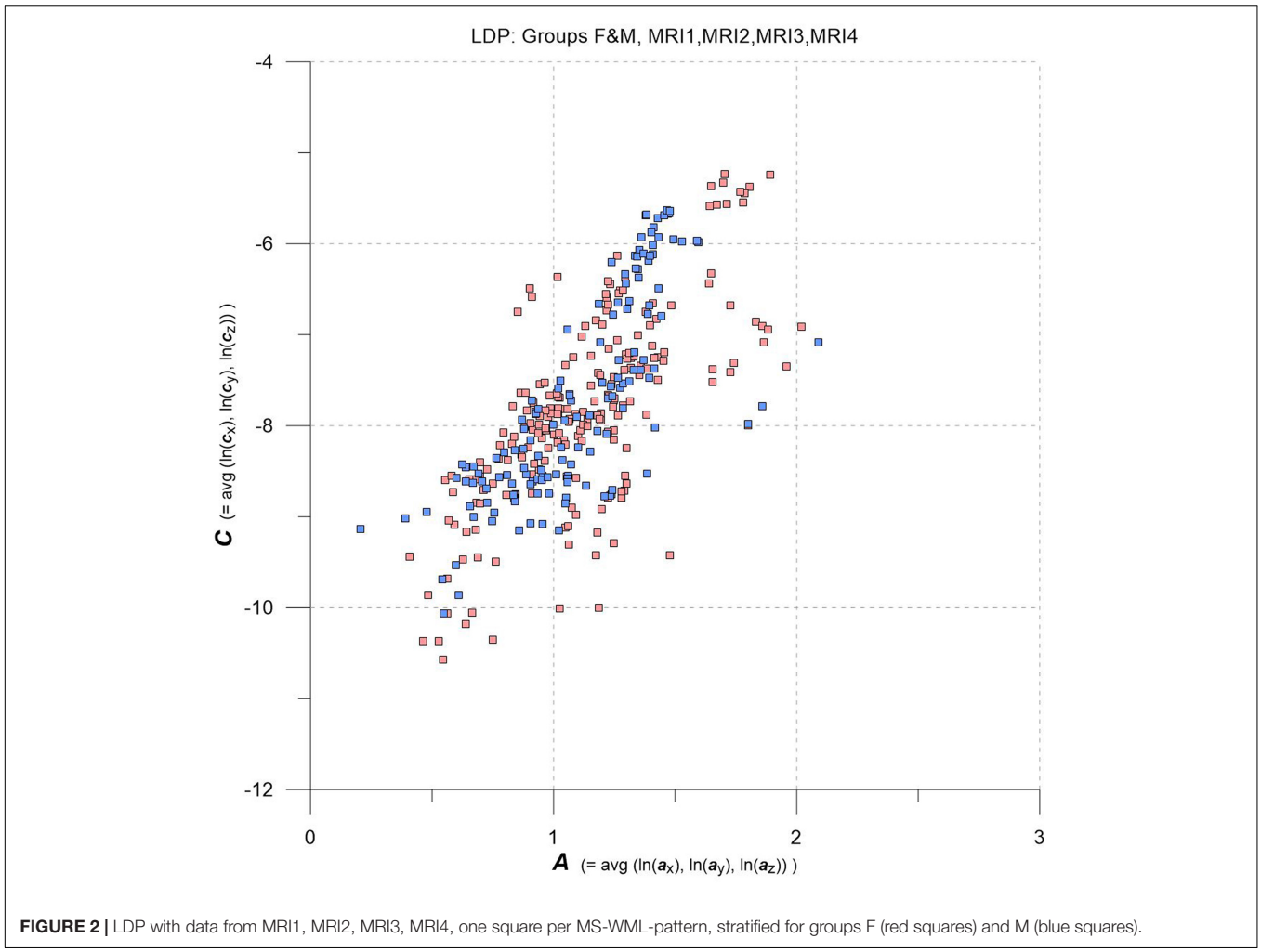

FIGURE 2 | LDP with data from MRI1, MRI2, MRI3, MRI4, one square per MS-WML-pattern, stratified for groups F (red squares) and M (blue squares).

the above context in the LDP. MS-WML pattern evolution of Patient1 is displayed with orange vectors, Patient2 with green vectors; numbers refer to MS-WML patterns in **Figure 1A**. In the LDP (**Figure 1B**), Patient1 and Patient2 evolution paths proceed in opposite directions. Patient1 vectors are generally pointing top right, indicating both increasing TLV and MS-WML pattern smoothness. The longest orange vector signals that prominent MS-WML pattern geometry changes occur between MRI2 and MRI3. By contrast, the evolution path of Patient2 MS-WML pattern is mainly running bottom left, with the longest green vector between MRI1 and MRI2. This is due to shrinkage of the big lesion and associated loss in TLV and loss in overall spatial correlation. Short vectors between MRI2-MRI3-MRI4 indicate only minor pattern changes occurring. The reversed vector direction between MRI3–MRI4 is consistent with two slightly increased lesions at posterior of pattern 241. Summing up, the LDP straightforwardly communicates different geometries, converse evolutions and dynamics of Patient1 and Patient2 MS-WML patterns.

As an overview, the LDP in **Figure 2** depicts all MS-WML patterns extracted from MRI1, MRI2, MRI3, and MRI4. The plot is stratified for groups F (red squares) and M (blue squares). At first glimpse, both groups display as strongly overlapping, elliptic point-clouds with an imaginary long axis trending 45 degrees, from about the lower left to the upper right corners of the LDP. Point densities are highest at and around the imaginary long axis, with a gentle fall-off toward both ends of the long axis. There is also a fall-off in F and M point densities perpendicular to the long axis, more distinct toward top left and dispersed toward bottom right. Closer inspection of **Figure 2** reveals that F points markedly overbalance M points along the lower fringe of the point cloud. In the LDP, MS-WML patterns that plot near the lower fringe of the cloud typically are dominated by relatively few, extended lesions

TABLE 2 | MS-WML pattern evolution of two MS-patients: variogram model parameters and total lesion volume (TLV) derived from MRI1 and MRI4.

	MRI1			MRI4		
	A	***C***	**TLV**	***A***	***C***	**TLV**
Patient1	1.06	−6.94	4.90	1.40	−5.87	9.16
Patient2	2.09	−7.08	4.05	1.24	−8.70	0.61

Compare with ***Figures 1A,B****.* ***A*** *= avg(ln(**a**$_x$), ln(**a**$_y$), ln(**a**$_z$)) and* ***C*** *= avg(ln(**c**$_x$), ln(**c**$_y$), ln(**c**$_z$)). See text for details.*

while patterns that plot near the upper fringe of the point cloud are characterized by many small lesions or complexly shaped MS-WML aggregates (Marschallinger et al., 2016; also check pattern 238 against pattern 518 in **Figure 1A**).

Tentatively, MS-WML patterns that are dominated by continuous, extended lesions should be more abundant in group F than in group M. To overcome the inherent limitations of visually interpreting MS-WML point-clouds in the LDP (**Figure 2**), we reviewed the marginal distributions with density plots. **Figure 3** suggests that both F and M groups have multimodal ***A*** and ***C*** distributions.

Going into more detail, we used multidimensional Gaussian Mixture Modeling (GMM) on ***A***, ***C*** data extracted at baseline (MRI1) to check groups F and M for possible clustering in the LDP space. Results are contrasted in **Figures 4A,B**.

Interestingly, at baseline GMM yields comparable clustering results for both F and M groups: a larger subgroup that stretches approximately along the diagonal of the LDP and a smaller subgroup that plots at comparatively high levels of ***A*** and ***C***. The larger subgroups are tagged F1 (pink) and M1 (light blue), and the smaller subgroups are F2 (red) and M2 (blue).

Normality tests (Shapiro–Wilk, Lilliefors, Anderson-Darling, all with $\alpha = 0.05$) on the respective marginal ***A*** and ***C*** distributions gave ambiguous results. Therefore, the evolution of ***A*** and ***C*** distributions in the above subgroups, from MRI1 (baseline) to MRI4 (end of study), is portrayed with box-whsiker plots (Chambers et al., 1983). The relevant F1, F2, M1, M2 distributions were matched on a non-parametric basis with robust statistical tests [Kruskal–Wallis (KW) and Mann–Whitney (MW) tests, all with $\alpha = 0.05$].

Figures 5A,B contrast the longitudinal evolution of the ***A*** distributions of subgroups F1, F2, M1, M2 at MRI1, MRI2, MRI4, MRI4. Aside from minor fluctuations, F1 and M1 show nearly constant longitudinal medians, IQRs and whiskers. Accordingly, KW- and MW-tests do not indicate significant differences for the longitudinal ***A*** distributions in F1 and M1. F2 and M2 present

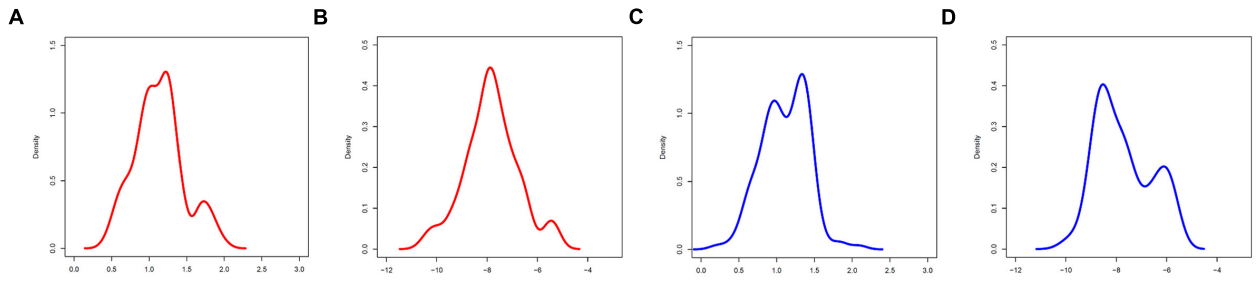

FIGURE 3 | Marginal ***A***,***C*** distributions of groups F (red) and M (blue). **(A,B)** ***A,C*** group F. **(C,D)** ***A,C*** group M.

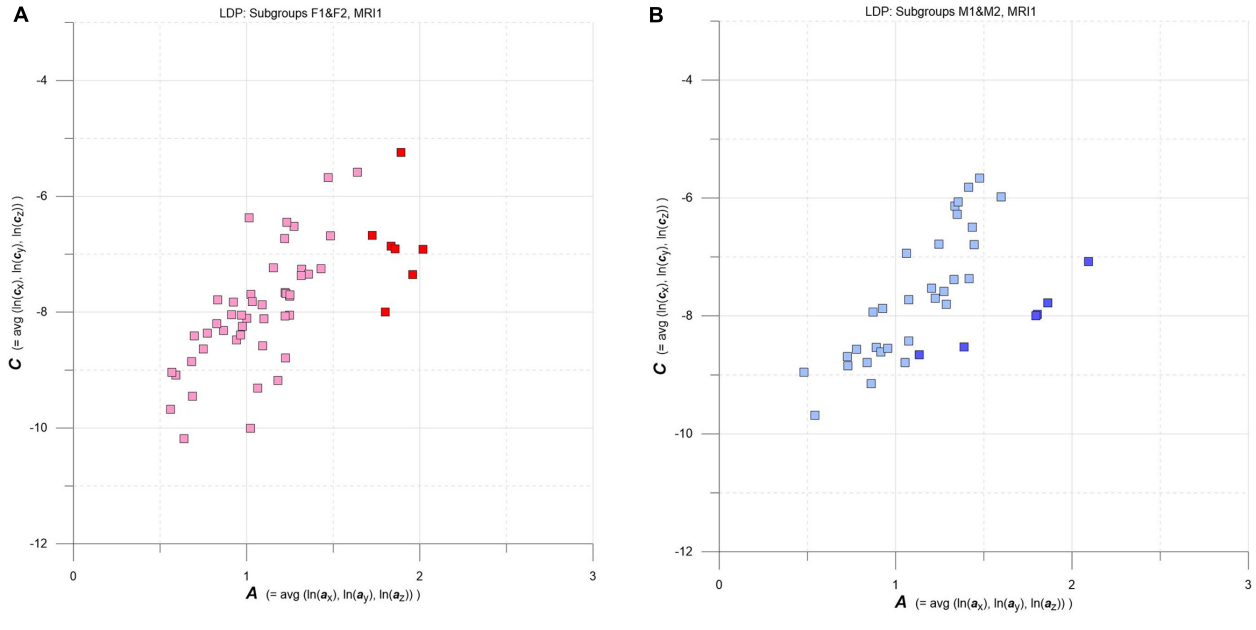

FIGURE 4 | (A,B) LDPs with F and M subgroups derived by GMM clustering. **(A)** Subgroups F1 and F2 (F1: pink squares, $n = 46$, average maximum a posteriori probability of class membership (MAP) = 0.992; F2: red squares, $n = 7$, average MAP = 0.911). **(B)** Subgroups M1 and M2 (M1: light blue squares, $n = 30$, average MAP = 0.989; F2: blue squares, $n = 6$, average MAP = 0.909). See text for details.

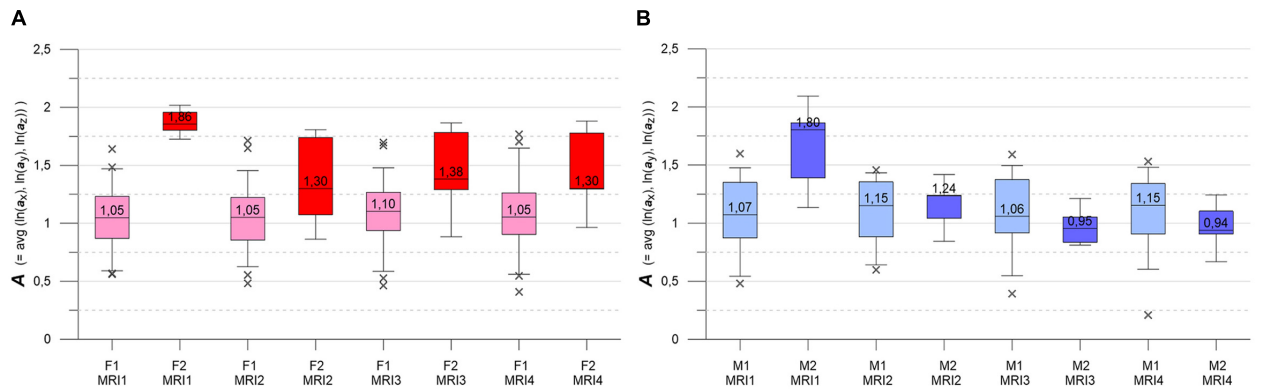

FIGURE 5 | (A,B) Box-whisker plots indicating longitudinal evolution of ***A*** distributions, from MRI1 to MRI4. Box height is interquartile range (IQR), line with value is median, whiskers mark 5 and 95% quantiles, crosses are outliers. (**A**, left) Subgroups F1 (pink, *n* = 46) and F2 (red, *n* = 7). (**B,** right) Subgroups M1 (light blue, *n* = 30) and M2 (blue, *n* = 6). See text for details.

more heterogeneously, with pronounced variations in medians, IQRs and whiskers. At baseline, both F2 and M2 start with high-level medians that decrease strongly at MRI2, followed by about constant values in F2 and a further decrease in M2. While F2 medians clearly remain higher than the respective F1 medians, M2 medians sink below M1 medians at MRI3. For both F2 and M2, KW-tests yield significant longitudinal differences. At all MRIs, MW-tests show significant differences between subgroups F1 and F2. MW-tests also show significant differences between M1 and M2 at MRI1 and between F2 and M2 at MRI3, MRI4.

Figures 6A,B present the longitudinal development of ***C*** distributions in subgroups F1, F2, M1, M2 at MRI1, MRI2, MRI3, MRI4. F1 and M1 show only minor longitudinal variation in medians, IQRs and whiskers, but F1 has a tendency of slightly increasing medians. KW- and MW-tests do not indicate significant differences for longitudinal ***C*** distributions in F1, M1. As compared to F1 and M1, F2 and M2 show accented variations in medians, IQRs and whiskers. F2 medians are longitudinally sinking but remain higher than respective F1 medians. M2 medians are also sinking (exception: MRI4) but are clearly lower than the respective M1 medians. MW-tests show significant differences between F1, F2 and F2, M2 at MRI1 and between M1, M2 at MRI2, MRI3, MRI4.

To assess the statistical significance of gender-based differences in the evolution of parameters ***A*** and ***C*** in groups F2 and M2, a longitudinal analysis was performed. A linear mixed model with fixed effects for centered time-point, gender and their interaction was used to estimate the group-level differences between genders. Subject-specific variation was accounted for by random effects for the intercept and centered time-point. Results are summarized graphically in **Figures 7A,B**: thin lines indicate the subject-specific evolution of parameters ***A*** and ***C*** for group F2 (red) and M2 (blue) individuals, from MRI1 to MRI4. Thick lines refer to the group-level change as estimated by the fixed effects – they indicate negative slopes for ***A*** and ***C*** in both groups F2, M2 without significant difference as well as a well-discernible offset (expected diff. between M2 and F2 between MRI2 and MRI3: −0.35 (95% CI: [−0.63, −0.08]) for parameter ***A***; −1.12 (95% CI: [−2.04, −0.21]) for parameter ***C***).

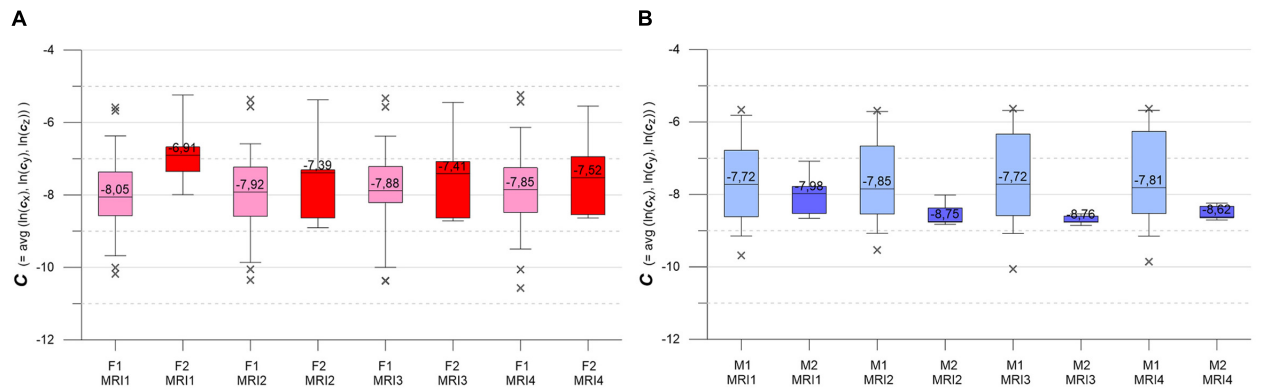

FIGURE 6 | (A,B) Box-whisker plots indicating longitudinal evolution of ***C*** distributions, from MRI1 to MRI4. (**A**, left) Subgroups F1 (pink, *n* = 46) and F2 (red, *n* = 7). **Figure 5B**, right: subgroups M1 (light blue, *n* = 30) and M2 (blue, *n* = 6). Graphics parameters as in **Figures 5A,B**, see text for details.

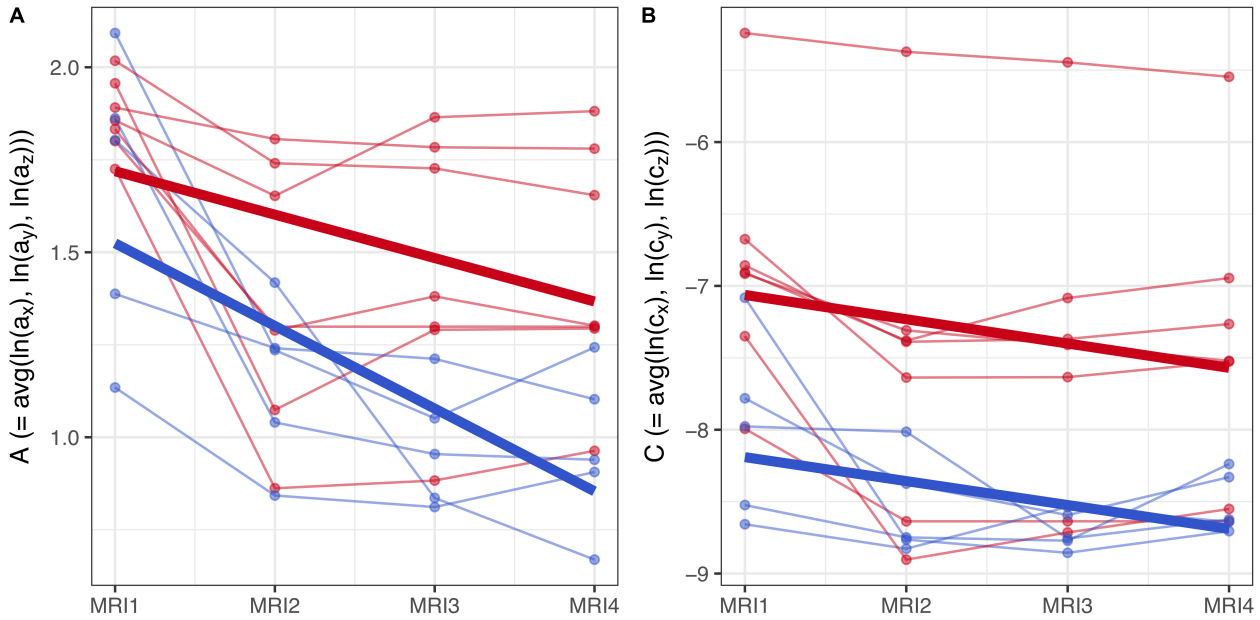

FIGURE 7 | (A,B) Longitudinal analysis of geostatistical parameters ***A*** and ***C*** in subgroups F2 and M2, from MRI1 to MRI4. See text for details.

Summing up, longitudinal analysis results are in accordance with EDA: in subgroups F2 and M2, females show significantly higher values of ***A*** and ***C*** than males.

As pointed out in **Figure 1B**, the evolution of MS-WML patterns can be conveniently visualized in the LDP by connecting longitudinal ***A***,***C*** data with vectors (**Figure 8**). Since the individual MS-WML patterns of F and M groups are in MNI geometry and time between MRI1 and MRI4 is 3 years, the dynamics of pattern change can be visually checked.

Figure 8 combines two LDPs that summarize individual-based and subgroup-based longitudinal MS-WML pattern evolution from baseline (MRI1) to study end (MRI4). **Figure 8A** shows

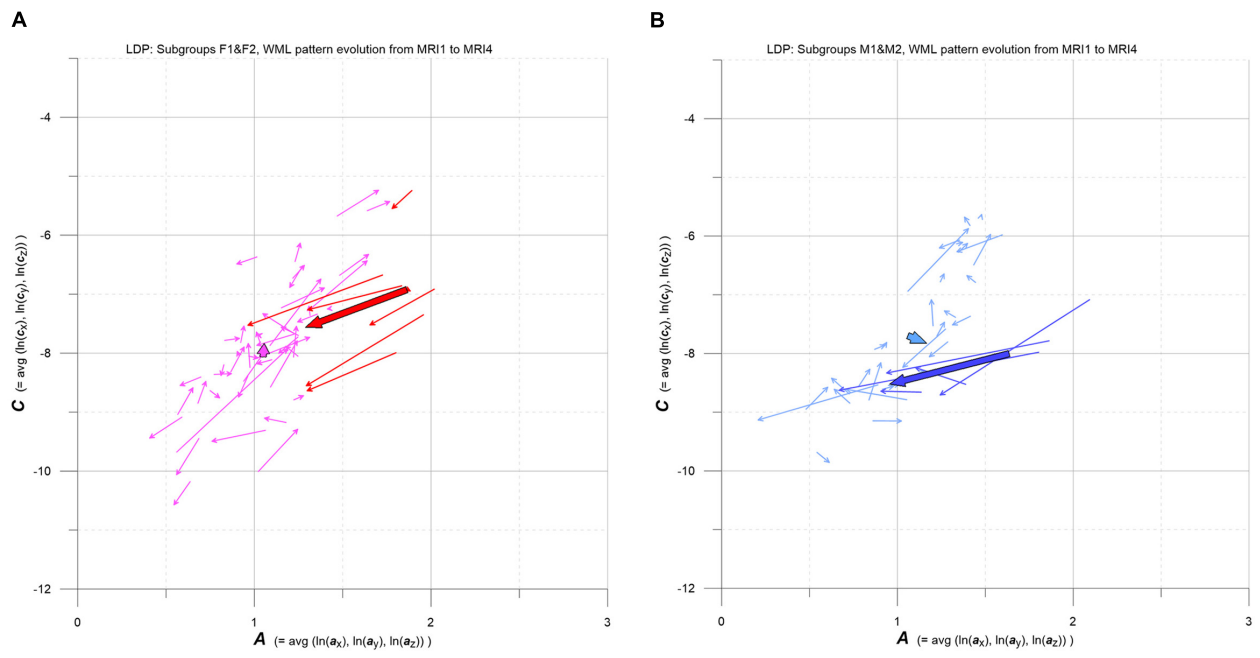

FIGURE 8 | (A,B) LDP-based MS-WML pattern evolution plot. Vectors indicate F1 (pink), F2 (red), M1 (light blue), and M2 (blue) individual and subgroup evolution in the 3-year observation period, from MRI1 to MRI4. One thin vector per individual, total vectors are bold, based on relevant medians. See text for details.

subgroups F1 (pink) and F2 (red), **Figure 8B** shows subgroups M1 (light blue) and M2 (blue). Vectors start at MRI1, arrow heads point to MRI4. Individual vectors are thin, subgroup total vectors are bold. Per subgroup, total vectors are defined by spatial medians of ***A***,***C*** at MRI1 and MRI4 (compare **Figure 5** and **Figure 6**). Individual vectors of subgroups F1, M1 roughly start along the LDP diagonal and show mixed directions and magnitudes. In consequence, total vectors of subgroups F1, M1 start at medium ***A***,***C*** levels and have minor magnitudes, indicating negligible changes: F1 points toward minimally increased ***A*** and ***C***, M1 points toward slightly increased ***A*** and decreased ***C***. By contrast, individual vectors of subgroups F2, M2 start at high ***A*** and medium ***C*** levels, and are mostly pointing to strongly decreased ***A***, and to less decreased ***C***. Hence F2 and M2 total vectors start at high ***A*** and medium ***C***, have increased magnitudes and face bottom-left. Notably, F2 starts and ends at clearly higher ***A***,***C*** than M2.

Subgroup average EDSS deltas broadly correspond to subgroup ***A*** deltas (**Table 3**): from MRI1 to MRI4, subgroups F1 and M1 show no/minor increase in ***A*** and slightly increased average EDSS, while subgroups F2 and M2 present clearly reduced ***A*** and reduced average EDSS.

DISCUSSION

The aim of this study was to evaluate gender-related MS-WML pattern morphology evolution in early MS. Using demographically comparable groups, MRI data acquired by standardized methodology and automatic MS-WML extraction, geostatistical variography revealed differences in the spatiotemporal evolution of MS-WML patterns among women and men with early-MS. The geostatistical work flow for quantifying MS-WML patterns is well-established and provides reliable measures on spatial correlation and TLV. Variography parameters ***A***,***C*** are considered appropriate for reducing the potentially complex three-dimensional structures of MS-WML patterns to two dimensions, for representing DIS in coherent form in the LDP.

We could use the LDP as an EDA tool for revealing the following differences in DIS and DIT: corresponding to gender and MS-WML pattern morphology at baseline, two female subgroups (F1, F2) and two male subgroups (M1, M2) are discerned. Subgroups F1, M1 and F2, M2 show clearly different evolution in space and time. At baseline, both F1 and M1 show similar, medium-level ***A***,***C*** values that remain practically unchanged till end of study – total vectors in the LDP indicate quasi-stationary behavior of F1, M1. By contrast, subgroups F2 and M2 show pronounced variations in the LDP: at baseline, both subgroups start with high-level ***A*** and medium-level ***C***, and evolve toward markedly lower ***A***,***C*** values at end of study. Both M2 and F2 total vectors indicate distinctly reduced pattern smoothness and TLV. Compared to M2, the F2 total vector starts and ends at significantly higher ***A***,***C*** levels, however.

TABLE 3 | Relations between subgroup ***A*** and EDSS at MRI1 and MRI4.

	MRI1		MRI4			
	A	**EDSS**	***A***	**EDSS**	**ΔA**	**ΔEDSS**
F1	1.05	1.4	1.05	1.5	0.00	0.1
F2	1.86	0.9	1.30	0.6	−0.56	−0.3
M1	1.07	1.2	1.15	1.5	0.08	0.3
M2	1.80	1.0	0.94	0.5	−0.86	−0.5

[ΔA = A(MRI4)−A(MRI1), ΔEDSS = EDSS(MRI4)−EDSS(MRI1)]. See text for details.

The dominant physical equivalent of increasing parameters ***A*** and ***C*** is lesion growth or confluence while decreasing ***A*** and ***C*** point to shrinking lesions or to breakup of lesion aggregates. Given MS-WML occur at preferred locations (Filli et al., 2012), notably alongside the CSF system which is stretched in y and z directions, MS-WML patterns are expected to show increased spatial correlation in these directions. Separate examination of x,y,z components of ***A*** complies with this expectation, in all subgroups. Generally, when matching total vectors in the MS-WML pattern evolution plot, in the 3-years observation period subgroups F1 and M1 show practically constant, medium-level MS-WML pattern smoothness and TLV, i.e., negligible change on average. In contrast, F2 and M2 that start with high-level MS-WML pattern smoothness and TLV, are characterized by strongly diminishing MS-WML pattern smoothness and reducing TLV – i.e., continued shrinking and breakup of MS-WML. From baseline to end of study, MS-WML patterns with spatially highly correlated, smooth lesions remain more abundant in F2 than in M2.

Striving for an interpretation of above results, group characteristics are recalled: groups studied here are early-MS with DMD and less than 2 years from first MS signs to MRI1. Of note, Frischer et al. (2015) describe that active WM MS plaques predominate in acute and early MS pathology. This could explain part of the MS-WML morphology evolution in F2 and M2, where dominant ***A*** and ***C*** reduction is observed from MRI1 to MRI2. Dunn et al. (2015) state that the autoimmune component which predominates in early-stage MS is more robust in women than in men and Antulov et al. (2009) show that WM atrophy is more advanced in female patients – this might account for the higher ***A*** and ***C*** values of F2 as compared to M2, over the whole 3-year observation period. Additional reasons for this phenomenon could be a distinct remyelination activity and presence of lesions with differing extent of activity among sexes. In this regard, a histopathological analysis by Kuhlmann et al. (2009) found that remyelination is slightly, but not significantly, more extensive in women than men in early MS lesions. A more recent study by Luchetti et al. (2018) reported a higher proportion of mixed active/inactive lesions compared to females. Last no least, the distinct reduction of ***A*** and ***C*** in F2 and M2 subgroups could relate to a stronger response to DMD of patients with smoother MS-WML. Interestingly, data on subgroup parameter ***A*** respectively EDSS at baseline and at end of study suggest a positive correlation. One problem in relating ***A*** and EDSS is the fact that ***A*** measures brain MS-WML pattern morphology only, while EDSS combines brain and spine performance. This might introduce unknown bias.

A limitation of the current approach to MS-WML pattern dynamics is that it relies on reproducible MRI input data. For example, matching longitudinal data involving different MRI equipment and varying MS-WML extraction methods, we could not find significant gender differences in MS-WML patterns. While the inherent strength of spatial summary statistics on MS-WML-patterns provided by variography is to communicate the "broad picture," this is counterbalanced by loss of spatial granularity: variography is not sensitive to location. In this respect, if more spatial granularity is necessary, MS-WML patterns need to be confined by ROIs. In a next step, these first explorative results on a sexually bimorphic evolution of MS-WML-patterns need to be verified with larger data sets in order to better quantify the uncertainties of estimates.

ETHICS STATEMENT

This study was carried out in accordance with the recommendations of Ethikkommission Land Salzburg. The protocol was approved by the Ethikkommission Land Salzburg. As this study involves only retrospective data and all subjects were anonymized before processing, the study was exempt from a detailed ethics statement (see translation below). Translation: "Research Projects that do not include clinical exams as by the Drug Law, Medical Products Law or new medical methods including non-interventional studies or applied medical research as by the Salzburg Clinics Law are not subject to evaluation by the Federal Country of Salzburg Ethics Committee" (Original in German).

AUTHOR CONTRIBUTIONS

RM, MM, and JS contributed to the conception and design of the study. VP and JK organized the database. RM performed geostatistical analysis. RM and JS wrote the first draft of the manuscript. MM wrote sections of the manuscript. PS performed longitudinal statistics and helped with general statistics. SM performed longitudinal MS-WML extraction. All authors contributed to manuscript revision, read and approved the submitted version.

FUNDING

This work was sponsored by the Paracelsus Medical University research funds (Project No. E-16/24/126-MAS).

ACKNOWLEDGMENTS

The authors would like to thank Prof. Eugen Trinka for continuous support.

REFERENCES

Antulov, R., Weinstock-Guttman, B., Cox, J. L., Hussein, S., and Durfee, J. (2009). Gender-related differences in MS: a study of conventional and nonconventional MRI measures. *Mult. Scler.* 15, 345–354. doi: 10.1177/1352458508099479

Caers, J. (2010). *Modeling Uncertainty in the Earth Sciences*. Hoboken, NJ: Wiley-Blackwell, 246.

Chambers, J. M., Cleveland, W. S., Kleiner, B., and Tukey, P. A. (1983). "Comparing data distributions," in *Graphical Methods for Data Analysis*, eds L. Breiman and L. Breiman (Belmont, CA: Wadsworth International Group), 62.

Cressie, N. A. C. (1993). *Statistics for Spatial Data*. Hoboken, NJ: Wiley, 920.

Deutsch, C. V., and Journel, A. G. (1997). *GSLIB Geostatistical Software Library and User's Guide*. New York, NY: Oxford University Press, 380.

Dolezal, O., Gabelic, T., Horakova, D., Bergsland, N., Dwyer, M. G., Zivadinov, R., et al. (2013). Development of gray matter atrophy in relapsing-remitting multiple sclerosis is not gender dependent: results of a 5-year follow-up study. *Clin. Neurol. Neurosurg.* 115(Suppl. 1)), 42–48. doi: 10.1016/j.clineuro.2013.09.020

Dunn, S. E., Lee, H., Pavri, F. R., and Zhang, M. A. (2015). Sex-based differences in multiple sclerosis (Part I): biology of disease incidence. *Curr. Top. Behav. Neurosci.* 26, 29–56. doi: 10.1007/7854-2015-371

Filli, L., Hofstetter, L., Kuster, P., and Bendfeldt, K. (2012). Spatiotemporal distribution of white matter lesions in relapsing-remitting and secondary progressive multiple sclerosis. *Mult. Scler.* 18, 1577–1584. doi: 10.1177/1352458512442756

Frischer, J. M., Weigand, S. D., Guo, Y., Kale, N., Parisi, J. E., and Luccincetti, C. (2015). Clinical and pathological insights into the dynamic nature of the white matter multiple sclerosis plaque. *Ann. Neurol.* 78, 710–721. doi: 10.1002/ana.24497

Gringarten, E., and Deutsch, C. V. (1999). Methodology for variogram interpretation and modeling for improved reservoir characterization. *Proc. SPE* 56654, 1–13. doi: 10.2118/56654-MS

Harbo, H. F., Gold, R., and Tintoré, M. (2013). Sex and gender issues in multiple sclerosis. *Ther. Adv. Neurol. Disord.* 6, 237–248. doi: 10.1177/1756285613488434

Kalincik, T., Vivek, V., Jokubaitis, V., Lechner-Scott, J., Trojano, M., Izquierdo, G., et al. (2013). Sex as a determinant of relapse incidence and progressive course of multiple sclerosis. *Brain* 136(Pt 12), 3609–3617. doi: 10.1093/brain/awt281

Kourgli, A., Belhadj-aissa, A., and Bouchemakh, A. (2004). "Optimizing texture primitives description based on variography and mathematical morphology," in *Image Analysis and Recognition*, eds A. Campilho and M. Kamel (Toronto, ON: ICIAR), 862.

Kuhlmann, T., Goldschmidt, T., Antel, J., Wegner, C., König, F., Metz, I., et al. (2009). Gender differences in the histopathology of MS? *J. Neurol. Sci.* 286, 86–91. doi: 10.1016/j.jns.2009.07.014

Louapre, C. (2018). Conventional and advanced MRI in multiple sclerosis. *Rev. Neurol.* 174, 391–397. doi: 10.1016/j.neurol.2018.03.009

Luchetti, S., Fransen, N. L., van Eden, C. G., Ramaglia, V., Mason, M., and Huitinga, I. (2018). Progressive multiple sclerosis patients show substantial lesion activity that correlates with clinical disease severity and sex: a retrospective autopsy group analysis. *Acta Neuropathol.* 135, 511–528. doi: 10.1007/s00401-018-1818-y

Marschallinger, R., Golaszewski, S. M., Kraus, J., Kronbichler, M., Kunz, A., Hofmann, P., et al. (2009). "Multiple sclerosis: a multidisciplinary approach to the analysis, 4D modeling and spatiotemporal simulation of lesion pattern evolution," in *Proceedings of the 4th SEECCM*, eds M. Papadrakakis, M. Kojic, and V. Papadopoulos (Kragujevac).

Marschallinger, R., Golaszewski, S. M., Kunz, A. B., Kronbichler, M., Ladurner, G., Kraus, J., et al. (2014). Usability and potential of geostatistics for spatial discrimination of multiple sclerosis lesion patterns. *J. Neuroimaging* 4, 278–286. doi: 10.1111/jon.12000

Marschallinger, R., Schmidt, P., Hofmann, P., Zimmer, C., Atkinson, P. M., Sellner, J., et al. (2016). A MS-lesion pattern discrimination

plot based on geostatistics. *Brain Behav.* 6:e00430. doi: 10.1002/brb3.430

Righart, R., Biberacher, V., Jonkman, L. E., Klaver, R., Schmidt, P., Mühlau, M., et al. (2017). Cortical pathology in multiple sclerosis detected by the T1/T2-weighted ratio from routine magnetic resonance imaging. *Ann. Neurol.* 82, 519–529. doi: 10.1002/ana.25020

Schmidt, P., Gaser, C., Arsic, M., Buck, D., and Forschler, A. (2012). An automated tool for detection of FLAIR-hyperintense white-matter lesions in multiple sclerosis. *NeuroImage* 59, 3774–3783. doi: 10.1016/j.neuroimage.2011.11.032

Schmidt-Nielson, K. (1984). *Scaling: Why is Animal Size So Important?* Cambridge: Cambridge University Press, 237.

Schoonheim, M. M. (2014). Sex-specific extent and severity of white matter damage in multiple sclerosis: implications for cognitive decline. *Hum. Brain Mapp.* 35, 2348–2358. doi: 10.1002/hbm.22332

Shirani, A., Zhao, Y., Kingwell, E., Fisk, J., Rieckmann, P., and Tremlett, H. (2012). Temporal trends of disability progression in multiple sclerosis: findings from British Columbia, Canada (1975-2009). *Mult. Scler* 18, 442–450. doi: 10.1177/1352458511422097

Thompson, A. J., Banwell, B. L., Barkhof, F., Carroll, W. M., Coetzee, T., Cohen, J. A., et al. (2018). Diagnosis of multiple sclerosis: 2017 revisions of the McDonald criteria. *Lancet Neurol.* 17, 162–173. doi: 10.1016/S1474-4422(17)30470-2

Tomassini, V., and Pozzilli, C. (2009). Sex hormones, brain damage and clinical course of multiple sclerosis. *J. Neurol. Sci.* 286, 35–39. doi: 10.1016/j.jns.2009.04.014

Trevisani, S., Cavalli, M., and Marchi, L. (2009). Variogram maps from LiDAR data as fingerprints of surface morphology on scree slopes. *Nat. Hazards Earth Syst. Sci.* 9, 129–133. doi: 10.5194/nhess-9-129-2009

Conflict of Interest Statement: The authors declare that the research was conducted in the absence of any commercial or financial relationships that could be construed as a potential conflict of interest.

frontiers in Molecular Neuroscience

ORIGINAL RESEARCH
published: 26 February 2019
doi: 10.3389/fnmol.2019.00027

Early Life Stress Delays Sexual Maturation in Female Mice

*Gabriela Manzano Nieves[1], Arielle Schilit Nitenson[1], Hye-In Lee[1], Meghan Gallo[2], Zachary Aguilar[1], Angelica Johnsen[2], Marilyn Bravo[1] and Kevin G. Bath[2]**

[1]Department of Neuroscience, Brown University, Providence, RI, United States, [2]Department of Cognitive, Linguistic and Psychological Sciences, Brown University, Providence, RI, United States

In humans, some forms of early life stress (ELS) have been linked with precocious puberty, altered brain maturation, and increased risk for a variety of forms of pathology. Interestingly, not all forms of ELS have been found to equally impact these metrics of maturation. In recent work, we have found that ELS in the form of limited bedding (LB) from P4 to P11, was associated with precocious hippocampus maturation in males and increased risk for depressive-like pathology and attentional disturbance in female mice. Here, we sought to test whether ELS in the form of LB also impacted the timing of sexual maturation in female mice. To establish rate of somatic and sexual development, distinct cohorts of mice were tested for weight gain, timing of vaginal opening, and development of estrous cycling. ELS animals weighed significantly less than controls at every timepoint measured. Onset of vaginal opening was tracked from P21 to 40, and ELS was found to significantly delay the onset of vaginal opening. To test the impact of ELS on estrous cycle duration and regularity, vaginal cytology was assessed in independent groups of animals using either a continuous sampling (daily from P40 to P57) or random sampling approach (single swab at P35, P50, or P75). ELS did impact measures of estrous cycling, but these effects were dependent upon the sampling method used. We also tested the impact of ELS on anxiety-like behaviors over development and across the estrous cycle. We observed a developmental increase in anxiety-like behavior in control but not ELS mice. No effect of estrous cycle stage was found on anxiety-like behavior for either group of mice. Together these results provide evidence that ELS in the form of LB delays somatic and sexual development. Additional work will be required to determine the mechanism by which ELS impacts these measures, and if these effects are common to other models of ELS in rodents.

Keywords: sexual maturation, estrous cycle, early life stress, anxiety, development, limited bedding

OPEN ACCESS

Edited by:
Jordan Marrocco, Rockefeller University, United States

Reviewed by:
Tania L. Roth, University of Delaware, United States
Debra A. Bangasser, Temple University, United States
Neil James MacLusky, University of Guelph, Canada

****Correspondence:***
Kevin G. Bath
kevin_bath@brown.edu

Received: *28 September 2018*
Accepted: *22 January 2019*
Published: *26 February 2019*

Citation:
Manzano Nieves G, Schilit Nitenson A, Lee H-I, Gallo M, Aguilar Z, Johnsen A, Bravo M and Bath KG (2019) Early Life Stress Delays Sexual Maturation in Female Mice. Front. Mol. Neurosci. 12:27. doi: 10.3389/fnmol.2019.00027

INTRODUCTION

In humans, a variety of forms of early life stress (ELS), ranging from famine to physical abuse, have been associated with effects on the timing of sexual maturation. A bulk of these studies have found that ELS is associated with precocious menarche (Moffitt et al., 1992; Ellis and Garber, 2000; Chisholm et al., 2005; Belsky et al., 2015). Precocious sexual development has been linked to increased risk for susceptibility to physical pathology, including increased lifetime risk for breast

and reproductive cancers and for emotional pathology, including increased risk for anxiety and depressive disorders (Kelsey et al., 1993; McPherson et al., 1996; Marshall et al., 1998; Collaborative Group on Hormonal Factors in Breast Cancer, 2012; Bodicoat et al., 2014). The relationship between the timing of sexual maturation and mental health outcomes have been posited to be related to a mismatch between real and perceived age of females at puberty (Caspi and Moffitt, 1991; Ge et al., 1996; Dick et al., 2000; Graber, 2013; Mendle et al., 2017). Understanding the environmental factors that impact the timing of sexual maturation, and associated change in risk for pathology holds great potential for both public policy and strategies for intervention.

Multiple life history theories have been proposed to account for effects of ELS on the timing of sexual maturation, including the predictive adaptive response (Gluckman and Hanson, 2004), energetics theory (Frisch, 1990) and the psychosocial acceleration theory (Mishra et al., 2009). In the predictive adaptive response theory, the quality of care giving serves as a signal to the developing organism about the quality of the external environment (Ellis and Del Giudice, 2014; Belsky et al., 2015; Shalev and Belsky, 2016). These signals serve to shape development by impacting the timing of somatic, neural, and behavioral maturation. In this model, ELS can serve as a signal of a low resource or dangerous environment and drive adaptive changes in the timing of reproductive maturation (e.g., delays in resource poor environments and acceleration in potentially dangerous environments). In the psychosocial acceleration theory, it is argued that high levels of stress should lead to accelerated sexual maturation. In this model, a harsh environment is a signal of increased risk of mortality, and by proxy, decreased longevity of the organism. One proposed evolutionary strategy to promote survival of the species is to promote earlier reproduction (Belsky et al., 1991). In support of this model, multiple published reports have found accelerated sexual maturation in females to be associated with prenatal stress, troubled family relations, mothers with mood disorders, higher allostatic load, and an absent father (Moffitt et al., 1992; Graber et al., 1995; Mezzich et al., 1997; Kim and Smith, 1998; Ellis and Garber, 2000; Allsworth et al., 2005; Chisholm et al., 2005; Costello et al., 2007; Belsky et al., 2015). As a counterpoint to the psychosocial acceleration theory, the energetics theory proposes that energy availability is the key determinant for the timing of sexual maturation (Frisch, 1990). As such, reduced access to nutrition or effects on metabolic function leading to low body weight or lower energy availability, should result in delayed sexual development. Thus, ELS in the form of food insecurity, poor parental care, or resource restriction may favor a delay in both somatic and sexual maturation. Support for this has come from work associating higher SES, lower marital discord, and greater parental support with decreased body mass and later sexual maturation (Ellis and Essex, 2007). In more recent work, children that were previously institutionalized children (PI) and subsequently adopted into United States households were studied. Investigators found that PI youth did not demonstrate the anticipated acceleration in pubertal development that may have been expected with exposure to high levels of ELS, and instead did not differ from control populations (Reid et al., 2017). Thus, not all forms of disruption in the quality or quantity of early life care will have uniform effects on the timing of sexual development. Alternatively, in this group, adoption into affluent or high care households was sufficient to prevent precocious pubertal-onset due to high SES or greater parental investment. Based upon the variety of types of ELS encountered, and differing effects on the timing of sexual maturation, we sought to determine whether a mouse model of ELS, in the form of limited bedding (LB), would alter the timing of sexual maturation.

Use of a rodent model allowed for the dissection of the somatic and physiological consequences of ELS in the form of LB (Harrison and Baune, 2014; Bath et al., 2017b; Walker et al., 2017) including direct effects on sexual maturation and secondary effects on the development of anxiety-like behaviors. Previous work in other models of ELS on sexual development in rodents, including altered licking and grooming or maternal separation, have found changes in copulatory behavior and effects on the timing of vaginal opening, but no effects on the weight of sexual organs in rats (Lau et al., 1996).

Here, we found that ELS in the form of LB led to delays in vaginal opening and decreased somatic weight. Furthermore, ELS was associated with changes in the time spent in different phases of the estrous cycle, but these effects were dependent upon the sampling method employed (continuous or random sampling). Assessing the effects of ELS on the development of anxiety-like behavior, an effect of age on anxiety-like behavior was found for control but not ELS mice. Further, no effect of estrous cycle phase was found for either group of mice. Together, the current findings add to our understanding of the effects of differing forms of ELS on the timing of sexual development. The current results also open up a number of questions regarding the mechanisms supporting changes in sexual development, what metrics should be used to track development, how they are sampled, and how these factors may impact neurobehavioral outcomes.

MATERIALS AND METHODS

Subjects

A total of 550 C57BL/6N virgin mice were used for this study. Subjects were sex segregated following weaning at age (P21). For any given cohort, multiple litters were sampled from (∼3–6 litters) to eliminate potential cohort effects. Cohorts ranged in size with 1–8 females per cohort. Testing of singly housed mice was limited. Example distribution of mice cohorts are shown in **Figures 3B**, **4B**. All animals were housed on a 12:12 h light:dark cycle and had *ad libitum* access to food and water throughout the study. Mice cages were housed in mixed female/male cage holding racks. Twenty-nine mice were used for **Figures 1A,B**. Sixty-five mice (36 control and 29 ELS) were sample across various days for **Figure 1C**, the exact number of mice sampled for a given age are shown in **Supplementary Table S1**. A total of 261 female and 94 male mice were used in **Figure 5**. Following the elevated plus maze (EPM) test, a subset of these mice was used for the random (**Figure 2**) and continuous

sampling to assess cycling (**Figures 3**, **4**). To achieve sufficient sample size for analysis, an additional 101 mice were sampled in **Figure 2**. A subset of the mice in **Figure 2** were continuously sampled for **Figures 3**, **4**. All animal procedures were approved by the Brown University Institutional Animal Care and Use Committee and were consistent with the National Institutes of Health Guide for the Care and Use of Laboratory Animals.

Limited Bedding (LB)

ELS was induced by providing LB material to dams when pups were between the ages of P4 to P11. This model induces a fragmentation in maternal care, where the dam exhibits a greater number of nest exits and entries compared with dams that have access to the full complement of bedding materials (Rice et al., 2008; Bath et al., 2016). Specifically, 4 days after the birth of a litter (P4), the dam and pups were transferred from their standard home cage with cob bedding and a 4 × 4 cm cotton nestlet to a cage containing a wire mesh floor and only a 3 × 4 cm cotton nestlet. The mice continued to have *ad libitum* access to food and water. Following 1 week (at P11), pups and dams were returned to their standard housing. The control reared mice (controls) were left undisturbed in a standard home cage during this period.

Vaginal Opening

To determine the onset of vaginal opening, two independent observers inspected the vaginal opening of mice for the visual appearance of an opening starting at postnatal day 21 and ending at postnatal day 45. To minimize stress and discomfort of mice, the vaginal status was assessed every other day. Upon visual observation of vaginal opening, status was verified by passing a small cotton swab along the outer opening of the vagina. The appearance of any opening was defined as the onset of vaginal opening. In **Figure 1**, the age and weight at which a vaginal opening onset was first detected was noted. For experiments in which vaginal smears were collected, a closed or partially open vaginal canal, which were insufficient for complete penetration for swabbing, resulted in a not available (N/A) designation. Vaginal smear collection required the vaginal canal to be completely open for samples to be collected. The number or proportion of mice from which smears could not be collected on a given day are indicated in each figure.

Estrous Cycle Monitoring

Estrous cycle was monitored using two different approaches. In a subset of mice, a random sampling approach was used in which vaginal smears were collected from mice at a single timepoint (postnatal day 35, 40, 50, or 75). The random sampling approach eliminated potential stimulatory effects, or effects of stress associated with repeated vaginal swabbing on cycle onset. In a separate cohort of mice, a repeated sampling (continuous) approach was used. For continuous sampling, vaginal smears were collected for either 18 (starting at P40) or 14 (starting at P75) consecutive days between the hours of 5 pm to 7 pm. All mice used for this study were previously unhandled.

Estrous cycle stage was determined by vaginal cytology. Vaginal cytology was assessed by dipping a sterile swab in water and gently swabbing the outer half of the vaginal canal. Vaginal samples were transferred to a microscope slide, air dried, stained using a Hema 3 staining kit (Fisher Scientific, Hampton, NH, USA), dehydrated, and then cover slipped prior to visualization on a light microscope at 10× magnification. Estrous cycle stage was assessed using previously established criteria (Bath et al., 2008; Aliagas et al., 2010; Byers et al., 2012) and were carried out by an observer blind to rearing condition and behavioral results. Vaginal smears were not collected from mice that did not have complete vaginal openings, these mice are labeled not available (N/A) in relevant figures. For explanation see "Vaginal Opening" section.

The number of cycles was defined as the number of times that proestrus or Diestrus preceded estrus. Whereas the length of the estrus cycle was analyzed as the number of days between proestrus to the next proestrus, or the number of days between proestrus to an estrus that directly followed Diestrus. In the example: P E M D P E M D E M D there are three cycles with the first cycle lasting 4 days. Only the length of the first complete cycle was analyzed for this study.

Elevated Plus Maze

To assess anxiety-like behavior during development, mice were tested on an EPM at either P28, P35, P50, P75–110. Mice were tested only once on this apparatus and an individual mouse contributed to only a single time point. The EPM apparatus was built in-house and consisted of two open (unprotected) and two closed (protected) arms, previously described (Manzano-Nieves et al., 2018). Greater time in the closed (protected) arms is defined as higher anxiety-like behavior while increasing time in the open arms is indicative of a lower anxiety-like state.

A trial began by placing a mouse in the center of the arena and allowing it to explore the maze for 7 min. The time spent in the protected vs. unprotected arms was assessed. Videos were recorded, and behavior was tracked using Noldus Ethovision XT 10.0 software. All trials were conducted under low light conditions (∼109 Lux). Time spent, visits and distance walked in the open and closed arms of the EPM were assessed using the mouse tracking module. Trials in which a mouse fell off the arena were discarded (6 out of 130 at P75), and the mouse was removed from the experiment. Within an hour of completing the behavioral test, vaginal cytology samples were obtained. Behavioral testing occurred between the hours of 3–7 pm, shortly before lights off in the housing facility.

Data Analysis

Data was analyzed using Prism software (Prism, GraphPad Software, La Jolla, CA, USA) and SPSS (IBM). Graphs and images were made using GraphPad Software. Differences in distributions were assessed using a Chi-square test. Differences in onset of vaginal openings was assesses using a Log-rank test. A two-way analyses of variance (ANOVA) followed by Sidak's multiple comparison test was used to assess differences in weight (**Figure 1A**). Multiple two-tailed unpaired *t*-tests with a Holm-Sidak multiple comparison correction were used for comparing the number of days spent in each cycle stage in **Figures 3E**, **4C** right, and **4D** right. All other *t*-tests used were also unpaired and two-tailed. In **Figure 5**, two-way ANOVAS

followed by *post hoc* Tukey tests were used to assess differences between groups.

RESULTS

Early Life Stress Delay Somatic Development

To determine the effect of ELS on somatic and sexual maturation, whole body weight and the timing of vaginal opening were measured. Body weight of control and ELS mice were measured across development (postnatal ages: 11, 12, 13, 14, 15, 16, 21, 28, 38, 43, and 60) **Figure 1A**. A main effect of age (two-way ANOVA- $F_{(11,367)} = 689.6$, $p < 0.0001$) was found with both groups gaining weight across development. However, weight between the groups differed ($F_{(1,367)} = 195$, $p < 0.0001$), with ELS mice weighing less than controls at all time points measured. No interaction between rearing condition and age were found ($F_{(11,367)} = 1.27$, $p = 0.25$). A subsequent Sidak's multiple comparisons *post hoc* test comparison revealed that ELS mice weighed significantly less than controls at every age tested (see **Supplementary Table S1**).

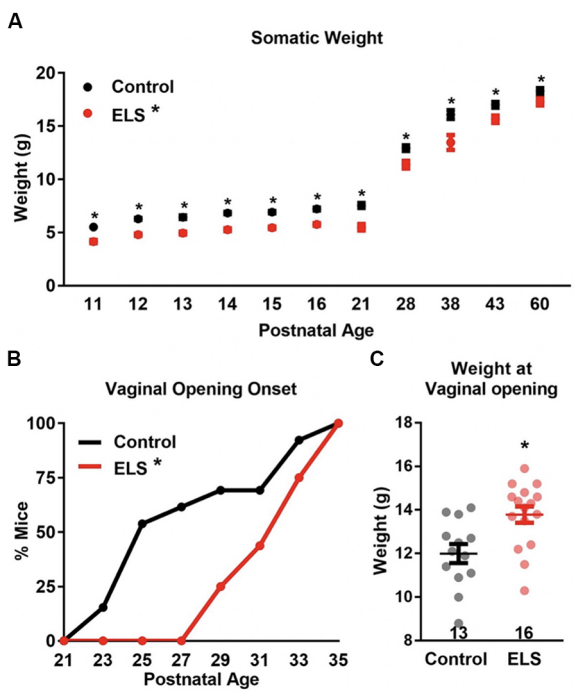

FIGURE 1 | Early life stress (ELS) decreases body weight and delays vaginal opening onset. **(A)** ELS females weigh consistently less than control females during development and into adulthood. Dots represent group means ± SEM (CR females, n = 12–34 per age; ELS females, n = 5–29 per age). **(B)** ELS delays vaginal opening onset in female mice. Graph represents the cumulative percentage of mice who had vaginal opening onsets by a given age. **(C)** The weight at which vaginal opening onset occurs was greater for ELS females than controls. *N* of the groups for panels **(B,C)** are presented in panel **(C)**. A two-way analyses of variance (ANOVA) followed by a *post hoc* multiple comparison test **(A)**, Log-rank **(B)**, and a two-tailed unpaired *t*-test **(C)** were used to assess statistical significance between groups $^*p < 0.05$.

Assessment of vaginal opening was determined by sampling animals on alternating days from postnatal day 21 to postnatal day 35. The appearance of any size vaginal fissure constituted the onset of vaginal opening. Vaginal openings were first observed in control mice at P23 and in ELS mice the first appearance of vaginal opening was observed at P29 (**Figure 1B**). A Log-rank test revealed that control females underwent vaginal openings at a younger age than ELS females ($X^2_{1,\,N\,=\,29} = 5.779$, $p = 0.0162$), suggesting that ELS females experience delayed somatic sexual development. Furthermore, the mean age at vaginal opening onset was significantly greater for ELS mice compared with controls (*t*-test: Control = 27.62 vs. ELS = 32.25; $t_{(27)} = 3.64$, $p = 0.0011$).

Diminished body weight has been shown to correlate with delayed or suppressed sexual maturation in humans (Frisch and McArthur, 1974; Vigersky et al., 1977; Warren, 1980). It is possible that lower body weights in ELS mice significantly contributed to the delay in vaginal openings. If the decrease in weight was driving the delay in vaginal opening, then it would be predicted that ELS mice should demonstrate vaginal opening at the same weight in which control mice exhibited vaginal opening. Surprisingly, the weight of ELS mice at the onset of vaginal opening was significantly greater than the mean weight of control mice at vaginal opening (*t*-test: $t_{(27)} = 3.13$, $p = 0.0042$; **Figure 1C**).

Early Life Stress Delays Onset of Estrous Cycling

To determine if ELS impacts the onset of estrous cycling, we used a random sampling (**Figure 2B**) approach. Representative images of vaginal cytology for each of the four estrous cycle stages are shown in **Figure 2A**. Random sampling of estrous stage allowed us to assess the distribution of cycle phase without the potential confounds of handling, repeated vaginal stimulation, or stress on this measure. For random sampling, cohorts were sampled a single time at either postnatal day 35, 50, or 75. The proportion of mice in each stage of the estrous cycle is presented for each age assessed (**Figure 2**). Chi square tests were performed to assess the effects of ELS on the proportion of mice in each stage of the estrous cycle.

During early adolescence (P35), ELS mice differed significantly from controls in the proportion of mice with complete vaginal openings ($X^2_{1,\,N\,=\,103} = 8.57$, $p = 0.0034$; **Figure 2C** top). Approximately 43% of ELS mice, but only 17% of control reared mice, did not have complete vaginal openings. As mice with incomplete vaginal openings could not be swabbed for cycle assessment, this decreased the number of mice from which vaginal smears could be obtained in the ELS group, hindering our ability to test for differences in cycle phase between the two groups. When mice without complete vaginal opening were excluded from the analysis, no differences between the groups were observed ($X^2_{3,\,N\,=\,74} = 6.58$, $p = 0.087$). However, this failure to detect a significant difference may have been the result of needing to exclude a large percentage of ELS female mice that did not have complete vaginal opening at P35 (43%). Given the resultant small sample size, the exact effect of ELS at this timepoint remains unclear. To determine

if the differences observed in early adolescence continued into adulthood, separate cohorts of mice were randomly sampled for estrous status at either P50 (late adolescence) or P75 (adults). Chi-square analysis of the distribution at P50 ($X^2_{3,\,N=92} = 0.36$, $p = 0.95$; **Figure 2B** middle) and P75 ($X^2_{3,\,N=170} = 0.14$, $p = 0.99$; **Figure 2B** bottom) indicated that rearing condition did not impact the distribution of cycle phases observed in those cohorts of mice.

ELS Alters the Periodicity of Estrous Cycling in Adolescence

The estrous cycle length shortens and becomes more regular as mice transition from young adulthood to full adulthood (approx. P120; Nelson et al., 1982). However, whether ELS impacts the development of a more regular and shorter cycle remains unknown. To test if ELS altered the number or length of estrous cycles, a continuous monitoring method was employed. Estrous cycle was tracked by daily collection of vaginal smears. To assess ELS effects on cycling during adolescence into young adulthood (P40–57; **Figure 3**), vaginal smears were collected for 18 consecutive days starting at P40. The total number of mice and the number of mice per cohort used are shown in **Figure 3B**. As adolescence represents a dynamic developmental stage, the data was binned into 6-day blocks (**Figure 3E**) to enable visualization of changes in the days spent in each cycle phase.

During development (P40–P57), no differences in the overall distribution ($X^2_4 = 2.007$, $p = 0.73$) or mean value of estrous cycles were observed ($t_{(62)} = 0.94$, $p = 0.35$; **Figure 3C**). Furthermore, ELS did not impact the overall percent of time that

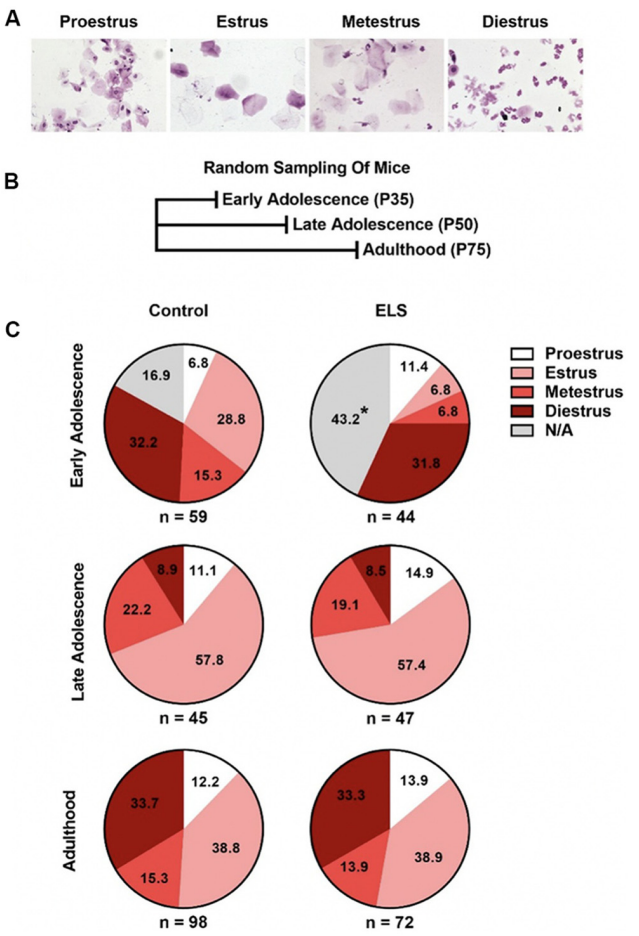

FIGURE 2 | ELS delays complete vaginal openings but does not affect the probability of being at a given estrous cycle. **(A)** Example pictures of the estrous cycle phases. **(B)** Schematic of random sampling protocol. Distinct cohorts of mice were used at each sampled age. **(C)** ELS early adolescent mice have a greater portion of females without complete vaginal openings and trend toward significant differences in the distribution of estrous cycle phases (top). ELS does not alter the distribution of females in a given estrous cycle phase during late adolescence (middle) or adulthood (bottom). Pie charts represent the portion of females in a given estrous cycle phase. *N* of the group is presented underneath each pie chart. Chi-squared test were used to assess statistical significance between groups $^*p < 0.05$.

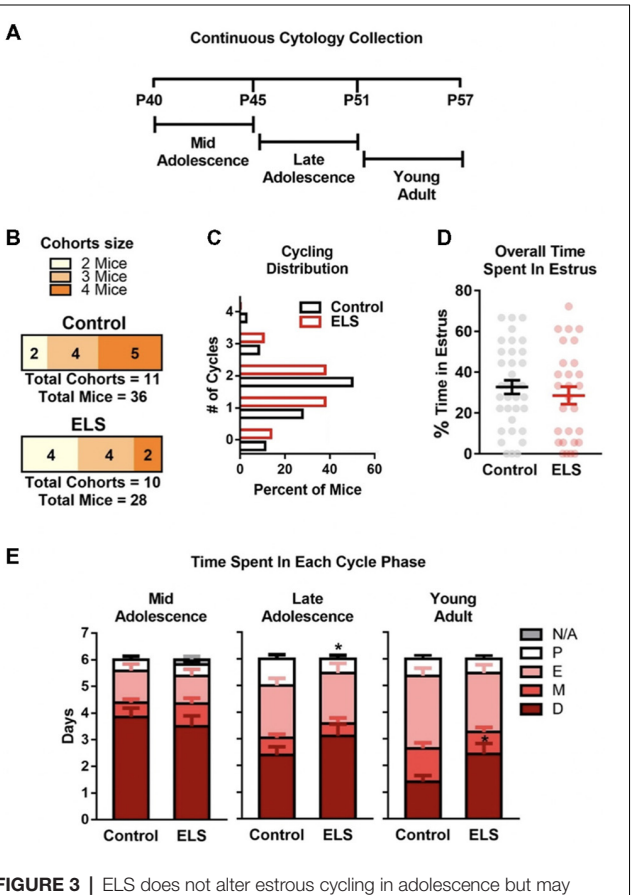

FIGURE 3 | ELS does not alter estrous cycling in adolescence but may affect length of cycle phases. **(A)** Schematic of continuous sampling protocol. Daily vaginal smears were obtained from postnatal day 40 to 57. **(B)** Description of total mice in each group and the number of mice in each cohort. **(C)** Graph depicting the percent of mice that were cycling. ELS did not alter the distribution or number of estrous cycles **(D)** or the overall time spent in estrous during the 18-day protocol (P40–57). **(E)** However, ELS did decrease the cumulative number of days mice spent in proestrus during late adolescence (P46–51). Furthermore, ELS increased the cumulative number of days spent in diestrus during young adulthood (P52–57). Lines and bars represent group means ± SEM. Dots in **(D)** represent individual values. The number of mice in each group is shown in panel **(B)**. Chi-square test was used to assess differences in distribution **(C)**. Unpaired two-tailed student *t*-test were used to assess statistical significance between groups $^*p < 0.05$.

mice spent in the estrus stage of the estrous cycle ($t_{(62)}$ = 0.78, p = 0.44; **Figure 3D**). During mid adolescence (P40–45; **Figure 3D** left), ELS and control mice spent approximately the same number of days in proestrus ($t_{(62)}$ = 0.064, p = 0.59), estrus ($t_{(62)}$ = 0.43, p = 0.59), metestrus ($t_{(62)}$ = 1.40, p = 0.59), and diestrus ($t_{(62)}$ = 0.70, p = 0.59). Furthermore, there was no differences in the number of days that mice spent without complete vaginal openings (N/A; $t_{(62)}$ = 1.60, p = 0.11). During late adolescence (P46–51; **Figure 3D** middle) ELS mice were found to spend less time in proestrus than controls ($t_{(62)}$ = 2.16, p = 0.034). ELS did not affect the time spent in any of the other estrous cycle phases; estrus ($t_{(62)}$ = 0.18, p = 0.86), metestrus ($t_{(62)}$ = 0.71, p = 0.48), or diestrus ($t_{(62)}$ = 1.36, p = 0.18). During young adulthood (P52–57; **Figure 3D** right) there was a significant difference in the amount of time ELS mice spent in diestrus ($t_{(62)}$ = 2.39, p = 0.020) compared to controls, with ELS spending on average more time in diestrus. ELS did not alter the time in proestrus ($t_{(62)}$ = 0.56, p = 0.58), estrus ($t_{(62)}$ = 1.19, p = 0.24), or metestrus ($t_{(62)}$ = 1.49, p = 0.14) during young adulthood.

ELS Rearing Does Not Affect Estrous Cycle Into Adulthood

To determine if ELS effects the estrous cycle of adult mice, the number of estrous cycles, estrus duration, and the time spent in each estrous stage were assessed. For assessing differences during adulthood (P75–89; **Figure 4**), vaginal smears were collected for 14 consecutive days starting at P75. As binning P75 data did not reveal effects of time only overall (14-day) data was analyzed and discussed.

To determine if there were differences in the estrous cycle of adult mice reared under control or ELS conditions, vaginal smears were collected daily from mice as detailed in **Figure 4A**. As the number of mice per cohort can alter cycling, the number of mice per cohort are presented in **Figure 4B**. The number and average length of the estrous cycles was compared for ELS and control reared mice. A t-test revealed that ELS rearing did not affect the distribution (X_3^2 = 0.20, p = 0.98; **Figure 4C** left), mean number (Control mean = 1.68 vs. ElS mean = 1.7; $t_{(69)}$ = 0.12, p = 0.91) or the mean time mice spent in estrus ($t_{(69)}$ = 0.082, p = 0.93; **Figure 4C** center). An analysis of the number of days spent in each of the four estrous cycle phases revealed no significant differences between ELS and controls during proestrus ($t_{(69)}$ = 0.43, p = 0.67), estrus ($t_{(69)}$ = 0.14, p = 0.89), metestrus ($t_{(69)}$ = 0.45, p = 0.65), or diestrus ($t_{(69)}$ = 0.12, p = 0.91; **Figure 4C** right). However, it is possible that our analysis is being skewed or masked by the high number of mice with irregular estrous cycles (defined as less than two cycles; see **Figure 4C** left). Therefore, we assessed possible cycling differences within the portion of mice that underwent two or more estrous cycles (Control = 61%, ELS = 60%; **Figure 4D**). We found that ELS mice did not significantly differ from control mice in the length of the estrous cycle ($t_{(41)}$ = 0.11, p = 0.91; **Figure 4D** left) or in the number of days spent in estrous ($t_{(41)}$ = 0.16, p = 0.87; **Figure 4D** center). Furthermore, an analysis of the number of days spent in each of the four estrous cycle phases, for the subset of mice that were regularly cycling, revealed no significant differences between ELS and controls (proestrus: $t_{(41)}$ = 0.28, p = 0.89; estrus: $t_{(41)}$ = 0.50, p = 0.98; metestrus: $t_{(41)}$ = 0.39, p = 0.98; diestrus: $t_{(41)}$ = 0.53, p = 0.98; **Figure 4D** right).

Age, but Not ELS Rearing or Estrous Cycle Stage, Impacts Anxiety-Like Behavior

Previous work has shown that estrous cycle stage can have a significant effect on the expression of anxiety-like behavior in mice (Gangitano et al., 2009; Bath et al., 2012). While ELS does impact the onset of vaginal opening and possibly the onset of stable estrous cycling, it does not appear to impact the duration of estrous cycling in adulthood (**Figure 4**). To determine if ELS rearing impacted the expression of anxiety-like behavior in mice, we used the EPM. Independent groups of mice were sampled across development, and estrous cycle phase was determined for each animal immediately following testing. A two-way ANOVA revealed a main effect of age on time spent in the open arms ($F_{(3,353)}$ = 7.88, $p < 0.0001$), with decreasing levels of open arm exploration as mice aged, suggesting that anxiety-like behavior increases with age. To determine what times points might be driving the main effect of age, we carried up follow-on *post hoc* testing collapsing across rearing condition. We found that at P28, mice spent significant more time in the open arms when compared to P35 (p = 0.0012), P50 (p = 0.0034), and P75 (p = 0.0012) mice. However, given that not all groups had the same n (**Figure 5A**), and that the effect of age may not be equal across all groups, we performed a *post hoc* Tukey to assess within group differences across ages. No main effect of rearing condition ($F_{(2,353)}$ = 0.52, p = 0.60) or interaction between rearing condition and age ($F_{(6,353)}$ = 0.71, p = 0.64) were found, suggesting that ELS rearing did not significantly affect anxiety-like behavior. To assess what ages where contributing to the main effect of age on anxiety-like behavior, we performed a *post hoc* Tukey test assessing the main effect was conducted. We found, after collapsing across conditions, that P28 mice spent significant more time in the open arms when compared to P35 (p = 0.0012), P50 (p = 0.0034), and P75 (p = 0.0012) mice. However, given that not all groups had the same n (**Figure 5A**), and that the effect of age may not be equal across all groups, we performed a *post hoc* Tukey to assess within group differences across ages (**Supplementary Table S2**). We found that control females spent a greater percentage of time in the open arms at P28 than at P35 (p = 0.012) and P75–110 (p = 0.016), and a trend towards more time in the open arms at P28 when compared to P50 (p = 0.061). For control males a difference between the percent time spent in the open arms was reported for P28 vs. P35 (p = 0.046), with P28 control animals spending more time in the open arms. In *post hoc* Tukey multiple comparison tests, no effects of sex or rearing condition were found at any of the ages tested (**Supplementary Table S3**). Additionally, no effects of the estrous cycle on anxiety like behavior were observed in adulthood (P75–110; **Figure 5A** right inset). A two-way ANOVA revealed that neither estrous cycle phase ($F_{(3,111)}$ = 0.51, p = 0.68) nor rearing condition ($F_{(1,111)}$ = 9.27 × 10^{-8}, p = 0.9998) effected the percent time females spent in the open arms. Furthermore, no interaction

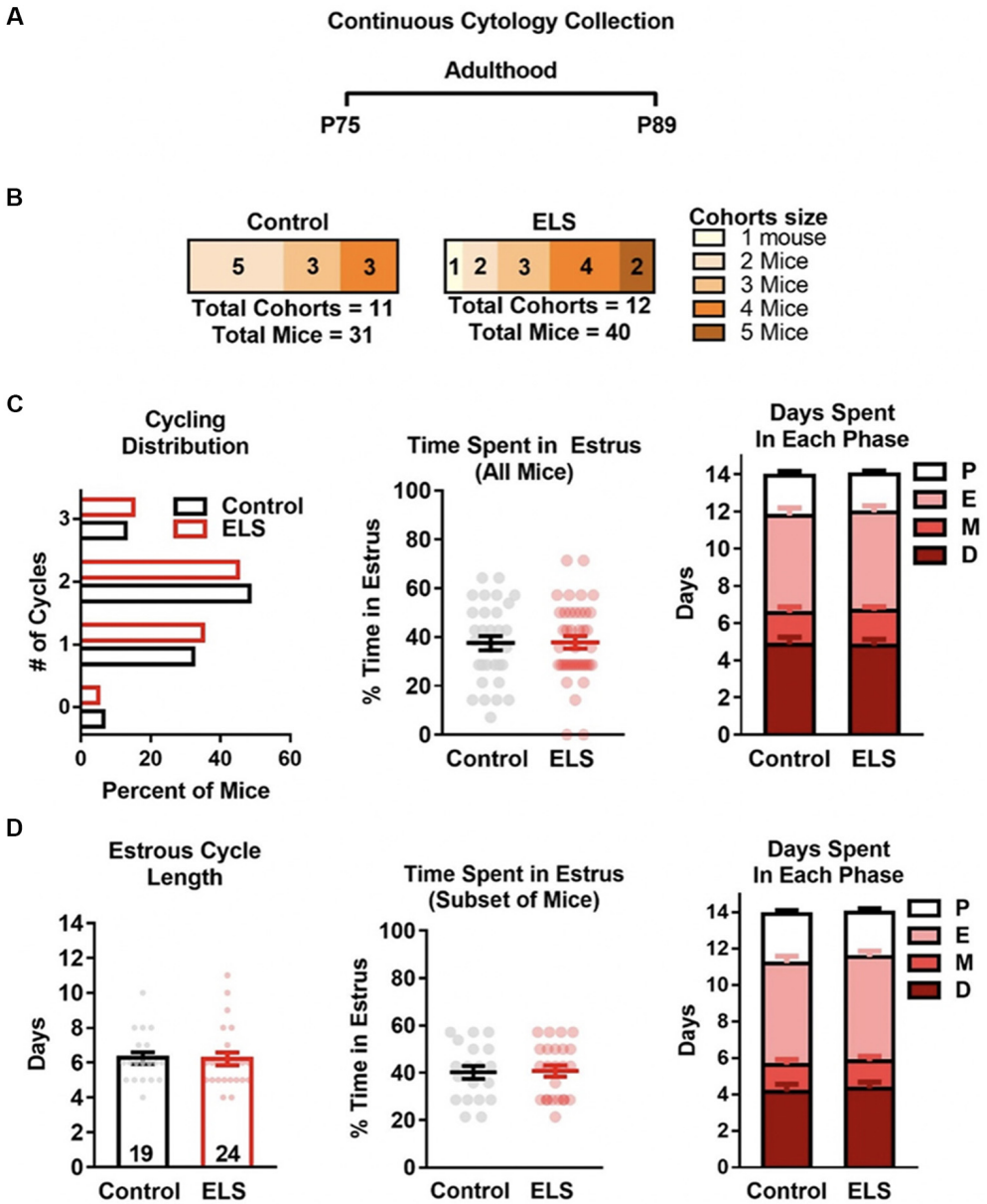

FIGURE 4 | ELS does not affect estrous cycling in adulthood. **(A)** Schematic of continuous sampling protocol. Daily vaginal smears were obtained from postnatal day 75 to 89. **(B)** Description of total mice in each group and the number of mice in each cohort. **(C)** Graph depicting the percent of mice that were cycling. ELS did not alter the distribution or mean number of estrous cycles (left), or the total time spent in the estrous cycle during the 14-day protocol (center). Furthermore, ELS did not change the cumulative number of days mice spent in each cycle phase (right). **(D)** Graphs depicting the effects of ELS in the subset of mice that had two or more cycles during the 14-day protocol. ELS did not alter the length of the estrous cycle (left), the time spent in estrus (center), nor the time spent in any of the other phases (right). Bars represent group means ± SEM. Dots represent individual values. The total *n* for graphs in **(C)** is depicted in panel **(B)**. The *n* of graphs in panel **(D)** are presented on the bars of (**D** left). Chi-square test was used to assess differences in distribution (**C** left); unpaired two-tailed student *t*-test were used to assess statistical significance between groups $^{*}p < 0.05$.

between estrous cycle and rearing condition was observed ($F_{(3,111)} = 0.51$, $p = 0.60$).

We also assessed rearing effects on percent entries into the open arms in the EPM. A two-way ANOVA revealed a main effect of age ($F_{(3,353)} = 6.021$, $p = 0.0005$) and interaction between group and age ($F_{(6,353)} = 2.78$, $p = 0.012$), suggesting that entries into the open arms decreased with increasing age of mice tested. No main effect of group was found ($F_{(2,353)} = 0.24$, $p = 0.79$). *post hoc* Tukey multiple comparison tests were used to assess simple effects of age and group. Significant age differences were only observed within control males, which had significantly more entries at P28 than at any other time

point (all $p < 0.05$). Control males also had significantly more entries at P50 than they did at P75–110. Furthermore, at P75–110 control males had decreased entries into the open arms when compared to control females ($p = 0.038$) and ELS females ($p = 0.0081$). This data suggests that the number of entries decreases with age in control males, but not control or ELS females. Furthermore, no effects of the estrous cycle on the number of entries into the open arms were observed in adulthood (P75–110; **Figure 5B** right inset). A two-way ANOVA revealed that neither estrous cycle phase ($F_{(3,111)} = 1.85$, $p = 0.14$) nor rearing condition ($F_{(1,111)} = 1.11$, $p = 0.29$) effected the number of entries into the open arms. Additionally, no interaction between estrous cycle and rearing condition was observed ($F_{(3,111)} = 1.016$, $p = 0.39$).

To determine if any of the observed effect of age, or failures to observe treatment or sex effects could be attributed to primary effects on locomotion, we tested for effects of these variables on the distance traveled by mice in the EPM. A two-way ANOVA revealed a main effect of group ($F_{(2,353)} = 3.92$, $p = 0.021$) and interaction between group and age ($F_{(6,353)} = 3.12$, $p = 0.0055$), suggesting that total distance walked in the EPM differed between groups. However, no main effect of age was found ($F_{(3,353)} = 2.20$, $p = 0.088$). A *post hoc* Tukey multiple comparison test was used to assess the differences between groups at a given age. At P28 we found that ELS females walked less than control males ($p = 0.013$) and control females ($p = 0.014$) of the same age. The difference between the distance walked persisted in P35, with control females walking significantly more than ELS females ($p = 0.032$). Only ELS females displayed age effects on distance walked. ELS females walked significantly more at P50 than at P28 ($p = 0.0029$) or P35 ($p = 0.037$). Interestingly, these changes in locomotion did not impact the number of entries or the percent time in the open arms. Further experiments will be needed to fully understand the impact of ELS on locomotor behavior during early adolescence and adolescence. To assess if the estrous cycle was impacting locomotion, we assessed the distance traveled in the EPM for control and ELS females in adulthood (P75–110; **Figure 5C** right inset). A two-way ANOVA revealed that neither estrous cycle phase ($F_{(3,111)} = 0.19$, $p = 0.90$) nor rearing condition ($F_{(1,111)} = 0.25$, $p = 0.61$) effected the number of entries into the open arms. Additionally, no interaction between estrous cycle and rearing condition was observed ($F_{(3,111)} = 0.18$, $p = 0.91$).

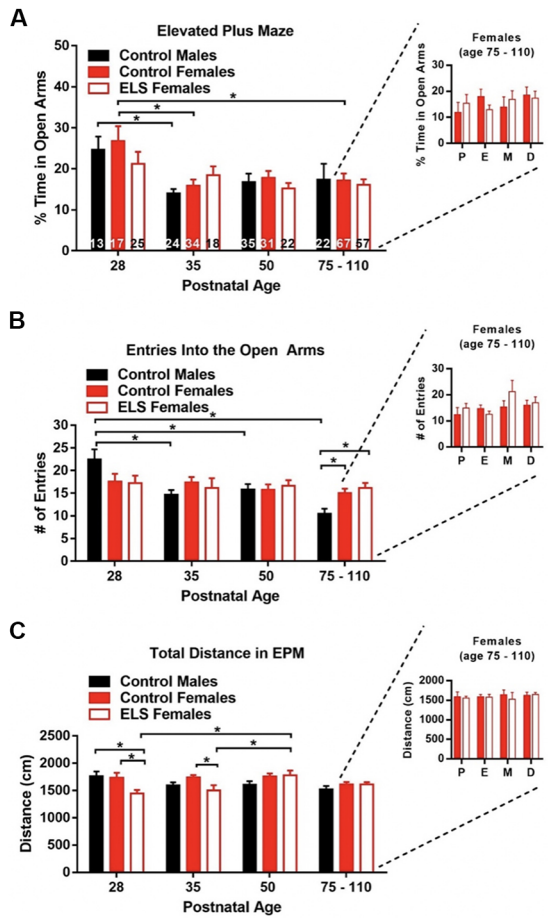

FIGURE 5 | Age only affects anxiety outcomes. **(A)** Time spent in the open arms (anxiogenic arms) of the elevated plus maze (EPM) decreases with age. This effect seems to be mainly driven by control animals. ELS does not affect the time spent in the open arms at any age. Estrous cycle phase was not seen to alter the time spent in the open arms in adult mice (right inset). **(B)** The number of entries into the open arms decreased with age for control males but not control or ELS females. ELS did not affect the entries into the open arms at any age when compared to control females. Estrous cycle phase was not seen to alter entries into the open arms in adult mice (right inset). **(C)** ELS decreased the distance walked for females at P28 and P35 when compared to control females. Estrous cycle phase was not seen to distance traveled in the EPM in adult mice (right inset). Bars represent group means ± SEM, the *n* of each group of the main figures are shown on the bars of panel **(A)**. Control females in the insets = 67, ELS females in the insets = 52. A two-way ANOVA followed by a *post hoc* multiple comparison test was used to assess statistical significance between and within groups $^*p < 0.05$.

DISCUSSION

Here, we assessed the impact of ELS in the form of LB on the timing of sexual maturation in female mice. ELS led to delays in vaginal opening, decreased body weight, and transient effects on estrous cycling. Time spent in different phases of the estrous cycle were largely restricted to the early adolescent period and unaltered during late adolescence and early adulthood. Interestingly, no effect of estrous cycle stage was found on anxiety-like behavior in control or ELS females. In fact, only increasing age was found to be associated with an increase in anxiety-like behavior. Together our findings add to the current literature and provide evidence that ELS in the form of LB delay aspects of sexual maturation in a mouse model.

To assess the effect of ELS on somatic development we tracked weight gain and the onset and completion of vaginal opening. We found that ELS delayed weight gain and the onset (**Figure 1B**) and completion (**Figure 2C**) of vaginal opening. This is in contrast with findings from a maternal separation paradigm, where investigators found an acceleration in the onset of vaginal opening (Grassi-Oliveira et al., 2016), but no effect on the completion of vaginal opening

(Rhees et al., 2001; Grassi-Oliveira et al., 2016). The disparities between these models may be related to differences in the form of stress encountered during development and what they signal to the developing organism. In the psychosocial acceleration theory, the repeated loss of the parent may signal either instability or greater probability of the loss of a caregiver, and thus the need to mature faster, exit the nest sooner, and possibly reproduce earlier. In the current work, limited access to bedding does not impact contact time between the dam and the pup or the total amount of care provided. However, this form of stress does impact weight gain of the pups, possibly through decreased nutrition provided by the dam, or effects on basal stress hormones levels, metabolism, or thermoregulation. Thus, this model may better approximate effects expected from the energetics theory of maturation, where decreased resources may elicit a delay in aspects of somatic maturation. Alternatively, the shift in sexual maturation that was observed could be interpreted in the context of the predictive adaptive response theory. It is possible that stress associated with the decrease in availability of resources may be promoting a delay in sexual development as a means of delaying reproduction in a low resource environment. This may provide advantages in the context of drought and famine when resources for caring for young are not available and provide a means to delay reproduction until such times pass. However, additional experiments altering the home-cage environment post ELS rearing would be necessary to test this hypothesis. The link between delay in vaginal opening and decreased body weight has previously been reported by various groups in pre-pubertal maternal separation in rodents (McIntosh et al., 1999; de Almeida Magalhães et al., 2017). Interestingly, studies in post-institutionalized children have reported similar decreases in body weight and no effect of institutional rearing on physical signs of puberty (Walker et al., 2007; Hayes and Tan, 2016; Reid et al., 2017). It is possible that environmental changes associated with adoption at a very young age may be sufficient to buffer against delays in sexual development, or that these effects may be mirroring an energetics model of reproductive development. Together these results suggest that ELS in the form of LB induces reduced weight gain over development, which may delay somatic signs of sexual development in a dose dependent manner. Studies comparing differing type, intensity, and length of ELS will be needed to completely parse out the relationship between these variables.

Over the course of development, there are significant changes in the regularity and duration of the estrous cycle in mice. As mice transition from late adolescence to adulthood, the cycle becomes shorter and more regular (Nelson et al., 1982). To test if ELS altered the amount of time mice spent in different phases of the estrous cycle during adolescence and young adulthood, we used two different approaches in two separate groups of mice, a cross-sectional (random sampling) and longitudinal (repeated sampling) approach. In the cross-sectional group (**Figure 2**), there was a trend for ELS effects on the distribution of mice in a given estrous phase during early adolescence ($p = 0.087$). However, this group suffered from under sampling due to many ELS mice (43%) not having complete vaginal openings. A larger sample size may have allowed us to view significant difference in the estrous phase distribution of ELS mice in early adolescence. In our continuously sampled group, we did not find any effects of ELS during the early adolescent period (**Figure 3**). It is possible that the effects observed in the cross-sectional group were missed in our continuously sampled group because of differences in the ages sampled. Whereas the cross-sectional group was sampled at P35 the longitudinal was first sampled at P40. However, the continuous sampling group, did reveal effects of decreased proestrus during late adolescence and increased diestrus in young adulthood. Because these effects only occurred in the continuously sampled group of mice, it is possible that continuous sampling acted as a secondary stressor. Therefore, the later effects observed in the continuously sampled data could have been a result of a condition by sampling method interaction.

In humans, anxiety disorders first emerge during pre-adolescence, with the median age of onset at 11 years of age (Kessler et al., 2005). Stress incurred early in life can increase the risk for developing anxiety-related behaviors (Agid et al., 1999; Draijer and Langeland, 1999; Widom, 1999; Heim and Nemeroff, 2001; Koenen and Widom, 2009). Curiously, our lab and others have found that ELS in the form of LBN is not associated with increased expression of anxiety-like behaviors in adulthood (Molet et al., 2016; Goodwill et al., 2018; Manzano-Nieves et al., 2018). However, a failure to exhibit an anxiety-like phenotype as an adult does not preclude the possibility that ELS impacts the expression of anxiety-like behavior over development (e.g., possible transient developmental expression of anxiety-like behaviors that may resolve by adulthood). To determine if ELS impacted the development of anxiety-like behavior, different groups of mice were tested once at either P28, P35, P50 or P75+. Rearing condition did not affect anxiety-like behavior at any of the ages tested. This both replicates and expands upon our previous findings, suggesting that a low resource model of ELS does not increase the propensity for anxiety-like behavior in a mouse model. However, we did observe an overall main effect of age on levels of anxiety-like behavior, whereby P28 mice showed significantly less anxiety than P35, P50 or P75+ mice. The decrease in anxiety at P28 may be reflective of a bias toward an increase in exploratory behavior at this age (Bath et al., 2017a). Decreasing anxiety and increasing exploration at P28 may be advantageous under non-stress conditions, as it promotes independence from dams and the discovery of new resources in the wild. Interestingly, ELS reared females specifically did not display an increase in anxiety-like behavior over development. These results may indicate that ELS is associated with an earlier elevation in anxiety-like behavior in female mice. Additional data from younger cohorts of mice would be required to directly test this hypothesis. Given that the variability of males and females are known to be explained by different facets of behavior in the EPM (Fernandes et al., 1999), assessing anxiety-like behavior in different behavioral paradigms (light/dark box or open field) will be necessary to conclusively determine the impacts of ELS and development on anxiety.

Together, the data presented here led us to conclude that ELS in the form of LB in females resulted in decreased weight gain and delayed sexual maturation, as indexed by the onset of vaginal opening. The effects of ELS on weight gain are consistent with our previous work in males (Bath et al., 2016). It is possible that the effects of ELS on weight gain, may be driving the observed delays in vaginal opening. Prior work has found that body weight may serve as a better predictor of puberty onset than chronological age (Kennedy and Mitra, 1963; Frisch, 1972), possibly due to effects on leptin levels, a hormone produced by adipose cells, that has been shown to be necessary for both puberty and fertility (Ahima et al., 1997; Yura et al., 2000; Farooqi, 2002; Smith et al., 2002). To directly test such a hypothesis, work manipulating both ELS and restoring body weight, through manipulations such as high fat diet, would be required. Future work will be needed to test this hypothesis.

AUTHOR CONTRIBUTIONS

GMN and KB conceived the project and designed the experiments. GMN performed behavioral experiments with the aid of H-IL. GMN and MG performed the "Vaginal Opening" section analysis experiment. GMN and ASN analyzed vaginal cytology. GMN obtained continuous vaginal smears with the aid of ZA, AJ and MB. GMN interpreted data, wrote and edited the manuscript with the aid of KB.

FUNDING

This work was supported by the Robert and Nancy Carney Fund for Scientific Innovation (KB), the Norman Prince Neuroscience Institute Translational Research Award (KB), R01-MH115914 (KB), R01-MH115049 (KB), F99-NS105219 (GMN) and by the National Science Foundation Graduate Research Fellowships Program Award (GMN).

ACKNOWLEDGMENTS

We would also like to thank Dr. Burwell for the use of her lab's microscopy equipment.

SUPPLEMENTARY MATERIAL

The Supplementary Material for this article can be found online at: https://www.frontiersin.org/articles/10.3389/fnmol.2019.00027/full#supplementary-material

REFERENCES

Agid, O., Shapira, B., Zislin, J., Ritsner, M., Hanin, B., Murad, H., et al. (1999). Environment and vulnerability to major psychiatric illness: a case control study of early parental loss in major depression, bipolar disorder and schizophrenia. *Mol. Psychiatry* 4, 163–172. doi: 10.1038/sj.mp.4000473

Ahima, R. S., Dushay, J., Flier, S. N., Prabakaran, D., and Flier, J. S. (1997). Leptin accelerates the onset of puberty in normal female mice. *J. Clin. Invest.* 99, 391–395. doi: 10.1172/jci119172

Aliagas, E., Torrejón-Escribano, B., Lavoie, E. G., de Aranda, I. G., Sévigny, J., Solsona, C., et al. (2010). Changes in expression and activity levels of ecto-5′-nucleotidase/CD73 along the mouse female estrous cycle. *Acta Physiol.* 199, 191–197. doi: 10.1111/j.1748-1716.2010.02095.x

Allsworth, J. E., Weitzen, S., and Boardman, L. A. (2005). Early age at menarche and allostatic load: data from the Third National Health and Nutrition Examination Survey. *Ann. Epidemiol.* 15, 438–444. doi: 10.1016/j.annepidem.2004.12.010

Bath, K. G., Chuang, J., Spencer-Segal, J. L., Amso, D., Altemus, M., McEwen, B. S., et al. (2012). Variant brain-derived neurotrophic factor (Valine66Methionine) polymorphism contributes to developmental and estrous stage-specific expression of anxiety-like behavior in female mice. *Biol. Psychiatry* 72, 499–504. doi: 10.1016/j.biopsych.2012.03.032

Bath, K. G., Mandairon, N., Jing, D., Rajagopal, R., Kapoor, R., Chen, Z. Y., et al. (2008). Variant brain-derived neurotrophic factor (Val66Met) alters adult olfactory bulb neurogenesis and spontaneous olfactory discrimination. *J. Neurosci.* 28, 2383–2393. doi: 10.1523/JNEUROSCI.4387-07.2008

Bath, K. G., Manzano-Nieves, G., and Goodwill, H. (2016). Early life stress accelerates behavioral and neural maturation of the hippocampus in male mice. *Horm. Behav.* 82, 64–71. doi: 10.1016/j.yhbeh.2016.04.010

Bath, K. G., Nitenson, A. S., Lichtman, E., Lopez, C., Chen, W., Gallo, M., et al. (2017a). Early life stress leads to developmental and sex selective effects on performance in a novel object placement task. *Neurobiol. Stress* 7, 57–67. doi: 10.1016/j.ynstr.2017.04.001

Bath, K. G., Russo, S. J., Pleil, K. E., Wohleb, E. S., Duman, R. S., and Radley, J. J. (2017b). Circuit and synaptic mechanisms of repeated stress: perspectives from differing contexts, duration, and development. *Neurobiol. Stress* 7, 137–151. doi: 10.1016/j.ynstr.2017.05.001

Belsky, J., Ruttle, P. L., Boyce, W. T., Armstrong, J. M., and Essex, M. J. (2015). Early adversity, elevated stress physiology, accelerated sexual maturation, and poor health in females. *Dev. Psychol.* 51, 816–822. doi: 10.1037/dev0000017

Belsky, J., Steinberg, L., and Draper, P. (1991). Childhood experience, interpersonal development, and reproductive strategy: and evolutionary theory of socialization. *Child Dev.* 62, 647–670. doi: 10.1111/j.1467-8624.1991.tb01558.x

Bodicoat, D. H., Schoemaker, M. J., Jones, M. E., McFadden, E., Griffin, J., Ashworth, A., et al. (2014). Timing of pubertal stages and breast cancer risk: the breakthrough generations study. *Breast Cancer Res.* 16:E18. doi: 10.1186/bcr3613

Byers, S. L., Wiles, M. V., Dunn, S. L., and Taft, R. A. (2012). Mouse estrous cycle identification tool and images. *PLoS One* 7:e35538. doi: 10.1371/journal.pone.0035538

Caspi, A., and Moffitt, T. E. (1991). Individual differences are accentuated during periods of social change: the sample case of girls at puberty. *J. Pers. Soc. Psychol.* 61, 157–168. doi: 10.1037//0022-3514.61.1.157

Chisholm, J. S., Quinlivan, J. A., Petersen, R. W., and Coall, D. A. (2005). Early stress predicts age at menarche and first birth, adult attachment, and expected lifespan. *Hum. Nat.* 16, 233–265. doi: 10.1007/s12110-005-1009-0

Collaborative Group on Hormonal Factors in Breast Cancer. (2012). Menarche, menopause, and breast cancer risk: individual participant meta-analysis, including 118 964 women with breast cancer from 117 epidemiological studies. *Lancet Oncol.* 13, 1141–1151. doi: 10.1016/s1470-2045(12)70425-4

Costello, E. J., Worthman, C., Erkanli, A., and Angold, A. (2007). Prediction from low birth weight to female adolescent depression: a test of competing hypotheses. *Arch. Gen. Psychiatry* 64, 338–344. doi: 10.1001/archpsyc.64.3.338

de Almeida Magalhães, T., Correia, D., de Carvalho, L. M., Damasceno, S., and Brunialti Godard, A. L. (2017). Maternal separation affects expression of stress response genes and increases vulnerability to ethanol consumption. *Brain Behav.* 8:e00841. doi: 10.1002/brb3.841

Dick, D. M., Rose, R. J., Viken, R. J., and Kaprio, J. (2000). Pubertal timing and substance use: associations between and within families across late adolescence. *Dev. Psychol.* 36, 180–189. doi: 10.1037//0012-1649.36.2.180

Draijer, N., and Langeland, W. (1999). Childhood trauma and perceived parental dysfunction in the etiology of dissociative symptoms in psychiatric inpatients. *Am. J. Psychiatry* 156, 379–385.

Ellis, B. J., and Del Giudice, M. (2014). Beyond allostatic load: rethinking the role of stress in regulating human development. *Dev. Psychopathol.* 26, 1–20. doi: 10.1017/s0954579413000849

Ellis, B. J., and Essex, M. J. (2007). Family environments, adrenarche, and sexual maturation: a longitudinal test of a life history model. *Child Dev.* 78, 1799–1817. doi: 10.1111/j.1467-8624.2007.01092.x

Ellis, B. J., and Garber, J. (2000). Psychosocial antecedents of variation in girls' pubertal timing: maternal depression, stepfather presence, and marital and family stress. *Child Dev.* 71, 485–501. doi: 10.1111/1467-8624.00159

Farooqi, I. S. (2002). Leptin and the onset of puberty: insights from rodent and human genetics. *Semin. Reprod. Med.* 20, 139–144. doi: 10.1055/s-2002-32505

Fernandes, C., González, M. I., Wilson, C. A., and File, S. E. (1999). Factor analysis shows that female rat behaviour is characterized primarily by activity, male rats are driven by sex and anxiety. *Pharmacol. Biochem. Behav.* 64, 731–738. doi: 10.1016/s0091-3057(99)00139-2

Frisch, R. E. (1972). Weight at menarche: similarity for well-nourished and undernourished girls at differing ages and evidence for historical constancy. *Pediatrics* 50, 445–450.

Frisch, R. E. (1990). The right weight: body fat, menarche and ovulation. *Baillieres. Clin. Obstet. Gynaecol.* 4, 419–439. doi: 10.1016/s0950-3552(05)80302-5

Frisch, R. E., and McArthur, J. W. (1974). Menstrual cycles: fatness as a determinant of minimum weight for height necessary for their maintenance or onset. *Science* 185, 949–951. doi: 10.1126/science.185.4155.949

Gangitano, D., Salas, R., Teng, Y., Perez, E., and De Biasi, M. (2009). Progesterone modulation of α5 nAChR subunits influences anxiety-related behavior during estrus cycle. *Genes Brain Behav.* 8, 398–406. doi: 10.1111/j.1601-183x.2009.00476.x

Ge, X., Conger, R. D., and Elder, G. H. Jr. (1996). Coming of age too early: pubertal influences on girls' vulnerability to psychological distress. *Child Dev.* 67, 3386–3400. doi: 10.2307/1131784

Gluckman, P. D., and Hanson, M. A. (2004). The developmental origins of the metabolic syndrome. *Trends Endocrinol. Metab.* 15, 183–187. doi: 10.1016/j.tem.2004.03.002

Goodwill, H. L., Manzano-Nieves, G., Gallo, M., Lee, H. I., Oyerinde, E., Serre, T., et al. (2018). Early life stress leads to sex differences in development of depressive-like outcomes in a mouse model. *Neuropsychopharmacology* doi: 10.1038/s41386-018-0195-5 [Epub ahead of print].

Graber, J. A. (2013). Pubertal timing and the development of psychopathology in adolescence and beyond. *Horm. Behav.* 64, 262–269. doi: 10.1016/j.yhbeh.2013.04.003

Graber, J. A., Brooks-Gunn, J., and Warren, M. P. (1995). The antecedents of menarcheal age: heredity, family environment, and stressful life events. *Child Dev.* 66, 346–359. doi: 10.2307/1131582

Grassi-Oliveira, R., Honeycutt, J. A., Holland, F. H., Ganguly, P., and Brenhouse, H. C. (2016). Cognitive impairment effects of early life stress in adolescents can be predicted with early biomarkers: impacts of sex, experience, and cytokines. *Psychoneuroendocrinology* 71, 19–30. doi: 10.1016/j.psyneuen.2016.04.016

Harrison, E. L., and Baune, B. T. (2014). Modulation of early stress-induced neurobiological changes: a review of behavioural and pharmacological interventions in animal models. *Transl. Psychiatry* 4:e390. doi: 10.1038/tp.2014.31

Hayes, P., and Tan, T. X. (2016). Timing of menarche in girls adopted from China: a cohort study. *Child Care Health Dev.* 42, 859–862. doi: 10.1111/cch.12393

Heim, C., and Nemeroff, C. B. (2001). The role of childhood trauma in the neurobiology of mood and anxiety disorders: preclinical and clinical studies. *Biol. Psychiatry* 49, 1023–1039. doi: 10.1016/s0006-3223(01)01157-x

Kelsey, J. L., Gammon, M. D., and John, E. M. (1993). Reproductive factors and breast cancer. *Epidemiol. Rev.* 15, 36–47. doi: 10.1093/oxfordjournals.epirev.a036115

Kennedy, G. C., and Mitra, J. (1963). Body weight and food intake as initiating factors for puberty in the rat. *J. Physiol.* 166, 408–418. doi: 10.1113/jphysiol.1963.sp007112

Kessler, R. C., Berglund, P., Demler, O., Jin, R., Merikangas, K. R., and Walters, E. E. (2005). Lifetime prevalence and age-of-onset distributions of DSM-IV disorders in the National Comorbidity Survey Replication. *Arch. Gen. Psychiatry* 62, 593–602. doi: 10.1001/archpsyc.62.7.768

Kim, K., and Smith, P. K. (1998). Childhood stress, behavioural symptoms and mother-daughter pubertal development. *J. Adolesc.* 21, 231–240. doi: 10.1006/jado.1998.0149

Koenen, K. C., and Widom, C. S. (2009). A prospective study of sex differences in the lifetime risk of posttraumatic stress disorder among abused and neglected children grown up. *J. Trauma. Stress* 22, 566–574. doi: 10.1002/jts.20478

Lau, C., Klinefelter, G., and Cameron, A. M. (1996). Reproductive development and functions in the rat after repeated maternal deprivation stress. *Fundam. Appl. Toxicol.* 30, 298–301. doi: 10.1006/faat.1996.0068

Manzano-Nieves, G., Gaillard, M., Gallo, M., and Bath, K. G. (2018). Early life stress impairs contextual threat expression in female, but not male, mice. *Behav. Neurosci.* 132, 247–257. doi: 10.1037/bne0000248

Marshall, L. M., Spiegelman, D., Goldman, M. B., Manson, J. E., Colditz, G. A., Barbieri, R. L., et al. (1998). A prospective study of reproductive factors and oral contraceptive use in relation to the risk of uterine leiomyomata. *Fertil. Steril.* 70, 432–439. doi: 10.1016/s0015-0282(98)00208-8

McIntosh, J., Anisman, H., and Merali, Z. (1999). Short- and long-periods of neonatal maternal separation differentially affect anxiety and feeding in adult rats: gender-dependent effects. *Dev. Brain Res.* 113, 97–106. doi: 10.1016/s0165-3806(99)00005-x

McPherson, C. P., Sellers, T. A., Potter, J. D., Bostick, R. M., and Folsom, A. R. (1996). Reproductive factors and risk of endometrial cancer. The Iowa Women's Health Study. *Am. J. Epidemiol.* 143, 1195–1202. doi: 10.1093/oxfordjournals.aje.a008707

Mendle, J., Ryan, R. M., and McKone, K. M. P. (2017). Age at menarche, depression, and antisocial behavior in adulthood. *Pediatrics* 141:e20171703. doi: 10.1542/peds.2017-1703

Mezzich, A. C., Giancola, P. R., Tarter, R. E., Lu, S., Parks, S. M., and Barrett, C. M. (1997). Violence, suicidality, and alcohol/drug use involvement in adolescent females with a psychoactive substance use disorder and controls. *Alcohol. Clin. Exp. Res.* 21, 1300–1307. doi: 10.1097/00000374-199710000-00021

Mishra, G. D., Cooper, R., Tom, S. E., and Kuh, D. (2009). Early life circumstances and their impact on menarche and menopause. *Womens Health* 5, 175–190. doi: 10.2217/17455057.5.2.175

Moffitt, T. E., Caspi, A., Belsky, J., and Silva, P. A. (1992). Childhood experience and the onset of menarche: a test of a sociobiological model. *Child Dev.* 63, 47–58. doi: 10.1111/j.1467-8624.1992.tb03594.x

Molet, J., Heins, K., Zhuo, X., Mei, Y. T., Regev, L., Baram, T. Z., et al. (2016). Fragmentation and high entropy of neonatal experience predict adolescent emotional outcome. *Transl. Psychiatry* 6:e702. doi: 10.1038/tp.2015.200

Nelson, J. F., Felicio, L. S., Randall, P. K., Sims, C., and Finch, C. E. (1982). A longitudinal study of estrous cyclicity in aging C57BL/6J mice: I. Cycle frequency, length and vaginal cytology. *Biol. Reprod.* 27, 327–339. doi: 10.1095/biolreprod27.2.327

Reid, B. M., Miller, B. S., Dorn, L. D., Desjardins, C., Donzella, B., and Gunnar, M. (2017). Early growth faltering in post-institutionalized youth and later anthropometric and pubertal development. *Pediatr. Res.* 82, 278–284. doi: 10.1038/pr.2017.35

Rhees, R. W., Lephart, E. D., and Eliason, D. (2001). Effects of maternal separation during early postnatal development on male sexual behavior and female reproductive function. *Behav. Brain Res.* 123, 1–10. doi: 10.1016/s0166-4328(00)00381-8

Rice, C. J., Sandman, C. A., Lenjavi, M. R., and Baram, T. Z. (2008). A novel mouse model for acute and long-lasting consequences of early life stress. *Endocrinology* 149, 4892–4900. doi: 10.1210/en.2008-0633

Shalev, I., and Belsky, J. (2016). Early-life stress and reproductive cost: a two-hit developmental model of accelerated aging? *Med. Hypotheses* 90, 41–47. doi: 10.1016/j.mehy.2016.03.002

Smith, G. D., Jackson, L. M., and Foster, D. L. (2002). Leptin regulation of reproductive function and fertility. *Theriogenology* 57, 73–86. doi: 10.1016/s0093-691x(01)00658-6

Vigersky, R. A., Andersen, A. E., Thompson, R. H., and Loriaux, D. L. (1977). Hypothalamic dysfunction in secondary amenorrhea associated with simple weight loss. *N. Engl. J. Med.* 297, 1141–1145. doi: 10.1056/NEJM197711242972103

Walker, C. D., Bath, K. G., Joels, M., Korosi, A., Larauche, M., Lucassen, P. J., et al. (2017). Chronic early life stress induced by limited bedding and nesting (LBN) material in rodents: critical considerations of methodology, outcomes and translational potential. *Stress* 20, 421–448. doi: 10.1080/10253890.2017.1343296

Walker, S. P., Chang, S. M., and Powell, C. A. (2007). The association between early childhood stunting and weight status in late adolescence. *Int. J. Obes.* 31, 347–352. doi: 10.1038/sj.ijo.0803383

Warren, M. P. (1980). The effects of exercise on pubertal progression and reproductive function in girls. *J. Clin. Endocrinol. Metab.* 51, 1150–1157. doi: 10.1210/jcem-51-5-1150

Widom, C. S. (1999). Posttraumatic stress disorder in abused and neglected children grown up. *Am. J. Psychiatry* 156, 1223–1229.

Yura, S., Ogawa, Y., Sagawa, N., Masuzaki, H., Itoh, H., Ebihara, K., et al. (2000). Accelerated puberty and late-onset hypothalamic hypogonadism in female transgenic skinny mice overexpressing leptin. *J. Clin. Invest.* 105, 749–755. doi: 10.1172/jci8353

Conflict of Interest Statement: The authors declare that the research was conducted in the absence of any commercial or financial relationships that could be construed as a potential conflict of interest.

frontiers in Molecular Neuroscience

PERSPECTIVE
published: 05 April 2019
doi: 10.3389/fnmol.2019.00077

Critical Period Regulation by Thyroid Hormones: Potential Mechanisms and Sex-Specific Aspects

Gervasio Batista[1] *and Takao K. Hensch*[1,2,3]*

[1]*Center for Brain Science, Department of Molecular Cellular Biology, Harvard University, Cambridge, MA, United States,*
[2]*FM Kirby Neurobiology Center, Department of Neurology, Boston Children's Hospital, Boston, MA, United States,*
[3]*International Research Center for Neurointelligence, University of Tokyo Institutes for Advanced Study, Tokyo, Japan*

Adequate perinatal levels of thyroid hormones (THs) are required for normal brain function and development. Studies in non-mammalian species suggest that TH might be involved in the regulation of critical periods (CPs) of heightened plasticity. Yet, it is largely unknown what mechanisms controlling such CPs might be under TH regulation. Here, we briefly review the influence of TH in early life across evolution. We discuss possible links between TH and known circuit and/or molecular mechanisms determining the timing of CPs of heightened brain plasticity. We focus on the role of parvalbumin-positive (PV) interneurons since their maturation defines CP onset and closure. Specifically, abnormal PV circuits are associated with low perinatal levels of TH, possibly because thyroid hypofunction may increase oxidative stress and/or dysregulate Otx2-mediated maturation of neuroprotective perineuronal nets. In addition, the level of cholinergic transmission is important for CP plasticity. Potentially, TH levels could affect gain changes in cholinergic transmission that can alter brain development. We believe that understanding how TH impacts CPs of circuit refinement will shed light onto the principles underlying normal developmental trajectories. Given that the thyroid gland expresses estrogen and androgen receptors, its activity can potentially be regulated differently between the sexes, contributing to sexually dimorphic behaviors.

Keywords: parvalbumin cell, perineuronal nets, oxidative stress, Otx2, acetylcholine

OPEN ACCESS

Edited by:
Jordan Marrocco,
Rockefeller University, United States

Reviewed by:
Yuri Bozzi,
University of Trento, Italy
Petra Wahle,
Ruhr University Bochum, Germany

***Correspondence:**
Takao K. Hensch
hensch@mcb.harvard.edu

Received: *06 December 2018*
Accepted: *11 March 2019*
Published: *05 April 2019*

Citation:
Batista G and Hensch TK (2019) Critical Period Regulation by Thyroid Hormones: Potential Mechanisms and Sex-Specific Aspects. Front. Mol. Neurosci. 12:77. doi: 10.3389/fnmol.2019.00077

INTRODUCTION

Thyroid hormones (THs) adjust a myriad of metabolic variables to suit environmental demands (Mullur et al., 2014). In the brain, TH milieu is particularly important for appropriate pre- and postnatal development and regulation of crucial cellular events (Zoeller, 2010). Thyroid gland hypofunction in pregnant women, for example, significantly increases autism risk (Román et al., 2013) and low perinatal TH levels are associated with persistent cognitive impairments and attentional deficits (reviewed in Salerno et al., 2016). Thus, it is clear that Thyroxine (T4) production, its conversion to Triiodothyronine (T3) and activation of Thyroid hormone receptors (THr) are vital processes to guarantee normal brain maturation. These events can be spatiotemporally regulated across development to control gene expression and shape brain organization. Precise orchestration of TH-signaling during windows of heightened plasticity might be particularly important. These critical periods (CPs) potently sculpt brain function in response

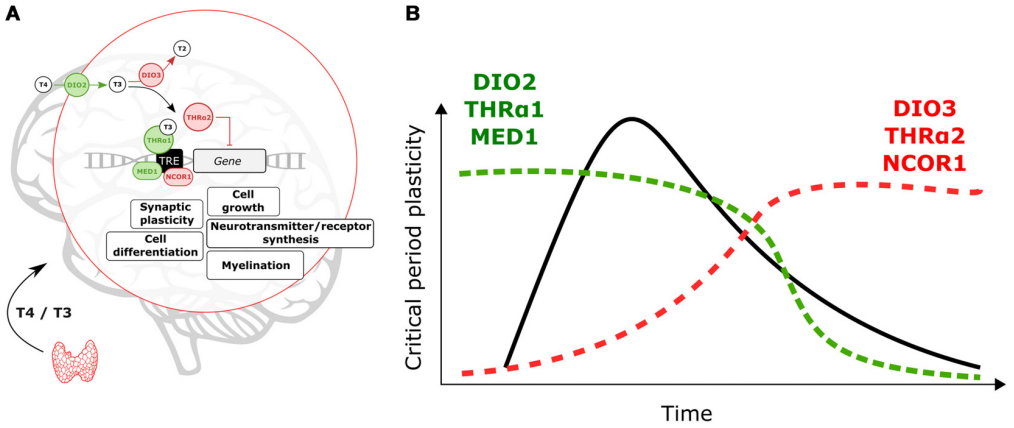

FIGURE 1 | Molecular events controlling locally thyroid hormone (TH)-signaling. **(A)** Deiodinases, THrα-variants and transcription co-regulators can enhance (green)/repress (red) T3-dependent transcription. **(B)** Expression levels of DIO2, THRα1 and MED1 are predicted to increase to support critical period (CP) onset and plasticity. After the CP breaks of TH-action (DIO3, THRα2 and nuclear receptor coregulator 1, NCOR1) could contribute to decreasing TH-signaling and T3-related changes in gene expression.

to early experience (Hensch, 2004) and may be dysregulated in psychiatric conditions (Marín, 2016). Hence, understanding the impact of TH on CP timing might yield new insights into the biological basis of brain disorders.

Here, we first review CPs where TH is known to play a major role. Second, we explore multiple molecular pathways by which CP plasticity could be linked to TH actions. Third, we consider regulation of thyroid gland function by sex hormones. Finally, we point to future directions that could shed light on the role of TH in the juvenile brain.

ACHIEVING SPATIOTEMPORAL SPECIFICITY THROUGH LOCAL REGULATION OF TH-SIGNALING

Changes in local T3 synthesis in the hypothalamus of birds mediate photoperiodic responses (Yoshimura et al., 2003). It is thus possible that on a developmental time scale local TH-signaling is achieved across cortical areas. As shown in **Figure 1A**, TH signaling is mediated by T3 the transcriptionally active hormone when bound to TH nuclear receptors (THr; Mullur et al., 2014). In the developing brain, the type-2 deiodinase (DIO2) locally converts T4 into T3 (Bárez-López et al., 2018). Instead, type-3 deiodinase (DIO3) is in charge of reducing cellular levels of T3 (Gereben et al., 2008). Levels of DIO2 and DIO3 can finely tune T3 availability at specific times during brain development (**Figure 1B**).

There are two types of THr, THrα and THrß. The THrα is widely expressed across the brain while THrß is predominantly expressed in subcortical brain areas (Flamant et al., 2017). Here, we will focus on THrα but it is possible that combinatorial effects of both receptor types shape brain maturation. Alternative splicing gives rise to two THrα variants, α1 and α2 (Hodin et al., 1990). T3-dependent transcription is mediated by THrα1 (Hodin et al., 1990). In contrast, the THrα2 variant does not bind to T3 and represses T3-dependent transcription (Hodin et al., 1990; Mullur et al., 2014). TH-signaling during CPs can be enhanced, or reduced, by altering expression levels of THrα1 and THrα2 (**Figure 1**).

In addition, transcription coregulators (enhancers/repressors) can tune T3-dependent transcription. The nuclear receptor coregulator 1 (NCOR1) is particularly important to regulate TH actions *in vivo* (Shimizu et al., 2015). Yet the expression of this repressor during brain development is poorly understood. The coactivator MED1 (Mediator of RNA polymerase II transcription subunit 1) enhances T3-dependent transcription (Park et al., 2005), which could contribute to enhance TH effects and oppose NCOR1 actions (**Figure 1**).

As shown in **Figure 1**, we expect that local enhancement of TH signaling is achieved early and during CPs through upregulation of DIO2, THRα1 and MED1. On the other hand, DIO3, THRα2 and NCOR1 upregulation upon CP closure can act as brakes for TH actions and associated changes in gene expression. We propose that from regulation of these elements, developmental changes in TH-signaling can contribute to the timing and plasticity of CPs. Moreover, it is possible that genetic and environmental insults disrupt local changes in TH signaling in early life to have major impacts on maturational brain trajectories.

TIME-CONSTRAINED EFFECTS OF THYROID HORMONES DURING DEVELOPMENT

TH-Signaling During CPs in Non-brain Tissue

Brief periods of high TH sensitivity characterize the maturation of body organs. A transient increase (between P5 and 13) in the THrα1/THrα2 ratio determines a CP for TH-dependent expression of hexose transporters within the jejunum of rats (Mochizuki et al., 2007). Similarly, renal development is also under TH control during a short period of time (Tan et al., 1997).

Before the kidney is innervated, THr regulates the expression of the adrenoreceptor α1, which transduce neurotrophic signals, exclusively within the first 3 weeks postpartum (Tan et al., 1997).

Time-Constrained Effects of TH in the Retina

In zebrafish, the thickness of the inner retinal layers responds to TH blockade within 65–66 h post fertilization but not in fully mature subjects (Reider and Connaughton, 2014). This CP was shown to be sensitive to temperature shifts (Reider and Connaughton, 2014), but the mechanisms underlying temperature sensitivity of TH actions remain unknown. Notably, the differential expression of THr-specific retinal layers is reported in chickens (Sjöberg et al., 1992) with limited explanation.

TH Actions and Cerebellar Development

Normal levels of perinatal TH are required for the correct development of cerebellar circuitry in rodents (Koibuchi, 2008). The dendritic complexity of Purkinje cells is heavily compromised in rats with low perinatal TH (Nicholson and Altman, 1972). Cerebellar connections might also be under TH control during the CP given that specific subsets of THr are expressed in different cells (Koibuchi, 2008). These findings indicate that dysregulation of thyroid function early in life may have a large impact on cerebellum-mediated motor function. Aberrant cerebellar development could lead to further cognitive impairments where this large processing structure is suspected to participate. The emergence of anomalous cerebellar-cortical communication during CPs has been linked to autistic disorders (Wang et al., 2014). Notably, dysregulation of TH signaling is also found in patients with autism (Yuen et al., 2015).

EARLY THYROID HORMONE LEVELS REGULATE COMPLEX BEHAVIORS

Thyroid function around birth is important for the development of a variety of behaviors across vertebrates. Perinatal TH are fundamental in humans (Törel Ergür et al., 2012), rodents (van Wijk et al., 2008), birds (Yamaguchi et al., 2012) and fish (Lema and Nevitt, 2004) to support different behaviors. Comparing the role of TH across these species could contribute to better understand their developmental role.

Perinatal Thyroid Hypofunction Has Long-Lasting Effects

Cognitive, verbal and motor deficits characterize patients with congenital hypothyroidism (Oerbeck et al., 2003; Kempers et al., 2006). Moreover, subclinical hypothyroidism of children and adolescents correlates with attention deficits (Törel Ergür et al., 2012). In rodents, low levels of TH lead to altered locomotion (Sadamatsu et al., 2006; van Wijk et al., 2008), impaired spatial memory (Sadamatsu et al., 2006) and reduced anxiety (Darbra et al., 1995). Genetic ablation of THrα and ß modify anxiety- and fear-related behaviors (Guadaño-Ferraz et al., 2003; Vasudevan et al., 2013). Interestingly, neonatal induced hypothyroidism also increases the number audiogenic seizures in adulthood (Yasuda et al., 2000), suggesting that TH deficits early in life may trigger a long-term imbalance between excitatory and inhibitory transmission.

Thyroid Hormone Functions During CPs in Non-mammalian Species

The role of TH during CPs is evolutionary conserved. Imprinting, the formation of a long-term memory within a sensitive period (Horn et al., 2001; Jin et al., 2016), requires activation of THr as demonstrated in chickens (Yamaguchi et al., 2012). This form of learning only occurs within the first 3 days after hatching unless chickens are treated with TH and the CP is reopened (Yamaguchi et al., 2012).

In salmon, where olfactory imprinting occurs (Bett et al., 2016), TH peak at the onset of the CP for memory formation (Lema and Nevitt, 2004). This has not been directly linked to experience-dependent behavioral plasticity, but T4 and T3 control cellular proliferation within the olfactory epithelium during the sensitive period (Lema and Nevitt, 2004). In turn, reorganization of peripheral olfactory processing could support imprinting by facilitating detection of specific odors.

Rising levels of TH have also been reported during the CP for song learning (Yamaguchi et al., 2017). While this correlation has not been shown to be causal, it is interesting that high levels of TH are present at the onset of several CPs (Lema and Nevitt, 2004; Yamaguchi et al., 2012, 2017). Thus, taken together the evidence gathered from mammalian and non-mammalian species supports that TH is highly active within the time-constrained developmental windows and regulate the organization of diverse and complex behaviors.

CP REGULATION THROUGH THYROID HORMONES: POTENTIAL LINKS

When vision from one eye is deprived during a specific window of time, binocular neurons in primary visual cortex (V1) lose their responsiveness to that visual input (Hubel and Wiesel, 1970). This process can lead to long-term blunted visual acuity, known as amblyopia (McKee et al., 2003). The study of ocular dominance plasticity (ODP) has shed light onto several circuits and molecular mechanisms controlling CPs. Here, we try to establish possible connections between such mechanisms and THr activation.

TH-Dependent Maturation of GABAergic Transmission Circuits

Pharmacological and genetic manipulation of inhibition bidirectionally affects CP timing for ODP (Hensch et al., 1998; Iwai et al., 2003; Hensch, 2005; Chattopadhyaya et al., 2007). While benzodiazepines can open V1 CP prematurely (Hensch et al., 1998), genetically-induced reduction of GABA synthesis delays ODP (Iwai et al., 2003; Chattopadhyaya et al., 2007). Several studies support a link between GABAergic transmission modulation and TH (reviewed in Wiens and Trudeau, 2006). Hence, TH could control CP timing through regulation of inhibitory transmission.

Glutamate is converted into GABA by the glutamate acid decarboxylate (GAD) enzyme. In vertebrates, the isoforms GAD65 and GAD67 mediate GABA synthesis (Fenalti et al., 2007). *In vitro* and *in vivo* studies demonstrated that TH regulates GAD expression in the brain (Wiens and Trudeau, 2006). Interestingly, GAD65 and GAD67 expression is more sensitive to TH around birth compared to adulthood (Wiens and Trudeau, 2006) and is spatiotemporally regulated in rats (Popp et al., 2009). Whether the spatiotemporal control of GAD expression and function responds to differential TH-signaling across brain regions remains to be tested.

In addition to GABA synthesis, TH can influence other aspects of inhibitory networks. Early in development TH shapes the morphology and connectivity of GABAergic cells (Westerholz et al., 2013). These effects are mediated by trkb and mTOR pathways (Westerholz et al., 2013). Interestingly, mTOR is also recruited by TH to promote behavioral plasticity during the CP for imprinting in chickens (Batista et al., 2018). Thus, TH/mTOR signaling appears to play a major role during early life, potentially, through regulation of GABAergic transmission. Supporting this view, a recent study showed that TH control a developmental switch in GABAa/GABAb receptors to open the CP for imprinting in chicks (Aoki et al., 2018).

PV Maturation Requires Normal Levels of TH

Increased inhibitory transmission mediates CP opening in V1 (Hensch et al., 1998). Yet ODP plasticity specifically involves the activation of GABA-receptors (GABARs) containing the subunit α1 (Fagiolini et al., 2004). This subunit is mostly expressed, and targeted, by parvalbumin-positive interneurons (PV; Fagiolini et al., 2004). The experience-dependent maturation of PV circuits opens the CP in V1 (Sugiyama et al., 2008) and plays a similar role in other brain areas (Spatazza et al., 2013). PV cells are particularly sensitive to perinatal TH levels. Hence, TH impact on PV neuron maturation might be crucial to set CP timing not only in V1 (**Figure 2**). In rat neocortex, perinatal-induced hypothyroidism decreases PV expression (Berbel et al., 1996; Royland et al., 2008). TH-mediated impairments in PV expression has been also found in the hippocampus of rats, an area extremely responsive to perinatal TH levels (Gould et al., 1990b; Gilbert et al., 2007; Sawano et al., 2013). Other brain regions where TH developmentally regulate PV expression include the hypothalamus (Harder et al., 2018) and the striatum (Bode et al., 2017). Given the importance of PV circuits in CP regulation, it is likely that perinatal TH deficits disrupt CP timing across brain regions, which can be adequately tested in sensory systems.

Otx2 Expression Is Regulated by TH

The transcription factor Otx2 is crucial for non-cell autonomous PV maturation (Sugiyama et al., 2008). Experience-dependent accumulation of Otx2 derived from the retina (Sugiyama et al., 2008) and choroid plexus (Spatazza et al., 2013) triggers the onset of the CP. Two facts relate TH and Otx2. Transthyretin, the protein transporting TH into the cerebrospinal fluid, is synthesized by the choroid plexus (Richardson et al., 2015). Yet, more importantly, Otx2 production can be regulated by THr activation as shown in midbrain stem cells (Chen et al., 2015). Whether TH controls Otx2 synthesis in the choroid plexus remains unknown. But given its role in midbrain (Chen et al., 2015), it is possible that TH acts as a permissive signal to set the onset of the CP by enhancing Otx2 production and PV maturation (**Figure 2**).

Oxidative Stress Is Affected by Thyroid Function

Fast-spiking properties of PV cells impose a heavy metabolic burden rendering them susceptible to oxidative stress (Cabungcal et al., 2013). This particular feature is thought to underlie their impairment in human patients with mental illness, such as psychosis (Andreazza et al., 2008; Yao and Keshavan, 2011). Unchecked oxidative stress within PV cells also leads to aberrantly extended V1 plasticity (Morishita et al., 2015), thus demonstrating the importance of redox regulation for normal CP timing. Human studies indicate that hypothyroid patients (Resch et al., 2002) and subclinical low levels of TH (Santi et al., 2012) are associated with a surge in oxidative stress. Mechanisms

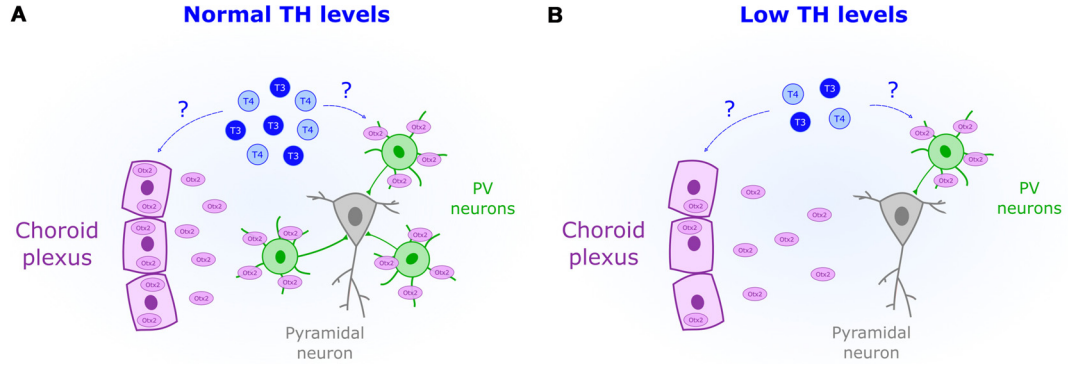

FIGURE 2 | Reduced perinatal levels of THs (blue) are associated with a decreased presence of parvalbumin-positive neurons (PV). **(A)** Normal levels of TH could act as permissive signals for CP onset by increasing Otx2 (purple) synthesis in the choroid plexus. **(B)** Downregulation of Otx2 expression in the choroid plexus could mediate the observed impairment in PV maturation under low levels of TH.

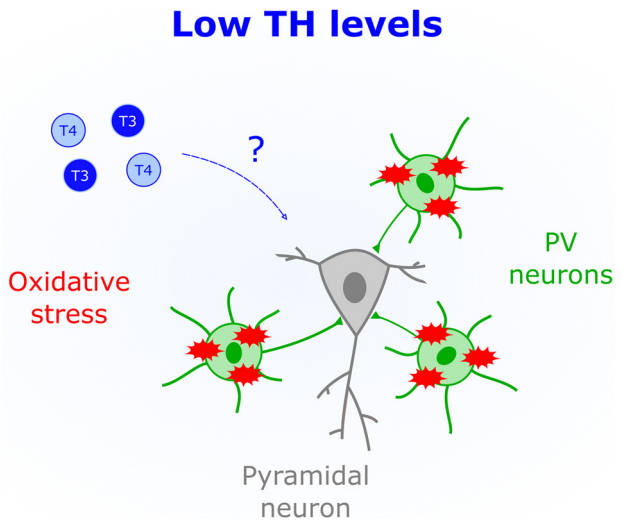

FIGURE 3 | Low levels of THs (blue) correlate with increased oxidative stress. The schematic shows that parvalbumin-positive cells (PV), but not pyramidal cells, are particularly sensitive to oxidative stress, which could mediate brain deficits triggered by low perinatal TH levels.

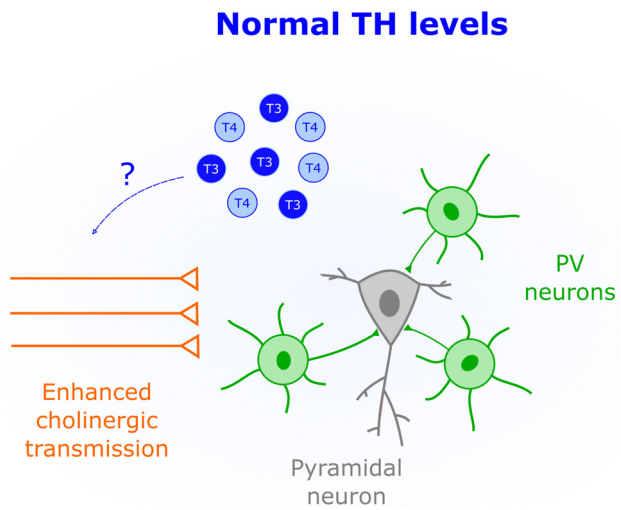

FIGURE 4 | Enhanced cholinergic transmission is characteristic of CPs. An important role of TH (blue) early in life could be to increase the acetylcholine synthesis and release.

underlying TH-mediated oxidative stress are not fully elucidated; however, it has been suggested that hypothyroidism reduces the presence of antioxidants (Mancini et al., 2016). One such agent, glutathione, impacts CP duration (Morishita et al., 2015). Therefore, TH actions in early life could include regulating antioxidant synthesis within PV circuits (**Figure 3**).

TH-Mediated Control of Cholinergic Transmission

Activation of cholinergic and muscarinic receptors by acetylcholine underlies synaptic plasticity and attention (Picciotto et al., 2012). Thus, changing the gain of cholinergic transmission over development appears is a powerful mechanism that constrains plasticity to specific time windows. Indeed, in V1 the protein Lynx1 dampens the activity of cholinergic receptors to close the CP (Morishita et al., 2010). Interestingly, non-pathological low levels of TH correlate with attention deficits in children and adolescents (Törel Ergür et al., 2012). This effect might be due to decreased cholinergic transmission since cell-specific optogenetics demonstrated that cholinergic inputs play an important role in attention (Luchicchi et al., 2014). It is thus possible that early life TH levels influence cholinergic transmission to regulate plasticity. Additional evidence supporting this view comes from *in vitro* studies where both release and synthesis of acetylcholine is enhanced by T4 application (Landa et al., 1991). Additionally, cholinergic deficits in the Snell Dwarf Mouse are corrected by T4 injections (Fuhrmann et al., 1986), suggesting that TH-mediated modulation of cholinergic transmission occurs *in vivo*. Further research is needed to establish a causal link between TH-mediated changes in cholinergic signaling and CP regulation (**Figure 4**).

INFLUENCES OF SEX HORMONES ON THYROID FUNCTION

Can the developmental role of TH contribute to sex differences in the brain? Is the thyroid gland sensitive to gonadal hormones? Do male and female thyroid glands respond differently to environmental insults? These sorts of questions remain largely unanswered, but they might be critical to uncovering how the role of TH during CPs could relate to sex-differences in the brain.

Sex-Specific Behavioral Plasticity in Birds During CPs

Filial imprinting in birds is tightly associated with TH levels (Yamaguchi et al., 2012). Historically, imprinting studies in chickens have not distinguished between male and female learning mechanisms. However, subtle differences have been reported (Miura and Matsushima, 2012). For example, male chickens have stronger innate preferences for biologically moving objects compared to females. It remains unclear whether these differences arise from TH-dependent organization of imprinted circuits or not. To address this, it would be important to assess whether thyroid function is comparable across sexes at hatching. In Zebra Finches, where males but not females develop a song over a CP, TH levels rise earlier in males (Yamaguchi et al., 2017). This increase in TH levels correlates with the appearance of PV in regions controlling song production (Balmer et al., 2009). Hence, it is possible that dimorphic TH levels contribute to sex-specific behaviors later controlled by PV maturation.

Gonadal Steroids Control Thyroid Gland Growth

Androgens and estrogens enhance thyroid stimulating hormone (TSH) effects on the thyroid gland in a sex-specific manner

(Banu et al., 2002; Sakhila Banu and Aruldhas, 2002). Receptors for gonadal steroids have been reported to enhance thyroid gland growth and function (Sakhila Banu and Aruldhas, 2002). Thus, when the production of gonadal hormones increases around puberty, thyroid gland growth is heightened (Sakhila Banu and Aruldhas, 2002). In turn, this may generate dimorphic developmental trajectories in males and females since the latter enter adolescence earlier (Brenhouse and Andersen, 2011). Yet it is unknown how androgens and estrogens interact with TH to sculpt the brain and whether this interaction underlies sexual dimorphism.

Sex-Specific Remodeling of Hippocampal Circuits

In mouse hippocampus, perinatal TH injections trigger sex- and sub-region specific effects (Gould et al., 1990b). Pyramidal cells in the CA3 area of male mice treated with thyroxine around birth, show fewer primary dendrites than females receiving the same treatment (Gould et al., 1990b). Notably, these structural changes could be tracked throughout life and are not detected in the nearby CA1 subregion (Gould et al., 1990b). Therefore, in addition to changes in thyroid function in adolescence, there is already a sexually dimorphic sensitivity to TH levels at birth that can cause long-lasting reorganization of neural circuits.

Thyroid Dysfunction Prevails in Women

Women exhibit a higher risk for thyroid malfunction compared to men (Bauer et al., 2014). The underlying mechanism for this susceptibility is under investigation. In rats, it has been demonstrated that an estrogen receptor-mediated increase in oxidative stress is responsible for the prevalence of thyroid dysfunction in females (Fortunato et al., 2014). This is particularly important considering that patients with bipolar disorders with comorbidity of thyroid problems is higher in women (Bauer et al., 2014). Further investigation is required to clarify the role of TH in female bipolar disorders (Bauer et al., 2014). One possible scenario is that sex-specific vulnerability to some psychiatric diseases arises from abnormal thyroid gland function in women.

Environmental Insults Can Trigger Sexually Dimorphic Thyroid Impairments

Neurotoxins affect the thyroid gland differently in men and women, thus leading to TH-mediated impairments in neurocognitive performance. Exposure to the industrial surfactant perfluorooctanoic acid is highly associated with thyroid dysfunction in women (Melzer et al., 2010). Similarly, exposure to radiation correlates with thyroid abnormalities in both men and women but is more prevalent within the latter (Lyon et al., 2006). These studies point to women as having an enhanced susceptibility to environmental risk factors. However, other unknown factors could be linked to thyroid dysfunction in men. For example, breathing second-hand smoke acutely enhances TH production in men (Flouris et al., 2008). Therefore, it might be the case that certain neurotoxins have sex-specific impacts on thyroid physiology indirectly leading to TH-mediated brain deficits.

CONCLUDING REMARKS AND FUTURE DIRECTIONS

Shifts in the onset and closure of windows of enhanced plasticity could lead to characteristic features of some neuropsychiatric disorders such as autism (LeBlanc and Fagiolini, 2011), schizophrenia and bipolar disorder (Yao and Keshavan, 2011; Morishita et al., 2015). A deeper understanding of the interaction between gonadal hormones and thyroid function can shed light onto novel principles underlying sex-differences in brain organization. Future research might fill the gap between CPs regulation and TH signaling. In addition, the circuits that are sensitive to perinatal T4 and T3 levels need to be identified. Given that hypothyroidism has been associated with functional and structural alterations within the cerebellum (Koibuchi, 2008), hippocampus (Gould et al., 1990a; Gilbert et al., 2007), cortex (Royland et al., 2008) and subcortical nuclei (Yasuda et al., 2000), TH are expected to have global impacts on brain functions. Recently, several studies suggest a link between gut microbiota and the brain (Dinan and Cryan, 2017). THs might also be important players in this poorly understood relationship. Research in humans and rodents suggest that intestinal microbiota influences thyroid function, the availability of iodine and selenium and T4 absorption (Virili and Centanni, 2015). This could be relevant not only for adult brain function but also early in life during the CPs of plasticity. In summary, neonatal thyroid function appears to be tightly related to developmental events that are constrained to specific windows of time across evolution. Yet more research is needed to understand how THs might regulate the mechanisms controlling CPs timing and plasticity.

AUTHOR CONTRIBUTIONS

GB and TH wrote the manuscript.

FUNDING

This work was supported by the JPB Foundation, Bezos Foundation and National Institute of Mental Health (NIMH) Silvio Conte Center (P50MH094271) to TH.

REFERENCES

Andreazza, A. C., Kauer-Sant'Anna, M., Frey, B. N., Bond, D. J., Kapczinski, F., Young, L. T., et al. (2008). Oxidative stress markers in bipolar disorder: a meta-analysis. *J. Affect. Disord.* 111, 135–144. doi: 10.1016/j.jad.2008.04.013

Aoki, N., Yamaguchi, S., Fujita, T., Mori, C., Fujita, E., Matsushima, T., et al. (2018). GABA-A and GABA-B receptors in filial imprinting linked with opening and closing of the sensitive period in domestic chicks (*Gallus gallus domesticus*). *Front. Physiol.* 9:1837. doi: 10.3389/fphys.2018.01837

Balmer, T. S., Carels, V. M., Frisch, J. L., and Nick, T. A. (2009). Modulation of perineuronal nets and parvalbumin with developmental song learning. *J. Neurosci.* 29, 12878–12885. doi: 10.1523/jneurosci.2974-09.2009

Banu, S. K., Govindarajulu, P., and Aruldhas, M. M. (2002). Testosterone and estradiol up-regulate androgen and estrogen receptors in immature and adult rat thyroid glands *in vivo*. *Steroids* 67, 1007–1014. doi: 10.1016/s0039-128x(02)00063-6

Bárez-López, S., Obregon, M. J., Bernal, J., and Guadaño-Ferraz, A. (2018). Thyroid hormone economy in the perinatal mouse brain: implications for cerebral cortex development. *Cereb. Cortex* 28, 1783–1793. doi: 10.1093/cercor/bhx088

Batista, G., Johnson, J. L., Dominguez, E., Costa-Mattioli, M., and Pena, J. L. (2018). Regulation of filial imprinting and structural plasticity by mTORC1 in newborn chickens. *Sci. Rep.* 8:8044. doi: 10.1038/s41598-018-26479-1

Bauer, M., Glenn, T., Pilhatsch, M., Pfennig, A., and Whybrow, P. C. (2014). Gender differences in thyroid system function: relevance to bipolar disorder and its treatment. *Bipolar Disord.* 16, 58–71. doi: 10.1111/bdi.12150

Berbel, P., Marco, P., Cerezo, J. R., and DeFelipe, J. (1996). Distribution of parvalbumin immunoreactivity in the neocortex of hypothyroid adult rats. *Neurosci. Lett.* 204, 65–68. doi: 10.1016/0304-3940(96)12318-1

Bett, N. N., Hinch, S. G., Dittman, A. H., and Yun, S.-S. (2016). Evidence of olfactory imprinting at an early life stage in pink salmon (*Oncorhynchus gorbuscha*). *Sci. Rep.* 6:36393. doi: 10.1038/srep36393

Bode, C., Richter, F., Spröte, C., Brigadski, T., Bauer, A., Fietz, S., et al. (2017). Altered postnatal maturation of striatal GABAergic interneurons in a phenotypic animal model of dystonia. *Exp. Neurol.* 287, 44–53. doi: 10.1016/j.expneurol.2016.10.013

Brenhouse, H. C., and Andersen, S. L. (2011). Developmental trajectories during adolescence in males and females: a cross-species understanding of underlying brain changes. *Neurosci. Biobehav. Rev.* 35, 1687–1703. doi: 10.1016/j.neubiorev.2011.04.013

Cabungcal, J. H., Steullet, P., Kraftsik, R., Cuenod, M., and Do, K. Q. (2013). Early-life insults impair parvalbumin interneurons via oxidative stress: reversal by N-acetylcysteine. *Biol. Psychiatry* 73, 574–582. doi: 10.1016/j.biopsych.2012.09.020

Chattopadhyaya, B., Di Cristo, G., Wu, C. Z., Knott, G., Kuhlman, S., Fu, Y., et al. (2007). GAD67-mediated GABA synthesis and signaling regulate inhibitory synaptic innervation in the visual cortex. *Neuron* 54, 889–903. doi: 10.1016/j.neuron.2007.05.015

Chen, C., Ma, Q., Chen, X., Zhong, M., Deng, P., Zhu, G., et al. (2015). Thyroid hormone-Otx2 signaling is required for embryonic ventral midbrain neural stem cells differentiated into dopamine neurons. *Stem Cells Dev.* 24, 1751–1765. doi: 10.1089/scd.2014.0489

Darbra, S., Balada, F., Garau, A., Gatell, P., Sala, J., and Marti-Carbonell, M. A. (1995). Perinatal alterations of thyroid hormones and behaviour in adult rats. *Behav. Brain Res.* 68, 159–164. doi: 10.1016/0166-4328(94)00166-d

Dinan, T. G., and Cryan, J. F. (2017). Gut-brain axis in 2016: brain-gut-microbiota axis — mood, metabolism and behaviour. *Nat. Rev. Gastroenterol. Hepatol.* 14, 69–70. doi: 10.1038/nrgastro.2016.200

Fagiolini, M., Fritschy, J.-M., Löw, K., Möhler, H., Rudolph, U., and Hensch, T. K. (2004). Specific GABAA circuits for visual cortical plasticity. *Science* 303, 1681–1683. doi: 10.1126/science.1091032

Fenalti, G., Law, R. H. P., Buckle, A. M., Langendorf, C., Tuck, K., Rosado, C. J., et al. (2007). GABA production by glutamic acid decarboxylase is regulated by a dynamic catalytic loop. *Nat. Struct. Mol. Biol.* 14, 280–286. doi: 10.1038/nsmb1228

Flamant, F., Gauthier, K., and Richard, S. (2017). Genetic investigation of thyroid hormone receptor function in the developing and adult brain. *Curr. Top. Dev. Biol.* 125, 303–335. doi: 10.1016/bs.ctdb.2017.01.001

Flouris, A. D., Metsios, G. S., Jamurtas, A. Z., and Koutedakis, Y. (2008). Sexual dimorphism in the acute effects of secondhand smoke on thyroid hormone secretion, inflammatory markers and vascular function. *Am. J. Physiol. Endocrinol. Metab.* 294, E456–E462. doi: 10.1152/ajpendo.00699.2007

Fortunato, R. S., Ferreira, A. C. F., Hecht, F., Dupuy, C., and Carvalho, D. P. (2014). Sexual dimorphism and thyroid dysfunction: a matter of oxidative stress? *J. Endocrinol.* 221, R31–R40. doi: 10.1530/joe-13-0588

Fuhrmann, G., Kempf, E., and Ebel, A. (1986). Effects of hormone therapy on the central cholinergic neurotransmission of the snell dwarf mouse. *J. Neurosci. Res.* 16, 527–539. doi: 10.1002/jnr.490160308

Gereben, B., Zeöld, A., Dentice, M., Salvatore, D., and Bianco, A. C. (2008). Activation and inactivation of thyroid hormone by deiodinases: local action with general consequences. *Cell. Mol. Life Sci.* 65, 570–590. doi: 10.1007/s00018-007-7396-0

Gilbert, M. E., Sui, L., Walker, M. J., Anderson, W., Thomas, S., Smoller, S. N., et al. (2007). Thyroid hormone insufficiency during brain development reduces parvalbumin immunoreactivity and inhibitory function in the hippocampus. *Endocrinology* 148, 92–102. doi: 10.1210/en.2006-0164

Gould, E., Allan, M. D., and McEwen, B. S. (1990a). Dendritic spine density of adult hippocampal pyramidal cells is sensitive to thyroid hormone. *Brain Res.* 525, 327–329. doi: 10.1016/0006-8993(90)90884-e

Gould, E., Westlind-Danielsson, A., Frankfurt, M., and McEwen, B. S. (1990b). Sex differences and thyroid hormone sensitivity of hippocampal pyramidal cells. *J. Neurosci.* 10, 996–1003. doi: 10.1523/jneurosci.10-03-00996.1990

Guadaño-Ferraz, A., Benavides-Piccione, R., Venero, C., Lancha, C., Vennström, B., Sandi, C., et al. (2003). Lack of thyroid hormone receptor α1 is associated with selective alterations in behavior and hippocampal circuits. *Mol. Psychiatry* 8, 30–38. doi: 10.1038/sj.mp.4001196

Harder, L., Dudazy-Gralla, S., Müller-Fielitz, H., Hjerling Leffler, J., Vennström, B., Heuer, H., et al. (2018). Maternal thyroid hormone is required for parvalbumin neurone development in the anterior hypothalamic area. *J. Neuroendocrinol.* 30:e12573. doi: 10.1111/jne.12573

Hensch, T. K. (2004). Critical period regulation. *Annu. Rev. Neurosci.* 27, 549–579. doi: 10.1146/annurev.neuro.27.070203.144327

Hensch, T. K. (2005). Critical period plasticity in local cortical circuits. *Nat. Rev. Neurosci.* 6, 877–888. doi: 10.1038/nrn1787

Hensch, T. K., Fagiolini, M., Mataga, N., Stryker, M. P., Baekkeskov, S., and Kash, S. F. (1998). Local GABA circuit control of experience-dependent plasticity in developing visual cortex. *Science* 282, 1504–1508. doi: 10.1126/science.282.5393.1504

Hodin, R. A., Lazar, M. A., and Chin, W. W. (1990). Differential and tissue-specific regulation of the multiple rat c-erbA messenger RNA species by thyroid hormone. *J. Clin. Invest.* 85, 101–105. doi: 10.1172/jci114398

Horn, G., Nicol, A. U., and Brown, M. W. (2001). Tracking memory's trace. *Proc. Natl. Acad. Sci. U S A* 98, 5282–5287. doi: 10.1073/pnas.091094798

Hubel, D. H., and Wiesel, T. N. (1970). The period of susceptibility to the physiological effects of unilateral eye closure in kittens. *J. Physiol.* 206, 419–436. doi: 10.1113/jphysiol.1970.sp009022

Iwai, Y., Fagiolini, M., Obata, K., and Hensch, T. K. (2003). Rapid critical period induction by tonic inhibition in visual cortex. *J. Neurosci.* 23, 6695–6702. doi: 10.1523/jneurosci.23-17-06695.2003

Jin, X., Pokala, N., and Bargmann, C. I. (2016). Distinct circuits for the formation and retrieval of an imprinted olfactory memory. *Cell* 164, 632–643. doi: 10.1016/j.cell.2016.01.007

Kempers, M. J. E., van der Sluijs Veer, L., Nijhuis-van der Sanden, M. W. G., Kooistra, L., Wiedijk, B. M., Faber, I., et al. (2006). Intellectual and motor development of young adults with congenital hypothyroidism diagnosed by neonatal screening. *J. Clin. Endocrinol. Metab.* 91, 418–424. doi: 10.1210/jc.2005-1209

Koibuchi, N. (2008). The role of thyroid hormone on cerebellar development. *Cerebellum* 7, 530–533. doi: 10.1007/s12311-008-0069-1

Landa, M. E., González Burgos, G., and Cardinali, D. P. (1991). *In vitro* effect of ithyroxine on cholinergic neurotransmission in rat sympathetic superior cervical ganglion. *Neuroendocrinology* 54, 552–558. doi: 10.1159/000125959

LeBlanc, J. J., and Fagiolini, M. (2011). Autism: a "critical period" disorder? *Neural Plast.* 2011:921680. doi: 10.1155/2011/921680

Lema, S. C., and Nevitt, G. A. (2004). Evidence that thyroid hormone induces olfactory cellular proliferation in salmon during a sensitive period for imprinting. *J. Exp. Biol.* 207, 3317–3327. doi: 10.1242/jeb.01143

Luchicchi, A., Bloem, B., Viaña, J. N. M., Mansvelder, H. D., and Role, L. W. (2014). Illuminating the role of cholinergic signaling in circuits of attention and emotionally salient behaviors. *Front. Synaptic Neurosci.* 6:24. doi: 10.3389/fnsyn.2014.00024

Lyon, J. L., Alder, S. C., Stone, M. B., Scholl, A., Reading, J. C., Holubkov, R., et al. (2006). Thyroid disease associated with exposure to the Nevada nuclear

weapons test site radiation: a reevaluation based on corrected dosimetry and examination data. *Epidemiology* 17, 604–614. doi: 10.1097/01.ede.0000240540.79983.7f

Mancini, A., Di Segni, C., Raimondo, S., Olivieri, G., Silvestrini, A., Meucci, E., et al. (2016). Thyroid hormones, oxidative stress, and inflammation. *Mediators Inflamm.* 2016:6757154. doi: 10.1155/2016/6757154

Marín, O. (2016). Developmental timing and critical windows for the treatment of psychiatric disorders. *Nat. Med.* 22, 1229–1238. doi: 10.1038/nm.4225

McKee, S. P., Levi, D. M., and Movshon, J. A. (2003). The pattern of visual deficits in amblyopia. *J. Vis.* 3, 380–405. doi: 10.1167/3.5.5

Melzer, D., Rice, N., Depledge, M. H., Henley, W. E., and Galloway, T. S. (2010). Association between serum perfluorooctanoic acid (PFOA) and thyroid disease in the U.S. National Health and Nutrition Examination Survey. *Environ. Health Perspect.* 118, 686–692. doi: 10.1289/ehp.0901584

Miura, M., and Matsushima, T. (2012). Preference for biological motion in domestic chicks: sex-dependent effect of early visual experience. *Anim. Cogn.* 15, 871–879. doi: 10.1007/s10071-012-0514-x

Mochizuki, K., Yagi, E., Sakaguchi, N., Mochizuki, H., Takabe, S., Kuranuki, S., et al. (2007). The critical period for thyroid hormone responsiveness through thyroid hormone receptor isoform α in the postnatal small intestine. *Biochim. Biophys. Acta* 1770, 609–616. doi: 10.1016/j.bbagen.2006.12.011

Morishita, H., Cabungcal, J.-H., Chen, Y., Do, K. Q., and Hensch, T. K. (2015). Prolonged period of cortical plasticity upon redox dysregulation in fast-spiking interneurons. *Biol. Psychiatry* 78, 396–402. doi: 10.1016/j.biopsych.2014.12.026

Morishita, H., Miwa, J. M., Heintz, N., and Hensch, T. K. (2010). Lynx1, a cholinergic brake, limits plasticity in adult visual cortex. *Science* 330, 1238–1240. doi: 10.1126/science.1195320

Mullur, R., Liu, Y.-Y., and Brent, G. A. (2014). Thyroid hormone regulation of metabolism. *Physiol. Rev.* 94, 355–382. doi: 10.1152/physrev.00030.2013

Nicholson, J. L., and Altman, J. (1972). The effects of early hypo- and hyperthyroidism on the development of the rat cerebellar cortex. II. Synaptogenesis in the molecular layer. *Brain Res.* 44, 25–36. doi: 10.1016/0006-8993(72)90363-0

Oerbeck, B., Sundet, K., Kase, B. F., and Heyerdahl, S. (2003). Congenital hypothyroidism: influence of disease severity and L-thyroxine treatment on intellectual, motor and school-associated outcomes in young adults. *Pediatrics* 112, 923–930. doi: 10.1542/peds.112.4.923

Park, S. W., Li, G., Lin, Y. P., Barrero, M. J., Ge, K., Roeder, R. G., et al. (2005). Thyroid hormone-induced juxtaposition of regulatory elements/factors and chromatin remodeling of Crabp1 dependent on MED1/TRAP220. *Mol. Cell* 19, 643–653. doi: 10.1016/j.molcel.2005.08.008

Picciotto, M. R., Higley, M. J., and Mineur, Y. S. (2012). Acetylcholine as a neuromodulator: cholinergic signaling shapes nervous system function and behavior. *Neuron* 76, 116–129. doi: 10.1016/j.neuron.2012.08.036

Popp, A., Urbach, A., Witte, O. W., and Frahm, C. (2009). Adult and embryonic GAD transcripts are spatiotemporally regulated during postnatal development in the rat brain. *PLoS One* 4:e4371. doi: 10.1371/journal.pone.0004371

Reider, M., and Connaughton, V. P. (2014). Effects of low-dose embryonic thyroid disruption and rearing temperature on the development of the eye and retina in zebrafish. *Birth Defects Res. B Dev. Reprod. Toxicol.* 101, 347–354. doi: 10.1002/bdrb.21118

Resch, U., Helsel, G., Tatzber, F., and Sinzinger, H. (2002). Antioxidant status in thyroid dysfunction. *Clin. Chem. Lab. Med.* 40, 1132–1134. doi: 10.1515/CCLM.2002.198

Richardson, S. J., Wijayagunaratne, R. C., D'Souza, D. G., Darras, V. M., and Van Herck, S. L. J. (2015). Transport of thyroid hormones via the choroid plexus into the brain: the roles of transthyretin and thyroid hormone transmembrane transporters. *Front. Neurosci.* 9:66. doi: 10.3389/fnins.2015.00066

Román, G. C., Ghassabian, A., Bongers-Schokking, J. J., Jaddoe, V. W. V., Hofman, A., De Rijke, Y. B., et al. (2013). Association of gestational maternal hypothyroxinemia and increased autism risk. *Ann. Neurol.* 74, 733–742. doi: 10.1002/ana.23976

Royland, J. E., Parker, J. S., and Gilbert, M. E. (2008). A genomic analysis of subclinical hypothyroidism in hippocampus and neocortex of the developing rat brain. *J. Neuroendocrinol.* 20, 1319–1338. doi: 10.1111/j.1365-2826.2008.01793.x

Sadamatsu, M., Kanai, H., Xu, X., Liu, Y., and Kato, N. (2006). Review of animal models for autism: implication of thyroid hormone. *Congenit. Anom.* 46, 1–9. doi: 10.1111/j.1741-4520.2006.00094.x

Sakhila Banu, K., and Aruldhas, M. M. (2002). Sex steroids regulate TSH-induced thyroid growth during sexual maturation in wistar rats. *Exp. Clin. Endocrinol. Diabetes* 110, 37–42. doi: 10.1055/s-2002-19993

Salerno, M., Capalbo, D., Cerbone, M., and De Luca, F. (2016). Subclinical hypothyroidism in childhood — current knowledge and open issues. *Nat. Rev. Endocrinol.* 12, 734–746. doi: 10.1038/nrendo.2016.100

Santi, A., Duarte, M. M. M. F., De Menezes, C. C., and Loro, V. L. (2012). Association of lipids with oxidative stress biomarkers in subclinical hypothyroidism. *Int. J. Endocrinol.* 2012:856359. doi: 10.1155/2012/856359

Sawano, E., Takahashi, M., Negishi, T., and Tashiro, T. (2013). Thyroid hormone-dependent development of the GABAergic pre- and post-synaptic components in the rat hippocampus. *Int. J. Dev. Neurosci.* 31, 751–761. doi: 10.1016/j.ijdevneu.2013.09.007

Shimizu, H., Astapova, I., Ye, F., Bilban, M., Cohen, R. N., and Hollenberg, A. N. (2015). NCoR1 and SMRT play unique roles in thyroid hormone action *in vivo*. *Mol. Cell. Biol.* 35, 555–565. doi: 10.1128/mcb.01208-14

Sjöberg, M., Vennström, B., and Forrest, D. (1992). Thyroid hormone receptors in chick retinal development: differential expression of mRNAs for alpha and N-terminal variant beta receptors. *Development* 114, 39–47.

Spatazza, J., Lee, H. H. C., Di Nardo, A. A., Tibaldi, L., Joliot, A., Hensch, T. K., et al. (2013). Choroid-plexus-derived Otx2 homeoprotein constrains adult cortical plasticity. *Cell Rep.* 3, 1815–1823. doi: 10.1016/j.celrep.2013.05.014

Sugiyama, S., Di Nardo, A. A., Aizawa, S., Matsuo, I., Volovitch, M., Prochiantz, A., et al. (2008). Experience-dependent transfer of Otx2 homeoprotein into the visual cortex activates postnatal plasticity. *Cell* 134, 508–520. doi: 10.1016/j.cell.2008.05.054

Tan, J. P., Seidler, F. J., Schwinn, D. A., Page, S. O., and Slotkin, T. A. (1997). A critical period for the role of thyroid hormone in development of renal α-adrenergic receptors. *Pediatr. Res.* 42, 93–102. doi: 10.1203/00006450-199707000-00015

Törel Ergür, A., Taner, Y., Ata, E., Melek, E., Erdoğan Bakar, E., and Sancak, T. (2012). Neurocognitive functions in children and adolescents with subclinical hypothyroidism. *J. Clin. Res. Pediatr. Endocrinol.* 4, 21–24. doi: 10.4274/jcrpe.497

van Wijk, N., Rijntjes, E., and Van De Heijning, B. J. M. (2008). Perinatal and chronic hypothyroidism impair behavioural development in male and female rats. *Exp. Physiol.* 93, 1199–1209. doi: 10.1113/expphysiol.2008.042416

Vasudevan, N., Morgan, M., Pfaff, D., and Ogawa, S. (2013). Distinct behavioral phenotypes in male mice lacking the thyroid hormone receptor α 1 or β isoforms. *Horm. Behav.* 63, 742–751. doi: 10.1016/j.yhbeh.2013.03.015

Virili, C., and Centanni, M. (2015). Does microbiota composition affect thyroid homeostasis? *Endocrine* 49, 583–587. doi: 10.1007/s12020-014-0509-2

Wang, S. S. H., Kloth, A. D., and Badura, A. (2014). The cerebellum, sensitive periods, and autism. *Neuron* 83, 518–532. doi: 10.1016/j.neuron.2014.07.016

Westerholz, S., de Lima, A. D., and Voigt, T. (2013). Thyroid hormone-dependent development of early cortical networks: temporal specificity and the contribution of trkB and mTOR pathways. *Front. Cell. Neurosci.* 7:121. doi: 10.3389/fncel.2013.00121

Wiens, S. C., and Trudeau, V. L. (2006). Thyroid hormone and γ-aminobutyric acid (GABA) interactions in neuroendocrine systems. *Comp. Biochem. Physiol. Part A Mol. Integr. Physiol.* 144, 332–344. doi: 10.1016/j.cbpa.2006.01.033

Yamaguchi, S., Aoki, N., Kitajima, T., Iikubo, E., Katagiri, S., Matsushima, T., et al. (2012). Thyroid hormone determines the start of the sensitive period of imprinting and primes later learning. *Nat. Commun.* 3:1081. doi: 10.1038/ncomms2088

Yamaguchi, S., Hayase, S., Aoki, N., Takehara, A., Ishigohoka, J., Matsushima, T., et al. (2017). Sex differences in brain thyroid hormone levels during early post-hatching development in zebra finch (*Taeniopygia guttata*). *PLoS One* 12:e0169643. doi: 10.1371/journal.pone.0169643

Yao, J. K., and Keshavan, M. S. (2011). Antioxidants, redox signaling, and pathophysiology in schizophrenia: an integrative view. *Antioxid. Redox Signal.* 15, 2011–2035. doi: 10.1089/ars.2010.3603

Yasuda, S., Ishida, N., Higashiyama, A., Morinobu, S., and Kato, N. (2000). Characterization of audiogenic-like seizures in naive rats evoked by activation of AMPA and NMDA receptors in the inferior colliculus. *Exp. Neurol.* 164, 396–406. doi: 10.1006/exnr.2000.7401

Yoshimura, T., Yasuo, S., Watanabe, M., Iigo, M., Yamamura, T., Hirunagi, K., et al. (2003). Light-induced hormone conversion of T4 to T3 regulates photoperiodic response of gonads in birds. *Nature* 426, 178–181. doi: 10.1038/nature02117

Yuen, R. K. C., Thiruvahindrapuram, B., Merico, D., Walker, S., Tammimies, K., Hoang, N., et al. (2015). Whole-genome sequencing of quartet families with autism spectrum disorder. *Nat. Med.* 21, 185–191. doi: 10.1038/nm.3792

Zoeller, R. T. (2010). New insights into thyroid hormone action in the developing brain: the importance of T3 degradation. *Endocrinology* 151, 5089–5091. doi: 10.1210/en.2010-0926

Conflict of Interest Statement: The authors declare that the research was conducted in the absence of any commercial or financial relationships that could be construed as a potential conflict of interest.

frontiers in Molecular Neuroscience

ORIGINAL RESEARCH
published: 11 April 2019
doi: 10.3389/fnmol.2019.00074

Sex and Estrous Cycle Effects on Anxiety- and Depression-Related Phenotypes in a Two-Hit Developmental Stress Model

Ivana Jaric[1†], *Devin Rocks*[1†], *Heining Cham*[2], *Alice Herchek*[1] *and Marija Kundakovic*[1*]

[1]Department of Biological Sciences, Fordham University, Bronx, NY, United States, [2]Department of Psychology, Fordham University, Bronx, NY, United States

Stress during sensitive developmental periods can adversely affect physical and psychological development and contribute to later-life mental disorders. In particular, adverse experiences during childhood dramatically increase the risk for the development of depression and anxiety disorders. Although women of reproductive age are twice as likely to develop anxiety and depression than men of the corresponding age, little is known about sex-specific factors that promote or protect against the development of psychopathology. To examine potential developmental mechanisms driving sex disparity in risk for anxiety and depression, we established a two-hit developmental stress model including maternal separation in early life followed by social isolation in adolescence. Our study shows complex interactions between early-life and adolescent stress, between stress and sex, and between stress and female estrogen status in shaping behavioral phenotypes of adult animals. In general, increased locomotor activity and body weight reduction were the only two phenotypes where two stressors showed synergistic activity. In terms of anxiety- and depression-related phenotypes, single exposure to early-life stress had the most significant impact and was female-specific. We show that early-life stress disrupts the protective role of estrogen in females, and promotes female vulnerability to anxiety- and depression-related phenotypes associated with the low-estrogenic state. We found plausible transcriptional and epigenetic alterations in psychiatric risk genes, *Nr3c1* and *Cacna1c*, that likely contributed to the stress-induced behavioral effects. In addition, two general transcriptional regulators, Egr1 and Dnmt1, were found to be dysregulated in maternally-separated females and in animals exposed to both stressors, respectively, providing insights into possible transcriptional mechanisms that underlie behavioral phenotypes. Our findings provide a novel insight into developmental risk factors and biological mechanisms driving sex differences in depression and anxiety disorders, facilitating the search for more effective, sex-specific treatments for these disorders.

Keywords: early life stress, adolescence, sex difference, anxiety, depression, estrogen, epigenetic, gene expression

OPEN ACCESS

Edited by:
Laura Musazzi,
University of Milan, Italy

Reviewed by:
Tania L. Roth,
University of Delaware, United States
Mathias V. Schmidt,
Max-Planck-Institut für Psychiatrie, Germany

***Correspondence:**
Marija Kundakovic
mkundakovic@fordham.edu

[†]*These authors have contributed equally to this work*

Received: *10 January 2019*
Accepted: *11 March 2019*
Published: *11 April 2019*

Citation:
Jaric I, Rocks D, Cham H, Herchek A and Kundakovic M (2019) Sex and Estrous Cycle Effects on Anxiety- and Depression-Related Phenotypes in a Two-Hit Developmental Stress Model. Front. Mol. Neurosci. 12:74. doi: 10.3389/fnmol.2019.00074

INTRODUCTION

Stressful experiences during sensitive developmental periods can have a major impact on later-life physical and mental health (Romeo and McEwen, 2006; McEwen, 2008). In particular, adverse experiences during childhood, such as abuse or neglect, dramatically increase the risk for the development of psychiatric disorders including depression, anxiety disorders, and substance abuse (Heim and Nemeroff, 2001; Lupien et al., 2009). It has been proposed that stress in early life induces increased reactivity within the hypothalamic-pituitary-adrenal (HPA) axis, sensitizing an individual to future stressful situations and challenges that may precipitate psychiatric disorders (Lupien et al., 2009). It is notable, though, that only a subset of individuals that experience early-life trauma develop a psychiatric condition in their adult life, and it is of great interest to reveal the factors that promote both risk and resilience to the effects of early life adversity.

The majority of psychiatric conditions linked to early-life adversity show a substantial sex bias in prevalence and severity, yet little is known about sex-specific factors that promote or protect against the development of psychopathology (Altemus et al., 2014). One of the major reasons for the dearth of knowledge in this area has been a traditional focus on male subjects in experimental neuroscience research (Beery and Zucker, 2011; Will et al., 2017). Some insights have been provided by the studies of depression and anxiety disorders, which show striking sex bias being twice as frequent in women than in men (Kuehner, 2017; Li and Graham, 2017). The increased risk in females emerges with the onset of puberty and various findings have suggested that natural hormonal shifts predispose females to stress-related, mood and anxiety disorders (Steiner et al., 2003; Altemus et al., 2014; Kuehner, 2017; Li and Graham, 2017). How sex hormones and stress may interact to bring about an increased vulnerability in females remains unknown.

To examine potential developmental mechanisms driving sex disparity in risk for anxiety and depression, we established a two-hit developmental stress model including maternal separation in early life followed by social isolation in adolescence. Repeated and prolonged separations of offspring from their mothers is one of the most frequently used rodent paradigms modeling aspects of childhood maltreatment in humans (Heim and Nemeroff, 2001; Kundakovic and Champagne, 2015). This model has been associated with disrupted brain development, and emotional and cognitive dysregulation in later life, showing translational validity (Heim and Nemeroff, 2001; Kundakovic and Champagne, 2015). However, the results have been inconsistent among different laboratories, largely due to different rodent strains used as well as different nature and timing of manipulation (Murthy and Gould, 2018). We use an established maternal separation protocol in C57BL/6 mice, combining maternal deprivation with disrupted maternal care, which was previously shown to induce depression-like behavior in early adolescent male and female animals (Kundakovic et al., 2013b). The rationale of the current study was to introduce another stress hit in adolescence and to examine whether increased female vulnerability to stress may emerge as females start experiencing cycling sex hormone levels following the onset of puberty. We chose a "suboptimal," mild adolescent stress paradigm, 3-week social isolation, previously shown to be insufficient to trigger behavioral abnormalities but exerting a synergistic disruptive effect on depression-related behavior when combined with another psychiatric risk factor (Niwa et al., 2013).

Our study provides a comprehensive analysis of the effects of early-life stress and adolescent stress, individually and in combination, on anxiety- and depression-related behavioral phenotypes in young adult male and female mice, accounting for the effects of the naturally cycling estrogen levels in females. Using several candidate genes of relevance to these behaviors, we also attempted to find molecular correlates that would link the effect of stressors to behaviors of interest. We examined both gene expression and DNA methylation in the ventral hippocampus, an area essential for emotional regulation, looking for a possible epigenetic link between stressful exposures and behavioral outcomes. We find complex interactions between two stressors, sex, and female estrogen status, and provide a new biological insight into the increased female vulnerability to stress and stress-related disorders.

MATERIALS AND METHODS

Study Design (**Figure 1**): to assess the effects of early-life stress and adolescent stress, individually and in combination, on behavioral and molecular outcomes, the following treatment groups were generated: (1) no stress (CON); (2) early life stress—maternal separation from postnatal day (PD) 1–14 (MS); (3) social isolation in adolescence from PD35–56 (SI); and (4) two-hit stress group—early life MS + SI in adolescence (MS_SI). In all groups, behavioral testing was performed from PD57–68, during the animals' light cycle, and in the following order (from least to most stressful): open-field test; elevated plus maze; sucrose preference; and forced swim test. Animals were sacrificed 2 days after the last behavioral test (PD70). Molecular analyses were performed on littermates that were not behaviorally tested to avoid the effect of behavioral testing on gene expression and DNA methylation. To avoid possible litter effects, a maximum of two pups per sex per litter were tested on behavioral measures, and one pup per sex per litter was used for molecular analyses.

Animals

Male (N = 40) and female (N = 80) C57BL/6 mice were ordered from Jackson Laboratories and housed in same-sex groups of five for 2.5 weeks prior to mating to habituate to the facility. Mating pairs consisting of two females and one male were separately housed and yielded N = 72 litters which were counted and weighed at PD0. Eighteen litters were randomly assigned to each group (CON, MS, SI, and MS_SI). Litters were weighed again on PD14, and individuals from the litters were weighed on weaning day, PD28, at which point they were housed in same-sex and same-group cages of five. Regardless of the treatment group, all animals were group-housed until PD35. Animals were kept on a 12:12 light/dark cycle (lights on at 8 a.m.) and given

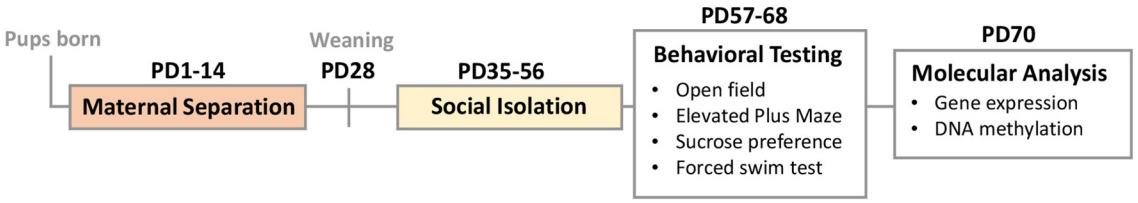

FIGURE 1 | Study design: two stress hits included early-life maternal separation (MS, PD1–14) and adolescent social isolation (SI, PD35–56). This design generated four groups of animals: no stress controls (CON), MS only, SI only, and combined two-hit stress MS_SI group. The majority of animals underwent behavioral testing from PD57–68 and their non-tested littermates were sacrificed for molecular analyses of the ventral hippocampus at PD70.

ad libitum access to food and water. This study was carried out in accordance with the recommendations of the Institutional Animal Care and Use Committee at Fordham University. The protocol was approved by the Institutional Animal Care and Use Committee at Fordham University.

Early-Life Stress

We used a previously established maternal separation protocol in C57BL/6 mice (Kundakovic et al., 2013b). Litters selected for early-life stress (MS and MS_SI groups) underwent maternal separation for 3 h every day for 2 weeks (PD1–14). During this time the dam was removed and placed in a temporary housing cage with food and water available. The time of day that maternal separation occurred was changed daily so that the stress was unpredictable. At a random time within the 3-h maternal separation window, dams were exposed to either restraint stress or forced swim to reduce the possibility of the dams giving compensatory maternal care to their litters following separation which was previously reported (Millstein and Holmes, 2007). In fact, we observed that this unpredictable stress disrupts maternal behavior for at least an hour after dams return to their pups; MS mothers spend more time out of nest and show reduced nurturing behaviors including less nursing, arched-back nursing, and licking/grooming, compared to control mothers (**Supplementary Figure S1**). Restraint stress lasted 20 min and involved placing the dam in a conical tube that restricted movement. Forced swim lasted 2 min and involved placing the dam in a 2 L glass beaker with 1 L of water, after which the dams were dried and returned to the temporary housing cage.

Adolescent Stress

Animals selected for adolescent stress (SI and MS_SI groups) underwent social isolation for 3 weeks starting at PD35 and ending at PD56. Social isolation involved placing individual animals in separate cages without cagemates. Socially isolated animals were given *ad libitum* access to food and water. At PD56, all animals were again housed in same-sex, same-treatment groups.

Open-Field Test

On PD57, animals from each group were tested using the Open Field paradigm. At the time of testing the animal was placed in the corner of the 40 cm × 40 cm × 35 cm glass box apparatus (Stoelting). The movement was tracked for 15 min using a camera and ANY-maze video tracking software (ANY-maze 5.1, Stoelting Co., Wood Dale, IL, USA). The size of the center zone in the open-field test was 20 cm × 20 cm. The total distance traveled, the amount of time the animal spent in the center of the maze vs. the periphery, and the latency to the first center entry was recorded. The results of the first 2 min of the test were used for the analysis.

Elevated Plus Maze Test

On PD60, animals from each group were tested using the Elevated Plus Maze paradigm. At the time of testing the animal was placed in the center of the apparatus, which was a raised (50 cm) plus-shaped platform with two 35 cm × 5 cm arms, one being protected by 15 cm walls (Stoelting). The movement was tracked for 5 min using a camera and ANY-Maze video tracking software. The total distance traveled, the amount of time the animal spent in the open arms of the maze vs. the closed arms, and the latency to the first open arm entry were recorded. The results of the first 2 min of the test was used for the analysis.

Sucrose Preference Test

From PD62–65, animals from each group were individually housed and given access to two water bottles with one containing 1% sucrose solution. Water bottles were weighed daily to assess sucrose preference. The position of the water bottles was switched each day to eliminate the possibility of attaining erroneous results due to place preference. The percentage of the sucrose solution consumed over the total volume of fluid consumed was reported as sucrose preference.

Forced Swim Test

On PD68, animals from each group were tested using the Forced Swim paradigm. Animals were placed in 2 L glass beakers filled with 1 L of water. The movement was tracked for 6 min using a camera and ANY-Maze video tracking software. The amount of time the animal spent frozen (immobile) and the latency to freeze were recorded. To ensure the accuracy of data obtained by automated video tracking of this test, the data were additionally evaluated and confirmed by watching the video recordings.

Estrous Cycle Stage Identification

To account for the sex hormone status of female animals, vaginal smears were taken immediately after behavioral testing or after sacrificing (for molecular analyses) for all female animals. Smears were analyzed by cytology and estrous cycle

stage was recorded following previously established protocols (McLean et al., 2012). Briefly, smears were allowed to dry and then stained with crystal violet dye. Smears were then analyzed using light microscopy. Proestrus is characterized by a high number of nucleated epithelial cells. Estrus is characterized by a high number of cornified epithelial cells. Metestrus is characterized by mostly cornified epithelial cells, some nucleated epithelial cells, and some leukocytes. Diestrus is characterized by cornified epithelial cells, nucleated epithelial cells, and many more leukocytes compared to metestrus. For the purpose of behavioral data analysis (for each test except for the sucrose preference test), female animals were classified into two groups based on the estrogen status on the day of test: (1) *high-estrogen status* (proestrus, diestrus/proestrus transition, and proestrus/estrus transition); and (2) *low-estrogen status* (diestrus, estrus, metestrus, estrus/metestrus transition, and metestrus/diestrus transition).

RNA and DNA Isolation

From each group, a subset of male (n = 8/group) and female (n = 12/group) animals which did not undergo behavioral testing were sacrificed at PD70 for molecular analysis. We checked the estrous cycle stage at the time of sacrificing, and as much as possible, we balanced the number of high- and low-estrogenic females in each group. Immediately after sacrifice, whole brains were isolated, frozen, and then stored at −80°C. The ventral hippocampus was later dissected, the tissue was immediately homogenized and DNA and RNA were extracted simultaneously using the Qiagen AllPrep DNA/RNA Mini Kit following the manufacturer's instructions. This served as the starting material for all subsequent molecular analyses.

Gene Expression Analysis

The analysis of gene expression was performed as described previously (Kundakovic et al., 2013a). Briefly, cDNA was synthesized from 500 ng of total RNA using the SuperScript III First-Strand Synthesis kit (Invitrogen, Carlsbad, CA, USA) following the manufacturer's protocol. qRT-PCR was then performed in QuantStudio 3 (Applied Biosystems, Foster City, CA, USA) using Fast SYBR Green Master Mix (Applied Biosystems, Foster City, CA, USA) and RT-PCR primers specific to the targeted genes (**Supplementary Table S1**). Relative mRNA expression was calculated using the standard ΔΔCT method. *Ppia* gene was used as a reference gene, previously shown not to be affected by early-life stressors (Kundakovic et al., 2013a,b). All data are expressed relative to the male control group.

DNA Methylation Analysis

DNA methylation analysis was performed at single-base resolution using the bisulfite pyrosequencing method as previously described (Kundakovic et al., 2013a). Briefly, 250 ng of genomic DNA was used for bisulfite conversion (EpiTect Bisulfite Kit, Qiagen) and 20 ng of bisulfite converted DNA was run in a PCR using the PyroMark PCR kit (Qiagen) and primers for genes of interest, one of which was biotinylated at the 5′ end. Biotinylated PCR products were processed on a vacuum workstation and pyrosequencing was performed on an Advanced PyroMark Q24 pyrosequencer using the advanced CpG reagents (Qiagen) and a specific sequencing primer. PCR and pyrosequencing primers for the mouse *Nr3c1* and *Cacna1c* genes are presented in **Supplementary Table S2**. Methylation levels of single CpG sites were quantified using PyroMark Q24 Advanced software (Qiagen).

Statistical Analysis

For all analyses, we did two-way analysis of variance (ANOVA) with group and sex as factors. We first looked for the group by sex interaction, and if the interaction was not significant, it was dropped from the model and we tested the main effects of group and sex. For the analyses of behavior (with the exception of sucrose preference), we did an additional two-way ANOVA analysis in females in which we assessed the effects of group and estrogen status and their interaction. If the group by estrogen interaction was not significant, it was dropped from the model, and we assessed the main effects of group and estrogen status. All *post hoc* tests were performed using Tukey's method. The analyses were performed in R version 3.5.1 and the graphs were generated using the R ggpubr package. Box plots show the first and third quartiles; the horizontal line is the median; the added, inner circles mark the mean with standard error for each box and small, outer circles mark possible outliers. The results were considered significant at a significance level of $P < 0.05$.

RESULTS

Body Weight

We monitored the effect of stressors on body weight throughout the study, including post-weaning (PD28), prior to social isolation (PD35), and after social isolation (PD56) time points (**Figure 2**). At all time points, males had higher body weight compared to females, and this relationship was not affected by any of the treatments (no significant group by sex interaction was found). Maternal separation led to significantly reduced body weight in both male and female offspring which was evident at PD28 ($P < 0.001$, **Figure 2A**) and persisted through PD35 ($P < 0.001$, **Figure 2B**) and PD56 ($P < 0.001$, **Figure 2C**). At PD56, we found that social isolation in males and females also led to a significant reduction in body weight compared to control mice ($P = 0.002$, **Figure 2C**). We found no significant difference between the effects of maternal separation and social isolation on body weight ($P = 0.6$, **Figure 2C**). However, the body weight reduction was most profound in mice that underwent the double-stress paradigm, surpassing the effects of a single exposure to either maternal separation ($P = 0.02$) or social isolation ($P < 0.001$, **Figure 2C**).

Anxiety-Like Behavior

In all four groups of animals, we performed two well-established tests for anxiety-like behavior: open-field and elevated plus maze tests.

Open Field

In the open field, we found no significant group by sex interaction on total distance traveled; however, we found a significant effect of group on this variable ($F_{(3,148)} = 2.87$, $P = 0.04$; **Figure 3A**). *Post hoc* test revealed that this effect

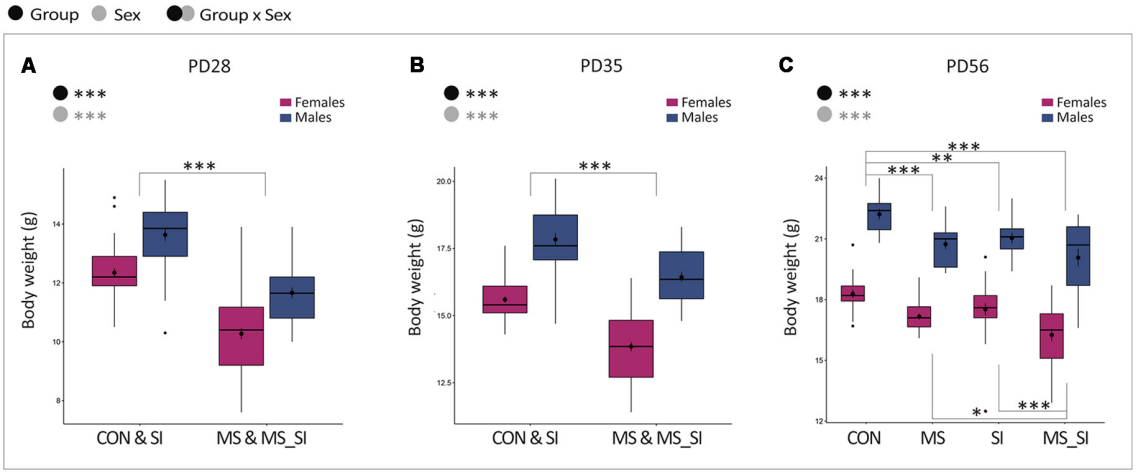

FIGURE 2 | The effect of maternal separation and social isolation on body weight. Body weight was examined after weaning **(A)**, prior to social isolation **(B)**, and before behavioral testing **(C)**. Note that PD28 and PD35 show the effects of MS only and the groups are merged to represent animals that did not undergo MS (CON and SI groups) vs. animals that underwent MS (MS and MS_SI groups). At PD56, social isolation was completed and four groups of animals are shown separately reflecting the effects of both MS and SI hits (N = 15–23/sex/group). Symbols in the upper left corner of each graph show significant main effects of group and sex or their interaction. Significant results of *post hoc* tests are presented in detail. CON, control; MS, maternal separation; SI, social isolation; MS_SI, combined maternal separation and social isolation. $^{*}P < 0.05$; $^{**}P < 0.01$; $^{***}P < 0.001$.

was driven by the double-stress (MS_SI) group which was marginally more active than any other group including CON ($P = 0.08$), MS ($P = 0.09$), and SI ($P = 0.08$). The average increase in the activity was higher in male MS_SI (11.07 ± 0.52 m) vs. CON (9.27 ± 0.60 m) comparison than in female MS_SI (11.15 ± 0.41 m) vs. CON (10.22 ± 0.90 m) comparison. There was no difference in activity between CON, MS, and SI groups ($P > 0.99$ for all comparisons). No significant effect of group or estrogen, or an interaction between group and estrogen were found when females were considered separately from males (**Figure 3B**).

When we analyzed the latency to the first entry into the center of the open field, no significant effect of group or sex nor their interaction was found with regard to this variable (**Figure 3C**). However, we found a significant effect of estrogen status ($F_{(1,82)} = 13.5$, $P < 0.001$); high-estrogenic females showed shorter latency time to enter the center compared to low estrogenic females (**Figure 3D**).

Finally, we analyzed the time spent in the center of the open field. We found no significant group by sex interaction and no significant main effects of group or sex on this variable (**Figure 3E**). However, when females were considered separately, we found a significant group by estrogen interaction ($F_{(3,79)} = 5.47$, $P = 0.002$; **Figure 3F**). In addition, both main effects of group ($F_{(3,79)} = 9.12$, $P < 0.001$) and estrogen status ($F_{(1,79)} = 39.34$, $P < 0.001$) were significant. In general, high estrogenic females showed more time spent in the center of the open field than low estrogenic females. Interestingly, in *post hoc* test, the effect of group was found to be significant in high-estrogenic females only; MS ($P < 0.001$), SI ($P = 0.003$), and MS_SI ($P = 0.01$) high estrogenic females were all found to spend significantly less time in the center of the open field than control high-estrogenic females. Another interesting observation is that a significant difference in the time spent in the center between high and low-estrogenic females was found only in control ($P < 0.001$) and SI ($P = 0.01$) groups, whereas this difference was lost in groups that were exposed to early life stress: MS ($P = 0.32$) and MS_SI ($P = 0.09$) groups (**Figure 3F**).

Elevated Plus Maze

No significant effect of group or sex nor their interaction was found on total distance traveled in the elevated plus maze (**Figure 4A**). There was a significant effect of estrogen status on activity in the maze ($F_{(1,82)} = 4.28$, $P = 0.04$) with high-estrogenic females showing marginally higher activity than low-estrogenic females (**Figure 4B**).

With regard to the latency to the first open arm entry, we found a significant group by sex interaction ($F_{(3,144)} = 3.35$, $P = 0.02$; **Figure 4C**). The effect of the group showed a trend toward significance in males only ($P = 0.07$) due to a longer latency to enter the open arm in SI male group compared to CON males ($P = 0.1$). Furthermore, the significant group by sex interaction that we observed was due to a sex difference induced in SI group, in which SI males showed significantly delayed latency to enter the open arms compared to SI female group ($P = 0.002$). No significant sex difference was found in CON, MS, or MS_SI groups ($P > 0.99$ for all comparisons). In addition, we found a significant effect of estrogen status in females ($F_{(1,82)} = 4.39$, $P = 0.04$); on average, high estrogenic females took longer to enter the open arm than low estrogen females (**Figure 4D**).

We found no significant group by sex interaction and no significant effect of group on time spent in the open arms of the elevated plus maze (**Figure 4E**). However, we found

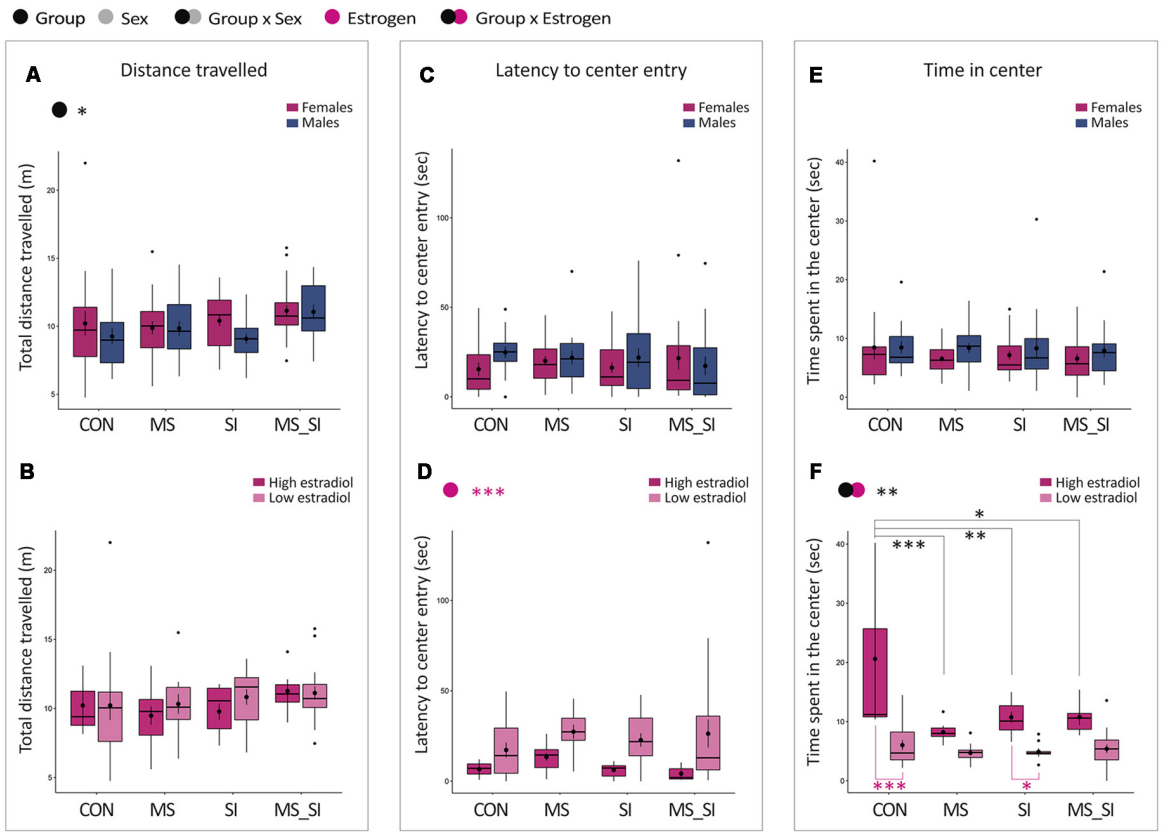

FIGURE 3 | Sex-specific and estrous cycle-dependent effects of maternal separation and social isolation on the open field behavior. Total distance traveled **(A,B)**, latency to the first center entry **(C,D)** and time spent in the center **(E,F)** were analyzed, either in all animals with group and sex as factors (upper panels—**A,C,E**) or in females with group and estrogen status as factors (lower panels—**B,D,F**); (N = 15–23/sex/group). Symbols in the upper left corner of each graph show significant main effects of group and sex/estrogen or their interaction. Significant results of *post hoc* tests are presented in detail. CON, control; MS, maternal separation; SI, social isolation; MS_SI, combined maternal separation and social isolation. $^{*}P < 0.05$; $^{**}P < 0.01$; $^{***}P < 0.001$.

a significant effect of sex ($F_{(1,148)} = 17.78$, $P < 0.001$), with females spending, on average, more time in the center of the maze than males (**Figure 4E**). This effect appears to be primarily driven by the estrogen status which was found to have a significant effect on time spent in the open arms in females ($F_{(1,82)} = 131.85$, $P < 0.001$), with high estrogenic females spending on average much longer time in the open arms than low estrogenic females (**Figure 4F**).

Depression-Like Behavior

Two well-established tests for depression-like behavior were performed in all four groups of animals: sucrose preference and forced swim test.

Sucrose Preference Test

This test represents a model of anhedonia in humans and we found a statistically significant interaction between the effects of group and sex on sucrose preference in our study ($F_{(3,145)} = 2.87$, $P = 0.04$; **Figure 5A**). This interaction was primarily driven by a sex difference in sucrose consumption observed in MS group; MS females showed a significantly decreased sucrose preference when compared to MS males ($P = 0.046$). Sex difference in sucrose preference did not exist in control group ($P = 0.99$) or in other treatment groups, SI ($P = 0.39$) and MS-SI ($P > 0.99$) groups. Of note, we did not examine the effect of estrogen status in this test because the test spans 3 days or more than a half of the mouse estrous cycle.

Forced Swim Test

We analyzed time spent immobile in the forced swim test and found a significant group by sex interaction in this test ($F_{(3,145)} = 3.07$, $P = 0.03$; **Figure 5B**). In *post hoc* tests, we found no significant difference between groups and only trend for an immobility time difference between males and females in the MS group ($P = 0.13$). In females, we found no significant group by estrogen interaction and no significant main effect of group. However, we found a significant effect of the estrogen status ($F_{(1,82)} = 211.80$, $P < 0.001$), with high-estrogenic females generally having significantly shorter immobility time in the forced swim test than low estrogenic females (**Figure 5C**).

Gene Expression Analysis

We determined the effects of early-life stress and adolescent stress on expression of the following candidate genes in the ventral hippocampus: *Bdnf* (encoding brain-derived

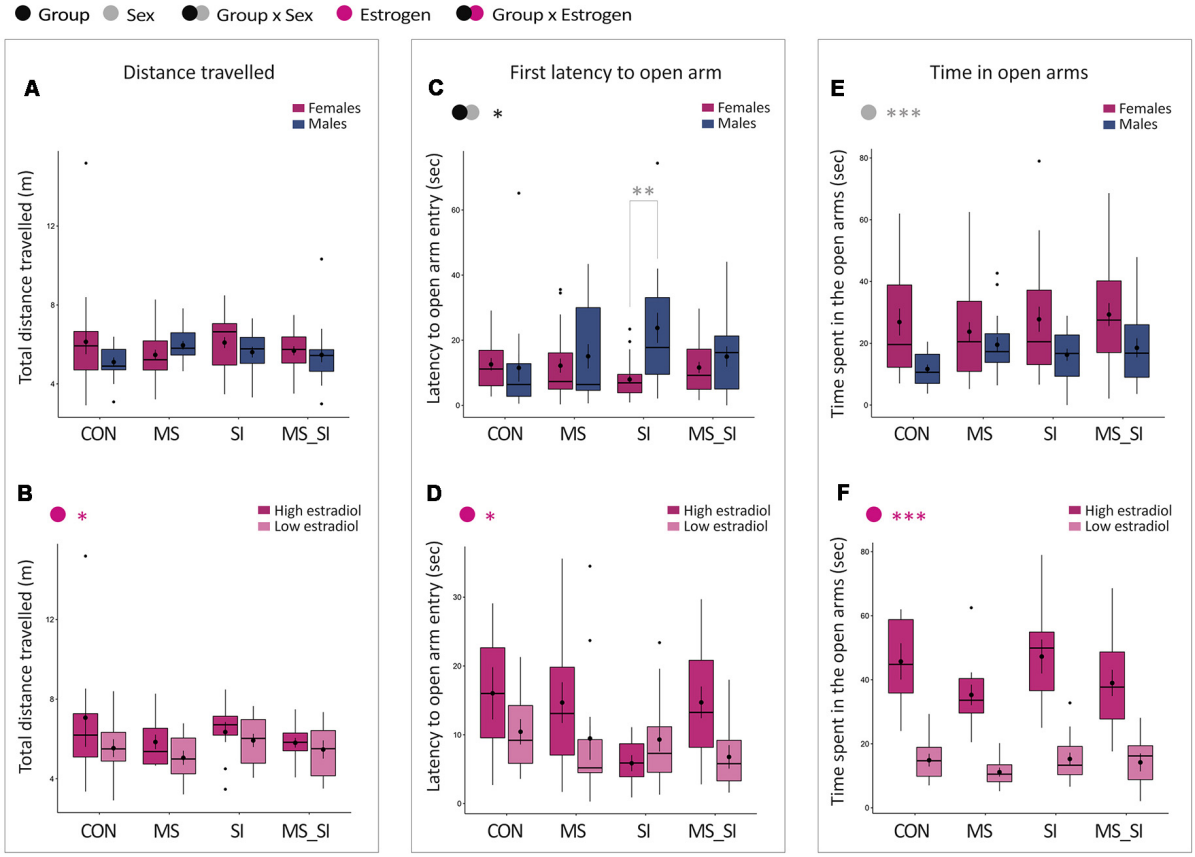

FIGURE 4 | Sex-specific effects of maternal separation and social isolation in the elevated plus maze test. Total distance traveled **(A,B)**, latency to the first open arm entry **(C,D)** and time spent in the open arms **(E,F)** were analyzed, either in all animals with group and sex as factors (upper panels—**A,C,E**) or in females with group and estrogen status as factors (lower panels—**B,D,F**); (*N* = 15–23/sex/group). Symbols in the upper left corner of each graph show significant main effects of group and sex/estrogen or their interaction. Significant results of *post hoc* tests are presented in detail. CON, control; MS, maternal separation; SI, social isolation; MS_SI, combined maternal separation and social isolation. $^{*}P < 0.05$; $^{**}P < 0.01$; $^{***}P < 0.001$.

neurotrophic factor); *Nr3c1* (encoding glucocorticoid receptor); *Egr1* (encoding early growth response protein 1); *Cacna1c* (encoding calcium voltage-gated channel subunit alpha1C), *Gria3* (encoding glutamate ionotropic receptor AMPA type subunit 3); and *Dnmt1* (encoding DNA methyltransferase 1). The ventral hippocampus was selected because it is strongly implicated in emotion regulation and anxiety-related behavior (Bannerman et al., 2003; Fanselow and Dong, 2010; Kheirbek et al., 2013). The *Bdnf* and *Nr3c1* genes have been previously implicated in the effects of early-life stress and in psychopathology (Weaver et al., 2004; Angelucci et al., 2005; McGowan et al., 2009; Roth et al., 2009; Boulle et al., 2012; Kundakovic et al., 2013b, 2015). *Egr1* has been reported to be sensitive to stress and encodes an immediate early gene product, a transcription factor which regulates expression of numerous genes including *Nr3c1* (Weaver et al., 2004; Gutièrrez-Mecinas et al., 2011; Xie et al., 2013; Rusconi et al., 2016). *Cacna1c* and *Gria3* are well-established psychiatric risk genes (Henley and Wilkinson, 2016; de Sousa et al., 2017; Dedic et al., 2018). Finally, *Dnmt1* encodes an epigenetic regulator that has been implicated in epigenetic effects of early-life stressors and in psychiatric disorders (Grayson and Guidotti, 2013; Kundakovic et al., 2013a; Dong et al., 2015).

We found no significant group by sex interaction and no significant effect of group or sex on the expression of *Bdnf* in the ventral hippocampus (**Figure 6A**). With regards to *Nr3c1*, there was no significant group by sex interaction, but there were significant main effects of both group ($F_{(3,75)} = 5.21$, $P = 0.003$) and sex ($F_{(1,75)} = 32.97$, $P < 0.001$) on the expression of this gene (**Figure 6B**). *Post hoc* test showed a significant difference between MS and CON groups only ($P = 0.001$). This effect was driven by an increased *Nr3c1* expression in the MS female group (1.39 ± 0.04) compared to CON female (1.08 ± 0.06) and CON male (1.00 ± 0.03) groups, whereas the MS male group had *Nr3c1* expression (1.08 ± 0.04) comparable to controls (**Figure 6B**). In general, female mice also had a higher *Nr3c1* expression in the ventral hippocampus than males ($P < 0.001$; **Figure 6B**). *Egr1* showed a similar pattern of expression to *Nr3c1*; there was no significant group by sex interaction but there were significant main effects of group ($F_{(3,68)} = 3.47$, $P = 0.02$) and sex ($F_{(1,68)} = 4.66$, $P = 0.03$) on the expression of this gene (**Figure 6C**). The only two

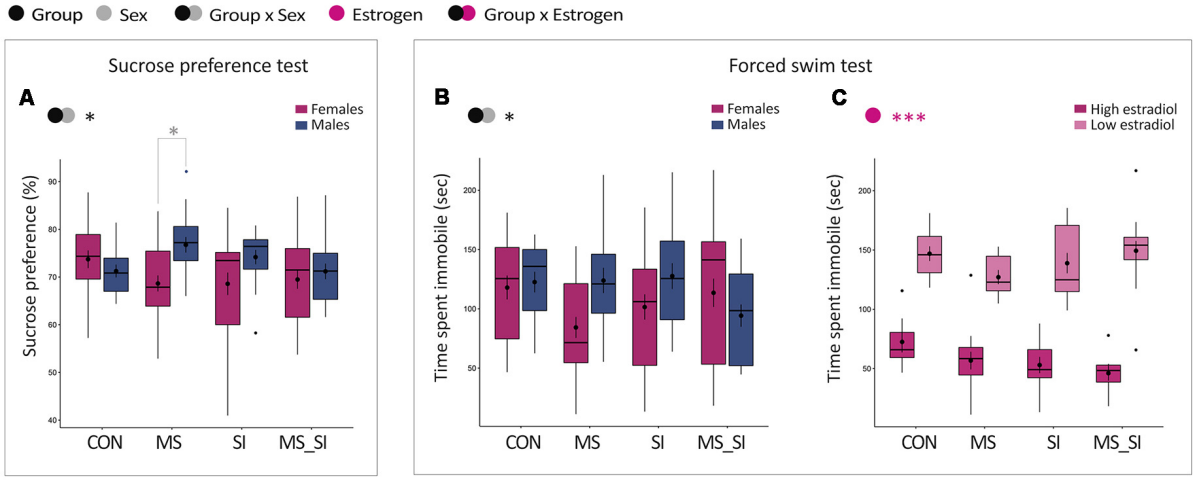

FIGURE 5 | Sex-specific effects of maternal separation and social isolation on depression-related phenotypes. Results of sucrose preference **(A)** and the forced swim **(B,C)** tests are shown. Sucrose preference was analyzed in all animals with group and sex as factors **(A)**. For the forced swim test, time spent immobile was analyzed in all animals with group and sex as factors **(B)** and in females with group and estrogen status as factors **(C)**; (*N* = 15–23/sex/group). Symbols in the upper left corner of each graph show significant main effects of group and sex/estrogen or their interaction. Significant results of *post hoc* tests are presented in detail. CON, control; MS, maternal separation; SI, social isolation; MS_SI, combined maternal separation and social isolation. $^{*}P < 0.05$; $^{***}P < 0.001$.

groups that showed a statistically significant difference in *Egr1* expression were MS and CON groups ($P = 0.02$) which, again, was driven by a higher expression in the MS female group (1.66 ± 0.21) compared to CON female (0.98 ± 0.06) and CON male (0.88 ± 0.05) groups and the MS male group had *Egr1* expression (1.03 ± 0.07) more comparable to controls (**Figure 6C**). In general, females had a higher *Egr1* expression compared to males (**Figure 6C**). The *Cacna1c* gene showed the most variable expression among the tested groups. We found a significant group by sex interaction for this gene ($F_{(3,72)} = 14.75$, $P < 0.001$; **Figure 6D**). In females, we found significantly reduced expression of this gene in all three treatment groups including MS ($P = 0.02$), SI ($P < 0.001$), and MS_SI ($P = 0.02$) compared to control female animals. In males, though, we found a significant reduction in *Cacna1c* expression in CON vs. MS comparison ($P < 0.001$) and in CON vs. SI comparison ($P < 0.001$) but there was no significant difference between CON and MS_SI groups ($P = 0.63$). However, the double-stress MS_SI male group had a significant higher expression than both single-stress exposed male groups—MS ($P < 0.001$) and SI ($P < 0.001$) groups. Of all groups, only CON ($P = 0.03$) and MS_SI groups ($P < 0.001$) showed a significant sex difference in *Cacna1c* expression; this difference was completely lost in MS and SI groups ($P > 0.99$ for both comparisons; **Figure 6D**). Unlike what we observed with *Cacna1c*, we found no significant group by sex interaction and no significant effect of group or sex on the expression of *Gria3* in the ventral hippocampus (**Figure 6E**). Finally, in terms of *Dnmt1* expression in the ventral hippocampus, there was no significant group by sex interaction but we found significant main effects of both group ($F_{(3,75)} = 19.68$, $P < 0.001$) and sex ($F_{(1,75)} = 9.60$, $P = 0.003$; **Figure 6F**). Two treatment groups SI ($P = 0.003$) and MS_SI ($P < 0.001$) showed a significant higher expression of *Dnmt1* than the control group; there was no significant difference between MS and control group ($P = 0.97$). Among the treatment groups, both SI ($P = 0.01$) and MS_SI groups ($P < 0.001$) had a significant higher expression of *Dnmt1* than MS group. The highest expression of *Dnmt1* was seen in the double-stress MS_SI group, significantly surpassing the effects of a single exposure to social isolation in the SI group ($P = 0.01$; **Figure 6F**).

DNA Methylation Analysis

To address possible epigenetic mechanisms underlying gene expression changes that we have observed, we performed DNA methylation analysis of the two candidate genes: *Nr3c1* and *Cacna1c*. We analyzed eight CpG sites located in the 5' regulatory region of the *Nr3c1* gene, containing the binding site for transcription factor Egr1 (or NGFI-A) overlapping CpG sites 7 and 8 (**Figure 7A**; Weaver et al., 2004; Kundakovic et al., 2013b). For CpG1 site, we found a significant group by sex interaction ($F_{(3,40)} = 4.67$, $P = 0.01$; **Figure 7A**). Specifically, MS_SI males had significantly higher methylation at this site than CON ($P = 0.02$) and SI ($P = 0.02$) males. In addition, MS_SI males had higher methylation levels than MS_SI females ($P = 0.003$), whereas sex difference was not found in any other group. We found no significant main effects of group or sex nor their interaction when we analyzed CpG site 2 (**Figure 7A**). We found a significant main effect of group ($F_{(3,43)} = 3.98$, $P = 0.01$) on methylation levels of CpG site 3, which was driven by increased methylation in MS_SI group compared to CON ($P = 0.02$) and SI ($P = 0.03$) groups (**Figure 7A**). For CpG site 4, we found a significant effect of both group ($F_{(3,43)} = 5.51$, $P = 0.003$) and sex ($F_{(1,43)} = 7.30$, $P = 0.01$; **Figure 7A**). We found significantly lower CpG 4 methylation in MS ($P = 0.003$), SI ($P = 0.04$), and MS_SI ($P = 0.01$)

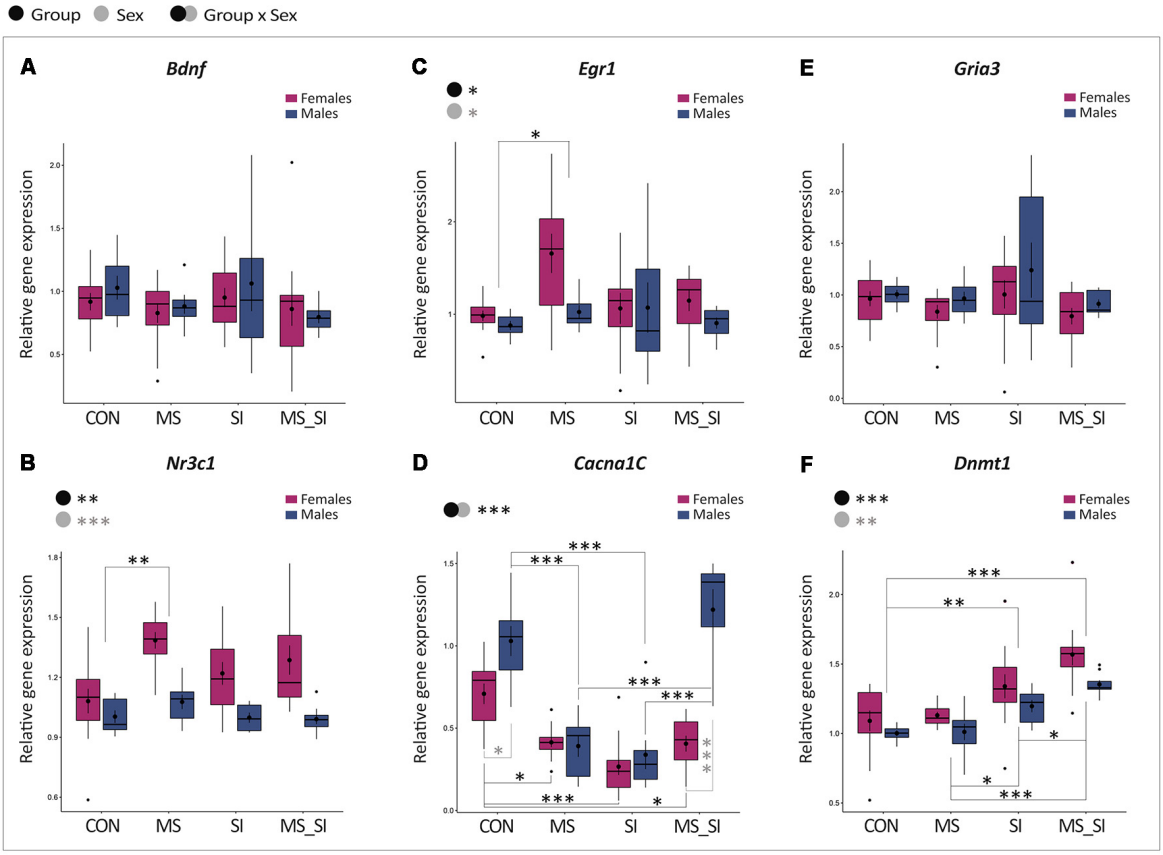

FIGURE 6 | Sex-specific effects of maternal separation and social isolation on gene expression in the ventral hippocampus. The expression of *Bdnf* **(A)**, *Nr3c1* **(B)**, *Egr1* **(C)**, *Cacna1c* **(D)**, *Gria3* **(E)**, and *Dnmt1* **(F)** was analyzed in the ventral hippocampus, using group and sex as factors (N = 12 females/group, N = 8 males/group). Symbols in the upper left corner of each graph show significant main effects of group and sex or their interaction. Significant results of *post hoc* tests are presented in detail. CON, control; MS, maternal separation; SI, social isolation; MS_SI, combined maternal separation and social isolation. $^{*}P < 0.05$; $^{**}P < 0.01$; $^{***}P < 0.001$.

groups compared to controls. In general, males had a higher methylation at CpG site 4 than females (P = 0.01). We found significant effect of both group ($F_{(3,43)}$ = 4.91, P = 0.01) and sex ($F_{(1,43)}$ = 5.77, P = 0.02) on CpG5 methylation (**Figure 7A**). This was driven by decreased methylation in the SI group compared to CON (P = 0.005) and MS_SI (P = 0.03) groups. In general, CpG 5 methylation was higher in males than in females. For CpG6, we found a significant effect of group ($F_{(3,43)}$ = 4.95, P = 0.005) and sex ($F_{(1,43)}$ = 4.12, P = 0.049; **Figure 7A**). The significant group difference was found in MS_SI to SI comparison only, where the SI group had significantly lower CpG6 methylation than MS_SI group (P = 0.002). Males had higher methylation levels than females. For CpG7 site, we found a significant group by sex interaction ($F_{(3,40)}$ = 4.32, P = 0.01). A significant effect of group was found in MS vs. CON group comparison in females only (P = 0.04), where we found significantly reduced CpG7 methylation in MS females (**Figure 7A**). CpG7 methylation was also marginally higher in MS_SI male group when compared to CON male group (P = 0.09). These results were consistent with observed sex difference, which was statistically significant within MS_SI group only (P = 0.001) and showed a trend toward significance in MS group (P = 0.06), with CpG7 methylation being higher in males of both groups. Finally, we found a significant group by sex interaction with regards to methylation of CpG site 8 ($F_{(3,40)}$ = 3.50, P = 0.02; **Figure 7A**). In *post hoc* test, we found only a significant decrease in CpG8 methylation in two female treatment groups—MS (P = 0.04) and MS_SI (P = 0.01)—compared to CON female group. No significant sex difference was observed in any of the groups.

We also analyzed four CpG sites in the first intron of the *Cacna1c* gene (**Figure 7B**). The analyzed region is within 1 kb from a transcription start site and is located in the CpG island shore having high homology between the mouse and human genome. In addition, these sites were previously shown to have cell-type specific methylation patterns (Nishioka et al., 2013). For CpG1, we found a significant main effect of group ($F_{(3,43)}$ = 3.43, P = 0.03) which was driven by a decreased CpG1 methylation found in MS_SI group compared to CON group (P = 0.02; **Figure 7B**). For CpG2, we found a marginally significant effect of group ($F_{(3,43)}$ = 2.79, P = 0.05) which was again driven by reduced CpG2 methylation in MS_SI group compared to CON

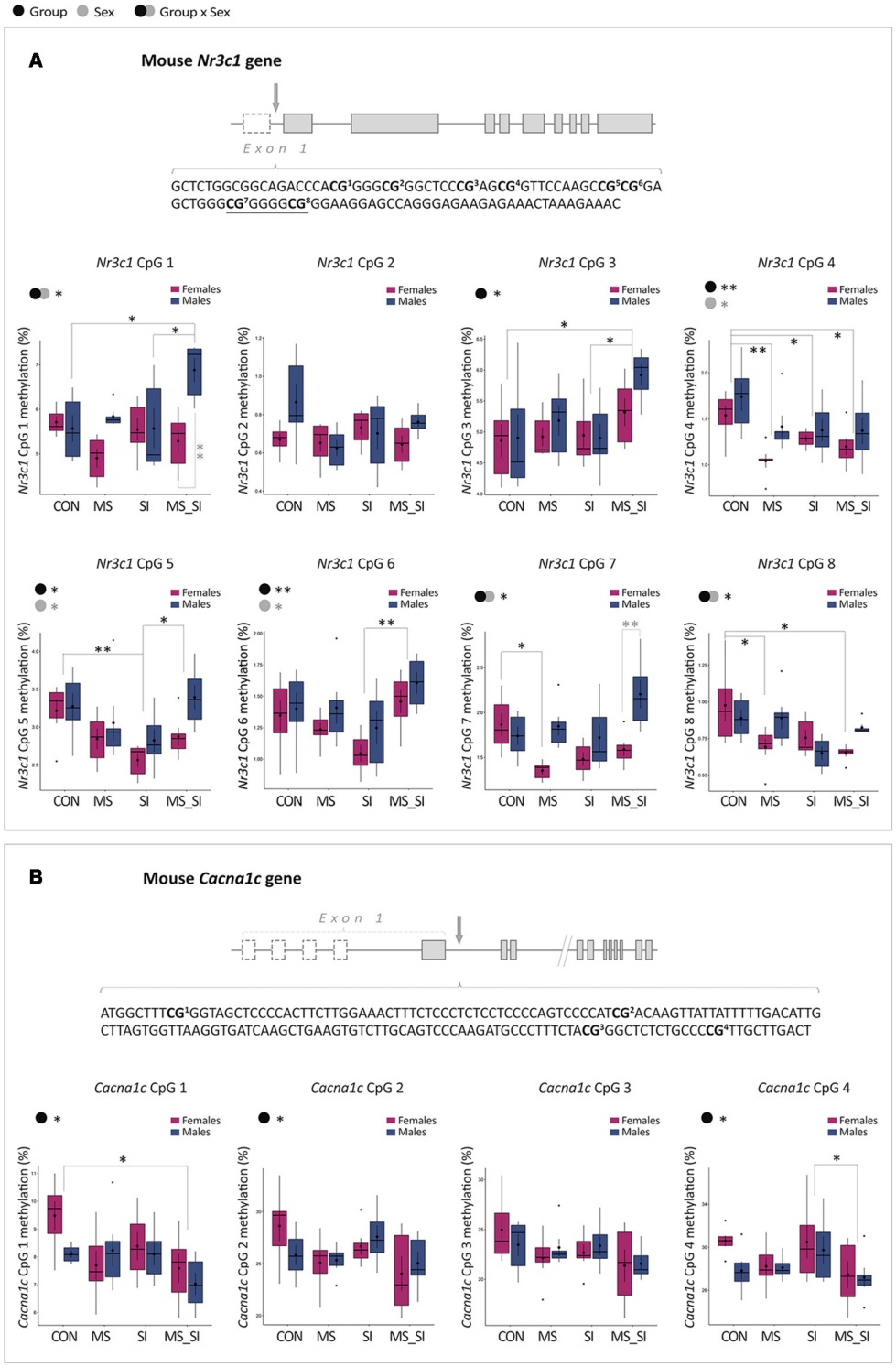

FIGURE 7 | Sex-specific effects of maternal separation and social isolation on DNA methylation of the *Nr3c1* and *Cacna1c* regulatory regions. **(A)** Schematic representation of the *Nr3c1* gene, the sequence of the analyzed CpG sites in the *Nr3c1* 5' regulatory region, and methylation levels of individual sites analyzed using group and sex as factors. Underlined sequence represents Egr1 binding site. **(B)** Schematic representation of the *Cacna1c* gene, the sequence of the analyzed CpG sites in the *Cacna1c* regulatory region, and methylation levels of individual sites analyzed using group and sex as factors ($N = 6$ sex/group; note: both genes have alternative first exons which are shown as dashed rectangles). Symbols in the upper left corner of each graph show significant main effects of group and sex or their interaction. Significant results of *post hoc* tests are presented in detail. CON, control; MS, maternal separation; SI, social isolation; MS_SI, combined maternal separation and social isolation. $^{*}P < 0.05$; $^{**}P < 0.01$.

group showing a trend toward significance ($P = 0.1$; **Figure 7B**). For CpG3, we found a similar trend with the main effect of group ($F_{(3,43)} = 2.2$, $P = 0.1$) due to a marginally significant reduction in CpG site 3 in MS_SI group compared to controls ($P = 0.07$; **Figure 7B**). There was also a significant effect of group on CpG4 methylation ($F_{(3,43)} = 2.92$, $P = 0.04$), again driven by reduced methylation in MS_SI group but this time compared to SI group ($P = 0.04$; **Figure 7B**). We found no significant effect of sex on methylation of any of the CpG sites analyzed in the *Cacna1c* gene.

DISCUSSION

In this study, we examined the effects of early-life stress and adolescent stress, individually and in combination, on body weight, anxiety- and depression-related behaviors, and expression and DNA methylation of genes implicated in stress-related psychiatric disorders. Overall, we found that a single, early-life stress exposure had the most profound effect on anxiety- and depression-related phenotypes in adult animals. Interestingly, the "second hit" of a suboptimal stress exposure in adolescence frequently attenuated the effects of early-life stress. Moreover, lasting effects of early-life stress are largely found to be female-specific and we have found significant effects of estrogen status on anxiety- and depression-like behavior in both control female animals and in those exposed to stress.

The current study is the continuation of our previous study which examined the effects of early-life maternal separation on early adolescent male and female offspring (Kundakovic et al., 2013b). The two developmental stressors that we used in the current study were sufficient to induce metabolic dysfunction in animals, as we have seen through the persistent reduction in body weight observed in all treatment groups. Interestingly, reduced body weight is a rare phenotype on which two stress hits worked synergistically, surpassing the effects of individual stress exposures. Another phenotype that emerged only in the double-hit stress group is hyperactivity in the open field test, with males being more strongly affected. While increased locomotor activity is a rather non-specific phenotype, which, interestingly, did not affect any of the indices of anxiety or depression-related behavior, this phenotype is seen after the treatment with psychostimulants and is reminiscent of hyperactivity seen in disorders such as attention deficit hyperactivity disorder (ADHD). Psychotic disorders and ADHD have been linked to developmental stress with males being more severely impacted (Bale et al., 2010), similar to what we observed in our study. Therefore, the double-stress paradigm that we constructed may be of relevance for studies of metabolic dysfunction and psychosis- or hyperactivity-related disorders but we found surprisingly small effects of this paradigm with regards to anxiety- and depression-related behaviors.

There are several possible explanations for the observed "buffering" effect of adolescent social isolation on the effect of early-life stress on anxiety- and depression-related phenotypes. First, 3 weeks of adolescent social isolation is a mild stressor. The only phenotype that we observed in the SI group is a marginally delayed latency to the open arm entry in males, which is as an index of increased anxiety-like behavior. Other than that, the behavioral effects of this paradigm were largely non-significant, in line with what was previously reported (Niwa et al., 2013). Our results suggest that mild stress in adolescence may decrease the risk for the development of anxiety and depression in individuals that experienced certain forms of early-life trauma. While this finding may be counterintuitive, it is consistent with the "mismatch hypothesis" of psychiatric disease (Schmidt, 2011; Nederhof, 2012). This hypothesis states that early-life environment induces adaptive phenotypic changes, preparing an individual for later-life environmental conditions (Nederhof, 2012). If the early-life and later-life environment match, the early-life stress may even be beneficial. However, the disorder may occur once the later-life conditions do not match the stressful environment experienced in early life. As an example, it was shown that rats who receive low levels of maternal care (form of early-life stress) exhibit enhanced learning under stressful conditions but impaired learning under normal conditions in later life (Champagne et al., 2008). There are also additional "two-hit stress" studies that showed increased stress resilience in animals that experienced early-life stress (Biggio et al., 2014; Hsiao et al., 2016; Santarelli et al., 2017). However, while the "mismatch hypothesis" is plausible to explain the lack of anxiety- and depression-related phenotypes in our two-hit stress model, it is likely that a stronger stressor during adolescence or adulthood would, indeed, worsen the phenotype induced by early-life stress, as seen in some studies (Peña et al., 2017). In addition, in humans, genetic vulnerability or resilience to depression and anxiety disorders, certainly play an important role in how early- and later-life stress affect the risk for the development of these disorders.

As compared to our previous study which showed that maternal separation induces decreased sucrose preference, a form of anhedonia or depression-like behavior, in both male and female early adolescent mice (Kundakovic et al., 2013b), here we show that this effect persists into adulthood only in female animals. It is well known that anxiety and depression show explicit sex bias with women of reproductive age being twice as likely as men of the corresponding age to develop these disorders. The mechanisms underlying this sex disparity are unknown, and the studies of early-life stress have not necessarily addressed this (Bale et al., 2010), particularly because a lot of studies were focused on male animals. Our study provides an important insight into this sex disparity, providing a clue about how early-life stress can be a sex-specific factor in driving vulnerability to anxiety and depression. Indeed, the early-life paradigm that we use, combining maternal separation with unpredictable maternal stress, turned out to be a good model to study increased female vulnerability to these disorders.

Among the most interesting sex-specific findings in our study is the effect of estrogen status and its interaction with early-life stress on anxiety- and depression-related behaviors in females. In fact, our most consistent finding is that the

high-estrogen phase of the cycle is associated with remarkably lower indices of anxiety and depression-like behavior compared to the low-estrogen phase. This was basically seen in all tests in which estrogen status was controlled for, including: open field (shorter latency and longer time spent in the center in high-estrogenic females); elevated plus maze (longer time spent in the open arms in high estrogenic females); and forced swim test (shorter time spent immobile in high estrogenic females). Our results are consistent with earlier studies in rats (Marcondes et al., 2001; Walf and Frye, 2006) and clearly indicate the importance of estrogen status for anxiety and mood regulation in females of reproductive age. Indeed, we can conclude that high estrogen levels have a protective, anxiolytic effect whereas a physiological drop in estrogen may increase the risk for the occurrence of anxiety and depression symptoms in females of reproductive age. This is in line with human data which show that a large number of women with major depression experience worsening of their symptoms in the premenstrual, low-estrogen phase of the cycle, even when antidepressant therapy is effective during the remainder of the cycle (Kornstein et al., 2005; Altemus et al., 2014). Importantly, hormonal fluctuations, rather than low hormone levels *per se*, seem to be critical for both pathogenesis and treatment of depression, considering that post-menopausal women with stable low hormone levels appear to lose sensitivity to estrogen (Morrison et al., 2004) and show a similar risk for depression when compared to men of their age (Deecher et al., 2008; Altemus et al., 2014).

Our study provides an important, novel insight into how stress can interact with the ovarian cycle to facilitate the increased anxiety and depression vulnerability in females. When we focused our analysis on female animals, we found that developmental stressors had a significant negative impact on anxiety-like behavior (time spent in the center of the open-field) in our female population. However, when we looked further into the estrous cycle effects, we found that stressors increased anxiety-like behavior only during the high-estrogen phase of the cycle when the anxiety levels are typically low. No effect of stress was found during the low-estrogen phase when the anxiety levels are already high. In addition, the most significant effect was found in the early-life stress group. And, even more interestingly, maternally separated animals (MS and MS_SI groups) showed a largely blunted, insignificant difference in anxiety levels between low and high estrogen phases, suggesting that the anxiolytic effect of estrogen is predominantly lost in groups that experience early life stress. Whether this is the consequence of lower estrogen levels or lost sensitivity to estrogen in response to early-life adversity remains to be further explored. Nevertheless, this finding reveals a possible sex-specific mechanism through which early-life adversity may contribute to sex disparity in risk for anxiety and depression by suppressing the "protective" effect of estrogen in women of reproductive age.

We further explored gene expression in the ventral hippocampus with an intent to find molecular correlates of the behavioral effects that we have observed. For this analysis, we did not look at the estrous cycle effects but have explored more general sex-specific patterns of gene expression that may contribute to the sex difference in vulnerability. Interestingly, although changes in hippocampal *Bdnf* expression have been found in many studies of early-life adversity (Onishchenko et al., 2008; Roth et al., 2009; Kundakovic et al., 2013b, 2015; Boersma et al., 2014), we found no significant changes in the expression of this gene in our study. This may be due to the fact that we focused our analysis on the ventral hippocampus while previous studies examined the entire hippocampus. Considering that the ventral and dorsal hippocampi are functionally distinct regions (Fanselow and Dong, 2010), showing distinct gene expression profiles (Cembrowski et al., 2016) and distinct responses to chronic stress (Czéh et al., 2015; Pinto et al., 2015), changes previously reported may largely stem from the stressor-induced alterations in the dorsal hippocampus. However, in MS females, we found an overexpression of *Nr3c1*, which is another gene that has been repeatedly associated with early-life stress in both animals and humans (Weaver et al., 2004; Champagne et al., 2008; McGowan et al., 2009; Suderman et al., 2012; Kundakovic et al., 2013b). This gene encodes the glucocorticoid receptor, directly involved in the negative feedback regulation of the HPA axis, providing one of the possible mechanisms for HPA axis dysregulation and consequent behavioral changes in the MS female group. Another interesting finding is that *Egr1* shows an almost identical expression pattern as *Nr3c1*. Considering that the *Nr3c1* regulatory region contains the binding site for Egr1 (also known as NGFI-A; Weaver et al., 2004; Kundakovic et al., 2013b), and Egr1 is induced by stress (Xie et al., 2013; Rusconi et al., 2016), this provides a plausible link between coordinate up-regulation of these two genes and anxiety- and depression-related phenotypes in the early-life stress female group.

The *Cacna1c* gene was another important candidate gene in our study. This gene has recently received a lot of attention, as it is considered to be one of the strongest genetics hits in psychiatry, associated with risk for bipolar disorder, major depression, and schizophrenia (Ferreira et al., 2008; Sklar et al., 2008; Green et al., 2010). Moreover, embryonic deletion of this gene in the mouse forebrain results in increased anxiety-like behavior and increased susceptibility to chronic stress (Dedic et al., 2018). Some clinical and animal studies have also found a significant interaction between sex and *Cacna1c* genotype (Dao et al., 2010; Witt et al., 2014; Takeuchi et al., 2018); for instance, female, but not male, *Cacna1c* heterozygous mice have been shown to display decreased risk-taking behavior and increased anxiety in multiple tests (Dao et al., 2010). Our study has revealed that this gene is very sensitive to developmental stress and that, depending on the number of hits, the effects of stress can be sex-specific. First, we observed that each individual stressor, maternal separation and social isolation, decreased Cacna1c mRNA levels in both sexes. Once these two stressors are combined, though, females still show reduced expression, but this effect is lost in males. These results provide a good example where deficiency in a single gene cannot be simply associated with behavioral phenotype. For instance, we can speculate that the down-regulation of *Cacna1c* expression contributed to increased anxiety-like behavior observed in

females of all groups and in SI males, with MS females being most significantly affected because these animals also show dysregulated expression of *Egr1* and *Nr3c1*. In addition, "normalized" *Cacna1c* expression is consistent with the lack of anxiety and depression-related phenotype in the double-stress male group. However, MS males also did not show any significant behavioral phenotype, despite reduced *Cacna1c* expression, suggesting that these animals may have expressed some protective or pro-resilient factors that "buffered" the effect of *Cacna1c* deficiency.

Finally, *Dnmt1* is the only gene which showed the largest expression changes in the double-hit stress group. Being an epigenetic regulator, Dnmt1 over-expression may affect the activity of many downstream target genes and, therefore, contribute to behavioral phenotypes. One possibility is that Dnmt1 up-regulation contributed to the hyperactivity seen in MS_SI group. This is consistent with the finding that the psychostimulant methamphetamine, which induces hyperactivity in rodents, also induces Dnmt1 mRNA levels in the rodent brain (Numachi et al., 2007). In addition, an increased *Dnmt1* expression has been found in psychosis (Veldic et al., 2005) and DNA methylation changes have been reported in many neuropsychiatric disorders including schizophrenia (Grayson and Guidotti, 2013) and ADHD (Heinrich et al., 2017; Chen et al., 2018), further providing a possible link between Dnmt1 dysregulation and the hyperactivity-related phenotype observed in our double-hit stress group.

In the last part of our study, we explored whether DNA methylation, an epigenetic mechanism, may contribute to the effects of developmental stressors on gene expression and behavioral outcomes. There are now a quite large number of studies suggesting that early-life experiences may exert long-term effects on brain and behavior *via* epigenetic mechanisms. Among those studies, changes in DNA methylation of the *Nr3c1* gene were the first to be linked to altered gene expression, HPA dysfunction, and anxiety-and depression-related phenotypes induced by early-life adversity in rats (Weaver et al., 2004) and humans (McGowan et al., 2009). Here we examined the region in mouse which is highly homologous (92%) to the previously reported exon 1_7 in rats (Weaver et al., 2004), and also containing the binding site for Egr1 (or NGFI-A) transcription factor encompassing two CpG sites (Weaver et al., 2004; Kundakovic et al., 2013b). Changes in DNA methylation within or adjacent to the transcription factor binding sites are particularly poised to affect transcriptional activity by preventing or facilitating the binding of transcription factors (Klose and Bird, 2006). While our results show complex group- and sex-specific patterns, it is notable that both sites in the Egr1 binding motif show female-specific reduction in methylation in the MS group. This finding is consistent with higher *Nr3c1* and *Egr1* expression in this group, and provides one of the possible mechanisms for the induced expression of the glucocorticoid gene and consequent behavioral alterations in early-life stress female group.

In terms of *Cacna1c* gene, there are reports of altered or more variable DNA methylation patterns in bipolar disorder (Starnawska et al., 2016) and depression (Córdova-Palomera et al., 2015) patients, respectively, compared to healthy subjects. We analyzed the region close to the transcription start site, with high homology between mice and humans, and shown to be differentially methylated between neurons and glia cells (Nishioka et al., 2013), hence, of possible functional relevance. We found subtle changes in DNA methylation of this gene in the double-stress hit group only, which cannot explain group- and sex-specific differences in *Cacna1c* gene expression that we have observed. However, it is possible that other regions of the *Cacna1c* gene, not examined in this study, may show differential methylation, which remains to be further explored. In addition, we would like to note that, although our DNA methylation analysis was limited to two regions and only 12 CpG sites total, our results suggest that epigenetic dysregulation may be prominent in the double-stress group, in line with changed gene expression of an epigenetic regulator, Dnmt1.

CONCLUSION

In conclusion, our study shows complex interactions between early-life and adolescent stress, between stress and sex, and between stress and female estrogen status in shaping behavioral phenotypes of adult animals. In our paradigm, early-life stress had the most significant impact on anxiety- and depression-related phenotypes and this was female-specific. We discovered that early-life stress disrupts the protective role of estrogen in females, and promotes female vulnerability to anxiety- and depression-related phenotypes associated with the low-estrogenic state. We found transcriptional and epigenetic alterations in psychiatric risk genes, *Nr3c1* and *Cacna1c*, that likely contributed to the stress-induced behavioral effects. In addition, two general transcriptional regulators, Egr1 and Dnmt1, were found to be dysregulated in maternally-separated females and in animals exposed to both stressors, respectively, providing insights into possible transcriptional mechanisms that underlie behavioral phenotypes. We envision future transcriptomics and epigenomics studies that will give more definitive answers regarding molecular signatures and mechanisms that drive developmental stress-induced vulnerability or resilience to anxiety and depression-related phenotypes. Our study highlights the importance of accounting for the effects of sex and female hormone status in the studies of the impact of stress on brain and behavior, and provides a foundation for the future studies of molecular mechanisms underlying sex disparity in anxiety and depression. This knowledge will be extremely important to enable the development of more effective, sex-specific treatments for these disorders.

AUTHOR CONTRIBUTIONS

IJ and MK designed the study. IJ, DR, AH, and MK performed the experiments. HC performed statistical analysis. IJ, DR, HC, and MK interpreted the data. IJ, HC, and MK constructed the figures. DR and MK wrote the article. MK conceived and directed the project. All authors revised and approved the final version of the article.

FUNDING

This study was supported by the NARSAD Young Investigator Grant from the Brain & Behavior Research Foundation to MK.

SUPPLEMENTARY MATERIAL

The Supplementary Material for this article can be found online at: https://www.frontiersin.org/articles/10.3389/fnmol.2019.00074/full#supplementary-material

REFERENCES

Altemus, M., Sarvaiya, N., and Neill Epperson, C. (2014). Sex differences in anxiety and depression clinical perspectives. *Front. Neuroendocrinol.* 35, 320–330. doi: 10.1016/j.yfrne.2014.05.004

Angelucci, F., Brene, S., and Mathe, A. A. (2005). BDNF in schizophrenia, depression and corresponding animal models. *Mol. Psychiatry* 10, 345–352. doi: 10.1038/sj.mp.4001637

Bale, T. L., Baram, T. Z., Brown, A. S., Goldstein, J. M., Insel, T. R., McCarthy, M. M., et al. (2010). Early life programming and neurodevelopmental disorders. *Biol. Psychiatry* 68, 314–319. doi: 10.1016/j.biopsych.2010.05.028

Bannerman, D. M., Grubb, M., Deacon, R. M., Yee, B. K., Feldon, J., and Rawlins, J. N. (2003). Ventral hippocampal lesions affect anxiety but not spatial learning. *Behav. Brain Res.* 139, 197–213. doi: 10.1016/s0166-4328(02)00268-1

Beery, A. K., and Zucker, I. (2011). Sex bias in neuroscience and biomedical research. *Neurosci. Biobehav. Rev.* 35, 565–572. doi: 10.1016/j.neubiorev.2010.07.002

Biggio, F., Pisu, M. G., Garau, A., Boero, G., Locci, V., Mostallino, M. C., et al. (2014). Maternal separation attenuates the effect of adolescent social isolation on HPA axis responsiveness in adult rats. *Eur. Neuropsychopharmacol.* 24, 1152–1161. doi: 10.1016/j.euroneuro.2014.03.009

Boersma, G. J., Lee, R. S., Cordner, Z. A., Ewald, E. R., Purcell, R. H., Moghadam, A. A., et al. (2014). Prenatal stress decreases Bdnf expression and increases methylation of Bdnf exon IV in rats. *Epigenetics* 9, 437–447. doi: 10.4161/epi.27558

Boulle, F., van den Hove, D. L., Jakob, S. B., Rutten, B. P., Hamon, M., van Os, J., et al. (2012). Epigenetic regulation of the BDNF gene: implications for psychiatric disorders. *Mol. Psychiatry* 17, 584–596. doi: 10.1038/mp.2011.107

Cembrowski, M. S., Wang, L., Sugino, K., Shields, B. C., and Spruston, N. (2016). Hipposeq: a comprehensive RNA-seq database of gene expression in hippocampal principal neurons. *Elife* 5:e14997. doi: 10.7554/elife.14997

Champagne, D. L., Bagot, R. C., van Hasselt, F., Ramakers, G., Meaney, M. J., de Kloet, E. R., et al. (2008). Maternal care and hippocampal plasticity: evidence for experience-dependent structural plasticity, altered synaptic functioning and differential responsiveness to glucocorticoids and stress. *J. Neurosci.* 28, 6037–6045. doi: 10.1523/JNEUROSCI.0526-08.2008

Chen, Y. C., Sudre, G., Sharp, W., Donovan, F., Chandrasekharappa, S. C., Hansen, N., et al. (2018). Neuroanatomic, epigenetic and genetic differences in monozygotic twins discordant for attention deficit hyperactivity disorder. *Mol. Psychiatry* 23, 683–690. doi: 10.1038/mp.2017.45

Córdova-Palomera, A., Fatjó-Vilas, M., Gastó, C., Navarro, V., Krebs, M. O., and Fañanas, L. (2015). Genome-wide methylation study on depression: differential methylation and variable methylation in monozygotic twins. *Transl. Psychiatry* 5:e557. doi: 10.1038/tp.2015.49

Czéh, B., Varga, Z. K., Henningsen, K., Kovács, G. L., Miseta, A., and Wiborg, O. (2015). Chronic stress reduces the number of GABAergic interneurons in the adult rat hippocampus, dorsal-ventral and region-specific differences. *Hippocampus* 25, 393–405. doi: 10.1002/hipo.22382

Dao, D. T., Mahon, P. B., Cai, X., Kovacsics, C. E., Blackwell, R. A., Arad, M., et al. (2010). Mood disorder susceptibility gene CACNA1C modifies mood-related behaviors in mice and interacts with sex to influence behavior in mice and diagnosis in humans. *Biol. Psychiatry* 68, 801–810. doi: 10.1016/j.biopsych.2010.06.019

de Sousa, R. T., Loch, A. A., Carvalho, A. F., Brunoni, A. R., Haddad, M. R., Henter, I. D., et al. (2017). Genetic studies on the tripartite glutamate synapse in the pathophysiology and therapeutics of mood disorders. *Neuropsychopharmacology* 42, 787–800. doi: 10.1038/npp.2016.149

Dedic, N., Pohlmann, M. L., Richter, J. S., Mehta, D., Czamara, D., Metzger, M. W., et al. (2018). Cross-disorder risk gene CACNA1C differentially modulates susceptibility to psychiatric disorders during development and adulthood. *Mol. Psychiatry* 23, 533–543. doi: 10.1038/mp.2017.133

Deecher, D., Andree, T. H., Sloan, D., and Schechter, L. E. (2008). From menarche to menopause: exploring the underlying biology of depression in women experiencing hormonal changes. *Psychoneuroendocrinology* 33, 3–17. doi: 10.1016/j.psyneuen.2007.10.006

Dong, E., Dzitoyeva, S. G., Matrisciano, F., Tueting, P., Grayson, D. R., and Guidotti, A. (2015). Brain-derived neurotrophic factor epigenetic modifications associated with schizophrenia-like phenotype induced by prenatal stress in mice. *Biol. Psychiatry* 77, 589–596. doi: 10.1016/j.biopsych.2014.08.012

Fanselow, M. S., and Dong, H. W. (2010). Are the dorsal and ventral hippocampus functionally distinct structures? *Neuron* 65, 7–19. doi: 10.1016/j.neuron.2009.11.031

Ferreira, M. A., O'Donovan, M. C., Meng, Y. A., Jones, I. R., Ruderfer, D. M., Jones, L., et al. (2008). Collaborative genome-wide association analysis supports a role for ANK3 and CACNA1C in bipolar disorder. *Nat. Genet.* 40, 1056–1058. doi: 10.1038/ng.209

Grayson, D. R., and Guidotti, A. (2013). The dynamics of DNA methylation in schizophrenia and related psychiatric disorders. *Neuropsychopharmacology* 38, 138–166. doi: 10.1038/npp.2012.125

Green, E. K., Grozeva, D., Jones, I., Jones, L., Kirov, G., Caesar, S., et al. (2010). The bipolar disorder risk allele at CACNA1C also confers risk of recurrent major depression and of schizophrenia. *Mol. Psychiatry* 15, 1016–1022. doi: 10.1038/mp.2009.49

Gutièrrez-Mecinas, M., Trollope, A. F., Collins, A., Morfett, H., Hesketh, S. A., Kersanté, F., et al. (2011). Long-lasting behavioral responses to stress involve a direct interaction of glucocorticoid receptors with ERK1/2-MSK1-Elk-1 signaling. *Proc. Natl. Acad. Sci. U S A* 108, 13806–13811. doi: 10.1073/pnas.1104383108

Heim, C., and Nemeroff, C. B. (2001). The role of childhood trauma in the neurobiology of mood and anxiety disorders: preclinical and clinical studies. *Biol. Psychiatry* 49, 1023–1039. doi: 10.1016/s0006-3223(01)01157-x

Heinrich, H., Grunitz, J., Stonawski, V., Frey, S., Wahl, S., Albrecht, B., et al. (2017). Attention, cognitive control and motivation in ADHD: linking event-related brain potentials and DNA methylation patterns in boys at early school age. *Sci. Rep.* 7:3823. doi: 10.1038/s41598-017-03326-3

Henley, J. M., and Wilkinson, K. A. (2016). Synaptic AMPA receptor composition in development, plasticity and disease. *Nat. Rev. Neurosci.* 17, 337–350. doi: 10.1038/nrn.2016.37

Hsiao, Y. M., Tsai, T. C., Lin, Y. T., Chen, C. C., Huang, C. C., and Hsu, K. S. (2016). Early life stress dampens stress responsiveness in adolescence: evaluation of neuroendocrine reactivity and coping behavior. *Psychoneuroendocrinology* 67, 86–99. doi: 10.1016/j.psyneuen.2016.02.004

Kheirbek, M. A., Drew, L. J., Burghardt, N. S., Costantini, D. O., Tannenholz, L., Ahmari, S. E., et al. (2013). Differential control of learning and anxiety along the dorsoventral axis of the dentate gyrus. *Neuron* 77, 955–968. doi: 10.1016/j.neuron.2012.12.038

Klose, R. J., and Bird, A. P. (2006). Genomic DNA methylation: the mark and its mediators. *Trends Biochem. Sci.* 31, 89–97. doi: 10.1016/j.tibs.2005.12.008

Kornstein, S. G., Harvey, A. T., Rush, A. J., Wisniewski, S. R., Trivedi, M. H., Svikis, D. S., et al. (2005). Self-reported premenstrual exacerbation of depressive symptoms in patients seeking treatment for major depression. *Psychol. Med.* 35, 683–692. doi: 10.1017/s0033291704004106

Kuehner, C. (2017). Why is depression more common among women than among men? *Lancet Psychiatry* 4, 146–158. doi: 10.1016/s2215-0366(16)30263-2

Kundakovic, M., and Champagne, F. A. (2015). Early-life experience, epigenetics, and the developing brain. *Neuropsychopharmacology* 40, 141–153. doi: 10.1038/npp.2014.140

Kundakovic, M., Gudsnuk, K., Franks, B., Madrid, J., Miller, R. L., Perera, F. P., et al. (2013a). Sex-specific epigenetic disruption and behavioral changes following low-dose in utero bisphenol A exposure. *Proc. Natl. Acad. Sci. U S A* 110, 9956–9961. doi: 10.1073/pnas.1214056110

Kundakovic, M., Lim, S., Gudsnuk, K., and Champagne, F. A. (2013b). Sex-specific and strain-dependent effects of early life adversity on behavioral and epigenetic outcomes. *Front. Psychiatry* 4:78. doi: 10.3389/fpsyt.2013.00078

Kundakovic, M., Gudsnuk, K., Herbstman, J. B., Tang, D., Perera, F. P., and Champagne, F. A. (2015). DNA methylation of BDNF as a biomarker of early-life adversity. *Proc. Natl. Acad. Sci. U S A* 112, 6807–6813. doi: 10.1073/pnas.1408355111

Li, S. H., and Graham, B. M. (2017). Why are women so vulnerable to anxiety, trauma-related and stress-related disorders? The potential role of sex hormones. *Lancet Psychiatry* 4, 73–82. doi: 10.1016/s2215-0366(16)30358-3

Lupien, S. J., McEwen, B. S., Gunnar, M. R., and Heim, C. (2009). Effects of stress throughout the lifespan on the brain, behaviour and cognition. *Nat. Rev. Neurosci.* 10, 434–445. doi: 10.1038/nrn2639

Marcondes, F. K., Miguel, K. J., Melo, L. L., and Spadari-Bratfisch, R. C. (2001). Estrous cycle influences the response of female rats in the elevated plus-maze test. *Physiol. Behav.* 74, 435–440. doi: 10.1016/s0031-9384(01)00593-5

McEwen, B. S. (2008). Understanding the potency of stressful early life experiences on brain and body function. *Metabolism* 57, S11–S15. doi: 10.1016/j.metabol.2008.07.006

McGowan, P. O., Sasaki, A., D'Alessio, A. C., Dymov, S., Labonté, B., Szyf, M., et al. (2009). Epigenetic regulation of the glucocorticoid receptor in human brain associates with childhood abuse. *Nat. Neurosci.* 12, 342–348. doi: 10.1038/nn.2270

McLean, A. C., Valenzuela, N., Fai, S., and Bennett, S. A. (2012). Performing vaginal lavage, crystal violet staining, and vaginal cytological evaluation for mouse estrous cycle staging identification. *J. Vis. Exp.* 67:e4389. doi: 10.3791/4389

Millstein, R. A., and Holmes, A. (2007). Effects of repeated maternal separation on anxiety- and depression-related phenotypes in different mouse strains. *Neurosci. Biobehav. Rev.* 31, 3–17. doi: 10.1016/j.neubiorev.2006.05.003

Morrison, M. F., Kallan, M. J., Ten Have, T., Katz, I., Tweedy, K., and Battistini, M. (2004). Lack of efficacy of estradiol for depression in postmenopausal women: a randomized, controlled trial. *Biol. Psychiatry* 55, 406–412. doi: 10.1016/j.biopsych.2003.08.011

Murthy, S., and Gould, E. (2018). Early life stress in rodents: animal models of illness or resilience? *Front. Behav. Neurosci.* 12:157. doi: 10.3389/fnbeh.2018.00157

Nederhof, E. (2012). The mismatch hypothesis of psychiatric disease. *Physiol. Behav.* 106, 689–690. doi: 10.1016/j.physbeh.2012.02.014

Nishioka, M., Shimada, T., Bundo, M., Ukai, W., Hashimoto, E., Saito, T., et al. (2013). Neuronal cell-type specific DNA methylation patterns of the Cacna1c gene. *Int. J. Dev. Neurosci.* 31, 89–95. doi: 10.1016/j.ijdevneu.2012.11.007

Niwa, M., Jaaro-Peled, H., Tankou, S., Seshadri, S., Hikida, T., Matsumoto, Y., et al. (2013). Adolescent stress-induced epigenetic control of dopaminergic neurons via glucocorticoids. *Science* 339, 335–339. doi: 10.1126/science.1226931

Numachi, Y., Shen, H., Yoshida, S., Fujiyama, K., Toda, S., Matsuoka, H., et al. (2007). Methamphetamine alters expression of DNA methyltransferase 1 mRNA in rat brain. *Neurosci. Lett.* 414, 213–217. doi: 10.1016/j.neulet.2006.12.052

Onishchenko, N., Karpova, N., Sabri, F., Castrén, E., and Ceccatelli, S. (2008). Long-lasting depression-like behavior and epigenetic changes of BDNF gene expression induced by perinatal exposure to methylmercury. *J. Neurochem.* 106, 1378–1387. doi: 10.1111/j.1471-4159.2008.05484.x

Peña, C. J., Kronman, H. G., Walker, D. M., Cates, H. M., Bagot, R. C., Purushothaman, I., et al. (2017). Early life stress confers lifelong stress susceptibility in mice via ventral tegmental area OTX2. *Science* 356, 1185–1188. doi: 10.1126/science.aan4491

Pinto, V., Costa, J. C., Morgado, P., Mota, C., Miranda, A., Bravo, F. V., et al. (2015). Differential impact of chronic stress along the hippocampal dorsal-ventral axis. *Brain Struct. Funct.* 220, 1205–1212. doi: 10.1007/s00429-014-0713-0

Romeo, R. D., and McEwen, B. S. (2006). Stress and the adolescent brain. *Ann. N Y Acad. Sci.* 1094, 202–214. doi: 10.1196/annals.1376.022

Roth, T. L., Lubin, F. D., Funk, A. J., and Sweatt, J. D. (2009). Lasting epigenetic influence of early-life adversity on the BDNF gene. *Biol. Psychiatry* 65, 760–769. doi: 10.1016/j.biopsych.2008.11.028

Rusconi, F., Grillo, B., Ponzoni, L., Bassani, S., Toffolo, E., Paganini, L., et al. (2016). LSD1 modulates stress-evoked transcription of immediate early genes and emotional behavior. *Proc. Natl. Acad. Sci. U S A* 113, 3651–3656. doi: 10.1073/pnas.1511974113

Santarelli, S., Zimmermann, C., Kalideris, G., Lesuis, S. L., Arloth, J., Uribe, A., et al. (2017). An adverse early life environment can enhance stress resilience in adulthood. *Psychoneuroendocrinology* 78, 213–221. doi: 10.1016/j.psyneuen.2017.01.021

Schmidt, M. V. (2011). Animal models for depression and the mismatch hypothesis of disease. *Psychoneuroendocrinology* 36, 330–338. doi: 10.1016/j.psyneuen.2010.07.001

Sklar, P., Smoller, J. W., Fan, J., Ferreira, M. A., Perlis, R. H., Chambert, K., et al. (2008). Whole-genome association study of bipolar disorder. *Mol. Psychiatry* 13, 558–569. doi: 10.1038/sj.mp.4002151

Starnawska, A., Demontis, D., Pen, A., Hedemand, A., Nielsen, A., Staunstrup, N., et al. (2016). CACNA1C hypermethylation is associated with bipolar disorder. *Transl. Psychiatry* 6:e831. doi: 10.1038/tp.2016.99

Steiner, M., Dunn, E., and Born, L. (2003). Hormones and mood: from menarche to menopause and beyond. *J. Affect. Disord.* 74, 67–83. doi: 10.1016/s0165-0327(02)00432-9

Suderman, M., McGowan, P. O., Sasaki, A., Huang, T. C., Hallett, M. T., Meaney, M. J., et al. (2012). Conserved epigenetic sensitivity to early life experience in the rat and human hippocampus. *Proc. Natl. Acad. Sci. U S A* 109, 17266–17272. doi: 10.1073/pnas.1121260109

Takeuchi, H., Tomita, H., Taki, Y., Kikuchi, Y., Ono, C., Yu, Z., et al. (2018). A common CACNA1C gene risk variant has sex-dependent effects on behavioral traits and brain functional activity. *Cereb. Cortex* doi: 10.1093/cercor/bhy189 [Epub ahead of print].

Veldic, M., Guidotti, A., Maloku, E., Davis, J. M., and Costa, E. (2005). In psychosis, cortical interneurons overexpress DNA-methyltransferase 1. *Proc. Natl. Acad. Sci. U S A* 102, 2152–2157. doi: 10.1073/pnas.0409665102

Walf, A. A., and Frye, C. A. (2006). A review and update of mechanisms of estrogen in the hippocampus and amygdala for anxiety and depression behavior. *Neuropsychopharmacology* 31, 1097–1111. doi: 10.1038/sj.npp.1301067

Weaver, I. C., Cervoni, N., Champagne, F. A., D'Alessio, A. C., Sharma, S., Seckl, J. R., et al. (2004). Epigenetic programming by maternal behavior. *Nat. Neurosci.* 7, 847–854. doi: 10.1038/nn1276

Will, T. R., Proaño, S. B., Thomas, A. M., Kunz, L. M., Thompson, K. C., Ginnari, L. A., et al. (2017). Problems and progress regarding sex bias and omission in neuroscience research. *eNeuro* 4:ENEURO.0278-0217.2017. doi: 10.1523/ENEURO.0278-17.2017

Witt, S. H., Kleindienst, N., Frank, J., Treutlein, J., Mühleisen, T., Degenhardt, F., et al. (2014). Analysis of genome-wide significant bipolar disorder genes in borderline personality disorder. *Psychiatr. Genet.* 24, 262–265. doi: 10.1097/YPG.0000000000000060

Xie, L., Korkmaz, K. S., Braun, K., and Bock, J. (2013). Early life stress-induced histone acetylations correlate with activation of the synaptic plasticity genes Arc and Egr1 in the mouse hippocampus. *J. Neurochem.* 125, 457–464. doi: 10.1111/jnc.12210

Conflict of Interest Statement: The authors declare that the research was conducted in the absence of any commercial or financial relationships that could be construed as a potential conflict of interest.

frontiers in Molecular Neuroscience

ORIGINAL RESEARCH
published: 01 May 2019
doi: 10.3389/fnmol.2019.00089

Perinatal Stress Programs Sex Differences in the Behavioral and Molecular Chronobiological Profile of Rats Maintained Under a 12-h Light-Dark Cycle

Sara Morley-Fletcher[1,2†], Jerome Mairesse[3†], Gilles Van Camp[1,2], Marie-Line Reynaert[1], Eleonora Gatta[4], Jordan Marrocco[5], Hammou Bouwalerh[1,2], Ferdinando Nicoletti[6,7‡] and Stefania Maccari[1,8‡]*

[1] UMR 8576, Unité de Glycobiologie Structurale et Fonctionnelle, Campus Cité Scientifique, CNRS, University of Lille, Lille, France, [2] University Lille – CNRS-UMR 8576, International Associated Laboratory (LIA) "Prenatal Stress and Neurodegenerative Diseases," Sapienza University of Rome – IRCCS Neuromed, Rome, Italy, [3] Division of Neonatology, Department of Pediatrics, University of Geneva, Geneva, Switzerland, [4] Department of Psychiatry, College of Medicine, Psychiatric Institute, Center for Alcohol Research in Epigenetics, University of Illinois at Chicago, Chicago, IL, United States, [5] Laboratory of Neuroendocrinology, The Rockefeller University, New York, NY, United States, [6] Department of Physiology and Pharmacology "V. Erspamer," Sapienza University of Rome, Rome, Italy, [7] Istituto di Ricovero e Cura a Carattere Scientifico (IRCCS), NEUROMED, Pozzilli, Italy, [8] Department of Science and Medical – Surgical Biotechnology, Sapienza University of Rome, Rome, Italy

OPEN ACCESS

Edited by:
Gi Hoon Son,
Korea University, South Korea

Reviewed by:
Henrik Oster,
Universität zu Lübeck, Germany
Han Kyoung Choe,
Daegu Gyeongbuk Institute of Science and Technology (DGIST), South Korea

***Correspondence:**
Stefania Maccari
stefania.maccari@univ-lille.fr

[†] These authors have contributed equally to this work

[‡] **Present address:**
Ferdinando Nicoletti and Stefania Maccari,
Co-director of International Associated Laboratory (LIA), University of Lille 1 – CNRS and Sapienza University of Rome – IRCCS Neuromed, Rome, Italy

Received: 28 November 2018
Accepted: 21 March 2019
Published: 01 May 2019

Citation:
Morley-Fletcher S, Mairesse J, Van Camp G, Reynaert M-L, Gatta E, Marrocco J, Bouwalerh H, Nicoletti F and Maccari S (2019) Perinatal Stress Programs Sex Differences in the Behavioral and Molecular Chronobiological Profile of Rats Maintained Under a 12-h Light-Dark Cycle. Front. Mol. Neurosci. 12:89. doi: 10.3389/fnmol.2019.00089

Stress and the circadian systems play a major role in an organism's adaptation to environmental changes. The adaptive value of the stress system is reactive while that of the circadian system is predictive. Dysfunctions in these two systems may account for many clinically relevant disorders. Despite the evidence that interindividual differences in stress sensitivity and in the functioning of the circadian system are related, there is limited integrated research on these topics. Moreover, sex differences in these systems are poorly investigated. We used the perinatal stress (PRS) rat model, a well-characterized model of maladaptive programming of reactive and predictive adaptation, to monitor the running wheel behavior in male and female adult PRS rats, under a normal light/dark cycle as well as in response to a chronobiological stressor (6-h phase advance/shift). We then analyzed across different time points the expression of genes involved in circadian clocks, stress response, signaling, and glucose metabolism regulation in the suprachiasmatic nucleus (SCN). In the unstressed control group, we found a sex-specific profile that was either enhanced or inverted by PRS. Also, PRS disrupted circadian wheel-running behavior by inducing a phase advance in the activity of males and hypoactivity in females and increased vulnerability to chronobiological stress in both sexes. We also observed oscillations of several genes in the SCN of the unstressed group in both sexes. PRS affected males to greater extent than females, with PRS males displaying a pattern similar to unstressed females. Altogether, our findings provide evidence for a specific profile of dysmasculinization induced by PRS at the behavioral and molecular level, thus advocating the necessity to include sex as a biological variable to study the set-up of circadian system in animal models.

Keywords: predictive adaptation, reactive adaptation, circadian rhythms, locomotor activity, chronobiological stressor, mRNA expression

INTRODUCTION

The optimal functioning of an organism is based on its ability to adapt to changes in the environment. The adaptation can be reactive to unexpected environmental changes, or predictive, as it prepares the organism to anticipate the daily changes in the environment (Moore-Ede, 1986). The glucocorticoid stress response is an essential mediator of allostatic processes (McEwen, 1998), which are engaged to allow the organism to find a new equilibrium in response to the specific stressor. This stress response is adaptive when it is transitory and shuts off quickly with the help of feedback loops (McEwen and Stellar, 1993; Maccari et al., 2003, 2017). However, in the long run, prolonged and/or uncontrollable sources of stress lead to a loss of organism's resistance and entering a phase of exhaustion that might account for many clinically relevant disorders at the behavioral, endocrine, metabolic, cardiovascular, and immune level (de Kloet, 1999; Russell et al., 2018). Glucocorticoids also have a circadian rhythm, and the circadian system is another major physiological system involved in the adaptation of the organism to environmental changes. In contrast to the stress system, whose adaptive value is reactive, the circadian system has a predictive adaptive role (Turek, 2016). As with the stress response, disruption of circadian rhythms leads to clinically relevant disorders including obesity, cardiovascular disease, inflammation, and cognitive impairments (Wirz-Justice and Van den Hoofdakker, 1999; Bunney and Potkin, 2008; Gerstner and Yin, 2010; Wulff et al., 2010; Medic et al., 2017). Circadian rhythms are under control of an internal clock present in nearly every cell, with a core mechanism governed by a genetic network. These clocks are organized hierarchically, with a central pacemaker located in the suprachiasmatic nuclei (SCN) of the hypothalamus at the top, that receive photic cues and in turn coordinate local circadian clocks in the periphery (Moore and Eichler, 1972; Klein et al., 1991; Buijs and Kalsbeek, 2001; Cirelli, 2009). Glucocorticoid hormones and body temperature, among other signals, act as internal systemic synchronizers to entrain peripheral clocks through the SCN (Dibner et al., 2010).

Stress-induced pathologies are often characterized by alterations in circadian rhythms (Weibel et al., 2002; Spiga et al., 2014; Liyanarachchi et al., 2017; Nicolaides et al., 2017), and the glucocorticoid stress response and many clock-controlled processes display sexual dimorphism (for a review, see Darnaudéry and Maccari, 2008; Mong et al., 2011; Heck and Handa, 2018). The corticosterone stress response is markedly greater in adult female rodents than in males (Heck and Handa, 2018), and in both rodents and humans the circadian rhythm of glucocorticoids secretion has higher amplitude in females (Mong et al., 2011; Vestergaard et al., 2017, respectively). In humans, women also display higher rates of sleep disorders than men and a differential ability to adapt to changing shift-work schedules and jet lag (Bailey and Silver, 2014). A sexual dimorphism and first demonstration of gonad-dependence of circadian rhythm concerns circadian locomotor activity in rodents (Albers et al., 1981; Wollnik and Turek, 1988). Gonadal steroids in the SCN seem to act through different mechanisms in males and females. Indeed, androgen receptors are densely located in the core SCN and therefore act on the SCN via a direct pathway, unlike the estrogen receptors that are located mostly extra-SCN and act on SCN afferents (Mong et al., 2011). Nevertheless, the number of studies that associate reactive and predictive adaptations is limited, with the females being underrepresented (Zucker and Beery, 2010; Beery and Zucker, 2011; Kiryanova et al., 2017; McCarthy et al., 2017).

An individual's capabilities to cope with environmental challenges are shaped during development by the interplay of genetic and epigenetic determinants (McEwen, 2016). Exposure to stressful events in early life strongly programs an individual's phenotype and adaptive capabilities by modifying reactive (Weaver et al., 2004; Seckl, 2008; Brunton et al., 2011; Maccari et al., 2017) as well as predictive adaptation (Van Reeth et al., 2000; Maccari and Morley-Fletcher, 2007). A well-characterized animal model of early programming of stress response is the PRS model in the rat (Maccari et al., 1995; for a review see Maccari et al., 2017), in which exposure to gestational stress and altered maternal behavior programs a life-long disruption in the reactive adaptation such as a hyperactive response to stress and a defective feedback of the hypothalamus-pituitary-adrenal (HPA) axis (Vallée et al., 1999; Gatta et al., 2018) together with long-lasting modifications in stress/anti-stress gene expression balance in the hippocampus (Mairesse et al., 2015; Gatta et al., 2018). The changes induced by PRS in predictive adaptation include a profound alteration of the sleep-wake cycle architecture together with increased sleep fragmentation when the animals reach adulthood (Dugovic et al., 1999; Mairesse et al., 2013) and alterations in the rhythm of plasma corticosterone secretion (Koehl et al., 1999). Nevertheless, there are no studies on changes in circadian rhythms at the molecular level in the PRS model.

Perinatal stress induces sex-specific effects on reactive and predictive adaptations as well as on sexual maturation induced by gonadal hormones (Reynaert et al., 2016). Indeed, PRS reduces the ratio of testosterone/dihydrotestosterone in males and estradiol levels in females. Such an effect is causally related to sex-dependent alterations in gene expression in the hypothalamus and in the hedonic sensitivity to palatable food (Reynaert et al., 2016). However, studies have generally been conducted in PRS males and have focused on reactive adaptation to a greater extent.

The aim of this study was to explore the influence of PRS on the circadian oscillations of gene expression in the SCN and on circadian locomotor behavior, in a sex-dependent manner. Of note, research on transcriptional rhythms has shown that more than half of all genes in the human and rodent genome follow a circadian pattern (Panda et al., 2002; Hughes et al., 2009; Summa and Turek, 2011; Zhang et al., 2014). Thus, we focused on genes belonging to four functional classes, namely the circadian clock, HPA axis stress response regulation, signaling and glucose metabolism in male and female adult PRS rats. We also monitored the running wheel behavior, first under a regular light/dark (L/D) cycle and then after an abrupt 6-h advance light shift (chronobiological stress).

MATERIALS AND METHODS

Ethics Statement

All the experiments performed in this study followed the guideline of the European Communities Council Directive 2010/63/EU. The protocol of perinatal stress, running wheel behavior and sample collection was approved by the Local Committee CEEA-75 (Comité d'Ethique en Experimentation Animale Nord-Pas de Calais, 75).

Animals and Perinatal Stress Procedure

Animals

In total, 48 nulliparous female Sprague-Dawley rats, weighing approximately 250 g, were purchased from a commercial breeder (Harlan, France). Animals were housed at constant temperature (22 ± 2°C) and under a regular 12 h light/dark (L/D) cycle (light on at 8:00 am). A vaginal smear using endocrine serum (NaCl 0.9%) was performed on the morning following mating with an experienced male. The day on which the smear was sperm positive was considered to be embryonic day 0 (E0). After mating, pregnant females were individually housed with *ad libitum* access to food and water at constant temperature (22°C ± 2°C), and under a regular 12 h light/dark cycle (light on at 08:00). On E11, pregnant females were randomly assigned to stress or control groups ($n = 24$ in each group). Control females were left undisturbed, with an exception made for weighing one time per week in order to follow gestation.

Perinatal Stress Procedure

The pregnant female group was subjected to a restraint stress procedure according to a standard protocol (Maccari et al., 1995; Morley-Fletcher et al., 2003). From day 11 of pregnancy until delivery, pregnant female rats were subjected to three stress sessions daily (45 min each), during which they were placed in plastic transparent cylinders with a conical extremity and exposed to bright light or were left undisturbed (control dams). Stress sessions were conducted during the light phase (between 09:00 and 15:00) with a minimum interval of 2 h between each stress session. The local ethical committee approved the gestational restraint procedure. Maternal behavior was monitored for 24 h every day during the first seven post-partum days. Constant monitoring was performed with small infrared cameras placed on the animal cage rack where cages containing lactating females were placed. Within each observation period, the behavior of each mother was scored every minute from post-partum day 1 to day 7 (60 observations/h with 2 h of observation per day, 1 h before lights off and 1 h after lights on). The active behavior of the mother (nursing behavior, grooming, licking, and carrying pups) was scored and the data obtained were expressed as percentages with respect to the total number of observations. Since gestational stress induces a reduction of maternal behavior (Gatta et al., 2018), we refer to the whole procedure as PRS having a prenatal and postnatal effect). In the present study, only male and female offspring from dams presenting a stress-reduced maternal behavior (with a cutoff below 40% of maternal care in the PRS group vs. a cutoff above 60% of maternal care in the control group), and from litters of 10–14 rats with a similar number of males and females, were used. Weaning of the offspring occurred at 21 days after birth.

Experimental Design

Separate sets of rats were used for behavioral studies ($n = 40$, 10 rat/sex/group) and transcriptomic analysis ($n = 60$, $n = 5$/group/time point). Within each litter, we took only two males and two females to minimize any litter effect (Chapman and Stern, 1979). Therefore, there were no more than two sibling within the same time point for the transcriptomic study. Housing conditions were two same-sex animals per cage from each perinatal and experimental group (CONT vs. PRS and behavioral or transcriptomic study) after weaning and until experiments started (at 4 months of age).

Running Wheel Activity

A first group of rats ($n = 10$/sex/group) was used to analyze the rhythm of circadian activity under a regular 12/12 L/D cycle (08:00–20:00). Rats were housed in light, air tight chambers equipped with continuously operating ventilating fans and single-housed in individual cages equipped with a running wheel that allowed continuous recording of locomotor activity via an on-line computer (Chronobiology kit, Stanford Software System, CA, United States), with light intensity set at 30–40 lux at cage floor level. Each chamber contained 10 single-cages, and males and females were housed separately. During the course of the experiments, food and water were provided *ad libitum*; room temperature (22°C) and humidity (60%) were kept constant. After 10–15 days of adaptation to the running wheels, the rhythm of activity was individually analyzed over 10 consecutive days. The onset of activity was identified with a 5 min resolution and was defined as the first time point at which the mean intensity of activity was above 10% of the maximum and remained above that point for at least 50% of the time during the following 30 min. The reversed procedure was used for the cessation (offset) of activity (first time point below 10% of maximum and activity remained below that point for at least 50% of the time during the following 30 min). The time elapsed between the onset and offset of activity was defined as the total time of nocturnal activity, the peak value of activity and peak hour of activity were directly determined on the actogram for each animal. The mean 24 h integrated activity was determined by adding the mean number of revolutions in the wheel, every 5 min over 10 consecutive days for each animal. The data were then plotted with a 30 min or 5 min resolution; this represented the mean number of wheel revolutions performed by the animals.

Exposure to a Chronobiological Stressor

At the end of the recording of normal activity, rats ($n = 10$/sex/group) were subjected to an abrupt 6-h advance shift in the L/D cycle. On the day of the shift, lights were turned-off 6 h before the current time, and the new 12 h L/D cycle (light on, 02:00) was maintained thereafter. The time to resynchronize to the new L/D cycle was defined as the number of days for the animal to exhibit a regular activity for at least three consecutive days. The time taken for re-entrainment to the new L/D cycle was individually assessed using the onset of activity criterion

determined as previously described. This criterion was defined as the smallest number of days required for the shifted activity onset to occur within 30 min of lights-off and to be stable for 3 days under the new L/D cycle.

Gene Expression Analysis in the Suprachiasmatic Nucleus (SCN)

A separate set of male and female CONT and PRS rats was used for gene expression analysis in the brain (n = 5 per group/time point) at three selected time points (15:00, 19:00 and 02:00) under a regular 12/12 L/D cycle (with light on at 08:00) in order to extract SCN during light phase (15:00), before the onset of dark phase (19:00) and during it (02:00).

The SCN of male and female CONT and PRS rats was rapidly dissected and kept frozen at −80°C. Special attention was taken for tissue collection at 2 am: in order to avoid any influence of light on gene expression, animals were killed under red light before tissue dissection, which did occurr under white light. RNA extraction was performed using the RNeasy Plus mini kit (Qiagen, France) following manufacturer's instructions. RNA concentration was determined using Nanodrop (ND-1000, Labtech, Germany), and quality verified by RIN (RNA Integrity Number; Bioanalyzer 2100, Agilent Technologies, France). All RNA samples had a quality score above 7.5 RIN. Retrotranscription was performed with the High-Capacity cDNA Reverse Transcription kit (Applied Biosystems, France). Transcript levels were measured by Custom Taqman qRT-PCR (Applied Biosystems, France). The following Taqman real-time PCR probes were obtained from Applied Biosystems:

Clock-Related Genes

Clock (Rn00573120_m1), aryl hydrocarbon receptor nuclear translocator-like (Bmal, Arntl, Rn00577590_m1), Cry1 (Rn01503063), period circadian regulator 1 (Per1, Rn01496757_m1), period circadian regulator 2 (Per2, Rn01426757_m1), period circadian regulator 3 (Per3, Rn00709499_m1), nuclear receptor subfamily 1-group D-member 1 (Rev-erbA-α, Nrd1, Rn00595671_m1), melatonin-1A receptor (Mel1AR, Rn01488022_m1), melatonin-1B receptor (Mel1BR, Rn01447987_m1), neuronal PAS domain protein 2 (Npas2, Rn01438223_m1).

HPA Axis Stress-Related Genes

Corticotropin releasing hormone receptor 1 (CrhR1, Rn00578611_m1), corticotropin releasing hormone receptor 2 (CrhR2, Rn00575617_m1), glucocorticoid receptor (GR, Nrc1, Rn00565562_m1), mineralocorticoid receptor (MR, Nrc2, Rn00561369_m1), Arginin vasopressin receptor 1a (Avpr1a, Rn00583910_m1), oxytocin receptor (OxtR, Rn00563503_m1).

Signaling-Related Genes

Metabotropic glutamate receptor 2 (mGluR2, Grm2, Rn01447672_m1), metabotropic glutamate receptor 3 (mGluR3, Grm3, Rn01755352_m1), metabotropic glutamate receptor 5 (mGluR5, Grm5, Rn00566628_m1), 5-hydroxytryptamine receptor 2C (Htr2c, Rn00562748_m1), mechanistic target of rapamycin (mTor, Rn00693900_m1), v-akt murine thymoma viral oncogene homolog 1 (Akt1, Rn00583646_m1), disrupted in schizophrenia 1 (Disc1, Rn00598264_m1), dickkopf WNT signaling pathway inhibitor 1 (Dkk1, Rn01501537_m1), early-growth transcription factor 1 (Ngf1A, Egr1, Rn00561139_m1), erb-b2 receptor tyrosine kinase 2 (Erbb2, Rn00566561_m1), erb-b2 receptor tyrosine kinase 3 (Erbb3, Rn00568107_m1), erb-b2 receptor tyrosine kinase 4 (Erbb4, Rn00572447_m1), solute carrier family 17-member 7, vesicle bound sodium-dependent inorganic phosphate cotransporter (vGlut1, Slc17a7, Rn01462431_m1), solute carrier family 1 member 3, glial high affinity glutamate transporter (Glast, Slc1a3, Rn00570130_m1).

Glucose Metabolism-Related Genes

Glycogen synthase kinase 3 beta (Gsk3ß, (Rn00583429_m1), insulin-like growth factor 1 (Igf1, Rn00710306_m1), insulin-like growth factor 1 receptor (Igf1R, Rn00583837_m1), insulin receptor (InsR, Rn00690703_m1), phosphoinositide-3-kinase regulatory subunit 1 (Pik3R1, Rn00564547_m1), solute carrier family 2, facilitated glucose transporter, member 1 (Glut1, Slc2a1, Rn01417099_m1), solute carrier family 2, facilitated glucose transporter, member 3 (Glut3, Slc2a3, Rn00567331_m1), solute carrier family 2, facilitated glucose transporter, member 4 (Glut4, Slc2a4, Rn00562597_m1), O-GlcNAcase (Oga, Mgea5, Rn00590870_m1), O-GlcNAc-transferase (Ogt, Rn00820779_m1), glutamine fructose-6-phosphate transaminase 1 (Gfpt1, Rn01765495_m1) and glutamine fructose-6-phosphate transaminase 2 (Gfpt2, Rn01456720_m1).

Transcript levels were normalized based on endogenous glyceraldehyde-3-phosphate dehydrogenase (Gapdh, Rn01462662_g1) and tyrosine 3-monooxygenase/tryptophan 5-monooxygenase activation protein (Ywhaz, Rn00755072_m1) expression.

Assay validity was assessed by using appropriate negative controls, in which cDNA was omitted. These negative controls were not read by the software. Acquisition of data (threshold cycle, Ct) was performed by StepOnePlus^{TM} software. A ΔCt (Ct of the considered gene – mean Ct (Gapdh and Ywhaz genes) was calculated.

Statistical Analysis

All data were analyzed using two-way Analysis Of Variance ANOVA, with group (CONT vs. PRS) and sex (Males vs. Females) as independent variables, and time (hours) as repeated measure. Fisher's LSD test was used to analyze the differences. Significance was set at a p-value of 0.05. In mRNA analysis, in order to subdivide data accounting for significant lower-order effects when F was larger than, trends with $0.05 < p < 0.08$ were also considered as significant (Snedecor and Cochran, 1967).

RESULTS

PRS Induces a Sex-Dependent Disruption of the Circadian Rhythm of Running Wheel Activity

The circadian rhythms of running wheel activity under a regular 12/12 LD cycle were individually analyzed in male and female

CONT unstressed and PRS rats over 10 consecutive days of continuous registration (**Figure 1A**). PRS induced changes in the circadian rhythm (*Group x Sex x Time effect*, $F_{(1,47)} = 13.241$, $p < 0.05$) with PRS males anticipating the light being switched off by starting the wheel running activity at 19:10 (**Figure 1B**); in contrast, all the other groups started around 20:00 (which is the precise time of light switch off). PRS females presented reduced number of wheel revolutions with respect to all other groups during the dark phase (**Figures 1A,C**). Indeed, there was a clear-cut effect of sex on the effect of PRS on the levels of activity defined by the number of wheel revolutions (**Figure 1C**); first, during the period of lower activity (light phase), both CONT and PRS females were more active than males. During the light phase, PRS increased activity in males, which reached levels of CONT females (*Group x Sex effect*, $F_{(1,36)} = 7.68$, $p < 0.01$). More interestingly, during the period of activity (dark phase), male PRS rats were more active than male CONT rats, in contrast, female PRS rats were less active than CONT females (*Group x Sex effect*, $F_{(1,36)} = 39.48$, $p < 0.01$). In addition, during the dark phase, CONT female rats were less active than CONT male rats. Overall, PRS males presented a phase advance and increased wheel activity, while PRS females were hypoactive and presented a more fragmented profile of activity than did CONT females (**Figure 1D**).

PRS Increases Vulnerability to Chronobiological Stress

We measured the number of days needed for the circadian rhythm of locomotor activity to become resynchronized after an abrupt 6-h advance shift in the L/D cycle (**Figure 2A**). Both PRS and sex influenced the time necessary for resynchronization (ANOVA, *Group x Sex effect*, $F_{(1,36)} = 6.316$, $p < 0.05$). In the CONT group, females required a longer time to resynchronize to the new light shift than the males did ($p < 0.05$). PRS increased the time to become resynchronized to the new L/D cycle in both sexes with PRS males reaching levels of CONT females. Moreover, the PRS effect occurred to a larger extent in female than in males ($p < 0.05$ vs. PRS males). Further, PRS females presented a more fragmented activity than PRS males (**Figure 2B**).

Effect of PRS and Sex on Circadian Gene Expression in the SCN

The expression of the 42 genes analyzed in the SCN during discrete time points (15:00, 19:00 and 02:00) is reported in **Table 1**, with genes such as *Gsk3ß, Igf1, mGluR2, mGluR3, Dkk1,* and *Glast* that were only influenced by PRS or sex (**Supplementary Figure S1**) and the other genes that followed a circadian rhythm in a sex-dependent manner and were also affected by PRS. Seven genes, did not show changes associated with PRS, sex, or time (*CrhR2, mGluR5, Htr2c, Erbb2, Erbb3, Erbb4, Gfpt1, Gfpt2*).

Signaling- and Glucose Metabolism -Related Genes

The expression of genes involved in signaling such as *mTor, Akt1, Disc1, Dkk1, mGluR2, mGluR3,* and *Glast* or in glucose metabolism, such as *Igf1, InsR, Gsk3ß* and *Glut1*, displayed a marked effect of both sex and PRS variables or sex only, whereas circadian oscillations were evident for *mTor, Glut1, Akt1, Disc1,* and *InsR*. As shown in **Supplementary Figure S1**, most of the sex-biased genes were down-regulated in females, with only *Dkk1* and *Igf1* being upregulated. Interestingly, PRS in males downregulated levels of gene expression compared to CONT males, with levels identical to CONT females (*mTor, Gsk3ß, and Glut1*).

Clock- and Glucose Metabolism-Related Genes

Interestingly, we observed circadian variations in gene expression that were influenced by both PRS and sex, in the genes that were measured and were involved in clock and glucose metabolism regulation, such as *Clock*, *Bmal*, *Mel1aR*, *Rev-erbA-α*, *Ngf1A*, and *Oga* (**Figure 3**). Among these genes, sex differences observed in the unstressed group for *Clock* and *Bmal* disappeared in the PRS group. mRNA levels of *Ngf1A* and *Oga* in PRS males showed opposing oscillations when compared to the CONT male group, and this occurred specifically before the onset of the dark phase (19:00) or during it (02:00). Additionally, PRS flipped the sex-specific profile observed in Rev-erbA-α and Mel1aR when compared to CONT, with PRS males showing the same profile that CONT females, and PRS females displaying an expression profile mimicking CONT males (ANOVA, *Group x Sex x Time effect*, Clock, $F_{(2,32)} = 3.229$, $p = 0.05$; Bmal, $F_{(2,32)} = 3.901$, $p < 0.05$; Ngf1A, $F_{(2,32)} = 3.595$, $p < 0.05$; Oga, $F_{(2,32)} = 5.355$, $p < 0.01$; Mel1aR, $F_{(2,32)} = 2.811$, $p = 0.07$; Rev-erbA-α, $F_{(2,32)} = 7.901$, $p < 0.01$).

HPA Axis Stress-Related Genes

The effects of PRS and sex were also observed on most of the genes involved in HPA axis activity and regulation that were included in the present study (**Figure 4**), such as *CrhR1*, *Nr3c2 (MR)*, *AvpR1a*. Here, sex differences observed in unstressed CONT rats in the levels of *CrhR1* and *MR,* which were upregulated in males but not in females, disappeared in the PRS group (ANOVA, CrhR1 (*Group x Sex effect*, $F_{(1,16)} = 18.012$, $p < 0.001$, *Time effect*, $F_{(2,32)} = 4.434$, $p < 0.05$); MR (*Group x Sex effect*, $F_{(1,16)} = 4.520$, $p < 0.05$, *Time effect*, $F_{(2,32)} = 3.140$, p = 0.06; AvpR1a, *Sex effect*, $F_{(1,16)} = 5.701$, $p < 0.05$, *Time effect*, $F_{(2,32)} = 11.228$, $p < 0.001$). On the other hand, Nr3c1 (GR) and OxtR displayed oscillations that were independent of the main variables effect of group or sex (ANOVA, *Time effect only*: GR, $F_{(2,32)} = 6.093$, $p < 0.01$; OxtR, $F_{(2,32)} = 2.965$, $p = 0.07$) and CrhR2 expression was unchanged.

DISCUSSION

We showed a sex- specific profile in the unstressed group that was either exacerbated or flipped by PRS. In unstressed animals, circadian wheel running behavior was greater during the day in females and higher during the night in males. Interestingly, PRS increased and decreased total locomotor activity in males and females, respectively, and it induced a significant phase advance in the rhythm of circadian activity

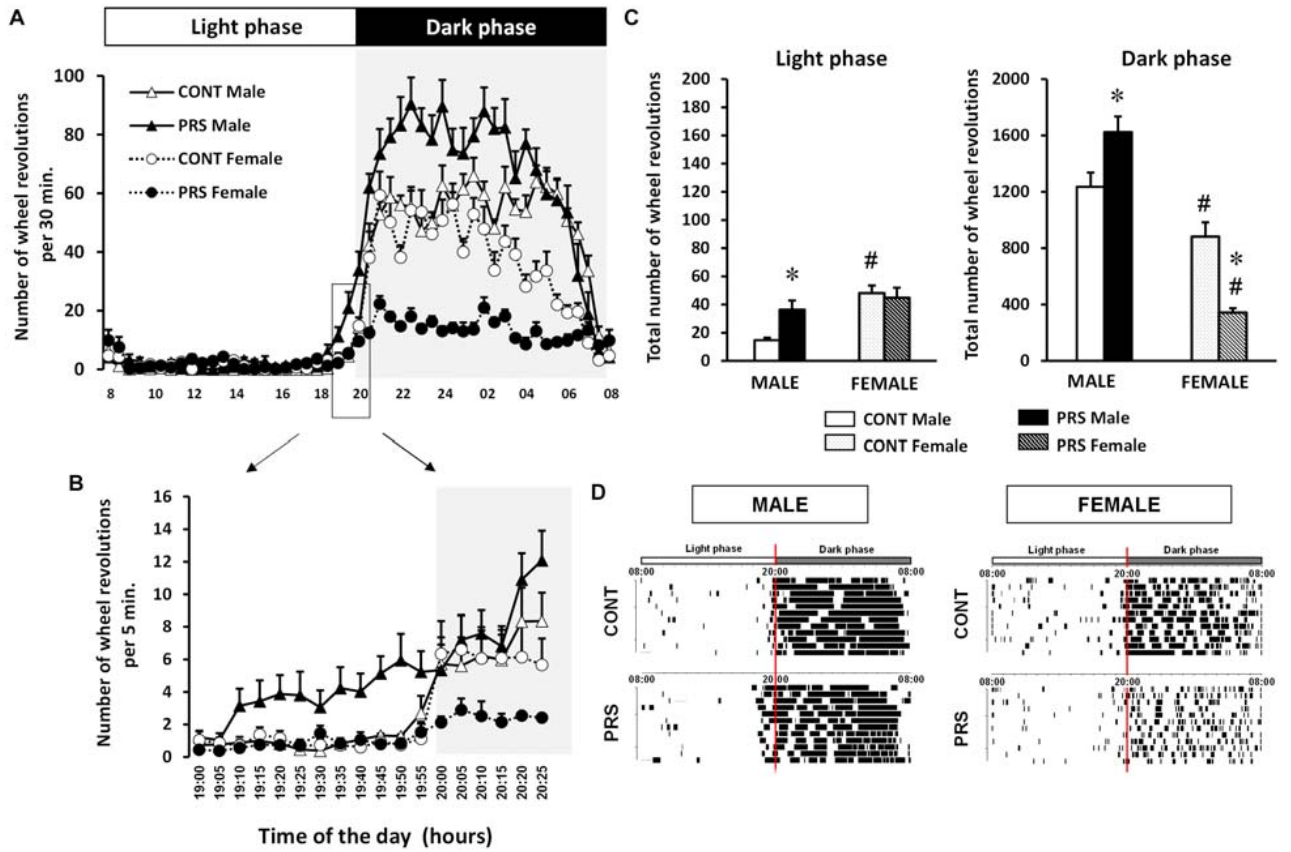

FIGURE 1 | Circadian locomotor activity in a wheel running paradigm in PRS and CONT animals of both sexes. **(A)** The 24 h representation of the mean number of wheel revolutions calculated over 10 consecutive days and plotted with a 30 min resolution, obtained from adult PRS and CONT rats of both sexes showing hyperactivity in PRS males and hypoactivity in PRS females. **(B)** Details of the light switch off period with data plotted with a 5 min resolution allowing a clear visualization of the advance in activity phase in male PRS animals. **(C)** Total number of wheel revolutions over 10 consecutive days during the period of inactivity (light phase) and activity (dark phase) showing the sex effect in the CONT group with females being more active in the light and less active in the dark phase. This effect was observed in the PRS group only in the dark phase, with females being hypoactive, and PRS males being always hyperactive. **(D)** Representative activity records of the circadian running wheel activity of male and female PRS and CONT rats over 10 consecutive days, where the phase advance in PRS males and fragmented activity in both PRS males and females is clearly observed. The first L/D cycle is shown at the top of each panel. Each horizontal line represents 24 h of the animal's life composed from the vertical bar, each representing a wheel revolution. Values are expressed as means ± S.E.M. $n = 10$ rats per group. $^{*}p < 0.05$ PRS *vs.* CONT within the same sex group; $^{\#}p < 0.05$ females *vs*. males within the CONT or PRS group.

exclusively in males. The advance phase observed in PRS males is responsible at least in part for their hyperactivity in the dark cycle. Since in the light period PRS males behaved similarly to unstressed females, PRS induced a dysmasculinization of males' profile. In the dark phase, PRS increased sex differences, with PRS males being hyperactive compared to PRS females, which were hypoactive with respect to all groups. The phase advance observed in PRS males is consistent with the altered circadian functioning of HPA axis activity observed in the PRS model (Koehl et al., 1999). Similar results have also been found using other models of early life stress (i.e., prenatal hypoxia, Joseph et al., 2002). The reduced locomotor activity observed in PRS females could also be related to the changes in the gonadal status that characterize the PRS model. Indeed, the reduced levels in estradiol and impaired estrous cycle observed in PRS females (Reynaert et al., 2016; Van Camp et al., 2018) is associated with the time and intensity of locomotor activity (Wollnik and Turek, 1988). Consistent with this, we have recently shown that a correction of estradiol levels in PRS females increased their rhythm of locomotor activity (Van Camp et al., 2018). The hyperactivity shown by PRS males may be related to the reduced testosterone levels observed in PRS males (Reynaert et al., 2016). In this line, in male mice, reduced testosterone levels induce a phase advance and increase levels of locomotor activity, while testosterone treatment corrects this profile (Butler et al., 2012).

Sex differences in the unstressed group were also observed in response to a chronobiological stress such as a 6-h advance phase shift, with females being more vulnerable than males since they required three more days to resynchronize to the new L/D cycle. The locomotor response to the chronobiological stress in unstressed females is consistent with the greater activation of the glucocorticoid response to stress that is generally observed in female rodents (Heck and Handa, 2018). Sex differences

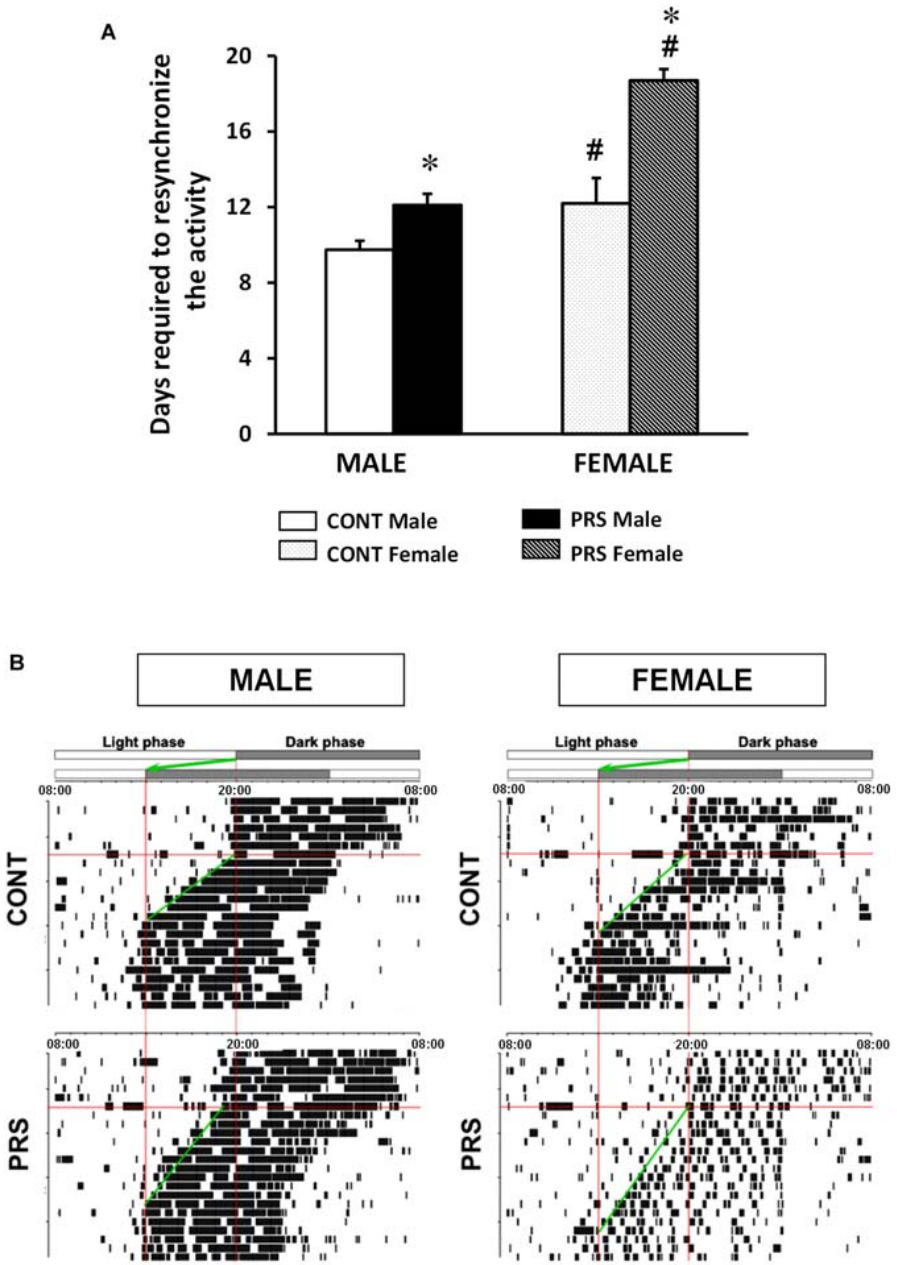

FIGURE 2 | Locomotor response to a chronobiological stressor in PRS and CONT animals of both sexes. **(A)** Circadian running wheel activity from CONT-unstressed and PRS rats of both sexes that were subjected to abrupt 6-h phase advance of the L/D cycle. PRS increased the time taken for resynchronization to the new L/D cycle in both sexes, showing increased sensitivity to the chronobiological stressor in PRS animals. Moreover, this occurred to a larger extent in females than in male PRS rats, with 7 days required by PRS females and 3 days by PRS males. **(B)** Representative activity records of the circadian running wheel activity on day 7. The first L/D cycle and the new L/D cycle, after a 6-h advance in the light period are shown at the top of each panel. Values are expressed as mean ± S.E.M. $n = 10$ rats per group. $^{*}p < 0.05$ PRS *vs.* CONT within the same sex group; $^{\#}p < 0.05$ females *vs.* males within the CONT or PRS group.

were observed also in PRS rats, with a greater number of days required by PRS females to re-entrain with respect to PRS males. However, we found that male and female PRS rats resynchronized their activity rhythm to the new L/D cycle more slowly than unstressed rats. Therefore, PRS males behaved like unstressed females. This specific pattern of increased time of resynchronization in the PRS animals is consistent with the increased stress corticosterone response and rhythm of secretion that has been reported in PRS animals and to a greater extent, in females (Koehl et al., 1997, 1999). Of note, significant increase in the number of days animals required in order to re-entrain to the new LD cycle following a phase shift, have been also observed in other prenatal stress paradigms in both mice and rats, following an 8-h advance/phase shift (chronic mild gestational

TABLE 1 | Effect of perinatal stress and sex on the temporal gene expression in the SCN.

		Males						**Females**						
		CONT			**PRS**			**CONT**			**PRS**			
Gene name	**Statistical effect**	**15**	**19**	**02**	**15**	**19**	**02**	**15**	**19**	**02**	**15**	**19**	**02**	**Taqman ID** (RnX_m1)
Clock	GST	1.00 ± 0.01	0.91 ± 0.03	1.16 ± 0.11	0.89 ± 0.01	0.94 ± 0.01	1.06 ± 0.06	0.98 ± 0.03	0.93 ± 0.05	**0.90$^{\#}$ ± 0.04**	0.93 ± 0.02	0.91 ± 0.05	**1.05* ± 0.04**	00573120
Bmal	GST	1.00 ± 0.04	0.79 ± 0.06	1.12 ± 0.13	0.97 ± 0.04	0.81 ± 0.04	1.13 ± 0.11	1.11 ± 0.03	**1.07$^{\#}$ ± 0.09**	0.96 ± 0.06	**0.89* ± 0.03**	0.88 ± 0.05	**1.28* ± 0.13**	00577590
Oga	GST	1.00 ± 0.03	0.95 ± 0.07	1.08 ± 0.11	1.05 ± 0.04	0.90 ± 0.02	1.00 ± 0.05	1.13 ± 0.04	1.01 ± 0.07	**0.89$^{\#}$ ± 0.04**	**0.94* ± 0.01**	0.96 ± 0.09	**1.09* ± 0.07**	00590870
Ngf1A	GST	1.00 ± 0.24	0.56 ± 0.08	0.52 ± 0.14	**0.66* ± 0.12**	0.73 ± 0.05	**0.91* ± 0.08**	0.76 ± 0.07	0.61 ± 0.09	0.56 ± 0.09	0.86 ± 0.11	0.80 ± 0.04	**0.62$^{\#}$ ± 0.04**	00561138
Rev-erbA-α	GST	1.00 ± 0.06	1.01 ± 0.09	0.55 ± 0.07	1.12 ± 0.07	**0.85* ± 0.05**	0.61 ± 0.06	1.12 ± 0.02	**0.85$^{\#}$ ± 0.04**	0.58 ± 0.02	1.04 ± 0.03	0.95 ± 0.08	0.52 ± 0.02	00595671
Mel1AR	GST	1.00 ± 0.37	0.77 ± 0.24	0.47 ± 0.09	1.38 ± 0.46	**1.74* ± 0.37**	0.59 ± 0.22	1.09 ± 0.22	**2.19$^{\#}$ ± 0.39**	0.68 ± 0.21	0.87 ± 0.28	**0.90*$^{\#}$ ± 0.26**	0.49 ± 0.02	01488022
CrhR1	GS/T	1.00 ± 0.06	0.91 ± 0.03	1.08 ± 0.06	**0.80* ± 0.03**	0.81 ± 0.04	**0.94* ± 0.09**	**0.84$^{\#}$ ± 0.02**	**0.75$^{\#}$ ± 0.03**	**0.86$^{\#}$ ± 0.04**	0.84 ± 0.03	0.83 ± 0.04	0.85 ± 0.03	00578611
MR	GS/T	1.00 ± 0.02	0.94 ± 0.03	1.07 ± 0.07	**0.86*** ± 0.01	0.90 ± 0.02	0.99 ± 0.07	0.97 ± 0.03	0.95 ± 0.04	0.96 ± 0.01	0.96 ± 0.02	0.95 ± 0.08	1.01 ± 0.04	00561369
Mtor	GS/T	1.00 ± 0.01	0.91 ± 0.03	1.00 ± 0.04	**0.87* ± 0.02**	0.92 ± 0.01	0.99 ± 0.05	0.93 ± 0.02	0.86 ± 0.03	**0.92$^{\#}$ ± 0.02**	0.95 ± 0.01	0.91 ± 0.03	0.92 ± 0.04	00693900
Glut1	GS/T	1.00 ± 0.06	1.13 ± 0.09	1.27 ± 0.17	0.84 ± 0.03	0.99 ± 0.04	1.15 ± 0.09	0.80 ± 0.02	**0.88$^{\#}$ ± 0.03**	**0.93$^{\#}$ ± 0.02**	0.84 ± 0.03	1.08 ± 0.17	0.93 ± 0.03	01417099
vGlut	GT/ST	1.00 ± 0.28	0.76 ± 0.11	2.40 ± 0.38	1.23 ± 0.50	0.94 ± 0.19	**3.62* ± 0.56**	1.66 ± 0.45	0.80 ± 0.13	**0.73$^{\#}$ ± 0.13**	1.77 ± 0.14	1.29 ± 0.17	**2.02*$^{\#}$ ± 0.23**	01462431
Mel1BR	ST	1.00 ± 0.16	1.08 ± 0.22	1.39 ± 0.48	1.32 ± 0.14	1.03 ± 0.15	1.30 ± 0.22	1.14 ± 0.18	1.14 ± 0.17	**0.82$^{\#}$ ± 0.13**	0.89 ± 0.09	1.18 ± 0.10	**0.73$^{\#}$ ± 0.09**	01447987
Npas2	ST	1.00 ± 0.02	0.83 ± 0.04	1.23 ± 0.13	0.88 ± 0.03	0.90 ± 0.04	1.23 ± 0.04	0.90 ± 0.01	0.86 ± 0.05	**0.97$^{\#}$ ± 0.03**	0.89 ± 0.01	0.86 ± 0.06	**1.04$^{\#}$ ± 0.06**	01438223
Disc1	ST	1.00 ± 0.09	0.95 ± 0.03	1.45 ± 0.25	0.88 ± 0.04	0.96 ± 0.09	1.48 ± 0.17	0.82 ± 0.03	1.01 ± 0.09	**0.98$^{\#}$ ± 0.02**	0.91 ± 0.05	1.04 ± 0.12	**0.92$^{\#}$ ± 0.09**	00598264
Glut4	ST	1.00 ± 0.15	1.61 ± 0.39	1.92 ± 0.34	1.06 ± 0.10	1.16 ± 0.09	2.15 ± 0.35	1.01 ± 0.08	1.34 ± 0.04	**1.27$^{\#}$ ± 0.13**	1.00 ± 0.12	1.31 ± 0.23	**1.08$^{\#}$ ± 0.11**	00562597
Igf1R	ST	1.00 ± 0.03	1.04 ± 0.05	1.26 ± 0.13	0.94 ± 0.02	0.95 ± 0.02	1.38 ± 0.17	1.01 ± 0.01	1.11 ± 0.03	1.11 ± 0.03	1.03 ± 0.02	**1.17$^{\#}$ ± 0.14**	**1.08$^{\#}$ ± 0.03**	00583837
Pik3R1	ST	1.00 ± 0.07	1.17 ± 0.07	1.32 ± 0.09	1.03 ± 0.04	1.11 ± 0.04	1.27 ± 0.07	**1.24$^{\#}$ ± 0.05**	1.14 ± 0.05	**1.11$^{\#}$ ± 0.03**	1.11 ± 0.05	1.23 ± 0.17	1.21 ± 0.04	00564547
Cry1	S/T	1.00 ± 0.04	1.23 ± 0.07	1.47 ± 0.22	1.00 ± 0.04	1.14 ± 0.07	1.39 ± 0.10	0.90 ± 0.03	1.05 ± 0.06	1.32 ± 0.05	0.89 ± 0.01	1.16 ± 0.10	1.33 ± 0.03	01503063
Per1	S/T	1.00 ± 0.08	1.13 ± 0.12	0.89 ± 0.08	0.85 ± 0.11	1.04 ± 0.05	1.03 ± 0.11	0.84 ± 0.06	0.92 ± 0.05	0.76 ± 0.01	0.86 ± 0.02	1.15 ± 0.16	0.79 ± 0.06	01496757
Avpr1a	S/T	1.00 ± 0.09	1.13 ± 0.10	1.32 ± 0.22	1.04 ± 0.05	1.05 ± 0.04	1.40 ± 0.10	1.14 ± 0.04	1.10 ± 0.02	1.51 ± 0.09	1.18 ± 0.07	1.18 ± 0.11	1.43 ± 0.08	00583910

(Continued)

TABLE 1 | Continued

		Males						Females						
		CONT			PRS			CONT			PRS			
Gene name	**Statistical effect**	**15**	**19**	**02**	**15**	**19**	**02**	**15**	**19**	**02**	**15**	**19**	**02**	**Taqman ID** (RnX_m1)
Akt1	S/T	1.00 ± 0.03	0.95 ± 0.01	1.07 ± 0.04	0.91 ± 0.03	0.92 ± 0.03	1.13 ± 0.13	**0.86$^{\#}$ ± 0.03**	0.89 ± 0.03	**0.93$^{\#}$ ± 0.02**	0.96 ± 0.01	0.91 ± 0.05	**0.93$^{\#}$ ± 0.02**	00583646
nsR	S/T	1.00 ± 0.02	0.90 ± 0.04	1.08 ± 0.12	0.91 ± 0.02	0.88 ± 0.02	0.97 ± 0.07	0.92 ± 0.03	0.85 ± 0.02	0.88 ± 0.02	0.88 ± 0.02	0.90 ± 0.05	0.95 ± 0.03	00690703
Gsk3b	GS	1.00 ± 0.02	1.01 ± 0.03	1.01 ± 0.02	0.95 ± 0.03	0.95 ± 0.04	0.92 ± 0.02	0.96 ± 0.01	0.88 ± 0.04	0.94 ± 0.03	0.93 ± 0.02	0.93 ± 0.06	0.91 ± 0.04	00583429
Igf1	S	1.00 ± 0.13	1.16 ± 0.16	1.08 ± 0.11	1.13 ± 0.08	1.18 ± 0.05	1.28 ± 0.12	1.80 ± 0.46	1.74 ± 0.19	1.59 ± 0.12	1.68 ± 0.25	1.75 ± 0.14	1.91 ± 0.25	00710306
mGlu2	S	1.00 ± 0.15	0.90 ± 0.12	1.04 ± 0.13	1.02 ± 0.07	0.70 ± 0.10	1.19 ± 0.39	0.92 ± 0.09	0.60 ± 0.11	0.52 ± 0.08	0.72 ± 0.10	0.79 ± 0.09	0.68 ± 0.07	01447672
mGlu3	S	1.00 ± 0.07	0.98 ± 0.08	1.11 ± 0.10	0.82 ± 0.04	0.81 ± 0.06	1.20 ± 0.26	0.89 ± 0.05	0.78 ± 0.10	0.82 ± 0.04	0.82 ± 0.04	0.95 ± 0.12	0.89 ± 0.06	01755352
Dkk1	S	1.00 ± 0.12	0.89 ± 0.09	1.46 ± 0.20	1.03 ± 0.11	0.87 ± 0.09	1.63 ± 0.38	1.04 ± 0.15	1.74 ± 0.39	1.17 ± 0.22	1.41 ± 0.19	1.22 ± 0.27	1.56 ± 0.09	01501537
Glast	S	1.00 ± 0.03	1.06 ± 0.03	1.05 ± 0.08	1.02 ± 0.03	0.99 ± 0.08	1.22 ± 0.14	0.98 ± 0.02	0.93 ± 0.03	0.97 ± 0.03	0.98 ± 0.02	0.99 ± 0.03	0.94 ± 0.02	00570130
Per2	T	1.00 ± 0.05	1.43 ± 0.13	1.12 ± 0.11	0.98 ± 0.08	1.27 ± 0.09	1.19 ± 0.11	1.03 ± 0.01	1.22 ± 0.05	1.00 ± 0.04	1.02 ± 0.02	1.38 ± 0.20	0.91 ± 0.05	01427704
Per3	T	1.00 ± 0.02	1.20 ± 0.07	1.09 ± 0.11	0.93 ± 0.05	1.11 ± 0.02	1.04 ± 0.07	0.97 ± 0.02	1.10 ± 0.05	1.07 ± 0.04	0.94 ± 0.01	1.25 ± 0.18	0.96 ± 0.03	00709499
GR	T	1.00 ± 0.03	1.04 ± 0.07	1.29 ± 0.12	0.95 ± 0.04	1.04 ± 0.07	1.16 ± 0.07	1.01 ± 0.05	1.08 ± 0.06	1.09 ± 0.06	0.95 ± 0.02	1.07 ± 0.10	1.04 ± 0.07	00565562
OxtR	T	1.00 ± 0.16	0.97 ± 0.16	0.76 ± 0.12	0.89 ± 0.12	1.23 ± 0.19	0.96 ± 0.20	0.87 ± 0.08	1.05 ± 0.11	0.75 ± 0.03	0.87 ± 0.07	1.22 ± 0.26	1.01 ± 0.11	00563503
Glut3	T	1.00 ± 0.03	0.88 ± 0.02	0.99 ± 0.04	0.87 ± 0.02	0.91 ± 0.03	0.99 ± 0.04	0.95 ± 0.02	0.87 ± 0.04	0.95 ± 0.03	0.93 ± 0.00	0.89 ± 0.03	0.91 ± 0.05	00567331
Ogt	T	1.00 ± 0.06	1.02 ± 0.04	1.24 ± 0.14	1.09 ± 0.06	1.26 ± 0.10	1.31 ± 0.18	1.28 ± 0.05	1.07 ± 0.09	1.17 ± 0.08	1.00 ± 0.03	1.18 ± 0.14	1.26 ± 0.11	00820779
mGlu5	–	1.00 ± 0.08	0.82 ± 0.05	0.88 ± 0.06	0.90 ± 0.06	0.91 ± 0.04	1.10 ± 0.16	0.94 ± 0.04	0.83 ± 0.07	0.88 ± 0.04	0.95 ± 0.04	0.82 ± 0.06	0.84 ± 0.03	00566628
Htr2c	–	1.00 ± 0.06	1.05 ± 0.06	1.10 ± 0.17	1.07 ± 0.09	1.03 ± 0.11	1.00 ± 0.22	0.93 ± 0.06	1.17 ± 0.17	0.92 ± 0.05	0.85 ± 0.01	1.23 ± 0.08	1.00 ± 0.07	00562748
CrhR2	–	1.00 ± 0.12	0.99 ± 0.08	0.89 ± 0.07	0.92 ± 0.11	1.05 ± 0.11	0.86 ± 0.02	1.00 ± 0.11	1.00 ± 0.12	1.00 ± 0.05	1.07 ± 0.07	1.00 ± 0.06	0.94 ± 0.03	00575617
ErbB2	–	1.00 ± 0.09	1.07 ± 0.07	1.00 ± 0.12	1.02 ± 0.03	1.02 ± 0.04	1.12 ± 0.11	0.97 ± 0.06	1.37 ± 0.15	1.07 ± 0.07	0.95 ± 0.07	1.15 ± 0.11	1.04 ± 0.05	00566561
ErbB3	–	1.00 ± 0.07	1.01 ± 0.09	1.27 ± 0.13	0.87 ± 0.05	0.93 ± 0.07	0.96 ± 0.11	1.01 ± 0.06	0.97 ± 0.07	1.09 ± 0.06	0.90 ± 0.04	1.07 ± 0.10	1.01 ± 0.09	00568107
ErbB4	–	1.00 ± 0.03	0.97 ± 0.03	1.12 ± 0.12	0.93 ± 0.03	0.91 ± 0.03	1.07 ± 0.10	1.08 ± 0.06	0.93 ± 0.02	0.92 ± 0.03	0.96 ± 0.02	0.99 ± 0.07	0.98 ± 0.06	00572447
Gfpt1	–	1.00 ± 0.03	0.99 ± 0.04	1.11 ± 0.08	0.96 ± 0.04	0.97 ± 0.03	1.06 ± 0.04	1.01 ± 0.04	0.97 ± 0.02	0.97 ± 0.02	0.99 ± 0.02	1.00 ± 0.06	1.00 ± 0.04	01765495
Gfpt2	–	1.00 ± 0.06	0.97 ± 0.04	1.10 ± 0.09	0.93 ± 0.03	0.90 ± 0.02	1.12 ± 0.11	0.90 ± 0.04	0.93 ± 0.03	0.95 ± 0.02	0.92 ± 0.04	1.00 ± 0.10	0.95 ± 0.06	01456720

*Expression of selected genes in the SCN of unstressed or PRS rats of both sexes was assayed by Custom Taqman qRT-PCR. For each sample, expression levels were normalized to the average levels of unstressed male rats obtained at 15:00 and expressed as Relative Quantitation (RQ). Genes are listed according to the main statistical effect: GST, Group × Stress × Time effect; GS, Group × Sex effect; GT, group × time; ST, sex × time effect; G, S, T for Group, Sex, or Time effect only. Data are means ± S.E.M of five determinations for each group. *$p < 0.05$ for PRS vs. CONT of the same-sex group; $^{\#}p < 0.05$ for females vs. males within the PRS or CONT group. Bolded values are those with greater significance.*

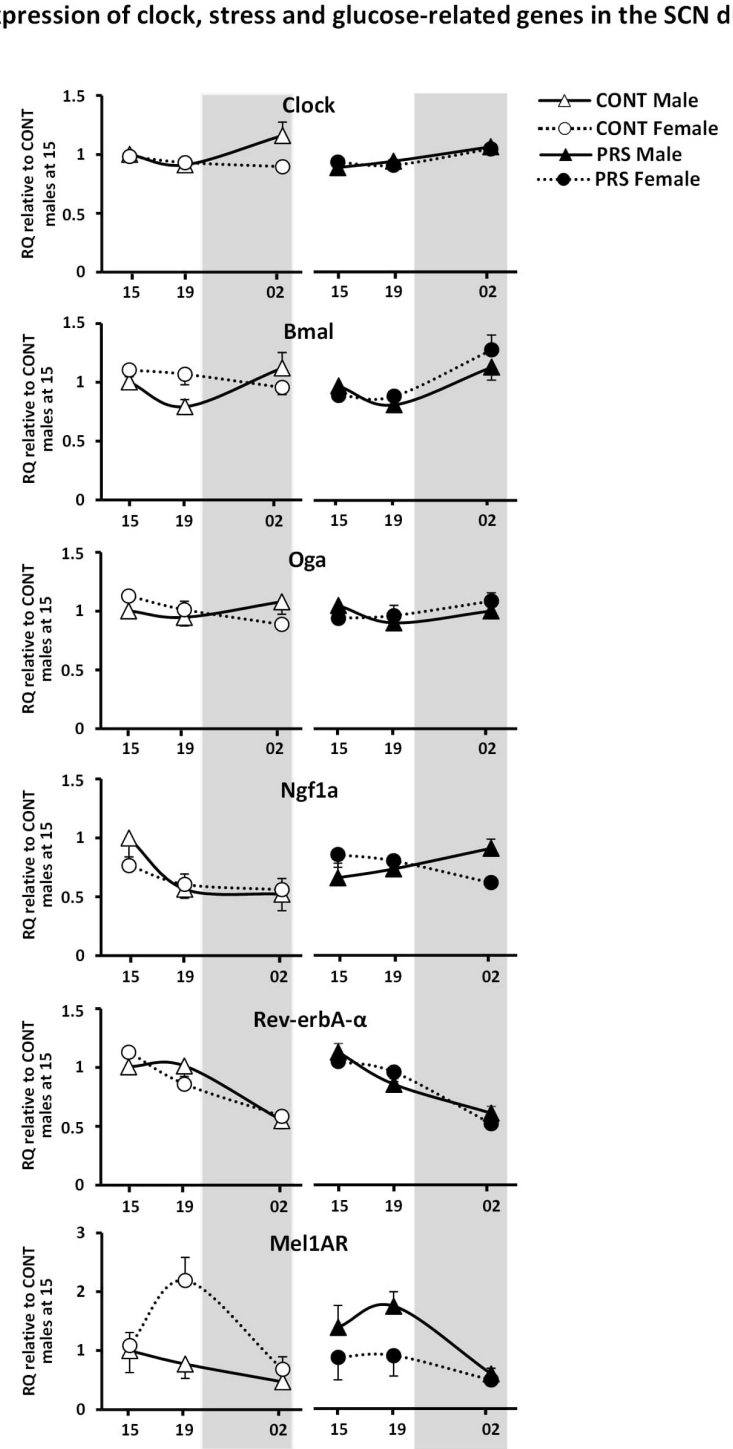

FIGURE 3 | Circadian expression of clock and glucose metabolism-related genes in the SCN of PRS and CONT animals of both sexes. Expression of selected genes in the SCN of CONT or PRS rats of both sexes was assayed by Custom Taqman qRT-PCR. Expression levels of each sample were normalized to the average levels in CONT male rats obtained at 15:00 and expressed as Relative Quantitation (RQ). Effect of PRS on gene expression was observed in both sexes for all the genes considered. PRS induced a dysmasculinization in the profile of expression for *Clock* and *Mel1aR* in males, which showed the same expression profile as CONT females. In *Bmal*, *Rev-erb*-α and *Mel1aR*, PRS females behaved as CONT males. Data are depicted as mean ± S.E.M of five determinations for each group.

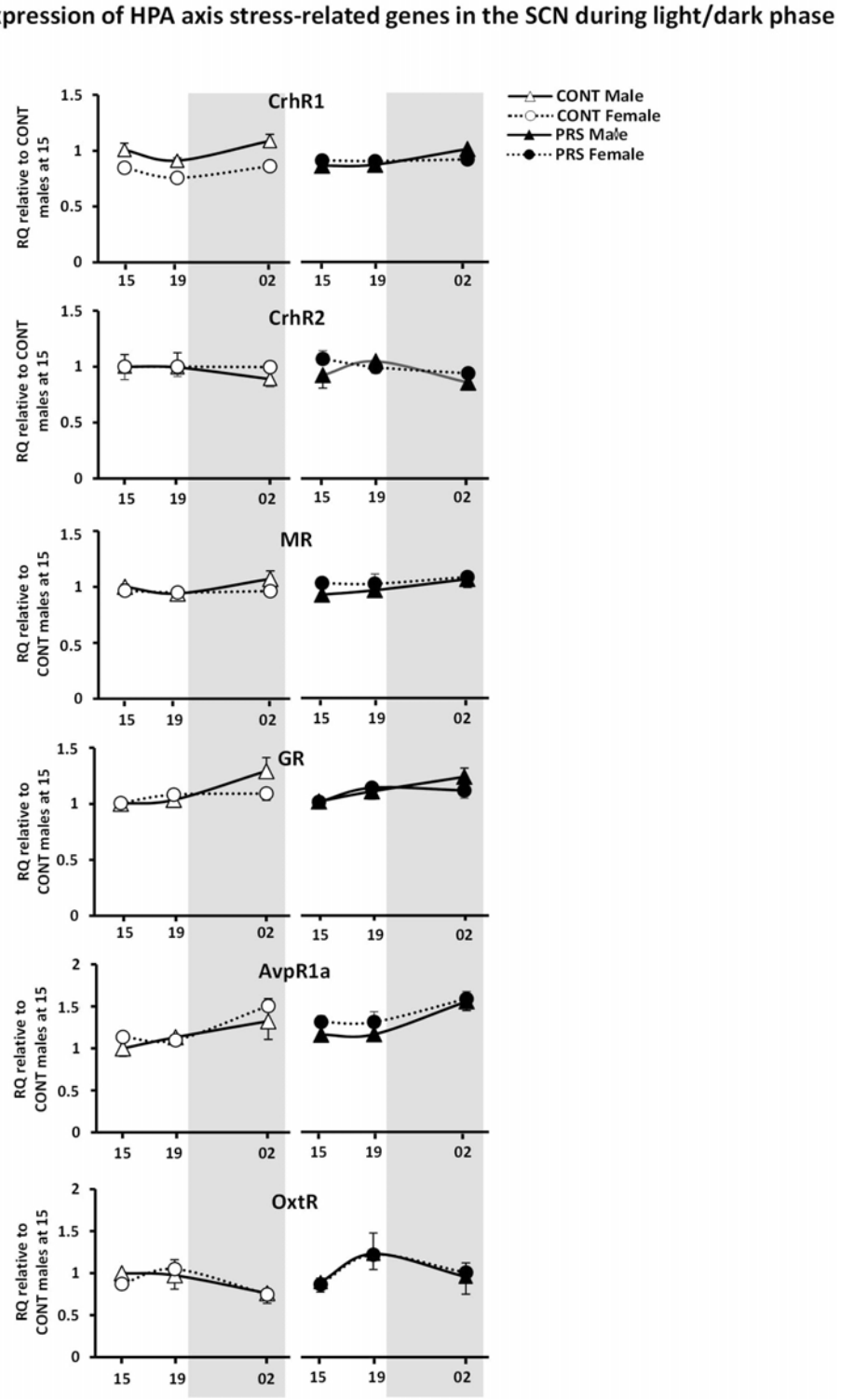

FIGURE 4 | Circadian expression of HPA axis stress-related genes in the SCN of PRS and CONT animals of both sexes. Expression of selected genes in the SCN of CONT or PRS rats of both sexes was assayed by Custom Taqman qRT-PCR. Expression levels of each sample were normalized to the average levels in CONT male rats obtained at 15:00 and expressed as Relative Quantitation (RQ). All genes presented oscillation with the time exception made for *CrhR2*. PRS induced a dysmasculinization in the profile of expression for *CrhR1* in males, which showed the same expression profile as CONT females. All values are represented as mean + S.E.M of five animals per group.

stress, Kiryanova et al., 2017) or an abrupt 6-h delay/phase shift (prenatal hypoxia Joseph et al., 2002).

Remarkably, the pattern of locomotor activity in PRS rats under a 12:12 h L/D cycle as well as in response to the chronobiological stress was erratic and fragmented, and this was particularly evident in female PRS rats. This specific fragmentation profile has already been shown for another circadian rhythm – the sleep-wake cycle – with PRS males showing discontinuous and shorter sleep when compared to unstressed animals (Dugovic et al., 1999; Mairesse et al., 2013). Moreover, fragmented circadian activity rhythms reflect age-related alterations in the biological clock, because circadian rhythms and sleep patterns change with age (Turek et al., 1995; Van Someren, 2000). Along these lines, the characteristic pattern of fragmentation in PRS rats would lean toward an accelerated aging of the circadian clock induced by PRS. This would broaden the concept of PRS-mediated accelerated aging processes to predictive adaptation, which has already been put forward at the level of reactive adaptation. Indeed, adult PRS males display prolonged secretion of plasma corticosterone in response to stress compared to unstressed aged animals (Vallée et al., 1999), and PRS females display reduced levels of estradiol already in adulthood (Reynaert et al., 2016) similar to unstressed females during aging (Van Camp et al., 2018).

The main actor in the regulation of central and peripheral circadian rhythms is the SCN. Interestingly, we observed patterns of oscillations for the genes analyzed in the SCN that were changed by PRS and in a sex-dependent manner. Indeed, the sex-specific profile of gene expression that was reported in almost all of the genes studied in the SCN in unstressed animals, was flipped by PRS, with PRS males displaying a pattern similar to that of unstressed females. As observed in the behavioral phenotype, this pattern of dysmasculinization also affected gene expression changes.

We observed that females had downregulated expression of the genes involved in signaling regulation, with only *Dkk1* and *Igf1* being upregulated. In particular, for glucose transporters, marked sex differences exist in the gene expression profiles in rodents' tissues (Nagai et al., 2014). Here PRS downregulated *mTor*, *Glut1,* and *Gsk3b* compared to unstressed males. Moreover, PRS males displayed a profile identical to unstressed females, again indicating a pattern of dysmasculinization. Down-regulation of *Glut1* in the SCN of PRS males suggests an impairment of glucose metabolism in the brain. Indeed, we previously reported downregulation of *GLUT1* in the placenta of male PRS fetuses (Mairesse et al., 2007).

Among the genes involved in clock and glucose regulation, we showed upregulation of *Clock* in unstressed males compared to unstressed females and upregulation of *Bmal*, *Oga*, and to a greater extent for *Mel1aR* in unstressed females. Levels of *Clock* in PRS males, were downregulated at night (02:00) with respect to unstressed males, thus displaying an unstressed female-like profile. Recent studies in rats indicate that *Clock* is expressed across brain tissues in a sex-specific pattern (Chun et al., 2015). PRS in males also downregulated *Ngf1A* during the day and higher levels during the night when compared to both unstressed animals and PRS females. Interestingly, *Bmal* and *Rev-erb-α* in PRS females displayed a masculinized profile, in that it mimicked the one observed in unstressed males. Remarkably, we observed that PRS completely flipped the sex-dependent expression of *Mel1aR* transcript levels, with PRS males showing the same profile as unstressed females with higher levels of Mel1aR expression, and PRS females displaying an expression profile similar to that of unstressed males, with reduced levels of the transcript. Within the stress response genes, we observed minor effects with upregulation of *CrhR1* mRNA levels in the SCN in males compared to females in the unstressed group. Overall, among all the genes studied, the unique profile in *Mel1aR* expression indicates that this gene is a key regulator in the programming of the circadian system induced by PRS.

CONCLUSION

Our results provide a first characterization of sex differences in the behavioral and molecular chronobiological profile in unstressed rats. PRS affected males to greater extent than females on the set-up of the circadian system, and lead to the dysmasculinization of PRS males related to locomotor activity phenotype, resynchronization to the new L/D cycle, and in gene expression in the SCN by suggesting a critical role for *Mel1aR in both sexes*. To our knowledge, this is the first demonstration of sex-dependent studies on predictive adaptation programmed by early life stress. Moreover, our results provide additional information, this time at the gene expression level, on the specific pattern of dysmasculinization, which has already been reported at the sexual, physiological, and behavioral level in animal studies of prenatal stress in the past decades (Ward, 1972, 1984; Becker and Kowall, 1977; Dahlöf et al., 1977; Dörner et al., 1983; Ward and Weisz, 1984; Koehl et al., 1997, 1999; Weinstock, 2001; Reznikov and Tarasenko, 2007). The disrupting effect induced by PRS has already been shown in reactive adaptation with its effects on stress response and glutamatergic transmission in the hippocampus. The results obtained in the present study extend this disruption to the main biological clock - and therefore to predictive adaptation. Overall, perturbation of the early life environment has profound consequences on the ability of the organism to react to changes (stress response) or anticipate those changes (circadian rhythms). Therefore, it is necessary to consider sex differences in translational research, in order to gain knowledge of this under-explored field. Animal models of stress- and sleep-disorders as well as sex differences satisfy translational criteria of validity and thus provide a great opportunity of investigation.

ETHICS STATEMENT

This study was carried out in accordance with the recommendations of the committee on animal experimentation CEEA75, Lille France. All experiments followed the rules of the European Communities Council Directive 2010/63/EU.

AUTHOR CONTRIBUTIONS

SM-F, JeM, GVC, JoM, FN, and SM designed the study and wrote the manuscript. SM-F, JeM, GVC, M-LR, EG, JoM, and HB conducted the experiments and analyzed the data.

FUNDING

This study was supported by the University of Lille, Sapienza University of Rome (Framework Agreement signed on February 15th, 2007), and the CNRS within the framework of the Prenatal Stress and Neurodegenerative Diseases International Associated Laboratory (LIA-PSND), co-directed by Professors SM (France) and FN (Italy). Behavioral assessments were carried out using the platform PHExMAR of the University of Lille. We are indebted to the Research Federation FRABio (University of Lille, CNRS, FR 3688, FRABio, Biochimie Structurale et Fonctionnelle des Assemblages Biomoléculaires) for providing the scientific and technical environment conducive to completing this body of work. Transcriptomic analysis was performed using the platform QPCR Imagif-CNRS, at Gif-sur-Yvette. English editing was provided by Editing Elsevier services.

SUPPLEMENTARY MATERIAL

The Supplementary Material for this article can be found online at: https://www.frontiersin.org/articles/10.3389/fnmol.2019.00089/full#supplementary-material

FIGURE S1 | Effect of PRS and sex differences on the expression levels of signaling- and glucose metabolism-related genes in the SCN. Expression of selected genes in the SCN of CONT or PRS rats of both sexes was assayed by Custom Taqman qRT-PCR. Expression levels of each sample were normalized to the average levels in CONT male rats obtained at 15:00 and expressed as Relative Quantitation (RQ). All genes displayed a marked effect of both sex and PRS variables or sex only. Here, gene expression is pulled over time variable. Most of the sex differences were in the direction of reduced expression levels for females, with only *Dkk1* and *Igf1* being upregulated in females. PRS males displayed reduced levels of expression for *mTor*, *Glut1*, and *Gsk3b* and therefore, displayed a profile identical to CONT females. Data are depicted as mean ± S.E.M of five determinations for each group (ANOVA, *Group x Sex effect*, mTor $F_{(1,16)} = 5.750$, $p < 0.05$; Glut1 $F_{(1,16)} = 5.051$, $p < 0.05$; Gsk3ß $F_{(1,16)} = 3.288$, $p = 0.07$; *Sex effect only*, mGlu2, $F_{(1,16)} = 9.268$, $p < 0.01$; mGlu3 $F_{(1,16)} = 5.894$, $p < 0.05$; Akt1, $F_{(1,16)} = 9.747$, $p < 0.01$; Disc, $F_{(1,16)} = 5.991$ $p < 0.05$; Dkk1, $F_{(1,16)} = 4.855$ $p < 0.05$; Glast, $F_{(1,16)} = 7.617$, $p < 0.01$; InsR, $F_{(1,16)} = 3.893$, $p = 0.06$; *Time effect*, mTor $F_{(2,32)} = 4.180$, $p < 0.05$; Glut1, $F_{(2,32)} = 6.046$, $p < 0.01$; Akt1, $F_{(2,32)} = 5.151$, $p < 0.05$; Disc1, $F_{(2,32)} = 8.906$, $p < 0.001$; InsR, $F_{(2,32)} = 4.050$, $p < 0.05$). $^{*}p < 0.05$ PRS vs. CONT within the same sex group; $^{\#}p < 0.05$ and $^{\#\#}p < 0.01$ females vs. males within the CONT or PRS group.

REFERENCES

Albers, H., Gerall, A., and Axelson, J. (1981). Effect of reproductive state on circadian periodicity in the rat. *Physiol. Behav.* 26, 21–25. doi: 10.1016/0031-9384(81)90073-1

Bailey, M., and Silver, R. (2014). Sex differences in circadian timing systems: implications for disease. *Front. Neuroendocrinol.* 35, 111–139. doi: 10.1016/j.yfrne.2013.11.003

Becker, G., and Kowall, M. (1977). Crucial role of the postnatal maternal environment in the expression of prenatal stress effects in the male rats. *J. Comp. Physiol. Psychol.* 91, 1432–1446. doi: 10.1037/h0077401

Beery, A. K., and Zucker, I. (2011). Sex bias in neuroscience and biomedical research. *Neurosci. Biobehav. Rev.* 35, 565–572. doi: 10.1016/j.neubiorev.2010.07.002

Brunton, P. J., Donadio, M. V. F., and Russell, J. A. (2011). Sex differences in prenatally programmed anxiety behaviour in rats: differential corticotropin-releasing hormone receptor mRNA expression in the amygdaloid complex. *Stress* 14, 634–643. doi: 10.3109/10253890.2011.604750

Buijs, R. M., and Kalsbeek, A. (2001). Hypothalamic integration of central and peripheral clocks. *Nat. Rev. Neurosci.* 2, 521–526. doi: 10.1038/35081582

Bunney, J. N., and Potkin, S. G. (2008). Circadian abnormalities, molecular clock genes and chronobiological treatments in depression. *Br. Med. Bull.* 86, 23–32. doi: 10.1093/bmb/ldn019

Butler, M. P., Karatsoreos, I. N., LeSauter, J., and Silver, R. (2012). Dose-dependent effects of androgens on the circadian timing system and its response to light. *Endocrinology* 153, 2344–2352. doi: 10.1210/en.2011-1842

Chapman, R. H., and Stern, J. M. (1979). Failure of severe maternal stress or ACTH during pregnancy to affect emotionality of male rat offspring: implications of litter effects for prenatal studies. *Dev. Psychobiol.* 12, 255–267. doi: 10.1002/dev.420120309

Chun, L. E., Woodruff, E. R., Morton, S., Hinds, L. R., and Spencer, R. L. (2015). Variations in phase and amplitude of rhythmic clock gene expression across prefrontal cortex, hippocampus, amygdala, and hypothalamic paraventricular and suprachiasmatic nuclei of male and female rats. *J. Biol. Rhyth.* 30, 417–436. doi: 10.1177/0748730415598608

Cirelli, C. (2009). The genetic and molecular regulation of sleep: from fruit flies to humans. *Nat. Rev. Neurosci.* 10, 549–560. doi: 10.1038/nrn2683

Dahlöf, L. G., Hård, E., and Larsson, K. (1977). Influence of maternal stress on offspring sexual behavior. *Anim. Behav.* 25, 958–968. doi: 10.1016/0003-3472(77)90047-1

Darnaudéry, M., and Maccari, S. (2008). Epigenetic programming of the stress response in male and female rats by prenatal restraint stress. *Brain Res. Rev.* 57, 571–585. doi: 10.1016/j.brainresrev.2007.11.004

de Kloet, E. R. (1999). Neurobiology of adaptation disorders. *Acta Neuropsychiatr.* 11, 11–14. doi: 10.1017/S0924270800036292

Dibner, C., Schibler, U., and Albrecht, U. (2010). The mammalian circadian timing system: organization and coordination of central and peripheral clocks. *Annu. Rev. Physiol.* 72, 517–549. doi: 10.1146/annurev-physiol-021909-135821

Dörner, G., Götz, F., and Döcke, W. D. (1983). Prevention of demasculinization and feminization of the brain in prenatally stressed male rats by perinatal androgen treatment. *Exp. Clin. Endocrinol.* 81, 88–90. doi: 10.1055/s-0029-1210211

Dugovic, C., Maccari, S., Weibel, L., Turek, F. W., and Van Reeth, O. (1999). High corticosterone levels in prenatally stressed rats predict persistent paradoxical sleep alterations. *J. Neurosci.* 19, 8656–8664. doi: 10.1523/JNEUROSCI.19-19-08656.1999

Gatta, E., Mairesse, J., Deruyter, L., Marrocco, J., Van Camp, G., Bouwalerh, H., et al. (2018). Reduced maternal behavior caused by gestational stress is predictive of life span changes in risk-taking behavior and gene expression due to altering of the stress/anti-stress balance. *Neurotoxicology* 66, 138–149. doi: 10.1016/j.neuro.2018.04.005

Gerstner, J. R., and Yin, J. C. P. (2010). Circadian rhythms and memory formation. *Nat. Rev. Neurosci.* 11, 577–588. doi: 10.1038/nrn2881

Heck, A. L., and Handa, R. J. (2018). Sex differences in the hypothalamic-pituitary-adrenal axis response to stress: an important role for gonadal hormones. *Neuropsychopharmacology* 44, 45–58. doi: 10.1038/s41386-018-0167-9

Hughes, M. E., DiTacchio, L., Hayes, K. R., Vollmers, C., Pulivarthy, S., Baggs, J. E., et al. (2009). Harmonics of circadian gene transcription in mammals. *PLoS Genet.* 5:e1000442. doi: 10.1371/journal.pgen.1000442

Joseph, V., Mamet, J., Lee, F., Dalmaz, Y., and Van Reeth, O. (2002). Prenatal hypoxia impairs circadian synchronisation and response of the biological clock to light in adult rats. *J. Physiol.* 543, 387–395. doi: 10.1113/jphysiol.2002.022236

Kiryanova, V., Smith, V. M., Dyck, R. H., and Antle, M. C. (2017). Circadian behavior of adult mice exposed to stress and fluoxetine during development. *Psychopharmacology* 234, 793–804. doi: 10.1007/s00213-016-4515-3

Klein, D. C., Moore, R. Y., and Reppert, S. M. (1991). *Suprachiasmatic Nucleus: The Mind 's Clock*. New York, NY: Oxford University Press.

Koehl, M., Barbazanges, A., Le Moal, M., and Maccari, S. (1997). Prenatal stress induces a phase advance of circadian corticosterone rhythm in adult rats which is prevented by postnatal stress. *Brain Res.* 759, 317–320. doi: 10.1016/S0006-8993(97)00394-6

Koehl, M., Darnaudéry, M., Dulluc, J., Van Reeth, O., Le Moal, M., and Maccari, S. (1999). Prenatal stress alters circadian activity of hypothalamo-pituitary-adrenal axis and hippocampal corticosteroid receptors in adult rats of both gender. *J. Neurobiol.* 40, 302–315. doi: 10.1002/(SICI)1097-4695(19990905)40:3<302::AID-NEU3>3.0.CO;2-7

Liyanarachchi, K., Ross, R., and Debono, M. (2017). Human studies on hypothalamo-pituitary-adrenal (HPA) axis. *Best Pract. Res. Clin. Endocrinol. Metab.* 31, 459–473. doi: 10.1016/j.beem.2017.10.011

Maccari, S., Darnaudery, M., Morley-Fletcher, S., Zuena, A. R., Cinque, C., and Van Reeth, O. (2003). Prenatal stress and long-term consequences: implications of glucocorticoid hormones. *Neurosci. Biobehav. Rev.* 27, 119–127. doi: 10.1016/S0149-7634(03)00014-9

Maccari, S., and Morley-Fletcher, S. (2007). Effects of prenatal restraint stress on the hypothalamus-pituitary-adrenal axis and related behavioural and neurobiological alterations. *Psychoneuroendocrinology* 32(Suppl. 1), S10–S15. doi: 10.1016/j.psyneuen.2007.06.005

Maccari, S., Piazza, P. V., Kabbaj, M., Barbazanges, A., Simon, H., and Le Moal, M. (1995). Adoption reverses the long-term impairment in glucocorticoid feedback induced by prenatal stress. *J. Neurosci.* 15, 110–116. doi: 10.1523/JNEUROSCI.15-01-00110.1995

Maccari, S., Polese, D., Reynaert, M. L., Amici, T., Morley-Fletcher, S., and Fagioli, F. (2017). Early-life experiences and the development of adult diseases with a focus on mental illness: the human birth theory. *Neuroscience* 342, 232–251. doi: 10.1016/j.neuroscience.2016.05.042

Mairesse, J., Gatta, E., Reynaert, M. L., Marrocco, J., Morley-Fletcher, S., Soichot, M., et al. (2015). Activation of presynaptic oxytocin receptors enhances glutamate release in the ventral hippocampus of prenatally restraint stressed rats. *Psychoneuroendocrinology* 62, 36–46. doi: 10.1016/j.psyneuen.2015.07.005

Mairesse, J., Lesage, J., Breton, C., Bréant, B., Hahn, T., Darnaudéry, M., et al. (2007). Maternal stress alters endocrine function of the feto-placental unit in rats. *Am. J. Physiol. Endocrinol. Metab.* 292, E1526–E1533. doi: 10.1152/ajpendo.00574.2006

Mairesse, J., Silletti, V., Laloux, C., Zuena, A. R., Giovine, A., Consolazione, M., et al. (2013). Chronic agomelatine treatment corrects the abnormalities in the circadian rhythm of motor activity and sleep/wake cycle induced by prenatal restraint stress in adult rats. *Int. J. Neuropsychopharmacol.* 16, 323–338. doi: 10.1017/S1461145711001970

McCarthy, M. M., Woolley, C. S., and Arnold, A. P. (2017). Incorporating sex as a biological variable in neuroscience: what do we gain? *Nat. Rev. Neurosci.* 12, 707–708. doi: 10.1038/nrn.2017.137

McEwen, B. S. (1998). Stress, adaptation, and disease. allostasis and allostatic load. *Ann. N.Y. Acad. Sci.* 1, 33–44. doi: 10.1111/j.1749-6632.1998.tb09546.x

McEwen, B. S. (2016). In pursuit of resilience: stress, epigenetics, and brain plasticity. *Ann. N.Y. Acad. Sci.* 1373, 56–64. doi: 10.1111/nyas.13020

McEwen, B. S., and Stellar, E. (1993). Stress and the individual. mechanisms leading to disease. *Arch. Intern. Med.* 153, 2093–2101. doi: 10.1001/archinte.1993.00410180039004

Medic, G., Wille, M., and Hemels, M. E. (2017). Short- and long-term health consequences of sleep disruption. *Nat. Sci. Sleep* 9, 151–161. doi: 10.2147/NSS.S134864

Mong, J. A., Baker, F. C., Mahoney, M. M., Paul, K. N., Schwartz, M. D., Semba, K., et al. (2011). Sleep, rhythms, and the endocrine brain: influence of sex and gonadal hormones. *J. Neurosci.* 31, 16107–16116. doi: 10.1523/JNEUROSCI.4175-11.2011

Moore, R. Y., and Eichler, V. B. (1972). Loss of a circadian adrenal corticosterone rhythm following suprachiasmatic lesions in the rat. *Brain Res.* 42, 201–206. doi: 10.1016/0006-8993(72)90054-6

Moore-Ede, M. C. (1986). Physiology of the circadian timing system: predictive versus reactive homeostasis. *Am. J. Physiol.* 250, R737–R752. doi: 10.1152/ajpregu.1986.250.5.R737

Morley-Fletcher, S., Darnaudery, M., Koehl, M., Casolini, P., Van Reeth, O., and Maccari, S. (2003). Prenatal stress in rats predicts immobility behavior in the forced swim test. effects of a chronic treatment with tianeptine. *Brain Res.* 989, 246–251. doi: 10.1016/S0006-8993(03)03293-1

Nagai, K., Yoshida, S., and Konishi, H. (2014). Gender differences in the gene expression profiles of glucose transporter GLUT class I and SGLT in mouse tissues. *Pharmazie* 69, 856–859.

Nicolaides, N. C., Charmandari, E., Kino, T., and Chrousos, G. P. (2017). Stress-related and circadian secretion and target tissue actions of glucocorticoids: impact on health. *Front. Endocrinol.* 8:70. doi: 10.3389/fendo.2017.00070

Panda, S., Antoch, M. P., Miller, B. H., Su, A. I., Schook, A. B., Straume, M., et al. (2002). Coordinated transcription of key pathways in the mouse by the circadian clock. *Cell* 109, 307–320. doi: 10.1016/S0092-8674(02)00722-5

Reynaert, M. L., Marrocco, J., Mairesse, J., Lionetto, L., Simmaco, M., Deruyter, L., et al. (2016). Hedonic sensitivity to natural rewards is affected by prenatal stress in a sex-dependent manner. *Addict. Biol.* 21, 1072–1085. doi: 10.1111/adb.12270

Reznikov, A. G., and Tarasenko, L. V. (2007). Hormonal protection of gender-related peculiarities of testosterone metabolism in the brain of prenatally stressed rats. *Neuro Endocrinol. Lett.* 28, 671–674.

Russell, A. L., Tasker, J. G., Lucion, A. B., Fiedler, J., Munhoz, C. D., Wu, T. J., et al. (2018). Factors promoting vulnerability to dysregulated stress reactivity and stress-related disease. *J. Neuroendocrinol.* 24:e12641. doi: 10.1111/jne.12641

Seckl, J. R. (2008). Glucocorticoids, developmental 'programming' and the risk of affective dysfunction. *Prog. Brain Res.* 167, 17–34. doi: 10.1016/S0079-6123(07)67002-2

Snedecor, G. W., and Cochran, W. G. (1967). *Statistical Methods*, 6th Edn. Ames Iowa: Iowa State Univ. Press.

Spiga, F., Walker, J. J., Terry, J. R., and Lightman, S. L. (2014). HPA axis-rhythms. *Compr. Physiol.* 4, 1273–1298. doi: 10.1002/cphy.c140003

Summa, K. C., and Turek, F. W. (2011). The genetics of sleep: insight from rodent models. *Sleep Med. Clin.* 6, 141–154. doi: 10.1016/j.jsmc.2011.04.004

Turek, F. W. (2016). Circadian clocks: not your grandfather's clock. *Science* 354, 992–993. doi: 10.1126/science.aal2613

Turek, F. W., Penev, P., Zhang, Y., Van Reeth, O., and Zee, P. (1995). Effects of age on the circadian system. *Neurosci. Biobehav. Rev.* 19, 53–58. doi: 10.1016/0149-7634(94)00030-5

Vallée, M., Maccari, S., Dellu, F., Simon, H., Le Moal, M., and Mayo, W. (1999). Long-term effects of prenatal stress and postnatal handling on age-related glucocorticoid secretion and cognitive performance: a longitudinal study in the rat. *Eur. J. Neurosci.* 11, 2906–2916. doi: 10.1046/j.1460-9568.1999.00705.x

Van Camp, G., Cigalotti, J., Bouwalerh, H., Mairesse, J., Gatta, E., Palanza, P., et al. (2018). Consequences of a double hit of stress during the perinatal period and midlife in female rats: mismatch or cumulative effect? *Psychoneuroendocrinology* 93, 45–55. doi: 10.1016/j.psyneuen.2018.04.004

Van Reeth, O., Weibel, L., Spiegel, K., Leproult, R., Dugovic, C., and Maccari, S. (2000). Interactions between stress and sleep: from basic research to clinical situations. *Sleep Med. Rev.* 4, 201–219. doi: 10.1053/smrv.1999.0097

Van Someren, E. J. (2000). Circadian and sleep disturbances in the elderly. *Exp. Gerontol.* 35, 1229–1237. doi: 10.1016/S0531-5565(00)00191-1

Vestergaard, M., Holm, S. K., Uldall, P., Siebner, H. R., Paulson, O. B., Baaré, W. F. C., et al. (2017). Glucocorticoid treatment earlier in childhood and adolescence show dose-response associations with diurnal cortisol levels. *Dev. Psychobiol.* 59, 1010–1020. doi: 10.1002/dev.21559

Ward, I. L. (1972). Prenatal stress feminizes and demasculinizes the behavior of males. *Science* 175, 82–84. doi: 10.1126/science.175.4017.82

Ward, I. L. (1984). The prenatal stress syndrome: current status. *Psychoneuroendocrinology* 9, 3–11. doi: 10.1016/0306-4530(84)90016-7

Ward, I. L., and Weisz, J. (1984). Differential effects of maternal stress on circulating levels of corticosterone, progesterone, and testosterone in male and female rat fetuses and their mothers. *Endocrinology* 114, 1635–1644. doi: 10.1210/endo-114-5-1635

Weaver, I. C., Cervoni, N., Champagne, F. A., D'Alessio, A. C., Sharma, S., Seckl, J. R., et al. (2004). Epigenetic programming by maternal behavior. *Nat. Neurosci.* 7, 847–854. doi: 10.1038/nn1276

Weibel, L., Maccari, S., and Van Reeth, O. (2002). Circadian clock functioning is linked to acute stress reactivity in rats. *J. Biol. Rhythms* 17, 438–446. doi: 10.1177/074873002237138

Weinstock, M. (2001). Alterations induced by gestational stress in brain morphology and behaviour of the offspring. *Prog. Neurobiol.* 65, 427–451. doi: 10.1016/S0301-0082(01)00018-1

Wirz-Justice, A., and Van den Hoofdakker, R. H. (1999). Sleep deprivation in depression: what do we know, where do we go? *Biol. Psychiatry* 46, 445–453.

Wollnik, F., and Turek, F. W. (1988). Estrous correlated modulations of circadian and ultradian wheel-running activity rhythms in LEW/Ztm rats. *Physiol. Behav.* 43, 389–396. doi: 10.1016/0031-9384(88)90204-1

Wulff, K., Gatti, S., Wettstein, J. G., and Foster, R. G. (2010). Sleep and circadian rhythm disruption in psychiatric and neurodegenerative disease. *Nat. Rev. Neurosci.* 11, 589–599. doi: 10.1038/nrn2868

Zhang, R., Lahens, N. F., Ballance, H. I., Hughes, M. E., and Hogenesch, J. B. (2014). A circadian gene expression atlas in mammals: implications for biology and medicine. *Proc. Natl. Acad. Sci. U.S.A.* 111, 16219–16224. doi: 10.1073/pnas.1408886111

Zucker, I., and Beery, A. K. (2010). Males still dominate animal studies. *Nature* 465:690. doi: 10.1038/465690a

Conflict of Interest Statement: The authors declare that the research was conducted in the absence of any commercial or financial relationships that could be construed as a potential conflict of interest.

frontiers in Human Neuroscience

ORIGINAL RESEARCH
published: 14 May 2019
doi: 10.3389/fnhum.2019.00144

Larger Amygdala Volume Mediates the Association Between Prenatal Maternal Stress and Higher Levels of Externalizing Behaviors: Sex Specific Effects in Project Ice Storm

Sherri Lee Jones[1,2†], Romane Dufoix[1,2†], David P. Laplante[2], Guillaume Elgbeili[2], Raihaan Patel[3,4], M. Mallar Chakravarty[3,4,5], Suzanne King[1,2] and Jens C. Pruessner[6]*

[1] Laboratory of Suzanne King, Department of Psychiatry, Douglas Mental Health University Institute, McGill University, Montreal, QC, Canada, [2] Laboratory of Suzanne King, Douglas Mental Health University Institute, Montreal, QC, Canada, [3] Computational Brain Anatomy Laboratory (CoBrA Lab), Douglas Mental Health University Institute, Montreal, QC, Canada, [4] Cerebral Imaging Center, Douglas Mental Health University Institute, Montreal, QC, Canada, [5] Department of Biological and Biomedical Engineering, McGill University, Montreal, QC, Canada, [6] Laboratory of Jens Pruessner, Department of Psychology, University of Konstanz, Konstanz, Germany

OPEN ACCESS

Edited by:
Jordan Marrocco,
The Rockefeller University,
United States

Reviewed by:
Dustin Scheinost,
Yale University, United States
María I. Cordero,
Manchester Metropolitan University,
United Kingdom

***Correspondence:**
Suzanne King
suzanne.king@mcgill.ca

[†] These authors have contributed equally to this work

Received: 08 October 2018
Accepted: 15 April 2019
Published: 14 May 2019

Citation:
Jones SL, Dufoix R, Laplante DP, Elgbeili G, Patel R, Chakravarty MM, King S and Pruessner JC (2019) Larger Amygdala Volume Mediates the Association Between Prenatal Maternal Stress and Higher Levels of Externalizing Behaviors: Sex Specific Effects in Project Ice Storm. Front. Hum. Neurosci. 13:144. doi: 10.3389/fnhum.2019.00144

Introduction: The amygdala is a brain structure involved in emotional regulation. Studies have shown that larger amygdala volumes are associated with behavioral disorders. Prenatal maternal depression is associated with structural changes in the amygdala, which in turn, is predictive of an increase in behavioral problems. Girls may be particularly vulnerable. However, it is not known whether disaster-related prenatal maternal stress (PNMS), or which aspect of the maternal stress experience (i.e., objective hardship, subjective distress, and cognitive appraisal), influences amygdala volumes. Nor is it known whether amygdala volumes mediate the effect of PNMS on behavioral problems in girls and boys.

Aims: To assess whether aspects of PNMS are associated with amygdala volume, to determine whether timing of exposure moderates the effect, and to test whether amygdala volume mediates the association between PNMS and internalizing and externalizing problems in 11½ year old children exposed *in utero*, to varying levels of disaster-related PNMS.

Methods: Bilateral amygdala volumes (AGV) and total brain volume (TBV) were acquired using magnetic resonance imaging, from 35 boys and 33 girls whose mothers were pregnant during the January 1998 Quebec Ice Storm. The mothers' disaster-related stress was assessed in June 1998. Child internalizing and externalizing problems were assessed at 11½ years using the Child Behavior Checklist (CBCL). Hierarchical regression analyses and mediation analyses were conducted on boys and girls separately, controlling for perinatal and postnatal factors.

Results: In boys, subjective distress was associated with larger right AGV/TBV when mothers where exposed during late pregnancy, which in turn explained higher levels of externalizing behavior. However, when adjusting for postnatal factors, the effect was no

longer significant. In girls, later gestational exposure to the ice storm was associated with larger AGV/TBV, but here, higher levels of objective PNMS were associated with more externalizing problems, which was, in part, mediated by larger AGV/TBV. No effects were detected on internalizing behaviors.

Conclusion: These results suggest that the effects of PNMS on amygdala development and externalizing symptoms, as assessed in boys and girls in early adolescence, can be influenced by the timing of the stress in pregnancy, and the particular aspect of the mother's stress experience.

Keywords: prenatal maternal stress, amygdala, internalizing, externalizing, adolescence

INTRODUCTION

There is strong evidence that prenatal maternal stress (PNMS) or anxiety during pregnancy has profound and long-lasting adverse consequences on offspring development (see Van den Bergh et al., 2017 for a recent review). For example, pregnancy-specific anxiety has been associated with increased adolescent depression levels in the offspring (Van Lieshout and Boylan, 2010; Van den Bergh et al., 2017) and an increase in externalizing problems in toddlers (Wadhwa et al., 2001; Gutteling et al., 2005; Chuang et al., 2011; Liu, 2011). As reviewed in Glover and Hill (2012), prospective studies worldwide show that mothers who are stressed, anxious, or depressed have children that are more likely to have symptoms of anxiety, depression, and increased stress reactivity. Some studies show that the associations are particularly sensitive to prenatal maternal anxiety (e.g., O'Connor et al., 2002; Van den Bergh and Marcoen, 2004). Many of those studies controlled for potential confounders associated with anxiety, such as smoking, alcohol use, and household income, and showed that the results persisted. Importantly, these effects even persist after controlling for genetic factors using prenatal cross-fostering studies (i.e., *in-vitro* fertilization) (Rice et al., 2010). Finally, Buss et al. (2012) reported that higher maternal cortisol levels during early pregnancy predicted more internalizing problems in girls at age 7, but not in boys, which was in part, mediated by amygdala volume (AGV).

The amygdala is an important limbic structure involved in processing of biologically relevant stimuli, emotional learning and memory (Davis and Whalen, 2001; Quirk and Beer, 2006), and is vulnerable to prenatal factors. Exposure to maternal depression has been shown to influence AGV and functionality. For example, chronic maternal depression is associated with increased AGV in 10 year old boys and girls (Lupien et al., 2011), and with deficits in amygdala connectivity and functionality at age 4½ years albeit only in girls (Soe et al., 2018). Prenatal exposure to maternal depression is associated with altered right amygdala microstructure at birth (Rifkin-Graboi et al., 2013), with AGV in childhood as well as with structural changes in the amygdala in the neonatal period and childhood (Rifkin-Graboi et al., 2013; Favaro et al., 2015; Posner et al., 2016; Scheinost et al., 2016; Wen et al., 2017). In a study considering maternal cortisol levels from saliva samples acquired at pregnancy weeks 15, 19, 25, 31, and 37, Buss et al. (2012) reported that exposure to higher levels of cortisol during earlier gestation was associated with larger right AGV in girls but not boys. Together these results suggest that the amygdalae of girls are particularly susceptible to the effects of maternal depression and pregnancy related cortisol levels.

Structural properties of the amygdala are also associated with psychopathology and subclinical psychopathological symptoms. For example, AGV is associated with psychiatric problems including depression (MacMillan et al., 2003; Rosso et al., 2005), anxiety disorders (De Bellis et al., 2000; Milham et al., 2005; Schienle et al., 2011), and aggression (Gopal et al., 2013), as well as sub-clinical symptoms of internalizing (e.g., anxiety and depression) (Spampinato et al., 2009) and externalizing (e.g., aggressive) behaviors (Matthies et al., 2012; Pardini et al., 2014; Thijssen et al., 2015).

The associations between perinatal stressors and/or naturally occurring maternal cortisol levels during pregnancy and AGV can explain psychopathological outcomes in the offspring. Interestingly, rodent studies suggest that PNMS may influence offspring development and subsequent behavioral outcomes by altering amygdala maturation as measured by AGV (Salm et al., 2004; Kraszpulski et al., 2009). Likewise, Buss et al. (2012) demonstrated that AGV mediated the relationship between maternal cortisol levels in early pregnancy and affective problems in 7 year-old girls, such that larger right AGV was associated with more affective problems. This finding is important as it shows that natural variations in cortisol during pregnancy can explain variation in AGV and in turn explain psychopathological symptoms, and highlights sex-specific effects as well as potential hemispheric lateralization.

While these findings link perinatal maternal depression and prenatal maternal cortisol to structural changes in the amygdala, and subsequent psychopathological symptoms in exposed offspring, these studies have their limitations. The use of maternal psychopathology as the stressor is confounded by potential genetic transmission from mother to child. Moreover, while the Buss et al. (2012) findings posit a potential mechanism—*in utero* exposure to heightened levels of maternal cortisol via the placenta (Cottrell and Seckl, 2009; Harris and Seckl, 2011)—maternal "stress" levels were not measured. Finally, although several studies suggest that the timing of a stressor *in utero* moderates the effects of maternal stress on childhood neurodevelopmental outcomes (Kinney et al., 2008; Cao et al.,

2014; Moss et al., 2018), studies of maternal depression in pregnancy cannot usually identify a specific onset date. As such, the temporal link between exposure to perinatal stressors, AGV, and childhood psychopathology symptoms with a sensitivity to timing of exposure, remains unclear.

This gap can be addressed in our PNMS study of children exposed to a natural disaster just prior to, and during gestation: Project Ice Storm. In January 1998, a series of ice storms resulted in electrical power failures for more than 3 million individuals for periods varying from 6 h, to more than five weeks, during the coldest months of the year. Mothers of the youth in our prospective, longitudinal study were at various stages of pregnancy and were quasi-randomly exposed to varying degrees of storm-related hardship. The ice storm serves as a "natural experiment," affecting women regardless of their personal characteristics while allowing for the women's disaster experience to be divided into various components (i.e., objective hardship exposure, cognitive appraisal of the event, and subjective distress from the event). As well, because the ice storm had a sudden onset, the timing of the onset of maternal stress can be assessed with great accuracy. Among the findings from Project Ice Storm, we have shown that increased objective hardship predicts delayed cognitive and language development in childhood (King and Laplante, 2005; Laplante et al., 2008), while both the women's objective hardship and subjective distress levels predict internalizing and externalizing problems in the children throughout childhood (King et al., 2012).

The goals of the present study were to test whether varying aspects of the PNMS experience affect AGV in 11½ year-old youth using a prospective longitudinal design, and whether AGV mediates the association between varying aspects of the PNMS experience and child internalizing and externalizing problems. We also hypothesized that the timing of the prenatal maternal stressor would moderate those associations.

MATERIALS AND METHODS

Participants

This study was carried out in accordance with the recommendations of The Code of Ethics of the World Medical Association, and approved by the Douglas Mental Health University Institute Research Ethics Board. All subjects gave written informed consent or written informed assent for participants under the age of 18 years, in accordance with the Declaration of Helsinki.

The initial Project Ice Storm cohort consisted of 178 children whose mothers were pregnant during the 1998 Quebec ice storm or became pregnant within 3 months of the ice storm and who responded to the questionnaire "reaction to the storm" sent on June 1, 1998. At 11½ years, 100 families were approached about participating in a standardized assessment and a structural brain magnetic resonance imaging (MRI) study. Of those, 90 children (male = 47; female = 43) underwent the cognitive and behavioral assessment, and 71 agreed to undergo the MRI protocol (male = 35; female = 36). Two children (both female) refused to undergo the scanning upon seeing the scanner. The scan of one girl was unusable because of excessive movement. An additional five participants (male = 4; female = 1) who were born preterm (before 37 weeks) with a low birth weight were excluded from the analyses as these birth outcomes have been shown to affect brain structure and integrity (Buss et al., 2007). The mother of one male participant did not complete the behavioral questionnaire (CBCL), leaving a total of 62 (30 male, 32 female) participants with valid behavioral data, and a 63 participants (31 males, 32 females) with valid MRI data.

There were 2 left-handed boys, and 3 left-handed girls. Thirty-three percent (21/63) of the participants were exposed to the storm prior to conception (boys: 11/31; girls: 10/32), 22.2% (14/63) during the first trimester (boys: 7/31; girls: 7/32), 23.8% (15/63) during the second trimester (boys: 8/31; girls: 7/32) and 20.6% (13/63) during the third trimester (boys: 5/31; girls: 8/32).

Instruments

Predictor Variables: Prenatal Maternal Stress (PNMS)

Objective hardship was assessed in June 1998 using Storm32 (Laplante et al., 2007), which assesses the mothers' responses to questions associated with four categories of exposure that were often used in other disaster studies: threat, loss, scope and change (Bromet and Dew, 1995). Scores for each category ranged from 0 to 8. A total score (max 32) was obtained by summing the categories.

Mothers' subjective distress was assessed in June 1998, using a validated French version (Brunet et al., 2003) of the 22-item Impact of Event Scale-Revised (IES-R; (Weiss and Marmar, 1997). This scale describes symptoms from three categories relevant to post-traumatic stress disorder (PTSD): hyper-arousal, avoidance, and intrusive thoughts or images. Thus, this scale reflects enduring PTSD symptoms in response to the ice storm crisis, which had begun 5 months earlier.

Mothers' cognitive appraisal of the ice storm crisis was assessed in the June 1998 questionnaire using the following question: "Overall, what were the consequences of the ice storm on you and your family?" Response options were on a 5-point Likert scale: "Very negative" (1), "Negative" (2), "Neutral" (3), "Positive" (4), and "Very positive" (5). This item was recoded into "negative" (0) or "neutral/positive" (1). We opted to treat cognitive appraisal as binary for two reasons. First, very few mothers reported that the crisis was either "very negative" (2) or "very positive" (1). Second, we wanted to isolate the "negative" appraisal from "neutral" and "positive" appraisals, because we believe negative cognitive appraisal is one of the components of the maternal stress experience that can influence child development.

Timing of *in utero* ice storm exposure was determined as the number of days between estimated date of conception and January 9th, 1998, the date at which the storm peaked; higher values indicate storm exposure later in pregnancy. To calculate estimated date of conception, 280 days (40 weeks) was subtracted from the women's due date.

Behavioral problems were assessed using the mother-rated 113-item Child Behavior Checklist (CBCL), the gold-standard for behavioral research, which yields scores on several subscales that combine to create Internalizing and Externalizing scales. The standardized scores with a mean of 50 and standard deviation of

10 were used in the analyses (Achenbach and Ruffle, 2000). Data for one boy were missing.

Control Variables

Socioeconomic status (SES) was measured with the Hollingshead scale (Hollingshead, 1975) using data from the June 1, 1998 (perinatal) and when the children were 11½ years of age (concurrent) questionnaires about maternal and paternal education and occupation. Note that the lower the score, the higher the SES. At recruitment, 1.6% (0/31 boys, 1/32 girls) were lower class, 3.2% (2/31 boys, 0/32 girls) were lower middle class, 31.7% (11/31 boys, 9/32 girls) were middle class, 46% (14/31 boys, 15/32 girls) were upper middle class, and 17.5% (4/31 boys, 7/32 girls) were upper class. At 11½ years, 3.4% (1/29 boys, 1/30 girls) were lower class, 11.9% (6/29 boys, 1/30 girls) were lower middle class, 30.5% (0/29 boys, 9/30 girls) were middle class, 32.2% (9/29 boys, 10/30 girls) were upper middle class, and 22.0% (4/29 boys, 9/30 girls) were upper class. Data for four families were missing.

The Life Experience Survey (LES) (Sarason et al., 1978) was used to control for any other major life events the mothers experienced during their pregnancies and between when the children were 2½ to 11½ years of age, The perinatal questionnaire was completed by the mothers when the children were 6 months of age. This questionnaire covered the period between conception and when the child was 6 months of age. The three postnatal questionnaires were completed by the mothers when the children were 5½, 8½, and 11½ years of age. Each questionnaire covered the previous 36 months. Perinatal data from one mother (girl) were missing. Data were missing from 29 mothers (14 boys, 15 girls) at 5½ years, 10 mothers (5 boys; 5 girls) at 8½ years, and one mother (boy) at 11½ years. In order to control for missing data, the average number of major events per year was calculated between ages 2½ and 11½.

Mothers' concurrent psychological symptoms were assessed when the children were aged 11½ using the General Health Questionnaire (GHQ-28; Goldberg, 1972). Each of its 28 items describes a psychological or somatic symptom, and subjects indicate on a 4-point Likert scale how much they have experienced it in the preceding 2 weeks. There are subscales for Anxiety, Depression, Somatic Complaints, and Dysfunction. In the present study, each item was rescored as either 0 (a rating of 0 or 1) or 1 (a rating of 2 or 3), according to the Goldberg method (Goldberg, 1972), resulting in a minimum possible score of 0 and a maximum possible score of 28. Data from two mothers (one girl, one boy) were missing.

The number of obstetric complications (e.g., hypertension, preeclampsia, cold or flu) was determined by maternal recall when their children were 6 months of age using an adaptation of the checklist used by Jacobsen and Kinney (1980) and, when available, by examination of medical charts. The total number of obstetric complications experienced by the women that were rated as moderate-to-severe using the McNeil-Sjöström Scale for Obstetric Complications (McNeil and Sjöström, 1995) were used in the analyses.

Smoking and alcohol habits in pregnancy were assessed in the 6 month postpartum questionnaire in order to capture the entire pregnancy. Women were asked to indicate the number of cigarettes smoked per day, and the number of drinks consumed per week.

Child handedness (e.g., right- or left-handed) was determined at age 11½ by observing which hand the child used to complete a visual-motor integration task.

MRI Image Acquisition

Anatomical MRI was performed at the *Unité de Neuroimagerie Fonctionelle* (UNF) *du Center de Recherche de l'Institut Universitaire de Gériatrie de Montréal* (CRIUGM). Brain imaging was done with a 3.0T Siemens MAGNETOM Trio TIM Syngo magnetic resonance imaging (MRI) scanner (Siemens, Erlangen, Germany), with a 12-channel head coil. For each participant, we obtained a 3D, T1-weighted Magnetization Prepared Rapid Gradient Echo [MPRAGE] sequence (TR/TE/TI = 2300/2.98/900 ms) (voxel size = 1 × 1 × 1 mm^3; sagittal acquisition; 176 slices; 256 × 256 mm grid). The raw images underwent automated correction for intensity non-uniformity and normalization for signal intensity (Sled et al., 1998).

MRI Image Analysis

The amygdala was automatically segmented using the multiple automatically generated templates (MAGeT) Brain pipeline (Chakravarty et al., 2013; Pipitone et al., 2014). Next, AGV were manually corrected (by RD) using a validated manual segmentation protocol (Pruessner et al., 2000), and a random subset were verified by an expert rater (JCP). Total Brain Volume (TBV) was obtained using the Brain Extraction based on non-local Segmentation Techniques (BEaST) method, which is based on non-local segmentation in a multi-resolution framework (Eskildsen et al., 2012). BEaST is designed to include cerebral spinal fluid (in the ventricles, cerebellar cistern, deep sulci, along surface of brain and brain stem), the brainstem, and cerebellar white and gray matter in the brain mask while excluding the skull, skin, fat, muscles, dura, eyes, bone, exterior blood vessels, and exterior nerves. After the BEaST masks were automatically created, the labels underwent quality control and manual corrections. Amygdala volumes were corrected for TBV (AGV/TBV) to account for individual differences in brain volume. The AGV/TBV variables were used in all analyses, and are referred to as normalized AGV.

Statistical Analyses

All analyses were carried out on boys and girls separately to account for the difference between male and female neurodevelopmental trajectories, and given the sex-specific effects reported in the literature (Buss et al., 2012; Favaro et al., 2015). First, descriptive analyses (mean, range, standard deviation) were conducted on outcome, predictor and control variables, and *t*-tests were run to compare boys' and girls' levels for each of those variables. Pearson zero-order correlations for normally distributed variables, as well as Spearman's rho non-parametric testing for variables violating normality were also conducted to test the association between all variables.

Prenatal Maternal Stress and Amygdala Volume (Regression Analyses)

To test the effects of PNMS on normalized AGV, the data for right and left normalized AGV were subjected to hierarchical regression analyses. Child handedness was controlled for in all analyses. Given the evidence that timing of exposure to the stressor might influence the response to PNMS, timing of exposure to the storm *in utero* was also included in the models regardless of its association with the brain, behavioral and cognitive outcomes. However, the mother's age at birth of child, pregnancy drinking and smoking habits, as well as her perinatal SES and number of life events, and concurrent psychological symptoms at 11½ years postpartum were used as covariates but kept only if they were correlated with brain outcomes. This method of selectively adding covariates to the models allowed for the conservation of power considering the limitations imposed by our sample size. The regression model steps were the same for right and left normalized AGV (the outcome variable): the covariates were entered first into the model (timing of exposure, then handedness, then covariates associated with the outcome sequentially), followed by objective hardship, subjective distress, and lastly, cognitive appraisal.

To assess the moderating effects of timing of exposure on the relationship between PNMS and right and left normalized AGV, interaction terms were added in the last step of the hierarchical regression, with either Objective hardship × Timing of exposure, Subjective distress × Timing of exposure or Cognitive appraisal × Timing of exposure as the interaction terms, entered in separate analyses.

In order to determine the confounding effect of postnatal environment on the effect of PNMS, concurrent SES at 11½ years postpartum, as well as postnatal maternal life events, were then added to the models if they were significantly correlated with AGV. Even though concurrent maternal psychological symptoms are postnatal, this variable was included in all models if significant, to address a potential responder bias issue.

Given the sample size, the equations were trimmed of any non-significant variables ($p > 0.1$) that were forced into the equation except for handedness, objective hardship, timing of exposure to the storm, and any PNMS variable included in the interaction term. To control for the number of moderation analyses, the Bonferroni correction was applied to the interaction term *p*-values.

Amygdala Volume and Behavioral Outcomes (Partial Correlations)

To test the effects of left or right AGV on internalizing and externalizing problems partial correlations were run, controlling for covariates that were significantly associated with the behavioral outcomes. As per the regression analyses, handedness and timing of exposure to the storm were always included as covariates, and analyses were run with and without postnatal measures to determine their confounding effect.

Mediating Effect of Amygdala Volumes on Association Between PNMS and Behavioral Problems

To test the extent to which changes in normalized AGV explained the effect of PNMS on behavior, simple mediation or moderated mediation analyses were used. Because the indirect effect is more likely to be significant if the two paths forming it are strongly associated, the mediation or moderated mediation was only tested when both paths of the indirect effect (path 1: PNMS or PNMS by timing interaction to normalized AGV from the regressions, and path 2: normalized AGV to behavior from the partial correlations) were significant or marginally significant. Covariates that were significantly correlated with either normalized AGV or the behavioral outcome were entered in the model, and then trimmed out if not-significant in the final model. Again, the models were run with and without postnatal measures.

For the moderation analyses, the SPSS PROCESS macro (Hayes and Preacher, 2013) was used to run multiple linear regressions and probe the interaction. For the mediation and moderated mediation analyses, PROCESS uses bootstrapping with 20,000 resamplings to calculate the 95% confidence interval for the indirect effect. All correlation and main effect analyses were set to $p < 0.05$. Analyses were conducted using SPSS 20.0.

RESULTS

Descriptive statistics for outcome, predictor, and control variables are presented for boys and girls separately in **Table 1**. There was a strong tendency for boys to have longer gestational ages at birth ($p = 0.054$ and to have higher internalizing problem scores ($p = 0.059$). There was also a weak tendency for mothers of boys to have lower concurrent SES ($p = 0.091$) and to have experienced more postnatal major life events (0.092). Boys and girls did not significantly differ on any other variable. Non-significant analyses are presented in **Supplementary Tables 1, 2**.

Boys

Prenatal Stress and Amygdala Volume (Regression Analyses)

As shown in **Table 2**, perinatal SES was correlated with left and right normalized AGV, thus, this variable was entered in both regression models. Additionally, concurrent SES and perinatal maternal life events were also correlated with left and right normalized AGV, and maternal psychological symptoms were associated with left normalized AGV, thus, those variables were entered accordingly into the two regression models adjusted for postnatal measures.

Right amygdala volume

In boys, the results of the hierarchical regressions for right normalized AGV are presented in **Table 3a**. In the first step, timing explained 6.5% ($p = 0.165$), in the second step handedness explained an additional 2.7% ($p = 0.373$) and in the third step, SES explained an additional 13.0% ($p = 0.043$) of the variance in normalized AGV, such that higher SES significantly predicted larger AGV. In the fourth step, mothers' objective hardship explained an additional 0.3% ($p = 0.755$) and in the fifth step

TABLE 1 | Descriptive statistics of variables, and results of *t*-test for sex differences.

Variables	Boys ($n = 31$)		Girls ($n = 32$)		*p*	*Cohen's d*
	Mean	SD	Mean	SD		
Right normalized AGV	0.070	0.007	0.072	0.008	0.274	0.278
Left normalized AGV	0.072	0.007	0.072	0.007	0.922	0.025
Objective stress storm32	11.839	4.810	11.031	4.816	0.508	0.168
Subjective stress IES-R	12.032	13.824	8.650	8.870	0.472	0.182
Number of days of pregnancy when ice storm happened (timing of PNMS)	78.450	102.849	94.590	103.788	0.538	0.156
Gestational age at birth (weeks)	40.226	0.976	39.754	0.927	0.054	0.495
Maternal psychological symptoms GHQ-28	0.106[b]	0.155	0.060[a]	0.115	0.192	0.338
Socioeconomic status (SES) Hollingshead scale (perinatal)	29.839	12.718	27.094	12.105	0.384	0.221
Socioeconomic status (SES) Hollingshead scale (concurrent)	34.31[c]	15.05	27.67[b]	14.60	0.091	0.448
Number of cigarettes/day	2.419	5.622	1.750	4.930	0.617	0.127
Number of glasses of alcohol/week	0.047	0.184	0.127	0.421	0.330	0.246
Maternal life events (perinatal)	6.516	4.098	5.468	2.961	0.248	0.294
Maternal life events (postnatal)	1.29[b]	0.89	0.9470	0.661	0.092	0.440
Obstetric complications	4.81	3.02	3.970	2.192	0.211	0.319
Maternal age at birth	29.000	5.320	30.196	4.311	0.330	0.247
Internalizing problems CBCL (T-scores)	54.73[b]	10.106	49.47	11.376	0.059	0.488
Externalizing problems CBCL (T-scores)	48.03[b]	8.732	45.81	8.716	0.320	0.255

Lower SES scores represent higher SES.
[a]*N = 31.*
[b]*N = 30.*
[c]*N = 29.*
AGV, Amygdala volume; IES-R, Impact of Event Scale-Revised; PNMS, Prenatal maternal stress; GHQ, General Health Questionnaire; CBCL, Achenbach Child Behavior Checklist.

subjective distress explained an additional 3.9% ($p = 0.207$) of the variance in the child's right normalized AGV. Finally, the subjective distress × timing interaction term explained a statistically significant increase of 12.9% ($p = 0.032$) of the variance. Since no significant main or interaction effects were found with cognitive appraisal, it was left out of the final analyses. The full model explained 40.2% of the variance of the boys' right normalized AGV.

We probed this interaction and found, as illustrated in **Figure 1**, that when the boys were exposed to the ice storm from pregnancy day 157 (week 22.42) onwards, there was a significant positive association between subjective distress and right normalized AGV: for boys exposed to the ice storm after pregnancy day 157, the greater their mothers' subjective distress, the larger the right normalized AGV. When the boys were exposed to the storm before pregnancy day 157, there was no significant effect of subjective distress on right normalized AGV. Additionally, when subjective distress scores were equal to or greater than a log value of 2.64 (original subjective stress scale 13.01), there was a significant ($p < 0.05$) effect of timing on right normalized AGV; for these boys, the later they were exposed to the ice storm in gestation, the larger the right normalized AGV.

When adjusting the model for postnatal measures, concurrent SES was no longer significant, so it was trimmed out of the model. Postnatal life events became marginally significant ($p = 0.056$), such that more yearly life events was associated with larger normalized AGV. However, adjusting for number of yearly postnatal life events, the subjective stress x timing interaction was no longer significant.

Left amygdala volume

For the left normalized AGV in boys, the hierarchical regression models revealed no significant main effects of PNMS measures, and no significant PNMS-by-timing interactions (data not shown).

Amygdala Volume and Behavioral Outcomes (Partial Correlations)

When testing the second path of the indirect effect we found that right and left normalized AGV in boys were associated with externalizing, but not internalizing, problems when controlling for timing of exposure, handedness, maternal psychological functioning, and maternal alcohol usage during pregnancy (**Table 4**). However, when adjusting for number of yearly postnatal maternal life events, the effect of normalized right AGV on externalizing became marginal.

Mediating Effect of Amygdala Volumes on Association Between PNMS and Externalizing Problems

Because a significant subjective distress by timing interaction effect was obtained on right normalized AGV, and that partial correlations showed that right normalized AGV was significantly associated with externalizing problems, a moderated mediation effect was tested in boys, moderating the first path by timing of exposure, and adjusting the model for handedness, SES, maternal psychological functioning, and maternal alcohol usage. However, since neither path in the model showed a significant effect of maternal psychological functioning, this covariate was

TABLE 2 | Pearson's and Spearman's rho correlation coefficients between all variables split by sex.

	1	2	3	4	5	6	7	8[b]	9[b]	10[b]	11[b]	12[b]	13[b]	14[b]	15[b]	16	17	18
1- Right normalized AGV[a]	–	0.796**	0.055	0.045	0.144	0.256	−0.354†	0.243	−0.408*	−0.425*	−0.204	0.072	0.118	0.410*	−0.131	–	0.251	0.432*
2- Left normalized AGV[a]	0.765**	–	0.089	0.135	0.077	0.203	−0.322†	0.434*	−0.355*	−0.445*	−0.288	0.182	0.238	0.477**	−0.266	–	0.330†	0.457*
3- Objective hardship[a]	0.087	0.146	–	0.373*	−0.406*	−0.108	0.198	0.409*	−0.206	−0.135	0.012	−0.278	0.060	0.197	−0.106	–	0.053	0.133
4- Subjective distress[a]	0.229	0.266	0.212	–	−0.140	−0.066	0.016	0.269	0.263	0.264	0.158	−0.034	0.330†	0.277	0.172	–	0.126	0.124
5- Cognitive appraisal	−0.207	−0.216	−0.303†	−0.021	–	0.286	−0.196	0.059	0.045	0.149	0.135	0.074	0.032	0.282	−0.189	–	0.072	0.223
6- Timing of PNMS[a]	0.441*	0.285	−0.259	0.000	−0.184	–	−0.087	0.095	−0.189	−0.180	−0.048	−0.031	−0.061	0.197	−0.128	–	0.079	−0.097
7- Gestational age at birth[a]	−0.008	−0.155	0.037	−0.243	0.265	0.074	–	0.033	−0.240	−0.326†	0.116	−0.066	0.048	−0.290	0.159	–	0.153	−0.154
8- Maternal psychological, GHQ[b]	−0.127	−0.063	0.001	0.373*	0.265	−0.130	−0.286	–	−0.243	−0.191	0.031	0.112	0.429*	0.634**	−0.109	–	0.529**	0.390*
9- Socioeconomic status (perinatal)[b]	0.310†	0.209	0.303†	0.379*	−0.084	0.091	0.076	0.157	–	0.843**	0.353†	−0.003	−0.272	−0.146	0.079	–	−0.261	−0.129
10- Socioeconomic status (concurrent)[b]	0.280	0.193	0.412*	0.604**	−0.023	−0.037	0.019	0.198	0.883**	–	0.324†	−0.002	−0.108	0.051	0.293	–	−0.306	−0.075
11- Smoking[b]	0.176	0.150	0.213	0.400*	0.111	−0.232	−0.300†	0.109	0.327†	0.524**	–	0.032	−0.135	−0.130	0.413*	–	−0.073	−0.274
12- Alcohol usage[b]	−0.100	−0.185	0.031	−0.175	−0.324†	−0.148	−0.324†	−0.018	−0.031	−0.106	0.105	–	0.195	0.087	0.108	–	0.397*	0.391*
13- Maternal life events (perinatal)[b]	0.090	0.171	−0.045	0.289	−0.170	0.291	−0.260	0.101	0.049	0.051	0.131	−0.185	–	0.428*	0.132	–	0.326†	0.269
14-Maternal life events (postnatal)[b]	−0.171	0.074	0.264	0.322†	−0.079	−0.341†	−0.004	0.393*	0.007	0.156	−0.107	−0.239	0.224	–	0.055	–	0.394*	0.389*
15-Obstetric complications[b]	−0.036	−0.166	0.028	−0.011	0.136	−0.093	0.183	0.158	0.008	0.143	0.236	−0.020	−0.269	−0.049	–	–	0.050	−0.154
16- Maternal age at birth[a]	−0.107	−0.246	−0.285	0.137	0.072	−0.046	−0.027	−0.006	−0.199	−0.134	0.059	0.049	−0.200	0.007	0.307†	–	0.207	0.109
17- Internalizing problems[a]	0.116	0.092	−0.039	0.291	−0.051	−0.048	−0.260	0.189	0.107	0.236	−0.036	−0.120	0.131	0.496**	0.134	0.048	–	0.583**
18- Externalizing problems[a]	0.403*	0.378*	0.070	0.396*	−0.174	−0.045	−0.215	0.215	0.150	0.281	0.210	−0.009	0.350*	0.378*	0.151	−0.254	0.636**	–

Correlations for boys (n = 31) are presented in the top right, and for girls (n = 32) in the bottom left. Lower socioeconomic status (SES) scores represent higher SES. AGV, Amygdala volume; PNMS, Prenatal Maternal Stress; GHQ, General Health Questionnaire.

[a] *Pearson.*

[b] *Spearman.*

† *p < 0.1, *p < 0.05, **p < 0.01.*

TABLE 3 | Summary of hierarchical regression analyses for (a) the normalized right amygdala volume in boys and for (b) the normalized right and (c) left amygdala volume in girls at 11 years of age.

Predictor variables	*β*	*B*	*SE of B*	*R*	R^2	ΔR^2	*F*	ΔF
(A) RIGHT NORMALIZED AGV—BOYS								
Step 1				0.256	0.065		2.027	
Timing	0.256	1.76E-05	1.20E-05					
Step 2				0.303	0.092	0.027	1.417	0.820
Timing	0.294	2.02E-05	1.30E-05					
Preferred hand	0.167	0.005	0.005					
Step 3				0.471	0.222	0.130	2.562†	4.498*
Timing	0.258	1.78E-05	1.20E-05					
Preferred hand	0.126	0.004	0.005					
SES (perinatal)	−0.363*	−2.02E-04*	9.50E-05					
Step 4				0.474	0.225	0.003	1.882	0.099
Timing	0.255	1.76E-05	1.20E-05					
Preferred hand	0.145	0.004	0.005					
SES (perinatal)	−0.376*	−2.10E-04*	1.00E-04					
Objective stress	−0.060	−8.78E-05	2.79E-04					
Step 5				0.523	0.273	0.049	1.880	1.677
Timing	0.257	1.77E-05	1.20E-05					
Preferred hand	0.173	0.005	0.005					
SES (perinatal)	−0.480*	−2.68E-04*	1.08E-04					
Objective stress	−0.193	−2.84E-04	3.14E-04					
Subjective stress	0.263	0.002	0.001					
Step 6				0.634	0.402	0.129	2.687*	5.159†
Timing	0.095	−4.40E-05	2.90E-05					
Preferred hand	0.096	0.003	0.005					
SES (perinatal)	−0.526*	−2.93E-04*	1.01E-04					
Objective stress	−0.049	−7.27E-05	3.05E-04					
Subjective stress	0.072	−0.002	0.002					
Subjective stress* timing	0.443†	2.57E-05†	1.10E-05					
Adjusted for postnatal life events				0.705	0.497	0.095	3.100*	4.057†
Timing	−0.074	−3.16E-05	2.88E-05					
Preferred hand	0.235	0.007	0.005					
SES (perinatal)	−0.444*	−2.47E-04*	1.00E-04					
Objective stress	−0.141	−2.09E-04	3.03E-04					
Subjective stress	0.028	−0.001	0.002					
Subjective stress* timing	0.329	1.88E-05	1.13E-05					
Postnatal life events	0.368†	0.003†	0.001					
(B) RIGHT NORMALIZED AGV—GIRLS								
Step 1				0.441	0.194		7.227*	
Timing	0.441*	3.19E-05*	1.20E-05					
Step 2				0.463	0.214	0.020	3.954*	0.742
Timing	0.443*	3.21E-05*	1.20E-05					
Preferred hand	0.142	0.004	0.004					
Step 3				0.543	0.295	0.081	3.904*	3.202†
Timing	0.528**	3.82E-05**	1.20E-05					
Preferred hand	0.259	0.007	0.004					
Objective stress	0.318†	4.96E-04†	2.77E-04					
(C) LEFT NORMALIZED AGV—GIRLS								
Step 1				0.285	0.081		2.648	
Timing	0.285	1.82E-5	1.10E-05					

(Continued)

TABLE 3 | Continued

Predictor variables	β	*B*	*SE of B*	*R*	R^2	ΔR^2	*F*	ΔF
Step 2				0.358	0.128	0.047	2.137	1.575
Timing	0.289	1.84E-5	1.10E-05					
Preferred hand	0.218	0.005	0.004					
Step 3				0.491	0.241	0.113	2.969*	4.168†
Timing	0.389*	2.48E-5*	1.10E-05					
Preferred hand	0.357†	0.008†	0.004					
Objective stress	0.376†	0.001†	2.54E-04					

AGV, amygdala volume.
*† $p < 0.10$. * $p < 0.05$ (2-tailed). ** $p < 0.01$ (2 tailed). Lower SES scores represent higher SES.*
*In (a) Bonferroni corrected on interaction p-value: † $p < 0.033$. * $p < 0.0167$ (2-tailed).*

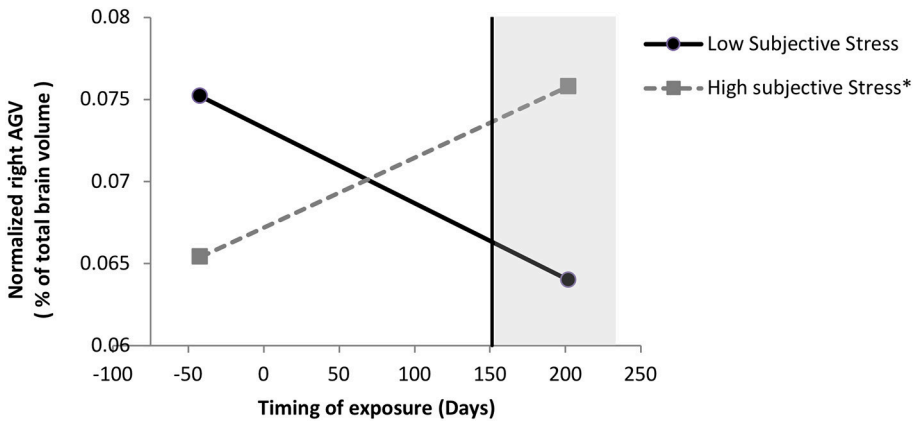

FIGURE 1 | Moderation of subjective stress' effect on normalized right AGV by timing of exposure in boys. Low and high stress lines are represented at the 10 and 90th sample percentile of subjective distress (measured with the Impact of Events Scale-Revised) respectively, which are at a log-transformed level of 0 and 3.33 (0 and 26.94 in original scale), respectively. Following a significant interaction between subjective stress and timing, probing the interaction revealed that when mothers were exposed to the storm from day 157 (week 22.42) onwards, the greater their mothers' subjective stress, the larger their right normalized AGV; the region of significance is represented by the vertical line. When mothers were exposed to the storm before day 157, which includes the mothers exposed to the storm during preconception, there was no significant effect of subjective stress on right normalized AGV. Additionally, when subjective stress scores were equal to or greater than a log value of 2.64 (original subjective stress scale 13.01), there was a significant ($p < 0.05$) effect of timing on right normalized AGV; for these boys, the later they were exposed to the storm in gestation, the larger the right normalized AGV; for these boys, the later they were exposed to the storm in gestation, the larger the right normalized AGV. *$p < 0.01$.

removed from the final model. The results indicated a significant moderated mediation effect (index of moderated mediation = 0.0135 and 95% confidence interval = [0.0006; 0.0369]), such that the mediation effect from higher subjective distress to more externalizing problems via larger right AGV was only significant for boys exposed on gestational day 212 (30.29 weeks) or later. However, since the moderation effect was no longer significant when adjusting for number of yearly postnatal life events, the mediation adjusting for postnatal measures was not tested.

Girls

Prenatal Stress and Amygdala Volume (Regression Analyses)

As shown in **Table 2**, no covariates were correlated with normalized AGV in girls, so no additional variables were added to the models.

Right amygdala volume

In girls, the results of the hierarchical regressions for right normalized AGV are presented in **Table 3b**. In the first step, timing explained 19.4% ($p = 0.012$), such that later exposure was significantly associated with larger right normalized AGV. In the second step, handedness explained 2.0% ($p = 0.396$) of the variance in right normalized AGV. In the last step, mothers' objective hardship explained an additional 8.1% ($p = 0.084$) of the variance in the girls' right normalized AGV: higher objective hardship was related to a larger right normalized AGV. Neither subjective distress, cognitive appraisal, nor any of the interaction terms were significantly related to the girls' right normalized AGV. The full model explained a total of 29.5% of the variance.

Left amygdala volume

Results of the hierarchical regression for left normalized AGV in girls are presented in **Table 3c**. In the first step, timing explained

TABLE 4 | Partial correlation coefficients between amygdala volume (AGV) and behavioral problems controlling for handedness, timing of exposure to the storm and additional covariates (see footnotes).

Sex child	Variables	Internalizing problems	Externalizing problems
PERINATAL MODEL			
Boys	Normalized right AGV	0.167[a,b]	0.452*[a,b]
	Normalized left AGV	0.154[a,b]	0.412*[a,b]
Girls	Normalized right AGV	0.177	0.561**[c]
	Normalized left AGV	0.144	0.384*[c]
ADJUSTING FOR POSTNATAL LIFE EVENTS			
Boys	Normalized right AGV	0.082[a,b,d]	0.355†[a,b,d]
	Normalized left AGV	0.075[a,b,d]	0.313*[a,b,d]
Girls	Normalized right AGV	0.203	0.568**[c]
	Normalized left AGV	0.074	0.344*[c]

† $p < 0.10$. * $p < 0.05$ (2-tailed). ** $p < 0.01$ (2-tailed).
[a] *Glasses of alcohol per week.*
[b] *Maternal psychological functioning (concurrent).*
[c] *Maternal life events (perinatal).*
[d] *Maternal life events (postnatal).*

8.1% ($p = 0.114$), and in the second step, handedness explained an additional 4.7% ($p = 0.220$) of the variance in left normalized AGV. In the last step, mothers' objective hardship explained an additional 11.3% ($p = 0.051$) of the variance: higher objective hardship was related to a larger left normalized AGV. The main effects of mothers' subjective distress and cognitive appraisal were not significantly related to the girls' left normalized AGV so they were left out of the model. None of the interaction terms were significantly related to the girls' left normalized AGV. The final model explained 24.1% of the variance in the girls' left normalized AGV.

Amygdala Volume and Behavioral Outcomes (Partial Correlations)

When testing the second path of the indirect effect we found that larger right normalized AGV predicted more externalizing problems in girls when controlling for timing, handedness, and maternal life events (**Table 4**). There was no effect on internalizing problems when controlling for timing and handedness. Results were very similar when adjusting for postnatal measures.

Mediating Effect of Amygdala Volumes on Association Between PNMS and Externalizing Problems

Because objective hardship was marginally associated with left and right normalized AGV, which were associated with externalizing problems, we tested for mediation effects, adjusting for timing of exposure, handedness, and maternal life events. However, in the model with left normalized AGV, neither path showed a significant maternal life events effect, so this covariate was removed from the final model. The analyses revealed that more objective hardship predicted larger left normalized AGV which in turn was associated with more externalizing problems (indirect effect = 0.286 and 95% confidence interval [0.0166; 0.9643]). The same mediation effect was also observed for the right normalized AGV (effect: 0.3831 and confidence interval [0.0106; 1.2727]). When adjusting for postnatal measures, the yearly number of postnatal life events was no longer significant, so it was trimmed out of the models. As such, the mediations through left and right AGV remain significant.

DISCUSSION

The first aim of this study was to determine whether there is an association between disaster-related PNMS and normalized AGV in boys and girls, and to investigate the extent to which timing of the ice storm *in utero* moderates the effects of PNMS on AGV. The second aim was to determine the extent to which AGV mediated the effects of disaster-related PNMS on child behavioral outcomes. By using a natural disaster as the source of stress, our method included the ability to test the relative contribution of three aspects of pregnant women's disaster-related PNMS experience (i.e., objective hardship, subjective distress, and cognitive appraisal) on AGV and on behavioral functioning of their children. Given the sudden onset of the ice storm, we were also able to test, and control for, the timing of *in utero* maternal stress exposure. Because boys and girls respond to PNMS differently, and because previous research has shown a sex-specific effect of maternal cortisol on AGV (Buss et al., 2012), and on internalizing/externalizing symptoms (reviewed in Glover and Hill, 2012) we tested our hypotheses in boys and girls separately. Our results suggest that there is a complex relationship between the predictors (the aspects of maternal stress experienced during pregnancy, and timing) and AGV in exposed boys and girls at 11½ years of age.

In Boys, Exposure to Higher Subjective PNMS in the Second Half of Pregnancy Is Associated With Larger Right Amygdala Volumes Which Predict More Externalizing Problems

Our first hypothesis was that higher levels of maternal objective hardship and/or subjective distress, and/or a negative cognitive appraisal of the crisis would explain variance in child AGV as normalized by total brain volume. No significant direct associations between our disaster-related PNMS measures and normalized AGV in boys were detected. From our correlational analyses we found that higher SES was associated with larger AGV, and when controlling for SES and objective PNMS exposure, an interaction between subjective PNMS and timing of exposure emerged. When exposure to the ice storm occurred at or after gestational week 22, higher maternal subjective distress predicted larger normalized right AGV. When subjective PNMS was >13 (which is not very severe), the later the exposure, the larger the AGV, such that AGV in those exposed earlier were below the sample's average while AGV in those exposed later were above the sample's average (**Figure 1**). The model explained 40% of the variance in normalized right AGV, with 13% attributed to SES, and 13% to the interaction between subjective PNMS

and timing. Interestingly, when adjusting the regression model for postnatal measures, concurrent SES was trimmed out of the model because it was no longer significant, and postnatal life events became marginally significant ($p = 0.056$), such that more yearly postnatal life events was associated with larger normalized AGV. However, adjusting for number of yearly postnatal life events, the interaction between subjective stress and timing was no longer significant. This suggests that maternal reported postnatal life events are an important factor contributing to right normalized amygdala volume in boys. Larger studies that specifically address the influences of prenatal factors, timing of PNMS exposure, and of postnatal life events directly related to the child are needed to better understand the influence of these factors on AGV in boys.

These data add to a growing body of literature showing that the amygdala is vulnerable to early life adverse experiences and prenatal factors, and suggest that the timing of exposure may be important. Maternal cortisol levels and prenatal maternal depression have been associated with structural and functional changes in the amygdala, and some have shown that the effects are specific to girls (e.g., Favaro et al., 2015; Wen et al., 2017; Soe et al., 2018). Limitations from those studies include, in the maternal depression studies (Lupien et al., 2011), the inability to test for timing effects, and in the maternal cortisol study (Buss et al., 2012), the lack of an independent maternal stressor. Our study suggests that the pregnant mother's subjective distress in response to a sudden onset stressor from mid-gestation onward is associated with larger AGV in boys. Furthermore, and consistent with previous studies (Buss et al., 2012; Rifkin-Graboi et al., 2013), the right amygdala seems particularly vulnerable to the effects of prenatal factors and early life adverse experiences. Our findings suggest that structural changes in the amygdala in boys may be particularly sensitive to maternal subjective distress experienced from a natural disaster, as of the 22nd week of gestation. The direction of our effect is consistent with that of Buss et al. (2012), who reported that higher levels of maternal cortisol levels in healthy mothers during pregnancy were associated with larger AGV at 7 years of age (albeit the effect was found in girls, but not boys), however their effect was detected earlier, at 15 weeks of gestation. Fetal cortisol is produced throughout the second trimester (weeks 12–20) (Johnston et al., 2018), with no difference between the sexes, and the fetal adrenal gland begins to secrete cortisol at increased levels as of 22 weeks gestation (Mesiano and Jaffe, 1997). One possibility explaining these sex-specific timing effects could involve sex differences in placental conversion of active maternal cortisol to inactive cortisone by 11B-hydroxysteroid dehydrogenase type 2 (11β-HSD2) (Clifton, 2010; Nugent and Bale, 2015). Another possibility may relate to amygdala circuitry, which expands from local to distal in the third trimester, developing connections with the frontal and temporal lobes before making connections with the contralateral amygdala (Scheinost et al., 2017). Thus, it is possible that in the face of maternal subjective distress, it is the summed contribution of both maternal and fetal cortisol levels that affects fetal male amygdala development and circuitry.

Prenatal factors can also differentially influence structural properties of the amygdala at different points in postnatal development. For example, in one rodent study that considered only males, mild prenatal environmental stressors (starting on gestational day 14/21) was associated with smaller lateral, basolateral, and central nuclei on postnatal day 25 (i.e., early pubertal period), but not at postnatal days 7, 45, or 60. Interestingly, in the basolateral amygdala, but not the lateral or central nuclei, prenatal stress was associated with a shorter nucleus at postnatal day 25, no difference on postnatal day 45, but longer nucleus on postnatal day 60 (Kraszpulski et al., 2009). Thus, PNMS may differentially affect structural properties of different amygdala nuclei throughout development. Although for rodents and humans, peak amygdala development occurs at different time points during gestation (in the second half of gestation in rats, and in the first trimester in humans, as reviewed in Charil et al., 2010), exposure to maternal perinatal stress or stress hormones can have a lasting impact on postnatal amygdala development in both species. Our data are consistent with those from studies of children who were initially raised in an impoverished institution as young infants, but who were then brought up in very high SES families: these children also had larger AGV in later life (Mehta et al., 2009; Tottenham and Sheridan, 2009). As such, the larger AGV we observe may be due to decreased cell proliferation and neuronal differentiation and increased gliogenesis due to stressors experienced during critical periods of perinatal development, as proposed by others (Salm et al., 2004; Kang et al., 2011; Buss et al., 2012). Although it is unclear how such structural changes may relate to externalizing problems, those changes may disrupt typical connectivity to other structures related to emotional regulation.

In boys, higher maternal subjective distress predicted higher externalizing scores through larger normalized right AGV, but only when the ice storm occurred at or after gestational week 30. This suggests that although maternal subjective distress can influence right AGV as of 22 weeks of gestation (as described above), the behavioral consequences of increased AGV are more likely to result from even later exposure (i.e., week 30). Whereas, there was no main effect of PNMS on internalizing or externalizing problems in boys, the partial correlations from both normalized left and right AGV predicted more externalizing problems, explaining 20% of the variance. Although the bivariate correlation suggested a tendency for left AGV to be associated with internalizing problems in boys, no association was detected from the partial correlations, suggesting that AGV was not associated with internalizing problems. Buss et al. (2012) did not observe associations between maternal cortisol and amygdala volume in boys, nor between maternal cortisol at any of the gestational ages and affective problems. Similarly, we did not find associations between PNMS and internalizing behaviors in our sample of boys. Yet our findings extend those of Buss et al. (2012) by showing that maternal subjective distress at a later period of gestation is associated with larger normalized AGV in 11½ year old boys, which in turn is associated with concurrent externalizing behaviors.

In Girls, Normalized Amygdala Volumes Mediate the Association Between Objective PNMS and Externalizing Problems

Our first hypothesis was that higher levels of maternal objective hardship and/or subjective distress, and/or a negative cognitive appraisal of the crisis would explain variance in the child's normalized AGV. The regression analyses revealed that when controlling for timing and handedness, greater objective hardship tended to predict larger right and left normalized AGV. Although there was no moderating effect of timing, a main effect of timing was detected in the hierarchical regression, such that later timing of exposure was associated with larger right and left normalized AGV. This timing effect is in contrast to Buss et al. (2012) who reported that maternal cortisol levels in earlier pregnancy were associated with larger AGV in girls at 7 years of age. As mentioned in section In Boys, Exposure to Higher Subjective PNMS in the Second Half of Pregnancy Is Associated With Larger Right Amygdala Volumes Which Predict More Externalizing Problems, these contrasting findings can be due to differences in the age of the participants when AGV was measured.

Our second hypothesis was that normalized AGV would mediate the association between PNMS and behavioral problems. The partial correlations revealed that when controlling for timing, handedness and maternal life events, larger right and left AGV were associated with more externalizing problems. The mediation analysis revealed that objective hardship was associated with larger left and right AGV, which in turn was associated with more externalizing problems at 11½ years of age. The existing literature suggests that more externalizing problems are associated with smaller AGV in adults (Matthies et al., 2012; Bobes et al., 2013; Gopal et al., 2013). However, prior to the current study only one study examined the mediating role of AGV between prenatal factors and behavior in children. Buss et al. (2012), in a group of healthy mothers and children, reported that higher maternal cortisol levels during early pregnancy were associated with larger right AGV which in turn was associated with more concurrent internalizing behaviors in 7 year old girls. That study considered naturally varying maternal cortisol levels collected at discrete periods during pregnancy (i.e., weeks 15, 19, 25, 31, and 39). The present study has the advantage of considering how a sudden-onset external stressor, outside of the mother's control, affected child development when exposed at varying prenatal periods. Here, we report that factors outside of the mother's control (i.e., her objective hardship experienced from the ice storm), and separate from her subjective response, is associated with larger normalized AGV and concurrent externalizing behaviors at 11½ years of age. Together these findings show that maternal factors during the prenatal period are important in the developing child's brain and behaviors.

The lack of associations with internalizing problems is surprising. We have previously reported with this sample that objective hardship and subjective distress are associated with internalizing problems when controlling for sex (King et al., 2012), whereas our bivariate correlations here suggest that subjective distress is more strongly associated with internalizing (and externalizing) in girls than in boys. Prospective studies have shown that maternal anxiety is a particularly strong predictor of child anxiety, regardless of sex (reviewed in Glover and Hill, 2012). Although the amygdala is thought to be an important structure associated with internalizing and externalizing problems, the directionality of those effects are not clear, which may be due to factors such as timing of the stressor, or the age of the child at the time of the assessment (Tottenham and Sheridan, 2009), or sex. Whereas some studies find smaller AGV in children and adolescents with mixed anxiety disorders (e.g., Mueller et al., 2013; Strawn et al., 2015), others report larger AGV in children with higher parent-reported anxiety (Qin et al., 2014). Both larger and smaller volumes have been reported in pediatric anxiety/depression (De Bellis et al., 2000; Milham et al., 2005), but sub-clinical internalizing problems appear to be associated with smaller AGV in otherwise healthy individuals (Spampinato et al., 2009; Merz et al., 2018). Similarly, it is smaller AGV that appears to be associated with higher levels of aggression in typical children (Matthies et al., 2012; Thijssen et al., 2015). Although the direction of these associations are unclear, Merz et al. (2018) recently reported that associations between environmental factors (i.e., SES) and AGV may vary by age. Our current findings suggests that larger, not smaller, AGV at 11½ may be predictive of concurrent aggressive behaviors, but not internalizing behaviors, particularly following *in utero* exposure to maternal stressors. Future studies are needed to disentangle the complex relationship between prenatal maternal stress and/or cortisol levels and behavioral problems as mediated through AGV, as their interaction with sex of the child, timing of exposure, and timing of assessment.

Sex-Specific Effects of the Maternal PNMS Experience on Child Outcomes

The various elements of the maternal stress experience (i.e., objective hardship, subjective distress, and cognitive appraisal) on the brain appear to be different for males and for females. We report that for girls, objective hardship seems to be the strongest predictor of AGV. For boys, subjective distress has some mild influence on AGV. Cognitive appraisal was not associated with AGV in neither sex. Our findings that only objective hardship, not subjective distress, was associated with externalizing behaviors via AGV in girls are surprising because they do not fit the conventional model of subjective distress and cortisol where more subjective distress during pregnancy causes an increase in maternal cortisol, which affects fetal development. This suggests that some distinct aspects of the objective hardship, perhaps unrelated to maternal cortisol levels, are influencing child prenatal development. Unfortunately, no other human studies have investigated the specific effect of objective maternal hardship on the offspring brain so it is difficult to discuss our findings in light of previous research. Interestingly, it was maternal subjective distress, and not objective hardship, in late pregnancy, that was associated with larger AGV and increased externalizing behaviors in boys. These sex-specific effects, and how they interact with timing of exposure *in utero*, warrant further investigation. In the only human PNMS study

on adult brain development, young women were found to have morphometric and functional changes in gray matter density within both the right and left amygdalae (Favaro et al., 2015), but men were not included in that study. Unfortunately, not only was the assessment of PNMS in that study retrospective, it also combined varying sources of stressors such as interpersonal problems (separation from partner), severe health problems, death of a loved one, abuse, or exposure to a natural disaster (Favaro et al., 2015). The design of our prospective longitudinal study allows the objective nature of the stress exposure to be isolated from the subjective distress of the woman and from her cognitive appraisal of the event, and the current data show that these different aspects of the maternal stress experience matter. In summary, our findings are consistent with those of Favaro et al. (2015), in that both the left and right amygdala are affected by PNMS in women, and we attribute this finding to the objective hardship exposure.

Both maternal subjective distress and objective hardship have been associated with cognitive and behavioral outcomes in the child (Watson et al., 1999; Wadhwa et al., 2001; Gutteling et al., 2005; Rice et al., 2007; Chuang et al., 2011; Liu, 2011). Moreover, in our previous Project Ice Storm studies, objective hardship was strongly correlated with physical, physiological and cognitive measures (Laplante et al., 2004, 2007, 2008, 2016; King and Laplante, 2005; King et al., 2009, 2012). Also, it was reported that objective hardship was strongly associated with DNA methylation (Cao-Lei et al., 2015, 2016), insulin secretion (Dancause et al., 2013), cytokine production (Veru et al., 2015), and earlier age at menarche (Duchesne et al., 2017), suggesting that the mechanisms through which objective hardship affects offspring development may bypass the maternal HPA axis and use other pathways to influence development of these systems. Lastly, our present findings linking subjective and/or objective PNMS with externalizing problems are supported by previous Project Ice Storm findings with assessments done 4½, 5½, 6½, 8½, and 9½ and 11½ years of age (King et al., 2012; Nguyen et al., 2018). Importantly, the current results suggest that different aspects of disaster-related PNMS can have sex-specific effects on neurodevelopment, and in turn explain variance in psychopathological symptoms (though the average T-scores lie within the normal range, as can be seen in **Table 1**).

Limitations

There are limitations to this work that need to be acknowledged. An important limitation regarding the sex specific effects is the sample size that limited our power to test the interaction with sex. However, based on the existing literature on sex-specific effects, we used statistical approaches that have been suggested as best practices in studies that were underpowered to test sex differences (i.e., sex disaggregation, Heidari et al., 2016; Day et al., 2017; Lee, 2018. Thus, our sex-specific analyses suggest that boys and girls are differentially affected by PNMS. We have reported the interactions in **Supplementary Table 3**, and note that the interaction between right normalized AGV and sex had the strongest effect size (R^2 change), consistent with the sex difference in right AGV reported by Buss et al. (2012). Moreover, the effect size we report for the interaction term was strongest for objective hardship, suggesting that this aspect of the maternal stress experience may be a particularly important driver in a potential sex difference. Future studies could use these reports to ensure sufficient power to specifically address sex differences.

Another important limitation to this study is that we did not collect maternal cortisol at the time of the stressor. This is a logistical limitation as the ice storm was a sudden-onset natural disaster and, due to delays in obtaining ethics approval, data collection only began 5 months after the disaster. In addition, although we were able to control for maternal reported life events, we did not have a direct measure of child self-reported life stressors in childhood. We used an indirect measure of child life events by using maternal related postnatal life events. These appear to be an important factor related to normalized amygdala volume in boys, and warrants further investigation. Another limitation is that we did not collect information on pubertal stage during the assessment at 11½ years of age. However, age at menarche was collected in 23 female participants at the 13½ year assessment. The mean age at menarche was 12. Only 5 out of the 23 female participants had attained menarche by the time of the MRI scan at age 11½. When looking at a scatterplot of the PNMS-by-AGV correlation, none of those 5 participants were outliers. No association was found between AGV in girls at age 11½ and their age at menarche (**Table 2**). Nonetheless, having pubertal stage information for the full sample may have improved our understanding of the effect seen, and may have helped remove the potential confounding effect of pubertal hormone surges on the brain and behavior. The lack of an unexposed control group is another important limitation to this study. And finally, although it is standard to correct brain region volumes for total brain volumes, it is possible that the volumetric changes we observed in amygdala volumes may be influenced by volumetric differences in other brain structures.

Strengths

Our study's main strength was the use of a sudden-onset, quasi-randomly distributed natural disaster as a stressor, rather than studying maternal psychological state or potentially non-independent life events. This allowed us to test for dose-response effects of PNMS on child neural and behavioral outcomes while reducing the influence of genetic factors. Moreover, we were able to assess the various elements of stress soon after the event occurred, thus providing us with a highly personalized, deep-level measure of the various stress levels. Additional strengths of our present study include its longitudinal prospective design with multiple assessment points between birth and childhood. This allowed us to include a number of maternal, familial, and postnatal child factors that may also influence child development, such as perinatal and concurrent SES, obstetric complications, gestational age at birth, maternal smoking and drinking habits during pregnancy, and maternal life events which were included as control variables in this study. Finally, segmentation of all child brain MRI was done with gold-standard manual segmentation. This may be especially important for the assessment of AGV because it has been suggested that automatic segmentation protocols are less reliable for smaller

subcortical structures (Tae et al., 2008), including the amygdala (Schoemaker et al., 2016).

CONCLUSION

Our present findings suggest that in boys, a mother's distress from a natural disaster, when experienced in the second half of pregnancy, can influence the development of her child's amygdala, which in turn mediates the association between subjective PNMS and externalizing behaviors when measured 11½ years later. In girls, the objective hardship experienced from a natural disaster predicted larger right and left normalized AGV, which in turn was associated with more externalizing behavior. This is, to the best of our knowledge, the first report linking PNMS with subsequent AGV and behavioral problems in childhood. Findings from the present study provide support for the hypothesis that susceptibility to behavioral problems may, in part, be programmed *in utero*, and that this effect may be mediated through the development of the amygdala. Furthermore, the study shows that exposure to a stressor during gestation exerts a lasting influence on child development. These results add to the growing awareness of the importance of the intrauterine environment and reveal a new pathway through which the maternal exposure to a stressor during pregnancy may affect the offspring, in a sex-specific manner.

DATA AVAILABILITY

We haven't obtained consent (mothers) or assent (children) to make the data available in publically accessible repositories, but they are available on request to the corresponding author.

ETHICS STATEMENT

This study was carried out in accordance with the recommendations of The Code of Ethics of the World Medical Association, and approved by the Douglas Mental Health University Institute Research Ethics Board. All subjects gave written informed consent or written informed assent for participants under the age of 18 years, in accordance with the Declaration of Helsinki.

AUTHOR CONTRIBUTIONS

SK designed and implemented Project Ice Storm. RD, DL, JP, and SK conceived of the current experiment. RD and RP ran the automated segmentation pipelines, which was overseen by MC. GE and RD ran the statistical analyses. RD did manual corrections of the amygdala and total brain volume segmentations derived from the automated segmentations, overseen by JP. SK, DL, MC, and JP provided intellectual contributions to the interpretation of data. RD interpreted the data and drafted an early version of the manuscript. SJ, SK, and DL provided intellectual contributions for the rationale, interpretation of the data, and prepared the final manuscript for submission.

FUNDING

The project was funded by grants from the March of Dimes Foundation (12-FY07-263), Canadian Institutes of Health Research (FRN 125892), and the McGill Stairs Memorial Fund. SJ was supported by a postdoctoral fellowship by the Fonds de recherche du Québec—Santé.

ACKNOWLEDGMENTS

The scanning protocol was designed by Arnaud Charil. The children were escorted through the scanning protocol at age 11½ by Rowena Lung, Karine Ferron, Gila Foomani, Weirquan Zeng, Marjolaine Massé, and Maria Papastergiou. The scans were obtained by MRI technicians André Cyr and Carollyne Hurst at the *Unité de Neuroimagerie Fonctionelle* (UNF) *du Centre de Recherche de l'Institut Universitaire de Gériatrie de Montréal* (CRIUGM). Child behavioral and cognitive testing was done by Jenifer Chappell and Isabelle Bouchard.

SUPPLEMENTARY MATERIAL

The Supplementary Material for this article can be found online at: https://www.frontiersin.org/articles/10.3389/fnhum.2019.00144/full#supplementary-material

REFERENCES

Achenbach, T. M., and Ruffle, T. M. (2000). The child behavior checklist and related forms for assessing behavioral/emotional problems and competencies. *Pediatr. Rev.* 21, 265–271. doi: 10.1542/pir.21-8-265

Bobes, M. A., Ostrosky, F., Diaz, K., Romero, C., Borja, K., Santos, Y., et al. (2013). Linkage of functional and structural anomalies in the left amygdala of reactive-aggressive men. *Soc. Cogn. Affect. Neurosci.* 8, 928–936. doi: 10.1093/scan/nss101

Bromet, E., and Dew, M. A. (1995). Review of psychiatric epidemiologic research on disasters. *Epidemiol. Rev.* 17, 113–119. doi: 10.1093/oxfordjournals.epirev.a036166

Brunet, A., St Hilaire, A., Jehel, L., and King, S. (2003). Validation of a French version of the impact of event scale-revised. *Can. J. Psychiatry* 48, 56–61. doi: 10.1177/070674370304800111

Buss, C., Davis, E. P., Shahbaba, B., Pruessner, J. C., Head, K., and Sandman, C. A. (2012). Maternal cortisol over the course of pregnancy and subsequent child amygdala and hippocampus volumes and affective problems. *Proc. Natl. Acad. Sci. U S A.* 109, E1312–E1319. doi: 10.1073/pnas.1201295109

Buss, C., Lord, C., Wadiwalla, M., Hellhammer, D. H., Lupien, S. J., Meaney, M. J., et al. (2007). Maternal care modulates the relationship between prenatal risk and hippocampal volume in women but not in men. *J. Neurosci.* 27, 2592–2595. doi: 10.1523/JNEUROSCI.3252-06.2007

Cao, X., Laplante, D. P., Brunet, A., Ciampi, A., and King, S. (2014). Prenatal maternal stress affects motor function in 5½-year-old children: Project Ice Storm. *Dev. Psychobiol.* 56, 117–125. doi: 10.1002/dev.21085

Cao-Lei, L., Dancause, K. N., Elgbeili, G., Massart, R., Szyf, M., Liu, A., et al. (2015). DNA methylation mediates the impact of exposure to prenatal maternal stress on BMI and central adiposity in children at age 13½ years: Project Ice Storm. *Epigenetics* 10, 749–761. doi: 10.1080/15592294.2015.1063771

Cao-Lei, L., Veru, F., Elgbeili, G., Szyf, M., Laplante, D. P., and King, S. (2016). DNA methylation mediates the effect of exposure to prenatal maternal stress on cytokine production in children at age 13½ years: Project Ice Storm. *Clin. Epigenetics* 8:54. doi: 10.1186/s13148-016-0219-0

Chakravarty, M. M., Steadman, P., van Eede, M. C., Calcott, R. D., Gu, V., Shaw, P., et al. (2013). Performing label-fusion-based segmentation using multiple automatically generated templates. *Hum. Brain Mapp.* 34, 2635–2654. doi: 10.1002/hbm.22092

Charil, A., Laplante, D. P., Vaillancourt, C., and King, S. (2010). Prenatal stress and brain development. *Brain Res. Rev.* 65, 56–79. doi: 10.1016/j.brainresrev.2010.06.002

Chuang, C.-H., Jeng, S.-F., Hsieh, W.-S., Liao, H.-F., Su, Y.-N., and Chen, P.-C. (2011). Maternal psychosocial factors around delivery, and the behavior of 2-year-old children. *Pediatr. Int.* 53, 656–661. doi: 10.1111/j.1442-200X.2010.03315.x

Clifton, V. L. (2010). Review: sex and the human placenta: mediating differential strategies of fetal growth and survival. *Placenta* 31, S33–S39. doi: 10.1016/j.placenta.2009.11.010

Cottrell, E. C., and Seckl, J. (2009). Prenatal stress, glucocorticoids and the programming of adult disease. *Front. Behav. Neurosci.* 3:19. doi: 10.3389/neuro.08.019.2009

Dancause, K. N., Veru, F., Andersen, R. E., Laplante, D. P., and King, S. (2013). Prenatal stress due to a natural disaster predicts insulin secretion in adolescence. *Early Hum. Dev.* 89, 773–776. doi: 10.1016/j.earlhumdev.2013.06.006

Davis, M., and Whalen, P. J. (2001). The amygdala: vigilance and emotion. *Mol. Psychiatry* 6, 13–34. 10.1038/sj.mp.4000812

Day, S., Mason, R., Tannenbaum, C., and Rochon, P. A. (2017). Essential metrics for assessing sex and gender integration in health research proposals involving human participants. *PLoS ONE* 12:e0182812. doi: 10.1371/journal.pone.0182812

De Bellis, M. D., Casey, B. J., Dahl, R. E., Birmaher, B., Williamson, D. E., Thomas, K. M., et al. (2000). A pilot study of amygdala volumes in pediatric generalized anxiety disorder. *Biol. Psychiatry* 48, 51–57. doi: 10.1016/S0006-3223(00)00835-0

Duchesne, A., Liu, A., Jones, S. L., Laplante, D. P., and King, S. (2017). Childhood body mass index at 5.5 years mediates the effect of prenatal maternal stress on daughters' age at menarche: Project Ice Storm. *J. Dev. Orig. Health Dis.* 8, 168–177. doi: 10.1017/S2040174416000726

Eskildsen, S. F., Coupé, P., Fonov, V., Manjón, J. V., Leung, K. K., Guizard, N., et al. (2012). BEaST: brain extraction based on nonlocal segmentation technique. *Neuroimage* 59, 2362–2373. doi: 10.1016/j.neuroimage.2011.09.012

Favaro, A., Tenconi, E., Degortes, D., Manara, R., and Santonastaso, P. (2015). Neural correlates of prenatal stress in young women. *Psychol. Med.* 45, 2533–2543. doi: 10.1017/S003329171500046X

Glover, V., and Hill, J. (2012). Sex differences in the programming effects of prenatal stress on psychopathology and stress responses: an evolutionary perspective. *Physiol. Behav.* 106, 736–740. doi: 10.1016/j.physbeh.2012.02.011

Goldberg, D. P. (1972). *The Detection of Psychiatric Illness by Questionnaire: A Technique for the Identification and Assessment of Non-Psychotic Illness*. Oxford: Oxford University Press.

Gopal, A., Clark, E., Allgair, A., D'Amato, C., Furman, M., Gansler, D. A., et al. (2013). Dorsal/ventral parcellation of the amygdala: relevance to impulsivity and aggression. *Psychiatry Res.* 211, 24–30. doi: 10.1016/j.pscychresns.2012.10.010

Gutteling, B. M., de Weerth, C., Willemsen-Swinkels, S. H. N., Huizink, A. C., Mulder, E. J. H., Visser, G. H. A., et al. (2005). The effects of prenatal stress on temperament and problem behavior of 27-month-old toddlers. *Eur. Child Adolesc. Psychiatry* 14, 41–51. doi: 10.1007/s00787-005-0435-1

Harris, A., and Seckl, J. (2011). Glucocorticoids, prenatal stress and the programming of disease. *Horm. Behav.* 59, 279–289. doi: 10.1016/j.yhbeh.2010.06.007

Hayes, A. F., and Preacher, K. J. (2013). "Conditional process modeling: using structural equation modeling to examine contingent causal processes," in *Quantitative Methods in Education and the Behavioral Sciences: Issues, Research, and Teaching. Structural Equation Modeling: A Second Course*, eds G. R. Hancock and R. O. Mueller (Charlotte, NC: IAP Information Age Publishing), 219–266.

Heidari, S., Babor, T. F., De Castro, P., Tort, S., and Curno, M. (2016). Sex and gender equity in research: rationale for the SAGER guidelines and recommended use. *Res. Integr. Peer Rev.* 1, 1–9. doi: 10.1186/s41073-016-0007-6

Hollingshead, A. B. (1975). *Four Factor Index of Social Status*. New Haven, CT: Yale University Press.

Jacobsen, B., and Kinney, D. K. (1980). Perinatal complications in adopted and non-adopted schizophrenics and their controls: preliminary results. *Acta Psychiatr. Scand.* 62, 337–346. doi: 10.1111/j.1600-0447.1980.tb07709.x

Johnston, Z. C., Bellingham, M., Filis, P., Soffientini, U., Hough, D., Bhattacharya, S., et al. (2018). The human fetal adrenal produces cortisol but no detectable aldosterone throughout the second trimester. *BMC Med.* 16:23. doi: 10.1186/s12916-018-1009-7

Kang, H. J., Kawasawa, Y. I., Cheng, F., Zhu, Y., Xu, X., Li, M., et al. (2011). Spatio-temporal transcriptome of the human brain. *Nature* 478, 483–489. doi: 10.1038/nature10523

King, S., Dancause, K., Turcotte-Tremblay, A.-M., Veru, F., and Laplante, D. P. (2012). Using natural disasters to study the effects of prenatal maternal stress on child health and development. *Birth Defects Res. C Embryo Today* 96, 273–288. doi: 10.1002/bdrc.21026

King, S., and Laplante, D. P. (2005). The effects of prenatal maternal stress on children's cognitive development: Project Ice Storm. *J. Biol. Stress* 8, 35–45. doi: 10.1080/10253890500108391

King, S., Mancini-Marïe, A., Brunet, A., Walker, E., Meaney, M. J., and Laplante, D. P. (2009). Prenatal maternal stress from a natural disaster predicts dermatoglyphic asymmetry in humans. *Dev. Psychopathol.* 21, 343–353. doi: 10.1017/S0954579409000364

Kinney, D. K., Miller, A. M., Crowley, D. J., Huang, E., and Gerber, E. (2008). Autism prevalence following prenatal exposure to hurricanes and tropical storms in Louisiana. *J. Autism Dev. Disord.* 38, 481–488. doi: 10.1007/s10803-007-0414-0

Kraszpulski, M., Dickerson, P. A., and Salm, A. K. (2009). Prenatal stress affects the developmental trajectory of the rat amygdala. *Stress* 9, 85–95. doi: 10.1080/10253890600798109

Laplante, D. P., Barr, R. G., Brunet, A., Galbaud du Fort, G., Meaney, M. L., Saucier, J.-F., et al. (2004). Stress during pregnancy affects general intellectual and language functioning in human toddlers. *Pediatr. Res.* 56, 400–410. doi: 10.1203/01.PDR.0000136281.34035.44

Laplante, D. P., Brunet, A., and King, S. (2016). The effects of maternal stress and illness during pregnancy on infant temperament: Project Ice Storm. *Pediatr. Res.* 79, 107–113. doi: 10.1038/pr.2015.177

Laplante, D. P., Brunet, A., Schmitz, N., Ciampi, A., and King, S. (2008). Project Ice Storm: prenatal maternal stress affects cognitive and linguistic functioning in 5½-year-old children. *J. Am. Acad. Child Adolesc. Psychiatry* 47, 1063–1072. doi: 10.1097/CHI.0b013e31817eec80

Laplante, D. P., Zelazo, P. R., Brunet, A., and King, S. (2007). Functional play at 2 years of age: effects of prenatal maternal stress. *Infancy* 12, 69–93. doi: 10.1080/15250000701298741

Lee, S. K. (2018). Sex as an important biological variable in biomedical research. *BMB Rep.* 51, 167–173. doi: 10.5483/BMBRep.2018.51.4.034

Liu, J. (2011). Early health risk factors for violence: conceptualization, review of the evidence, and implications. *Aggress. Violent Behav.* 16, 63–73. doi: 10.1016/j.avb.2010.12.003

Lupien, S. J., Parent, S., Evans, A. C., Tremblay, R. E., Zelazo, P. D., Corbo, V., et al. (2011). Larger amygdala but no change in hippocampal volume in 10-year-old children exposed to maternal depressive symptomatology since birth. *Proc. Natl. Acad. Sci. U S A.* 108, 14324–14329. doi: 10.1073/pnas.1105371108

MacMillan, S., Szeszko, P. R., Moore, G. J., Madden, R., Lorch, E., Ivey, J., et al. (2003). Increased amygdala: hippocampal volume ratios associated with severity of anxiety in pediatric major depression. *J. Child Adolesc. Psychopharmacol.* 13, 65–73. doi: 10.1089/104454603321666207

Matthies, S., Rüsch, N., Weber, M., Lieb, K., Philipsen, A., Tuescher, O., et al. (2012). Small amygdala – high aggression? The role of the amygdala in modulating aggression in healthy subjects. *World J. Biol. Psychiatry* 13, 75–81. doi: 10.3109/15622975.2010.541282

McNeil, T. F., and Sjöström, K. (1995). *The McNeil–Sjöström OC Scale: A Comprehensive Scale for Measuring Obstetric Complications*. Malmö: Department of Psychiatry; Lund University; Malmö General Hospital.

Mehta, M. A., Golembo, N. I., Nosarti, C., Colvert, E., Mota, A., Williams, S. C. R., et al. (2009). Amygdala, hippocampal and corpus callosum size following severe early institutional deprivation: the English and Romanian Adoptees study pilot. *J. Child Psychol. Psychiatry* 50, 943–951. doi: 10.1111/j.1469-7610.2009.02084.x

Merz, E. C., Tottenham, N., and Noble, K. G. (2018). Socioeconomic status, amygdala volume, and internalizing symptoms in children and adolescents. *J. Clin. Child Adolesc. Psychol.* 47, 312–323. doi: 10.1080/15374416.2017.1326122

Mesiano, S., and Jaffe, R. B. (1997). Developmental and functional biology of the primate fetal adrenal cortex. *Endocr. Rev.* 18, 378–403. doi: 10.1210/edrv.18.3.0304

Milham, M. P., Nugent, A. C., Drevets, W. C., Dickstein, D. S., Leibenluft, E., Ernst, M., et al. (2005). Selective reduction in amygdala volume in pediatric anxiety disorders: a voxel-based morphometry investigation. *Biol. Psychiatry* 57, 961–966. doi: 10.1016/j.biopsych.2005.01.038

Moss, K. M., Simcock, G., Cobham, V. E., Kildea, S., Laplante, D. P., and King, S. (2018). Continuous, emerging, and dissipating associations between prenatal maternal stress and child cognitive and motor development: the QF2011 Queensland Flood Study. *Early Hum. Dev.* 119, 29–37. doi: 10.1016/j.earlhumdev.2018.02.022

Mueller, S. C., Aouidad, A., Gorodetsky, E., Goldman, D., Pine, D. S., and Ernst, M. (2013). Gray matter volume in adolescent anxiety: an impact of the brain-derived neurotrophic factor Val(66)Met polymorphism? *J. Am. Acad. Child Adolesc. Psychiatry* 52, 184–195. doi: 10.1016/j.jaac.2012.11.016

Nguyen, T.-V., Jones, S. L., Elgbeili, G., Monnier, P., Yu, C., Laplante, D. P., et al. (2018). Testosterone–cortisol dissociation in children exposed to prenatal maternal stress, and relationship with aggression: Project Ice Storm. *Dev. Psychopathol.* 30, 981–994. doi: 10.1017/S0954579418000652

Nugent, B. M., and Bale, T. L. (2015). The omniscient placenta: metabolic and epigenetic regulation of fetal programming. *Front. Neuroendocrinol.* 39, 28–37. doi: 10.1016/j.yfrne.2015.09.001

O'Connor, T. G., Heron, J., Glover, V., and Alspac Study Team. (2002). Antenatal anxiety predicts child behavioral/emotional problems independently of postnatal depression. *J. Am. Acad. Child Adolesc. Psychiatry* 41, 1470–1477. doi: 10.1097/00004583-200212000-00019

Pardini, D. A., Raine, A., Erickson, K., and Loeber, R. (2014). Lower amygdala volume in men is associated with childhood aggression, early psychopathic traits, and future violence. *Biol. Psychiatry* 75, 73–80. doi: 10.1016/j.biopsych.2013.04.003

Pipitone, J., Park, M. T. M., Winterburn, J., Lett, T. A., Lerch, J. P., Pruessner, J. C., et al. (2014). Multi-atlas segmentation of the whole hippocampus and subfields using multiple automatically generated templates. *Neuroimage* 101, 494–512. doi: 10.1016/j.neuroimage.2014.04.054

Posner, J., Cha, J., Roy, A. K., Peterson, B. S., Bansal, R., Gustafsson, H. C., et al. (2016). Alterations in amygdala-prefrontal circuits in infants exposed to prenatal maternal depression. *Transl. Psychiatry* 6:e935. doi: 10.1038/tp.2016.146

Pruessner, J. C., Li, L. M., Serles, W., Pruessner, M., Collins, D. L., Kabani, N., et al. (2000). Volumetry of hippocampus and amygdala with high-resolution MRI and three-dimensional analysis software: minimizing the discrepancies between laboratories. *Cereb. Cortex* 10, 433–442. doi: 10.1093/cercor/10.4.433

Qin, S., Young, C. B., Duan, X., Chen, T., Supekar, K., and Menon, V. (2014). Amygdala subregional structure and intrinsic functional connectivity predicts individual differences in anxiety during early childhood. *Biol. Psychiatry* 75, 892–900. doi: 10.1016/j.biopsych.2013.10.006

Quirk, G. J., and Beer, J. S. (2006). Prefrontal involvement in the regulation of emotion: convergence of rat and human studies. *Curr. Opin. Neurobiol.* 16, 723–727. doi: 10.1016/j.conb.2006.07.004

Rice, F., Harold, G. T., Boivin, J., van den Bree, M., Hay, D. F., and Thapar, A. (2010). The links between prenatal stress and offspring development and psychopathology: disentangling environmental and inherited influences. *Psychol. Med.* 40, 335–345. doi: 10.1017/S0033291709005911

Rice, F., Jones, I., and Thapar, A. (2007). The impact of gestational stress and prenatal growth on emotional problems in offspring: a review. *Acta Psychiatr. Scand.* 115, 171–183. doi: 10.1111/j.1600-0447.2006.00895.x

Rifkin-Graboi, A., Bai, J., Chen, H., Hameed, W. B., Sim, L. W., Tint, M. T., et al. (2013). Prenatal maternal depression associates with microstructure of right amygdala in neonates at birth. *Biol. Psychiatry* 74, 837–844. doi: 10.1016/j.biopsych.2013.06.019

Rosso, I. M., Cintron, C. M., Steingard, R. J., Renshaw, P. F., Young, A. D., and Yurgelun-Todd, D. A. (2005). Amygdala and hippocampus volumes in pediatric major depression. *Biol. Psychiatry* 57, 21–26. doi: 10.1016/j.biopsych.2004.10.027

Salm, A. K., Pavelko, M., Krouse, E. M., Webster, W., Kraszpulski, M., and Birkle, D. L. (2004). Lateral amygdaloid nucleus expansion in adult rats is associated with exposure to prenatal stress. *Dev. Brain Res.* 148, 159–167. doi: 10.1016/j.devbrainres.2003.11.005

Sarason, I. G., Johnson, J. H., and Siegel, J. M. (1978). Assessing the impact of life changes: development of the life experiences survey. *J. Consult. Clin. Psychol.* 46, 932–946. doi: 10.1037/0022-006X.46.5.932

Scheinost, D., Kwon, S. H., Lacadie, C., Sze, G., Sinha, R., Constable, R. T., et al. (2016). Prenatal stress alters amygdala functional connectivity in preterm neonates. *NeuroImage Clin.* 12, 381–388. doi: 10.1016/j.nicl.2016.08.010

Scheinost, D., Sinha, R., Cross, S. N., Kwon, S. H., Sze, G., Constable, R. T., et al. (2017). Does prenatal stress alter the developing connectome? *Pediatric Res.* 81, 214–226. doi: 10.1038/pr.2016.197

Schienle, A., Ebner, F., and Schäfer, A. (2011). Localized gray matter volume abnormalities in generalized anxiety disorder. *Eur. Arch. Psychiatry Clin. Neurosci.* 261, 303–307. doi: 10.1007/s00406-010-0147-5

Schoemaker, D., Buss, C., Head, K., Sandman, C. A., Davis, E. P., Chakravarty, M. M., et al. (2016). Hippocampus and amygdala volumes from magnetic resonance images in children: assessing accuracy of FreeSurfer and FSL against manual segmentation. *Neuroimage* 129, 1–14. doi: 10.1016/j.neuroimage.2016.01.038

Sled, J. G., Zijdenbos, A. P., and Evans, A. C. (1998). A nonparametric method for automatic correction of intensity nonuniformity in MRI data. *IEEE Trans. Med. Imaging* 17, 87–97. doi: 10.1109/42.668698

Soe, N. N., Wen, D. J., Poh, J. S., Chong, Y.-S., Broekman, B. F., Chen, H., et al. (2018). Perinatal maternal depressive symptoms alter amygdala functional connectivity in girls. *Hum. Brain Mapp.* 39, 680–690. doi: 10.1002/hbm.23873

Spampinato, M. V., Wood, J. N., De Simone, V., and Grafman, J. (2009). Neural correlates of anxiety in healthy volunteers: a voxel-based morphometry study. *J. Neuropsychiatry Clin. Neurosci.* 21, 199–205. doi: 10.1176/jnp.2009.21.2.199

Strawn, J. R., Hamm, L., Fitzgerald, D. A., Fitzgerald, K. D., Monk, C. S., and Phan, K. L. (2015). Neurostructural abnormalities in pediatric anxiety disorders. *J. Anxiety Disord.* 32, 81–88. doi: 10.1016/j.janxdis.2015.03.004

Tae, W. S., Kim, S. S., Lee, K. U., Nam, E.-C., and Kim, K. W. (2008). Validation of hippocampal volumes measured using a manual method and two automated methods (FreeSurfer and IBASPM) in chronic major depressive disorder. *Neuroradiology* 50, 569–581. doi: 10.1007/s00234-008-0383-9

Thijssen, S., Ringoot, A. P., Wildeboer, A., Bakermans-Kranenburg, M. J., El Marroun., Hofman, A., et al. (2015). Brain morphology of childhood aggressive behavior: a multi-informant study in school-age children. *Cogn. Affect. Behav. Neurosci.* 15, 564–577. doi: 10.3758/s13415-015-0344-9

Tottenham, N., and Sheridan, M. A. (2009). A review of adversity, the amygdala and the hippocampus: a consideration of developmental timing. *Front. Hum. Neurosci.* 3:68. doi: 10.3389/neuro.09.068.2009

Van den Bergh, B. R. H., and Marcoen, A. (2004). High antenatal maternal anxiety is related to ADHD symptoms, externalizing problems, and anxiety in 8- and 9-year-olds. *Child Dev.* 75, 1085–1097. doi: 10.1111/j.1467-8624.2004.00727.x

Van den Bergh, B. R. H., van den Heuvel, M. I., Lahti, M., Braeken, M., de Rooij, S. R., Entringer, S., et al. (2017). Prenatal developmental origins of behavior and mental health: the influence of maternal stress in pregnancy. *Neurosci. Biobehav. Rev.* doi: 10.1016/j.neubiorev.2017.07.003. [Epub ahead of print].

Van Lieshout, R. J., and Boylan, K. (2010). Increased depressive symptoms in female but not male adolescents born at low birth weight in the offspring of a national cohort. *Can. J. Psychiatry* 55, 422–430. doi: 10.1177/070674371005500705

Veru, F., Dancause, K., Laplante, D. P., King, S., and Luheshi, G. (2015). Prenatal maternal stress predicts reductions in CD4+ lymphocytes, increases in innate-derived cytokines, and a Th2 shift in adolescents: Project Ice Storm. *Physiol. Behav.* 144, 137–145. doi: 10.1016/j.physbeh.2015.03.016

Wadhwa, P. D., Culhane, J. F., Rauh, V., Barve, S. S., Hogan, V., Sandman, C. A., et al. (2001). Stress, infection and preterm birth: a biobehavioural perspective. *Paediatr. Perinat. Epidemiol.* 15, 17–29. doi: 10.1046/j.1365-3016.2001.00005.x

Watson, J. B., Mednick, S. A., Huttunen, M., and Wang, X. (1999). Prenatal teratogens and the development of adult mental illness. *Dev. Psychopathol.* 11, 457–466.

Weiss, D. S., and Marmar, C. R. (1997). "The impact of event scale—revised," in *Assessing Psychological Trauma and PTSD*, eds J. P. Wilson and T. M. Keane (New York, NY: Guilford Press), 399–411.

Wen, D. J., Poh, J. S., Ni, S. N., Chong, Y.-S., Chen, H., Kwek, K., et al. (2017). Influences of prenatal and postnatal maternal depression on amygdala volume and microstructure in young children. *Transl. Psychiatry* 7:e1103. doi: 10.1038/tp.2017.74

Conflict of Interest Statement: The authors declare that the research was conducted in the absence of any commercial or financial relationships that could be construed as a potential conflict of interest.

frontiers in Molecular Neuroscience

ORIGINAL RESEARCH
published: 17 July 2019
doi: 10.3389/fnmol.2019.00166

Differential Neuroinflammatory Response in Male and Female Mice: A Role for BDNF

Andrea Carlo Rossetti[1†], Maria Serena Paladini[1], Ada Trepci[2†], Anne Mallien[3], Marco Andrea Riva[2], Peter Gass[3] and Raffaella Molteni[1]*

[1] Department of Medical Biotechnology and Translational Medicine, University of Milan, Milan, Italy, [2] Department of Pharmacological and Biomolecular Sciences, University of Milan, Milan, Italy, [3] Department of Psychiatry and Psychotherapy, Central Institute of Mental Health, Medical Faculty Mannheim, Heidelberg University, Heidelberg, Germany

OPEN ACCESS

Edited by:
Jordan Marrocco, The Rockefeller University, United States

Reviewed by:
Aleksander A. Mathé, Karolinska Institute (KI), Sweden
Xin Du, Monash University, Australia

***Correspondence:**
Raffaella Molteni
raffaella.molteni@unimi.it

†Present address:
Andrea Carlo Rossetti, Central Institute of Mental Health, Medical Faculty Mannheim, Heidelberg University, Heidelberg, Germany; HITBR Hector Institute for Translational Brain Research gGmbH, Mannheim, Germany; German Cancer Research Center (DKFZ), Heidelberg, Germany
Ada Trepci, Department of Physiology and Pharmacology, Karolinska Institutet, Stockholm, Sweden

Received: *11 March 2019*
Accepted: *17 June 2019*
Published: *17 July 2019*

Citation:
Rossetti AC, Paladini MS, Trepci A, Mallien A, Riva MA, Gass P and Molteni R (2019) Differential Neuroinflammatory Response in Male and Female Mice: A Role for BDNF. Front. Mol. Neurosci. 12:166. doi: 10.3389/fnmol.2019.00166

A growing body of evidence supports the close relationship between major depressive disorder (MDD), a severe psychiatric disease more common among women than men, and alterations of the immune/inflammatory system. However, despite the large number of studies aimed at understanding the molecular bases of this association, a lack of information exists on the potential cross-talk between systems known to be involved in depression and components of the inflammatory response, especially with respect to sex differences. Brain-derived neurotrophic factor (BDNF) is a neurotrophin with a well-established role in MDD etiopathology: it is altered in depressed patients as well as in animal models of the disease and its changes are restored by antidepressant drugs. Interestingly, this neurotrophin is also involved in the inflammatory response. Indeed, it can be secreted by microglia, the primary innate immune cells in the central nervous system whose functions may be in turn regulated by BDNF. With these premises, in this study, we investigated the reciprocal impact of BDNF and the immune system by evaluating the neuroinflammatory response in male and female BDNF-heterozygous mutant mice acutely treated with the cytokine-inducer lipopolysaccharide (LPS). Specifically, we assessed the potential onset of an LPS-induced sickness behavior as well as changes of inflammatory mediators in the mouse hippocampus and frontal cortex, with respect to both genotype and sex. We found that the increased inflammatory response induced by LPS in the brain of male mice was independent of the genotype, whereas in the female, it was restricted to the heterozygous mice with no changes in the wild-type group, suggestive of a role for BDNF in the sex-dependent effect of the inflammatory challenge. Considering the involvement of both BDNF and neuroinflammation in several psychiatric diseases and the diverse incidence of such pathologies in males and females, a deeper investigation of the mechanisms underlying their interaction may have a critical translational relevance.

Keywords: brain-derived neurotrophic factor, lipopolysaccharide, sex, neuroinflammation, hippocampus

INTRODUCTION

Major depressive disorder (MDD) is a severe psychiatric disease affecting almost 10% of the general population and estimated to become the second leading cause of disability by 2020 (Bromet et al., 2011). In addition to the symptom heterogeneity among patients and to its complex etiology (Otte et al., 2016), MDD presents a sexually dimorphic nature, characterized by a twofold greater risk in females to develop the pathology (Brody et al., 2018; LeGates et al., 2019). On this basis and given the different immunological response in terms of innate and adaptive systems among sexes (Klein and Flanagan, 2016), it is plausible that sex-based differences in immune response might play an important role to the diverse vulnerability/incidence to psychiatric disorders (Derry et al., 2015; Rubinow and Schmidt, 2019). In the last years, growing evidence suggests that alterations in the inflammatory/immune response may contribute to the susceptibility for different psychiatric conditions, including MDD (Müller, 2014). Particularly, the increased levels of peripheral and central inflammatory markers observed in a large subset of MDD subjects (Raison et al., 2006; Howren et al., 2009; Dowlati et al., 2010), the high co-morbidity between MDD and various non-psychiatric illnesses associated with inflammatory conditions (Anisman, 2008; Berge and Riise, 2015; Réus et al., 2017), and the development of MDD in a high percentage of patients under interferon regimen (Raison et al., 2009; Udina et al., 2012) clearly support the relevance of a neuroinflammatory component in MDD. In addition, while changes in immune/inflammatory response have been found in MDD experimental models based on both the genetic and the environmental components of the disease (Chourbaji et al., 2011; Couch et al., 2013; Macchi et al., 2013; Rossetti et al., 2016; Wang et al., 2018), several studies indicate the immune/inflammatory system as a potential target for the pharmacological treatment of MDD (Molteni et al., 2013; Kv et al., 2018; Rossetti et al., 2018a,b; Lu et al., 2019).

It is known that this complex psychopathology affects multiple molecular systems such as neurotransmitters, hormones, and mediators of neuronal plasticity. Among those, the neurotrophin brain-derived neurotrophic factor (BDNF) plays a crucial role. Indeed, BDNF levels are reduced in depressed subjects and the neurotrophin represents a key step in long-term adaptive changes brought about by antidepressant drugs (Berton and Nestler, 2006; Martinowich et al., 2007; Molendijk et al., 2014; Castrén and Kojima, 2017). In addition, BDNF is dramatically affected by inflammatory insults (Calabrese et al., 2014; Lima Giacobbo et al., 2018): the administration of lipopolysaccharide (LPS) or pro-inflammatory cytokines in rodents has been shown to decrease its levels in the cortex and hippocampus (Guan and Fang, 2006; Schnydrig et al., 2007; Patterson, 2015), while the therapeutic treatment with interferons alters BDNF expression in human subjects (Capuron et al., 2004; Kenis et al., 2011; Lotrich et al., 2013). Moreover, microglial cells, the macrophage resident population within the brain and one of the crucial components of the neuroinflammatory response, express BDNF mRNA, secrete the neurotrophin following stimulation, and are regulated by BDNF signaling (Nakajima et al., 2001; Ferrini and De Koninck, 2013).

On this basis, the main goal of our study was to investigate the potential link between neuroinflammation and BDNF in male and female mice by evaluating if and how the inflammatory response might be altered in conditions characterized by compromised expression of the neurotrophin. Accordingly, we assessed the brain inflammatory response of male and female BDNF$^{+/-}$ mice, which exhibit an approximately 50% reduction of BDNF protein and mRNA (Korte et al., 1995; Lyons et al., 1999; Sairanen et al., 2005; Chourbaji et al., 2012), after an acute systemic injection of LPS in comparison with wild-type mice. This experimental setting might actually provide important information regarding the sex-dependent pathological consequences of a dysregulated immune/inflammatory response, pointing out the role of BDNF. In line with our approach, it has been reported that some biological functions of the neurotrophin are different in male and female. For instance, the administration of BDNF may alleviate the pain induced by acetic acid in male rats but has no effect in females (Li et al., 2010). Moreover, different basal protein levels of the neurotrophin have been detected in humans (Hayley et al., 2015) and in rodents (Szapacs et al., 2004; Franklin and Perrot-Sinal, 2006) as well as a different activation of the BDNF signaling (Hill and van den Buuse, 2011).

Based on these considerations, we hypothesized that the altered interaction between the inflammatory system and BDNF may represent a potential candidate contributing to the sex-dependent differences in the inflammatory response that, in turn, might be associated with several psychiatric disorders such as MDD.

MATERIALS AND METHODS

Animals

Wild-type and *BDNF*$^{+/-}$ male and female littermate mice on a C57BL/6N background were bred as described earlier (Chourbaji et al., 2004). All the animals were housed individually at the age of 13–19 weeks in standard macrolon cages (type II—26 cm × 20 cm × 14 cm) with bedding and nesting material (paper tissue). They were acclimatized at least for 2 weeks to a reserved 12-h dark–light cycle (lights off 8 am to 8 pm) at 22 ± 1°C room temperature and the humidity was 35% as described earlier (Chourbaji et al., 2005). Animals received a standard pellet diet and water *ad libitum*. Lastly, to reduce the number of experimental biases, all the experiments were performed using blind numbers. All animal experiments were approved by the Animal Welfare Office of the Regierungspräsidium Karlsruhe, Germany.

LPS Treatment and Behavioral Evaluation

After the acclimatization phase, wild-type and heterozygous mice were randomly divided to receive saline or LPS (LPS from *Escherichia coli*; serotype 026:B6; Sigma Aldrich). The bacterial toxin was dissolved in sterile, endotoxin-free isotonic saline and injected i.p. from 1 mg/ml stock solution. We decided to use a dosage of 400 μg/kg as a low dose of LPS able to induce only

TABLE 1 | Sequences of forward and reverse primers and probes used in qRT-PCR analyses.

Gene	Forward primer	Reverse primer	Probe
*Cd11b**	CATCCCATGACCTTCCAAGAG	GTGCTGTAGTCACACTGGTAG	CCACACTCTGTCCAAAGCCTTTTGC
*Cx3cl1**	TCTTCCATTTGTGTACTCTGCT	GGACTCCTGGTTTAGCTGATAG	TGTCGCACATGATTTCGCATTTCGTC
*Cx3cr1**	GTTATTTGGGCGACATTGTGG	ATGTCAGTGATGCTCTTGGG	TCTGGTGGGAAATCTGGTTGGTGGTC
*β-Actin**	ACCTTCTACAATGAGCTGCG	CTGGATGGCTACGTACATGG	TCTGGGTCATCTTTTCACGGTTGGC
*Il-1β***		Mm00434228_m1	
*Il-6***		Mm00446190_m1	
*Tnf-α***		Mm00443258_m1	

Purchased from Eurofins MWG Operon (Germany) and Applied Biosystem (Italy)**.*

TABLE 2 | Baseline body weight of the animals used in this study.

	Wild type	*BDNF*$^{+/-}$
Males	28.48 ± 3.26	30.02 ± 3.73
Females	23.34 ± 1.95	25.90 ± 3.45

The body weight was assessed before the beginning of the study. The data are presented as average weight ± standard deviation of 12 animals/group.

subtle changes in body weight and locomotor activity few hours from the administration, which disappeared within 24 h (Couch et al., 2016). In a pilot study, we compared this dosage with 830 μg/kg, which is similar to the amount used in several studies, finding that the two doses had the same impact on the body weight and locomotion (data not shown). The lowest dose of LPS was chosen as it is less aversive to the subjects and in order to avoid a massive activation of the inflammatory response that could have masked the molecular impact of the genotype and/or the sex of the animals. With this experimental design, we obtained eight groups of animals: wild-type mice treated with saline (male, $n = 5$; female, $n = 6$) or LPS (male, $n = 6$; female, $n = 6$); *BDNF*$^{+/-}$ mice that received saline (male, $n = 6$; female, $n = 6$) or the bacterial toxin (male, $n = 6$; female, $n = 6$).

We assessed body weight before the beginning of the experiment (baseline), 1 h before LPS administration, and 6 and 24 h after the immune challenge. Moreover, 6 h after the injection, animals were tested with the Open Field (OF) test to evaluate alterations in the locomotor activity as previously reported (Zueger et al., 2005; Richter et al., 2011). Briefly, after a period of acclimatization to the room (30 min), mice were individually placed in a square-shaped, white, illuminated (25 lx) arena, measuring 50 × 50 cm^2. The test, conducted in the active phase of the animals, was monitored from above for 10 min and recorded by a video camera (Sony CCD IRIS). For each subject, total distance moved and velocity were analyzed by a blinded experimenter using the image processing

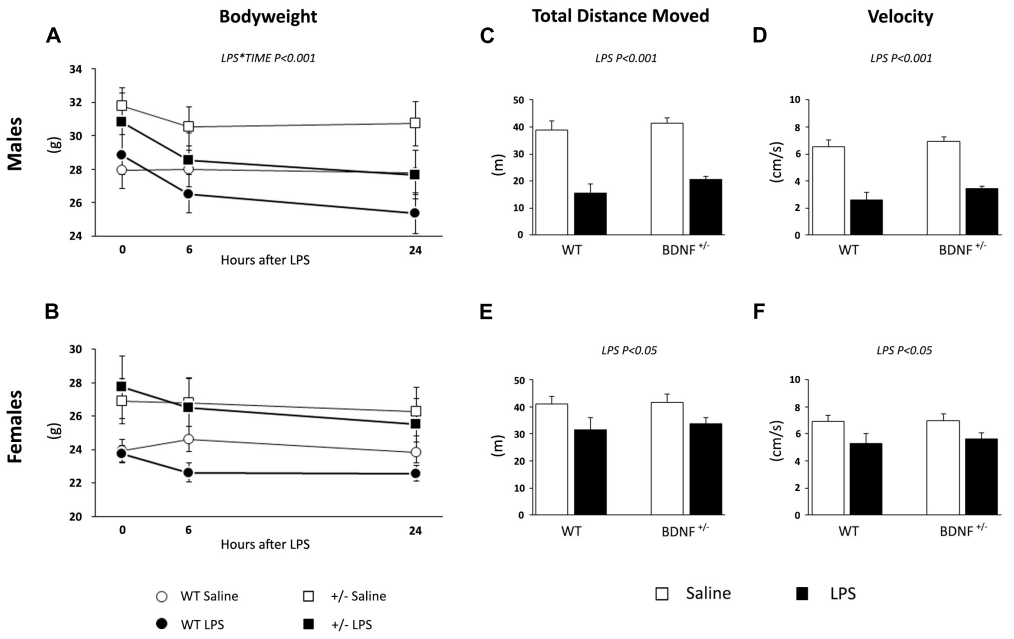

FIGURE 1 | Evaluation of LPS-induced sickness behavior through body weight and locomotor activity. The body weight of both male **(A)** and female **(B)** animals was measured before LPS injection, 6 and 24 h after the immune challenge. After 6 h from the injection, we tested saline and LPS-treated animals performance with the OF test to assess the total distance traveled (males, **C**; females, **E**) and the velocity (males, **D**; females, **F**) as parameters of locomotion.

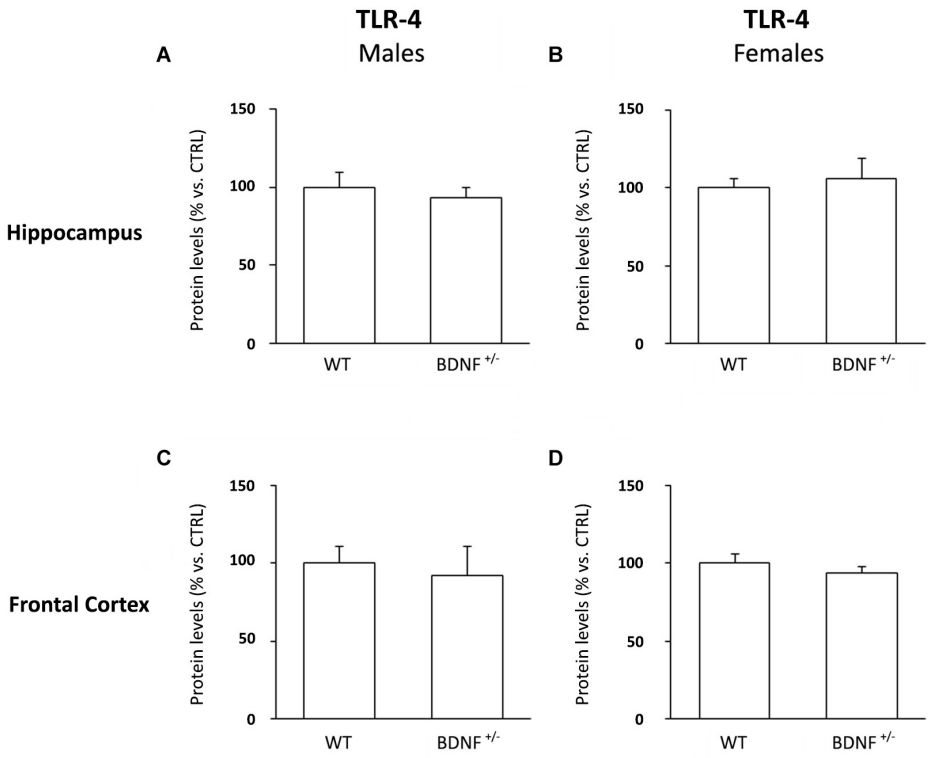

FIGURE 2 | Western Blot Analysis of TLR-4 Basal Levels in the Hippocampus and in the Frontal Cortex. The protein levels of the toll like-4 receptor (TLR-4) were measured in the hippocampus and in the frontal cortex of male **(A,C)** and female **(B,D)** wild-type (WT) and BDNF heterozygous (BDNF$^{+/-}$) mice treated with saline. The data, expressed as a percentage of the saline-injected wild-type mice (CTRL, set at 100%), represent the mean ± SEM of at least five independent determinations.

system Etho Vision 3.0 (Noldus Information Technology). Animals were sacrificed 24 h after LPS injection, the brains were harvested, and the hippocampus and frontal cortex were dissected on ice from both the hemispheres. The tissues were rapidly frozen on dry ice and stored at −80°C until the molecular analyses.

RNA Preparation and Gene Expression Analyses

For gene expression analyses, total RNA was isolated from the different brain regions by single-step guanidinium isothiocyanate/phenol extraction using PureZol RNA isolation reagent (Bio-Rad Laboratories S.r.l.) according to the manufacturer's instructions and quantified by spectrophotometric analysis. The samples were then processed for real-time polymerase chain reaction (PCR) as previously reported (Rossetti et al., 2016) to assess mRNA levels of target genes.

Briefly, an aliquot of each sample was treated with DNase to avoid DNA contamination and subsequently analyzed by TaqMan qRT-PCR instrument (CFX384 real-time system, Bio-Rad Laboratories S.r.l.) using the iScript one-step RT-PCR kit for probes (Bio-Rad Laboratories S.r.l). Samples were run in 384-well format in triplicate as multiplexed reactions with a normalizing internal control (β-*Actin*). Thermal cycling was initiated with incubation at 50°C for 10 min (RNA retrotranscription), and then at 95°C for 5 min (TaqMan polymerase activation). After this initial step, 39 cycles of PCR were performed. Each PCR cycle consisted of heating the samples at 95°C for 10 s to enable the melting process and then for 30 s at 60°C for the annealing and extension reactions. A comparative cycle threshold (Ct) method was used to calculate the relative target gene expression. Probe and primer sequences used were purchased from Applied Biosystem Italia and Eurofins MWG-Operon. A complete list of primers and probes is presented in **Table 1**.

Protein Extraction and Western Blot Analysis

Protein extracts were obtained as previously described (Rossetti et al., 2018a,b). Briefly, brain samples were manually homogenized using a glass–glass potter in a pH 7.4 cold isotonic buffer and then sonicated for 10 s at a maximum power of 10–15% (Bandelin Sonoplus). The homogenate was clarified by centrifugation to obtain a pellet (P1) enriched in nuclear components, which was resuspended in a hypotonic buffer. The supernatant (S1) was then centrifuged (13,000 × *g*; 15 min) to obtain a clarified fraction of cytosolic proteins (S2). The

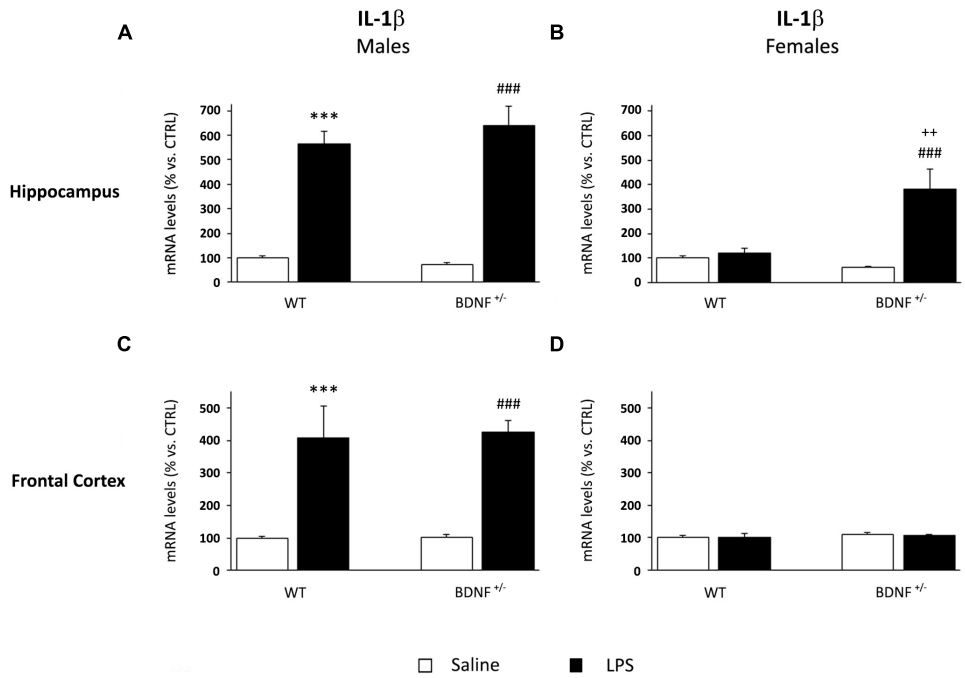

FIGURE 3 | Gene expression analysis of IL-1β in the hippocampus and in the frontal cortex. The mRNA levels of the pro-inflammatory cytokine IL-1β were measured in the hippocampus and in the frontal cortex of male **(A,C)** and female **(B,D)** wild-type (WT) and BDNF heterozygous (BDNF$^{+/-}$) mice 24 h after a single injection of lipopolysaccharide (LPS, 400 μg/kg i.p). in comparison with mice treated with saline. The data, expressed as a percentage of the saline-injected wild-type mice (CTRL, set at 100%), represent the mean ± SEM of at least six independent determinations. $^{***}P < 0.001$ vs. CTRL; $^{###}P < 0.001$ vs. BDNF$^{+/-}$; $^{++}P < 0.01$ vs. WT/LPS (Two-way ANOVA with PLSD).

pellet (P2), corresponding to the crude membrane fraction, was resuspended in the same buffer used for the nuclear fraction. Total protein content was measured according to the Bradford Protein Assay procedure (Bio-Rad Laboratories), using bovine serum albumin as calibration standard. For the protein analysis, 10 μg of P2 protein lysates were run under reducing conditions on polyacrylamide gels and then transferred onto nitrocellulose membranes. Unspecific binding sites were blocked with 10% non-fat dry milk and then the membranes were incubated overnight with the primary antibody (TLR-4 Santa Cruz cat. sc-10741; 1:1,000), followed by a 1-h incubation at room temperature with a peroxidase-conjugated anti-rabbit IgG. Immunocomplexes were visualized by chemiluminescence using the ETA C2.0 (Cyanagen). Protein levels were calculated by measuring the optical density of the immunocomplexes using chemiluminescence (Chemidoc MP Imaging System, Bio-Rad Laboratories) and results were standardized on β-Actin (Sigma cat. A5441; 1:10000) bands at 43 kDa as internal control.

Statistical Analyses

Behavioral data were analyzed using repeated measurement ANOVA (Time*LPS*Genotype): one-way ANOVA (Treatment) or two-way ANOVA (LPS*Genotype). When appropriate, Bonferroni *post hoc* tests were used to evaluate furtherdifferences between groups.

Molecular data were analyzed by two-way ANOVA, with treatment (Saline vs. LPS) or genotype (wild type vs. *BDNF*$^{+/-}$) as independent factors. When appropriate, direct contrasts were analyzed with Fisher's protected least significant difference (PLSD). All the molecular analyses were carried out in individual animals (independent determinations), and for graphic clarity, data are presented as mean percent ± standard error (SEM) of control group, with significance threshold set at $P < 0.05$.

RESULTS

LPS Administration Alters the Body Weight and the Locomotion of Both Male and Female Animals

First, we have assessed the ability of LPS to induce the so-called sickness behavior by measuring the body weight of the animals and monitoring their locomotor activity in the OF test 6 h after the inflammatory challenge. Although it is known from the literature that at this time point LPS may cause behavioral consequences, our aim was to evaluate the influence of sex or genotype.

At baseline, wild-type and heterozygous mice showed differences in body weight that were statistically significant only in female animals as a result of the BDNF partial deletion (Genotype: $F_{1,20} = 6.940$, $P < 0.05$; **Table 2** and **Figures 1A,B**). After LPS administration, we observed a decrease of body weight over time in male (LPS*Time, $F_{1,19} = 17.046$, $P < 0.001$;

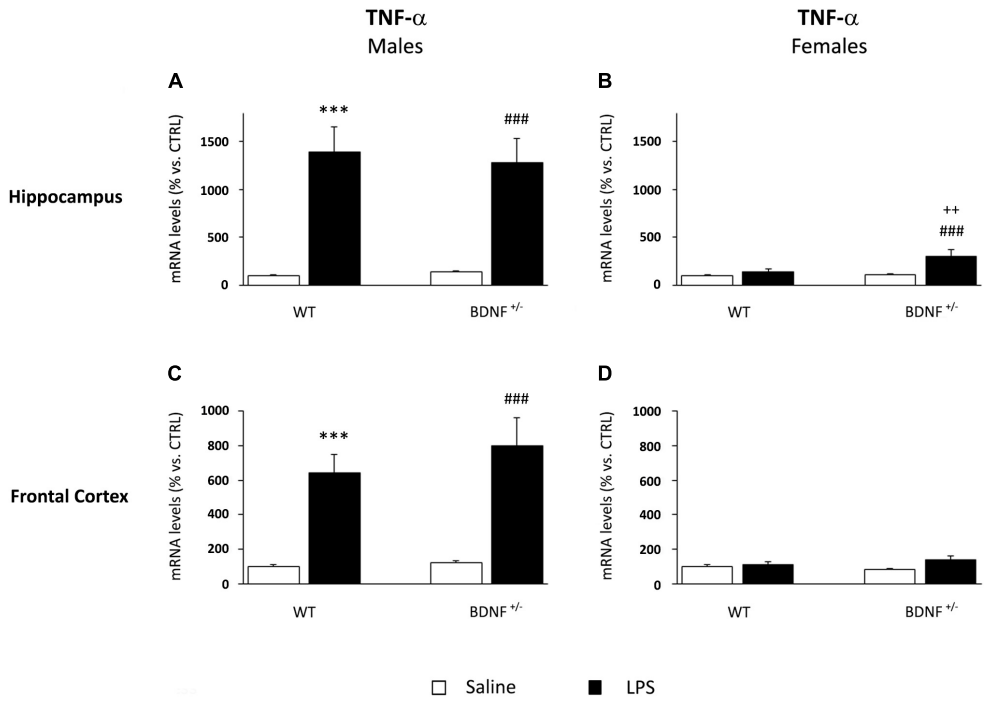

FIGURE 4 | Gene expression analysis of TNF-α in the hippocampus and in the frontal cortex. The mRNA levels of the pro-inflammatory cytokine TNF-α were measured in the hippocampus and in the frontal cortex of male **(A,C)** and female **(B,D)** wild-type (WT) and BDNF heterozygous (BDNF$^{+/-}$) mice 24 h after a single injection of lipopolysaccharide (LPS, 400 μg/kg i.p). in comparison with mice treated with saline. The data, expressed as a percentage of the saline-injected wild-type mice (CTRL, set at 100%), represent the mean ± SEM of at least six independent determinations. $^{***}P < 0.001$ vs. CTRL; $^{###}P < 0.01$ vs. BDNF$^{+/-}$; $^{++}P < 0.01$ vs. WT/LPS (Two-way ANOVA with PLSD).

Figure 1A), while in female mice, the impact of the immune challenge was blunted by the basal genotype effect (**Figure 1B**).

In the OF test, we analyzed the total distance moved and the velocity of the animals 6 h after the exposure to the bacterial toxin. As shown in **Figure 1C**, the total distance moved by male mice treated with LPS was reduced when compared to the locomotion of saline-treated mice (LPS, $F_{1,23} = 74.485$, $P < 0.001$; **Figure 1C**) irrespective of the genotype. A similar, but milder effect was observed for female animals; indeed, LPS treatment significantly affected the distance traveled ($F_{1,20} = 7.566$, $P < 0.05$; **Figure 1E**) in both wild-type and heterozygous mice.

LPS also modulated the velocity of the animals during the locomotion test, which was reduced in both male ($F_{1,19} = 73.859$, $P < 0.001$; **Figure 1D**) and female mice ($F_{1,20} = 7{,}582$, $P < 0.05$; **Figure 1F**) without any effect of the genotype. Similar to what was previously observed, the magnitude of the LPS-induced changes was higher in male animals.

Wild-Type and Heterozygous Mice Have the Same Basal Levels of TLR-4, Without Gender Differences

To exclude the idea that LPS could have acted on a different receptor background, we examined the protein levels of toll-like receptor 4 (TLR-4), the endogenous receptor for the bacterial toxin.

As shown in **Figure 2**, we did not find any difference among the experimental groups.

The Immune Challenge Differentially Affects the Cytokine Expression Profile in the Hippocampus and Frontal Cortex of Male and Female Heterozygous Mice

Next, we investigated if sex or genotype may also influence also the molecular impact of the inflammatory challenge. With this aim, we analyzed the gene expression of the pro-inflammatory cytokines IL-1β, TNF-α, and IL-6 in the hippocampus and in the frontal cortex of wild-type and mutant mice of both sexes. The molecular analyses were performed 24 h after the immune challenge to avoid the peak of cytokine expression usually observed in the first hours from LPS injection, which could confound the influence of the other two variables.

IL-1β gene expression was significantly modulated by LPS administration in the hippocampus of both wild-type and heterozygous male mice ($F_{1,19} = 179.8$, $P < 0.001$). Specifically, the challenge markedly increased the pro-inflammatory cytokine without differences between the two genotypes (WT/LPS +465% vs. WT/SAL, $P < 0.001$; *BDNF*$^{+/-}$/LPS +571% vs. *BDNF*$^{+/-}$/SAL, $P < 0.001$; **Figure 3A**). Conversely, a different profile was observed in the hippocampus of female mice where the significant effect of the LPS injection ($F_{1,18} = 14.17$, $P < 0.01$) was restricted to the mutant animals, as indicated

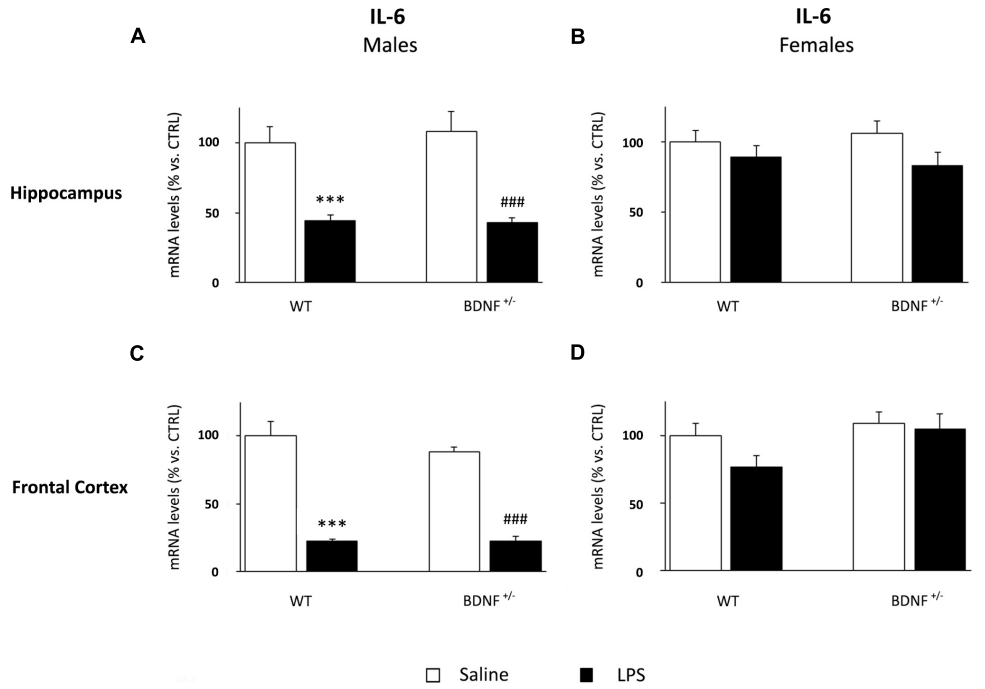

FIGURE 5 | Gene expression analysis of IL-6 in the hippocampus and in the frontal cortex. The mRNA levels of the pro-inflammatory cytokine IL-6 were measured in the hippocampus and in the frontal cortex of male **(A,C)** and female **(B,D)** wild-type (WT) and BDNF heterozygous (BDNF$^{+/-}$) mice 24 h after a single injection of lipopolysaccharide (LPS, 400 μg/kg i.p). in comparison with mice treated with saline. The data, expressed as a percentage of the saline-injected wild-type mice (CTRL, set at 100%), represent the mean ± SEM of at least six independent determinations. $^{***}P < 0.001$ vs. CTRL; $^{###}P < 0.001$ vs. BDNF$^{+/-}$ (Two-way ANOVA with PLSD).

by the significant treatment*genotype interaction ($F_{1,18} = 10.85$, $P < 0.01$). Indeed, as shown in **Figure 3**, IL-1β mRNA levels were significantly induced by LPS only in the heterozygous mice (*BDNF*$^{+/-}$/LPS +324% vs. *BDNF*$^{+/-}$/SAL, $P < 0.001$; +262% vs. WT/LPS, $P < 0.01$; **Figure 3B**) with no changes in wild-type animals. Moreover, it has to be noted that the magnitude of the cytokine induction in female mice was lower with respect to male animals, although its basal expression was similar.

In the frontal cortex of male mice, IL-1β expression was similar to that observed in the hippocampus. LPS administration, indeed, significantly increased the mRNA of the pro-inflammatory cytokine ($F_{1,22} = 45.49$, $P < 0.001$) in both wild-type (WT/LPS +309% vs. WT/SAL, $P < 0.001$) and heterozygous male mice (*BDNF*$^{+/-}$/LPS +324% vs. *BDNF*$^{+/-}$/SAL, $P < 0.001$; **Figure 3C**) without differences between the two experimental groups. Conversely, no changes in IL-1β levels were found in the frontal cortex of female mice exposed to LPS (**Figure 3D**).

Similarly to what was observed for IL-1β, the mRNA levels of TNF-α were significantly up-regulated by the LPS treatment in male mice ($F_{1,20} = 42.58$, $P < 0.001$), an effect independent of the genotype. In fact, the inflammatory challenge strongly induced the expression of TNF-α in the hippocampus in both wild-type (WT/LPS +1287% vs. WT/SAL, $P < 0.001$; **Figure 4A**) and mutant mice (*BDNF*$^{+/-}$/LPS +1142% vs. *BDNF*$^{+/-}$/SAL, $P < 0.001$; **Figure 4A**) without any significant difference between the genotypes. On the contrary, in female mice, the increased TNF-α gene expression by LPS was limited to the mutant animals, as indicated by the significant effects of LPS ($F_{1,18} = 6.74$, $P < 0.05$), genotype ($F_{1,18} = 10.7$, $P < 0.01$), and interaction between LPS*Genotype ($F_{1,18} = 4.95$, $P < 0.05$). Again, this increase was less pronounced with respect to the modulations observed in male mice (*BDNF*$^{+/-}$/LPS +186% vs. *BDNF*$^{+/-}$/SAL, $P < 0.01$; +164% vs. WT/LPS $^{**}P < 0.01$; **Figure 4B**).

In the frontal cortex, the gene expression profile of TNF-α was qualitatively comparable to that observed in the hippocampus, although the effect of the inflammatory challenge was lower. As shown in **Figure 4C**, we found a significant increase of TNF-α mRNA levels after LPS injection ($F_{1,22} = 42.43$, $P < 0.001$) in both wild-type (WT/LPS +544% vs. WT/SAL, $P < 0.001$) and mutant male mice (*BDNF*$^{+/-}$/LPS +678% vs. *BDNF*$^{+/-}$/SAL, $P < 0.001$). Interestingly, a slight but significant modulation of TNF-α by LPS ($F_{1,21} = 4.45$, $P = 0.05$) was also observed in heterozygous female mice (*BDNF*$^{+/-}$/LPS +55% vs. *BDNF*$^{+/-}$/SAL, $P < 0.01$; **Figure 4D**).

The expression of IL-6 was differentially modulated by LPS administration if compared to the other cytokines. Indeed, the inflammatory challenge significantly decreased IL-6 mRNA levels ($F_{1,19} = 42.84$, $P < 0.001$) in both wild-type (WT/LPS -56% vs. WT/SAL, $P < 0.001$) and heterozygous mice (*BDNF*$^{+/-}$/LPS -65% vs. *BDNF*$^{+/-}$/SAL, $P < 0.001$; **Figure 5A**). On the contrary, we did not observe any significant change in female mice (**Figure 5B**).

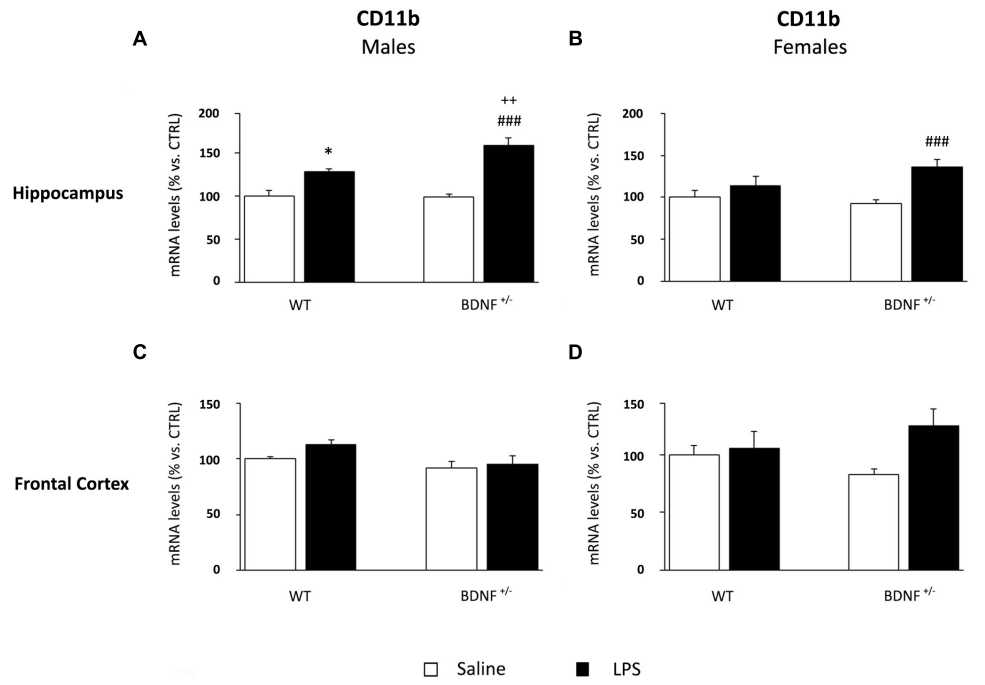

FIGURE 6 | Gene expression analysis of CD11b in the hippocampus and in the frontal cortex. The mRNA levels of the microglial marker CD11b were measured in the hippocampus and in the frontal cortex of male **(A,C)** and female **(B,D)** wild-type (WT) and BDNF heterozygous (BDNF$^{+/-}$) mice 24 h after a single injection of lipopolysaccharide (LPS, 400 μg/kg i.p). in comparison with mice treated with saline. The data, expressed as a percentage of the saline-injected wild-type mice (CTRL, set at 100%), represent the mean ± SEM of at least six independent determinations. $^{*}P < 0.05$ vs. CTRL; $^{###}P < 0.001$ vs. BDNF+/−/LPS; $^{++}P < 0.01$ vs. WT/LPS (two-way ANOVA with PLSD).

In line with the observed expression profile in the hippocampus, the expression of IL-6 was significantly down-regulated by LPS also in the frontal cortex of male mice ($F_{1,19} = 123.9$, $P < 0.001$). The impact of the immune challenge altered the expression of the cytokine in wild-type (WT/LPS -77% vs. WT/SAL, $P < 0.001$) as well as mutant animals (*BDNF*$^{+/-}$/LPS -66% vs. *BDNF*$^{+/-}$/SAL, $P < 0.001$; **Figure 5C**), an effect even greater in this brain region, when compared to the hippocampus. IL-6 expression was not affected in the frontal cortex of female mice (**Figure 5D**).

LPS Administration Differentially Modulates Microglial Markers in Male and Female Brain, With a Specific Influence of the Genotype

Considering the pivotal role of microglia in the immune response within the central nervous system, we analyzed the expression of a marker of microglia activation, namely, CD11b, and two molecules involved in the control of microglia response, such as fractalkine (CX3CL1) and its receptor (CX3CR1).

The analyses on the hippocampus of male mice indicated that the expression of CD11b was significantly modulated by the inflammatory challenge ($F_{1,23} = 48.93$, $P < 0.001$) and by the genotype ($F_{1,23} = 5.05$, $P < 0.05$). As shown in **Figure 6A**, CD11b expression was increased in both wild-type (WT/LPS +27% vs. WT/SAL, $P < 0.01$) and *BDNF* heterozygous mice (*BDNF*$^{+/-}$/LPS +60% vs. *BDNF*$^{+/-}$/SAL, $P < 0.001$). Interestingly, this effect was significantly higher in the mutant animals (*BDNF*$^{+/-}$/LPS +31% vs. WT/LPS, $P < 0.01$) as indicated by the LPS*Genotype interaction ($F_{1,23} = 6.85$, $P < 0.05$). In the hippocampus of female mice, the expression of the microglial marker was significantly affected by the immune challenge ($F_{1,23} = 13.06$, $P < 0.01$) only in mutant animals (*BDNF*$^{+/-}$/LPS +44% vs. *BDNF*$^{+/-}$/SAL, $P < 0.001$; **Figure 6B**). Conversely, in the frontal cortex, we did not observe any significant modulation of the expression of CD11b by LPS or by the genotype, neither in male nor in female mice (**Figures 6C,D**).

The gene expression analyses of fractalkine in the hippocampus of male mice indicated a significant impact of the genotype ($F_{1,22} = 8.72$, $P < 0.01$). Indeed, the basal levels of CX3CL1 were significantly higher only in BDNF heterozygous mice if compared to control mice (*BDNF*$^{+/-}$/SAL +36% vs. WT/SAL, $P < 0.01$; **Figure 7A**). Conversely, the mRNA levels of CX3CL1 in female mice were modulated by LPS administration ($F_{1,23} = 5.07$, $P < 0.05$) only in wild-type animals (WT/LPS -16% vs. WT/SAL, $P < 0.05$; **Figure 7B**). No significant changes were found in the prefrontal cortex (**Figures 7C,D**).

Despite the slight modulation of fractalkine observed in the hippocampus of male mice, the inflammatory challenge had significant effect on CX3CR1 ($F_{1,22} = 34.17$,

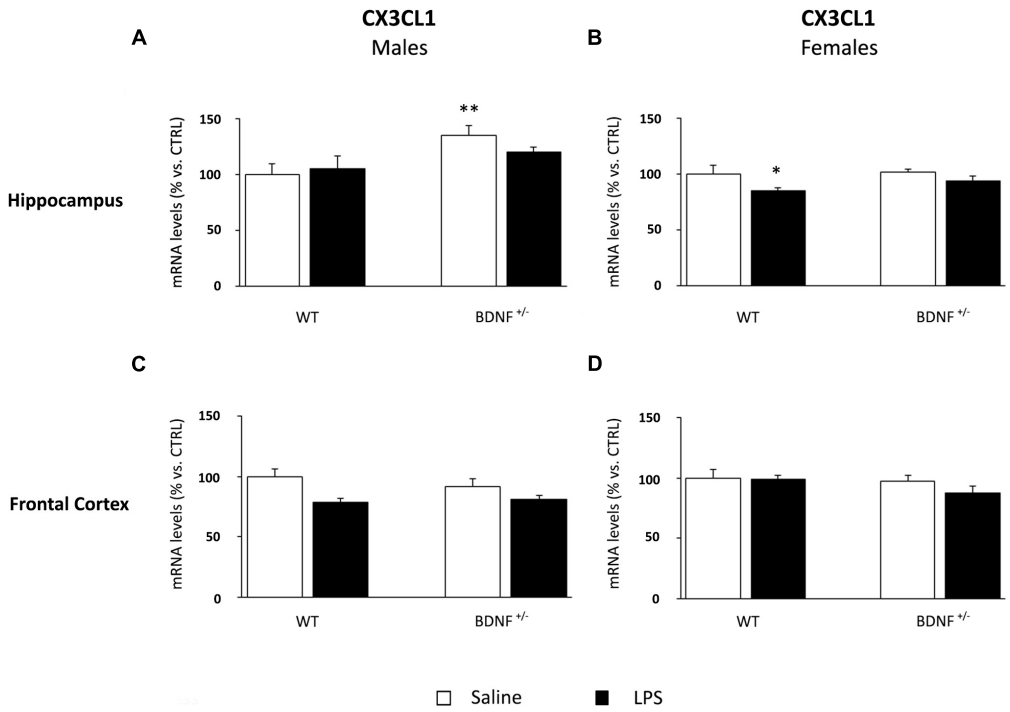

FIGURE 7 | Gene expression analysis of CX3CL1 in the hippocampus and in the frontal cortex. The mRNA levels of CX3CL1 were measured in the hippocampus and in the frontal cortex of male **(A,C)** and female **(B,D)** wild-type (WT) and BDNF heterozygous (BDNF$^{+/-}$) mice 24 h after a single injection of lipopolysaccharide (LPS, 400 μg/kg i.p). in comparison with mice treated with saline. The data, expressed as a percentage of the saline-injected wild-type mice (CTRL, set at 100%), represent the mean ± SEM of at least six independent determinations. *$P < 0.05$ and **$P < 0.01$ vs. CTRL (two-way ANOVA with PLSD).

$P < 0.001$). Specifically, the mRNA levels of the receptor were significantly increased by LPS in both wild-type (WT/LPS +50% vs. WT/SAL, $P < 0.001$; **Figure 8A**) and BDNF heterozygous mice (*BDNF*$^{+/-}$/LPS +45% vs. *BDNF*$^{+/-}$/SAL, $P < 0.001$; **Figure 8A**). In female mice, the hippocampal CX3CR1 expression was up-regulated following the treatment ($F_{1,24} = 5.54$, $P < 0.05$), but only in heterozygous mice (*BDNF*$^{+/-}$/LPS +22% vs. *BDNF*$^{+/-}$/SAL, $P < 0.05$; **Figure 8B**).

Although we observed a similar modulation also in the frontal cortex of male (**Figure 8C**) and female mice (**Figure 8D**), neither the impact of the immune challenge nor the *BDNF* mutation significantly affected the expression of fractalkine receptor.

DISCUSSION

In this study, we show that the partial deletion of BDNF influences the inflammatory response to LPS in a sex-specific manner. Specifically, we found that the molecular impact of the inflammatory challenge was different in the two sexes: high in male mice independently from the genotype, almost null in wild-type female mice, and mild in the BDNF heterozygous female mice. This effect was mainly observed in the hippocampus, suggesting a pivotal role for the neurotrophin in the inflammatory response of this area of the female brain.

The systemic injection of LPS in the rodent mimics a gram-negative bacterial infection that induces a massive inflammatory response with a release of pro-inflammatory cytokines and the insurgence of the so-called "sickness behavior," characterized by decreased motor activity, social withdrawal, reduced food and water intake, and altered cognition within a few hours from the LPS administration (Dantzer et al., 2008). Likewise, we found reduced body weight and decreased locomotor activity 6 h after the LPS administration, an effect independent from genotype but influenced by sex. It is important to mention that animals of both sexes were single caged. While single housing could have been more favorable for male mice due to less social distress and aggressive behaviors (Chourbaji et al., 2005; Kamakura et al., 2016; Kappel et al., 2017), individual housing could have affected the behavior of female mice. Nevertheless, the baseline levels of the parameters analyzed in the OF were comparably similar between sexes, suggesting that the housing condition apparently did not alter the behavioral outcomes analyzed in our study. Male mice showed a stronger induction of sickness behavior if compared to the female counterpart, as indicated by a greater weight loss and a worse OF performance, in line with previous published data (Cai et al., 2016). Similarly, the neuroinflammatory response was stronger in males than in females when assessed at molecular levels. Thus, the mRNA levels of IL-1β and TNF-α were increased in the hippocampus and frontal cortex of male mice but not in

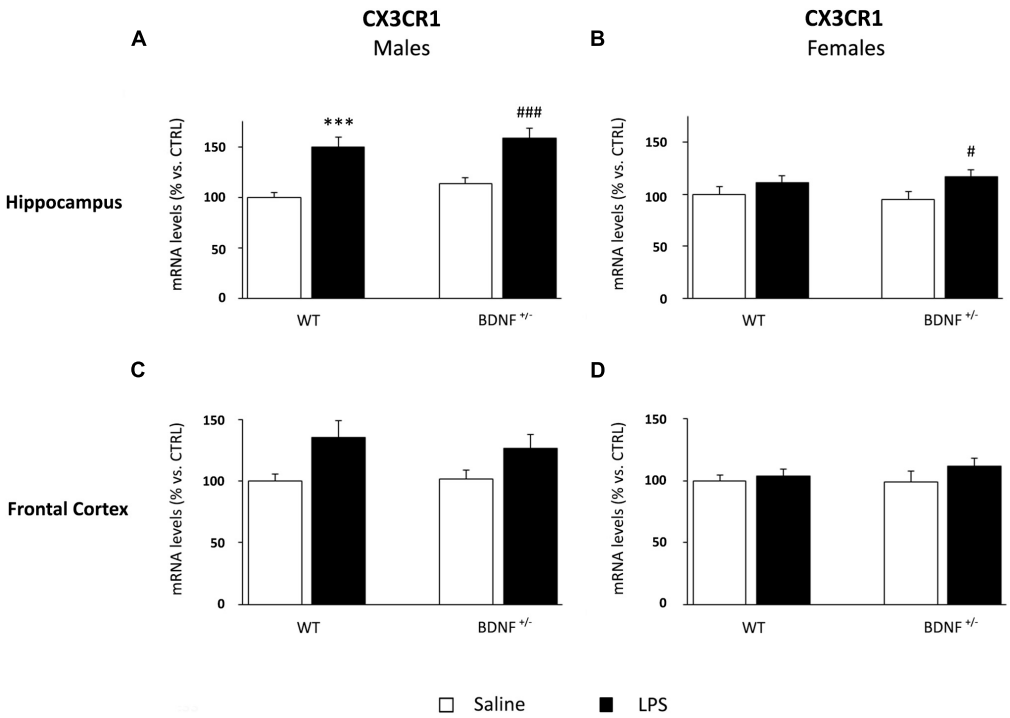

FIGURE 8 | Gene expression analysis of CX3CR1 in the hippocampus and in the frontal cortex. The mRNA levels of CX3CR1 were measured in the hippocampus and in the frontal cortex of male **(A,C)** and female **(B,D)** wild-type (WT) and BDNF heterozygous (BDNF$^{+/-}$) mice 24 h after a single injection of lipopolysaccharide (LPS, 400 μg/kg i.p). in comparison with mice treated with saline. The data, expressed as a percentage of the saline-injected wild-type mice (CTRL, set at 100%), represent the mean ± SEM of at least six independent determinations. $^{***}P < 0.001$ vs. CTRL; $^{\#}P < 0.05$ and $^{\#\#\#}P < 0.001$ vs. BDNF$^{+/-}$ mice (two-way ANOVA with PLSD).

females. These changes were paralleled by a strong decrease of IL-6 transcripts in male mice 24 h after LPS, an effect that was already reported in other studies (Schneiders et al., 2015) and could probably be ascribed to the inhibitory activity of the suppressor of cytokine signaling 3 (SOCS3), a protein controlling the negative feedback regulation of IL-6 (Babon et al., 2014). Since it has been shown that TNF-α is able to induce SOCS3 protein levels, thus modulating IL-6 pathway (Dagvadorj et al., 2010), the cross-talk between these two cytokines might explain the decrease of IL-6 observed only in the brain of male mice where the levels of TNF-α were dramatically increased.

It has to be noted that, despite the observed sex-dependent differences in LPS response, the toxin is acting on the same receptor background, as no basal changes in the expression of TLR-4, the endogenous receptor for LPS, were observed in any experimental group.

The differences in the inflammatory response among the sexes are actually well known (Klein and Flanagan, 2016); however, beside a role for genetic and/or hormonal mediators, a lack of information exists regarding the underlying mechanisms.

Among the molecular systems that might contribute to such differential response, our data suggest a role for the neurotrophin BDNF. Indeed, the *BDNF*$^{+/-}$ female mice showed a significant LPS-dependent increase of the abovementioned cytokines, mainly in the hippocampus, an effect that—to our knowledge—has never been reported. To further analyze the different expression profile between male and female heterozygous mice, we focused our attention on microglia, the immune resident cell population of the brain. In addition to their role as first-line immune defense within the CNS, these cells are involved in several mechanisms of neuronal homeostasis such as neural plasticity, synaptic remodeling and architecture, neurogenesis, and apoptosis (Paolicelli et al., 2011; Tay et al., 2018). As a consequence, their abnormal activation may impact key processes contributing to the pathophysiology of several diseases. In our study, the mRNA levels of CD11b, a marker of microglia activation, were increased after LPS in the hippocampus of male mice of both genotypes, with an expression profile comparable to that observed for the inflammatory cytokines IL-1β and TNF-α. Interestingly, only heterozygous female mice showed increased hippocampal levels of CD11b, a result that enlightens the enhanced susceptibility of mutant females. To confirm this modulation, we also analyzed the expression of fractalkine (CX3CL1) and its receptor (CX3CR1). CX3CL1 is mainly produced by neurons to bind its receptor on microglia surface, in order to control its activation state (Biber et al., 2007; Paolicelli et al., 2014). Interestingly, while fractalkine did not show clear modulations, CX3CR1 followed the expression profile of CD11b, in light of the specific expression of fractalkine receptor

in this cellular population (Wolf et al., 2013). Accordingly, a different activation of microglia may contribute to the sex-dependent effect of LPS. Microglia cells show sex differences from the developmental stages in the rodent fetal brain: while males have more microglia in the developing brain, females boost the number of activated microglia during adulthood (Lenz and McCarthy, 2015). Moreover, adult microglia present several differences between males and females in terms of morphology, function, and transcriptional signature (Bilbo, 2017; Hanamsagar et al., 2017; Guneykaya et al., 2018). Our findings provide new information showing that BDNF may differently influence the microglia response in males and females, supporting the capability of the neurotrophin to act also at the immune level. In this sense, Lai et al. (2018) recently demonstrated that BDNF participates in the modulation of inflammatory homeostasis, with an anti-inflammatory activity on microglia through the erythropoietin (EPO) and sonic hedgehog (Shh) signaling pathways. Moreover, BDNF is also able to modulate the internal Ca^{2+} influx in microglia cells, thus controlling the release of pro-inflammatory molecules from activated microglia. These functions would suggest that BDNF might have—in the female—an anti-inflammatory impact through the control of microglial activation (Mizoguchi et al., 2009). Accordingly, the molecular susceptibility of heterozygous females to the LPS administration might be a potential consequence of differences in BDNF activity among the sexes. Interestingly, it has been shown that basal BDNF protein levels are doubled in females compared to males (Chourbaji et al., 2012), a finding that could be associated to the "masculinized" inflammatory response of female mutant mice lacking the neurotrophin. This observation supports the idea of a sex-dependent mechanism of action of the neurotrophin (Chan and Ye, 2017). In this sense, sex hormones might play a pivotal role in the control of BDNF expression. First, given that the BDNF gene contains an estrogen responsive element, the higher levels of circulating estrogens in females may control its expression with a transcriptional mechanism (Sohrabji et al., 1995). A caveat of our study is that we did not examine the estrous cycle of the female mice when LPS was administered. Further studies will be necessary to investigate the interaction between estrogens and BDNF in an inflammatory context, specifically taking into consideration the reported protective anti-inflammatory activity of these hormones (Vegeto et al., 2008; Villa et al., 2015). On the other hand, testosterone—whose levels are higher in males—can be converted into estrogen in specific brain regions by the enzyme aromatase, thus modulating BDNF expression with an estrogen-mediated mechanism also in males (Wei et al., 2017). Therefore, considering the sexual dimorphism of estrogen receptor and aromatase (Wu et al., 2009), BDNF transcription might be controlled with a sex-specific mechanism. Interestingly, not only the expression *per se*, but also the activation of the BDNF signaling differs from males to females. Specifically, Hill and co-workers demonstrated that male *BDNF*$^{+/-}$ mice have increased activation of the cognate receptor of the neurotrophin, tropomyosin receptor kinase B (TrkB), when compared to female mutant mice. Despite the fact that the mechanism responsible for this increase has not been clarified, the authors suggest a potential contribution of steroid hormones (Hill and van den Buuse, 2011). This observation could, at least in part, explain the increased susceptibility in female mice in our study, since a basal increased TrkB activity in male mice could compensate for the lack of BDNF due to the mutation.

Based on the involvement of the immune/inflammatory system in the different vulnerability of the male and female brain to develop neurological and psychiatric disorders (Zagni et al., 2016), our results reveal a sex-dependent activity of BDNF on neuroinflammation suggestive of a potential new role for the neurotrophin in the sexual dimorphism of the central nervous system. Although the underlying molecular mechanism is still unknown, this finding might be of great interest for future studies aimed at developing therapeutic strategies for brain disorders with higher prevalence in women, in which BDNF plays a key role.

DATA AVAILABILITY

No datasets were generated or analyzed for this study.

AUTHOR CONTRIBUTIONS

AR, PG, MR, and RM designed the study and wrote the protocol. AM and AT performed the LPS treatments; the behavioral test and the sample preparation; and carried out the related statistical analyses. AR, MP, and AT performed the gene expression assessments and carried out the related statistical analyses. AR, RM, PG, and MR wrote or contributed to the writing of the manuscript. All authors contributed to and have approved the final version of the manuscript.

FUNDING

This work was in part supported by a grant from the Deutsche Forschungsgemeinschaft (Forschergruppe 2591, project GA427/12-1) to PG and a grant from the Italian Ministry of Instruction, University and Research (PRIN grant number 20152HKF3Z) to RM.

REFERENCES

Anisman, H. (2008). Cascading effects of stressors and inflammatory immune system activation: implications for major depressive disorder. *J. Psychiatry Neurosci.* 34, 4–20.

Babon, J. J., Varghese, L. N., and Nicola, N. A. (2014). Inhibition of IL-6 family cytokines by SOCS3. *Semin. Immunol.* 26, 13–19. doi: 10.1016/j.smim.2013.12.004

Berge, L. I., and Riise, T. (2015). Comorbidity between Type 2 Diabetes and depression in the adult population: directions of the association and its

possible pathophysiological mechanisms. *Int. J. Endocrinol.* 2015:164760. doi: 10.1155/2015/164760

Berton, O., and Nestler, E. J. (2006). New approaches to antidepressant drug discovery: beyond monoamines. *Nat. Rev. Neurosci.* 7, 137–151. doi: 10.1038/nrn1846

Biber, K., Neumann, H., Inoue, K., and Boddeke, H. W. (2007). Neuronal 'On' and 'Off' signals control microglia. *Trends Neurosci.* 30, 596–602. doi: 10.1177/1759091419843393

Bilbo, S. D. (2017). Sex differences in microglial appetites during development: inferences and implications. *Brain. Behav. Immun.* 64, 9–10. doi: 10.1016/j.bbi.2017.05.010

Brody, D. J., Pratt, L. A., and Hughes, J. P. (2018). Prevalence of depression among adults aged 20 and over: United States, 2013–2016. *NCHS Data Brief* 303, 1–8.

Bromet, E., Andrade, L. H., Hwang, I., Sampson, N. A., Alonso, J., de Girolamo, G., et al. (2011). Cross-national epidemiology of DSM-IV major depressive episode. *BMC Med.* 9:90. doi: 10.1186/1741-7015-9-90

Cai, K. C., van Mil, S., Murray, E., Mallet, J. F., Matar, C., and Ismail, N. (2016). Age and sex differences in immune response following LPS treatment in mice. *Brain Behav. Immun.* 58, 327–337. doi: 10.1016/j.bbi.2016.08.002

Calabrese, F., Rossetti, A. C., Racagni, G., Gass, P., Riva, M. A., and Molteni, R. (2014). Brain-derived neurotrophic factor: a bridge between inflammation and neuroplasticity. *Front. Cell. Neurosci.* 8:430. doi: 10.3389/fncel.2014.00430

Capuron, L., Ravaud, A., Miller, A. H., and Dantzer, R. (2004). Baseline mood and psychosocial characteristics of patients developing depressive symptoms during interleukin-2 and/or interferon-alpha cancer therapy. *Brain Behav. Immun.* 18, 205–213. doi: 10.1016/j.bbi.2003.11.004

Castrén, E., and Kojima, M. (2017). Brain-derived neurotrophic factor in mood disorders and antidepressant treatments. *Neurobiol. Dis.* 97(Pt B), 119–126. doi: 10.1016/j.nbd.2016.07.010

Chan, C. B., and Ye, K. (2017). Sex differences in brain-derived neurotrophic factor signaling and functions. *J. Neurosci. Res.* 95, 328–335. doi: 10.1002/jnr.23863

Chourbaji, S., Brandwein, C., and Gass, P. (2011). Altering BDNF expression by genetics and/or environment: impact for emotional and depression-like behaviour in laboratory mice. *Neurosci. Biobehav. Rev.* 35, 599–611. doi: 10.1016/j.neubiorev.2010.07.003

Chourbaji, S., Hellweg, R., Brandis, D., Zörner, B., Zacher, C., Lang, U. E., et al. (2004). Mice with reduced brain-derived neurotrophic factor expression show decreased choline acetyltransferase activity, but regular brain monoamine levels and unaltered emotional behavior. *Brain Res. Mol. Brain Res.* 121, 28–36. doi: 10.1016/j.molbrainres.2003.11.002

Chourbaji, S., Hörtnagl, H., Molteni, R., Riva, M. A., Gass, P., and Hellweg, R. (2012). The impact of environmental enrichment on sex-specific neurochemical circuitries—Effects on brain-derived neurotrophic factor and the serotonergic system. *Neuroscience* 220, 267–276. doi: 10.1016/j.neuroscience.2012.06.016

Chourbaji, S., Zacher, C., Sanchis-Segura, C., Spanagel, R., and Gass, P. (2005). Social and structural housing conditions influence the development of a depressive-like phenotype in the learned helplessness paradigm in male mice. *Behav. Brain Res.* 164, 100–106. doi: 10.1016/j.bbr.2005.06.003

Couch, Y., Anthony, D. C., Dolgov, O., Revischin, A., Festoff, B., Santos, A. I., et al. (2013). Microglial activation, increased TNF and SERT expression in the prefrontal cortex define stress-altered behaviour in mice susceptible to anhedonia. *Brain. Behav. Immun.* 29, 136–146. doi: 10.1016/j.bbi.2012.12.017

Couch, Y., Trofimov, A., Markova, N., Nikolenko, V., Steinbusch, H. W., Chekhonin, V., et al. (2016). Low-dose lipopolysaccharide (LPS) inhibits aggressive and augments depressive behaviours in a chronic mild stress model in mice. *J. Neuroinflammation* 13:108. doi: 10.1186/s12974-016-0572-0

Dagvadorj, J., Naiki, Y., Tumurkhuu, G., Noman, A. S., Iftakhar-E-Khuda, I., Komatsu, T., et al. (2010). Tumor necrosis factor-a augments lipopolysaccharide-induced suppressor of cytokine signalling 3 (SOCS-3) protein expression by preventing the degradation. *Immunology* 129, 97–104. doi: 10.1111/j.1365-2567.2009.03154.x

Dantzer, R., O'Connor, J. C., Freund, G. G., Johnson, R. W., and Kelley, K. W. (2008). From inflammation to sickness and depression: when the immune system subjugates the brain. *Nat. Rev. Neurosci.* 9, 46–56. doi: 10.1038/nrn2297

Derry, H. M., Padin, A. C., Kuo, J. L., Hughes, S., and Kiecolt-Glaser, J. K. (2015). Sex differences in depression: does inflammation play a role? *Curr. Psychiatry Rep.* 17:78. doi: 10.1007/s11920-015-0618-5

Dowlati, Y., Herrmann, N., Swardfager, W., Liu, H., Sham, L., Reim, E. K., et al. (2010). A meta-analysis of cytokines in major depression. *Biol. Psychiatry* 67, 446–457. doi: 10.1016/j.biopsych.2009.09.033

Ferrini, F., and De Koninck, Y. (2013). Microglia control neuronal network excitability via BDNF signalling. *Neural Plast.* 2013:429815. doi: 10.1155/2013/429815

Franklin, T. B., and Perrot-Sinal, T. S. (2006). Sex and ovarian steroids modulate brain-derived neurotrophic factor (BDNF) protein levels in rat hippocampus under stressful and non-stressful conditions. *Psychoneuroendocrinology* 31, 38–48. doi: 10.1016/j.psyneuen.2005.05.008

Guan, Z., and Fang, J. (2006). Peripheral immune activation by lipopolysaccharide decreases neurotrophins in the cortex and hippocampus in rats. *Brain Behav. Immun.* 20, 64–71. doi: 10.1016/j.bbi.2005.04.005

Guneykaya, D., Ivanov, A., Hernandez, D. P., Haage, V., Wojtas, B., Meyer, N., et al. (2018). Transcriptional and translational differences of microglia from male and female brains. *Cell Rep.* 24, 2773–2783.e6. doi: 10.1016/j.celrep.2018.08.001

Hanamsagar, R., Alter, M. D., Block, C. S., Sullivan, H., Bolton, J. L., and Bilbo, S. D. (2017). Generation of a microglial developmental index in mice and in humans reveals a sex difference in maturation and immune reactivity. *Glia* 65, 1504–1520. doi: 10.1002/glia.23176

Hayley, S., Du, L., Litteljohn, D., Palkovits, M., Faludi, G., Merali, Z., et al. (2015). Gender and brain regions specific differences in brain derived neurotrophic factor protein levels of depressed individuals who died through suicide. *Neurosci. Lett.* 600, 12–16. doi: 10.1016/j.neulet.2015.05.052

Hill, R. A., and van den Buuse, M. (2011). Sex-dependent and region-specific changes in TrkB signaling in BDNF heterozygous mice. *Brain Res.* 1384, 51–60. doi: 10.1016/j.brainres.2011.01.060

Howren, M. B., Lamkin, D. M., and Suls, J. (2009). Associations of depression with C-reactive protein, IL-1, and IL-6: a meta-analysis. *Psychosom. Med.* 71, 171–186. doi: 10.1097/PSY.0b013e3181907c1b

Kamakura, R., Kovalainen, M., Leppäluoto, J., Herzig, K. H., and Mäkelä, K. A. (2016). The effects of group and single housing and automated animal monitoring on urinary corticosterone levels in male C57BL/6 mice. *Physiol. Rep.* 4:e12703. doi: 10.14814/phy2.12703

Kappel, S., Hawkins, P., and Mendl, M. T. (2017). To group or not to group? Good practice for housing male laboratory mice. *Animals* 7:E88. doi: 10.3390/ani7120088

Kenis, G., Prickaerts, J., van Os, J., Koek, G. H., Robaeys, G., Steinbusch, H. W., et al. (2011). Depressive symptoms following interferon-α therapy: mediated by immune-induced reductions in brain-derived neurotrophic factor? *Int. J. Neuropsychopharmacol.* 14, 247–253. doi: 10.1017/S1461145710000830

Klein, S. L., and Flanagan, K. L. (2016). Sex differences in immune responses. *Nat. Rev. Immunol.* 16, 626–638. doi: 10.1038/nri.2016.90

Korte, M., Carroll, P., Wolf, E., Brem, G., Thoenen, H., and Bonhoeffer, T. (1995). Hippocampal long-term potentiation is impaired in mice lacking brain-derived neurotrophic factor. *Proc. Natl. Acad. Sci. U.S.A.* 92, 8856–8860. doi: 10.1073/pnas.92.19.8856

Kv, A., Madhana, R. M., Js, I. C., Lahkar, M., Sinha, S., and Naidu, V. G. M. (2018). Antidepressant activity of vorinostat is associated with amelioration of oxidative stress and inflammation in a corticosterone-induced chronic stress model in mice. *Behav. Brain Res.* 344, 73–84. doi: 10.1016/j.bbr.2018.02.009

Lai, S. W., Chen, J. H., Lin, H. Y., Liu, Y. S., Tsai, C. F., Chang, P. C., et al. (2018). Regulatory effects of neuroinflammatory responses through brain-derived neurotrophic factor signaling in microglial cells. *Mol. Neurobiol.* 55, 7487–7499. doi: 10.1007/s12035-018-0933-z

LeGates, T. A., Kvarta, M. D., and Thompson, S. M. (2019). Sex differences in antidepressant efficacy. *Neuropsychopharmacology* 44, 140–154. doi: 10.1038/s41386-018-0156-z

Lenz, K. M., and McCarthy, M. M. (2015). A starring role for microglia in brain sex differences. *Neuroscientist* 21, 306–321. doi: 10.1177/1073858414536468

Li, F., Zhang, J. W., Wei, R., Luo, X. G., Zhang, J. Y., Zhou, X. F., et al. (2010). Sex-differential modulation of visceral pain by brain derived neurotrophic factor (BDNF) in rats. *Neurosci. Lett.* 478, 184–187. doi: 10.1016/j.neulet.2010.05.013

Lima Giacobbo, B., Doorduin, J., Klein, H. C., Dierckx, R. A. J. O., Bromberg, E., and de Vries, E. F. J. (2018). Brain-derived neurotrophic factor in brain disorders: focus on neuroinflammation. *Mol. Neurobiol.* 56, 3295–3312. doi: 10.1007/s12035-018-1283-6

Lotrich, F. E., Albusaysi, S., and Ferrell, R. E. (2013). Brain-derived neurotrophic factor serum levels and genotype: association with depression during interferon-α treatment. *Neuropsychopharmacology* 38, 985–995. doi: 10.1038/npp.2012.263

Lu, Y., Xu, X., Jiang, T., Jin, L., Zhao, X. D., Cheng, J. H., et al. (2019). Sertraline ameliorates inflammation in CUMS mice and inhibits TNF-α-induced inflammation in microglia cells. *Int. Immunopharmacol.* 67, 119–128. doi: 10.1016/j.intimp.2018.12.011

Lyons, W. E., Mamounas, L. A., Ricaurte, G. A., Coppola, V., Reid, S. W., Bora, S. H., et al. (1999). Brain-derived neurotrophic factor-deficient mice develop aggressiveness and hyperphagia in conjunction with brain serotonergic abnormalities. *Proc. Natl. Acad. Sci. U.S.A.* 96, 15239–15244. doi: 10.1073/pnas.96.26.15239

Macchi, F., Homberg, J. R., Calabrese, F., Zecchillo, C., Racagni, G., Riva, M. A., et al. (2013). Altered inflammatory responsiveness in serotonin transporter mutantrats. *J. Neuroinflammation* 10:116. doi: 10.1186/1742-2094-10-116

Martinowich, K., Manji, H., and Lu, B. (2007). New insights into BDNF function in depression and anxiety. *Nat. Neurosci.* 10, 1089–1093. doi: 10.1038/nn1971

Mizoguchi, Y., Monji, A., Kato, T., Seki, Y., Gotoh, L., Horikawa, H., et al. (2009). Brain-derived neurotrophic factor induces sustained elevation of intracellular Ca2+ in rodent microglia. *J. Immunol.* 183, 7778–7786. doi: 10.4049/jimmunol.0901326

Molendijk, M. L., Spinhoven, P., Polak, M., Bus, B. A., Penninx, B. W., and Elzinga, B. M. (2014). Serum BDNF concentrations as peripheral manifestations of depression: evidence from a systematic review and meta-analyses on 179 associations (N = 9484). *Mol. Psychiatry* 19, 791–800. doi: 10.1038/mp.2013.105

Molteni, R., Macchi, F., Zecchillo, C., Dell'agli, M., Colombo, E., Calabrese, F., et al. (2013). Modulation of the inflammatory response in rats chronically treated with the antidepressant agomelatine. *Eur. Neuropsychopharmacol.* 23, 1645–1655. doi: 10.1016/j.euroneuro.2013.03.008

Müller, N. (2014). Immunology of major depression. *Neuroimmunomodulation* 21, 123–130. doi: 10.1159/000356540

Nakajima, K., Honda, S., Tohyama, Y., Imai, Y., Kohsaka, S., and Kurihara, T. (2001). Neurotrophin secretion from cultured microglia. *J. Neurosci. Res.* 65, 322–331. doi: 10.1002/jnr.1157

Otte, C., Gold, S. M., Penninx, B. W., Pariante, C. M., Etkin, A., Fava, M., et al. (2016). Major depressive disorder. *Nat. Rev. Dis. Primers* 2:16065. doi: 10.1038/nrdp.2016.65

Paolicelli, R. C., Bisht, K., and Tremblay, M. È (2014). Fractalkine regulation of microglial physiology and consequences on the brain and behavior. *Front. Cell. Neurosci.* 8:129. doi: 10.3389/fncel.2014.00129

Paolicelli, R. C., Bolasco, G., Pagani, F., Maggi, L., Scianni, M., Panzanelli, P., et al. (2011). Synaptic pruning by microglia is necessary for normal brain development. *Science* 333, 1456–1458. doi: 10.1126/science.1202529

Patterson, S. L. (2015). Immune dysregulation and cognitive vulnerability in the aging brain: interactions of microglia, IL-1β, BDNF and synaptic plasticity. *Neuropharmacology* 96(Pt A), 11–18. doi: 10.1016/j.neuropharm.2014.12.020

Raison, C. L., Borisov, A. S., Majer, M., Drake, D. F., Pagnoni, G., Woolwine, B. J., et al. (2009). Activation of central nervous system inflammatory pathways by interferon-alpha: relationship to monoamines and depression. *Biol. Psychiatry* 65, 296–303. doi: 10.1016/j.biopsych.2008.08.010

Raison, C. L., Capuron, L., and Miller, A. H. (2006). Cytokines sing the blues: inflammation and the pathogenesis of depression. *Trends Immunol.* 27, 24–31. doi: 10.1016/j.it.2005.11.006

Réus, G. Z., Dos Santos, M. A. B., Strassi, A. P., Abelaira, H. M., Ceretta, L. B., and Quevedo, J. (2017). Pathophysiological mechanisms involved in the relationship between diabetes and major depressive disorder. *Life Sci.* 183, 78–82. doi: 10.1016/j.lfs.2017.06.025

Richter, S. H., Garner, J. P., Zipser, B., Lewejohann, L., Sachser, N., Touma, C., et al. (2011). Effect of population heterogenization on the reproducibility of mouse behavior: a multi-laboratory study. *PLoS One* 6:e16461. doi: 10.1371/journal.pone.0016461

Rossetti, A. C., Paladini, M. S., Colombo, M., Gruca, P., Lason-Tyburkiewicz, M., Tota-Glowczyk, K., et al. (2018a). Chronic stress exposure reduces parvalbumin expression in the rat hippocampus through an imbalance of redox mechanisms: restorative effect of the antipsychotic lurasidone. *Int. J. Neuropsychopharmacol.* 21, 883–893. doi: 10.1093/ijnp/pyy046

Rossetti, A. C., Paladini, M. S., Racagni, G., Riva, M. A., Cattaneo, A., and Molteni, R. (2018b). Genome-wide analysis of LPS-induced inflammatory response in the rat ventral hippocampus: modulatory activity of the antidepressant agomelatine. *World J. Biol. Psychiatry* 19, 390–401. doi: 10.1080/15622975.2017.1298839

Rossetti, A. C., Papp, M., Gruca, P., Paladini, M. S., Racagni, G., Riva, M. A., et al. (2016). Stress-induced anhedonia is associated with the activation of the inflammatory system in the rat brain: restorative effect of pharmacological intervention. *Pharmacol. Res.* 103, 1–12. doi: 10.1016/j.phrs.2015.10.022

Rubinow, D. R., and Schmidt, P. J. (2019). Sex differences and the neurobiology of affective disorders. *Neuropsychopharmacology* 44, 111–128. doi: 10.1038/s41386-018-0148-z

Sairanen, M., Lucas, G., Ernfors, P., Castrén, M., and Castrén, E. (2005). Brain-derived neurotrophic factor and antidepressant drugs have different but coordinated effects on neuronal turnover, proliferation, and survival in the adult dentate gyrus. *J. Neurosci.* 25, 1089–1094. doi: 10.1523/jneurosci.3741-04.2005

Schneiders, J., Fuchs, F., Damm, J., Herden, C., Gerstberger, R., Soares, D. M., et al. (2015). The transcription factor nuclear factor interleukin 6 mediates pro- and anti-inflammatory responses during LPS-induced systemic inflammation in mice. *Brain. Behav. Immun.* 48, 147–164. doi: 10.1016/j.bbi.2015.03.008

Schnydrig, S., Korner, L., Landweer, S., Ernst, B., Walker, G., Otten, U., et al. (2007). Peripheral lipopolysaccharide administration transiently affects expression of brain-derived neurotrophic factor, corticotropin and proopiomelanocortin in mouse brain. *Neurosci. Lett.* 429, 69–73. doi: 10.1016/j.neulet.2007.09.067

Sohrabji, F., Miranda, R. C., and Toran-Allerand, C. D. (1995). Identification of a putative estrogen response element in the gene encoding brain-derived neurotrophic factor. *Proc. Natl. Acad. Sci. U.S.A.* 92, 11110–11114. doi: 10.1073/pnas.92.24.11110

Szapacs, M. E., Mathews, T. A., Tessarollo, L., Ernest Lyons, W., Mamounas, L. A., Andrews, A. M., et al. (2004). Exploring the relationship between serotonin and brain-derived neurotrophic factor: analysis of BDNF protein and extraneuronal 5-HT in mice with reduced serotonin transporter or BDNF expression. *J. Neurosci. Methods* 140, 81–92. doi: 10.1016/j.jneumeth.2004.03.026

Tay, T. L., Béchade, C., D'Andrea, I., St-Pierre, M. K., Henry, M. S., Roumier, A., et al. (2018). Microglia gone rogue: impacts on psychiatric disorders across the lifespan. *Front. Mol. Neurosci.* 10:421. doi: 10.3389/fnmol.2017.00421

Udina, M., Castellví, P., Moreno-España, J., Navinés, R., Valdés, M., Forns, X., et al. (2012). Interferon-induced depression in chronic hepatitis C: a systematic review and meta-analysis. *J. Clin. Psychiatry* 73, 1128–1138. doi: 10.4088/jcp.12r07694

Vegeto, E., Benedusi, V., and Maggi, A. (2008). Estrogen anti-inflammatory activity in brain: a therapeutic opportunity for menopause and neurodegenerative diseases. *Front. Neuroendocrinol.* 29:507–519. doi: 10.1016/j.yfrne.2008.04.001

Villa, A., Rizzi, N., Vegeto, E., Ciana, P., and Maggi, A. (2015). Estrogen accelerates the resolution of inflammation in macrophagic cells. *Sci. Rep.* 5:15224. doi: 10.1038/srep15224

Wang, Y. L., Han, Q. Q., Gong, W. Q., Pan, D. H., Wang, L. Z., Hu, W., et al. (2018). Microglial activation mediates chronic mild stress-induced depressive- and anxiety-like behavior in adult rats. *J. Neuroinflammation* 15:21. doi: 10.1186/s12974-018-1054-3

Wei, Y. C., Wang, S. R., and Xu, X. H. (2017). Sex differences in brain-derived neurotrophic factor signaling: functions and implications. *J. Neurosci. Res.* 95, 336–344. doi: 10.1002/jnr.23897

Wolf, Y., Yona, S., Kim, K. W., and Jung, S. (2013). Microglia, seen from the CX3CR1 angle. *Front. Cell. Neurosci.* 7:26. doi: 10.3389/fncel.2013.00026

Wu, M. V., Manoli, D. S., Fraser, E. J., Coats, J. K., Tollkuhn, J., Honda, S., et al. (2009). Estrogen masculinizes neural pathways and sex-specific behaviors. *Cell* 139, 61–72. doi: 10.1016/j.cell.2009.07.036

Zagni, E., Simoni, L., and Colombo, D. (2016). Sex and gender differences in central nervous system-related disorders. *Neurosci. J.* 2016:2827090. doi: 10.1155/2016/2827090

Zueger, M., Urani, A., Chourbaji, S., Zacher, C., Roche, M., Harkin, A., et al. (2005). Olfactory bulbectomy in mice induces alterations in exploratory behavior. *Neurosci. Lett.* 374, 142–146. doi: 10.1016/j.neulet.2004.10.040

Conflict of Interest Statement: MR has received compensation as a speaker/consultant from the Lundbeck, Otzuka, Sumitomo Dainippon Pharma, and Sunovion, and he has received research grants from the Lundbeck, Sumitomo Dainippon Pharma, and Sunovion.

The remaining authors declare that the research was conducted in the absence of any commercial or financial relationships that could be construed as a potential conflict of interest.

Advantages of publishing in Frontiers

OPEN ACCESS
Articles are free to read for greatest visibility and readership

FAST PUBLICATION
Around 90 days from submission to decision

HIGH QUALITY PEER-REVIEW
Rigorous, collaborative, and constructive peer-review

TRANSPARENT PEER-REVIEW
Editors and reviewers acknowledged by name on published articles

Frontiers
Avenue du Tribunal-Fédéral 34
1005 Lausanne | Switzerland

Visit us: www.frontiersin.org
Contact us: frontiersin.org/about/contact

REPRODUCIBILITY OF RESEARCH
Support open data and methods to enhance research reproducibility

DIGITAL PUBLISHING
Articles designed for optimal readership across devices

FOLLOW US
@frontiersin

IMPACT METRICS
Advanced article metrics track visibility across digital media

EXTENSIVE PROMOTION
Marketing and promotion of impactful research

LOOP RESEARCH NETWORK
Our network increases your article's readership